Compressible Flow

Prof. S. A. E. Miller, Ph.D.

University of Florida

Department of Mechanical and Aerospace Engineering

Theoretical Fluid Dynamics and Turbulence Group

https://saemiller.com

Fall of 2024

“The curve described by a simple molecule of air or vapor is regulated in a manner just as certain as the planetary orbits; the only difference between them is that which comes from our ignorance.”

–Pierre-Simon Marquis de Laplace, 1820, Essai Philosophique sur les Probabilits, Paris

Figure 1: Pierre-Simon Marquis de Laplace.

Table of Contents I

Table of Contents II

Table of Contents III

Table of Contents IV

Class Summary

- Who am I?
- Class overview (syllabus)
- Visualizations of compressible flow

“The great bird will take its first flight on the back of a great swan; filling the universe with wonders; filling all writings with its fame and bringing eternal glory to the nest from which it came”

Leonardo da Vinci

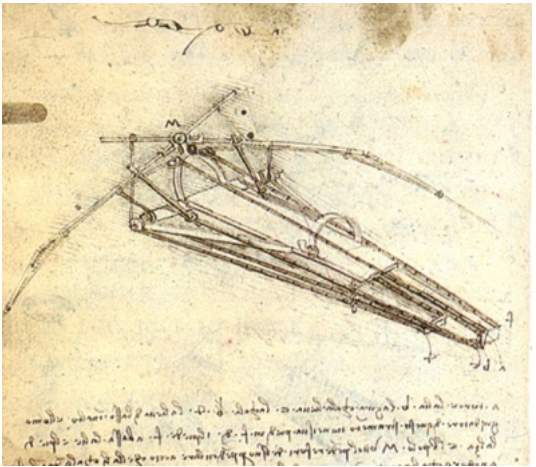

Figure 2: Leonardo da Vinci.

Brief Biography

- UF MAE Prof.
- Previous life NASA
  - NASA Civil Servant from 2009 - 2016
  - Research Aerospace Engineer - Theoretical Aeroacoustics
- Education
  - Ph.D. (NASA Grant)
  - Aerospace Engineering, Penn State
  - M.S. (NREL Grant)
  - Aerospace Engineering, Penn State
  - B.S. Mechanical Engineering, Michigan State University
  - Studies at Tagonrog Russia and Eastern Michigan University
- Early life in Michigan

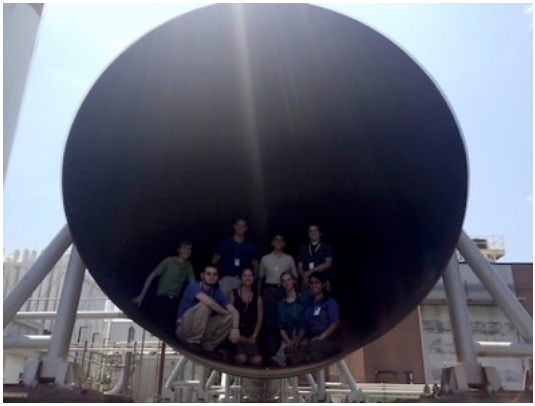

Figure 3: The student group of Prof. Miller at NASA Langley Research Center. Located at the exit of the 8-ft Hypersonic Wind Tunnel.

Turbulence

The last great challenge in classical physics "I am an old man now, and when I die and go to heaven there are two matters on which I hope for enlightenment. One is quantum electrodynamics, and the other is turbulent motion of fluids. And about the former I am rather optimistic." *1932 address to the British Association for the Advancement of Science*

Sir Horace Lamb, FRS
Hydrodynamics and Dynamical Theory of Sound

My Research - Theoretical Fluid Dynamics and Turbulence Group

- Interested in understanding turbulence physically and mathematically
- Interested in understanding how sound is produced by and propagated through turbulent fields
- Central questions within the field of fluid dynamics
- Multiple ways to solve problems - analytical, computationally, and experimentally
- My research focuses on analytical and computational (combined) methods
- This class focuses on analytical, semi-empirical methods, physics, applications, and limited numerics.

Class Outline I

- Introduction
  - Who Am I, syllabus, movies, visualizations
  - What is fluid, flow based on Mach number, compressibility, Mach number, continuum assumption
  - Mathematical models of fluids, derivation of NSE
  - Eqns. of motion, Boltzmann equation, specific forms, acoustics, Bernoulli, Thermo
  - Thermodynamics laws one and two, isentropic, RTT, examples
  - 1D flow, wave prop, speed of sound, Mach waves
- Isentropic Flow
  - Intro. Isentropic flow, examples, RTT derivation, converging-diverging streamtubes, examples
  - Stagnation conditions, error in Bernoulli for comp flows
  - Critical conditions, choking, isentropic calculator, note on table use
  - De Leval, isentropic nozzle operation and rocket engine
  - Applications to supersonic wind tunnel, wind tunnel efficiency, transition to shocks
- Normal shock waves (NSW)

Class Outline II

- What is a shock, shock tubes, compression, expansion
- Shock tubes in practice, bow shock, NSW equation formulation, asymptotic limits
- Stag. prop. across NSW, NSW plots, entropy, shock strength, shock thickness, example
- Hugoniot, Weak & strong NSW, moving NSW
- Induced velocity, reflected shocks, Rayleigh Pitot
- Air blast similarity theory, CD-nozzles standing shocks
- Off-design nozzles, shocks in nozzles and ducts, $T - S$ diagram, examples
- Applications Wind Tunnels
- Applications - Isentropic flow, nozzles, supersonic inlets, ballistic range, midterm review / questions

- Oblique Shock Waves
  - OSW examples, Mach angle, OSW diagram, theory, $\theta - \beta - \mathcal{M}$ graphs
  - Attached vs bluff body shocks, $\theta - \beta - \mathcal{M}$ solutions, shock polar, hodograph, reflections
  - Multiple shock systems, slip lines, λ, Mach intersection
  - Detachment, three-dimensions, explanation of charts and figures
- Prandtl-Meyer Expansion Waves
  - PMEF intro, theory, Meyer function, solution approach

Class Outline III

- Shock expansion theory, diamond airfoils, wave drag, maximum expansion
- Expansions in nozzles, application of shock-expansion systems
- Off-design shock-expansions from nozzles
- Method of characteristics with nozzle example

- Compressible ‘pipe’ flow
  - Rayleigh Flow
  - Fanno flow, boundary Layers
  - Examples of Rayleigh and Fanno flow
  - Combined Rayleigh and Fanno Flow, Prandtl number and Rayleigh relation, isothermo flow
- Transonic flow
  - Transonic flow definitions, theory, historical context
  - Area rule, supercritical airfoil, numerical examples using theory
- Hypersonic Flow
  - Introduction, examples, $\mathcal{M}$ number independence, observations
  - Newton, K, similarity, oblique shocks, expansions

Class Outline IV

- Hypersonic heat-transfer, leading edge bluntness, shock wave interaction
- Supersonic Flow – supersonic flow past wings of finite span, sweep, similarity theory
- Schlieren – special topic on schlieren - schlieren concepts, types of schlieren, sensitivity
- CFD – Special topic on CFD and class review

Syllabus

Discussion of the syllabus

This class is based on...

Numerous journal articles, online articles, history, my professional experience, and personal knowledge. The class is inspired by Professor G. Settles (retired) of the Pennsylvania State University

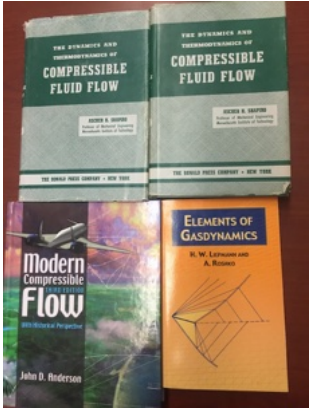

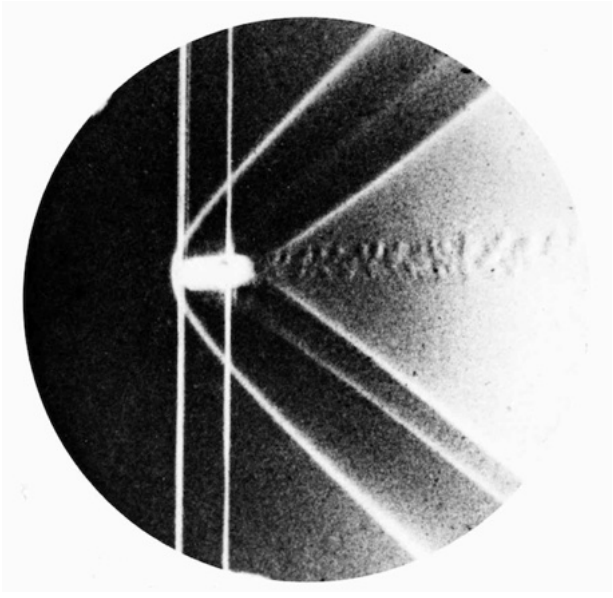

Figure 4: Schlieren image created by Dr. Earnst Mach.

Some Introductory Youtube Videos

- Schlieren optics https://www.youtube.com/watch?v=mLp_rSBzteI
- Schlieren of a match https://www.youtube.com/watch?v=TQJAokQQbmI
- Structure and Dynamics of a Deflagrated Flame Evolution https://www.youtube.com/watch?v=aQrKBR3Qsg8
- Supersonic jet impingement https://www.youtube.com/watch?v=61tsXGUc6nU
- SpaceX engine test https://youtu.be/e7kqFt3nID4?t=3
- NACA airfoil transonic schlieren https://youtu.be/BsIabrtezIQ?t=15
- Russian hypersonics https://www.youtube.com/watch?v=FfiYy0NfTbs
- Volcano Eruption in Papua New Guinea https://www.youtube.com/watch?v=BUREX8aFbMs

Figure 5: SR–71 and XB–70.

Figure 6: SR–71 inlet.

Figure 7: XLR–99 engine that powers the X–15. The world's first restartable and throttle ready liquid rocket engine.

Figure 8: Boeing X-20 Dyna-Soar (“Dynamic Soarer”) was a United States Air Force (USAF) program to develop a spaceplane that could be used for a variety of military missions, including aerial reconnaissance, bombing, space rescue, satellite maintenance, and as a space interceptor to sabotage enemy satellites.

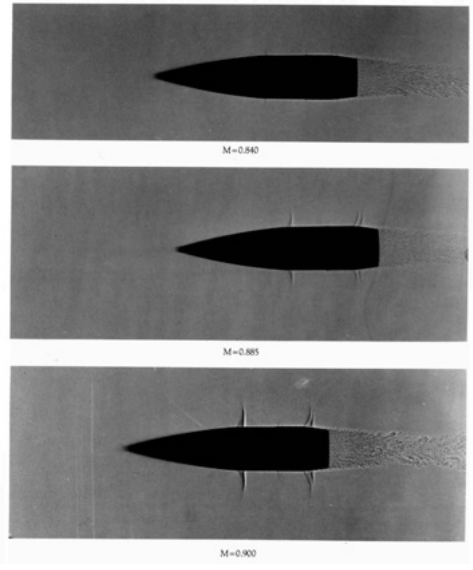

Figure 9: Schlieren images of flow over a projectile. A. C. Charters, in von Kármán 1947

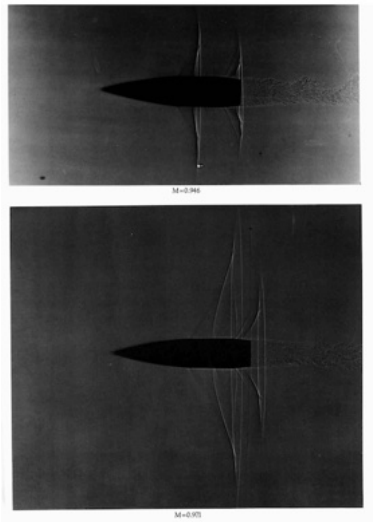

Figure 10: Schlieren images of flow over a projectile. A. C. Charters, in von Kármán 1947

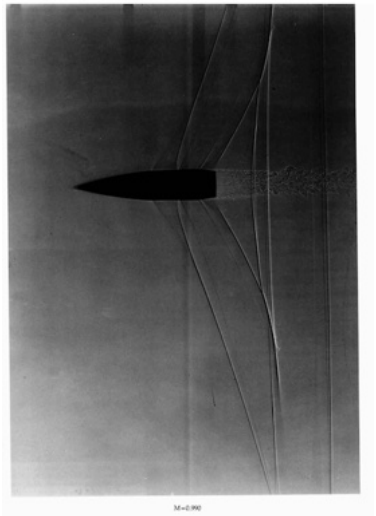

Figure 11: Schlieren image. A. C. Charters, in von Kármán 1947

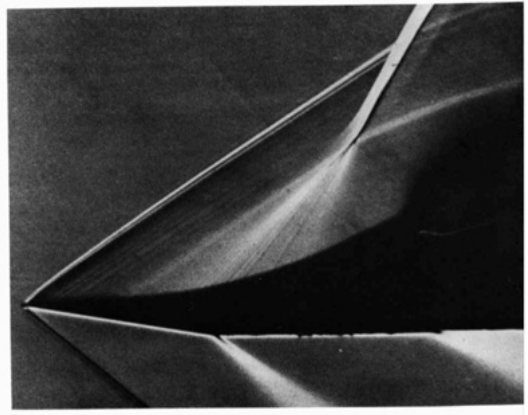

Figure 12: “Steady formation of an oblique shock wave. A cylindrical concave surface in a supersonic wind tunnel at Mach number 1.96 produces a converging fan of compression waves, which are made visible by schlieren photography with the knife edge parallel to the free stream. They focus roughly as a centered compression, forming a strong oblique shock wave that turns the stream through 22.5 degrees. The surface extends upstream as a flat plate at zero incidence so that the weak shock wave from the slightly blunt leading edge will not obscure the view. The surface is roughened to make the boundary layer turbulent, so that it will not separate. Johannesen 1952.”

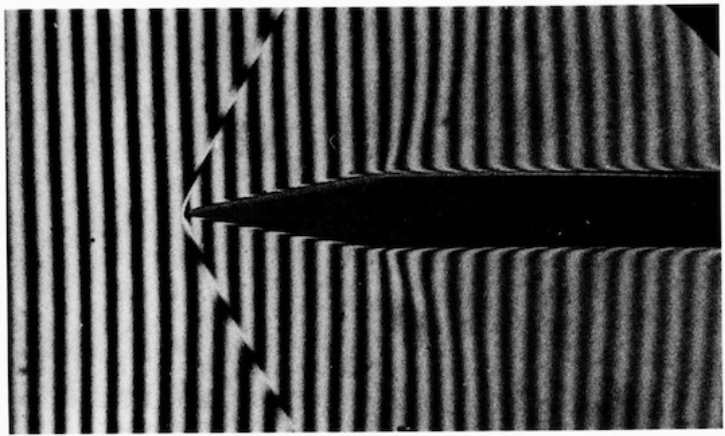

Figure 13: Symmetric shock waves on a wedge. A shock tube semi-vertex angle. A steady flow has been established 100 is here used as a transient wind tunnel. An interferogram microseconds after the incident shock wave passed the tip. shows air flowing at $M = 1.45$ over a wedge-plate of 10° Bleakney, Weimer Fletcher 1949.

Figure 14: Diffraction of a shock wave inside a box. A shock at the right are slip lines generated as the diffracted shock wave in nitrogen is diffracted through a window at one wave oscillated in shape moving across the box, which end of a rectangular box and reflected from the other end. have been perturbed by shock waves passing over them A shadowgraph shows a remarkable pattern of shock roughly at right angles. Several examples of separated waves, slip lines, and vortices, but one that is altogether boundary-layer flow are also evident. Photograph by Russell determinate and reproducible. The three rope-like traces E. Duff in Laporte's laboratory.

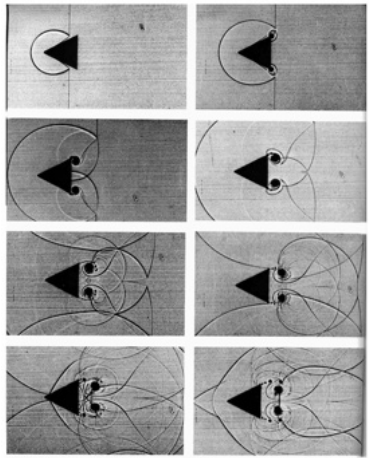

Figure 15: Diffraction of a shock wave by a finite wedge. Photographs by H. Schardin, in Oertel 1966.

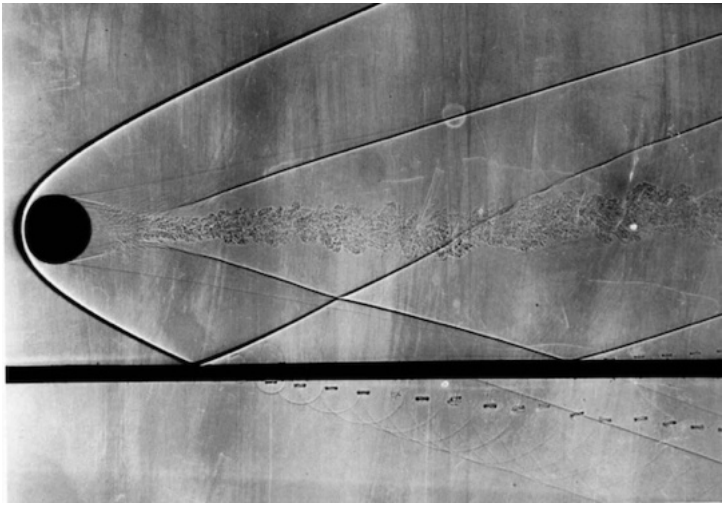

Figure 16: Sphere flying over a perforated plate. A shadowgraph shows a $9/16$-inch sphere shot past a plate with a line of $1/16$-inch holes spaced $1/4$ inch apart. The pressure of the bow wave produces below the plate the classical diagram of the Mach cone as the envelope of a series of expanding spherical acoustic waves. This was used to measure the Mach number, which is seen to be 3. A tiny vortex ring moving downward is formed at each hole, followed at the right by a secondary ring moving upward. Photograph from U.S. Army Ballistic Research Laboratory.

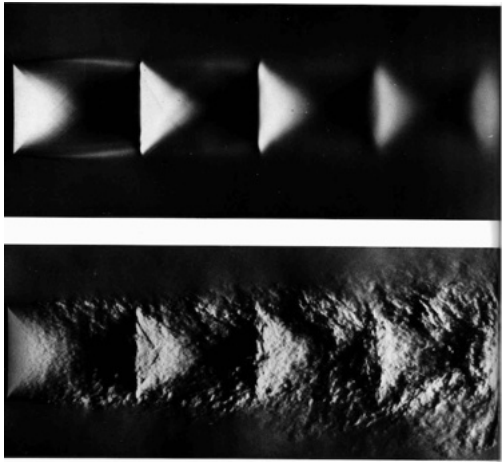

Figure 17: Long- and short-duration photographs of a with an exposure time of 10^{-2} s, shows the mean flow, with supersonic jet. Dry air flows from a converging conical a series of expansion and compression waves. The lower nozzle with an exit diameter of 1 cm. The ratio of stagnation photograph, at 0.5×10^{-6} s, shows the more complicated atmospheric pressure is 3.13, giving an axisymmetric jet of Mach number 1.4. The upper shadowgraph, with an exposure time of 10^{-2} s, shows the mean flow, with a series of expansion and compression waves. The lower photograph, at 0.5×10^{-6} s, shows the more complicated instantaneous structure. Photographs by N. Johannesen

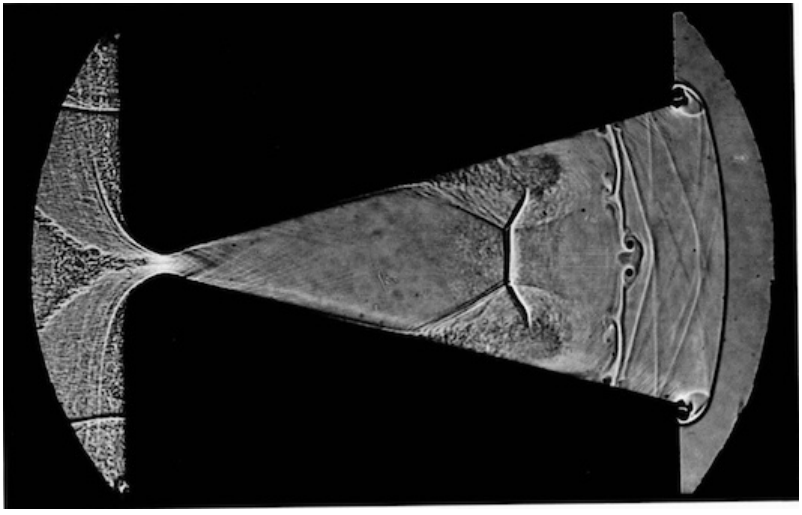

Figure 18: Starting process in a nozzle. The incident shock directed upstream but being swept downstream, and causwave, traveling at a shock Mach number of 3 , has just ing the boundary layers to separate. Mach waves from the passed through a plane nozzle. Behind it are several con- walls show the supersonic flow established downstream of tact surfaces containing vortices. Between them and the nozzle throat is a second shock wave.

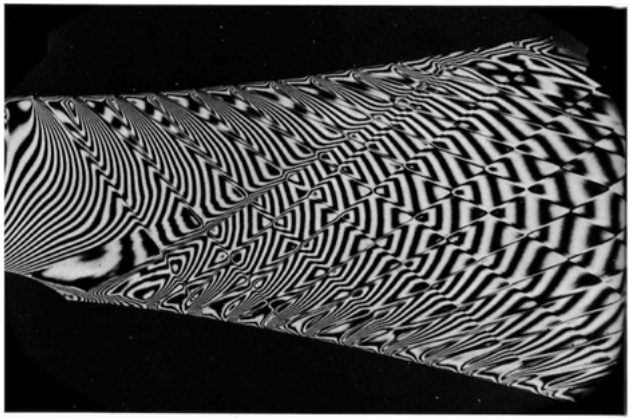

Figure 19: Supersonic nozzle with wall disturbances. This engine. Triangular grooves about 0.3 mm deep have been interferogram shows the flow through a plane Laval nozzle scratched into the walls to generate weak shock waves with a disturbing cylinder on the lower boundary in the throat region, as a model for a disturbed rocket.

Figure 20: Plasma wake of the Space Shuttle reentry as observed from the International Space Station.

Next Time

- Flow regime definitions
- Compressibility
- Mach number

Class Overview

Introduction

- Flow regime definitions
- Compressibility
- Mach number

“Before writing on winged creatures, make a book on insensate objects that descend through the air without wind (in other words the laws of gravity and falling bodies) and another on those that descend with the wind (in other words the laws of air resistance and aerodynamics).”

Leonardo da Vinci

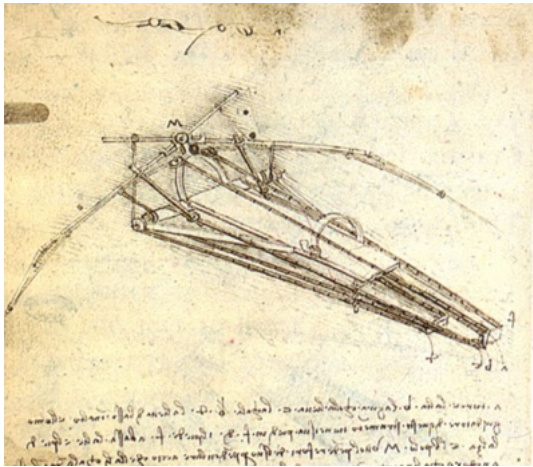

Figure 21: Da Vinci, Flying Machine, 1485.

Fluid Basics

- What is a fluid? Any substance that deforms continually under shear stress
- E.g. Plasmas, liquids, gases
- We mostly focus on gas in this class
- Most liquids show almost no change in density, ρ, with change in pressure, p
- Most liquids are considered to be incompressible for practical prediction purposes
- Gases change readily with pressure
- Close equation requires a gas law - e.g. ideal gas law

$$p = \rho RT \tag{1}$$

- Compressible flows are those where ρ changes in time and/or space

Compressibility

What is compressibility? Let τ_c be compressibility

$$\tau_c = -\frac{1}{v}\frac{dv}{dp} \tag{2}$$

where v is volume, τ_c is compressibility, and p is pressure. Here, v is not the velocity component.

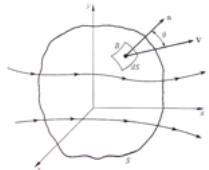

Figure 22: Control volume.

Compressibility

- Isothermal Compressibility – T is held constant
- Isentropic Compressibility – Constant entropy
- Compressibility is a property of the fluid
- e.g. Water $\tau_c \sim 5 \times 10^{-10}$ m^2 / N at ATM
- Air $\tau_c \sim 10^{-5}$ m^2 / N at ATM

τ_c in terms of density is

$$\tau_c = \frac{1}{\rho}\left(\frac{d\rho}{dp}\right) \tag{3}$$

We can write

$$d\rho = \rho \tau_c dp \tag{4}$$

If you cannot perform this mathematical step please consult your math textbooks.

Molecules and Collisions

- Avogadro's number, 6.025×10^{23}, molecules in a gram molecular weight of gas,
  - Standard temperature 0 deg. C and pressure 760 Torr occupies 22,414 cm^3, which means 2.7×10^{19} molecules/cm^3.
- Hence cube's edge is only 0.001 cm contains 2.7×10^{10} molecules.
- At standard conditions, mean free path for gases such as air is approximately 10^{-5} cm, which is smaller than the edge of the 0.001 cm cube.
- Total number of collisions γ per second in a cubic centimeter is $\gamma = \nu\bar{c}/2\lambda$, where ν is the number of molecules in a cubic centimeter, $\bar{c}$ is the mean velocity (for air roughly $\left(5 \times 10^4\right)$ cm / s, and λ is 10^{-5} cm.
- For these representative numbers, $\gamma = 6.75 \times 10^{28}$ collisions per second cm^3, and the collision frequency for a molecule is 5×10^9 per s.
- A 0.001 cm cube, we have is 6.75×10^{19} collisions / s.

Pressure Gradients

Some important notes on pressure gradients

- Most flows contain pressure gradients
- Many flows are driven by pressure gradients
- Strong gradients of p will create density changes
- This is not the case in incompressible flow (eg ρ is a constant)
- Consider a portion of the right hand side of the momentum equation

$$-\frac{\partial p}{\partial x_i}\delta_{ij} \tag{5}$$

- Note term δ_{ij}, which is the Kronecker delta function

Mach Number

$$M = \frac{\text{gas velocity}}{\text{speed of sound}} = \frac{u}{c} \tag{6}$$

where u is velocity and c or a are local speed of sound. Or

$$M_\infty = \frac{u_\infty}{c_\infty} \tag{7}$$

- Be aware of the difference between local and global Mach number
- Consider flow to be compressible if $M > 0.3$, however there are exceptions
- Turbulent Mach number, M_t, or turbulent Reynolds number, Re_t
- If flow speed is low enough then can be treated incompressible

Subsonic Flow

Introducing the global Mach number, M_∞, your new friend

$$M_\infty \lessapprox 0.8 \tag{8}$$

- Mach number less than unity everywhere, strict definition $M < 1$
- All streamlines are "smooth" and continuous on $\mathcal{C}^1$
- Compressible (maybe)

Transonic Flow

$$0.8 \lessapprox M_\infty \lessapprox 1 + \tag{9}$$

- Subsonic M_∞
- Expansion of flow results in supersonic regions
- Shock terminates back to subsonic flow (usually)
- If M_∞ increases then shock moves to end of the flight vehicle and forms a bow shock
- Streamlines are non-continuous in $\mathcal{C}^1$ on discontinuities and continuous elsewhere

Supersonic Flow

$$M_\infty > 1 \tag{10}$$

- Flow everywhere is $M > 1$ (this is not a rigorous definition)
- Flow in front of the shock is unaware of the shock
- Flow after shocks are very aware of the shock
  - Called the region of influence
- Tremendous mathematical differences relative to subsonic flow
  - Referred to as hyperbolic or elliptic

Hypersonic Flow

$$M_\infty > 5 \tag{11}$$

- Many characterizations and confusion about what hypersonics is!
- At high speeds the flow eventually becomes “Mach number independent”
- Ionize gas (sometimes)
- Dissociate gas (perhaps)
- T, p, ρ increase by large amounts across shockwave – we will define these later
- Example - Oxygen will liquify within air at $M \approx 5$

Hypervelocity Flow

$$20 \lessapprox M_\infty \leq \infty \tag{12}$$

- Rarified flow-field
- Continuum breaks down
- Navier-Stokes equations invalid, but are a useful approximation
- Monte-Carlo or Boltzman approach required
- Briefly discuss this flow near the end of the class

Flows at Various Mach Numbers

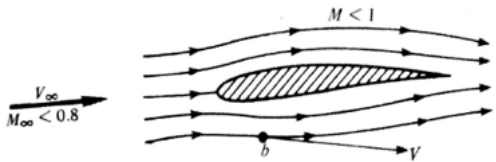

Figure 23: Subsonic flow.

Flows at Various Mach Numbers

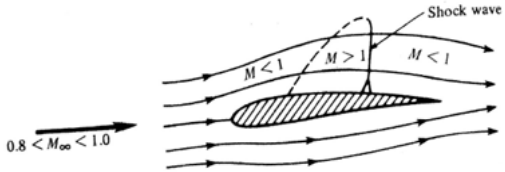

Figure 24: Transonic flow.

Flows at Various Mach Numbers

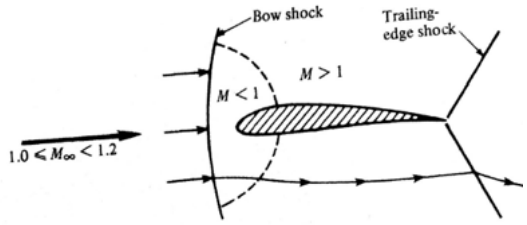

Figure 25: Transonic flow.

Flows at Various Mach Numbers

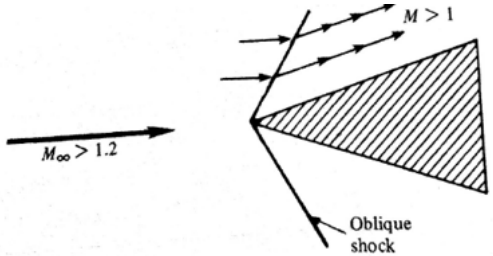

Figure 26: Supersonic flow.

Flows at Various Mach Numbers

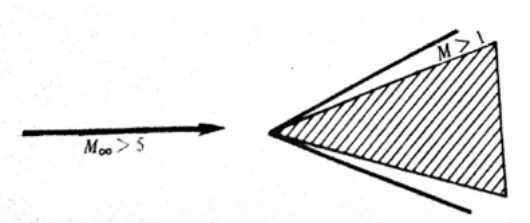

Figure 27: Hypersonic flow.

Continuum Assumption I

- Fluids are made of molecules (atomic theory)
- Continuum assumption holds in almost all cases discussed
- Continuum assumption is true as long as mean free path between molecules is much less than scales of the flow
- Examine rarefied gas dynamics for situations where assumption breaks down

Strict definition - Fluid is the continual deformation of Euclidian space

Continuum Assumption I

- Most aerospace flows are Newtonian

$$\tau \approx \mu \frac{du}{dy} \tag{13}$$

  is a linear relationship where τ is the shear stress in a simplified parallel shear flow
- Non-Newtonian fluids are difficult to handle
- In practice, fluids have viscosity
- Without viscosity fluids are Eulerian and Euler equations model them
  - Example liquid Helium near zero K

William Thomson, 1st Baron Kelvin

26 June 1824 – 17 December 1907, Scots-Irish

- Mathematical physicist, engineer, academic, president RS
- Knighted 1866 by Queen Victoria
- Title refers to the river Kelvin, which flows close by his laboratory at the University of Glasgow
- 650 articles and 70 patents
- Widely known for determining absolute zero as approximately –273.15 degree C

S.A.E. Miller, Ph.D., saem@ufl.edu

William Thomson, 1st Baron Kelvin

26 June 1824 – 17 December 1907, Scots-Irish

"In physical science a first essential step in the direction of learning any subject is to find principles of numerical reckoning and practicable methods for measuring some quality connected with it. I often say that when you can measure what you are speaking about and express it in numbers you know something about it; but when you cannot measure it, when you cannot express it in numbers, your knowledge is of a meagre and unsatisfactory kind: it may be the beginning of knowledge, but you have scarcely, in your thoughts, advanced to the stage of science, whatever the matter may be."

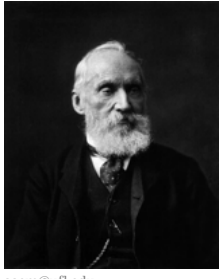

S.A.E. Miller, Ph.D., saem@ufl.edu

Knudsen Number

- K_n is dimensionless ratio of the mean free path by the physical length scale
- If K_n is large then the flow is rarified
- Typically in the atmosphere (STP) $\lambda \approx 1 \times 10^{-8}$ m

$$K_n = \frac{\lambda}{L} \tag{14}$$

where λ is the mean free path and L is the physical length scale. For a Boltzmann gas

$$\boxed{K_n = \frac{k_B T}{2^{1/2} \pi d^2 p_o L}} \tag{15}$$

where k_B is the Boltzmann constant, T is the static temperature, d is the particle diameter, and p is the total pressure. $k_B = 1.38064852 \times 10^{-23}$ m^2 kg s^{-2} K^{-1}.

Knudsen Number I

We can relate the Mach number and Reynolds number through K_n. Let the molecular average speed be $\bar{c}$

$$\bar{c} = \sqrt{\frac{8k_BT}{\pi m}} \tag{16}$$

where m is the molecular mass. Mean free path can be written

$$\lambda = \frac{\mu}{\rho}\sqrt{\frac{\pi m}{2k_BT}} \tag{17}$$

If we divide both sides of Eqn. 17 by L and assume $M = u_\infty/c$, where $c = \sqrt{\gamma k_BT/M} = \sqrt{\gamma RT/M}$ and then note the ratio of M/Re as

$$\frac{M}{Re} = \frac{u_\infty/c_\infty}{\rho u_\infty L/\mu} = \frac{\mu}{\rho L}\sqrt{\frac{m}{\gamma k_BT}} \tag{18}$$

Knudsen Number II

If we multiply the right hand side by $(\gamma\pi/2)^{1/2}$. We obtain

$$K_n = \frac{\mu}{\rho L}\sqrt{\frac{m}{\gamma k_B T}}\sqrt{\frac{\gamma\pi}{2}} \tag{19}$$

Thus we can write

$$\boxed{K_n = \frac{M}{Re}\left(\frac{\gamma\pi}{2}\right)^{1/2}} \tag{20}$$

Knudsen Number

- For $K_n > 10$, we should treat the flow as rarefied, otherwise we will treat the flow using statistical and continuum mechanics.
- Almost all the flows of interest are treatable as statistical and as a continuum except for high-altitude high Mach number reentry.
- Turbulence is by definition a continuum phenomenon, which greatly simplifies the calculation of $K_n > 10$ flows.

Boundary Layer

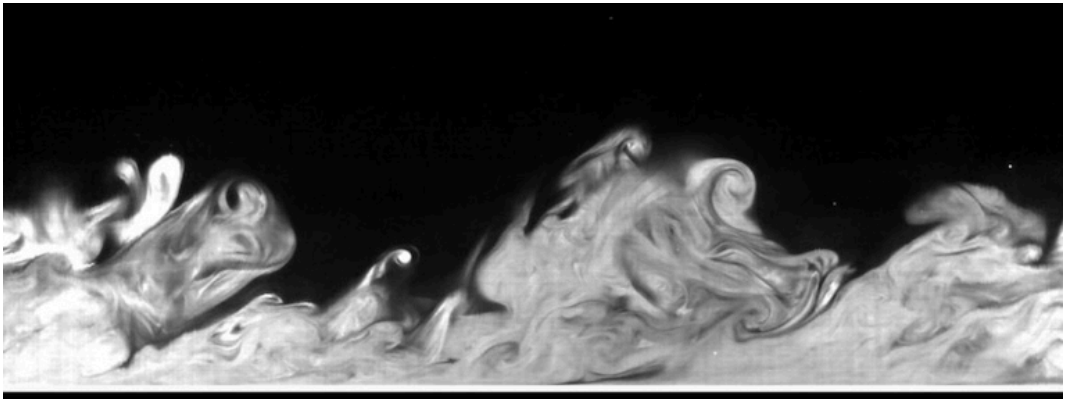

Figure 28: A high–speed camera captured this dye injected turbulent boundary layer. Courtesy of Prof. Mitchell.

Boundary Layer

- Recall no slip condition that $\boldsymbol{u} = 0$ at the wall

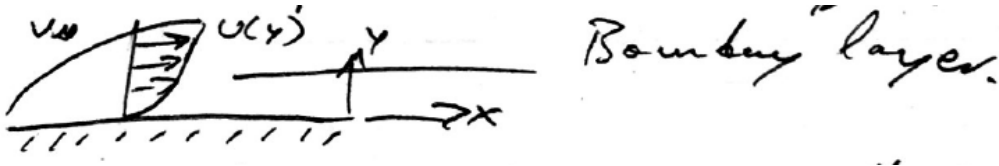

- The turbulent boundary layer must be predicted to accurately capture drag
- A thin layer in a fluid near the solid boundary
- Proposed by Ludwig Prandtl (1875 to 1953)

Incompressible versus Compressible Flow

Incompressible Flow

- Unknowns field-variables are p and $\boldsymbol{u}$

Compressible Flow

- At least 4 unknowns including p, $\boldsymbol{u}$, T, ρ, and more depending on assumptions
- Require that we formulate an energy equation and equation of state
- If combustion occurs then likely tens to millions of additional equations per chemical species
- Does not include electromagnetics
- Does not include nuclear effects
- Does not include multiphase

Class Summary

- Flow regime definitions
- Compressibility
- Mach number

Next Time

- The Navier-Stokes equations (NSE)
- Differential form and integral form

Class Overview

The Navier–Stokes equations holds its master in its own bonds, shackling the mind and brain so that the inner freedom of the very strongest must suffer.

- The Navier–Stokes equations (NSE)
- Differential form and integral form

Mathematical Models of Fluid Dynamics

- Seek mathematical models in the form of sets of partial differential equations that we can use to model and hopefully predict the dynamics of fluids
- Field-variables – typically 5
  - ρ – density
  - $\boldsymbol{u}$ – velocity
  - E – total energy
- Generally cannot solve these equations analytically
  - No general solution exists
  - Only solutions with very specific assumptions
- Boundary conditions must also be developed but we will define these in later classes

“I was capable of being moved, mathematically, as it were, by the belief that a particular course was right; and I do believe that God put these views in my mind, working by means of that which was in me to supply that which was wanting,”

Lucasian Professor George Gabriel Stokes

“Then it is right that you should even now draw back, nor heed though I should go to the grave a thinking machine unenlivened and uncheered and unwarmed by the happiness of domestic affection,” (on receiving reply of his 55 page essay to his future wife on why they should not be marreid)

Lucasian Professor George Gabriel Stokes

Claude Louis Marie Henri Navier

10 February 1785 – 21 August 1836, French

- Engineer and physicist who specialized in mechanics
- Known for Navier-Stokes equations
- École polytechnique, and in 1804 continued his studies at the École Nationale des Ponts et Chaussées, from which he graduated in 1806
- Construction of bridges at Choisy, Asnières and Argenteuil
- Professor of calculus and mechanics at the École Polytechnique
- Named on Eiffel tower

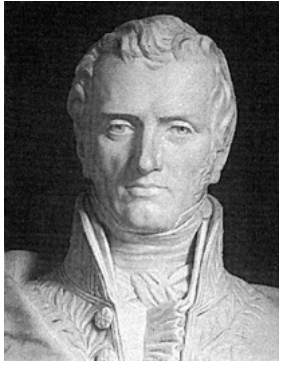

S.A.E. Miller, Ph.D., saem@ufl.edu

George Gabriel Stokes

13 August 1819 – 1 February 1903, British

- Physicist and mathematician, fluids, optics
- Navier-Stokes equations
- Stokes spent all of his career at the University of Cambridge, where he served as Lucasian Professor of Mathematics
- President Royal Society
- President of the Victoria Institute, which had been founded to defend evangelical Christian principles against challenges from the new sciences, especially the Darwinian theory of biological evolution
- Married Mary Susanna Robinson, daughter of the Rev Thomas Romney Robinson, 5 children

S.A.E. Miller, Ph.D., saem@ufl.edu

Derivation of Navier-Stokes Equations I

- Fluid flow can be represented mathematically as a continuous transformation of three-dimensional Euclidean space into itself.
- This transformation is parametrized by a real parameter t that represents time.
- Assume that there is a fixed rectangular coordinate system (x_1, x_2, x_3), which we denote as the position denoted by x
- We parameterize the position of a particle P that moves through the fluid from time $t = 0$ to some other time t, $-\infty < t < \infty$
- Its new position is another position x
- x is determined as a function of X (new position) and t as $x = x(X, t)$ or $x_i = x_i(X, t)$

Transformation and Jacobian I

- If X is fixed and t varies then the path of the particle is specified
- Fixed t the equation determines a transformation of a region initially occupied by the fluid into its position at time t
- Assume that the parameterization is continuous and invertible and the inverse exists, $X = X(x, t)$ and $X_i = X_i(x, t)$
- Assume that x_i and X_i are sufficiently smooth to differentiate

Transformation and Jacobian II

From the condition that the transformation possesses a differentiable inverse we can define its Jacobian

$$J = J(X,t) = \det\left(\frac{\partial x_i}{\partial X_j}\right) \tag{21}$$

where $0 < J < \infty$.

- We call the material coordinate of the particle X (its initial position)
- The spatial coordinates x are referred to as the position or place of the particle

Derivation of Navier-Stokes Equations I

Because of the transformation, we defined for x and X, each of the hydrodynamic variables is expressed in terms of material coordinates

$$f(x,t) = f(x(X,t),t) = F(X,t) \tag{22}$$

Therefore, we may for example write the velocity u at time t of a particle initially at X through this definition as

$$u(x,t) = U(X,t) = \frac{d}{dt}x(X,t) \text{ with } x = x(X,t) \tag{23}$$

Here, X is the parameter representing a given fixed particle, and this is the reason we use the ordinary derivative.

Derivation of Navier-Stokes Equations I

If we have a velocity field, $u(x,t)$, we can determine the principle transformation solving the ordinary differential equation

$$\frac{d}{dt}x(X,t) = u(x(X,t),t) \tag{24}$$

with $x(X,0) = X$, where X is a parameter. We shall always write

$$\frac{d}{dt}F(X,t) \text{ and } \frac{\partial}{\partial t}f(x,t) \tag{25}$$

where f and F are related. We then have

$$\frac{d}{dt}F(X,t) = \frac{d}{dt}f(x(X,t),t) = \frac{\partial f}{\partial x_i}(x(X,t),t)\frac{dx_i}{dt} + \frac{\partial f}{\partial t}(x(X,t),t) \tag{26}$$

Material (Total) Derivative I

We may now obtain a general formula

$$\frac{d}{dt}F(X,t) = \frac{D}{Dt}f(x,t) \tag{27}$$

where

$$\boxed{\frac{D}{Dt}f(x,t) \equiv \frac{\partial f}{\partial t}(x,t) + u(x,t)\cdot\nabla f(x,t)} \tag{28}$$

which is called the material derivative of f.

Transport Theorem I

Theorem 1.

Let $\Omega(t)$ denote an arbitrary volume that is moving with the fluid and let $f(x,t)$ be a scalar or vector function of position and time. The transport theorem states that

$$\boxed{\begin{aligned} &\frac{d}{dt}\int_{\Omega(t)} f(x,t)dx \\ &= \int_{\Omega(t)} \left(\frac{\partial f}{\partial t}(x,t) + u(x,t)\cdot\nabla f(x,t) + f(x,t) div\, u(x,t) \right) dx \end{aligned}} \tag{29}$$

Transport Theorem II

The transport theorem can also be written as

$$\boxed{\begin{aligned}&\frac{d}{dt}\int_{\Omega(t)} f(x,t)dx \\ &= \int_{\Omega(t)} \frac{\partial f}{\partial t}(x,t)dx + \int_{\partial\Omega(t)} f(x,t)u(x,t)\cdot n(x,t)dS\end{aligned}} \tag{30}$$

where $n(x,t)$ is the outward unit normal to $\partial\Omega(t)$ at $x \in \partial\Omega(t)$.

Transport Theorem Proof I

Proof – Consider the transform $x : \Omega(0) \rightarrow \Omega(t), x = x(X,t)$. Then

$$\begin{aligned} \int_{\Omega(t)} f(x,t)dx &= \int_{\Omega(0)} f(x(X,t),t)J(X,t)dX \\ &= \int_{\Omega(0)} F(X,t)J(X,t)dX \end{aligned} \tag{31}$$

and we can now find

$$\begin{aligned} \frac{d}{dt}\int_{\Omega(t)} f(x,t)dx &= \frac{d}{dt}\int_{\Omega(0)} F(X,t)J(X,t)dX \\ = \int_{\Omega(0)} \frac{d}{dt}F(X,t)J(X,t) &+ F(X,t)\frac{d}{dt}J(X,t)dX \end{aligned} \tag{32}$$

Transport Theorem Proof II

So we now have

$$\begin{aligned}
&\int_{\Omega(0)} \frac{d}{dt} F(X,t) J(X,t) dX \\
&= \int_{\Omega(0)} \left(\frac{\partial f}{\partial t}(x(X,t),t) + u(x(X,t),t) \cdot \nabla f(x(X,t),t) \right) J(X,t) dX \\
&= \int_{\Omega(t)} \left(\frac{\partial f}{\partial t}(x,t) + u(x,t) \cdot \nabla f(x,t) \right) dx
\end{aligned} \tag{33}$$

All that remains is to prove the Euler formula

$$\frac{d}{dt} J(X,t) = \operatorname{div} u(x(X,t),t) J(X,t) \tag{34}$$

Derivation of Navier-Stokes Equations – Compressibility I

The fluid is called incompressible if for any domain $\Omega(0)$ and any t

$$\boxed{\text{volume } \Omega(t) = \text{volume } \Omega(0)} \tag{35}$$

which is the mathematical definition for incompressible flow (not the less rigorous $\rho =$ constant.

Jean le Rond d'Alembert Condition I

Noting that from the transport theorem we can write using

$$\begin{aligned}\frac{d}{dt}\int_{\Omega(t)} f(x,t)dx &= \frac{d}{dt}\int_{\Omega(0)} F(X,t)J(X,t)dX \\ &= \int_{\Omega(0)} \frac{d}{dt}F(X,t)J(X,t) + F(X,t)\frac{d}{dt}J(X,t)dX\end{aligned} \tag{36}$$

and find with $f(x,t) \equiv 1$

$$\frac{d}{dt}\text{volume}\Omega(t) = \frac{d}{dt}\int_{\Omega(t)} dx = \int_{\Omega(0)} \frac{d}{dt}J(X,t)dX \tag{37}$$

Based on the Euler formula and $0 < J < \infty$ and the fact of the arbitrariness of choice of the domain $\Omega(t)$ via $(\Omega(0))$ a necessary and sufficient condition for the fluid to be incompressible is

$$\boxed{\text{div } u(x,t) = 0 \text{ or } \nabla \cdot u(x,t) = 0} \tag{38}$$

Continuity – Conservation of Mass I

Let $\rho = \rho(x,t)$ be the mass per unit volume of the fluid at point x and time t. Then the mass of any finite volume Ω is

$$m = \int_{\Omega} \rho(x,t)dx \tag{39}$$

The principle of the conservation of mass states that the mass of a fluid in a material volume Ω does not change as Ω moves with the fluid

$$\frac{d}{dt}\int_{\Omega(t)} \rho(x,t)dx = 0 \tag{40}$$

Continuity – Conservation of Mass I

Using the transport theorem (Eqn. 30) we can then write

$$\int_{\Omega(t)} \left(\frac{\partial \rho}{\partial t} + \text{div}\,(\rho u) \right) dx = 0 \tag{41}$$

therefore

$$\frac{\partial \rho}{\partial t} + \text{div}\,(\rho u) = 0 \tag{42}$$

as the integrand must be zero.

Continuity – Conservation of Mass I

The principle of conservation of mass can also be expressed as follows. Let Ω be a fixed volume, then

$$\frac{d}{dt}\int_{\Omega}\rho(x,t)dx = -\int_{\partial\Omega}\rho u \cdot ndS \tag{43}$$

which is the rate of change of mass in a fixed volume Ω and is equal to the mass flux through its surface. We note the general formula

$$\frac{d}{dt}\int_{\Omega(t)}\rho f dx = \int_{\Omega(t)}\rho\frac{D}{Dt}f dx \tag{44}$$

Conservation of Momentum I

- Conservation of linear momentum principle – Forces acting on an element of continuous medium are of two kinds
  - External
  - Body forces

f represents a force per unit mass then it acts on an element Ω as

$$\int_{\Omega} \rho f dx \tag{45}$$

Internal or contact forces are acting on an element of volume Ω through its bounding surface.

Conservation of Momentum I

Let n be the unit outward normal at a point of the surface $\partial\Omega$ and t_n the force per unit area exerted there by the material volume outside $\partial\Omega$.

The surface force exerted on the volume Ω can be expressed by the integral

$$\int_{\partial\Omega} t_n dS \tag{46}$$

The Cauchy principle says that t_n depends on any given time only on the position and the orientation of the surface element dS eg

$$t_n = t_n(x, t, n) \tag{47}$$

Conservation of Momentum I

Principle of conservation of linear momentum says that, "the rate of change of linear momentum of a material volume equals the resultant force on the volume," Newton.

We assume f is known

$$\frac{d}{dt}\int_{\Omega(t)} \rho u dx = \int_{\Omega(t)} \rho f dx + \int_{\partial\Omega(t)} t_n dS \tag{48}$$

Recall the formula previously developed

$$\frac{d}{dt}\int_{\Omega(t)} \rho f dx = \int_{\Omega(t)} \rho \frac{D}{Dt} f dx \tag{49}$$

Combining these two equations we obtain

$$\int_{\Omega(t)} \rho \frac{Du}{Dt} dx = \int_{\Omega(t)} \rho f dx + \int_{\partial\Omega(t)} t_n dS \tag{50}$$

Conservation of Momentum I

We note the important fact that the vector t_n is the normal stress and can be expressed as a linear function of n in the form

$$t_n(x,t,n) = n(x,t)T(x,t) \tag{51}$$

where $T = T_{ij}$ is the tensor called the stress tensor.
Let l^3 be the volume of $\Omega = \Omega(t)$. Divide both sides by l^2 and let the volume go to zero, we find

$$\lim_{|\Omega|\to 0} l^{-2} \int_{\partial\Omega} t_n dS = 0 \tag{52}$$

Stress forces are in local equilibrium.

Conservation of Momentum I

- Let Ω be a domain containing a fluid and consider a regular tetrahedron with vertex at an arbitrary point $x \in \partial\Omega$ with its three faces parallel to the coordinate plates.
- Let the slanted face have normal $n = (n_1, n_2, n_3)$ and area Σ.
- Normals of the other faces are $-e_1$, $-e_2$, and $-e_3$ with areas $n_1\Sigma$, $n_2\Sigma$, and $n_3\Sigma$
- Applying the above equation to the family of tetrahedrons obtained by lettering $\Sigma \to 0$ we obtain

$$t(n) + n_1 t(-e_1) + n_2 t(-e_2) + n_3 t(-e_3) = 0 \tag{53}$$

where $t(n) = t_n = t_n(x, t, n)$, $t(-h) = t_{-h}$ for $h \in (e_1, e_2, e_3)$ and $n_i > 0$
$t(n)$ can be expressed as a linear function of n.

Conservation of Momentum I

We can now write our previous momentum equation with Green's theorem as

$$\int_{\Omega(t)} \rho \frac{Du}{Dt} dx = \int_{\Omega(t)} (\rho f + \text{ div } T)\, dx \tag{54}$$

and integrating both sides we have

$$\rho \frac{Du}{Dt} = \rho f + \text{ div } T \tag{55}$$

or

$$\rho \left(\frac{\partial}{\partial t} u_i + \sum_{j=1}^{3} u_j \frac{\partial}{\partial x_j} u_i \right) = \rho f_i + T_{ji,j}, \text{ for } i = 1, 2, 3 \tag{56}$$

which is the Cauchy equation of motion in differential form.

Augustin-Louis Cauchy

21 August 1789 – 23 May 1857, French

"very often the laws derived by physicists from a large number of observations are not rigorous, but approximate."

- Professor at École Polytechnique
- Founded complex analysis, Wave theory, mechanics, elasticity
- 800 research articles and 5 textbooks
- Fled France in the 1830 revolution and later returned (Royalist)

S.A.E. Miller, Ph.D., saem@ufl.edu

Conservation of Momentum I

- Need to formulate T but it depends on the type of fluid of interest
- In the simplest model the contact forces act perpendicular to the surface elements

$$t(n) = -p(x)n \tag{57}$$

where p is the pressure.

- The minus sign is chosen so that when $p > 0$ the contact forces on a closed surface tend to compress the fluid inside.
- p represents the pressure exerted from outside on a surface of the element on the fluid.
- All fluids at rest exhibit this stress behavior
  - A fluid parcel of always experiences a stress normal to itself, and this stress is independent of the orientation.
- This is called hydrostatic.

Conservation of Momentum I

The equation of motion for a perfect fluid is now

$$\rho\left(\frac{\partial u}{\partial t}+(u\cdot\nabla)\,u\right)=\rho f-\nabla p \tag{58}$$

where

$$(u\cdot\nabla)u_i=\sum_{j=1}^{3}u_j\frac{\partial}{\partial x_j}u_i,\ \text{for } i=1,2,3 \tag{59}$$

This can also be written in Einstein (index) notation as $u_j u_{ij}$.

Conservation of Momentum I

- All real fluids can exert tangential stresses across surface elements when in motion and then the tensor T is not diagonal.

The stress tensor may always be written in the form

$$T_{ij} = -p\delta_{ij} + P_{ij} \tag{60}$$

where P_{ij} is called the viscous stress tensor.

- We assume that $T_{ij} = T_{ji}$, which is symmetrical.

Note that we can also write the Cauchy equation of motion as

$$\frac{\partial}{\partial t}\rho u_i = \rho f_i + (T_{ji} - \rho u_j u_i)_{,j} \tag{61}$$

Note that the last term on the right hand side is almost always put on the left hand side.

Conservation of Energy I

- The first law of thermodynamics states that the increase of total energy in a material volume is the sum of the heat transferred and the work done on the volume.
- We denote q by the heat flux and E by the specific internal energy.

We can then find the balance expressed by the first law as

$$\begin{aligned} &\frac{d}{dt}\int_{\Omega(t)} \rho\left(\frac{1}{2}|u|^2 + E\right) dx \\ &= \int_{\Omega(t)} \rho f \cdot u dx + \int_{\partial\Omega(t)} t_n \cdot u dS - \int_{\partial\Omega(t)} q \cdot n dS \end{aligned} \tag{62}$$

The integral (first) on the RHS is the rate at which the body force does work and the second represents the work done by the stress, and the third is the total heat flux into the volume.

Conservation of Energy I

We can write this equation using the theorem of stress means with $F = u_i$ and rearranging the terms through the use of the transport theorem

$$\begin{aligned} \frac{d}{dt}\int_{\Omega(t)} \rho \frac{1}{2}|u|^2 dx = \int_{\Omega(t)} \rho \frac{1}{2}\frac{D}{Dt}|u|^2 dx \\ = \int_{\Omega(t)} \rho f_i u_i dx - \int_{\Omega(t)} T_{ji} u_{i,j} dx + \int_{\partial\Omega(t)} u_i (t_n)_i dS \end{aligned} \tag{63}$$

It can be seen that the rate of change of kinetic energy in the material volume is the sum of three parts

- The rate at which the body forces do work
- The rate which the internal stresses do work
- The rate at which the surface stresses do work

Conservation of Energy I

Through the use of the transport theorem and the Green's theorem we find

$$\int_{\Omega(t)} \left(\rho \frac{DE}{Dt} + \nabla \cdot q - T : (\nabla u) \right) dx = 0 \tag{64}$$

where $T : (\nabla u)$ is the dyadic notation for $T_{ji} u_{i,j}$, the scalar product of T and ∇u.
Thus we have

$$\rho \frac{DE}{Dt} = -\nabla \cdot q + T : \nabla u \tag{65}$$

We can typically use Fourier's law for heat conduction

$$\rho \frac{DE}{Dt} = \nabla \cdot (k \nabla \Theta) + T : \nabla u \tag{66}$$

In this form Θ is the static thermodynamic temperature.

Summary of Equations of Motion - Differential

Continuity

$$\frac{\partial \rho}{\partial t} + \text{div}(\rho u) = 0 \tag{67}$$

Momentum

$$\frac{\partial}{\partial t}\rho u_i + \left(\rho u_i u_j\right)_{,j} = \rho f_i + (T_{ji})_{,j} \tag{68}$$

Energy

$$\rho \frac{DE}{Dt} = \nabla \cdot (k \nabla \Theta) + T : \nabla u \tag{69}$$

where $T_{ij} = -p\delta_{ij} + P_{ij}$ is the stress tensor P_{ij} is the viscous stress tensor.

Summary of Equations of Motion - Integral

Continuity

$$\int_{\Omega(t)} \left(\frac{\partial \rho}{\partial t} + \operatorname{div}(\rho u) \right) dx = 0 \tag{70}$$

Momentum

$$\int_{\Omega(t)} \rho \frac{Du}{Dt} dx = \int_{\Omega(t)} (\rho f + \operatorname{div} T) \, dx \tag{71}$$

Energy

$$\int_{\Omega(t)} \left(\rho \frac{DE}{Dt} + \nabla \cdot q - T : (\nabla u) \right) dx = 0 \tag{72}$$

Existence and Smoothness of the Navier-Stokes Equation

EXISTENCE AND SMOOTHNESS OF THE NAVIER–STOKES EQUATION

CHARLES L. FEFFERMAN

The Euler and Navier–Stokes equations describe the motion of a fluid in $\mathbb{R}^n$ ($n = 2$ or 3). These equations are to be solved for an unknown velocity vector $u(x,t) = (u_1(x,t))_{1\le i\le n} \in \mathbb{R}^n$ and pressure $p(x,t) \in \mathbb{R}$, defined for position $x \in \mathbb{R}^n$ and time $t \ge 0$. We restrict attention here to incompressible fluids filling all of $\mathbb{R}^n$. The *Navier–Stokes equations* are then given by

$$\frac{\partial}{\partial t}u_i + \sum_{j=1}^{n} u_j \frac{\partial u_i}{\partial x_j} = \nu\Delta u_i - \frac{\partial p}{\partial x_i} + f_i(x,t) \qquad (x \in \mathbb{R}^n, t \ge 0), \tag{1}$$

$$\operatorname{div} u = \sum_{i=1}^{n} \frac{\partial u_i}{\partial x_i} = 0 \qquad (x \in \mathbb{R}^n, t \ge 0) \tag{2}$$

with initial conditions

$$u(x,0) = u^0(x) \qquad (x \in \mathbb{R}^n). \tag{3}$$

Here, $u^0(x)$ is a given, C^∞ divergence-free vector field on $\mathbb{R}^n$, $f_i(x,t)$ are the components of a given, externally applied force [e.g. gravity], ν is a positive coefficient (the viscosity), and $\Delta = \sum_{i=1}^{n} \frac{\partial^2}{(\partial x_i)^2}$ is the Laplacian in the space variables. The *Euler equations* are equations (1), (2), (3) with ν set equal to zero.

Equation (1) is just Newton's law $f = ma$ for a fluid element subject to the external force $f = (f_i(x,t))_{1\le i\le n}$ and to the forces arising from pressure and friction. Equation (2) just says that the fluid is incompressible. For physically reasonable solutions, we want to make sure $u(x,t)$ does not grow large as $|x| \to \infty$. Hence, we will restrict attention to forces f and initial conditions u^0 that satisfy

$$|\partial_x^\alpha u^0(x)| \le C_{\alpha K}(1+|x|)^{-K} \qquad \text{on } \mathbb{R}^n, \text{ for any } \alpha \text{ and } K \tag{4}$$

and

$$|\partial_x^\alpha \partial_t^m f(x,t)| \le C_{\alpha m K}(1+|x|+t)^{-K} \qquad \text{on } \mathbb{R}^n \times [0,\infty), \text{ for any } \alpha, m, K. \tag{5}$$

We accept a solution of (1), (2), (3) as physically reasonable only if it satisfies

$$p, u \in C^\infty(\mathbb{R}^n \times [0,\infty)) \tag{6}$$

and

$$\int_{\mathbb{R}^n} |u(x,t)|^2 dx < C \quad \text{for all } t \ge 0 \quad \text{(bounded energy)}. \tag{7}$$

Alternatively, to rule out problems at infinity, we may look for spatially periodic solutions of (1), (2), (3). Thus, we assume that $u^0(x)$, $f(x,t)$ satisfy

$$u^0(x+e_j) = u^0(x), \quad f(x+e_j,t) = f(x,t) \quad \text{for } 1 \le j \le n \tag{8}$$

Figure 29: Clay Math Inst. Millenium Problem

Existence and Smoothness of the Navier-Stokes Equation

2 CHARLES L. FEFFERMAN

$\{e_j = j^{th}$ unit vector in $\mathbb{R}^n\}$.

In place of (4) and (5), we assume that u° is smooth and that

$$|\partial_x^\alpha \partial_t^\beta f(x,t)| \leq C_{\alpha\beta K}(1+|t|)^{-K} \quad \text{on } \mathbb{R}^3 \times [0,\infty), \text{ for any } \alpha, \beta, K. \tag{9}$$

We then accept a solution of (1), (2), (3) as physically reasonable if it satisfies

$$u(x,t) = u(x+e_j,t) \quad \text{on } \mathbb{R}^3 \times [0,\infty) \text{ for } \quad 1 \leq j \leq n \tag{10}$$

and

$$p, u \in C^\infty(\mathbb{R}^n \times [0,\infty)). \tag{11}$$

A fundamental problem in analysis is to decide whether such smooth, physically reasonable solutions exist for the Navier–Stokes equations. To give reasonable leeway to solvers while retaining the heart of the problem, we ask for a proof of one of the following four statements.

(A) Existence and smoothness of Navier–Stokes solutions on $\mathbb{R}^3$. Take $\nu > 0$ and $n = 3$. Let $u^\circ(x)$ be any smooth, divergence-free vector field satisfying (4). Take $f(x,t)$ to be identically zero. Then there exist smooth functions $p(x,t), u_i(x,t)$ on $\mathbb{R}^3 \times [0,\infty)$ that satisfy (1), (2), (3), (6), (7).

(B) Existence and smoothness of Navier–Stokes solutions in $\mathbb{R}^3/\mathbb{Z}^3$. Take $\nu > 0$ and $n = 3$. Let $u^\circ(x)$ be any smooth, divergence-free vector field satisfying (8); we take $f(x,t)$ to be identically zero. Then there exist smooth functions $p(x,t)$, $u_i(x,t)$ on $\mathbb{R}^3 \times [0,\infty)$ that satisfy (1), (2), (3), (10), (11).

(C) Breakdown of Navier–Stokes solutions on $\mathbb{R}^3$. Take $\nu > 0$ and $n = 3$. Then there exist a smooth, divergence-free vector field $u^\circ(x)$ on $\mathbb{R}^3$ and a smooth $f(x,t)$ on $\mathbb{R}^3 \times [0,\infty)$, satisfying (4), (5), for which there exist no solutions (p,u) of (1), (2), (3), (6), (7) on $\mathbb{R}^3 \times [0,\infty)$.

(D) Breakdown of Navier–Stokes Solutions on $\mathbb{R}^3/\mathbb{Z}^3$. Take $\nu > 0$ and $n = 3$. Then there exist a smooth, divergence-free vector field $u^\circ(x)$ on $\mathbb{R}^3$ and a smooth $f(x,t)$ on $\mathbb{R}^3 \times [0,\infty)$, satisfying (8), (9), for which there exist no solutions (p,u) of (1), (2), (3), (10), (11) on $\mathbb{R}^3 \times [0,\infty)$.

Those problems are also open and very important for the Euler equations ($\nu = 0$), although the Euler equation is not on the Clay Institute's list of prize problems.

Let me sketch the main partial results known regarding the Euler and Navier–Stokes equations, and conclude with a few remarks on the importance of the questions.

Figure 30: Clay Math Inst. Millenium Problem

Class Summary

- The Navier-Stokes equations (NSE)
- Differential form and integral form

Next Time

- Equations of motion – Application viewpoint
- Acoustics – Everything you need to know for this class
- Bernoulli equation and implications
- Thermodynamics – A review

Class Overview

Introduction

- Equations of motion
- Boltzmann
- Acoustics
- Bernoulli
- Thermodynamics

“The object that strikes the air develops a force equal to that of the air that strikes the object. Observe how the beating of its wings against the air suffices to bear up the weight of the eagle in the highest and thinnest air. Observe too that, conversely, the air fills the sails and pushes the heavily laden ship. From this you can understand that man, with great wings, acting against the resistance of air, might overcome it victoriously and rise above it,”

Leonardo da Vinci

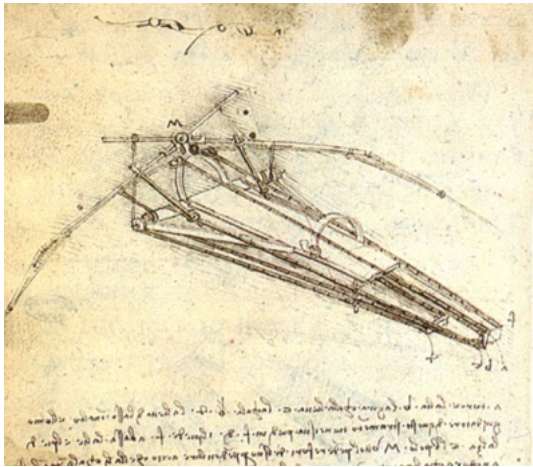

Figure 31: Leonardo da Vinci’s designs for an Ornithopter.

Basic Definitions

- Fluid - Any substance that deforms continuously under shear stress
  - Liquid
  - Gas
  - Plasma
- Compressible versus incompressible
  - Most simplistic definition for compressible flow is density varies as function of time at a particular spatial location – this is sufficient condition for compressible flow
  - Showed that mathematically that $V(t_1) = V(t_2)$ is the rigorous definition

Basic Definitions

- Subsonic versus supersonic - Specific regions of the flow-field have the property $M > u/c$
  - Exact transonic condition is $M = 1$
  - Transonic flow most always has regions of $M \neq 1$
  - Set of trivial solutions exist where $M = 1$, everywhere
- Steady flow - Statistically stationary set or subset of flow-field where the statistical properties (even turbulent) are independent of time
  - All turbulent flows are unsteady, but can be considered statistically invariant or statistically steady

Viscosity

Measure of a fluids resistance to shear when the fluid is in motion

$$\tau = \mu \frac{\partial u}{\partial y}$$

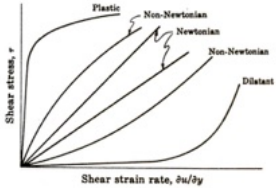

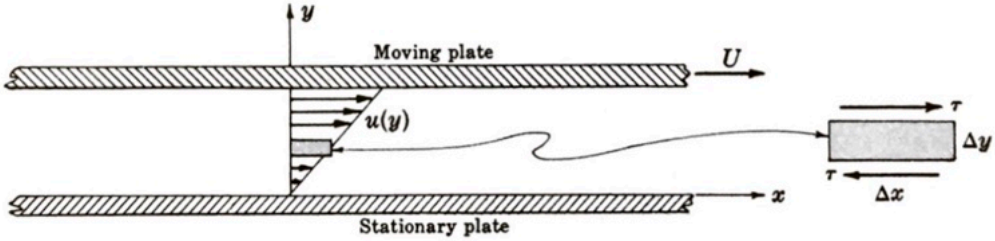

Fig. 1-1. Flow between parallel plates to illustrate viscosity. The velocity u is linear across the channel, zero at the bottom and U at the top. A small element shows the shear stress.

Flow Regimes

Laminar Flow – Flow moves in infinitely many layers
(think 'laminate')

Transitional – Flow is undergoing an instability from laminar to turbulent or is alternating between laminar and turbulent states

Turbulent – The wavenumber energy spectrum contains non-zero energy at all wavenumbers. Simply put it is highly chaotic.

Laminar

Turbulent

External versus Internal Flows

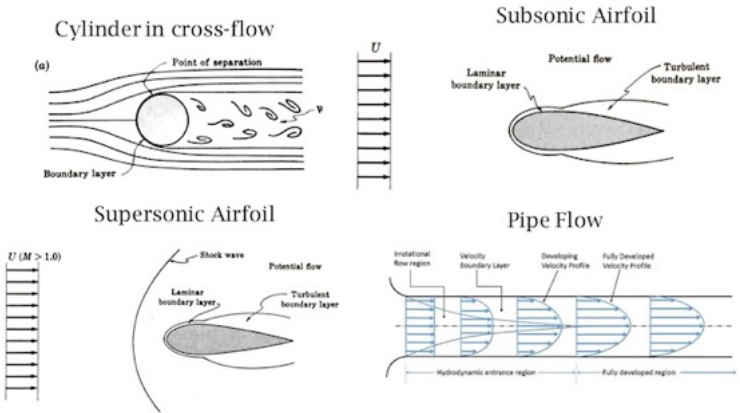

Examples

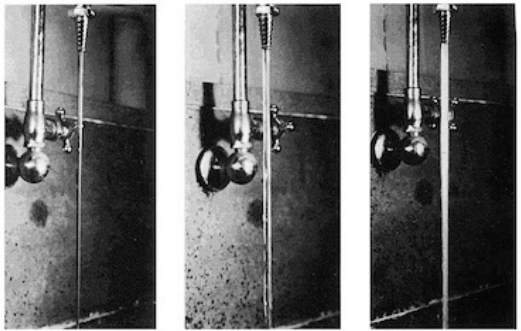

Figure 32: Flow regime examples from a faucet.

Differential Form - Continuity

Conservation of mass

$$\frac{\partial \rho}{\partial t} + \frac{\partial}{\partial x_i}(\rho u_i) = 0 \tag{73}$$

Vector notation

$$\frac{\partial \rho}{\partial t} + \nabla \cdot (\rho \mathbf{u}) = 0 \tag{74}$$

Cartesian form

$$\frac{\partial \rho}{\partial t} + \frac{\partial}{\partial x}(\rho u) + \frac{\partial}{\partial y}(\rho v) + \frac{\partial}{\partial z}(\rho w) = 0 \tag{75}$$

Incompressible

$$\frac{\partial u}{\partial x} + \frac{\partial v}{\partial y} + \frac{\partial w}{\partial z} = 0 \tag{76}$$

Steady

$$\nabla \cdot (\rho \mathbf{u}) = 0 \tag{77}$$

Differential Form - Momentum

Remember stress tensor notations

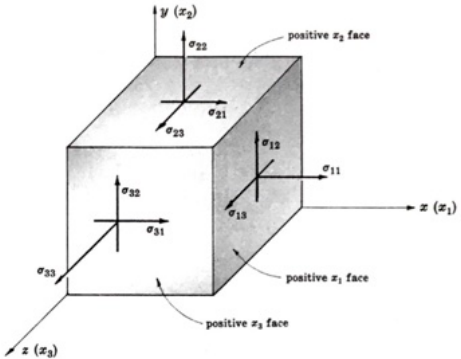

$$\sigma_{ij} = \begin{bmatrix} \sigma_{11} & \sigma_{12} & \sigma_{13} \\ \sigma_{21} & \sigma_{22} & \sigma_{23} \\ \sigma_{31} & \sigma_{32} & \sigma_{33} \end{bmatrix}$$

Differential Form - Momentum

Einstein notation

$$\rho \frac{Du_i}{Dt} = \rho\left(\frac{\partial u_i}{\partial t} + u_j \frac{\partial u_i}{\partial x_j}\right) = \frac{\partial \sigma_{ij}}{\partial x_j} + B_i \tag{78}$$

Cartesian form (expanded)

$$\rho \frac{Du}{Dt} = \rho\left(\frac{\partial u}{\partial t} + u\frac{\partial u}{\partial x} + v\frac{\partial u}{\partial y} + w\frac{\partial u}{\partial z}\right) = \frac{\partial \sigma_{11}}{\partial x} + \frac{\partial \sigma_{12}}{\partial y} + \frac{\partial \sigma_{13}}{\partial z} + B_x \tag{79}$$

$$\rho \frac{Dv}{Dt} = \rho\left(\frac{\partial v}{\partial t} + u\frac{\partial v}{\partial x} + v\frac{\partial v}{\partial y} + w\frac{\partial v}{\partial z}\right) = \frac{\partial \sigma_{21}}{\partial x} + \frac{\partial \sigma_{22}}{\partial y} + \frac{\partial \sigma_{23}}{\partial z} + B_y \tag{80}$$

$$\rho \frac{Dw}{Dt} = \rho\left(\frac{\partial w}{\partial t} + u\frac{\partial w}{\partial x} + v\frac{\partial w}{\partial y} + w\frac{\partial w}{\partial z}\right) = \frac{\partial \sigma_{31}}{\partial x} + \frac{\partial \sigma_{32}}{\partial y} + \frac{\partial \sigma_{33}}{\partial z} + B_z \tag{81}$$

Vector form

$$\frac{D\mathbf{u}}{Dt} = \frac{\partial \mathbf{u}}{\partial t} + (\mathbf{u}\cdot\nabla)\mathbf{u} = \frac{\partial \mathbf{u}}{\partial t} + \nabla(u^2/2) - \mathbf{u}\times\nabla\times\mathbf{u} \tag{82}$$

Note that

$$\sigma_{ij} = -p\delta_{ij} + \mu\left(\frac{\partial u_i}{\partial x_j} + \frac{\partial u_j}{\partial x_i} - \frac{2}{3}\delta_{ij}\frac{\partial u_k}{\partial x_k}\right) + \zeta\delta_{ij}\frac{\partial u_k}{\partial x_k} \tag{83}$$

Differential Form - Energy

Energy equation for specific energy e

$$\rho \frac{De}{Dt} = -\frac{\partial}{\partial x_i} q_i - p \frac{\partial u_i}{\partial x_i} - u_i \frac{\partial p}{\partial x_i} + u_i \frac{\partial \sigma'_{ji}}{\partial x_j} + \Phi + q''' \tag{84}$$

where e is the internal energy.

- $\Phi = \sigma^i_{ij} \partial u_j / \partial x_i$ is the dissipation function and is the rate at which the shear stress does irreversible work on the fluid
- $\sigma_{ij} = -p\delta_{ij} + \sigma'_{ij}$ is stress divided into pressure and pure shear
- q''' is internal heat generation rate per unit volume
- $\boldsymbol{q} = -\kappa \Delta^2 T$ is a great approximation (Fourier's Law)

Many many many versions of the energy equation that solve for p, T, enthalpy

$$\rho \frac{Dh}{Dt} = \frac{Dp}{Dt} + \kappa \nabla^2 T - \nabla \cdot \mathbf{q}_r + q''' + \Phi \tag{85}$$

$$\rho c_p \frac{DT}{Dt} + \kappa \nabla^2 T - \nabla \cdot \mathbf{q}_r + q''' \Phi \tag{86}$$

Differential Form - Entropy

Entropy – used for differential form analysis
If θ is entropy rate production per unit volume then we can write

$$\int_{C.V} \theta d\mathcal{V} - \int_{C.S.} \frac{\mathbf{q}}{T} \cdot d\mathbf{A} = \frac{\partial}{\partial t} \int_{C.V.} \rho s d\mathcal{V} + \int_{C.S.} \rho s \mathbf{V} \cdot d\mathbf{A} \tag{87}$$

Assume Fourier's law

$$\theta = \frac{\Phi}{T} + \frac{\mathbf{q} \cdot \mathbf{q}}{\kappa T^2} = \frac{\Phi}{T} + \kappa \frac{(\nabla T)^2}{T^2} \tag{88}$$

The entropy production rate in terms of the coupled irreversibilities of heat currents and viscous dissipation

The Navier-Stokes Equations

Continuity

$$\frac{\partial \rho}{\partial t} + \frac{\partial \rho u_j}{\partial x_j} = 0 \tag{89}$$

Momentum equation

$$\frac{\partial \rho u_i}{\partial t} + \frac{\partial \rho u_i u_j}{\partial x_j} = -\frac{\partial p}{\partial x_j}\delta_{ij} + \frac{\partial \tau_{ij}}{\partial x_j} \tag{90}$$

Energy equation

$$\frac{\partial \rho e_o}{\partial t} + \frac{\partial \rho u_j e_o}{\partial x_j} = -\frac{\partial u_j p}{\partial x_j} - \frac{\partial q_j}{\partial x_j} + \frac{\partial u_i \tau_{ij}}{\partial x_j} \tag{91}$$

where e_o is the total energy per unit mass $e_o = e + u_k u_k/2$

$$\tau_{ij} = 2\mu S^*_{ij} \qquad S^*_{ij} = \frac{1}{2}\left(\frac{\partial u_i}{\partial x_j} + \frac{\partial u_j}{\partial x_i}\right) - \frac{1}{3}\frac{\partial u_k}{\partial x_k}\delta_{ij} \qquad q_j = -c_p \frac{\mu}{\mathcal{P}_r}\frac{\partial T}{\partial x_j}$$

$$\mathcal{P}_r = c_p \mu \lambda^{-1}$$

Navier-Stokes Equations

We use the following definitions. Shear stress

$$\frac{\partial u_i \tau_{ij}}{\partial x_j} \tag{92}$$

Total energy per unit mass, e_o

$$e_o = e + \frac{u_i u_i}{2} \tag{93}$$

$\tau_{ij} = 2\mu S_{ij}, S_{ij} = \frac{1}{2}\left(\frac{\partial u_i}{\partial x_j} + \frac{\partial u_j}{\partial x_i}\right) - \frac{1}{3}\frac{\partial u_i}{\partial x_i}\delta_{ij}$

$q_j = -c_p \frac{\mu}{Pr}\frac{\partial T}{\partial x_j}, Pr = \frac{c_p \mu}{\lambda}, \lambda =$ thermal conductivity

$\gamma = c_p/c_v, p = \rho RT, e = c_v T,$ and $R = c_p - c_v$

Leopold Kronecker

7 December 1823 – 29 December 1891, German

"God made the integers, all else is the work of man."

- Number theory, algebra, logic
- Born Prussia (now Legnica, Poland) in a wealthy Jewish family
- Kronecker did not follow his interest in research but managed family farm estate
- Married his cousin Fanny Prausnitzer with six children
- Dirichlet introduced Kronecker to the Berlin elite.
- Published numerous papers resulting from his independent research
- Converted to Christianity year he died
- Named for Kronecker are the Kronecker limit formula, Kronecker's congruence, Kronecker delta, Kronecker comb, Kronecker symbol, Kronecker product, Kronecker's method for factorizing polynomials, Kronecker substitution, Kronecker's theorem in number theory, Kronecker's lemma, and Eisenstein–Kronecker numbers.

S.A.E. Miller, Ph.D., saem@ufl.edu

Acoustics

- Acoustic waves are extremely important in the field of compressible flow and fluid dynamics
- Do equations of motion contain acoustics?
- Do acoustic waves exist in an incompressible flow?
- Waves can compress or expand the flow
- Waves in fluids can be very large $p \approx 1 \times 10^{5}$ Pa or extremely tiny $p \approx 1 \times 10^{-5}$ Pa
- What happens to the speed of sound in an incompressible flow?

Boltzmann Equation

Distribution Function – We define a distribution function $f(x, v, t)$ such that $f\, d^3x\, d^3v$ is the average number of particles contained in a volume element d^3x about x. A velocity-space element d^3v about v at time t. Properties of the gas can then be found

$$n(\mathbf{x}, t) = \int_{-\infty}^{\infty} f(\mathbf{x}, \mathbf{v}, t) d^3v$$
$$\rho(\mathbf{x}, t) = mn(\mathbf{x}, t)$$
$$\mathbf{u}(\mathbf{x}, t) = n^{-1} \int_{-\infty}^{\infty} f((\mathbf{x}, \mathbf{v}, t)\mathbf{v} d^3v = \langle \mathbf{v} \rangle$$

Note n is 'number density' of the particles, m is mass of single particle

Velocity is average plus a random quantity $v = u + w$

Boltzmann Equation

For flows with no collision we can derive Vlasovls equation

$$\frac{\partial f}{\partial t} + v^i \frac{\partial f}{\partial x^i} + a^i \frac{\partial f}{\partial v^i} = 0 \tag{94}$$

where a is an acceleration of F/m, and F is force acting on the particles

- To account for collisions we must have a term that accounts for particles that end up in other volume elements.
- Add RHS term that gives net rate at which particles are entered into another element

$$\frac{\partial f}{\partial t} + v^i \frac{\partial f}{\partial x^i} + a^i \frac{\partial f}{\partial v^i} = \left(\frac{Df}{Dt}\right)_{coll} \tag{95}$$

which is the Boltzmann transport equation

Boltzmann Equation

The collision integral for binary collisions - net rate at which particles are entering into the phase-space element under consideration

$$\left(\frac{Df}{Dt}\right)_{coll} = R_{in} - R_{out} \tag{96}$$

where R_{in} and R_{out} are the rates at which particles are scattered in and out of a volume in 'phase space.' We can also write R_{out} as

$$R_{out} d^3x_1 d^3v_1 = \left(\iiint f_1 f_2 \, q \, b \, db \, d\Phi d^3v_2 \right) d^3x_1 v_1 \tag{97}$$

where b is a range of impact parameters and $q = |v_2 - v_1|$. It can be shown that the collision term can be written

$$\left(\frac{Df_1}{Dt}\right)_{coll} = \iiint (f_1' f_2' - f_1 f_2) q \, b \, db \, d\Phi d^3v_2 \tag{98}$$

where the subscripts denote families of ranges of velocities

Boltzmann Equation

Note that taking 'moments' of the Boltzmann equation will recover the Navier-Stokes equations. Multiply by a quantity $Q(v_1)$ and integrate (moment)

$$\int Q\left(\frac{\partial f_1}{\partial t} + v_1^i \frac{\partial f_1}{\partial x^i} + a^i \frac{\partial f_1}{\partial v_1^i}\right) d^3 v_1 = \int Q\left(\frac{Df_1}{Dt}\right)_{coll} d^3 v_1$$

Assume that Q is conserved and we can find a conservation equation. Using partial integration of all three terms, make use of the fact that t, ξ, and v_i are independent variables (change the order of integration and differentiation with respect to different variables) and $v_i \to \infty, f \to 0$ that (Q & f) vanishes

$$\frac{\partial}{\partial t}(n\langle Q\rangle) + \frac{\partial}{\partial x^i}(n\langle Qv^i\rangle) - na^i\langle\frac{\partial Q}{\partial v^i}\rangle = 0$$

Example - now let $Q = m$, and insert into this equation, and set $nm = \mu$

$$\frac{\partial \rho}{\partial t} + \nabla \cdot (\rho \mathbf{u}) = 0$$

We will not work with Boltzmann equation more, but remember that there are growing resources and CFD techniques to make predictions using Boltzmann equation.

Ludwig Boltzmann

Ludwig Eduard Boltzmann (February 20, 1844 – September 5, 1906) was an Austrian physicist and philosopher whose greatest achievement was in the development of statistical mechanics, which explains and predicts how the properties of atoms (such as mass, charge, and structure) determine the physical properties of matter (such as viscosity, thermal conductivity, and diffusion).

Most famous for definition of entropy

$$S = k \log W$$

Figure 33: Prof. Cedric Villani by the Boltzmann grave. Note the equation on grave!

Examples

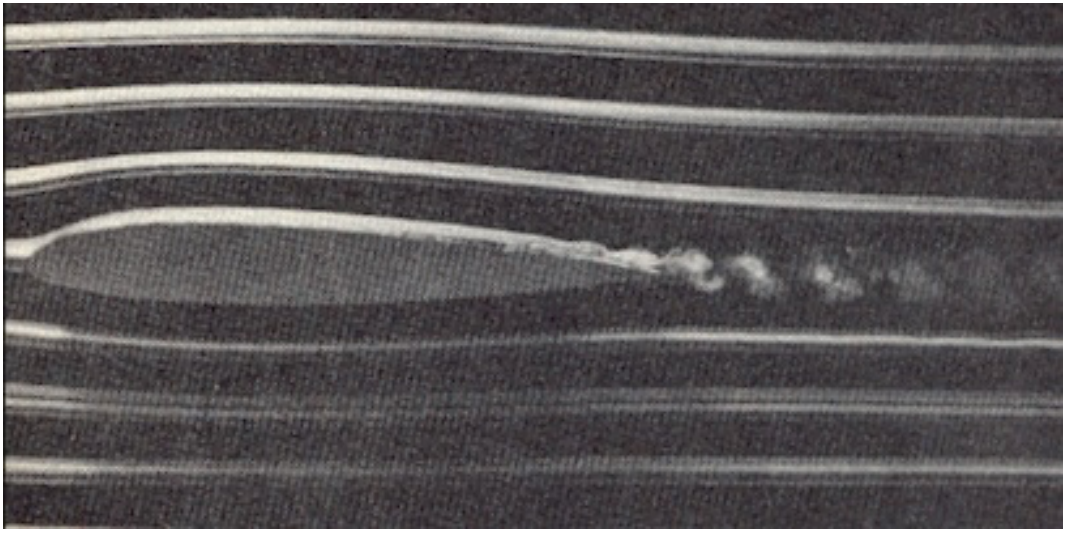

Figure 34: Flow over an airfoil.

Example

Error of Bernoulli equation in incompressible flow. Consider the flow with the following properties over a wing

- Assume standard atmosphere
- p_∞, T_∞, and ρ_∞ are static thermodynamic variables
- $u_\infty = 100$ mi/hr
- We measure a maximum velocity over the wing as 150 mi/hr

What is the percentage pressure change between free-stream and the max velocity point?

Example Continued

Air speeds are very low. Assume that the flow is incompressible. For example purposes, apply Bernoulli equation (please recall assumptions of this equation and how it was derived)

$$\text{Recall } \boxed{p_1 + \frac{1}{2}\rho u_1^2 = p_2 + \frac{1}{2}\rho u_2^2} \quad \underline{\text{only valid for incompressible flow}}$$

Now, $p_2 - p_1 = \frac{1}{2}\rho(u_2^2 - u_1^2)$ at standard sea level $\rho_\infty = 0.002377$ slug / ft^3. Note 60 mi/hr = 88 ft/s yields u_1 = 100 mi/hr = 147 ft/s, $u_2 = 220$ ft/s

$$\therefore p_2 - p_1 = 31.8 \text{lb/ft}^2$$

$$p_\infty = 2116 \text{ lb/ft}^2 \leftarrow p \text{ ATM}$$

$$\therefore \frac{p_2 - p_1}{p_1} = \frac{31.8}{2116} = 0.015 \implies 1.5\% \text{ pressure change!}$$

Use of Bernoulli equation in high speed flow will lead to significant error. Lesson: $\triangle p$ is small and $\triangle \rho$ is smaller, so can neglect it for the purposes of this analysis.

Additional Thoughts for this Example

- Unlike incompressible flow, kinetic internal energies play a large role in compressible flow
- These thermal variables interact with other field-variables
- Variables are strongly connected through the gas law and energy equation

A Perfect Fluid Deserves a Perfect Law

A perfect gas is one in which intermolecular forces are neglected. For example

$$pV = RT \tag{99}$$

where V is the specific volume, R is gas constant, T is static thermodynamic temperature, and p is static thermodynamic pressure.

- We have previously introduced pressure, p, through the derivation of fluid stress
- T is a thermodynamic quantity (statistical) and is a measure of the kinetic energy within the gas, which is different than for example $\frac{1}{2}\overline{u}^2$
- Many forms of perfect gas law.
  - Most useful here is $\boxed{p = \rho RT}$

Gas Constants and Gas Law

If equation deals with moles use universal gas constant

$$R = 8314 \text{ J/Kg mol K} \tag{100}$$

If equation deals with mass then use

$$\text{e.g. } \underline{\text{air}}\ R = 287 \text{ J/Kg K} \tag{101}$$

If equation deals with particles use Boltzman constant K

$$K_b = 1.38 \times 10^{-23} \text{ J/K} \tag{102}$$

How accurate is ideal gas law?

- For low pressures and high temperatures deviates at most 1% $\rightarrow$... Very low pressures or high temperatures use real gas laws.
- What do we do in hypersonic flows? Use mixture or system of ideal gas laws!

Internal Energy and Enthalpy

- e is internal energy per unit mass of gas, consists of kinetic, rotational, vibrational energies of the system of molecules. Function of T and V
- h is enthalpy per unit mass. Function of T and p

Assume non-chemically reacting flow and e and h are functions of T only. Then

$$e = e(T) \tag{103}$$

$$h = h(T) \tag{104}$$

$$de = c_v dT \tag{105}$$

$$dh = c_p dT \tag{106}$$

Ratio of Specific Heats

If c_v and c_p are constant then

- $c_p = \frac{dh}{dT}\Big|_{\text{constant p}}$
- $c_v = \frac{de}{dT}\Big|_{\text{constant V}}$
- $\boxed{e = c_v T}$
- $\boxed{h = c_p T}$

This system is called calorically perfect. As a general rule for air in aerospace engineering (flows about Earth)

- $T < 1000K$ - perfect
- $1000K < T < 2500K$ - thermally perfect
- $T > 2500K$ - chemically reacting

Ratio of Specific Heats

For thermally or calorically perfect gas

$$c_p = \frac{\gamma R}{\gamma - 1} \tag{107}$$

and

$$c_v = \frac{R}{\gamma - 1} \tag{108}$$

where $\gamma = c_p/c_v$ (1.4 for air but really 1.39 from quantum–mechanics theory) for diatomic gas. γ varies from 1 to 5 / 3.

Class Summary

- Navier-Stokes
- Boltzmann
- Acoustics
- Bernoulli
- Thermodynamics

Next Time

- Laws of thermodynamics – a review and compressible flow insight
- Isentropy
- Reynolds transport theorem
- Examples

Class Overview

Introduction

- Laws of thermodynamics – a review and compressible flow insight
- Isentropy
- Reynolds transport theorem
- Examples

“My attention (was) drawn to various mechanical phenomena, for the explanation of which I discovered that a knowledge of mathematics was essential,”

Osborne Reynolds

First Law of Thermodynamics

The first law of thermodynamics written in an algebraic form is

$$\boxed{\delta q + \delta w = de} \tag{109}$$

where δq is the heat added to system, δw is the work done on the system, and de is the change in internal energy.

Processes

Please recall these fundamental definitions of thermodynamic processes

- Adiabatic – No heat added or removed from system
- Reversible – No dissipation
- Isentropic – Both adiabatic and reversible

Second Law - Entropy

The second law of thermodynamics following Boltzmann is

$$S = K \log W \tag{110}$$

Within this class we follow $dS \geq \delta q/T$, where T is system temperature and $dS \geq 0$. Using the first law and $\delta q_{rev} = TdS$ we can show

$$TdS = de + pdV \tag{111}$$

and

$$TdS = dh - Vdp \tag{112}$$

For thermally perfect gas

$$\boxed{\Delta s = c_p \ln \frac{T_2}{T_1} - R \ln \frac{p_2}{p_1}} \tag{113}$$

$$\Delta s = c_v \ln \frac{T_2}{T_1} + R \ln \frac{V_2}{V_1} \tag{114}$$

Ludwig Eduard Boltzmann

February 20, 1844 – September 5, 1906, Austrian

- Development of statistical mechanics, which explains and predicts how the properties of atoms (such as mass, charge, and structure) determine the physical properties of matter (such as viscosity, thermal conductivity, and diffusion)
- At 25 appointed full Professor of Mathematical Physics at the University of Graz, Chair of Theoretical Physics at the University of Munich, 1885 he became a member of the Imperial Austrian Academy of Sciences, and in 1887 he became the President of the University of Graz. He was elected a member of the Royal Swedish Academy of Sciences
- Major equations – Boltzmann equation and entropy

S.A.E. Miller, Ph.D., saem@ufl.edu

Isentropic flows

In isentropic flows, we can find the following changes between states one and two (thermodynamic relation)

$$\frac{p_2}{p_1} = \left(\frac{\rho_2}{\rho_1}\right)^{\gamma} = \left(\frac{T_2}{T_1}\right)^{\frac{\gamma}{\gamma-1}} \tag{115}$$

where the subscripts represent states and the variables are those of the typical field-variables.

Thermodynamics Summary

Summary of the thermodynamic laws

- "Zero law" – Two systems are in thermal equilibrium with common third system then two systems are in thermal equilibrium with each other
- First law – Conservation of energy. Cannot be created or destroyed. Thermodynamic changes in e, q, and w
- Second law – $\frac{dS}{dt} \geq 0$
- Third law – Entropy goes to zero as T goes to zero ($\lim_{T \to 0} S = 0$)

Isentropic process implies there is no change in entropy

$$\triangle S = 0 \tag{116}$$

Famous Joke about Thermodynamics

What are the three laws of thermodynamics?

Famous Joke about Thermodynamics

What are the three laws of thermodynamics?

“You can’t win, you can’t break even, and you can’t get out of the game.”

Osborne Reynolds

23 August 1842 – 21 February 1912, Irish

- Born in Belfast
- Studied the conditions in which the flow of fluid in pipes transitioned from laminar flow to turbulent flow, kinetic theory of gas
- At 25, he was appointed professor of engineering at Owens College in Manchester (now the University of Manchester), first professor in UK university to hold the title of "Professor of Engineering"
- Proposed RANS
- Known for Re number

Painted by John Collier, a most famous British Pre-Raph. Artist!

S.A.E. Miller, Ph.D., saem@ufl.edu

Reynold's Transport Theorem

- You are expected to know this theory and how to apply it from your previous classes
- It is also known as the transport theorem if certain assumptions are not made, which was presented previously

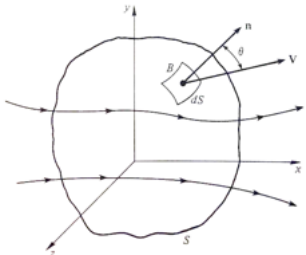

$\forall-$Volume of element, $\hat{\underline{n}}-$unit vector normal at B, $\underline{u}$ velocity at B, $\rho-$density at B, $S-$closed surface, and fixed control volume.

Integral Form - Continuity

Net rate of mass flow out of control surface is equal to the time rate of decrease of mass inside the control volume

$$\int_{CS} \rho \mathbf{u} \cdot d\mathbf{A} = -\frac{\partial}{\partial t} \int_{CV} \rho dV \qquad (117)$$

$$\boxed{\frac{d}{dt} \int_{\forall} \rho d\forall + \int_{S} \rho \boldsymbol{u} \cdot d\boldsymbol{S} = 0} \qquad (118)$$

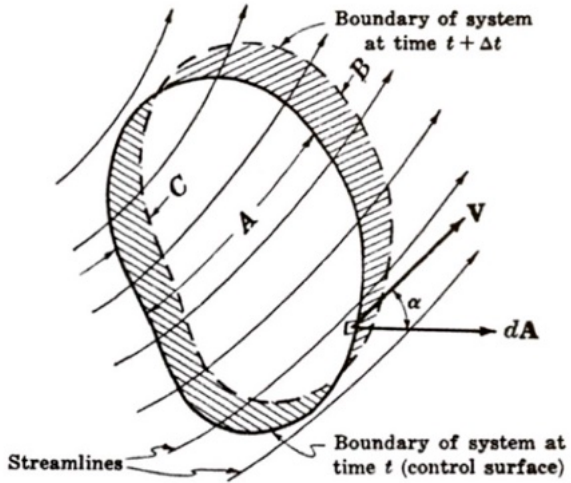

Integral Form - Momentum

Basis is Newton's second law. Conservation law for momentum

$$\boxed{\frac{d}{dt}\int_{\forall}\rho\boldsymbol{u}d\forall+\int_{\boldsymbol{S}}\boldsymbol{u}\left(\rho\boldsymbol{u}\cdot d\boldsymbol{S}\right)=\int_{\forall}\rho\boldsymbol{f}d\forall-\int_{\boldsymbol{S}}pd\boldsymbol{S}+F_{\text{visc}}} \tag{119}$$

where ρ is density, $\boldsymbol{u}$ is the velocity vector, $\boldsymbol{S}$ is the surface vector (outward), $\boldsymbol{f}$ is the body force vector (external), p is static pressure (always absolute), and F_{visc} is a lumped viscous term.

Integral Form - Momentum - Alternative

$$\boxed{\mathbf{F}_s + \int_{CS} \mathbf{B} dV = \frac{\partial}{\partial t} \int_{CV} \rho \mathbf{u} dV + \int_{CS} \rho \mathbf{u}\mathbf{u} \cdot d\mathbf{A}} \tag{120}$$

where **B** is body force per unit volume and F_s is total surface force (pressure and shear). Note that if the flow is steady we might write

$$\mathbf{F}_s = \int_{CS} \rho \mathbf{u}\mathbf{u} \cdot d\mathbf{A} \tag{121}$$

We might alternatively write a conservation law for angular momentum

$$\int_{CS} \boldsymbol{r} \times d\mathbf{F}_s + \int_{CV} \boldsymbol{r} \times \mathbf{B} dV = \frac{\partial}{\partial t} \int_{CV} \boldsymbol{r} \times \rho \mathbf{u} dV + \int_{CS} \boldsymbol{r} \times \rho \mathbf{u}\mathbf{u} \cdot d\mathbf{A} \tag{122}$$

Integral Form - Energy

The energy equation in integral form is

$$\boxed{\begin{aligned}&\frac{d}{dt}\int_{\forall}\rho\left(e+\frac{u^2}{2}\right)d\forall+\int_{\boldsymbol{S}}\rho\left(e+\frac{u^2}{2}\right)\boldsymbol{u}\cdot d\boldsymbol{S}\\&=\int_{\forall}\dot{q}\rho d\forall-\int_{S}p\boldsymbol{u}\cdot d\boldsymbol{S}+\int_{\forall}\rho(\boldsymbol{f}\cdot\boldsymbol{u})d\forall+\dot{Q}+\dot{w}\end{aligned}} \tag{123}$$

where ρ is denstiy, e is internal energy, $\boldsymbol{u}$ is the velocity, $\boldsymbol{S}$ is the surface vector (outward), $\dot{q}$ is heat transfer rate, p is static pressure (absolute), f is external body force, Q is heat added to the system, and w is work done by the system. Check units before evaluation!

Integral Form - Energy - Alte

Based on first law of thermodynamics

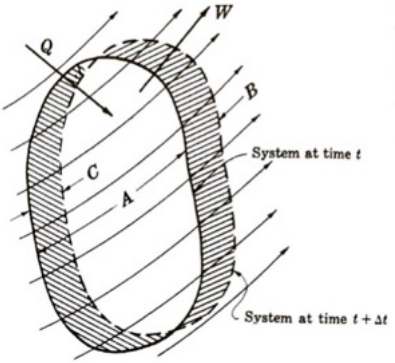

$Q - W = \Delta E$

$Q =$ heat added to the system

$W =$ work done by the system

$\Delta E =$ change in the energy of the system

$E = U + (1/2)mu^2 + mgz$

$U =$ internal energy associated with molecular and atomic behaviour

$(1/2)mu^2 =$ kinetic energy

$mgz =$ potential energy associated with the location in the earth's gravitational field

$$\boxed{\frac{dQ}{dt} - \frac{dW_s}{dt} = \frac{\partial}{\partial t}\int_{CV} \rho e dV + \int_{CS} \rho(e + p/\rho)\boldsymbol{u} \cdot dA} \tag{124}$$

$$e = U + \frac{1}{2}u^2 + gz \tag{125}$$

The time rate of heat added to the system minus the work done by the system is equal to the time rate of change of the stored energy in the control volume plus the net rate of efflux of stored energy and flow work out of the control volume.

Integral Form - Entropy

Second law of thermodynamics

$$dS - \frac{dQ}{T} \geq 0 \tag{126}$$

Entropy change minus the heat transferred to the system divided by the temperature is equal or greater than zero

$$\boxed{\frac{\partial}{\partial t}\int_{CV} \rho s dV + \int_{CS} \rho s u \cdot dA - \int_{CS} q/T \cdot dA \geq 0} \tag{127}$$

Q is the heat flux vector and s is the specific entropy (per unit mass)

Reynolds Transport Solution Strategy

- Define problem (most important)
- Draw control volume
- Write down integral equations and gas law
  - Mass
  - Momentum
  - Energy
- Cross out terms that are negligible or that cancel
- Estimate terms that are unknown
- Solver for unknowns – 1 to 6 equations in general for ideal gas compressible flows
- Hints - in general but not always
  - Mass flow rates, densities, etc. will be found through conservation of mass equation
  - Momentum, forces, drag, lift, etc. found through momentum equation
  - Energies, kinetic, internal, enthalpy, work, heat transfer, found through energy equation

Examples

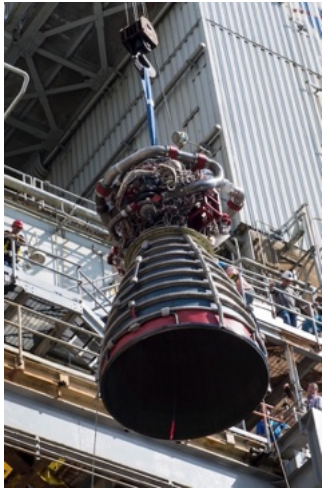

Figure 35: NASA Engine test - engine being moved to stand. Site NASA.gov

Examples

Figure 36: The General Electric GEnx (“General Electric Next-generation”) is an advanced dual rotor, axial flow, high-bypass turbofan jet engine in production by GE Aviation for the Boeing 787 and 747-8.

Examples

Figure 37: The General Electric F404 and F412 are a family of afterburning turbofan engines in the 10,500-19,000 lbf class. The series are produced by GE Aviation. Partners include Volvo Aero, which builds the RM12 variant. The F404 was developed into the larger F414 turbofan, as well as the experimental GE36 civil propfan.

Example – Basic Thrust Calculation

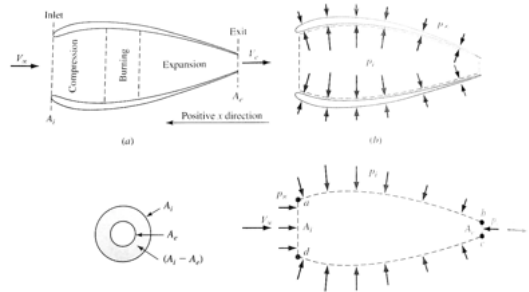

$$\frac{d}{dt}\int_{\forall}\rho\boldsymbol{u}d\forall+\int_{\boldsymbol{S}}\boldsymbol{u}\left(\rho\boldsymbol{u}\cdot d\boldsymbol{S}\right)=\int_{\forall}\rho\boldsymbol{f}d\forall-\int_{\boldsymbol{S}}pd\boldsymbol{S}+F_{\text{visc}} \tag{128}$$

$\sum F$ = momentum flux $\rightarrow$ Thrust $+ A_e(p_e - p_\infty) = \dot{m}V_e$

given $\dot{m} = 1400$ kg/s, $p_\infty = 101$ kPa, $p_e = 50$ kPa

$u_e = 1450$ m/s, $D_e = 2.4$ m, $A_e = 4.52$ m^2

$\therefore$ Thrust $= (50000 - 101000)4.52 + 1400(1450) = 1.8 \times 10^6$ N ($\sim$ 400,000 lbf).

Examples I

- Penn State supersonic wind tunnel has a compressed air storage tank with a volume of $57\ \mathrm{m}^3\ (2000\mathrm{ft}^3)$.
- In operation at Mach 2.5 and $p_t = 448$ kPa$(70\mathrm{psia})$, the mass flow rate out of the tank is $\dot{m} = 10\ \mathrm{kg/s}$.
- If a test begins at $p_{\text{tank}} = 1790$ kPa and ends at $p_{\text{tank}} = 690$ kPa (typical operation), how long does the test last?

Examples II

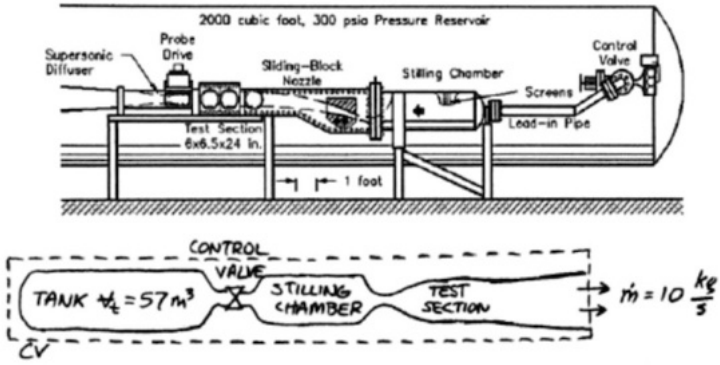

Figure 38: PSU Gas Dynamics Lab Supersonic Wind Tunnel.

Examples III

$$\frac{d}{dt}\int_{\forall}\rho d\forall + \int_{S}\rho \boldsymbol{u}\cdot d\boldsymbol{S} = 0 \tag{129}$$

Conditions change in the tank, so the RTT unsteady term is nonzero (+ entering the CV and − leaving it):

$$\iint \rho\vec{v}\cdot\vec{n}dA = -\dot{m} = V_{\text{tank}}\frac{\Delta\rho_{\text{tank}}}{\Delta t} \tag{130}$$

We are given Δp but need $\Delta\rho$. Assume the tank is adiabatic so T_{tank} is approximately constant and apply the perfect-gas state equation

$$\rho_{tank} = \frac{p_{tank}}{RT_{tank}} \tag{131}$$

so

$$-\dot{m} = \frac{V_{tank}}{RT_{tank}}\frac{\delta p_{tank}}{\delta t} \tag{132}$$

Examples IV

This can be integrated, since p_{tank} is solely a function of time:

$$-\dot{m}\int_0^{t_f} dt = \frac{V_{\text{tank}}}{RT_{\text{tank}}} \cdot \int_{p_1}^{p_f} dP \tag{133}$$

which yields

$$-\Delta t = \frac{V_{tank}}{\dot{m}RT_{tank}} \left(p_f - p_i\right)_{tank} \tag{134}$$

Evaluating this with the tank volume of $57\ \text{m}^3$, $T_{\text{tank}} = 300\ \text{K}$, the mass flow rate of $\dot{m} = -10\ \text{kg/s}$, $p_{\text{i}} = 1790\ \text{kPa}$ and $p_{\text{f}} = 690\ \text{kPa}$ yields:

$$\Delta t = \frac{57(690 - 1790)}{-10 \cdot 287 \cdot 300} = 73\ \text{s} \tag{135}$$

in good agreement with experimental results.

Examples I

- The plate is parallel to the flow.
- Uniform velocity $\mathbf{V} = U_0\mathbf{i}$
- Boundary layer of thickness, $y = \delta$
- Find the drag force D in terms of the flow properties ρ, U_0, and δ and the plate and dimensions L and b

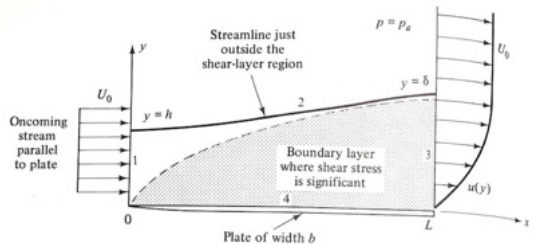

Figure 39: Boundary layer development on flat plate.

Examples II

Solution approach

- Like most practical cases, this problem requires a combined mass and momentum balance.
- A proper selection of control volume is essential, and we select the four-sided region from 0 to h to δ to L and back to the origin O
- We follow a streamline passing through $(x, y) = (0, h)$ which is outside the shear layer and has no mass flow across it
- The pressure is uniform so there is no net pressure force

Examples III

$$\frac{d}{dt}\int_{\forall}\rho \boldsymbol{u} d\forall + \int_{\boldsymbol{S}} \boldsymbol{u}\left(\rho \boldsymbol{u}\cdot d\boldsymbol{S}\right) = \int_{\forall}\rho \boldsymbol{f} d\forall - \int_{\boldsymbol{S}} p d\boldsymbol{S} + F_{\text{visc}} \tag{136}$$

The flow is assumed incompressible and steady and there are only fluxes through the entry and exit face of the control volume

$$\begin{aligned}\sum F_x = -D &= \rho\int\int_1 u(\boldsymbol{u}\cdot\boldsymbol{n})dA + \rho\int\int_3 u\left(\boldsymbol{u}\cdot\boldsymbol{n}\right)dA \\ &= \rho\int_0^h U_o(-U_o)bdy + \rho\int_0^\delta u(u)bdy\end{aligned} \tag{137}$$

Examples I

Evaluating the first integral and rearranging gives After defining the control volume, we write down all control volume equations, and cross out ones we do not need or make additional assumptions to cross out terms. We arrive at for drag the momentum equation

$$\frac{d}{dt}\int_{\forall}\rho\boldsymbol{u}d\forall+\int_{\boldsymbol{S}}\boldsymbol{u}\left(\rho\boldsymbol{u}\cdot d\boldsymbol{S}\right)=\int_{\forall}\rho\boldsymbol{f}d\forall-\int_{\boldsymbol{S}}pd\boldsymbol{S}+F_{\text{visc}} \tag{138}$$

And isolate for drag

$$D=\rho U_0^2bh-\rho b\int_0^{\delta}u^2dy \tag{139}$$

The height h is not known with respect to the shear-layer thickness δ. This is found by applying mass conservation, since the control volume forms a stream tube

$$\rho\iint_{\mathbb{S}}(u\cdot\mathrm{n})dA=0=\rho\int_0^h\left(-U_0\right)bdy+\rho\int_0^{\delta}ubdy \tag{140}$$

Examples II

$$U_0 h = \int_0^{\delta} u dy \tag{141}$$

After canceling b and ρ and evaluating the first integral. Introduce this value of h for a cleaner result

$$D = \rho b \int_0^{\delta} u \left(U_0 - u\right) dy \Big|_{x=L} \tag{142}$$

Examples I

- This result was first derived by Theodore von Karman in 1921
- Relates the friction drag on one side of a flat plate to the integral of the momentum defect $u\,(U_0 - u)$ across the trailing cross section of the flow past the plate.
- As $U_0 - u$ vanishes as y increases, the integral has a finite value.
- Example of momentum-integral theory for boundary layers.
- Illustrate the magnitude of this drag force, we use a simple approximation for the outlet-velocity profile $u(y)$, which simulates low-speed or laminar shear flow

$$u \approx U_0 \left(\frac{2y}{\delta} - \frac{y^2}{\delta^2} \right) \qquad \text{for } 0 \leq y \leq \delta \tag{143}$$

Substituting and letting $\eta = y/\delta$ for convenience, we obtain

$$D = \rho b U_0^2 \delta \int_0^1 \left(2\eta - \eta^2\right)\left(1 - 2\eta + \eta^2\right) d\eta = \frac{2}{15} \rho U_0^2 b \delta \tag{144}$$

Examples II

- Predicts within 1% of the accepted result from laminar boundary-layer theory.
- Led to the wide use of Karman's integral theory in the analysis of viscous flows.
- D increases with the shear-layer thickness δ, which increases with plate length.

Class Summary

- Laws of thermodynamics – a review and compressible flow insight
- Isentropy
- Reynolds transport theorem
- Examples

Next Time

- One-dimensional flow
- Wave propagation
- Speed of sound
- Mach waves

Class Overview

Introduction

- One-dimensional flow
- Wave propagation
- Speed of sound
- Mach waves

“I know of nothing more terrible than the poor creatures who have learned too much. Instead of the sound powerful judgement which would probably have grown up if they had learned nothing, their thoughts creep timidly and hypnotically after words, principles and formulae, constantly by the same paths. What they have acquired is a spider’s web of thoughts too weak to furnish sure supports, but complicated enough to provide confusion.”

Ernst Mach

One-Dimensional Flow and Quasi-One-Dimensional Flow

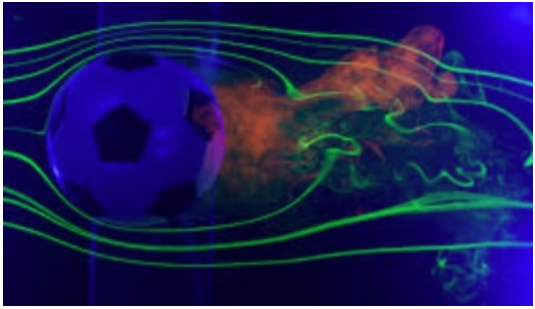

Figure 40: Smoke visualization around a soccer ball - some streamlines can be considered to be in quasi-one-dimensional flow.

Example: One-Dimensional Flow and Quasi-One-Dimensional Flow

Figure 41: Natural gas pipelines.

Application of Reynold's Transport Theory

Application of theory to streamtube, variation of streamtube with area, and a differential element.

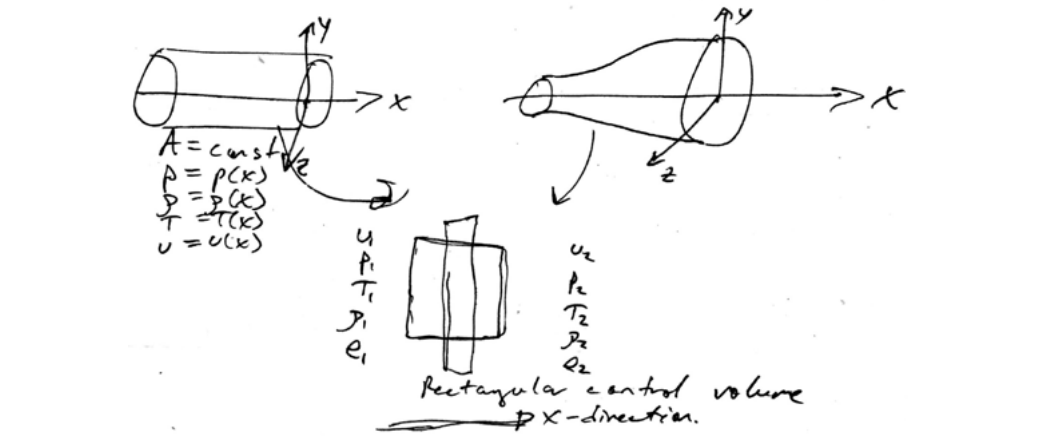

Figure 42: Simple control surfaces for the application of Reynold's transport theorem.

Application of Reynold's Transport Theory

Assume that the flow is steady or statistically stationary. Continuity equation in integral form is

$$\oint_S \rho \underline{u} \cdot d\underline{S} = 0 \rightarrow -\rho_1 u_1 A + \rho_2 u_2 A = 0 \tag{145}$$

It is clear we can write $\rho_1 u_1 = \rho_2 u_2$, which is the continuity equation for steady one-dimensional flow.

Application of Reynold's Transport Theory

Let us examine the momentum equation in integral form

$$\oint_S (\rho \underline{u} \cdot d\underline{S})\underline{u} - \oint_S p d\underline{S} = 0 \tag{146}$$

Let us choose the x direction as the direction of the flow

$$\rho_1(-u_1 A)u_1 + \rho_2(u_2 A)u_2 = -(-p_1 A + p_2 A) \tag{147}$$

Rearranging we find

$$p_1 + \rho_1 u_1^2 = p_2 + \rho_2 u_2^2 \tag{148}$$

which is the x momentum equation for steady (statistically) one dimensional flow.

Application of Reynold's Transport Theory

The integral equation for conservation of energy is

$$\dot{Q} - \oint_S p\underline{u} \cdot d\underline{S} = \oint_S \rho \left(e + \frac{u^2}{2} \right) \underline{u} \cdot d\underline{S} \tag{149}$$

Let us evaluate the surface integrals

$$\dot{Q} - (-p_1 u_1 A + p_2 u_2 A) = -\rho_1 \left(e_1 + \frac{u_1^2}{2} \right) u_1 A + \rho_2 \left(e_2 + \frac{u_2^2}{2} \right) u_2 A \tag{150}$$

Rearranging and dividing by the continuity equation (as derived previously) $(\rho_1 u_1 = \rho_2 u_2)$ yields

$$\frac{\dot{Q}}{\rho_1 u_1 A} + \frac{p_1}{\rho_1} + e_1 + \frac{u_1^2}{2} = \frac{p_2}{\rho_2} + e_2 + \frac{u_2^2}{2} \tag{151}$$

Let q be the heat added per unit mass.

Application of Reynold's Transport Theory

Recall the relation between enthalpy h, internal energy e, and pv, which is $h = e + pv$. Using this relation with the energy equation we obtain

$$h_1 + \frac{u_1^2}{2} + q = h_2 + \frac{u_2^2}{2} \tag{152}$$

which is the energy equation for steady one-dimensional flow. We now have a system of algebraic equations that have been reduced from integral equations.

Application of Reynold's Transport Theory

We assumed

- One-dimensional
- Steady
- No viscous terms
- Constant area
- No body forces
- No shaft work

Have we made any other assumptions? How did we arrive at these algebraic set of equations from our initial complicated partial differential equations?

Consider the Speed of Sound

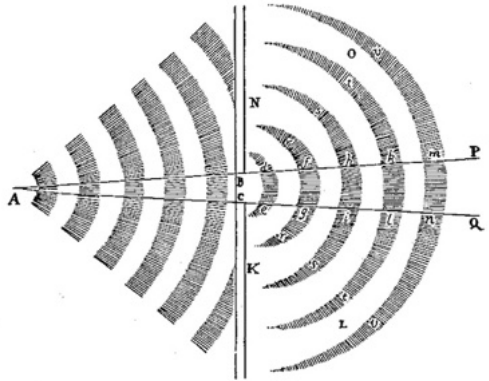

Figure 1-2 Sketch in Newton's *Principia* (1686) of the passage of waves through a hole. The source is at point *A*; the hole is described by points *B* and *C*; *de*, *fg*, *hi*, etc., describe the "tops of several waves, divided from each other by as many intermediate valleys or hollows." *(Adapted from Sir Isaac Newton's Principia, 4th ed., 1726, reprinted 1871, by MacLehose, Glasgow, p. 359.)*

Figure 43: Study in acoustics of Newton in his famous publication.

Differential Speed of Sound

- Consider a gas, a plasma, or a liquid (e.g. air in the room)
- Disturbance in the air or a solid object acting on the air can induce waves
- Different kinds of waves travel at different speeds, here we consider acoustic waves

Consider a differential change between states 1 and 2 or before and after the wave.

1	2
c	$c + dc$
p	$p + dp$
ρ	$\rho + d\rho$
T	$T + dT$
In front of wave	Behind wave

Speed of Sound

Note that there are two reference frames we can consider

- Standing on the wave
- Watching the wave propagate past

Recall conservation of mass $\rho_1 u_1 = \rho_2 u_2$ Let us replace u with c and the differential change, $\rho c = (\rho + d\rho)(c + dc)$. Now expand the result $\rho c = \rho c + c d\rho + \rho dc + \cancelto{0}{d\rho dc}$ and linearize, we find.

$$c = -\rho \frac{dc}{d\rho} \tag{153}$$

Can also write momentum equations as

$$p + \rho c^2 = (p + dp) + (\rho + d\rho)(c + dc)^2 \tag{154}$$

We neglect products again and solve for dc

$$dc = \frac{dp + c^2 d\rho}{-2c\rho} \tag{155}$$

Speed of Sound

Combine these two relations based on mass and momentum

$$c = -\rho\left[\frac{dp/d\rho + c^2}{-2c\rho}\right] \tag{156}$$

Solve for c^2

$$c^2 = \frac{dp}{d\rho} \tag{157}$$

Note sound waves are very small disturbances

- Irreversible, dissipative, viscous, thermal conduction are small
- No heat addition

We assume that the process is isentropic (for acoustic waves that are linear).

Speed of Sound and Incompressibility

We should view

$$c^2 = \frac{dp}{d\rho}\Big|_{isentropic} \tag{158}$$

given these assumptions.

- The speed of sound is a measure of the compressibility of the gas.
- Recall $\rho = 1/\nu \therefore d\rho = -d\nu/\nu^2$

$$c^2 = \partial p/\partial\rho = -\partial p/\partial\nu\nu^2 = -\nu/(1/\nu)/(\partial\nu/\partial p) \tag{159}$$

As $\tau_s \to 0$ sound speed becomes infinite $\to$ incompressible. For calorically perfect gas we can write

$$pV^\gamma = \text{constant} \tag{160}$$

Mach Number

Differentiate and noting $V = 1/\rho$ we obtain

$$\left(\frac{dp}{d\rho}\right)_S = \frac{\gamma p}{\rho} \implies c = \sqrt{\frac{\gamma p}{\rho}} \tag{161}$$

Note $\frac{p}{\rho} = RT \implies c = \sqrt{\gamma RT}$ perfect gas.

Result shows that speed of sound goes as $c \propto T^{1/2}$. For air $c_\infty \cong 343$ m/s. Mach number of vehicles is measured against c_∞.

Mach Number

Analyze Mach number in terms of energies of the flow. Let

$$\left(\frac{u^2/2}{e}\right) = \frac{u^2/2}{c_v T}$$
$$= \frac{u^2/2}{RT/(\gamma-1)} = \frac{(\gamma/2)u^2}{c^2/(\gamma-1)} = \frac{\gamma(\gamma-1)}{2}M^2 \tag{162}$$

We find an interesting interpretation of Mach number

$$M^2 \propto \frac{\text{kinetic energy}}{\text{internal energy}} \tag{163}$$

Ernst Waldfried Josef Wenzel Mach

18 February 1838 – 19 February 1916, Austrian

- Physicist and philosopher - interference, diffraction, polarization and refraction
- Professor of Mathematics at the University of Graz
- Deduced and experimentally confirmed the existence of a shock wave of conical shape
- Mach opposed Ludwig Boltzmann and others who proposed an atomic theory of physics
- Psychologists remember Mach for the optical illusion called Mach bands
- Albert Einstein, "it is justified to consider Mach as the precursor of the general theory of relativity" (Any phenomena that would seem attributable to absolute space and time)

After an 1897 lecture by Ludwig Boltzmann at the Imperial Academy of Science in Vienna he yells, "*I don't believe that atoms exist!*"

S.A.E. Miller, Ph.D., saem@ufl.edu

Disturbances in a Fluid - Notation

Consider small body moving through a gas. Acoustic waves from the body propagate at the speed of sound.

- u speed of body
- c speed of sound
- t time
- For illustration purposes, consider sound emitted at constant intervals generated at $t, 2t, \ldots nt$

Disturbances in a Fluid - Subsonic

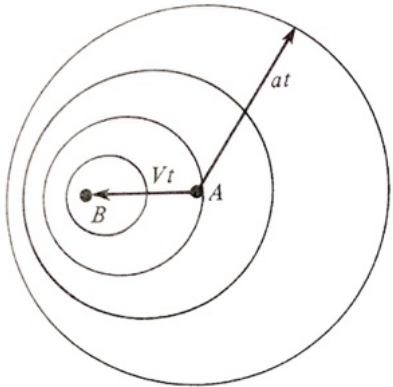

Figure 44: Diagram showing radiation of various disturbances with ambient subsonic Mach number.

Note that these waves never coalesce.

Disturbances in a Fluid - Supersonic

Now small protrusions on surfaces create Mach waves. These waves are not shock waves.

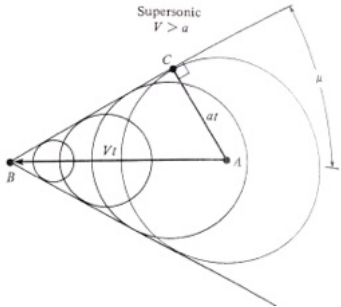

Figure 45: Diagram showing radiation of various disturbances with ambient Supersonic Mach number.

This case has angle α that is found by

$$\sin\alpha = \frac{c}{u} = M^{-1} \tag{164}$$

Mach Waves Observed During Launch

Figure 46: Mach waves are labeled when this Atlas rocket approaches the transonic condition. They radiated in front of the rocket through the atmosphere in the direction of flight.

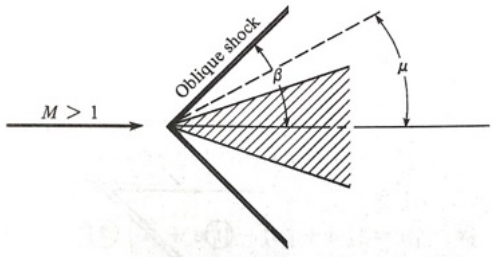

Figure 47: A two-dimensional wedge in supersonic flow. Consider the physical formation of the shock wave and its relation to disturbances.

Example

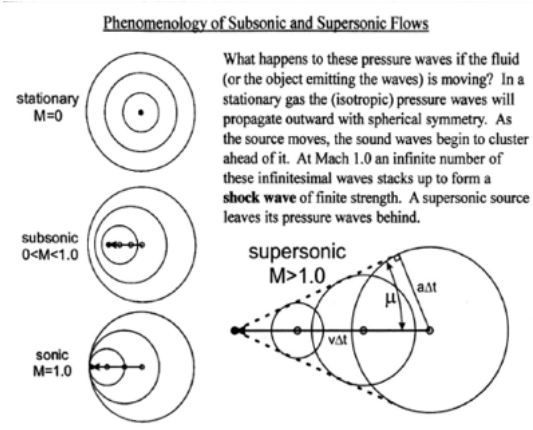
Phenomenology of Subsonic and Supersonic Flows
stationary
M=0
subsonic
0<M<1.0
sonic
M=1.0
What happens to these pressure waves if the fluid (or the object emitting the waves) is moving? In a stationary gas the (isotropic) pressure waves will propagate outward with spherical symmetry. As the source moves, the sound waves begin to cluster ahead of it. At Mach 1.0 an infinite number of these infinitesimal waves stacks up to form a shock wave of finite strength. A supersonic source leaves its pressure waves behind.
supersonic
M>1.0
aΔt
μ
vΔt

Example

- For air, $\gamma = 1.4$ and $T = 288$ K $(60°\text{F})$, find c.
  - $c \equiv \sqrt{\gamma RT} = \sqrt{1.4\left(287\frac{m^2}{s^2K}\right)288K} = 340\frac{m}{s}$
- Car driver goes to 200mph on $80°$F day. Is the airflow over these cars compressible or incompressible?
  - $u = 200\text{mph} = 89.4$ m/s; $T = 80°\text{F} = 300$ K
  - $c \equiv \sqrt{\gamma RT} = \sqrt{1.4\left(287\frac{\text{m}^2}{\text{s}^2K}\right)300K} = 347\frac{\text{m}}{\text{s}}$
  - $M = u/c = 89.4/347 = 0.26$
  - Well below the onset of compressibility (engineering approximation).

Example

Aircraft max Mach number is 0.91 at sea level. Find max velocity of aircraft at 5° C and 45° C.

- $u_{\text{max}}|_{\text{sea level}} = M_{\text{max}} c_{\text{sea level}} = 0.91\sqrt{\gamma R T_{\text{sea level}}}$
- For $5^\circ C = 278$ K
- $u_{\text{max}} = 0.91\sqrt{1.4(287)(278)} = 304$ m/s
- For $45^\circ C = 318$ K
- $u_{\text{max}} = 0.91\sqrt{1.4(287)(318)} = 325$ m/s
- Speed records are best set on days that are hot.

Example

A weak pressure wave contains a 0.05 kPA pressure rise. Air is approximately 30° C and pressure is 105 kPa. Find the velocity behind the wave.

Solution

Conservation of mass gives

$$\dot{m} = \rho c = (\rho + d\rho)(c - du) \tag{165}$$

du = velocity difference

conservation of momentum

$$p - (p + dp) = \dot{m}[(c - du) - c] \tag{166}$$

$\therefore dp = \dot{m} du = \rho c du, du = \frac{1}{\rho c} dp$

Density is $\rho = \frac{p}{RT} = \frac{105 \times 10^3}{287303K} = 1.209 \text{ kg/m}^3$

$c = \sqrt{\gamma RT} = \sqrt{1.4(287)(303)K} = 348.7 \text{ m/s}$

$\therefore du = \frac{1}{1.209(348.7)} \underbrace{(0.05 \times 10^3)}_{0.05\text{kPa}} = 0.119 \text{ m/s}$

Example

An observer on the ground finds that an airplane flying horizontally at an altitude of 5 km has travelled 12 km from the overhead position before the sound of plane is first heard. Estimate the speed at which the plane is flying. Assume atmosphere temperature of $T = 271.9$ K. Here, $c = \sqrt{\gamma RT} = \sqrt{1.4 \times 287 \times 271.9} = 330.6$ m/s Mach angle...

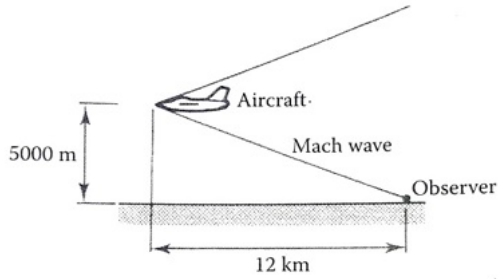

$\tan\alpha = \frac{5}{12} = 0.417$ Now, $\alpha = 1/M \therefore \tan\alpha = \frac{1}{M^2-1} \therefore M = 2.6$ velocity $= 2.6 \times 330.6 = 859.6$ m/s.

Modern superguns (for more on this topic see "space gun" on Wikipedia)

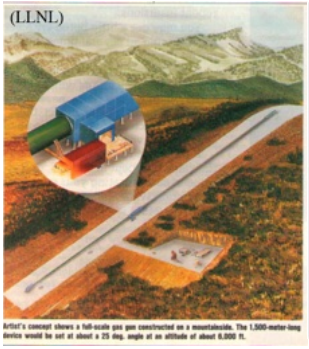

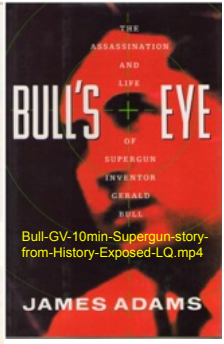

Bull-GV-10min-Supergun-story-from-History-Exposed-LQ.mp4

Example – Asteroid

A near–Earth asteroid on August 10, 1972 was seen by a large number of people including camera–bearing tourists in the Grand Teton national park. Estimates give the altitude as 100 km, speed 14.8 km/s, mass 1 billion kg (1 million tons), and diameter of tens of meters. Find the Mach number of the asteroid. If you could see the wave system it generated, how would it appear?

Figure 48: An asteroid over the Grand Teton National Park.

Solution: The "standard atmosphere" tables (available on the web) give the temperature as ~ 180K at 100 km (the edge of space).

$a = \sqrt{\gamma RT}$ = sqrt(1.4 x 287 x 180) = 270 m/sec $M = V/a = 14800/270 = 55$

Mach 55! The asteroid was in what we call the hypervelocity flow regime. Up close, a very strong shock wave heats it to white-hot radiance. Not far downstream, however, we can assume the shock weakens to the Mach angle.

$\mu = \sin^{-1}\left(\frac{1}{M}\right) = 1°$ Shown below is a sketch of the trailing wave system

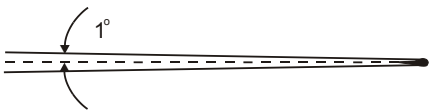

*Ceplecha, Z., "Earth-grazing daylight fireball of August 10, 1972," *Astronomy and Astrophysics*, **283** (1994), pp. 287-288.

If this asteroid had actually hit the Earth, its kinetic energy would have been transformed into a huge explosion. How huge?

$KE = \frac{1}{2}mV^2 \sim 10^{17}$ J

The explosive TNT produces about 4 million J/kg. Dividing this into the above, the asteroid impact would have had the equivalent of 24 megatons of TNT, similar to the largest US hydrogen bomb ever developed.

From the movie "Armageddon": Armageddon-Paris-clip

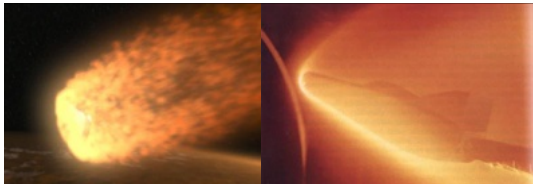

Other examples of kinetic heating, clockwise from top left: NASA Mars Phoenix probe, NASA arc tunnel, burning hypersonic model in ballistic range (AEDC), Space Shuttle Columbia disaster. Video: Phoenix-Mars-aerobraking-2

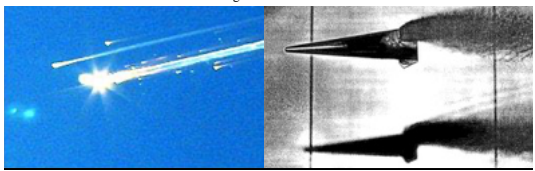

Assumptions

What assumptions have we made or violated?

- Atmospheres have non-uniform properties (e.g. T)
- Observe sonic boom and not really Mach waves

Figure 49: The turbulent atmosphere. Sound waves are refracted and reflected as they travel through the turbulent atmosphere.

Class Summary

- One-dimensional flow
- Wave propagation
- Speed of sound
- Mach waves

Next Time

- Introduction to isentropic flow
- Reynolds transport theory for isentropic flow and its derivation
- Convergent-divergent streamtubes

Class Overview

Isentropic Flow

- Introduction to isentropic flow
- Reynolds transport theory for isentropic flow and its derivation
- Convergent-divergent streamtubes
- Examples

"You should call it entropy, for two reasons. In the first place your uncertainty function has been used in statistical mechanics under that name, so it already has a name. In the second place, and more important, no one really knows what entropy really is, so in a debate you will always have the advantage."

Suggesting to Claude Shannon a name for his new uncertainty function, as quoted in Scientific American Vol. 225 No. 3, (1971), p. 180.

Regions of Isentropic Flow

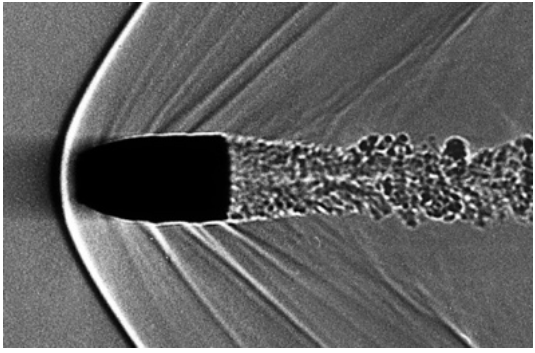

Figure 50: Schlieren image of a bullet.

Regions of Isentropic Flow

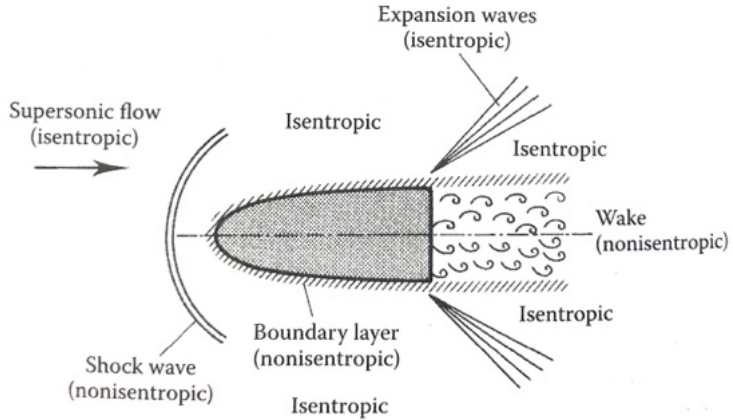

Figure 51: A schematic of a bullet.

Regions of Isentropic Flow

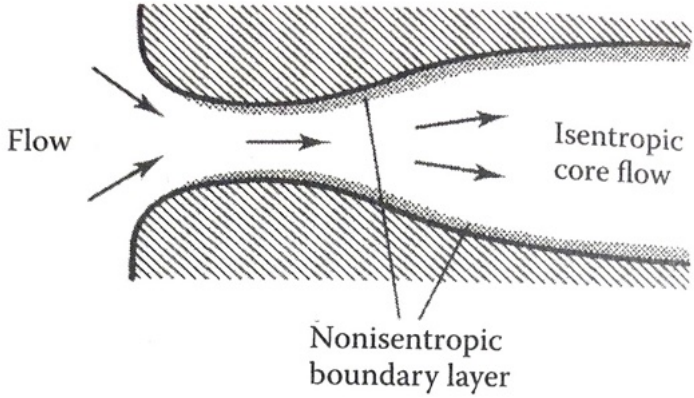

Figure 52: A schematic of a nozzle flow.

One-Dimensional vs Quasi-One-Dimensional

Important points

- Constant area assumption is a restriction
- Area changes have effect on the flow
- Variation of area is useful for examining rocket nozzles and wind tunnels
- Flows have properties of conservation mass, momentum, and energy
- View flows as a stream tube that varies with area

Example Streamtube

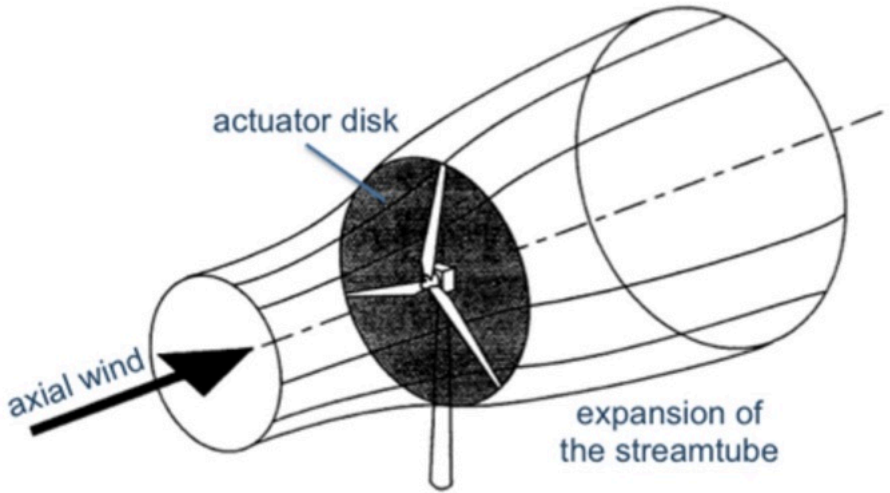

Figure 53: Streamtube with an actuator disk modeling a wind-turbine airflow.

Quasi-One-Dimensional Streamtube Control Surface

We now seek to understand how the total energy changes in a streamtube

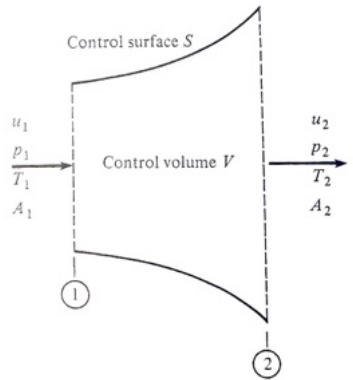

Figure 54: Stream tube with control surface.

Mass and Momentum Equations

Conservation of mass

$$-\int\int_S \rho \underline{u} \cdot d\underline{S} = \frac{d}{dt}\int_\forall \rho d\forall \tag{167}$$

Integration results in

$$\boxed{\rho_1 u_1 A_1 = \rho_2 u_2 A_2} \tag{168}$$

Momentum equation

$$\int\int_S (\rho \underline{u} \cdot d\underline{S})\underline{u} + \int_\forall \frac{d\rho \underline{u}}{dt} d\forall = \int_\forall \rho \underline{f} d\forall - \int_S p d\underline{S} \tag{169}$$

Assuming steady and no body forces

$$\boxed{p_1 A_1 + \rho_1 u_1^2 A_1 + \int_{A_1}^{A_2} p dA = p_2 A_2 + \rho_2 u_2^2 A_2} \tag{170}$$

pressure force on sides of control volume between locations 1 and 2

Energy Equation I

We write the energy equation as

$$\begin{aligned}&\int_{\forall} \dot{q}\rho d\forall - \int_S p\underline{u}\cdot d\underline{S} + \int_{\forall}\rho(\underline{f}\cdot\underline{u})d\forall \\ &= \int_{\forall}\frac{d}{dt}\left[\rho\left(e+\frac{u^2}{2}\right)\right]d\forall + \int_S \rho\left(e+\frac{u^2}{2}\right)\underline{u}\cdot d\underline{S}\end{aligned} \tag{171}$$

Assumptions – Steady, adiabatic, and no body forces yields

$$p_1u_1A_1 + \rho_1u_1A_1\left(e_1+\frac{u_1^2}{2}\right) = p_2u_2A_2 + \rho_2u_2A_2\left(e_2+\frac{u_2^2}{2}\right) \tag{172}$$

Divide by continuity relation and noting $h = e + p/\rho$, where h is enthalpy and $\rho = v^{-1}$.

Energy Equation Continued

Results in

$$\boxed{h_1 + \frac{u_1^2}{2} = h_2 + \frac{u_2^2}{2}} \tag{173}$$

Energy equation for steady quasi-one dimensional flow implies total stagnation enthalpy, h_o is constant

$$\boxed{h_o = \text{constant}} \tag{174}$$

An important implication – steady adiabatic flow has constant enthalpy along streamlines.

Seek a Differential Form I

We now seek a differential equation to understand area effect changes. Continuity implies

$$\rho u A = \text{constant} \tag{175}$$

and

$$\therefore d(\rho u A) = 0 \tag{176}$$

Seek a Differential Form II

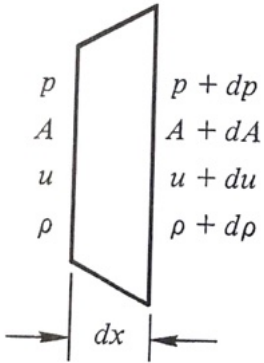

Figure 55: Differential element of streamtube with varying area.

- Momentum equation, applied to control volume in the streamwise (x) direction

Seek a Differential Form III

- Drop second order terms
- Perform difference of the continuity equation multiplied by u

We find

$$dp = -\rho u du \tag{177}$$

This equation is a simplification of the Euler equations.

Leonhard Euler

15 April 1707 – 18 September 1783, Swiss

"Read Euler, read Euler, he is the master of us all." ~Laplace

- Mathematician, physicist, astronomer, logician, and engineer
- Calculus, graph theory, topology, analytic number theory, mathematical terminology, notation, particularly, mechanics, fluid dynamics, optics, astronomy, and music theory
- Most prolific mathematician of all time, collected works fill 80+, volumes, more than anybody
- Most of his adult life in Saint Petersburg, Russia, and in Berlin, then the capital of Prussia
- Married Katharina Gsell, a painter from the Academy Gymnasium. Only 5 of their 13 children survived childhood
- Devout Christian who believed the Bible to be inspired

S.A.E. Miller, Ph.D., saem@ufl.edu

Seek a Differential Form

Differentiating the energy equation

$$uAd\rho + \rho Adu + \rho udA = 0 \tag{178}$$

then divide by ρuA results in

$$dh + udu = 0 \tag{179}$$

We now seek an area-velocity relation. Recall, continuity $d(\rho uA) = 0$, so we write

$$\frac{d\rho}{\rho} + \frac{du}{u} + \frac{dA}{A} = 0 \tag{180}$$

Eliminate $\frac{d\rho}{\rho}$ by using momentum relation yields

$$\frac{dp}{\rho} = \frac{dp}{\rho}\frac{d\rho}{d\rho} = -udu \tag{181}$$

Seek a Differential Form

We made the isentropic assumption so all changes in p result in isentropic changes in density

$$\therefore \frac{dp}{d\rho} = \left(\frac{dp}{d\rho}\right)_S = c^2 \text{ (recall from previous lecture)} \tag{182}$$

Combining previous two equations yields,

$$c^2 \frac{d\rho}{\rho} = -udu \tag{183}$$

or

$$\frac{d\rho}{\rho} = \frac{-udu}{c^2} = \frac{-u^2 du}{c^2 u} = -M^2 \frac{du}{u} \tag{184}$$

Seek a Differential Form

Substitute this into the term for $\partial\rho/\rho$

$$\frac{d\rho}{\rho} + \frac{du}{u} + \frac{dA}{A} = 0 \tag{185}$$

yields

$$\boxed{\frac{dA}{A} = (M^2 - 1)\frac{du}{u}} \tag{186}$$

This equation is the area-velocity relation. Also called Mach number area relation.

Implications of Area-Velocity Relation

- For $M \to 0$ then A is a constant
  - Corresponds to incompressible result.
- For $0 \leq M < 1$, subsonic flow, increase in velocity (du) is associated with a decrease in area.
  - Recall fluid mechanics course: in subsonic flow a diffuser will slow down the flow.
- For $M > 1$, an increase in velocity results in an increase in area!
  - This is a bit counter intuitive but a very important result.
- For $M = 1$ (sonic flow), $\frac{dA}{A} = 0$, which is minimum or maximum in area distribution.
  - This implies that the minimum solution is the one corresponding to reality.

Convergent-Divergent Ducts

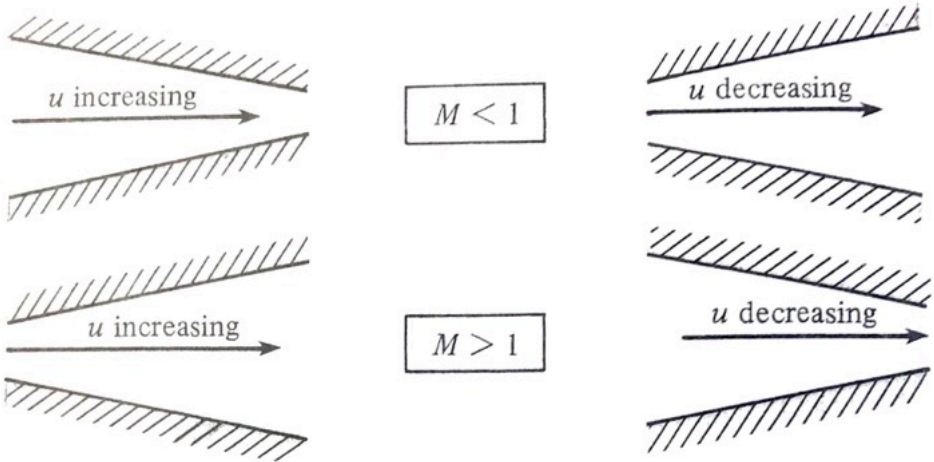

Figure 56: Variation of velocity in the streamwise direction with varying area and dependence on M.

Implications

Some notes

- For gas to expand from subsonic to supersonic, it must pass through a convergent-divergent duct
- The minimum area is called the "throat," denoted as A_t or A^* (if $M = 1$)
- For flow to slow down from supersonic to subsonic isentropically, it must pass through a throat (minimum A).
- These observations imply a shape for a rocket nozzle

Implications

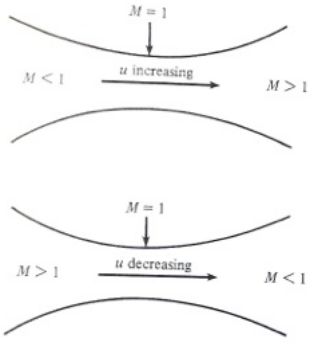

Figure 57: Two of a few possible flows.

Isentropic Relations

- Isentropic relations can be related to Mach numbers
- Derive by isentropic relation then substituting and eliminating stagnation quantity along streamlines of T_o

$$\frac{p_2}{p_1} = \left[\frac{1+\frac{1}{2}(\gamma-1)M_1^2}{1+\frac{1}{2}(\gamma-1)M_2^2}\right]^{\frac{\gamma}{\gamma-1}} \tag{187}$$

$$\frac{\rho_2}{\rho_1} = \left[\frac{1+\frac{1}{2}(\gamma-1)M_1^2}{1+\frac{1}{2}(\gamma-1)M_2^2}\right]^{\frac{1}{(\gamma-1)}} \tag{188}$$

$$\frac{T_2}{T_1} = \frac{1+\frac{1}{2}(\gamma-1)M_1^2}{1+\frac{1}{2}(\gamma-1)M_2^2} \tag{189}$$

I do not prefer students use this method in practice or in class, as we will develop more powerful methods later!

Isentropic Relations

Using these equations, we can directly relate ratios of static thermodynamic properties

$$\frac{T_2}{T_1} = \left(\frac{\rho_2}{\rho_1}\right)^{\gamma-1} = \left(\frac{p_2}{p_1}\right)^{(\gamma-1)/\gamma} \tag{190}$$

and from continuity

$$\left(\frac{\rho_2}{\rho_1}\right)\left(\frac{u_2}{u_1}\right) = \frac{A_1}{A_2} \tag{191}$$

- By knowing the ratio of Mach numbers then all the ratios of isentropic flow are known.
- These can be developed independently from this approach.

Example

Gas has molar mass of 39.9 and $\gamma = 1.67$. It is discharged from a large chamber with pressure 500 kPa and temperature 30° C through a nozzle. Using one-dimensional isentropic flow find

a) The M, T, and u at a point in the nozzle where p is 80 kPa.
b) Mass flow rate, $\dot{m}$, if nozzle diameter, D, is 12 mm.

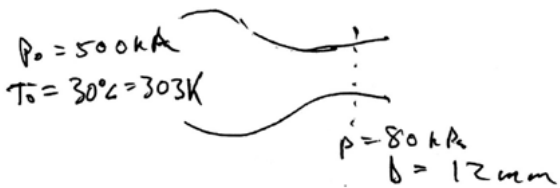

Solution

Rearrange

$$\frac{p_2}{p_1} = \left(\frac{1+\frac{1}{2}(\gamma-1)M_1^2}{1+\frac{1}{2}(\gamma-1)M_2^2}\right)^{\frac{\gamma}{\gamma-1}} \tag{192}$$

$$\rightarrow M = \left(\left(\frac{2}{\gamma-1}\right)\left(\frac{p_o}{p}^{\frac{\gamma-1}{\gamma}} - 1\right)\right)^{\frac{1}{2}} \tag{193}$$

$$= \left(\left(\frac{2}{0.67}\right)\left(\frac{500}{80}\right)^{0.4} - 1\right)^{\frac{1}{2}} = 1.8$$

$$T = T_o\left(1+\frac{8-1}{2}M^2\right)^{-1} = 303\text{ K}\left(1+\frac{0.67}{2}(1\times 8^2)\right)^{-1} = 145.3\text{ K} \tag{194}$$

Calculate the speed of sound

$$c = \sqrt{\gamma RT} = \sqrt{1.667\frac{8314}{39.9}145.3} = 224.9\text{ m/s} \tag{195}$$

Solution

Recall that $M = u/c$

$$\therefore u = Mc = 1.8(224.9 \text{ m/s}) = 404.7 \text{ m/s}. \tag{196}$$

b) Density at cross-section from ideal gas law

$$\rho = \frac{p}{RT} = \frac{80 \times 10^3 \text{ Pa}}{(8314/39.9)155.3} = 2.64 \text{ kg/m}^3 \tag{197}$$

Recall that $\dot{m} = \rho u A$

$$\dot{m} = 2.64 \times 404.7 \left(\frac{\pi 0.012^2}{4} \right) = 0.121 \text{ kg/s} \tag{198}$$

Example

A gas with molar mass of 4 and $\gamma = 1.3$ flows through a variable air duct. At one point in the flow the velocity is 150 m/s, the pressure is $p = 100$ kPa, and the T is 15 deg. C. Find:

- M at this point.
- At another point the T is $-10°$ C. Find M, p, u at this second point using isentropic theory.

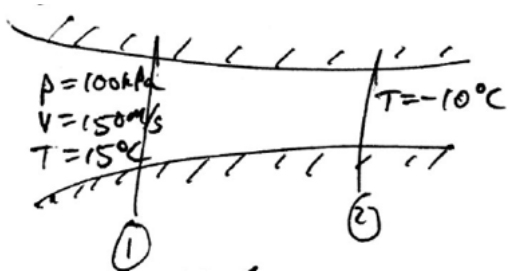

Solution

For the gas constant

$$R = \frac{\mathfrak{R}}{m} = \frac{8314}{4} = 2078.5 \text{ J / kg } \cdot \text{K} \tag{199}$$

Now seek $M_1 = \frac{u_1}{c_1} = \frac{150}{\sqrt{1.3 \times 2078.5 \times 288}} = 0.17$

Let us now examine section 2. Seek the speed of sound c_2

$$c_2 = c_1 \left(\frac{T_2}{T_1} \right)^{\frac{1}{2}} = 843 \text{ m/s} \tag{200}$$

Solution

Let's find M_2. Recall the relation we just developed

$$\frac{T_2}{T_1} = \left(\frac{1 + \frac{\gamma - 1}{2} M_1^2}{1 + \frac{\gamma - 1}{2} M_2^2} \right) \tag{201}$$

Solving for M_2

$$M_2 = \left(\frac{\left(1 + \frac{\gamma - 1}{2} M_1^2 \right) \frac{T_1}{T_2} - 1}{(\gamma - 1)/2} \right)^{1/2} = 0.8157 \tag{202}$$

$$u_2 = M_2 c_2 = 687.2 \text{ m/s} \tag{203}$$

Isentropic relation

$$p_2 = \left(\frac{c_2}{c_1} \right)^{\frac{2\gamma}{\gamma - 1}}, p_2 = \left(\frac{843}{882.15} \right)^{8.67} 100 = 67.5 \text{ kPa} \tag{204}$$

Example

Air flows through a nozzle that has inlet area of $A_i = 10$ cm^2. Inlet properties are $u = 80$ m/s, $T = 28^\circ$ C, and $p = 700$ kPa. At the outlet we measure $p = 250$ kPa. Find mass flow rate, $\dot{m}$, and exit velocity u_e.

Solution

Mass flow rate can immediately be found.

$$\dot{m} = \rho_1 u_1 A_1 = \frac{p_1}{RT_1} u_1 A_1 = \frac{700 \times 10^3}{287(301)} 80 \times 10^{-3} = 0.648 \text{ kg/s} \tag{205}$$

Seeking the Mach number

$$M_1 = \frac{u_1}{c_1} = \frac{80}{\sqrt{\gamma RT}} = \frac{80}{(1.4(287)(301))^{\frac{1}{2}}} = 0.23 \tag{206}$$

Solution

Recall isentropic relation

$$\frac{p_2}{p_1} = \left(\frac{1 + \frac{\gamma - 1}{2} M_1^2}{1 + \frac{\gamma - 1}{2} M_2^2} \right)^{\frac{\gamma}{\gamma - 1}} \tag{207}$$

We do not know M_2, solving yields $M_2 = 1.335$

Isentropic nozzle $\frac{T_2}{T_1} = \left(\frac{p_2}{p_1} \right)^{\frac{\gamma - 1}{\gamma}}$

$$\therefore T_2 = 301 \left(\frac{250}{700} \right)^{\frac{1}{3.5}} = 224.3 \text{ K} \tag{208}$$

Solving for u_2 $u_2 = M_2 c_2 = 1.335 \sqrt{1.4(287)224.3} = 400.8$ m/s

Class Summary

- Introduction to isentropic flow
- Reynolds transport theory for isentropic flow and its use
- Convergent-divergent streamtubes
- Examples

Next Time

- Stagnation (total) conditions
- Pitot-static tubes
- Examples

Class Overview

- Isentropic flow
- Stagnation (total) conditions
- Pitot-static tubes
- Examples

“Without encroaching upon grounds appertaining to the theologian and the philosopher, the domain of natural sciences is surely broad enough to satisfy the wildest ambition of its devotees. The work may be hard, and the discipline severe; but the interest never fails, and great is the privilege of achievement,”

John Strutt, 3rd Baron Rayleigh

Stagnation Point Video

Stagnation point video in video folder 2_2

Stagnation or Total Conditions

We aim to develop relations for the 'stagnation' or 'total' values of thermodynamic quantities (and others). This will yield an important and useful tool in our field. Recall

$$h_1 + \frac{u_1^2}{2} = h_2 + \frac{u_2^2}{2} \tag{209}$$

For calorically perfect gas, $h = c_p T$,

$$c_p T_1 + \frac{u_1^2}{2} = c_p T_2 + \frac{u_2^2}{2} \tag{210}$$

Can be written using ideal gas law

$$\frac{\gamma R T_1}{\gamma - 1} + \frac{u_1^2}{2} = \frac{\gamma R T_2}{\gamma - 1} + \frac{u_2^2}{2} \tag{211}$$

Stagnation or Total Conditions

Using speed of sound

$$\frac{c_1^2}{\gamma - 1} + \frac{u_1^2}{2} = \frac{c_2^2}{\gamma - 1} + \frac{u_2^2}{2} \tag{212}$$

Can also be written using $c = \sqrt{\gamma p/\rho}$

$$\frac{\gamma}{\gamma - 1}\left(\frac{p_1}{\rho_1}\right) + \frac{u_1^2}{2} = \frac{\gamma}{\gamma - 1}\left(\frac{p_2}{\rho_2}\right) + \frac{u_2^2}{2} \tag{213}$$

If there is not heat transfer (addition) then this holds for isentropic flow.

Stagnation or Total Conditions

Now consider the fluid being brought adiabatically to Mach one with speed of sound $c^*(u_2 = c^*)$. We find

$$\frac{c^2}{\gamma - 1} + \frac{u^2}{2} = \frac{\gamma + 1}{2(\gamma - 1)} c^{*2} \tag{214}$$

where c^*(speed of sound) can now be found in the flow-field given c and u. Now imagine we try the opposite situation where the fluid is brought to rest isentropically. Let T and u be static values of temperature and velocity then

$$c_p T + \frac{u^2}{2} = c_p T_o \tag{215}$$

Remember, stagnation or total conditions are those that correspond to conditions when fluid is brought isentropically to rest.

Stagnation or Total Conditions

Using this equation and $c_p = \gamma R/(\gamma - 1)$ we find

$$\begin{aligned} \frac{T_o}{T} &= 1 + \frac{u^2}{2c_pT} = 1 + \frac{u^2}{2\gamma RT/(\gamma - 1)} \\ &= 1 + \frac{u^2}{2c^2/(\gamma - 1)} = 1 + \frac{\gamma - 1}{2}\left(\frac{u}{c}\right)^2 \end{aligned} \tag{216}$$

$$\boxed{\frac{T_o}{T} = 1 + \frac{\gamma - 1}{2}M^2} \tag{217}$$

This is an important equation that relates the total (stagnation) to static temperature at a point in the flow as a function of M. Now, recall that for isentropic processes

$$\frac{p_o}{p} = \left(\frac{\rho_o}{\rho}\right)^{\gamma} = \left(\frac{T_o}{T}\right)^{\frac{\gamma}{\gamma-1}} \tag{218}$$

Stagnation or Total Conditions

- Using a similar approach for T, we can find the relations for p and ρ.
- We can use the isentropic relations to relate ratios of T_o/T to other static field-variables.

We find

$$\boxed{\frac{p_o}{p} = \left(1 + \frac{\gamma - 1}{2} M^2\right)^{\frac{\gamma}{\gamma - 1}}} \tag{219}$$

$$\boxed{\frac{\rho_o}{\rho} = \left(1 + \frac{\gamma - 1}{2} M^2\right)^{\frac{1}{\gamma - 1}}} \tag{220}$$

- These relations are so important that they are shown in the "Ames" tables, which are named after NASA Ames Research Center.
- They are shown in the isentropic tables given to you in this class.

A Note on Purely Isentropic Flow through Nozzles

We now consider nozzles, where the flow is fully isentropic throughout.

- The primary purpose of a nozzle is to accelerate a flow.
- Nozzles used in wind tunnels, propulsion systems, and in many other applications
- Isentropic systems have $\Delta S = 0$, so there are no losses or shocks
- Many nozzles in practice have losses (boundary layers, shocks, etc.) that we will consider later in the course

Example

A perfect gas has $\gamma = 1.4$. It moves at $\mathcal{M} = 3$. The static properties are $T = 250$ K, $p = 101$ kPa, and $\rho = 1.4077$ kg/m^3. Determine the stagnation (total) conditions T_o, p_o, and ρ_o.

Solution

$$\frac{T_o}{T} = 1 + \frac{\gamma - 1}{2} M^2 = (0.3571)^{-1} \tag{221}$$

$$\frac{p_o}{p} = \left(1 + \frac{\gamma - 1}{2} M^2\right)^{\frac{\gamma}{\gamma - 1}} = (0.02722)^{-1} \tag{222}$$

$$\frac{\rho_o}{\rho} = \left(1 + \frac{\gamma - 1}{2} M^2\right)^{\frac{1}{\gamma - 1}} = (0.07623)^{-1} \tag{223}$$

So, $T_o = T\left(\frac{T_o}{T}\right) = 250 \text{ K } \frac{1}{0.3571} = 700 \text{ K}$

$p_o = 101 \text{ kPa } \left(\frac{1}{0.02722}\right) = 3710.5 \text{ kPa}$

$\rho_o = \rho\left(\frac{\rho_o}{\rho}\right) = 1.4077 \frac{1}{0.07623} = 18.4665 \text{ kg/m}^3$

Examples of Stagnation Conditions

Air flows over an airfoil. The free-stream air has a Mach number of 0.85 ($M_\infty = 0.85$) and static pressure $p_\infty = 80$ kPa. Find the largest pressure acting on the body.

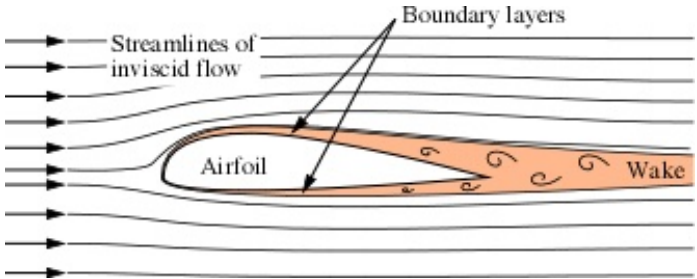

Figure 58: Streamlines over an airfoil with moderate separation.

Solution

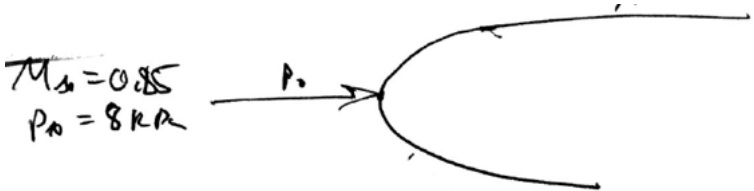

$$\frac{p_o}{p} = \left(1 + \frac{\gamma - 1}{2} M^2\right)^{\frac{\gamma}{(\gamma-1)}} \tag{224}$$

$$\frac{p_o}{p} = \left(1 + \frac{1.4 - 1}{2} 0.85^2\right)^{\frac{1.4}{(1.4-1)}} = 1.604 \tag{225}$$

We find $p_o = 80$ kPa(1.604) = 128.3 kPa

- We can apply this concept to wind tunnel flows e.g. the Pitot tube (subsonic)

Pitot Tube

Recall the equation for p_o/p as a function of M

$$\frac{p_o}{p} = \left(1 + \frac{\gamma - 1}{2} M^2\right)^{\frac{\gamma}{(\gamma-1)}} \tag{226}$$

Solve for M

$$M = \left(\frac{2}{\gamma - 1}\left(\left(\frac{p_o}{p}\right)^{\frac{\gamma-1}{\gamma}} - 1\right)\right)^{1/2} \tag{227}$$

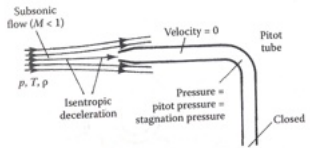

Pitot-Static Tube

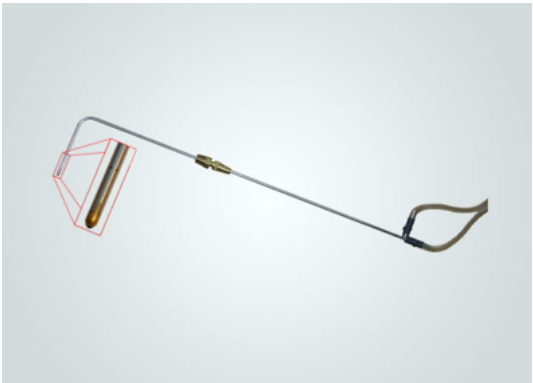

Figure 59: Pitot-static tube with close-up of total and static pressure ports.

Pitot-Static Tube

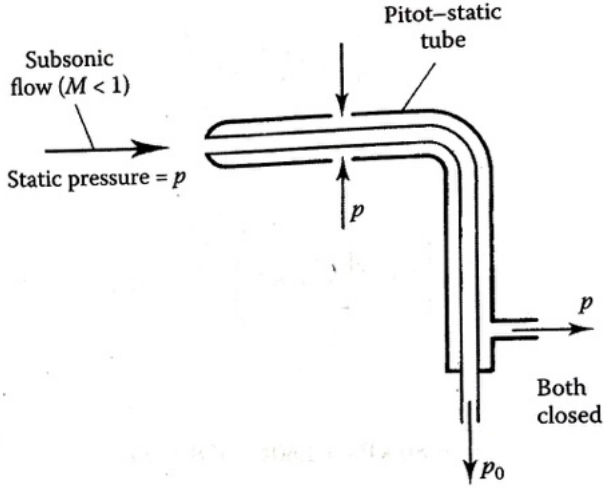

Figure 60: Simplified schematic of the Pitot-static tube.

Pitot-Static Tube

Figure 61: Pitot-static tube on a Boeing aircraft.

Pitot-Static Tube

Figure 62: Pitot-static tube on X-15.

Pitot-Static Tube

Figure 63: F–117.

Pitot-Static Tube

Figure 64: F–117 Pitot tubes.

Pitot-Static Tube

Figure 65: Lockheed–Martin YF–12, interceptor. Predecessor to the SR–71.

Pitot-Static Tube

Figure 66: Lockheed–Martin YF–12, interceptor. Predecessor to the SR–71.

Example

A Pitot-static tube is placed in a subsonic airflow. The static pressure and temperature in the flow are 80 kPa and 12 deg. C, respectively. We measure the difference between the total and static pressures as 200 mmHg. Find u_∞ and Mach number, M_∞.

Solution

Recall from fluid statics

$$p_o - p = \rho_m g \triangle H \tag{228}$$

where ρ_m = density of mercury = 13,580 kg/m^3, g = gravity constant ms^{-2}, $\triangle H$ = height of Mercury

$$\therefore p_o - p = 13580 \times 9.81 \times 0.2 = 26.64 \text{ kPa} \tag{229}$$

Example Continued

Find the appropriate ratio of stagnation to static pressure

$$\frac{p_o - p}{p} = \frac{26.64 \text{ kPa}}{80 \text{ kPa}} \rightarrow \frac{p_o}{p} = 1.3331 \tag{230}$$

Now we can find M as

$$M_\infty = \sqrt{\left(\frac{2}{\gamma - 1}\right)\left(\left(\frac{p_o}{p}^{\frac{\gamma-1}{\gamma}}\right) - 1\right)} = 0.654 \tag{231}$$

and finally u_∞

$$u_\infty = M_\infty c_\infty = M\sqrt{\gamma R T_\infty} = 0.654\sqrt{1.4(287)285} = 221.3 \text{ m/s} \tag{232}$$

To find M, we need p_o and p, which is something we typically measure. To find u_∞, we require T at the probe location.

Daniel Bernoulli

8 February 1700 – 17 March 1782, Swiss

- Mathematician and physicist and was one of the many prominent mathematicians in the Bernoulli Brothers.
- Applications of mathematics to mechanics, especially fluid mechanics, and for his pioneering work in probability and statistics.
- Bernoulli's principle, a particular example of the conservation of energy.
- Friend of Leonhard Euler
- In Hydrodynamica (1738) - basis for the kinetic theory of gases
- With Euler developed the Euler-Bernoulli beam equation

S.A.E. Miller, Ph.D., saem@ufl.edu

Error of Bernoulli Equation I

We examine error when using incompressible theory. The classical Bernoulli result is

$$u_\infty = \sqrt{\frac{2(p_o - p)}{\rho_\infty}} \tag{233}$$

Now we need to find the corresponding equation that includes compressible effects

$$p_o - p = p\left(\frac{p_o}{p} - 1\right) = \left(\frac{1}{2}\rho u^2\right)\left(\frac{2p}{\rho u^2}\right)\left\{\left[1 + \frac{\gamma - 1}{2}M^2\right]^{\frac{\gamma}{\gamma - 1}} - 1\right\} \tag{234}$$

Replacing p, ρ, and u in the second term with the $\gamma - M$ relation yields

$$p_o - p = \frac{1}{2}\rho u^2\left\{\left(\frac{2}{\gamma M^2}\right)\left[\left(1 + \frac{\gamma - 1}{2}M^2\right)\right]^{\frac{\gamma}{\gamma - 1}} - 1\right\} \tag{235}$$

We find

$$u_\infty = \sqrt{\frac{2(p_o - p)}{\rho}}\left\{\left(\frac{2}{\gamma M^2}\right)\left[1 + \frac{\gamma - 1}{2}M^2\right]^{\frac{\gamma}{\gamma - 1}} - 1\right\}^{\frac{-1}{2}} \tag{236}$$

Error of Bernoulli Equation II

Recall the incompressible result of Bernoulli

$$u_\infty = \sqrt{\frac{2\left(p_o - p\right)}{\rho}} \tag{237}$$

We define the error as

$$\epsilon = \left| \frac{u_{\text{compressible}} - u_{\text{incompressible}}}{u_{\text{compressible}}} \right| = \left| 1 - \frac{u_{\text{incompressible}}}{u_{\text{compressible}}} \right| \tag{238}$$

And using our relations for u_∞

$$\epsilon = \left| 1 - \left\{ \left(\frac{2}{\gamma M^2} \right) \left(\left[1 + \frac{\gamma - 1}{2} M^2 \right]^{\frac{\gamma}{\gamma - 1}} - 1 \right) \right\}^{\frac{1}{2}} \right| \tag{239}$$

We find that the error depends on M and γ.

Error of Bernoulli Equation

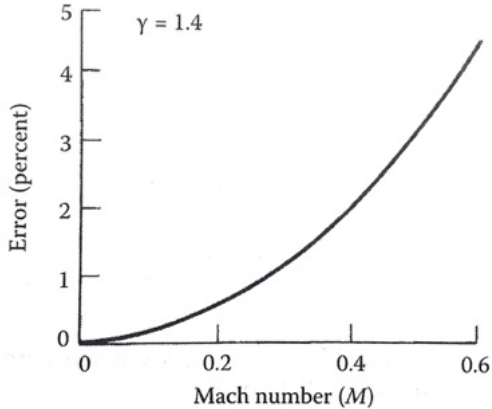

Figure 67: Error with Mach number of measured compressibility effect.

Example I

A Pitot-static tube measures $p = 96$ kPa and $p_o - p = 32$ kPa. $T_\infty = 27^\circ$ C. Find air velocity using incompressible and compressible theory.

Solution

First, find ρ using ideal gas law

$$\rho = \frac{p}{RT} = 1.115 \text{ kg/m}^3 \tag{240}$$

a) incompressible $\boxed{u_\infty = 239.6}$ m/s using Eqn. 237

b) compressible $\frac{p_o - p}{p} = \frac{p_o}{p} - 1 = \frac{32}{96} \rightarrow p_o/p = 1.3333.$

$$\frac{p_o}{p} = \left(1 + \frac{\gamma - 1}{2} M^2\right)^{\frac{\gamma}{\gamma - 1}} \tag{241}$$

Solving for M yields 0.654

$$u_\infty = Mc = 0.654\sqrt{1.4(287)(300)} = \boxed{u_\infty = 225.7} \text{ m/s} \tag{242}$$

Please note the differences in velocities.

Class Summary

- Stagnation (total) conditions
- Pitot-static tubes
- Examples

Next Time

- Critical conditions
- Choking
- Compressible flow calculator
- Overview and use of tables

“The whole problem of aerodynamics, both subsonic and supersonic, may be summed up in one sentence: Aerodynamics is the science of slowing-down the air without loss, after it has once been accelerated by any device, such as a wing or a wind tunnel. It is thus good aerodynamic practice to avoid accelerating the air more than is necessary.”

– W. F. Hilton, 1951

Class Overview

- Critical conditions
- Choking
- Compressible flow calculator
- Examples
- On the use of tables

Critical Conditions

- Critical conditions correspond to those where the flow accelerates or decelerates to the transonic condition ($M = 1$).
- Total or stagnation values are constant in isentropic flows.
- We require another stagnation condition, the stagnation speed of sound c_o.

$$\frac{c_o^2}{\gamma - 1} = \frac{c^2}{\gamma - 1} + \frac{u^2}{2} \tag{243}$$

Note this equation we developed previously (and is on the equation sheet).

Critical Conditions

Now for Mach 1 conditions we have

$$\left(\frac{c_o}{c^*}\right)^2 = \frac{T_o}{T^*} = \frac{\gamma+1}{2} \tag{244}$$

$$\frac{p_o}{p^*} = \left(\frac{\gamma+1}{2}\right)^{\frac{\gamma-1}{\gamma}} \text{ and } \frac{\rho_o}{\rho^*} = \left(\frac{\gamma+1}{2}\right)^{\gamma-1} \tag{245}$$

What are these values for $\gamma = 1.4$ (air)

$$\frac{T^*}{T_o} = 0.833, \frac{p^*}{p_o} = 0.528, \text{ and } \frac{\rho^*}{\rho_o} = 0.634 \tag{246}$$

and finally

$$M^2 = \frac{2}{[(\gamma+1)/M^{*2}] - (\gamma-1)} \tag{247}$$

where M^* = characteristic Mach number

Critical Conditions

The critical conditions are easy to find. Simply place unity for M_2 in static-thermodynamic isentropic Mach number relations

$$\frac{T^*}{T} = \left(\frac{2}{\gamma + 1} + \frac{\gamma - 1}{\gamma + 1} M^2 \right) \tag{248}$$

$$\frac{c^*}{c} = \left(\frac{2}{\gamma + 1} + \frac{\gamma - 1}{\gamma + 1} M^2 \right)^{\frac{1}{2}} \tag{249}$$

$$\frac{p^*}{p} = \left(\frac{2}{\gamma + 1} + \frac{\gamma - 1}{\gamma + 1} M^2 \right)^{\frac{\gamma}{\gamma - 1}} \tag{250}$$

$$\frac{\rho^*}{\rho} = \left(\frac{2}{\gamma + 1} + \frac{\gamma - 1}{\gamma + 1} M^2 \right)^{\frac{1}{\gamma - 1}} \tag{251}$$

Critical Conditions at $M = 0$

- A set of critical conditions occur when the Mach number reaches zero in an isentropic flow.
- If a transonic flow is brought to rest isentropically, we find relations between a choked flow static properties and its stagnation.

$$\frac{T^*}{T_o} = \frac{2}{\gamma + 1} \tag{252}$$

$$\frac{c^*}{c_o} = \left(\frac{2}{\gamma + 1}\right)^{1/2} \tag{253}$$

$$\frac{p^*}{p_o} = \left(\frac{2}{\gamma + 1}\right)^{\frac{\gamma}{\gamma - 1}} \tag{254}$$

$$\frac{\rho^*}{\rho_o} = \left(\frac{2}{\gamma + 1}\right)^{\frac{1}{\gamma - 1}} \tag{255}$$

Mass Flow Rate

- The mass flow rate, $\dot{m}$, can be written as a function of stagnation properties and Mach number.
- Seek the mass flow rate at any cross-section of a variable area stream tube

$$\dot{m} = \rho A u = \frac{p}{RT} A M \sqrt{\gamma R T} \tag{256}$$

We substitute values for the local properties

$$\dot{m} = \frac{p_o}{\sqrt{R T_o}} A \gamma^{1/2} M \left(1 + \frac{\gamma - 1}{2} M^2\right)^{(\gamma+1)/(2-2\gamma)} \tag{257}$$

Mass Flow Rate

This equation can be written as

$$\boxed{\frac{\dot{m}T_o^{1/2}}{p_o A} = f(\gamma, M)} \tag{258}$$

- Recall that p/p_o and T/T_o are similarly expressed as functions of γ and M.
- We will attempt to relate most relations to M.
- Usually $\dot{m}$ is not tabulated as obtained from these properties.

Area Ratio

- We select the throat of the duct as a reference state, naming the area at the throat A_t and when choked as A^*
- This is the reference throat area whether or not the flow is transonic at A_t
- Via the steady-flow continuity equation for flow through a duct, $\dot{m}$ must be the same at any cross-section

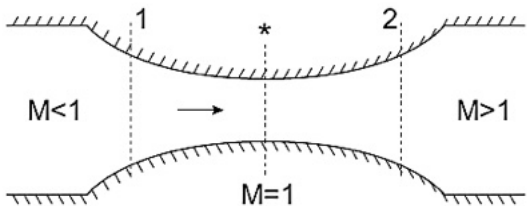

Figure 68: Flow through a generic converging-diverging duct, which is choked.

Area Ratio

Now rewrite our equation for $\dot{m}$ by solving for duct cross-sectional area A, we find

$$A = \frac{\dot{m}}{\gamma^{1/2} M \left(1 + \frac{\gamma-1}{2} M^2\right)^{(\gamma+1)/(2-2\gamma)}} \tag{259}$$

This equation involves the area, mass flow rate, M, and γ. But how is it related to the reference area?

Area Ratio

Write the ratio of the area at location A relative to the area of the throat A^* using Eqn. 259

$$\boxed{\frac{A}{A^*} = \frac{1}{M}\left(\frac{(\gamma+1)/2}{1+\frac{\gamma-1}{2}M^2}\right)^{(\gamma+1)/(2-2\gamma)}} \tag{260}$$

which is the famous Mach number area relation.

- $A/A*$ is a function of γ and M just like previously developed equations.
- Equation has two roots - one for subsonic flow ahead of the throat and one for supersonic flow downstream of the throat.

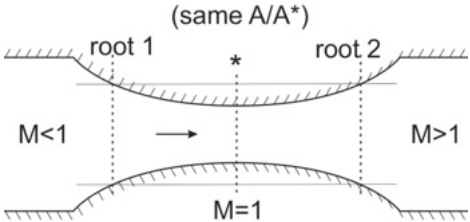

Figure 60

Notes on Isentropic Flow

- Variations of flow properties with Mach number and relation to one another are important to know.
- Area ratio A/A^* is one of the most important properties.
- A/A^* is a function of M only for constant γ
  - Mach number M is a function of area ratio only and γ.
  - For $M < 1$ approaching a sonic throat ($M = 1$), and in supersonic flow thereafter ($M > 1$), the M of the flow is controlled by the area ratio, regardless of how much power is applied to move the fluid.
- This is a very different aspect of high-speed flow relative to basic fluid mechanics that requires special attention.
- Let us know examine a chart showing how these flow-field variables change with M

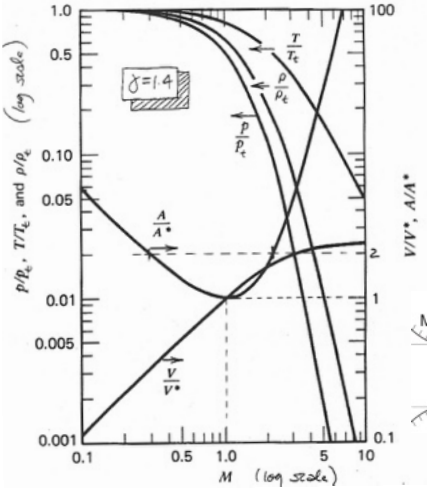

Figure 70: Isentropic flow properties as functions of Mach number for $\gamma = 1.4$

DEPRESSURIZATION —

Russian space chief vows to find "full name" of technician who caused ISS leak

"We want to find out the full name of who is at fault—and we will."

ERIC BERGER - 9/4/2018, 5:10 PM

Enlarge / The source of the leak on the International Space Station.

Last week, a pressure leak occurred on the International Space Station. It was slow and posed no immediate threat to the crew, with the atmosphere leaving the station at a rate such that depressurization of the station would have taken 14 days.

Eventually, US and Russian crew members traced the leak to a 2mm breach in the orbital module of the Soyuz MS-09 vehicle that had flown to the space station in June. The module had carried Russian cosmonaut Sergey Prokopyev, European Space Agency astronaut Alexander Gerst, and NASA's Serena M. Auñón-Chancellor.

The crew on the station was in no danger, and, over the course of several hours, Russian engineers devised a fix that involved epoxy. A preliminary analysis concluded that the vehicle is safe for return to Earth (the orbital

FURTHER READING
Russian editor: Our space program is entering the "Dark Ages"

a tiny bit of orbital debris. However, recent Russian news reports have shown that the problem was, in fact, a manufacturing defect. It remains unclear whether the hole was an accidental error or intentional. There is evidence that a technician saw the drilling mistake and covered the hole with glue, which prevented the problem from being detected during a vacuum test.

"We are able to narrow down the cause to a technological mistake of a technician. We can see the mark where the drill bit slid along the surface of the hull," Dmitry Rogozin, head of the Russian space agency Roscosmos, told RIA Novosti. (A translation of the Russian articles in this story was provided to Ars by Robinson Mitchell). "We want to find out the full name of who is at fault—and we will."

Ongoing technical problems

NASA spokesman Dan Huot, based in Houston where the space station program is managed, deferred all comment on the issue to Roscosmos.

The spacecraft was manufactured by Energia, a Russian corporation. A former employee of the company who is now a professor at Moscow State University told another Russian publication that these kinds of incidents have occurred before at Energia.

"I have conducted investigations of all kinds of spacecraft, and after landing, we discovered a hole drilled completely through the hull of a re-entry module," the former Energia employee, Viktor Minenko, said in Gazeta.RU. "But the technician didn't report the defect to anyone but sealed up the hole with epoxy. We found the person, and after a commotion he was terminated," said Minenko.

In this case, the technician used glue instead of epoxy. As the Soyuz hull is made from an aluminum alloy, it could have been properly repaired on Earth by welding, had the technician reported the mistake.

FURTHER READING
Russia's Proton rocket, which predates Apollo, will finally stop flying

The Soyuz manufacturing issue represents another significant problem for the Russian space agency's suppliers and its quality control processes. Already, the manufacturer of Proton rockets, Khrunichev, has had several serious problems that have led to launch failures. Rogozin was recently installed as the leader of Roscosmos to try to clean up corruption and address these kinds of issues.

He has his work cut out for him.

Example

A gas is contained in a large vessel stored at $p = 300$ kPa and $T = 50$ deg. C. The gas is expanded isentropically through $M = 1$ via a convergent opening. Find p, T, and u at the choked condition if the gas is air and helium.

Solution

As we have expanded to $M = 1$ we have obtained a critical condition. We can use our stagnation-critical condition equations

$$\frac{p^*}{p_o} = \left(\frac{2}{\gamma + 1}\right)^{\frac{\gamma}{\gamma - 1}} \tag{261}$$

$$\gamma_{\text{air}} = 1.4 \rightarrow p^*_{\text{air}} = 300 \text{ kPa} \left(\frac{2}{2.4}\right)^{\frac{1.4}{0.4}} = 158.5 \text{ kPa} \tag{262}$$

$$\gamma_{\text{He}} = 1.667 \rightarrow p^*_{\text{He}} = 300 \left(\frac{2}{2.667}\right)^{\frac{1.667}{0.667}} = 146.1 \text{ kPa} \tag{263}$$

Solution

The temperatures

$$\frac{T^*}{T_o} = \frac{\gamma}{\gamma + 1} \tag{264}$$

$$T^*_{\text{air}} = 323\ \text{K}\left(\frac{2}{2.4}\right) = 269.2\ \text{K} \tag{265}$$

$$T^*_{\text{He}} = 323\ \text{K}\left(\frac{2}{2.667}\right) = 242.2\ \text{K} \tag{266}$$

Now seek the velocities, $u = Mc = c$ as we have $M = 1$

$$u_{\text{air}} = (1.4(8314.3/28.97)269.2\ \text{K})^{\frac{1}{2}} = 328.9\ \text{m/s} \tag{267}$$

$$u_{\text{He}} = (1.667(8314.3/4)242.2\ \text{K})^{\frac{1}{2}} = 916.1\ \text{m/s} \tag{268}$$

Example

A channel with cross-sectional area $A = 50$ cm^2 carries an airflow flow at $M = 0.5$, $p = 50$ kPa, and $T = 300$ K.

a) Find the mass flow rate, $\dot{m}$, through the channel.

b) If the channel now converges, at what area will the Mach number reach 1.0?

c) What will happen to the mass flow rate if the cross sectional area is smaller than that of part b)?

Solution

a) Find $\dot{m}$

- Use the given formula for mass flow rate
- We are given $M = 0.50$, $A = 50$ cm^2, $\gamma = 1.4$, $R = 287$ J / kg / K for air
- Consult the isentropic flow tables at $M = 0.5$ or the equation to find $p_o/p = 1.1862$ and $T_o/T = 1.0504$, and we find $p_o = 59.3$ kPa and $T_o = 315$ K
- Now use our developed mass flow rate equation and find $\dot{m} = 0.504$ kg/s
- Careful of units, use kg-m-s units, do not confuse cm^2 and m^2, and recall that a Pascal is 1 kg/(m s^2)

Solution

b) Use the Mach number area relation at $M = 0.5$ to find $A/A^* = 1.34$, and we find $A^* = 50/1.34 = 37.3$ cm^2

c) At Mach 1.0 the channel carries its maximum mass flow rate per unit area under the given upstream conditions.

- If the channel is reduced to an area smaller than A^*, two things must happen
  - The mass flow rate is reduced
  - Mach number upstream of the sonic condition falls below the given value of Mach 0.5 (Why? A/A^* changed but throat still choked.)

Example

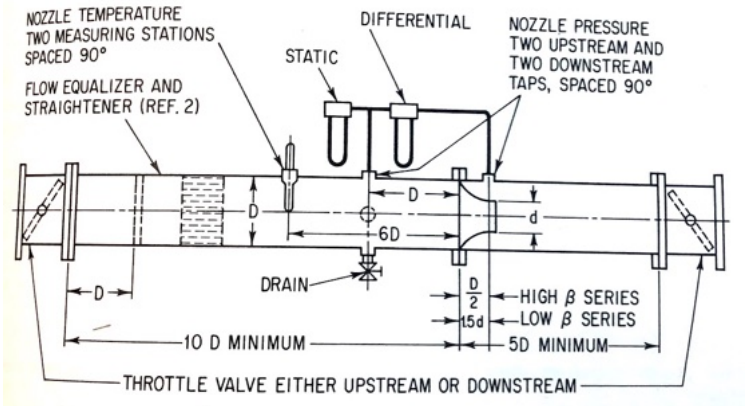

Figure 71: Flow meter from the de Laval Engineering Handbook (flow-meters). Notice the convergent nozzle.

Example

The chemical process to produce a new drug requires you to design the apparatus to deliver exactly 360 kg/hr of oxygen gas ($\gamma = 1.4$, $R = 260$ J/ kg / K to a chemical reactor. The oxygen is stored in pressurized cylinders at 32 deg. F. A regulator holds $p_o = 0.70$ MPa. Apply your knowledge of isentropic flow to achieve this design goal.

Solution

- Use the principle of constant mass flux through a choked nozzle
- Note that everything to the right of the A in the mass flow equation is known. Recall

$$A = \frac{\dot{m}}{\gamma^{1/2} M \left(1 + \frac{\gamma-1}{2} M^2\right)^{(\gamma+1)/(2-2\gamma)}} \tag{269}$$

- The right hand side can be lumped into the constant 0.685 when $M = 1$ for this γ
- This yields a simple and handy mass flux equation for $\gamma = 1.4$ gas flow at a choked throat

$$\dot{m} = 0.685 \frac{p_o A^*}{\sqrt{R T_o}} \tag{270}$$

Solution

- T_o is given as 32 deg. F or 273 K
- $\dot{m}$ is given as 360 kg/hr or 0.1 kg/s.
- Oxygen cylinders are supplied with 15 MPa pressure, which can be set at $p_o = 0.70$ MPa by a regulator.
- Solving this simplified mass flow equation for A^* yields $A^* = 5.55 \times 10^{-5}$ m^2, from which the sonic throat diameter is 8.4 mm.
- This is in the range of the so-called "sonic flow prover" nozzles
  - Such a nozzle can be bought with a throat diameter of a few mm
  - The stagnation pressure can be adjusted accordingly to get the required $\dot{m}$.

Online Calculators

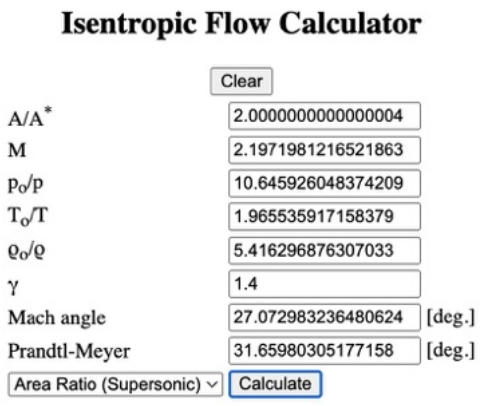

Figure 72: Miller's calculator at https://saemiller.com/flow/SAEMiller_Comp_Calc.html

Online Calculators

Calculator Example: UTIAS $M = 1.5$ tunnel, $\gamma = 1.4$:

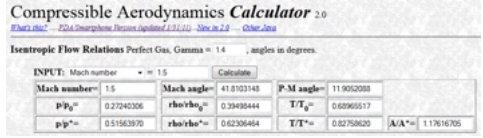

Calculator Example: P&W RL-10 rocket motor, $\gamma = 1.33$, $A/A^* = 40$:

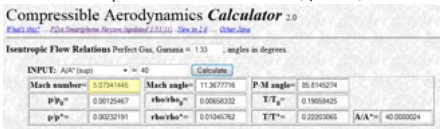

Figure 73: Calculator Example: P W RL-10 rocket motor, $\gamma = 1.33$, $A/A* = 40$ VT calculator at by Googling "compressible flow calculator" Try using it to check your homework solutions.

$\gamma =$	1.4000					Isentropic					Normal Shock					P-M	Ray.-Pitot
M	p_o/p	T_o/T	ρ_o/ρ	c_o/c	A/A^*	M_2	p_2/p_1	T_2/T_1	ρ_2/ρ_1	p_{o2}/p_{o1} A_{o2}/A_{o1}	A_{o2}/A^*_{o2}	ν deg.	p_{o2}/p_1
0.000	1.0000	1.0000	1.0000	1.0000	∞								
0.025	1.0006	1.0001	1.0003	1.0000	23.1568								
0.050	1.0018	1.0005	1.0013	1.0002	11.5914								
0.075	1.0039	1.0011	1.0028	1.0006	7.7421								
0.100	1.0070	1.0020	1.0050	1.0010	5.8218								
0.125	1.0110	1.0031	1.0078	1.0016	4.6732								
0.150	1.0158	1.0045	1.0113	1.0022	3.9103								
0.175	1.0216	1.0061	1.0154	1.0031	3.3680								
0.200	1.0283	1.0080	1.0201	1.0040	2.9635								
0.225	1.0359	1.0101	1.0255	1.0050	2.6509								
0.250	1.0444	1.0125	1.0315	1.0062	2.4027								
0.275	1.0539	1.0151	1.0382	1.0075	2.2013								
0.300	1.0644	1.0180	1.0456	1.0090	2.0351								
0.325	1.0759	1.0211	1.0537	1.0105	1.8959								
0.350	1.0884	1.0245	1.0624	1.0122	1.7780								
0.375	1.1019	1.0281	1.0718	1.0140	1.6771								
0.400	1.1166	1.0320	1.0819	1.0159	1.5901								
0.425	1.1325	1.0361	1.0928	1.0179	1.5146								
0.450	1.1498	1.0405	1.1043	1.0200	1.4487								
0.475	1.1670	1.0451	1.1167	1.0223	1.3908								
0.500	1.1882	1.0500	1.1297	1.0247	1.3398								
0.525	1.2066	1.0551	1.1436	1.0272	1.2948								
0.550	1.2265	1.0605	1.1582	1.0298	1.2549								
0.575	1.2512	1.0661	1.1736	1.0325	1.2196								
0.600	1.2753	1.0720	1.1898	1.0354	1.1882								
0.625	1.3012	1.0781	1.2069	1.0383	1.1603								
0.650	1.3283	1.0845	1.2248	1.0414	1.1356								
0.675	1.3569	1.0911	1.2436	1.0446	1.1137								
0.700	1.3871	1.0980	1.2633	1.0479	1.0944								
0.725	1.4189	1.1051	1.2839	1.0512	1.0773								
0.750	1.4523	1.1125	1.3054	1.0548	1.0624								
0.775	1.4874	1.1201	1.3279	1.0584	1.0494								
0.800	1.5243	1.1280	1.3514	1.0621	1.0382								
0.825	1.5631	1.1361	1.3758	1.0659	1.0287								
0.850	1.6038	1.1445	1.4013	1.0698	1.0207								
0.875	1.6465	1.1531	1.4279	1.0738	1.0141								
0.900	1.6913	1.1620	1.4555	1.0780	1.0089								
0.925	1.7382	1.1711	1.4843	1.0822	1.0049								
0.950	1.7874	1.1805	1.5143	1.0865	1.0023								
0.975	1.8390	1.1901	1.5452	1.0909	1.0005								
1.000	1.8929	1.2000	1.5774	1.0954	1.0000	1.0000	1.0000	1.0000	1.0000	1.0000	1.0000	1.8929	1.3975	1.4.0602	2.1281	0.6068	1.4588	2.3485	0.5258	0.4141	2.0166	3.1806	0.3508	36.1387	7.7437
1.025	1.9494	1.2101	1.6109	1.1001	1.0005	0.9758	1.0391	1.0165	1.0418	1.0000	0.1751	1.9494	2.400	1.4.0220	2.1520	0.7937	1.4670	2.4031	0.5231	0.5333	2.0403	3.2119	0.5401	36.7465	7.8969
1.050	2.0085	1.2205	1.6457	1.1048	1.0020	0.9531	1.1196	1.0328	1.0840	0.9999	0.4874	2.0083	2.425	1.5.2037	2.1761	0.9857	1.4752	2.4582	0.5205	0.6943	2.0641	3.2428	0.5297	37.3489	8.0518
1.075	2.0704	1.2311	1.6817	1.1096	1.0045	0.9318	1.1816	1.0490	1.1264	0.9995	0.6813	2.0694	2.450	1.5.8041	2.2005	1.1830	1.4834	2.5168	0.5179	0.8363	2.0885	3.2733	0.5193	37.9459	8.2083
1.100	2.1351	1.2420	1.7191	1.1145	1.0079	0.9118	1.2450	1.0649	1.1691	0.9989	0.8362	2.1328	2.475	1.6.4339	2.2251	1.7.3856	1.4917	2.5760	0.5154	0.9799	2.1129	3.3035	0.5091	38.5374	8.3664
1.125	2.2028	1.2531	1.7579	1.1194	1.0122	0.8929	1.3089	1.0808	1.2120	0.9980	1.8390	2.1984	2.500	1.7.0839	2.2500	7.5938	1.5000	2.6367	0.5130	7.1250	2.1375	3.3333	0.4990	39.1286	8.5261
1.150	2.2736	1.2645	1.7980	1.1245	1.0175	0.8759	1.3763	1.0966	1.2550	0.9967	2.3810	2.2661	2.525	1.7.7631	2.2751	2.8075	1.5084	2.6990	0.5106	2.7716	2.1624	3.3628	0.4891	39.7044	8.6875
1.175	2.3476	1.2761	1.8396	1.1297	1.0235	0.8581	1.4441	1.1123	1.2983	0.9950	2.9558	2.3358	2.550	1.8.4662	2.3005	8.0270	1.5167	2.7630	0.5083	7.4198	2.1875	3.3919	0.4793	40.2798	8.8505
1.200	2.4250	1.2880	1.8827	1.1349	1.0304	0.8422	1.5133	1.1280	1.3416	0.9928	3.5582	2.4077	2.575	1.9.1962	2.3261	8.2524	1.5252	2.8286	0.5061	7.6931	2.2128	3.4206	0.4696	40.8499	9.0151
1.225	2.5058	1.3001	1.9274	1.1402	1.0382	0.8270	1.5841	1.1437	1.3851	0.9902	4.1841	2.4812	2.600	1.9.9540	2.3520	8.4839	1.5336	2.8960	0.5039	7.7200	2.2383	3.4490	0.4601	41.4147	9.1803
1.250	2.5903	1.3125	1.9736	1.1456	1.0468	0.8126	1.6563	1.1594	1.4286	0.9871	4.8299	2.5568	2.625	2.0.7496	2.3781	8.7214	1.5421	2.9650	0.5017	7.8724	2.2641	3.4770	0.4508	41.9742	9.3492
1.275	2.6785	1.3251	2.0214	1.1511	1.0561	0.7990	1.7289	1.1751	1.4721	0.9835	5.4928	2.6342	2.650	2.1.5569	2.4045	8.9652	1.5506	3.0339	0.4996	8.0263	2.2902	3.5047	0.4416	42.5285	9.5186
1.300	2.7707	1.3380	2.0708	1.1567	1.0663	0.7860	1.8050	1.1909	1.5157	0.9794	6.1703	2.7136	2.675	2.2.4040	2.4311	9.2155	1.5592	3.1085	0.4976	8.1816	2.3164	3.5320	0.4325	43.0776	9.6897
1.325	2.8670	1.3511	2.1220	1.1624	1.0773	0.7736	1.8816	1.2067	1.5593	0.9748	6.8602	2.7948	2.700	2.3.2829	2.4580	9.4723	1.5678	3.1830	0.4956	8.3383	2.3429	3.5590	0.4236	43.6215	9.8624
1.350	2.9676	1.3645	2.1749	1.1681	1.0890	0.7618	1.9596	1.2226	1.6028	0.9697	7.5697	2.8778	2.725	2.4.1946	2.4851	9.7358	1.5764	3.2594	0.4937	8.4966	2.3696	3.5856	0.4148	44.1602	10.0367

$\gamma =$	1.4000					Isentropic					Normal Shock					P-M	Ray.-Pitot
M	p_o/p	T_o/T	ρ_o/ρ	c_o/c	A/A^*	M_2	p_2/p_1	T_2/T_1	ρ_2/ρ_1	p_{o2}/p_{o1} A_{o2}/A_{o1}	A_{o2}/A^*_{o2}	ν deg.	p_{o2}/p_1
1.375	3.0726	1.3781	2.2296	1.1739	1.1016	0.7505	2.0391	1.2386	1.6463	0.9642	8.2701	2.9261
1.400	3.1823	1.3920	2.2861	1.1798	1.1149	0.7397	2.1200	1.2547	1.6897	0.9582	8.8670	3.0492
1.425	3.2967	1.4061	2.3446	1.1858	1.1291	0.7294	2.2024	1.2709	1.7330	0.9517	9.7101	3.1376
1.450	3.4162	1.4205	2.4049	1.1918	1.1440	0.7196	2.2863	1.2872	1.7763	0.9448	10.4381	3.2278
1.475	3.5409	1.4351	2.4673	1.1980	1.1597	0.7101	2.3716	1.3036	1.8192	0.9375	11.1701	3.3196
1.500	3.6710	1.4500	2.5317	1.2042	1.1762	0.7011	2.4583	1.3202	1.8621	0.9298	11.9052	3.4133
1.525	3.8068	1.4651	2.5983	1.2104	1.1935	0.6924	2.5466	1.3369	1.9048	0.9217	12.6425	3.5086
1.550	3.9485	1.4805	2.6670	1.2168	1.2116	0.6841	2.6363	1.3538	1.9473	0.9132	13.3812	3.6057
1.575	4.0963	1.4961	2.7379	1.2232	1.2305	0.6761	2.7274	1.3708	1.9896	0.9044	14.1207	3.7045
1.600	4.2504	1.5120	2.8111	1.2296	1.2502	0.6684	2.8200	1.3880	2.0317	0.8952	14.8604	3.8050
1.625	4.4112	1.5281	2.8867	1.2362	1.2708	0.6611	2.9141	1.4053	2.0736	0.8857	15.5996	3.9072
1.650	4.5789	1.5445	2.9646	1.2428	1.2922	0.6540	3.0096	1.4228	2.1152	0.8760	16.3379	4.0110
1.675	4.7537	1.5611	3.0450	1.2494	1.3145	0.6471	3.1066	1.4405	2.1566	0.8660	17.0748	4.1166
1.700	4.9360	1.5780	3.1280	1.2562	1.3376	0.6405	3.2050	1.4583	2.1977	0.8557	17.8099	4.2238
1.725	5.1260	1.5951	3.2136	1.2630	1.3616	0.6342	3.3049	1.4764	2.2385	0.8452	18.5428	4.3327
1.750	5.3241	1.6125	3.3018	1.2698	1.3865	0.6281	3.4063	1.4946	2.2791	0.8346	19.2732	4.4433
1.775	5.5306	1.6301	3.3928	1.2768	1.4123	0.6222	3.5091	1.5130	2.3193	0.8237	20.0007	4.5556
1.800	5.7458	1.6480	3.4865	1.2837	1.4390	0.6165	3.6133	1.5316	2.3592	0.8127	20.7251	4.6695
1.825	5.9700	1.6661	3.5832	1.2908	1.4666	0.6110	3.7191	1.5504	2.3988	0.8015	21.4460	4.7851
1.850	6.2037	1.6845	3.6828	1.2979	1.4952	0.6057	3.8263	1.5693	2.4381	0.7902	22.1633	4.9023
1.875	6.4471	1.7031	3.7854	1.3050	1.5247	0.6006	3.9349	1.5885	2.4771	0.7788	22.8768	5.0212
1.900	6.7006	1.7220	3.8912	1.3122	1.5553	0.5956	4.0450	1.6079	2.5157	0.7674	23.5861	5.1418
1.925	6.9647	1.7411	4.0001	1.3195	1.5868	0.5908	4.1566	1.6275	2.5540	0.7558	24.2913	5.2640
1.950	7.2398	1.7605	4.1124	1.3268	1.6193	0.5862	4.2696	1.6473	2.5919	0.7442	24.9920	5.3878
1.975	7.5262	1.7801	4.2279	1.3342	1.6529	0.5817	4.3841	1.6673	2.6295	0.7325	25.6882	5.5133
2.000	7.8244	1.8000	4.3469	1.3416	1.6875	0.5774	4.5000	1.6875	2.6667	0.7209	26.3798	5.6404
2.025	8.1349	1.8201	4.4694	1.3491	1.7232	0.5731	4.6174	1.7079	2.7035	0.7092	27.0665	5.7692
2.050	8.4581	1.8405	4.5956	1.3567	1.7600	0.5691	4.7363	1.7285	2.7400	0.6975	27.7484	5.8996
2.075	8.7946	1.8611	4.7254	1.3642	1.7979	0.5651	4.8566	1.7494	2.7761	0.6858	28.4253	6.0317
2.100	9.1447	1.8820	4.8590	1.3719	1.8369	0.5613	4.9785	1.7705	2.8119	0.6742	29.0971	6.1654
2.125	9.5090	1.9031	4.9965	1.3795	1.8772	0.5576	5.1016	1.7917	2.8473	0.6626	29.7638	6.3007
2.150	9.8881	1.9245	5.1380	1.3873	1.9185	0.5540	5.2263	1.8132	2.8823	0.6511	30.4253	6.4377
2.175	10.2825	1.9461	5.2836	1.3950	1.9611	0.5505	5.3524	1.8349	2.9170	0.6396	31.0815	6.5763
2.200	10.6927	1.9680	5.4333	1.4029	2.0050	0.5471	5.4800	1.8569	2.9512	0.6281	31.7325	6.7165
2.225	11.1194	1.9901	5.5873	1.4107	2.0501	0.5438	5.6091	1.8790	2.9851	0.6168	32.3781	6.8583
2.250	11.5631	2.0125	5.7457	1.4186	2.0964	0.5406	5.7396	1.9014	3.0186	0.6055	33.0184	7.0018
2.275	12.0243	2.0351	5.9085	1.4266	2.1441	0.5374	5.8716	1.9240	3.0518	0.5944	33.6533	7.1469
2.300	12.5043	2.0580	6.0759	1.4346	2.1931	0.5344	6.0050	1.9468	3.0845	0.5833	34.2828	7.2937
2.325	13.0030	2.0811	6.2481	1.4426	2.2435	0.5315	6.1399	1.9698	3.1169	0.5723	34.9069	7.4420
2.350	13.5214	2.1045	6.4250	1.4507	2.2953	0.5286	6.2763	1.9931	3.1490	0.5615	35.5255	7.5920
2.375	14.0602	2.1281	6.6068	1.4588	2.3485	0.5258	6.4141	2.0166	3.1806	0.5508	36.1387	7.7437
2.400	14.6200	2.1520	6.7937	1.4670	2.4031	0.5231	6.5533	2.0403	3.2119	0.5401	36.7465	7.8969
2.425	15.2017	2.1761	6.9857	1.4752	2.4592	0.5205	6.6941	2.0641	3.2428	0.5297	37.3489	8.0518
2.450	15.8061	2.2005	7.1830	1.4834	2.5168	0.5179	6.8363	2.0885	3.2733	0.5193	37.9459	8.2083
2.475	16.4339	2.2251	7.3856	1.4917	2.5760	0.5154	6.9799	2.1129	3.3035	0.5091	38.5374	8.3664
2.500	17.0839	2.2500	7.5938	1.5000	2.6367	0.5130	7.1250	2.1375	3.3333	0.4990	39.1236	8.5261
2.500	17.7631	2.2751	7.8075	1.5084	2.6990	0.5106	7.2716	2.1624	3.3628	0.4891	39.7044	8.6875
2.550	18.4662	2.3005	8.0270	1.5167	2.7630	0.5083	7.4198	2.1875	3.3919	0.4793	40.2798	8.8505
2.575	19.1962	2.3261	8.2524	1.5252	2.8286	0.5061	7.5695	2.2128	3.4206	0.4696	40.8499	9.0151
2.600	19.9540	2.3520	8.4839	1.5336	2.8960	0.5039	7.7200	2.2383	3.4490	0.4601	41.4147	9.1803
2.625	20.7406	2.3781	8.7214	1.5421	2.9650	0.5017	7.8724	2.2641	3.4770	0.4508	41.9742	9.3492
2.650	21.5569	2.4045	8.9652	1.5506	3.0339	0.4996	8.0263	2.2902	3.5047	0.4416	42.5285	9.5186
2.675	22.4040	2.4311	9.2155	1.5592	3.1085	0.4976	8.1816	2.3164	3.5320	0.4325	43.0776	9.6897
2.700	23.2829	2.4580	9.4723	1.5678	3.1830	0.4956	8.3383	2.3429	3.5590	0.4236	43.6215	9.8624
2.725	24.1946	2.4851	9.7358	1.5764	3.2594	0.4937	8.4966	2.3696	3.5856	0.4148	44.1602	10.0367

Class Summary

- Critical conditions
- Choking
- Compressible flow calculator
- Examples
- On the use of tables

Next Time

- de Laval nozzles
- Isentropic nozzle operations
- Rocket engines

Class Overview

Isentropic

- de Laval nozzles
- Isentropic nozzle operations
- Rocket engines

“The rocket worked perfectly, except for landing on the wrong planet.”

Wernher von Braun

Commenting on V2 landing on London 1944, Apollo in Perspective: Spaceflight Then and Now (1999)

Figure 74: DeLaval company cow with logo in background. This cow likely loves aerospace engineering.

DeLaval - From the Company Web

"DeLaval is the worldwide leader in milking equipment and solutions for dairy farmers, which make sustainable food production possible, ensuring milk quality and animal health. DeLaval solutions are used by millions of dairy farmers around the globe every day. DeLaval was founded more than 130 years ago in Sweden, when the visionary Gustaf de Laval patented the cream separator. Today, DeLaval has 4,500 employees and operates in more than 100 markets. DeLaval, alongside Tetra Pak and Sidel, is part of the Tetra Laval Group." https://www.delaval.com/en-us/about-us/ (Jan 29, 2019)

Karl Gustaf Patrik de Laval

9 May 1845 – 2 February 1913, Swedish

- Engineer and inventor contributions to design of steam turbines and dairy machinery
- Enrolled at the Institute of Technology in Stockholm (later the Royal Institute of Technology, KTH) in 1863, receiving a degree in mechanical engineering in 1866
- Royal Swedish Academy of Sciences, held national office, being elected to Swedish parliament, from 1888 to 1890, a member of the senate
- 1890 - a nozzle to increase the steam jet to supersonic speed
- Died in Stockholm in 1913

S.A.E. Miller, Ph.D., saem@ufl.edu

Historical Notes on de Laval

- Origin of convergent-divergent (CD) nozzle
- Designed CD nozzles for steam turbine
- Swedish
- Worked in industry (mining) and left for PhD
- Started own company in Stockholm that made cream separators
- Held Swedish senate positions
- Had no real knowledge (or at least proof) that supersonic flow actually existed in his nozzle

Original de Laval Nozzle Patent

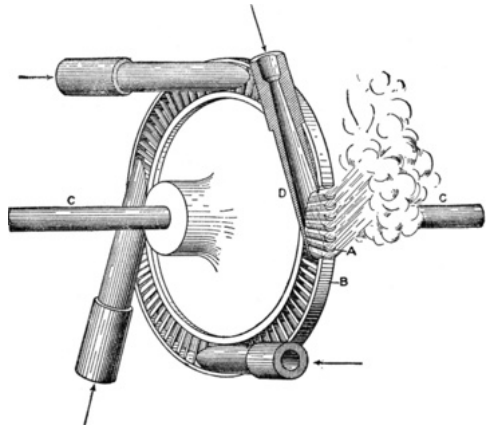

Figure 75: Source - Derr, Louis Cyclopedia of Engineering (Chicago, IL: American Technical Society, 1911)

NPO Energomash Engine

Figure 76: NPO Energomash test of RD-91 engine.

Figure 77: NPO Energomash floor models - Dr. Miller has toured this facility before it was open to westerners.

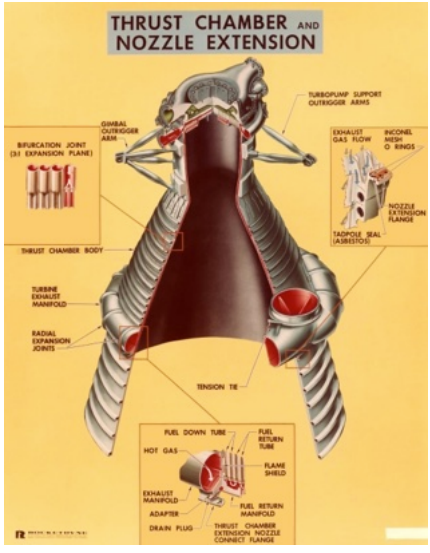

Figure 78: F1 Rocketdyne cut-away.

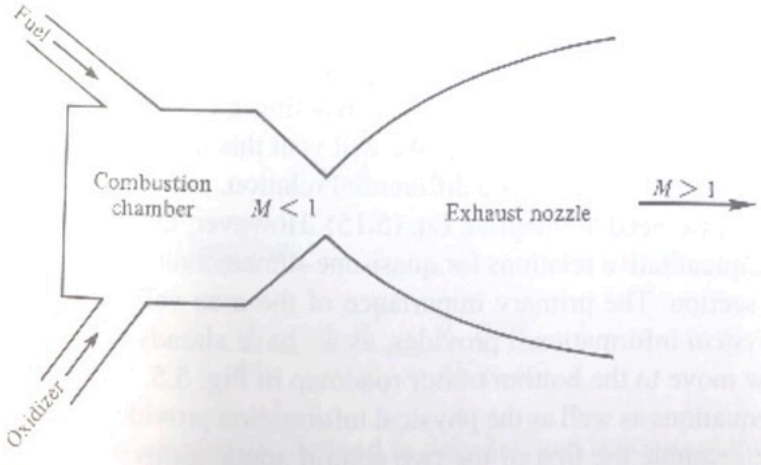

Figure 79: Bell shaped nozzles.

Subsonic and Supersonic Nozzles

Figure 80: Convergent-divergent nozzle.

Subsonic and Supersonic Nozzles

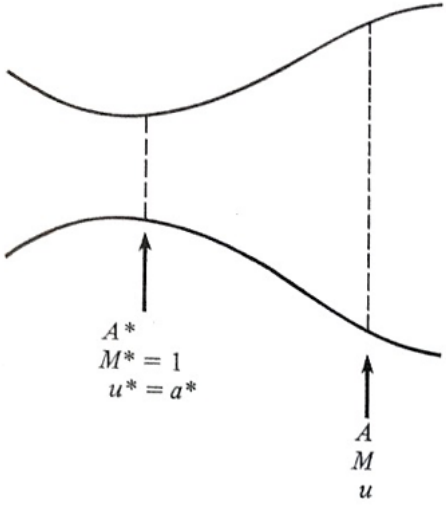

Figure 81: Converging-diverging nozzle schematic with critical (choke) and expansion locations.

Mach Number Area Relation

Seek the Mach number area relation. We can choke the flow at minimum area, A, called A^*. Mass conservation states

$$\rho^* u^* A^* = \rho u A \tag{271}$$

Please recall that when choked $u^* = c^*$

$$\frac{A}{A^*} = \frac{\rho^*}{\rho}\frac{c^*}{u} = \frac{\rho^*}{\rho_o}\frac{\rho_o}{\rho}\frac{c^*}{u} \tag{272}$$

Flow is isentropic and stagnation values are constant, including ρ_o. We previously developed the critical relation for density as

$$\frac{\rho_o}{\rho^*} = \left(\frac{\gamma - 1}{2}\right)^{\frac{1}{(\gamma-1)}} \tag{273}$$

Mach Number Area Relation

Also recall that we developed the relation for c^* as

$$\left(\frac{u}{c^*}\right)^2 = M^{*2} = \frac{\frac{\gamma+1}{2}M^2}{1+\frac{\gamma-1}{2}M^2} \tag{274}$$

Square the equation involving the ratio of A/A^*

$$\left(\frac{A}{A^*}\right)^2 = \left(\frac{\rho^*}{\rho_o}\right)^2\left(\frac{\rho_o}{\rho}\right)^2\left(\frac{c^*}{u}\right)^2 \tag{275}$$

Substitute in our relations of the ratios on the right hand side

$$\left(\frac{A}{A^*}\right)^2 = \left(\frac{2}{\gamma+1}\right)^{\frac{2}{\gamma-1}}\left(1+\frac{\gamma-1}{2}M^2\right)^{\frac{2}{\gamma-1}}\left(\frac{1+\frac{\gamma-1}{2}M^2}{\frac{\gamma+1}{2}M^2}\right) \tag{276}$$

Mach Number Area Relation

We now simplify the expression

$$\boxed{\left(\frac{A}{A^*}\right)^2 = \frac{1}{M^2}\left(\left(\frac{2}{\gamma+1}\right)\left(1+\frac{\gamma-1}{2}M^2\right)\right)^{\frac{\gamma+1}{\gamma-1}}} \tag{277}$$

- This is the Mach number area relation
- Equation shows $M = \pm(A/A^*)$.
- Two values of M correspond to solutions of the equation
- Note the tabulation in the isentropic tables of NASA Ames and in your handout
- There are no mathematical or physical solutions for $A/A^* < 1$

Mach Number Area Relation

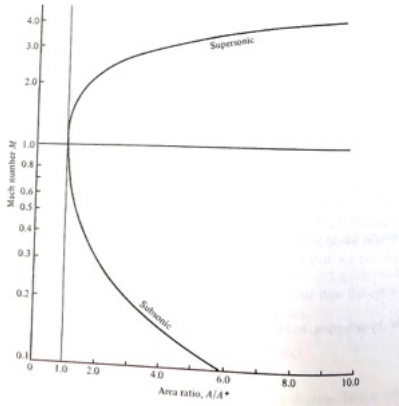

Figure 82: Graph of the Mach number area relation.

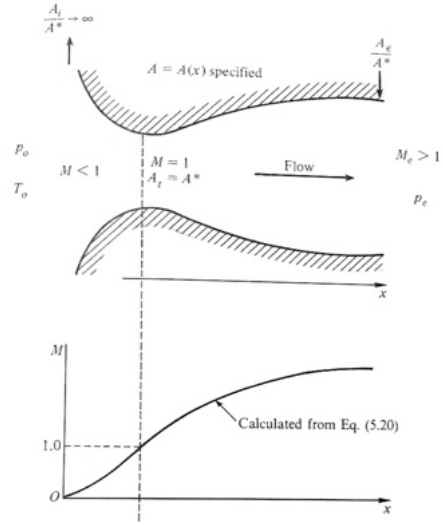

Figure 83: Variation of M in a typical convergent-divergent nozzle with transonic throat.

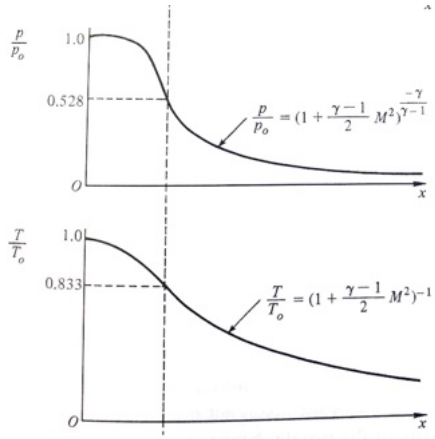

Figure 84: Variation of T and p within convergent-divergent nozzle.

Subsonic Flow in Convergent-Divergent Nozzle

- Ideally, the flow in the nozzle expands isentropically but this is not always the case.
- The nozzle can operate subsonically, and the flow-field is very different compared to the supersonic case.

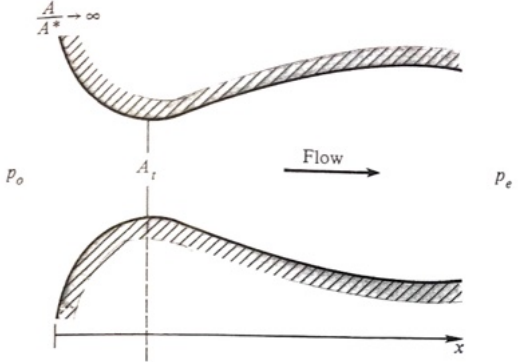

Figure 85: Diagram of a convergent-divergent nozzle.

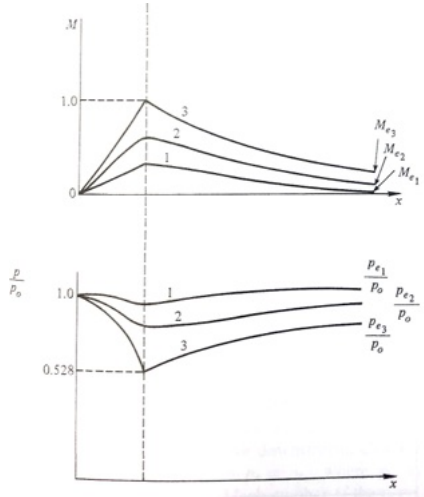

Figure 86: Variation of flow through a convergent-divergent nozzle in the subsonic and transonic regime.

Subsonic Nozzle Flow - Isentropic

- For subsonic cases area throat $A_t = A_1$.
  - This is because flow is not choked.
- Subsonic flow encounters diverging duct
- Divergent section acts as a diffuser
- There are infinite number of isentropic solutions for subsonic nozzle flow.
- Only one isentropic solution exists for supersonic nozzle flow.
  - A/A^* is only controlling factor.
- Non-isentropic solutions contain shock waves.

Shocks Inside Nozzles

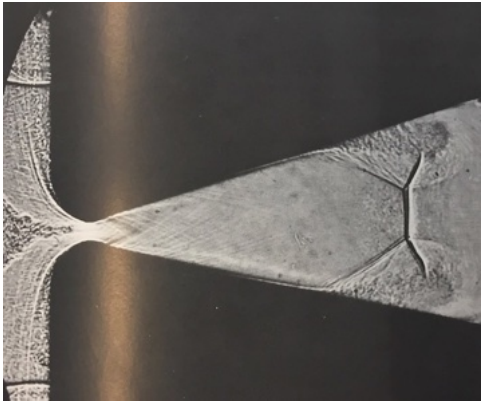

Figure 87: The normal shockwave resides in the nozzle and may cause the flow to separate.

Subsonic Nozzle Flow with Shock Wave

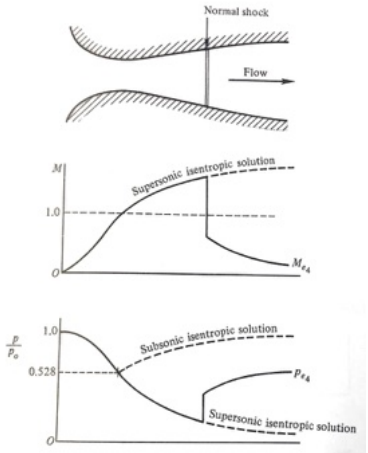

Figure 88: Variation of flows within a convergent-divergent nozzle with a normal shock.

Mass Flow Rate within Nozzles

- Mass flow increases as p_∞ decreases or p_o increases
- Easiest to assess $\dot{m}$ based on throat conditions (but not in practice)
  - Normal operation

$$\dot{m} = \rho_t A_t u_t \tag{278}$$

  - When choked

$$\dot{m} = \rho^* A^* u^* \tag{279}$$

- M at throat restricted to $0 \leq M \leq 1$
  - Because M is restricted at the throat, we are unable to increase $\dot{m}$ with increasing NPR (p_o/p_∞)

Example

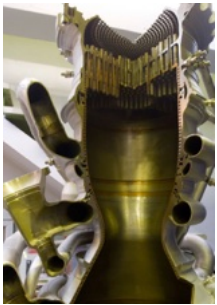

Figure 89: Rocket engine cut-away showing combustion chamber.

Example

A rocket engine uses hydrogen and oxygen. The combustion chamber has pressure and temperature of 3517 K and 25 atm. The molecular weight of the combustion product is 16 and $\gamma = 1.22$. The pressure at the exit of the engine is (1.174×10^{-2}) atm. The area of throat is 0.4 m^2. Assuming a calorically perfect gas and isentropic flow, calculate:

a) Exit Mach number
b) Exit velocity
c) $\dot{m}$
d) Nozzle exit area.

Solution I

Cannot use isentropic tables as they are for air ($\gamma = 1.40$).
a) Exit Mach number predicted by equation for nozzle pressure ratio.

$$\frac{p_o}{p_e} = \left(1 + \frac{\gamma - 1}{2} M_e^2\right)^{\frac{\gamma}{\gamma - 1}} \tag{280}$$

$$\therefore M_e^2 = \frac{2}{\gamma - 1}\left[\left(\frac{p_o}{p_e}\right)^{\frac{\gamma - 1}{\gamma}} - 1\right]$$

$$= \frac{2}{0.22}\left[\left(\frac{25}{1.174 \times 10^{-2}}\right)^{\frac{0.22}{1.22}} - 1\right] \tag{281}$$

$$= 27.166$$

$M_e = 5.21$
Technically, this is what we call the fully-expanded Mach number, M_j, and is not the true value of M_e

Solution I

b) Exit velocity

$$\frac{T_e}{T_o} = \left(\frac{p_e}{p_o}\right)^{\frac{\gamma-1}{\gamma}} = \left(\frac{1.174 \times 10^{-2}}{25}\right)^{0.180} = 0.2517 \tag{282}$$

$$T_e = 0.2517 T_o = 0.2517(3517) = 885.3 \text{ K} \tag{283}$$

Find $R = \frac{\mathfrak{R}}{M} = \frac{8314}{16} = 519.6$ J/kg K

$$c_e = \sqrt{\gamma R T_e} = \sqrt{1.22(519.6)(885.3)} = 749.1 \text{ m/s} \tag{284}$$

$$u_e = M_e c_e = (5.21)(749.1) = 3903 \text{ m/s} \tag{285}$$

These are technically fully expanded properties.

Solution I

c) Find $\dot{m}$

We are given throat area. Recall we are choked. First find

$$\rho_o = \frac{p_o}{RT_o} = \frac{(25)(1.01 \times 10^5)}{519.6(3517)} = 1.382 \text{ kg/m}^3 \tag{286}$$

Now

$$\frac{\rho^*}{\rho_o} = \left(\frac{2}{\gamma+1}\right)^{\frac{1}{\gamma-1}} = \left(\frac{2}{2.22}\right)^{4.545} = 0.622 \tag{287}$$

- $\rho^* = 0.622\rho_o = 0.666(1.382) = 0.860 \text{ kg/m}^3$
- $\frac{T^*}{T_o} = \frac{2}{\gamma+1} = \frac{2}{2.22} = 0.9$
- $T^* = 0.9T_o = 0.9(3517) = 3168 \text{ K}$

$$c^* = \sqrt{\gamma RT^*} = (1.22(519.6)(3168))^{\frac{1}{2}} = 1417 \text{ m/s} \tag{288}$$

$$\dot{m} = \rho A u = \rho^* A^* c^* = 0.860(0.4)(1417) = 487.4 \text{ kg/s} \tag{289}$$

Solution I

d) Find the exit area A_e, $\dot{m}$ = constant. Recall

$$\dot{m} = \dot{m}^* = \rho_e A_e u_e = 487.4 \text{ kg/s} \tag{290}$$

$$\rho_e = \frac{p_e}{RT_e} = \frac{(1.174 \times 10^{-2})(1.01 \times 10^5)}{(519.6)(885.3)} = 0.00258 \text{ kg/m}^3 \tag{291}$$

$$A_e = \frac{\dot{m}}{\rho_e u_e} = \frac{487.4}{0.00258(3903)} = 48.4 \text{ m}^2 \tag{292}$$

Example

A convergent-divergent nozzle has area ratio of $A/A_t = 2$, $p_o = 1$ atm, and $p_\infty = p_b = 0.95$ atm. What is Mach number at the throat and at the exit (that is M_t and M_e)?

Solution

If flow is supersonic in divergent portion then from isentropic table at $\frac{A}{A^*} = 2 \rightarrow \frac{p_o}{p_e} = 10.69$

$$\therefore p_e = \frac{p_o}{10.69} = \frac{1}{10.69} = 0.0935 \text{ atm.} \tag{293}$$

- This p_e value is less than p_∞. So, we do not have the sub-sup flow.
- Is the flow completely subsonic?
- For all subsonic flow A_t must be great than A^*
- From table $\frac{p_o}{p_e} = \frac{1 \text{ Atm}}{0.951 \text{ atm}} = 1.053 \rightarrow \frac{A_e}{A^*} \cong 2.17$, but our nozzle is $A/A^* = 2$. So, flow is subsonic everywhere.
- Since $\frac{p_o}{p_e} = 1.053 \overset{\text{table}}{\rightarrow} M_e = 0.28$
- At the throat $\frac{A_t}{A^*} = 1.085 \rightarrow M_t = 0.72$

Example

Consider a convergent-divergent (CD) nozzle with an area ratio of $\frac{A_e}{A^*} = 1.60$. Calculate the nozzle pressure ratio (NPR) required for sonic flow at the throat and subsonic flow everywhere else.

Solution

For $M = 1$ at the throat $A_t = A^*$

$$\therefore \frac{A_e}{A_t} = \frac{A_e}{A^*} = 1.6 \tag{294}$$

From the isentropic relations or table we see that

$$\frac{p_o}{p_\infty} = 1.1117 \tag{295}$$

which is the NPR.

- How would changing NPR alter the flow?
- How would changing total temperature ratio (TTR, T_o/T_∞) alter the flow?

Class Summary

- de Laval nozzles
- Isentropic nozzle operations
- Rocket engines

Next Time

- Supersonic wind tunnels – isentropic
- Efficiency
- Transition to shocks

Class Overview

- Supersonic wind tunnels – isentropy
- Efficiency
- Transition to shocks

“Basic research is what I am doing when I don’t know what I am doing.”

Wernher von Braun

New York Times, 16th December 1957

Supersonic Windtunnel Demonstration

Let us view a video from “Engineering Fluid Dynamics University of Twente. Published on Feb 9, 2016. MSc student Ella Giskes explaining the schlieren system on the supersonic windtunnel of the University of Twente. Images show the bow shock and others around a pitot tube in a supersonic flow.”

https://www.youtube.com/watch?v=_9FJgxwnD6A

Supersonic Wind Tunnel

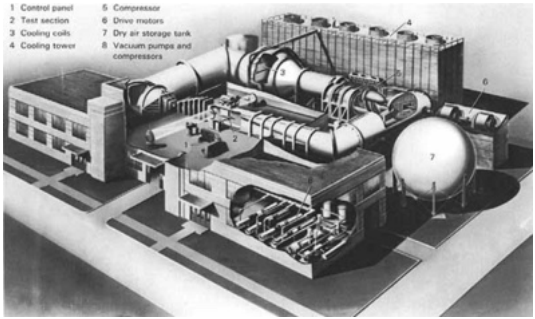

Figure 90: The 6 by 6 foot supersonic wind tunnel of NASA Ames Research Center.

Supersonic Wind Tunnel

Figure 91: The compressor's stator case is open for inspection and maintenance. Compressor Number 1 is similar, though it is driven by four of these motors. Altogether, the seven motors can deliver a total of 290,500 horsepower.

Supersonic Wind Tunnel

Figure 92: NASA Glenn Research Center 8 by 6 test section.

Supersonic Wind Tunnel

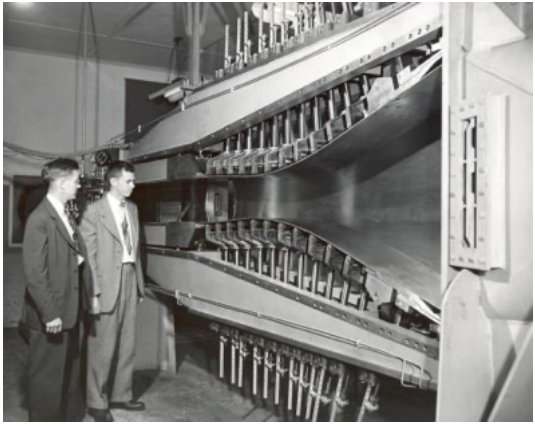

Figure 93: Supersonic test section at JPL.

Basic Wind Tunnel Schematic for Supersonic Flow

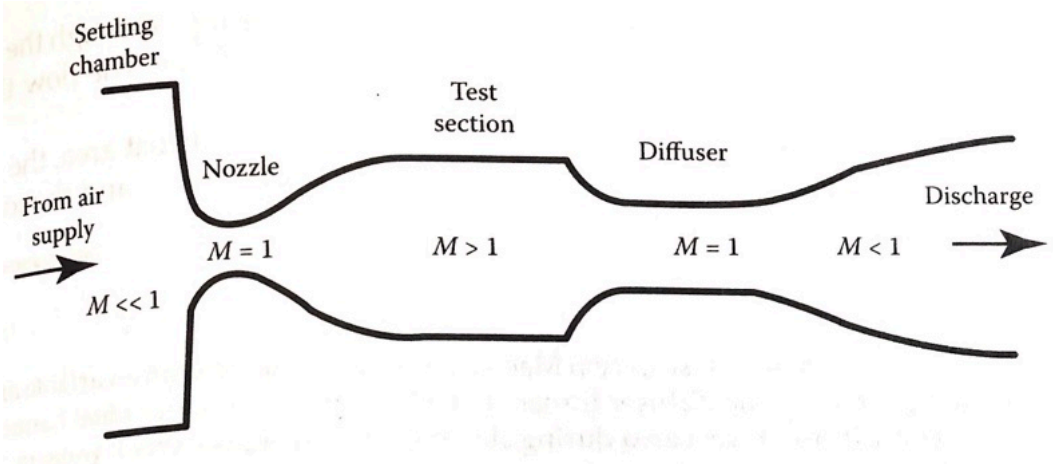

Figure 94: Ideal supersonic wind tunnel operation.

Ducts with More Than One Constriction

Given the duct with $A_2 > A_1$ shown below, what are the possible isentropic flow conditions assuming p_o fixed and p_b variable?

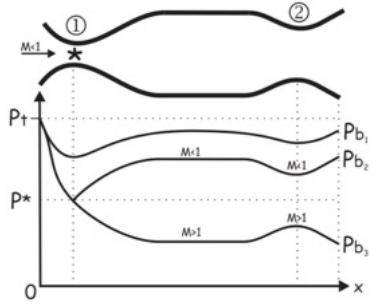

Figure 95: Variation of pressure (isentropic) in a double divergent duct.

- For ducts with multiple constrictions, find the smallest one: it will choke first.
- A restriction of area does not mean that it is transonic.

Ducts with More Than One Constriction

Given the duct with $A_2 = A_1$ shown below, what are the possible isentropic flow conditions assuming p_o fixed and p_∞ variable?

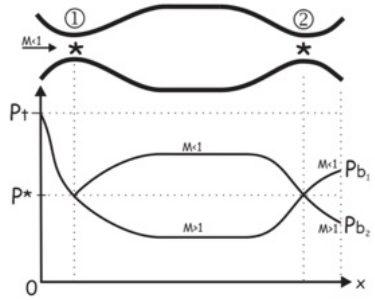

Figure 96

- As $A_2 = A_1$, if A_1 chokes then so does A_2 in isentropic flow.
- Four different pressure curves are possible, all isentropic with $M \geq 1$ somewhere.

These two solutions, with $A_1 = A_2$ and $M < 1$ between the two throats depends on the values of p_b and how the tunnel is started.

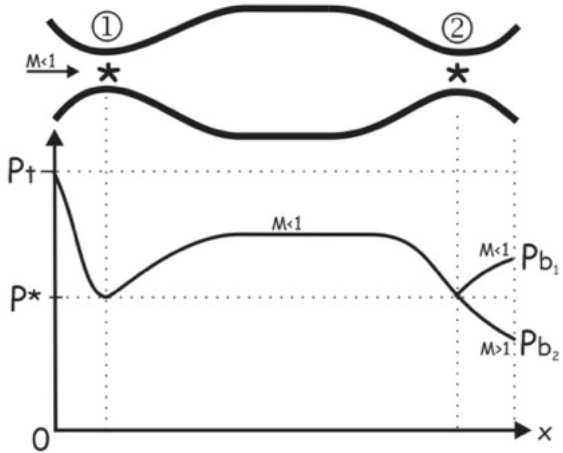

Figure 97: Subsonic tunnel operation.

- Two solutions, with $A_1 = A_2$ and $M > 1$ between the two throats, are not possible unless the duct geometry can be altered to "swallow" a starting shock wave, then restored.

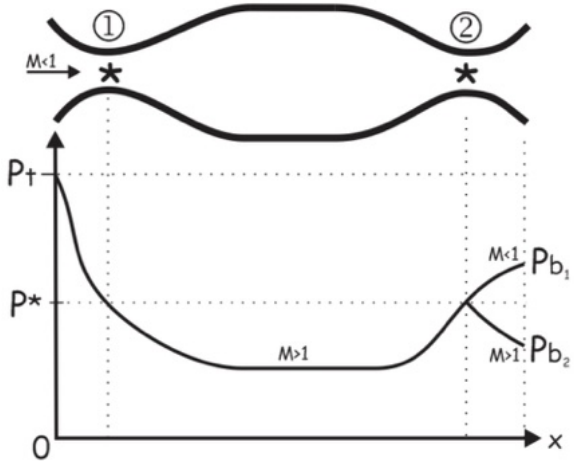

Figure 98: Supersonic tunnel operation.

- $A_2 < A_1$, and A_2 is choked. We do not know if the flow incoming at left is subsonic or supersonic, we have to consider both cases.
- Back pressure can end up high (p_{b1}) or low (p_{b2}), so once again there are four possible isentropic solutions.

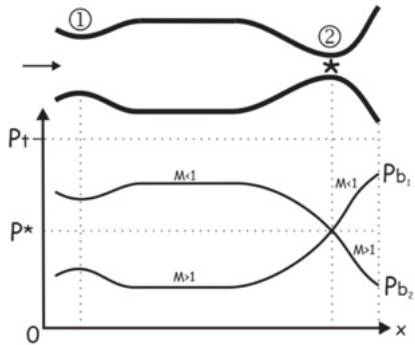

Figure 99: Flows with second throat transonic.

Mass Flow Rate versus Exit Pressure

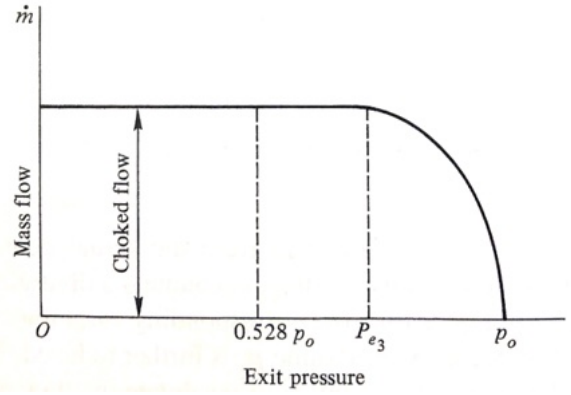

Figure 100: The variation of mass flow rate, $\dot{m}$, with the variation of back pressure, p_b.

Additional Thoughts

- Nozzle walls must be designed correctly to maintain isentropic flow.
- Shape of the walls can cause shock waves to form so they must be carefully designed.
  - Method of characteristics (MOC) discussed later.
- There are select companies in the world that specialize in building wind tunnels
- People who build wind tunnels and understand their design are highly sought after because they became experts through a lifetime of learning and dedication.

Example

A supersonic wind tunnel is designed to produce Mach 2.5 flow in the test section with standard sea level conditions. Using basic isentropic theory, calculate the exit area and conditions necessary to achieve these design goals.

Solution

From supersonic portion of isentropic tables for $M_e = 2.5 \implies A_e/A^* = 2.637$, $\frac{p_o}{p_e} = 17.09$, $\frac{T_o}{T_e} = 2.25$, we assume $p_e = 1$ atm and $T_e = 288$ K. (sea level conditions)

$$p_o = \frac{p_o}{p_e} p_e (17.09)(1) = 17.09 \text{ atm} \tag{296}$$

$$T_o = \frac{T_o}{T_e} T_e = 2.25(288) = 648 \text{ K} \tag{297}$$

- Ideally (isentropic) our stagnation properties are defined at the inlet and the back static pressures are ambient values.
- May not work very well for a recirculating tunnel, but certain types of supersonic tunnels use these conditions closely - can you think of their configuration?

Diffusers

- Recall
  - Diffusers in subsonic flow lower velocity
  - Diffusers in supersonic flow accelerate flow
  - Mathematical and physical reason for these facts
- Diffuser goal is to slow flow with little losses as possible
- Ideally compress flow

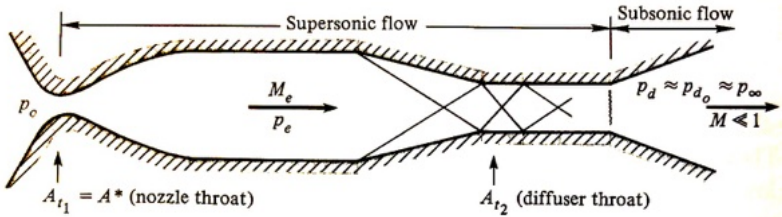

Figure 101: A supersonic wind tunnel test section. Note locations of shocks. (from Anderson)

Diffuser Efficiency

- We turn our attention to the efficiency of the diffuser, which is critical for supersonic wind tunnel operations.
- We use our isentropic theory to define an efficiency.

The efficiency is defined as η_D

$$\eta_D = \frac{(p_{do}/p_o)_{\text{actual}}}{(p_{o2}/p_{o1})_{\text{normal shock at tunnel exit}}} \tag{298}$$

where $p_{do}/p_o =$ total pressure across diffuser.

- Typically $\eta_D > 1$ but for hypersonic tunnels $\eta_D < 1$
  - This is strange but accepted in the community
- In supersonic wind tunnels $A_{t2} > A_{t1}$. Why?
  - Due to entropy generation, which primarily occurs in the diffuser.
  - Primary driver of entropy are shocks and boundary layers.

The Ratio of Areas

We intend to find the ratio of the throat areas of a supersonic wind tunnel. Recall the conservation of mass. We place it in a curious form

$$\rho_1^* A_{t1} c_1^* = \rho_2^* A_{t2} c_2^* \tag{299}$$

and

$$\frac{A_{t2}}{A_{t1}} = \frac{\rho_1^*}{\rho_2^*} \frac{c_1^*}{c_2^*} \tag{300}$$

Assume that the flow is adiabatic, which implies T^* is a constant, and using speed of sound relation

$$\therefore \frac{A_{t2}}{A_{t1}} = \frac{\rho_1^*}{\rho_2^*} \tag{301}$$

Using the equation of state and combining with the previous equation we find

$$\frac{\rho_1^*}{\rho_2^*} = \frac{p_1^*/RT_1^*}{p_2^*/RT_2^*} = p_1^*/p_2^* \tag{302}$$

The Ratio of Areas

Combining these relations we find

$$\frac{A_{t2}}{A_{t1}} = \frac{p_1^*}{p_2^*} \tag{303}$$

For optimal operations the Mach numbers must be unity at the throats ($M_1 = M_2 = 1$). Now we know

$$\frac{p_{o1}}{p_1^*} = \left(1 + \frac{\gamma - 1}{2} M_1^2\right)^{\frac{\gamma}{\gamma - 1}} = \left(\frac{\gamma + 1}{2}\right)^{\frac{\gamma}{\gamma - 1}} \tag{304}$$

$$\frac{p_{o2}}{p_2^*} = \left(1 + \frac{\gamma - 1}{2} M_2^2\right)^{\frac{\gamma}{\gamma - 1}} = \left(\frac{\gamma + 1}{2}\right)^{\frac{\gamma}{\gamma - 1}} \tag{305}$$

Recall definition of $*$ (sup $*$), the critical condition.

The Ratio of Areas

Combining these relations we find the ratio of areas

$$\boxed{\frac{A_{t2}}{A_{t1}} = \frac{p_{o1}}{p_{o2}}} \tag{306}$$

- p_o within the tunnel decreases with increasing S (entropy generation)
- Increase of S is due to turbulence, boundary layers, and shock waves (and what else?)
- Second throat must be larger than first throat for tunnel operation
- Imagine a wind tunnel with diffuser throat smaller than first!
  - Never able to achieve supersonic test section
- η_D is a very strongly sensitive to A_{t2}, due to a sensitivity analysis

Efficiency

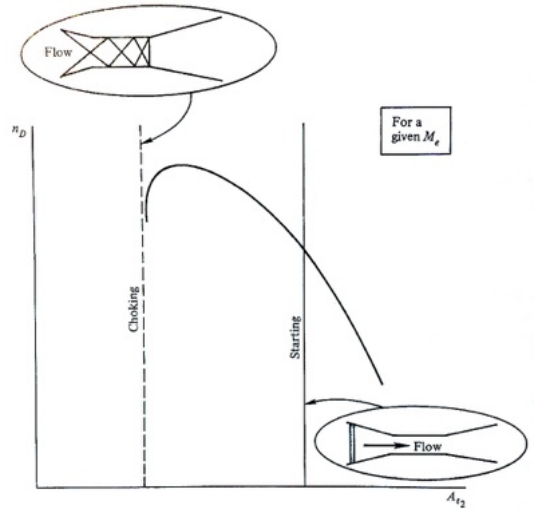

Figure 102: Graph of efficiency of the diffuser system (from Anderson).

Starting the Wind Tunnel

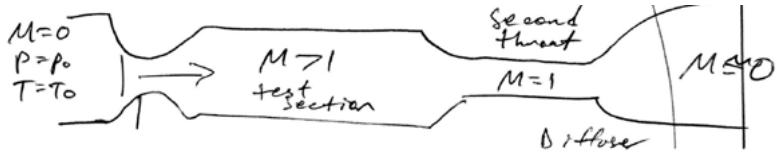

Figure 103: Professor Miller's sketch.

- For small tunnels a valve is released
- Results in a traveling normal shock that propagates through the tunnel
- A_{t2} must be large enough for the shock to pass through the tunnel

Shock Propagation and Efficiency of the Diffuser

We make the following observations from experiments

- Turbulent
- Highly 3D
- Filled with oblique shock waves
- Design usually involves numerical situations and trial and error.

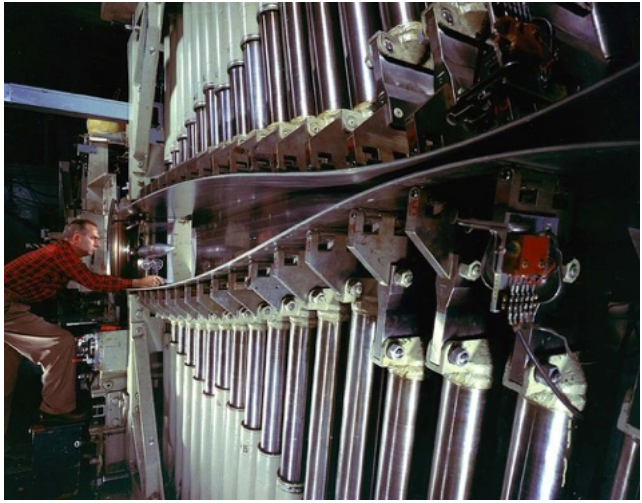

Figure 104: Source: NASA.gov.

Class Overview

- Supersonic wind tunnels – isentropy
- Efficiency
- Transition to shocks

Next Time

- What is a shock
- Shock tubes
- Compression
- Expansion

Class Overview

Normal Shock Waves

- What is a shock
- Shock tubes
- Compression
- Expansion

“von Neumann gave me an interesting idea: that you don’t have to be responsible for the world that you’re in. So I have developed a very powerful sense of social irresponsibility as a result of von Neumann’s advice. It’s made me a very happy man ever since. But it was von Neumann who put the seed in that grew into my active irresponsibility!”

Part 3: “Feynman, The Bomb, and the Military,” Los Alamos from Below, page 132.

What is a shock wave

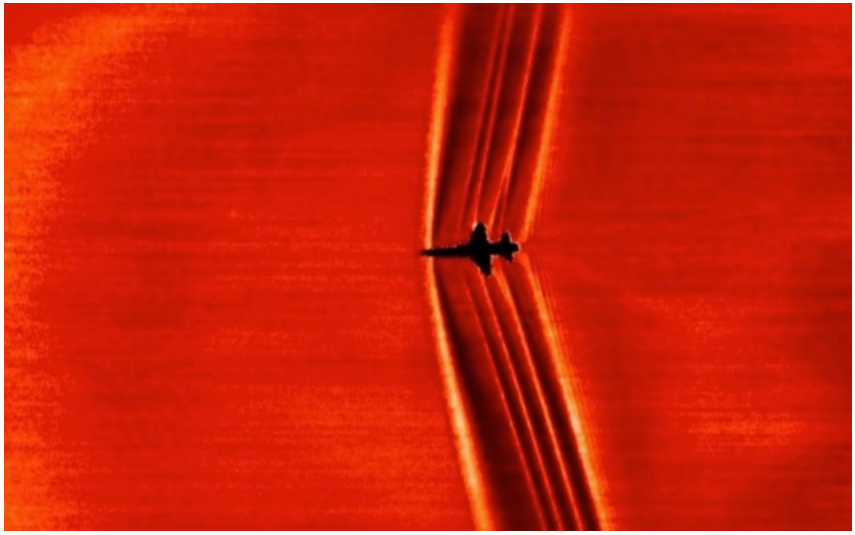

Figure 105: Shockwaves as seen from an earth observer with the sun.

What is a shock wave

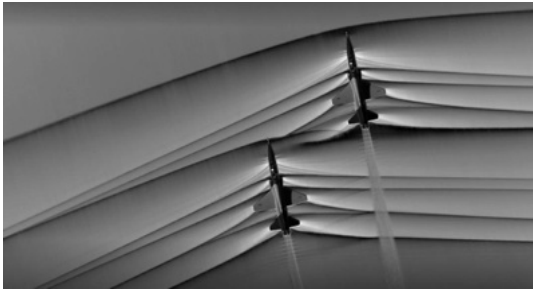

Figure 106: Using the schlieren photography technique, NASA was able to capture the first air-to-air images of the interaction of shockwaves from two supersonic aircraft flying in formation. These two U.S. Air Force Test Pilot School T-38 aircraft are flying in formation, approximately 30 feet apart, at supersonic speeds, or faster than the speed of sound, producing shockwaves that are typically heard on the ground as a sonic boom. This image was captured during the fourth phase of the Air-to-Air Background Oriented Schlieren flights, or AirBOS which took place at NASA's Armstrong Flight Research Center in Edwards, California. These flights were flown, in part, to better understand how shocks interact with aircraft plumes, as well as with each other.

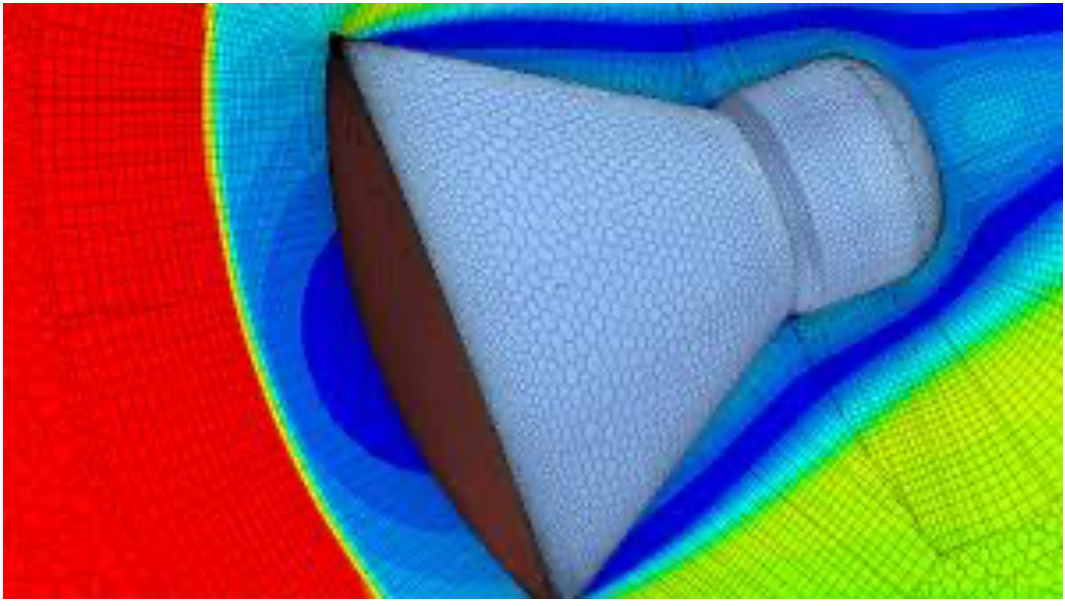

Figure 107: Bow shock in front of a reentry vehicle from a computational fluid dynamics solution.

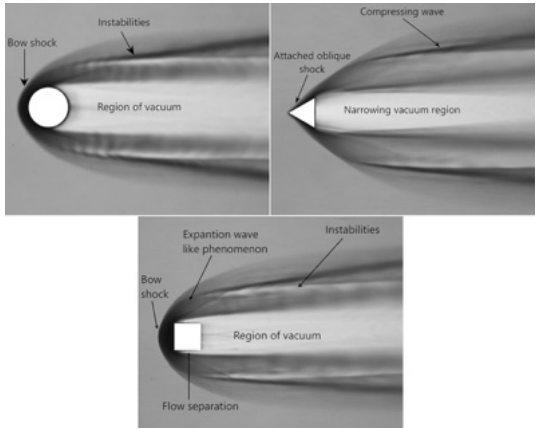

Figure 108: Bow shock vs attached oblique shock. From Garai, P., Verma, S. & Kumar, S. J Vis (2019) 22: 729. https://doi.org/10.1007/s12650-019-00558-5

Figure 109: USS Iowa.

Sandia National Labs Shock Tube

"Sandia National Labs, Published on Nov 17, 2017. The Sandia blast tube facility provides experimental conditions to simulate extreme blast environments. The validation & qualification experimental sciences complex combines large scale environmental test facilities with advanced engineering & diagnostics to solve complex national security problems. Utilizing advanced engineering and modeling, precision shockwaves are bombarded onto test units. Watch in slow motion how a 100 lb. explosive charge is shaped into precise Mach 3 wavefront using high speed photography and synthetic Schlieren wavefront imaging. Advanced data fusion methods show how the wavefront progresses relative to measured pressure data and shockwave physics models. SAND2017-2479 V"

https://www.youtube.com/watch?v=CkhCiSneJJg

Observations of Shocks

- Bow shock is nearly normal to the flow direction
- Oblique shock – oblique angle relative to incoming flow direction
- Near nose of aircraft shock is nearly normal
- Normal shock – portion of the flow, which is perpendicular to the free-stream
- Why examine normal shocks first?
  - We simply apply our previously developed one-dimensional theory
- Shock process results in very large and almost discrete changes in the field variables
  - Thickness over a single to tens of mean-free-paths
- Subsonic flows, pressure matched by gradual changes
- Supersonic flows are matched by very abrupt changes (shocks)

Particular Observations of Shocks

- Shocks are discontinuities in the fluid
  - Derivation showed that the Navier-Stokes equations can be interpreted as deformations of Euclidean space
- Shocks can form due to a coalescence of weak compression waves
- Formation of normal shock (one type)
  - Due to weak compression waves
  - Example, imagine we have a long tube with moving wall
  - Typically called “shock tubes”

Shock Tube

Figure 110: The Free-Piston Driven Hypersonic Shock Tunnel 3 (Photo: SK Karthick/LHSR)

Shock Tube

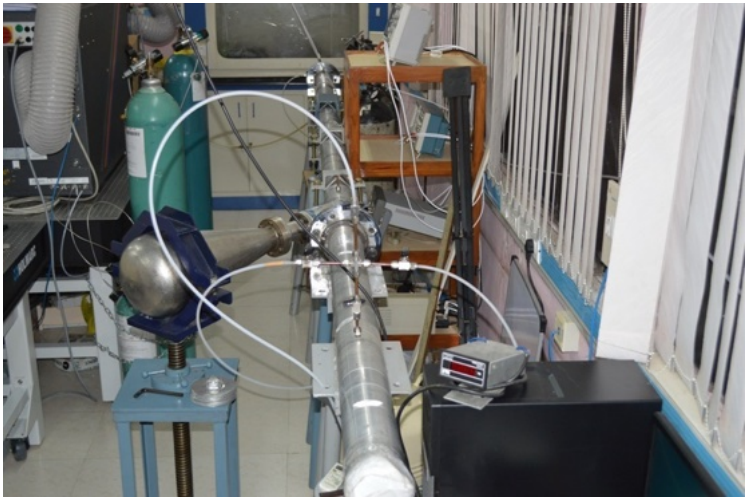

Figure 111: 2.1 m long shock tube at UF.

Shock Tube Operation

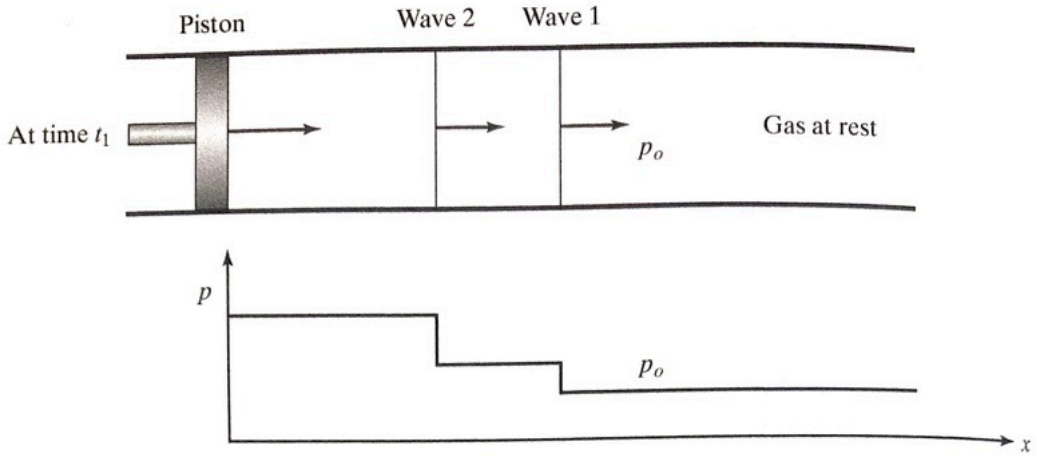

Figure 112: Diagram of a shock tube with discrete compression waves.

Shock Tube Operation

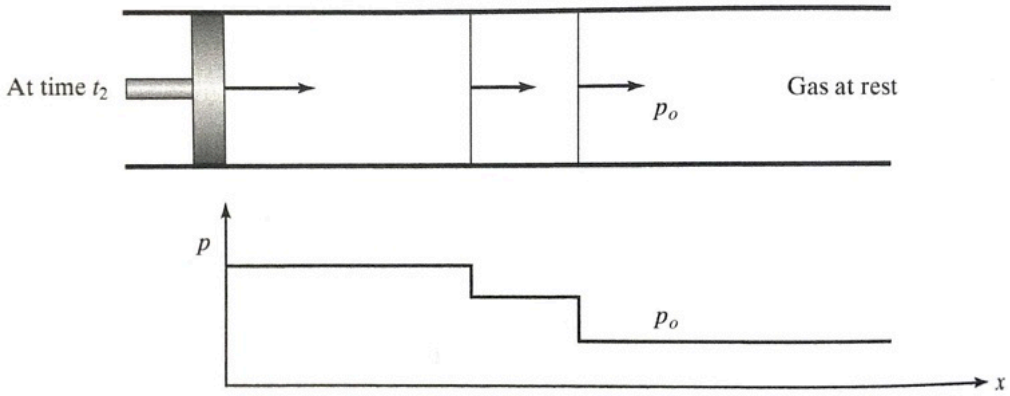

Figure 113: Diagram of a shock tube with discrete compression waves.

Shock Tube Operation

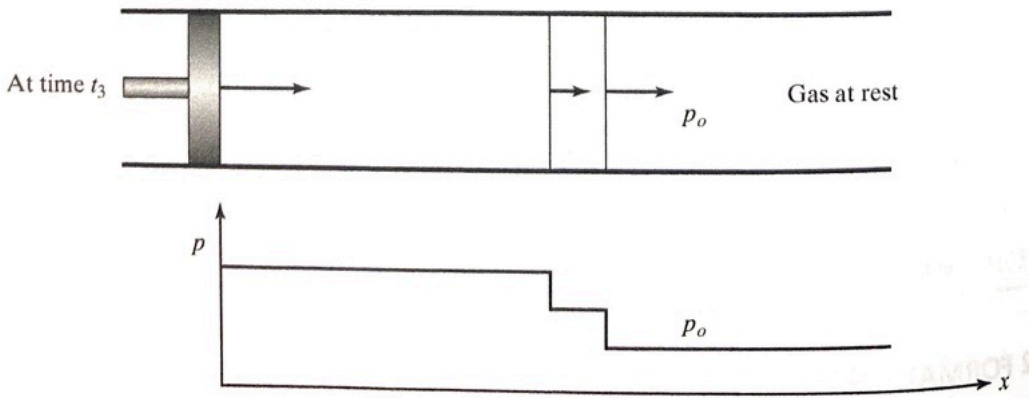

Figure 114: Diagram of a shock tube with discrete compression waves.

Shock Tube Operation

- Fluid initially at rest
- Piston moves to right with small velocity magnitude du
- Piston accelerates at a higher velocity, $du + \epsilon$, $\epsilon =$ small increment
- du's cause waves to travel down the tube
- Waves travel at local speed of sound, c, plus the ambient velocity, u
  - There is an "induced velocity behind a compression wave"
  - Induced velocity due to gas being compressed by wave, it has slightly higher temperature
- $\therefore c_1 > c_\infty$ after each wave
- Each compression wave travels faster than the previous wave
- Piston accelerates rapidly and we can graph the changes

Δu with x

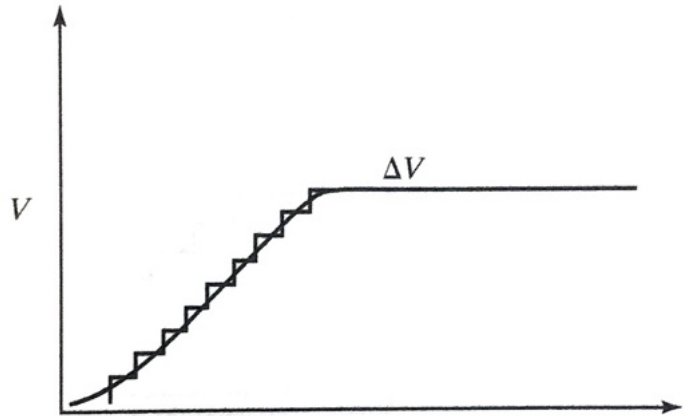

Figure 115: Changes in velocity with respect to the axial direction within a shock tube undergoing compression.

Coalesce of Shock Tube Disturbances

Given the acceleration of the piston and the increasing wave speed the waves will coalesce

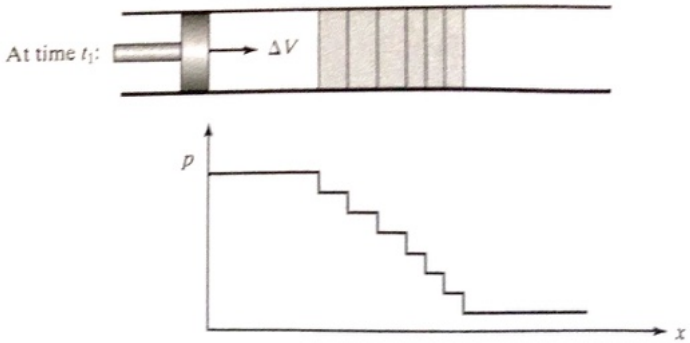

Figure 116: Coalescence of waves within tube.

Coalescence of Shock Tube Disturbances

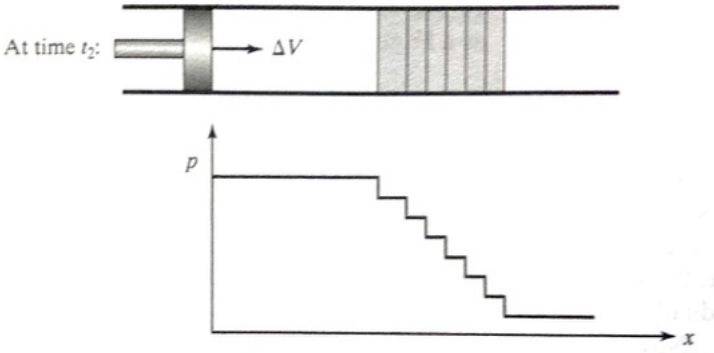

Figure 117: Coalescence of waves within tube.

Coalescence of Shock Tube Disturbances

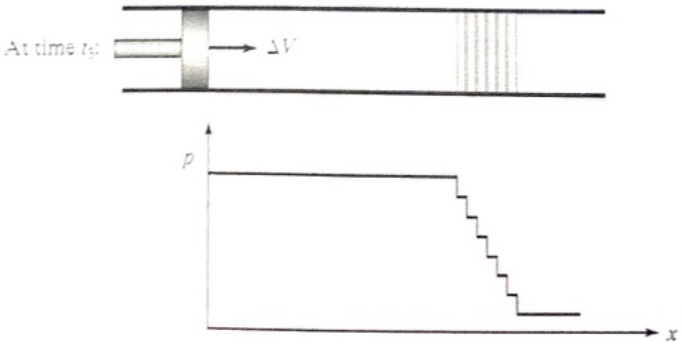

Figure 118: Coalescence of waves within tube.

On Compression Waves

- Compression process is balanced by effect of heat conduction and viscous effects within the wave
- A normal shock wave is formed via the waves coalescing
- Velocity vector on the wave is normal to the wave front
- Also, expansion of pressure waves are balanced by heat conduction and viscous effects

The Expansion Wave

Consider what happens when the piston moves in the opposite direction of the fluid.

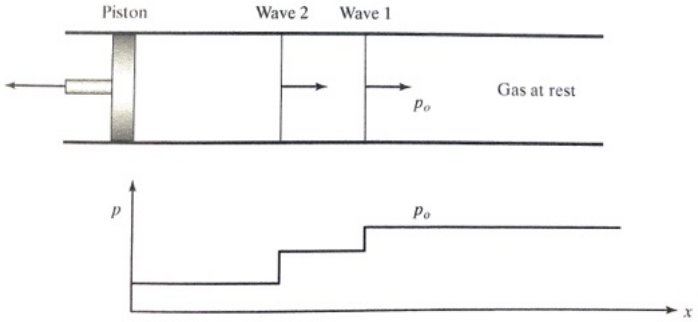

Figure 119: The expansion wave is formed when the piston moves in the opposite direction.

The Expansion Wave

Consider what happens when the piston moves in the opposite direction of the fluid.

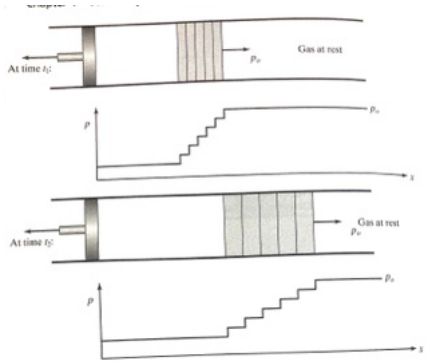

Figure 120: The expansion wave is formed when the piston moves in the opposite direction.

Expansion Wave – Shock Tube

- Another type of wave can form that is opposite the shock wave
- Called an “expansion wave”
- Flow is expanded, what does that mean?
- Speed of sound is lowered
- Expansion waves spread out over time (and/or space) and will never coalesce
- Shock formation is impossible
- We devote a module to it later in the class – Prandtl-Meyer expansion waves

Class Summary

- What is a shock
- Shock tubes
- Compression
- Expansion

Next Time

- Shock tubes in practice
- Bow shocks
- Normal shock wave equations formulation
- Asymptotic limits

Class Overview

Normal Shock Waves

- Shock tubes in practice
- Bow shocks
- Normal shock wave equation formulation
- Asymptotic limits

“Science is the belief in the ignorance of experts,”

Richard Feynman

“What is Science” presented at the fifteenth annual meeting of the National Science Teachers Association, in New York City (1966), published in The Physics Teacher, volume 7, issue 6 (1969), p. 313-320

Shock Tubes in Practice

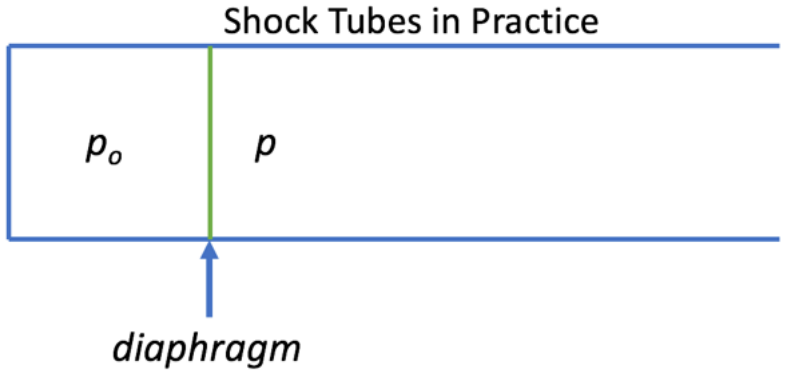

Figure 121: Diagram of a diaphragm based shock tube.

Shock Tubes – Diaphragm Based

- Diaphragm is ruptured
  - Shock will have pressure rise p_o/p_∞
- What happens now?
- Single shock propagates through tube
- Reality is a little bit different than our ideal analysis

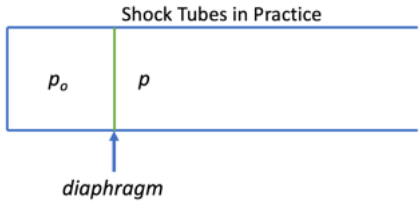

Figure 122

Shock Tube Diaphragm

Figure 123: “Aluminum foil used as a diaphragm between shock tube pipe segments.” Achim Hering CC BY-SA 4.0.

- Shocks in these systems contain hydrodynamic instabilities
- Flow-field is not really as ideal as we describe it
- Shock tubes offer great ways to study blast waves (kind of shock wave) and carry different pressure ratios

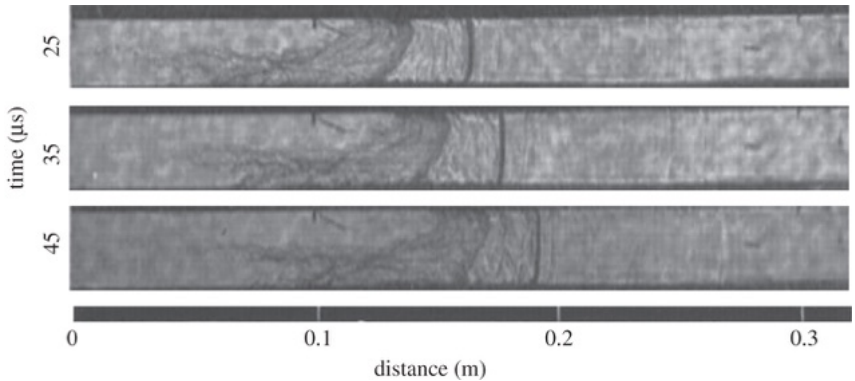

Figure 124: Series of schlieren images of shock wave propagation in a shock tube.

Shocks Attached to Subsonic Aircraft (Transonic)

- Shock is very thin, $\approx 10^{-7}$ m for this condition.
- Approximately a few mean-free-paths.

Figure 125: Shock wave attached to the wing of a commercial aircraft.

Shocks Attached to Subsonic Aircraft (Transonic)

Figure 126: NOAA 2018.

Normal Shock Wave Continuity

Shock waves instantaneously turn the flow. We expect streamlines to be discontinuous at shocks.

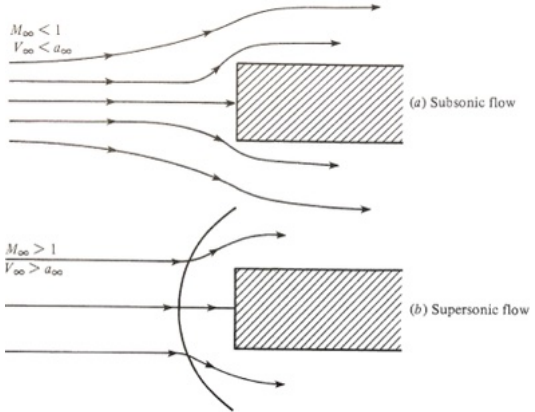

Figure 127: Streamlines about a bluff body.

Disturbances Near Normal Shocks

- Bodies and fluid disturbances (eg turbulence) create acoustic waves as they travel
- Waves travel upstream for $M_\infty < 1$
- Waves cannot propagate upstream when $u_\infty > c_\infty$ and $M_\infty \geq 1$
- Waves travel at the eigenvalues of $u_\infty - c_\infty$ and $c_\infty + u_\infty$
- Vorticity and entropy waves travel at $\overline{u}$
- This can be shown via the eigenvalues of the coefficient matrix of the LNSE system u, $u + c$, and $u - c$

Field-Variable Properties Across the Shock

Shock tube experiments show the following changes of field-variables across a normal shock wave

State 1	State 2
p_1	$p_2 > p_1$
T_1	$T_2 > T_1$
ρ_1	$\rho_2 > \rho_1$
u_1	$u_2 < u_1$
$M_1 > 1$	$M_2 < 1$

We seek to quantify these values through theory

Shock Wave Analysis

- Assume we know conditions in front of the shock
- Assume heat addition is zero.
  - It is difficult to add heat to the flow (but not impossible, e.g. laser).
  - Therefore the shock wave is adiabatic.
- We form normal shock wave equations from one-dimensional flow equations.
- Our objective is to find the relations in the form $M_2 = f(M_1)$

Equations of Motion

Continuity

$$\rho_1 u_1 = \rho_2 u_2 \tag{307}$$

Momentum

$$p_1 + \rho_1 u_1^2 = p_2 + \rho_2 u_2^2 \tag{308}$$

Energy

$$h_1 + \frac{u_1^2}{2} = h_2 + \frac{u_2^2}{2} \tag{309}$$

Gas law for closure

Shock Wave Analysis

For calorically perfect gas we know

$$p = \rho RT \text{ and } h = c_p T \tag{310}$$

We now have five equations and five unknowns. Divide momentum equation by continuity equation

$$\frac{p_1}{\rho_1 u_1} - \frac{p_2}{\rho_2 u_2} = u_2 - u_1 \tag{311}$$

Note that $c = \sqrt{\frac{\gamma p}{\rho}}$ and substituting in yields

$$\frac{c_1^2}{\gamma u_1} - \frac{c_2^2}{\gamma u_2} = u_2 - u_1 \tag{312}$$

Recall energy equation in an alternative form

$$\frac{c^2}{\gamma - 1} + \frac{u^2}{2} = \frac{\gamma + 1}{2(\gamma - 1)} c^{*2} \tag{313}$$

Shock Wave Analysis

Write before and after the shock

$$c_1^2 = \frac{\gamma+1}{2}c^{*2} - \frac{\gamma-1}{2}u_1^2 \tag{314}$$

and

$$c_2^2 = \frac{\gamma+1}{2}c^{*2} - \frac{\gamma-1}{2}u_2^2 \tag{315}$$

- As flow is adiabatic, c^{*2} is the same constant value across the shock.
- This is a critical concept, where the critical condition of the speed of sound is conserved.
- c^* allows us to relate conditions across the shock.

Shock Wave Analysis

Substitute these two previous relations into continuity-momentum relation and we find

$$\frac{\gamma+1}{2}\frac{c^{*2}}{\gamma u_1}-\frac{\gamma-1}{2\gamma}u_1-\frac{\gamma+1}{2}\frac{c^{*2}}{\gamma u_2}+\frac{\gamma-1}{2\gamma}u_2=u_2-u_1 \tag{316}$$

Simplifying

$$\frac{\gamma+1}{2\gamma u_1 u_2}(u_2-u_1)c^{*2}+\frac{\gamma-1}{2\gamma}(u_2-u_1)=u_2-u_1 \tag{317}$$

Divide by (u_2-u_1) yields

$$\frac{\gamma+1}{2\gamma u_1 u_2}c^{*2}+\frac{\gamma-1}{2\gamma}=1 \tag{318}$$

Solve for c^{*2}

$$c^{*2}=u_1 u_2 \tag{319}$$

Shock Wave Analysis

We have found the Prandtl relation. We can then directly find the following

$$\boxed{M_2^* = (M_1^*)^{-1}} \tag{320}$$

Recall the relation between M and characteristic M

$$M^2 = \frac{2}{[(\gamma+1)/M^{*2}] - (\gamma-1)} \tag{321}$$

Solving for M^* yields

$$M^{*2} = \frac{(\gamma+1)M^2}{2+(\gamma-1)M^2} \tag{322}$$

Substituting this relation into $M_2^* = (M_1^*)^{-1}$ yields

$$\frac{(\gamma+1)M_2^2}{2+(\gamma-1)M_2^2} = \left[\frac{(\gamma+1)M_1^2}{2+(\gamma-1)M_1^2}\right]^{-1} \tag{323}$$

Shock Wave Analysis

We solve for M_2 and find a relation as a function of M_1

$$\boxed{M_2^2 = \frac{\frac{\gamma-1}{2}M_1^2 + 1}{\gamma M_1^2 - \frac{\gamma-1}{2}}} \tag{324}$$

Notes...

- For constant γ and calorically perfect gas, M_2 is only a function of M_1
- This equation can also be applied to Mach waves
- Observe M_1 increases M_2 decreases
- $M_1 \to \infty$ then $M_2 \to \sqrt{\frac{\gamma-1}{2\gamma}} \sim 0.378$ for air
- M_1 is most important parameter for normal shocks

Shock Wave Analysis

We seek other thermodynamic variables across the normal shock. Using the Prandtl relation $c^{*2} = u_1 u_2$ and conservation of mass $\rho_1 u_1 = \rho_2 u_2$ we find

$$\frac{\rho_2}{\rho_1} = \frac{u_1}{u_2} = \frac{u_1^2}{u_1 u_2} = \frac{u_1^2}{c^{*2}} = M_1^{*2} \tag{325}$$

Substituting $M^{*2} = \frac{(\gamma+1)M^2}{2+(\gamma-1)M^2}$ into above relation gives

$$\boxed{\frac{\rho_2}{\rho_1} = \frac{u_1}{u_2} = \frac{(\gamma+1)M_1^2}{2+(\gamma-1)M_1^2}} \tag{326}$$

We now have a powerful equation to derive field-variable ratios. Let us now seek the pressure ratios across the shock.

Shock Wave Analysis

Consider the momentum equation

$$p_2 - p_1 = \rho u_1^2 - \rho_2 u_2^2 \tag{327}$$

and combining with $M_2^* = (M_1^*)^{-1}$ with $\rho_2/\rho_1 = u_1/u_2$ yields

$$p_2 - p_1 = \rho u_1 (u_1 - u_2) = \rho_1 u_1^2 \left(1 + \frac{u_2}{u_1}\right) \tag{328}$$

Divide by p_1 and use $c_1^2 = \gamma p_1/\rho_1$ We then obtain

$$\frac{p_2 - p_1}{p_1} = \gamma M_1^2 \left(1 - \frac{u_2}{u_1}\right) \tag{329}$$

Shock Wave Analysis

Noting relation for u_2/u_1 we find

$$\boxed{\frac{p_2}{p_1} = 1 + \frac{2\gamma}{\gamma+1}(M_1^2 - 1)} \tag{330}$$

which is the pressure ratio across normal shock.
The temperature ratio can be found using the equation of state

$$\frac{T_2}{T_1} = \underbrace{\left(\frac{p_2}{p_1}\right)\left(\frac{\rho_1}{\rho_2}\right)}_{\text{We know these two ratio}} \tag{331}$$

We find

$$\boxed{\frac{T_2}{T_1} = \frac{h_2}{h_1} = \left[1 + \frac{2\gamma}{\gamma+1}(M_1^2 - 1)\right]\left[\frac{2 + (\gamma-1)M_1^2}{(\gamma+1)M_1^2}\right]} \tag{332}$$

Summary for Normal Shock Relations

We have now found ratios of ρ, p, T, and M_2 as functions of M_1 only.

- Quantities hold for calorically perfect gases
- Thermally perfect gas normal shock wave relations depend on M_1 and T_1
- Chemically reacting flows normal shock relations depend on M_1, T_1, and p_1
- Closed form expressions cannot be obtained and numerical techniques are required
- For standard air our results are valid roughly for $M \lessapprox 5$
  - This is approximately where community members view the onset of hypersonics, $M_\infty > 5$

Examine Asymptotics for our Relations

We consider the particular case when M approaches infinity. This has applications for high-speed flows, and is generally an interesting exercise to gain insight into the physics.

$$\lim_{M_1 \to \infty} M_2 = \sqrt{\frac{\gamma - 1}{2\gamma}} = 0.378 \text{ air / diatomic} \tag{333}$$

$$\lim_{M_1 \to \infty} \frac{\rho_2}{\rho_1} = \frac{\gamma + 1}{\gamma - 1} = 6 \text{ air / diatomic} \tag{334}$$

$$\lim_{M_1 \to \infty} \frac{p_2}{p_1} = \infty \tag{335}$$

and

$$\lim_{M_1 \to \infty} \frac{T_2}{T_1} = \infty \tag{336}$$

Examine Asymptotics for our Relations

We now consider what happens when our Mach number approaches unity from the supersonic condition.

For Mach waves we find

$$\frac{M_1}{M_2} = \frac{\rho_2}{\rho_1} = \frac{p_2}{p_1} = \frac{T_2}{T_1} = 1 \tag{337}$$

Note our equations of motion can be solved for $M_1 < 1$. This is non-physical, why?

Entropy Across Shocks

Recall second law of thermodynamics (what assumptions have we made for this equation?)

$$S_2 - S_1 = c_p \ln \frac{T_2}{T_1} - R \ln \frac{p_2}{p_1} \tag{338}$$

Using derived relations for T_2/T_1 and p_2/p_1 we find

$$\boxed{\begin{aligned} S_2 - S_1 = \Delta S = c_p \ln \left\{ \left[1 + \frac{2\gamma}{\gamma+1}(M_1^2 - 1) \right] \left[\frac{2 + (\gamma-1)M_1^2}{(\gamma+1)M_1^2} \right] \right\} \\ -R \ln \left[1 + \frac{2\gamma}{\gamma+1}(M_1^2 - 1) \right] \end{aligned}} \tag{339}$$

Entropy Across Shocks

- This equation shows that the entropy change across shocks are a function of M_1 (given our previous assumptions.)
  - If $M_1 = 1$ then $S_2 - S_1 = 0$
  - If $M_1 < 1$ then $S_2 - S_1 < 0$
  - If $M_1 > 1$ then $S_2 - S_1 > 0$
- For second law to be valid $M_1 \geq 1$
- Entropy increase is due to the large gradients of field variables across the shock – change in T and p
- Entropy increase occurs completely inside the shock wave

Class Summary

- Shock tubes in practice
- Bow shocks
- Normal shock wave equations formulation
- Asymptotic limits

Next Time

- Stagnation properties (total) across normal shock waves
- Graphs of normal shock waves
- Entropy
- Shock strength
- Shock thickness
- Examples

Class Overview

- Stagnation properties (total) across normal shock waves
- Graphs of normal shock waves
- Entropy
- Shock strength
- Shock thickness
- Examples

“Discrepancy between theory and practice, which in sound physical and mechanical science is a delusion, has a real existence in the minds of men; and that fallacy, through rejected by their judgments, continues to exert and influence over their acts,”

William John Macquorn Rankine

Introductory Lecture on the Harmony of Theory and Practice in Mechanics (1856), p. 4

Variation of Stagnation Conditions

- We previously developed properties for stagnation or total conditions within isentropic flow
- The total conditions are constant within the isentropic flows
- We seek stagnation properties across stationary normal shock waves
- This is a strange concept because we know that $\Delta S > 0$ across a shock

Stagnation for Supersonic Flow

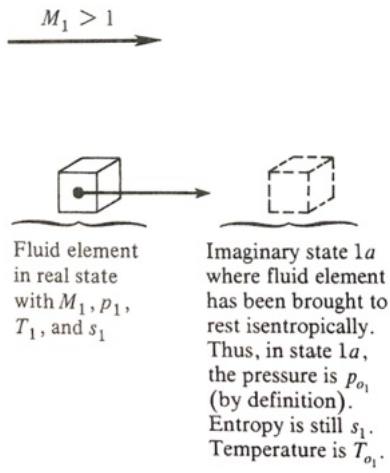

Figure 128: Stagnation before the shock.

Stagnation for Subsonic Flow

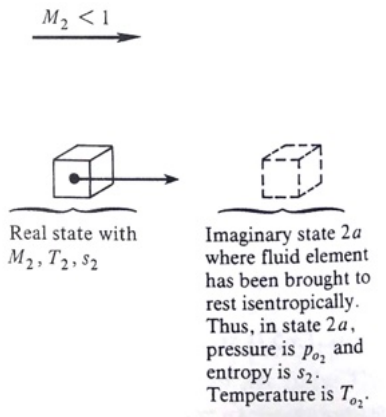

Figure 129: Subscripts denote fluid is being isentropically brought to rest before or after the shock wave.

Alteration of Stagnation Temperature Across Shocks

We pose the question: How does T_{o2} compare to T_{o1}, and other properties across the shock? We examine the energy equation

$$c_p T_1 + \frac{u_1^2}{2} = c_p T_2 + \frac{u_2^2}{2} \tag{340}$$

Remember the definition of total or stagnation temperature

$$c_p T_o = c_p T + \frac{u^2}{2} \tag{341}$$

It is clear that

$$T_{o1} = T_{o2} \tag{342}$$

which implies that the total temperature across a stationary normal shock wave is constant.

Alteration of Stagnation Temperature Across Shocks

Consider the total enthalpy change across a shock wave. If we have a perfect gas then we can use the definition of $h_o = c_p T_o$ It is clear that stagnation enthalpy is also conserved across a stationary normal shock.

$$\boxed{c_p T_{o1} = c_p T_{o2} \text{ (enthalpy)} \rightarrow h_{o1} = h_{o2}} \tag{343}$$

These relations are not true for

- Chemically reacting flows
- Thermally perfect flows
- Non-stationary or moving shock waves

Entropy and Pressure

We have shown that stagnation temperature is conserved. We can write

$$\frac{T_{o2}}{T_{o1}} = 1 \tag{344}$$

We now examine our entropy equation, that is simplified because of conservation of T_o

$$S_2 - S_1 = -R \ln \frac{p_{o2}}{p_{o1}} \tag{345}$$

and solving for the stagnation pressure ratio

$$\frac{p_{o2}}{p_{o1}} = \exp[-(S_2 - S_1)/R] \tag{346}$$

It is clear that the total or stagnation pressure decreases across a shock wave. These equations are tabulated in the "Ames Tables" for $\gamma = 1.4$ and our own class tables.

Entropy and Pressure

The general relationship is on your formula sheet, and holds for all flows in this course, not just normal shocks

$$\boxed{\frac{s_2 - s_1}{R} = -\ln\frac{p_{o2}}{p_{o1}}} \tag{347}$$

- Shows that the stagnation pressure will always decrease across a normal shock.
- The amount of this decrease is a direct measure of the entropy increase across the shock wave.
- The entropy increase across the shock is effectively a measure of the strength of the shock wave.
  - In isentropic flow, for example, $s_2 = s_1$, and requires that $p_{o1} = p_{o2}$

The Normal Shock Relations

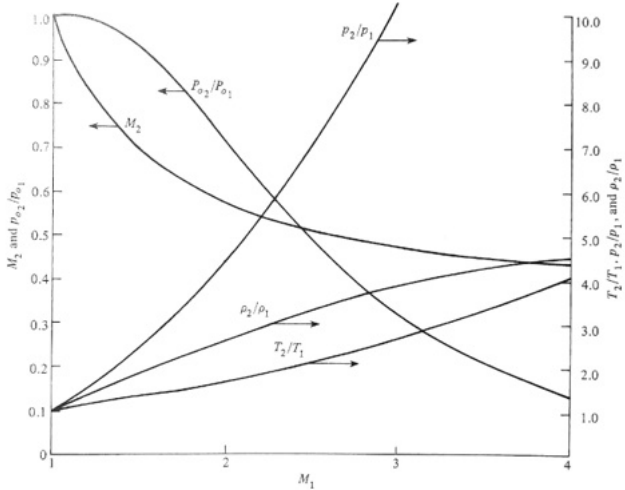

Figure 130: Variation of field-variables with M_1 (Anderson).

Variation of Mach Number

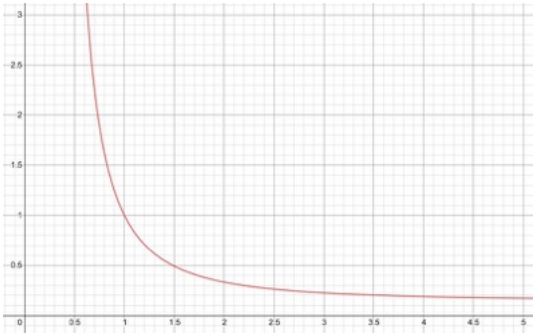

Figure 131: Variation of M_2 with M_1. Note x-axis is M_1 and y-axis is M_2.

Based on the equation

$$M_2^2 = \frac{M_1^2 + \frac{2}{\gamma - 1}}{\frac{2\gamma}{\gamma - 1} M_1^2 - 1} \tag{348}$$

Variation of Entropy

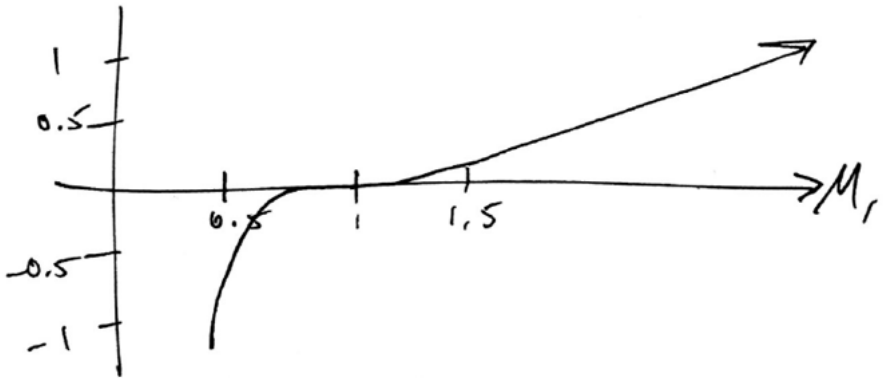

Figure 132: $(S_2 - S_1)/R$ as a function of M_1.

Different Measures of Normal-Shock Wave Strength

Typically we measure in terms of Δs, p_{o2}/p_{o1}, p_2/p_1, or M_1

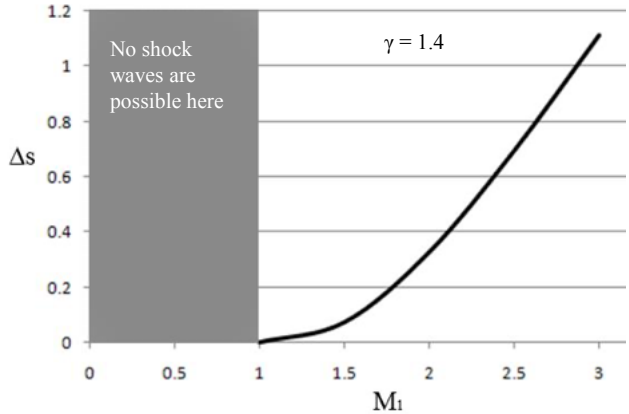

Figure 133: Variation of entropy with M_1 across a standing normal shock wave.

Stagnation Pressure Ratio versus M_1

We have found p_{o2}/p_{o1} as a function of entropy but we seek it as a function of M_1. Recall the momentum equation

$$p_1 + \rho_1 u_1^2 = p_2 + \rho_2 u_2^2 \tag{349}$$

and the energy equation for a perfect gas via $c = (\gamma p/\rho)^{1/2}$

$$p + \rho u^{2*} = p(1 + \gamma M^2) \tag{350}$$

We combine these two equations

$$p_1(1 + \gamma M_1^2) = p_2(1 + \gamma M_2^2) \tag{351}$$

and solve for the static pressure ratio

$$\frac{p_2}{p_1} = \frac{1 + \gamma M_1^2}{1 + \gamma M_2^2} \tag{352}$$

Stagnation Pressure Ratio versus M_1

- We previously derived a static pressure ratio and combined it with the Mach number relation.
- The Mach number relation is $M_2^2 = \frac{M_1^2 + \frac{2}{M_1}}{M_1^2\left(\frac{2\gamma}{\gamma-1}\right) - 1}$.

We find

$$\frac{p_2}{p_1} = \frac{2\gamma M_1^2}{\gamma+1} - \frac{\gamma-1}{\gamma+1} \tag{353}$$

Expand our stagnation pressure relation as a multiplication of fractions and substitute in our known relations

$$\frac{p_{o2}}{p_{o1}} = \left(\frac{p_{o2}}{p_2}\right)\left(\frac{p_2}{p_1}\right)\left(\frac{p_1}{p_{o1}}\right) \tag{354}$$

Stagnation Pressure Ratio versus M_1

We substitute in our relations for each fraction that we previously derived

$$\frac{p_{o2}}{p_{o1}} = \left(1 + \frac{\gamma - 1}{2} M_2^2\right)^{\frac{\gamma}{\gamma-1}} \left(\frac{2\gamma M_1^2}{\gamma + 1} - \frac{\gamma - 1}{\gamma + 1}\right) \left(\frac{1}{1 + \frac{\gamma-1}{2} M_1^2}\right)^{\frac{\gamma}{\gamma-1}} \tag{355}$$

And finally substituting our relation for M_2 we find

$$\boxed{\frac{p_{o2}}{p_{o1}} = \left[\frac{\frac{\gamma+1}{2} M_1^2}{1 + \frac{\gamma-1}{2} M_1^2}\right]^{\frac{\gamma}{\gamma-1}} \left[\frac{1}{\frac{2\gamma}{\gamma+1} M_1^2 - \frac{\gamma-1}{\gamma+1}}\right]^{\frac{1}{\gamma-1}}} \tag{356}$$

which is the relation of stagnation pressure across a normal stationary shock wave in a perfect gas.

- Remember our assumptions when finding this equation.
- This is also summarized in the Ames tables.

Notes on Error

- The ratio of stagnation pressure across a normal shock wave can be written directly as a function of M_1 and γ.
- It is difficult to see the behavior of these normal-shock jump conditions by examining the equations themselves, let us plot them
- In a later class we will examine the Rankine-Hugoniot relationship between pressure and density, but for now it is

$$\frac{p_2}{p_1} = \frac{\frac{\gamma+1}{\gamma-1}\frac{\rho_2}{\rho_1} - 1}{\frac{\gamma+1}{\gamma-1} - \frac{\rho_2}{\rho_1}} \tag{357}$$

Rankine-Hugoniot Curve

- The Rankine-Hugoniot Curve for a normal shock wave, compared with isentropic flow for $\gamma = 1.4$
- Weak shocks ($M_1 < 1.4$) are almost isentropic: At $M_1 = 1.4$ the p_o loss is only 5%, whereas at $M_1 = 3.0$ it is 67%
- A normal shock wave at $M_1 = 1.0$ is vanishingly weak
- Weak shock waves can be desirable in certain situations

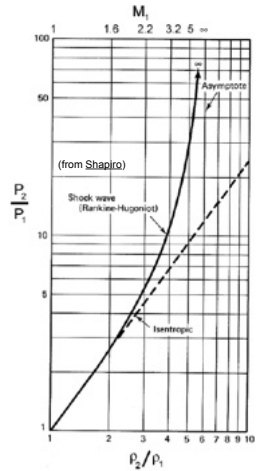

Figure 134

Numerical Prediction

Here is an example using the Calculator to find all the jump conditions across a normal shock at $M_1 = 2.0$ and $\gamma = 1.4$.

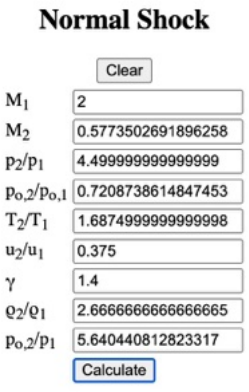

Figure 135: Example compressible flow calculator.

Ames Tables

TABLE II.—SUPERSONIC FLOW

$\gamma = 7/5$

M or M_1	$\frac{p}{p_t}$	$\frac{\rho}{\rho_t}$	$\frac{T}{T_t}$	β	$\frac{q}{p_t}$	$\frac{A}{A_*}$	$\frac{V}{a_*}$	ν	μ	M_2	$\frac{p_2}{p_1}$	$\frac{\rho_2}{\rho_1}$	$\frac{T_2}{T_1}$	$\frac{p_{t_2}}{p_{t_1}}$	$\frac{p_1}{p_{t_2}}$
1.00	0.5283	0.6339	0.8333	0	0.3698	1.000	1.00000	0	90.00	1.000	1.000	1.000	1.000	1.000	0.5283
1.01	.5221	.6287	.8306	.1418	.3728	1.000	1.00831	.04473	81.93	.9901	1.023	1.017	1.007	1.000	.5221
1.02	.5160	.6234	.8278	.2010	.3758	1.000	1.01658	.1257	78.64	.9805	1.047	1.033	1.013	1.000	.5160
1.03	.5099	.6181	.8250	.2468	.3787	1.001	1.02481	.2294	76.14	.9712	1.071	1.050	1.020	1.000	.5100
1.04	.5039	.6129	.8222	.2857	.3815	1.001	1.03300	.3510	74.06	.9620	1.095	1.067	1.026	.9999	.5039
1.05	.4979	.6077	.8193	.3202	.3842	1.002	1.04114	.4874	72.25	.9531	1.120	1.084	1.033	.9999	.4980
1.06	.4919	.6024	.8165	.3516	.3869	1.003	1.04925	.6367	70.63	.9444	1.144	1.101	1.039	.9997	.4920
1.07	.4860	.5972	.8137	.3807	.3895	1.004	1.05731	.7973	69.16	.9360	1.169	1.118	1.046	.9996	.4861
1.08	.4800	.5920	.8108	.4079	.3919	1.005	1.06533	.9680	67.81	.9277	1.194	1.135	1.052	.9994	.4803
1.09	.4742	.5869	.8080	.4337	.3944	1.006	1.07331	1.148	66.55	.9196	1.219	1.152	1.059	.9992	.4746
1.10	.4684	.5817	.8052	.4583	.3967	1.006	1.08124	1.336	65.38	.9118	1.245	1.169	1.065	.9989	.4689
1.11	.4626	.5766	.8023	.4818	.3990	1.010	1.08913	1.532	64.28	.9041	1.271	1.186	1.071	.9986	.4632
1.12	.4568	.5714	.7994	.5044	.4011	1.011	1.09699	1.735	63.23	.8966	1.297	1.203	1.078	.9982	.4576
1.13	.4511	.5663	.7966	.5262	.4032	1.013	1.10479	1.944	62.25	.8892	1.323	1.221	1.084	.9978	.4521
1.14	.4455	.5612	.7937	.5474	.4052	1.015	1.11256	2.160	61.31	.8820	1.350	1.238	1.090	.9973	.4467
1.15	.4398	.5562	.7908	.5679	.4072	1.017	1.12029	2.381	60.41	.8750	1.376	1.255	1.097	.9967	.4413
1.16	.4343	.5511	.7879	.5879	.4090	1.020	1.12797	2.607	59.55	.8682	1.403	1.272	1.103	.9961	.4360
1.17	.4287	.5461	.7851	.6074	.4108	1.022	1.13561	2.839	58.73	.8615	1.430	1.290	1.109	.9953	.4307
1.18	.4232	.5411	.7822	.6264	.4125	1.025	1.14321	3.074	57.94	.8549	1.458	1.307	1.115	.9946	.4255
1.19	.4178	.5361	.7793	.6451	.4141	1.026	1.15077	3.314	57.18	.8485	1.485	1.324	1.122	.9937	.4204
1.20	.4124	.5311	.7764	.6633	.4157	1.030	1.15828	3.558	56.44	.8422	1.513	1.342	1.128	.9928	.4154
1.21	.4070	.5262	.7735	.6812	.4171	1.033	1.16575	3.806	55.74	.8360	1.541	1.359	1.134	.9918	.4104
1.22	.4017	.5213	.7706	.6989	.4185	1.037	1.17319	4.057	55.05	.8300	1.570	1.376	1.141	.9907	.4055
1.23	.3964	.5164	.7677	.7162	.4198	1.040	1.18057	4.312	54.39	.8241	1.598	1.394	1.147	.9896	.4006
1.24	.3912	.5115	.7648	.7332	.4211	1.043	1.18792	4.569	53.75	.8183	1.627	1.411	1.153	.9884	.3958

Figure 136: Supersonic isentropic portion of the Ames tables.

Example

A normal shock wave is standing in the test section of a supersonic wind tunnel. Upstream of the shock wave we measure $M_1 = 3$, $p_1 = 0.5$ atm, and $T_1 = 200$ K. Find M_2, p_2, T_2, and u_2 downstream of the shock.

Solution

The solution is easy if we use tables or equations we have derived. For $M_1 = 3 \rightarrow \frac{p_2}{p_1} = 10.33$, $\frac{T_2}{T_1} = 2.679$, and $M_2 = 0.4752$

$$p_2 = \frac{p_2}{p_1} p_1 = 10.33(0.5) = 5.165 \text{ atm} \tag{358}$$

$$T_2 = \frac{T_2}{T_1} T_1 = 2.679(200) = 535.8 \text{ K} \tag{359}$$

$$c_2 = \sqrt{\gamma R T_2} = \sqrt{1.4(287)535.8} = 464 \text{ m/s} \tag{360}$$

$$u_2 = M_2 c_2 = 0.4752(464) = 220 \text{ m/s} \tag{361}$$

Note how we constructed our solutions with ratios multiplied by the known values.

Shock Wave Thickness

We now consider the question of the dissipative effects that account for the increase in the shock.

- In the absence of viscosity and heat conduction, compression waves tend to become infinitely steep
- Analysis underlying this result was based on a form of the equation of motion containing only pressure and inertial forces
- As the wave becomes very steep, viscous stresses must become appreciable, no matter how small the viscosity
- Heat condition effects must become substantial, no matter how small thermal conductivity is
- Thus a particle of fluid undergoes adiabatic effects

Shock Wave Thickness

- As viscosity and heat condition effects wipe out discontinuities in velocity and temperature, they resist steepening of the compression wave
- Steepening is controlled by viscous and heat condition effects
- When a compression wave has reached a stationary form, the spreading influences the viscosity and heat conduction is balanced by steepening influence of pressure and inertia forces

Shock Wave Thickness - Order of Magnitude

- Estimate the order of magnitude of the shock thickness
- A stationary form, pressure, viscous, and inertial terms in the equations of motion must be of comparable magnitude

Shock Wave Thickness

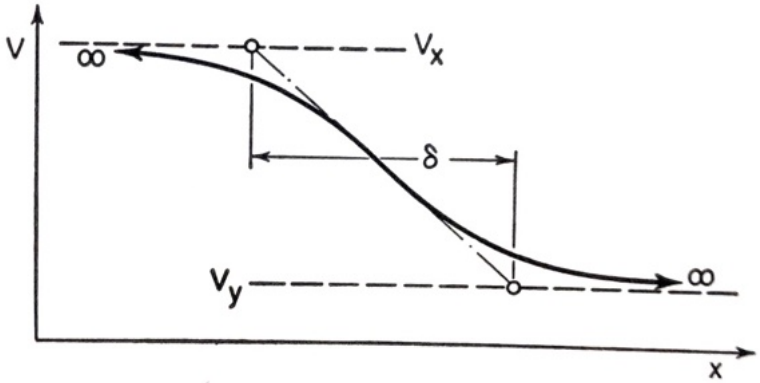

Figure 137: Description of the shock thickness.

The velocity curve approaches the end values of V_x and V_y asymptotically, so the thickness is really finite

Shock Wave Thickness - Order of Magnitude

- The entire change in velocity occurs in a very short distance
- We define a characteristic shock thickness δ

$$\delta = \frac{V_x - V_y}{(dV/dx)_{max}} \tag{362}$$

Since the longitudinal viscous stress is of the same order of magnitude as the inertial stress

$$\frac{4}{3}\mu^* \frac{d}{dx}\left(\frac{dV}{dx}\right) \approx \rho^* V^* \frac{dV}{dx} \tag{363}$$

Shock Wave Thickness - Order of Magnitude

Evaluating the derivatives in order of magnitude fashion and assuming that $4/3 \approx 1$ then we find

$$\mu^* \frac{(V_x - V_y)/\delta}{\delta} \approx \rho^* V^* \frac{V_x - V_y}{\delta} \tag{364}$$

from which we find

$$Re_{shock} = \frac{\rho^* V^* \delta}{\mu^*} \approx 1 \tag{365}$$

which says that the Reynolds number of the shock is based on the thickness and the fluid properties at T^* is on the order unity

Shock Wave Thickness - Order of Magnitude

We introduce relations form kinetic energy theory of gases and we can show by order of magnitude

$$\frac{\delta^*}{l^*} \approx \frac{5}{8} Re_{shock} \tag{366}$$

where l is the mean molecular path.

- It is clear that the shock thickness is on the order of a mean free path
- Thermodynamic equilibrium does not prevail within a shock, and the analysis of a shock from continuum considerations at best gives approximate results for the shock structure
- Kinetic theory or even quantum mechanics will be necessary for further analysis

Shock Thickness - Perfect Gas

- Structure of shock waves can be investigated by solving the exact NSE
- Results are more accurate than our analysis
- Shapiro and Kline have developed the following formula relation shock thickness as a function of other variables

$$\frac{\rho_x c_x \delta}{\mu_x} = \frac{D}{(\gamma+1)M_x^*} \frac{M_x^*+1}{M_x^*-1}\left[\left(\frac{\gamma+1}{2}\right)\left(1-\frac{\gamma-1}{\gamma+1}M_x^{*2}\right)\right]^{1/2-n} \left[1 \pm \sqrt{1+\frac{8\gamma(\gamma+1)}{3Pr^*}\frac{1}{D^2}\frac{(M_x^*-1)^2}{M_x^*}}\right] \tag{367}$$

where

$$D = \frac{4}{3} + \frac{2\gamma}{Pr^*} - \frac{\gamma+1}{2Pr^*}\frac{M_x^{*2}+1}{M_x^*} \tag{368}$$

and n is the exponent in a viscosity temperature relationship of $\mu \approx T^n$

Shock Thickness - Perfect Gas

For very weak shocks this equation may be approximated as

$$\frac{\rho_x c_x \delta}{\mu_x} \approx \frac{4}{\gamma+1}\left(\frac{4}{3}+\frac{\gamma+1}{Pr^*}\right)\frac{1}{M_x^*-1} \tag{369}$$

- The thickness of a weak shock is inversely proportional to the strength of the shock if we choose the strength to be measured by $M_x^* - 1$
- Extremely weak shocks have shock thickness at normal pressure and temperature

Shock Thickness - Perfect Gas

If we use constants for air then we find these typical values. Typical results of thickness of shock wave. Note that x denotes properties before a shock and y after.

M_x^*	M_x	$\rho_x c_x \delta/\mu_x$	$\frac{\delta/l_x}{4}$
1.36	1.5	8.0	4
1.63	2	4.6	2
1.96	3	3.1	2
2.14	4	2.9	2
2.24	5	2.9	2
2.30	6	2.9	2
2.33	7	3.0	2
2.36	8	3.1	2
2.38	9	3.3	2
2.39	10	3.4	2
2.45	∞	∞	∞

Shock Wave Thickness

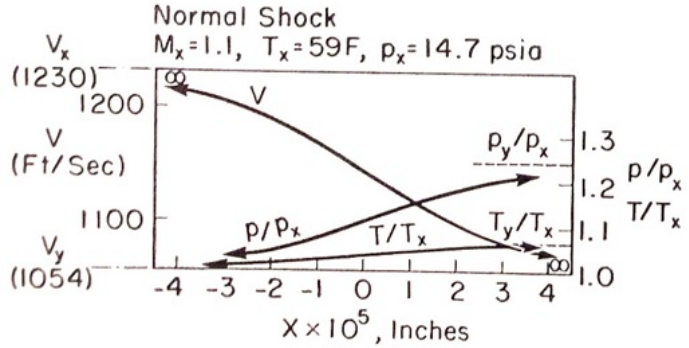

Figure 138: Thickness of a compression shock at normal atmospheric pressure and temperature is very small and thus justifies the approximation that the shock is a discontinuity in continuum mechanics.

Shock Wave Thickness

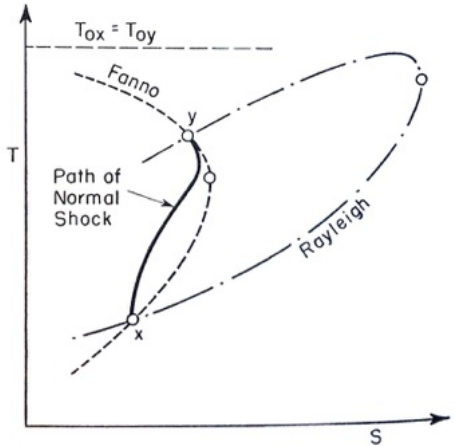

Figure 139: Variation of properties across a normal shock. $T - S$ diagram.

Shock Wave Thickness

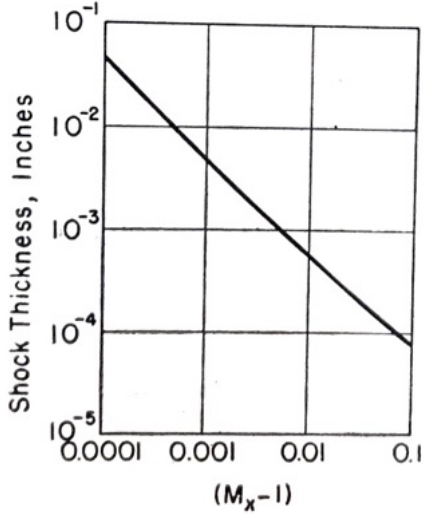

Figure 140: Thickness of a normal shock at standard atmospheric pressure and temperature.

Class Summary

- Stagnation properties (total) across normal shock waves
- Graphs of normal shock waves
- Entropy
- Shock strength
- Shock thickness
- Examples

Next Time

- Hugoniot
- Weak and strong normal shock waves
- Moving normal shock waves

Class Overview

- Hugoniot
- Weak and strong normal shock waves
- Moving normal shock waves

“A hypothetical theory is necessary, as a preliminary step, to reduce the expression of the phenomena to simplicity and order before it is possible to make any progress in framing an abstractive theory,”

William John Macquorn Rankine

Outlines of the Science of Energetics, in Proceedings of the Philosophical Society of Glasgow (1855)

Pierre-Henri Hugoniot

June 5, 1851 – February 1887, French

- Inventor, mathematician, and physicist who worked on fluid mechanics
- Professor of mechanics and ballistics at the School of Artillery Lorient, Deputy Director of the Central Laboratory of the artillery Navy (Captain), assistant professor of mechanical engineering at the Ecole Polytechnique
- Formulated Rankine-Hugoniot equation in "The propagation of movement in bodies, particularly in perfect gases."
- Died at 36

Hugoniot
courtesy of Ecole Polytechnique Archives

S.A.E. Miller, Ph.D., saem@ufl.edu

William John Macquorn Rankine

5 July 1820 – 24 December 1872, Scottish

- Civil engineering, physics, mathematics, thermodynamics and laws, botany, music theory, number theory, Rankine cycle
- Singer, pianist, cellist
- Regius Professor of Civil Engineering and Mechanics at the University of Glasgow
- A prominent legal and banking family
- Reduce the phenomena of heat to a mathematical form
- Queen Victoria's visit to Scotland, he organized a large bonfire situated on Arthur's Seat, constructed with radiating air passages under the fuel. The bonfire served as a beacon to initiate a chain of other bonfires across Scotland.
- Volunteer rifleman and founder of naval architecture in Scotland.

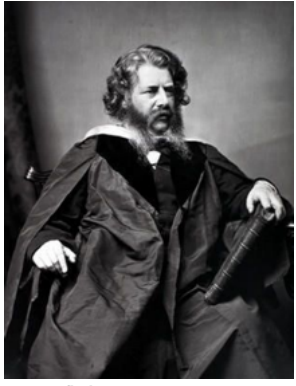

S.A.E. Miller, Ph.D., saem@ufl.edu

Hugoniot Equation

- Previously created relations involving Mach number and velocities
- Wave can be written of in terms of thermodynamic quantities only

From the continuity equation we can write

$$u_2 = u_1(\rho_2/\rho_1) \tag{370}$$

Substitute into the momentum equation

$$p_1 + \rho_1 u_1^2 = p_2 + \rho_2 \left(\frac{\rho_2}{\rho_1} u_1 \right)^2 \tag{371}$$

Solving for u_1^2

$$u_1^2 = \frac{p_2 - p_1}{\rho_2 - \rho_1} \left(\frac{\rho_2}{\rho_1} \right) \tag{372}$$

Hugoniot Equation

Also seek an equation for u_2. Write the continuity equation again

$$u_1 = u_2 \frac{\rho_2}{\rho_1} \tag{373}$$

and find a similar formula for u_2

$$u_2^2 = \frac{p_2 - p_1}{\rho_2 - \rho_1}\left(\frac{\rho_1}{\rho_2}\right) \tag{374}$$

Using the energy equation

$$h_1 + \frac{u_1^2}{2} = h_2 + \frac{u_2^2}{2} \tag{375}$$

Combining energy equation and relations for u_1^2 and u_2^2 yield

$$e_1 + \frac{p_1}{\rho_1} + \frac{1}{2}\left(\frac{p_2 - p_1}{\rho_2 - \rho_1}\left(\frac{\rho_2}{\rho_1}\right)\right) = e_2 + \frac{p_2}{\rho_2} + \frac{1}{2}\left(\frac{p_2 - p_1}{\rho_2 - \rho_1}\left(\frac{\rho_1}{\rho_2}\right)\right) \tag{376}$$

Hugoniot Equation

Simplifying Eqn. 376 yields

$$e_2 - e_1 = \frac{p_1 + p_2}{2}\left(\frac{1}{\rho_1} - \frac{1}{\rho_2}\right) \tag{377}$$

and we find the Hugoniot equation

$$\boxed{e_2 - e_1 = \frac{p_1 + p_2}{2}\underbrace{(\nu_1 - \nu_2)}_{\text{specific volumes}}} \tag{378}$$

- Relates thermodynamic properties across the shock
- No assumption of gas type
- A physical description is “change in internal energy is mean pressure across the shock times change in specific volume”
- Equilibrium thermodynamics – any state variable can be written as a function of any other two

Hugoniot Curve

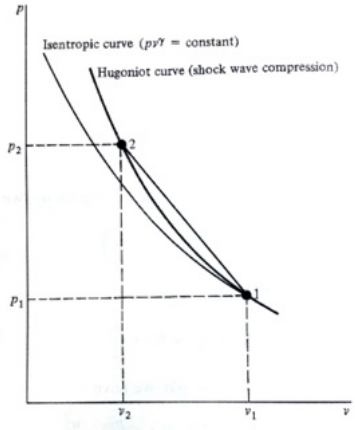

Figure 141: The Hugoniot curve for a shock wave.

Hugoniot Relation of Thermodynamic Variable

Let us seek the ratio of static thermodynamic pressure. Recall

$$u_1^2 = \frac{p_2 - p_1}{\rho_2 - \rho_1}\left(\frac{\rho_2}{\rho_1}\right) \tag{379}$$

substitute in $\nu = \frac{1}{\rho}$ and rearrange

$$\underbrace{\frac{p_2 - p_1}{\nu_2 - \nu_1}}_{\text{Slope of Hugoniot curve}} = -\left(\frac{\nu_1}{\nu_2}\right)^2 \tag{380}$$

Hugoniot Relation of Thermodynamic Variable

Assume that the gas is calorically perfect. We have

$$e = c_v T \tag{381}$$

and

$$T = pV/R \tag{382}$$

Substituting, we find the Hugoniot relation

$$\boxed{\frac{p_2}{p_1} = \frac{\left(\frac{\gamma+1}{\gamma-1}\right)\frac{\nu_1}{\nu_2} - 1}{\left(\frac{\gamma+1}{\gamma-1}\right) - \frac{\nu_1}{\nu_2}}} \tag{383}$$

where ν are the specific volumes before and after the shock, respectively.

Hugoniot Relation Across a Shock

- Let us show the Hugoniot equation holds with our previous developments
- Recall from a previous example where we found the following relations for a $M_1 = 3$ shockwave

$M_1 = 3$	$M_2 = 0.4752$
$p_1 = 0.5$ atm	$p_2 = 5.165$ atm
$T_1 = 200$ K	$T_2 = 535.8$ K
$u_1 = 850.4$ m/s	$u_2 = 220$ m/s
$\rho_1 = 0.8798$ kg/m^3	$\rho_2 = 3.392$ kg/m^3

Do these relations make physical sense?

Hugoniot Relation Across a Shock

Check previously developed approach with the Hugoniot relation. First find the ratio of specific volumes

$$\frac{\rho_2}{\rho_1} = \frac{\nu_1}{\nu_2} = \frac{3.392}{0.8798} = 3.855 \tag{384}$$

And now using the Hugoniot relation for the ratio of static thermodynamic pressures

$$\frac{p_2}{p_1} = \frac{\left(\frac{\gamma+1}{\gamma-1}\right)\frac{\nu_1}{\nu_2} - 1}{\left(\frac{\gamma+1}{\gamma-1}\right) - \frac{\nu_1}{\nu_2}} = \frac{\frac{2.4}{0.4}3.855 - 1}{\frac{2.4}{0.4} - 3.855} \boxed{= 10.32} \tag{385}$$

For calorically perfect approach

$$\frac{p_2}{p_1} = \boxed{10.33} \tag{386}$$

Summary of Rankine-Hugoniot Equations

$$\frac{p_2}{p_1} = \frac{2\gamma}{\gamma+1}M_1^2 - \frac{\gamma-1}{\gamma+1} = \frac{\frac{\gamma+1}{\gamma-1}\frac{\rho_2}{\rho_1} - 1}{\frac{\gamma+1}{\gamma-1} - \frac{\rho_2}{\rho_1}} \tag{387}$$

$$\frac{T_2}{T_1} = \frac{\left(1 + \frac{\gamma-1}{2}M_1^2\right)\left(\frac{2\gamma}{\gamma-1}M_1^2 - 1\right)}{M_1^2\left(\frac{2\gamma}{\gamma-1} + \frac{\gamma-1}{2}\right)} \tag{388}$$

$$\frac{\rho_2}{\rho_1} = \frac{\nu_1}{\nu_2} = \frac{(\gamma+1)M_1^2}{(\gamma-1)M_1^2 + 2} \tag{389}$$

Limiting Forms of Stationary Normal Shock Waves

Strength of shock waves defined by ratio of $\triangle p$ across shock divided by upstream pressure p_1. We write

$$\frac{p_2}{p_1} = \frac{2\gamma M_1^2}{\gamma+1} - \frac{\gamma-1}{\gamma+1} \rightarrow \boxed{\frac{p_2 - p_1}{p_1} = \frac{2\gamma}{\gamma+1}(M_1^2 - 1)} \tag{390}$$

Please be careful, this is different than strong versus weak shocks in upcoming oblique shock theory.

Strong Shocks

Consider what happens when M_1 approaches ∞

$$\lim_{M_1 \to \infty} M_2 \cong \sqrt{\frac{\gamma - 1}{2\gamma}} \tag{391}$$

$$\lim_{M_1 \to \infty} \frac{T_2}{T_1} \to \infty \tag{392}$$

$$\lim_{M_1 \to \infty} \frac{p_2}{p_1} \to \infty \tag{393}$$

$$\lim_{M_1 \to \infty} \frac{\rho_2}{\rho_1} = \frac{u_1}{u_2} = \frac{\gamma + 1}{\gamma - 1} \tag{394}$$

$$\lim_{M_1 \to \infty} \frac{p_{o2}}{p_{o1}} = \exp[-(S_2 - S_1)/R] \cong \left(\frac{\gamma + 1}{\gamma - 1}\right)^{\frac{\gamma}{\gamma - 1}} \left(\frac{\gamma + 1}{M_1^2 2\gamma}\right)^{\frac{1}{\gamma - 1}} \tag{395}$$

Remember in this limit gas will disassociate.

Weak Shocks

Let us examine the other case involving the weak shock. Recall the equation relating Mach numbers across the stationary normal shock.

$$M_2^2 = \frac{M_1^2 + \frac{2}{\gamma-1}}{\frac{2\gamma}{\gamma-1}M_1^2 - 1}. \tag{396}$$

Replace M_1^2 with $1 + \epsilon$, where ϵ is a small positive real value. We find

$$M_2^2 = \frac{1 + \epsilon + \frac{2}{\gamma-1}}{\frac{2\gamma}{\gamma-1}(1+\epsilon) - 1} = \left(1 + \frac{\gamma-1}{\gamma+1}\epsilon\right)\left(1 + \frac{2\gamma}{\gamma+1}\epsilon\right)^{-1} \tag{397}$$

$$\cong 1 + \left(\frac{\gamma-1}{\gamma+1} - \frac{2\gamma}{\gamma+1}\right)\epsilon = 1 - \epsilon \tag{398}$$

$$= 2 - M_1^2 \tag{399}$$

Weak Shocks

We perform a similar perturbation analysis for the other thermodynamic ratios

$$\frac{p_2}{p_1} = 1 + \frac{2\gamma}{\gamma+1}(M_1^2 - 1) \tag{400}$$

$$\frac{T_2}{T_1} = 1 - 2\left(\frac{\gamma-1}{\gamma+1}\right)(M_1^2 - 1) \tag{401}$$

$$\frac{u_2}{u_1} = 1 - \frac{2}{\gamma+1}(M_1^2 - 1) \tag{402}$$

and

$$\frac{\rho_2}{\rho_1} = 1 + \frac{2}{\gamma+1}(M_1^2 - 1) \tag{403}$$

Weak Shocks

The entropy relation is

$$\frac{S_2 - S_1}{R} \cong \frac{\gamma + 1}{12\gamma^2}\left(\frac{p_2 - p_1}{p_1}\right)^3 \tag{404}$$

The Hugoniot equation is now

$$\frac{\triangle p}{p} = \frac{\gamma \triangle \rho}{\rho} \tag{405}$$

Notice this equation does not involve T. And for very weak shocks it is shown that

$$M_1 \cong 1 + \epsilon \tag{406}$$

Moving Normal Shock Waves

Consider shocks that move relative to the observer

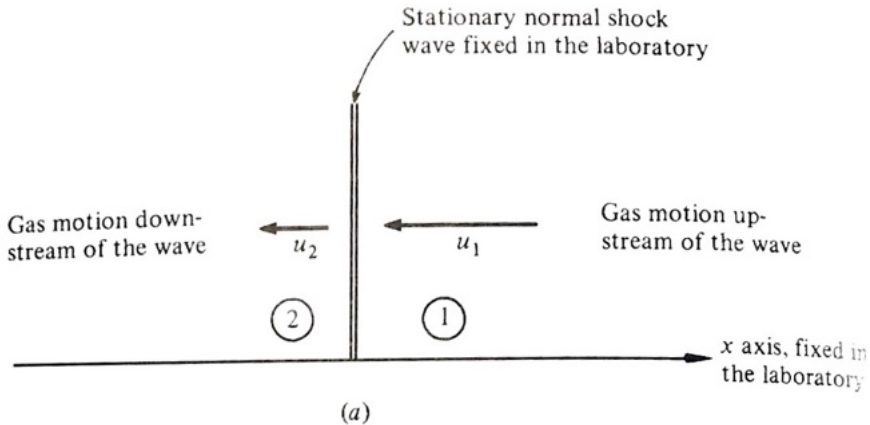

Figure 142: Schematic of the stationary normal shock.

Moving Normal Shock Waves

- Introduce new variable, u_p, which is the induced velocity of the fluid behind the shock wave.
- W is the velocity of the wave

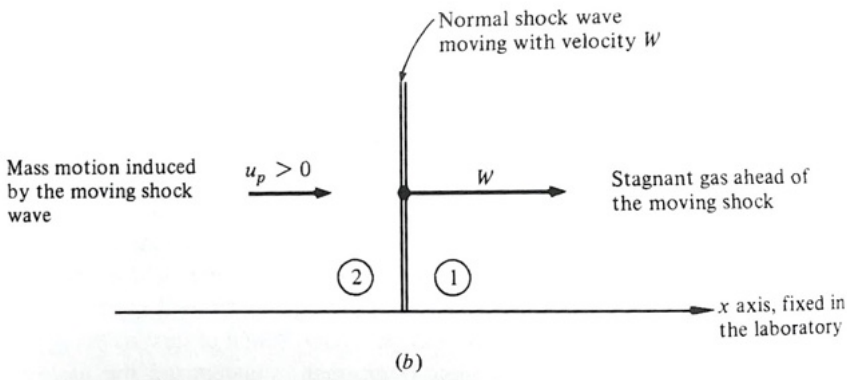

Figure 143: Schematic of the moving normal shock wave.

Moving Normal Shock Waves

Notes on moving normal shock waves

- Same physics, but we learn much by changing our references
- For stationary shock set $u_1 = 0$
  - Must move at velocity W to obtain corresponding properties as corresponding stationary case
- For stationary wave properties depend on x
- For moving wave properties depend on x and t

We can now introduce the new relation between u_1 and W

$$|u_1| = |W|, \tag{407}$$

where W is the velocity of the shock wave.

Moving Normal Shock Waves

- Now analyze mathematically the problem of moving normal shock waves.
- Recall conservation equations derived for the normal shock wave.

Mass

$$\rho_1 u_1 = \rho_2 u_2 \tag{408}$$

Momentum

$$p_1 + \rho_1 u_1^2 = p_2 + \rho_2 u_2^2 \tag{409}$$

and energy

$$h_1 + \frac{u_1^2}{2} = h_2 + \frac{u_2^2}{2} \tag{410}$$

Moving Normal Shock Waves

- Previously, u_1 and u_2 are relative velocities before and after the shock wave.
- Shock wave is now moving
- u_1 and u_2 remain relative to the shock wave.
- Let
  - W be the velocity of gas ahead of shock wave, relative to the wave
  - $W - u_p$ be the velocity of gas behind the shock wave, relative to the wave

Moving Normal Shock Waves

Substitute these new relations into our equations of motion. We obtain for mass

$$\rho_1 W = \rho_2 (W - u_p) \tag{411}$$

momentum

$$p_1 + \rho_1 W^2 = p_2 + \rho_2 (W - u_p)^2 \tag{412}$$

and energy

$$h_1 + \frac{W^2}{2} = h_2 + \frac{(W - u_p)^2}{2} \tag{413}$$

Here, our new governing equations are for a shock wave with velocity W.

Moving Normal Shock Waves

Let us rewrite the continuity equation as

$$W - u_p = W\left(\frac{\rho_1}{\rho_2}\right) \tag{414}$$

or

$$W = (W - u_p)\frac{\rho_2}{\rho_1} \tag{415}$$

Substitute this form of the continuity equation into the momentum equation

$$p_1 + \rho_1 W^2 + p_2 + \rho_2 W^2 \left(\frac{\rho_1}{\rho_2}\right)^2 \tag{416}$$

Moving Normal Shock Waves

We now rearrange the resulting equation that is a combination of the continuity and momentum equation. Solving for the difference of p

$$p_2 - p_1 = \rho_1 W^2 \left(1 - \frac{\rho_1}{\rho_2}\right) \tag{417}$$

Then W is

$$W^2 = \frac{p_2 - p_1}{\rho_1 \left(1 - \frac{\rho_1}{\rho_2}\right)} \tag{418}$$

Now simplifying into a form that is easier for calculations

$$W^2 = \frac{p_2 - p_1}{\rho_2 - \rho_1} \left(\frac{\rho_2}{\rho_1}\right) \tag{419}$$

We find an interesting form for ratios of pressure and density with W.

Moving Normal Shock Waves

Let us resubstitute the form of W^2 with the continuity equation

$$(W - u_p)^2(\rho_2/\rho_1)^2 = \frac{p_2 - p_1}{\rho_2 - \rho_1}\left(\frac{\rho_2}{\rho_1}\right) \tag{420}$$

Dividing both sides by $(\rho_1/\rho_2)^2$

$$(W - u_p)^2 = \frac{p_2 - p_1}{\rho_2 - \rho_1}\left(\frac{\rho_1}{\rho_2}\right) \tag{421}$$

We have obtained an equation that relates differences in u_p and W dependent on density and pressure.

Moving Normal Shock Waves

Combine this equation with the energy equation

$$e_1 + \frac{p_1}{\rho_1} + \frac{1}{2}\left(\frac{p_2 - p_1}{\rho_2 - \rho_1}\left(\frac{\rho_2}{\rho_1}\right)\right) = e_2 + \frac{p_2}{\rho_2} + \frac{1}{2}\left(\frac{p_2 - p_1}{\rho_2 - \rho_1}\left(\frac{\rho_1}{\rho_2}\right)\right) \tag{422}$$

which we can simplify to

$$e_2 - e_1 = \frac{p_1 + p_2}{2}\left[\frac{1}{\rho_1} - \frac{1}{\rho_2}\right] \tag{423}$$

or

$$e_2 - e_1 = \frac{p_1 + p_2}{2}(\nu_1 - \nu_2) \tag{424}$$

We have once again found the Hugoniot equation! Thermodynamic properties are independent of the frame of reference.

Moving Normal Shock Waves

- No known analytical solution to this set of equations
- Equations must be solved numerically

If we assume a calorically perfect gas

$$e = c_v T \text{ and } V = RT/p \tag{425}$$

We can solve for

$$\boxed{\frac{T_2}{T_1} = \frac{p_2}{p_1}\left(\frac{\frac{\gamma+1}{\gamma-1} + \frac{p_2}{p_1}}{1 + \frac{\gamma+1}{\gamma-1}\frac{p_2}{p_1}}\right)} \tag{426}$$

and

$$\boxed{\frac{\rho_2}{\rho_1} = \frac{1 + \frac{\gamma+1}{\gamma-1} + \frac{p_2}{p_1}}{\frac{\gamma+1}{\gamma-1} + \frac{p_2}{p_1}}} \tag{427}$$

which give the ratios of thermodynamic pressures across the moving shock in terms of the pressure ratio.

Moving Normal Shock Waves

Solution approach follows exactly one we used before for stationary shocks.

- For stationary shocks M_1 is most important parameter
- For moving shocks p_2/p_1 is most important parameter
- Moving shock wave has a new Mach number which we call

$$\boxed{M_S = \frac{W}{c_1}} \tag{428}$$

where c_1 is the speed of sound before the moving shock

Let us find the induced velocity behind the shock

Moving Normal Shock Waves

Likewise, following the previous derivation of normal shock relation and using M_S we find

$$\frac{p_2}{p_1} = \frac{2\gamma}{\gamma+1}(M_S^2 - 1) + 1 \tag{429}$$

and solving for M_S

$$\boxed{M_S = \left(\frac{\gamma+1}{2\gamma}\left(\frac{p_2}{p_1} - 1\right) + 1\right)^{\frac{1}{2}}} \tag{430}$$

And now solving for W

$$\boxed{W = c_1\left(\frac{\gamma+1}{2\gamma}\left(\frac{p_2}{p_1} - 1\right) + 1\right)^{\frac{1}{2}}} \tag{431}$$

We have now related the wave velocity to the pressure ratio.

Moving Normal Shock Waves

Now using the continuity equation we can write

$$u_p = W\left(1 - \frac{\rho_1}{\rho_2}\right) \tag{432}$$

Substituting relations for T_2/T_1 and W into this equation yields

$$\boxed{u_p = \frac{c_1}{\gamma}\left(\frac{p_2}{p_1} - 1\right)\left(\frac{\frac{2\gamma}{\gamma+1}}{\frac{p_2}{p_1} + \frac{\gamma-1}{\gamma+1}}\right)^{\frac{1}{2}}} \tag{433}$$

Therefore $u_p = f(c_1, p_2/p_1, \gamma)$.

Class Summary

- Hugoniot
- Weak and strong normal shock waves
- Moving normal shock waves

Next Time

- Induced velocity behind shocks
- Reflected shock waves
- Rayleigh Pitot formula

Class Overview

- Induced velocity behind shocks
- Reflected shock waves
- Rayleigh-Pitot equation

“The more important fundamental laws and facts of physical science have all been discovered, and these are now so firmly established that the possibility of their ever being supplanted in consequence of new discoveries is exceedingly remote. Nevertheless, it has been found that there are apparent exceptions to most of these laws, and this is particularly true when the observations are pushed to a limit, i.e., whenever the circumstances of experiment are such that extreme cases can be examined.” Lord Rayleigh

Induced Velocity Behind a Shock

Figure 144: Induced velocity behind a nuclear explosion blast wave causes the trees to bend and break.

Moving Shock Waves

All shock waves are in motion, but if we change our reference we can learn new physics

- Velocity induced by shock wave, behind the shock
- Inducted velocity can be very large
- Velocity induced is always in the direction of the wave
- Can we find Mach number behind the wave if we know the velocity and temperature rise? Let us try ...

Moving Shock Waves

Seek M_p, induced Mach number after a moving shock wave

$$M_p = \frac{u_p}{c_2} = \frac{u_p}{c_1}\frac{c_1}{c_2} = \frac{u_p}{c_1}\sqrt{\frac{T_1}{T_2}} \tag{434}$$

Substituting relations for T_2/T_1 and u_p into this expression

$$\boxed{M_p = \frac{u_p}{c_2}} = \frac{1}{\gamma}\left(\frac{p_2}{p_1} - 1\right)\left(\frac{\frac{2\gamma}{\gamma+1}}{\frac{p_2}{p_1} + \frac{\gamma-1}{\gamma+1}}\right)^{\frac{1}{2}}\left[\frac{1 + \frac{\gamma+1}{\gamma-1}\frac{p_2}{p_1}}{\frac{\gamma+1}{\gamma-1}\left(\frac{p_2}{p_1}\right) + \left(\frac{p_2}{p_1}\right)^2}\right]^{\frac{1}{2}} \tag{435}$$

Moving Shock Waves

What is the maximum possible induced Mach number? Let us take the limit

$$\lim_{p_2/p_1 \to \infty} \left(\frac{u_p}{c_2} \right) = \left(\frac{2}{\gamma(\gamma - 1)} \right)^{\frac{1}{2}} \tag{436}$$

- Limit is $M_p = 1.89$ for $\gamma = 1.40$
- How does M_p change with varying γ?
- Outcome, induced Mach number and flow-field can be supersonic
- $M_p > 1$ is very unlikely in practice, but more common in high-speed flight-vehicles

Moving Shock Waves

Important notes on total conditions

- h_o conserved in standing normal shock
- h_o not conserved for moving normal shocks, $h_{o2} = h_2 + \frac{u_p^2}{2}$
- p_o is not conserved across a moving normal shock
- p_{o2} also must be calculated from known properties of the induced mass motion
- How do we find the total properties? Via energy equation

$$\rho \frac{Dh_o}{Dt} = \frac{dp}{dt} \tag{437}$$

$\therefore$ Flow is unsteady. Therefore $\frac{dp}{dt} \neq 0$ and $\therefore \frac{Dh_o}{Dt} \neq 0$

Moving Shock Waves

We have found these equations and in summary...

TABLE 5.2 Comparison of Equations across Moving and Stationary Normal Shocks

Moving Normal-Shock Relations	Stationary Normal-Shock Relations
$M_1 = \frac{0}{a_1} = 0$	$M_1 = \frac{S}{a_1}$
$p_{o1} = p_1$	$p_{o1} = p_1\left(1 + \frac{\gamma - 1}{2}M_1^2\right)^{\gamma/(\gamma-1)}$
$T_{o1} = T_1$	$T_{o1} = T_1\left(1 + \frac{\gamma - 1}{2}M_1^2\right)$
$T_2 = T_1\left[1 + \frac{\gamma - 1}{2a_1^2}(2SV - V^2)\right]$	$T_2 = T_1\frac{2(\gamma - 1)}{(\gamma + 1)^2}\frac{\left(1 + \frac{\gamma - 1}{2}M_1^2\right)\left(\frac{2\gamma}{\gamma - 1}M_1^2 - 1\right)}{M_1^2}$
$M_2 = \frac{V}{a_2}$	$M_2 = \frac{S - V}{a_2} = \sqrt{\frac{M_1^2 + \frac{2}{\gamma - 1}}{\frac{2\gamma}{\gamma - 1}M_1^2 - 1}}$
$p_2 = p_1\left(1 + \gamma\frac{SV}{a_1^2}\right)$	$p_2 = p_1\left[\frac{2\gamma}{\gamma + 1}M_1^2 - \frac{(\gamma - 1)}{(\gamma + 1)}\right]$
$p_{o2} = p_2\left(1 + \frac{\gamma - 1}{2}\frac{V^2}{a_2^2}\right)^{\gamma/(\gamma-1)}$	$p_{o2} = p_2\left(1 + \frac{\gamma - 1}{2}M_2^2\right)^{\gamma/(\gamma-1)}$
$T_{o2} = T_2\left(1 + \frac{\gamma - 1}{2}\frac{V^2}{a_2^2}\right)$	$T_{o2} = T_2\left(1 + \frac{\gamma - 1}{2}M_2^2\right)$

Figure 145: Summary of moving shock relations relative to stationary shock relations.

Incident and Reflected Shocks

What happens when a shock wave reflects from a surface or a fluid structure?

- Consider linear acoustics
  - In acoustics the boundary condition is $\frac{dp}{d\hat{n}} = 0$
  - Unfortunately not always applicable
- The shock wave is a nonlinear phenomenon

Examine an experiment

Reflected Shock Waves

The shock wave travels through the shock tube and reflects. What happens to the shock?

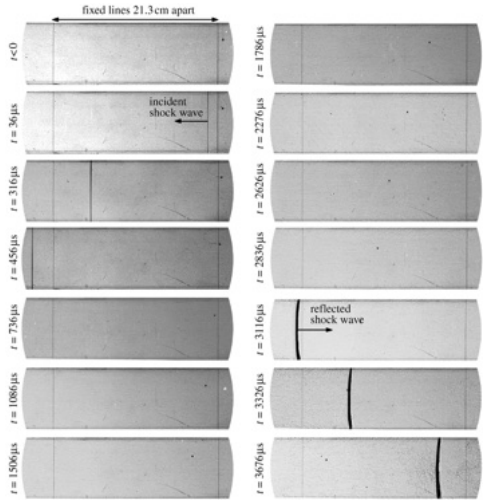

Figure 146: Schlieren images from a movie of a reflected shock.

Incident Shock

Diagram showing the initial position of the shock wave, which is moving to the right.

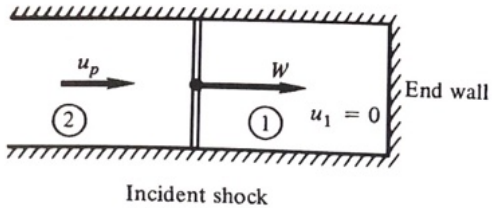

Figure 147: Schematic of the incident moving normal shock wave before impingement.

Reflected Shock

Diagram of the shock wave after reflection.

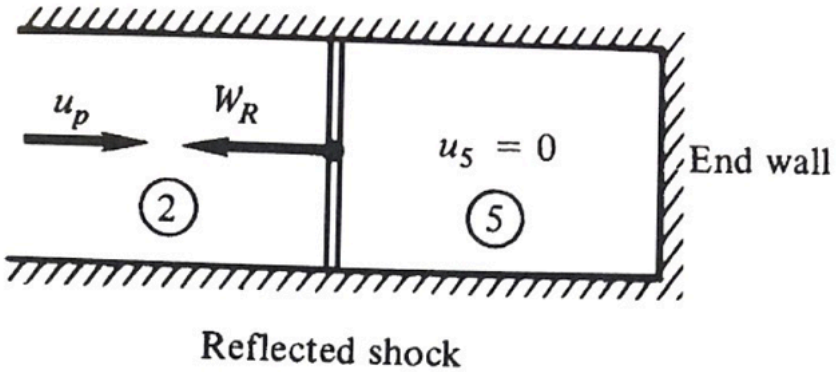

Figure 148: Schematic of the reflected moving normal shock wave after impingement.

Reflected Shock Waves

Additional notes on reflected waves

- $u = 0$ to the right of reflected shock (why?)
  - Conservation of mass
- W_R is velocity of the reflected shock opposed to W
- Strength of reflected shock must be dependent on $u_r = 0$
  - Why? Related to induced velocity behind reflected shock
- We can understand the physics by considering the wave motion on a graph of t versus x

Reflected Shock Waves

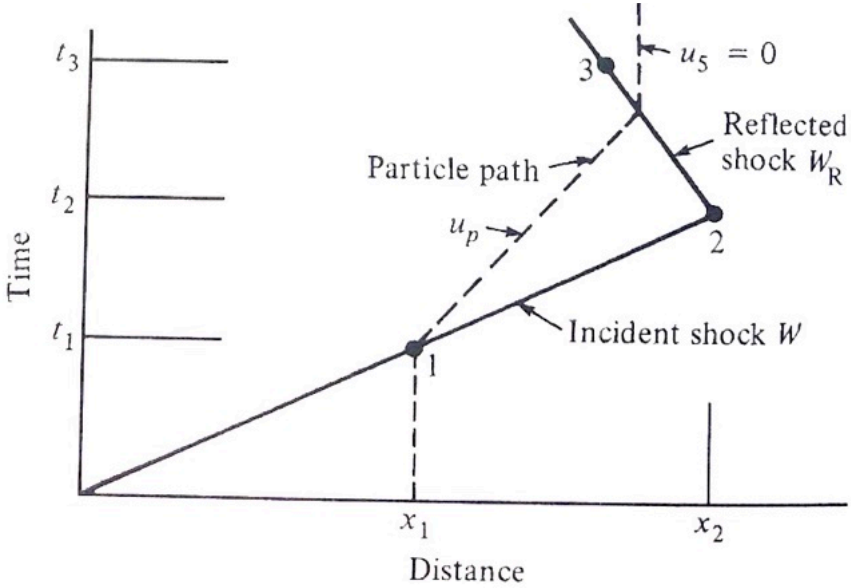

Reflected Shock Waves – Diagram of $x - t$

- Dashed line is the particle path
- Slopes are $1/W$ and $1/W_R$, respectively
- $|W_R| < |W|$, as observed in experiments
  - Do our predictions support our observation?
- $W_R + u_p$ is the velocity of the gas ahead of the shock wave relative to the wave
- W_R is the velocity of the gas behind the shock wave relative to the wave

Equations for Reflected Shock Waves

Let us analyze the reflected shock problem. The continuity equation is

$$\rho_1(W_R + u_p) = \rho_2 W_R \tag{438}$$

momentum equation

$$p_1 + \rho_2(W_R + u_p)^2 = p_2 + \rho_2 W_R^2 \tag{439}$$

and energy equation

$$h_1 + \frac{(W_R + u_p)^2}{2} = h_2 + \frac{W_R^2}{2} \tag{440}$$

where the incident shock Mach number is

$$M_S = \frac{W}{c_1} \tag{441}$$

and the reflected shock Mach number is

$$M_R = (W_R + u_p)/c_R \tag{442}$$

Reflected Shock Waves

- Does this system of equations have an analytical solution?
  - No.
  - Must use numerical approach if no assumptions are made
- Assumption: fluid is a calorically perfect gas
- Use the same solution approach that we previously developed

We find relation between reflected Mach number and incident Mach number

$$\frac{M_R}{M_R^2-1} = \frac{M_S}{M_S^2-1}\left(1+\frac{2(\gamma-1)}{(\gamma+1)^2}(M_S^2-1)\left(\gamma+\frac{1}{M_S^2}\right)\right)^{\frac{1}{2}} \tag{443}$$

Try and recover this equation yourself. The implication of this equation - the reflected shock properties are only a function of incident shock properties.

Reflected Shock Waves

Using the equations for moving normal shock waves developed previously, we find the relation

$$\triangle p_R = \frac{\left(\frac{3\gamma-1}{\gamma+1}\right)\triangle p - \frac{\gamma-1}{\gamma+1}}{1+\left(\frac{\gamma-1}{\gamma+1}\right)\triangle p} \tag{444}$$

Here $\triangle p_R$ is only function of $\triangle p$.

Reflected Shock Waves

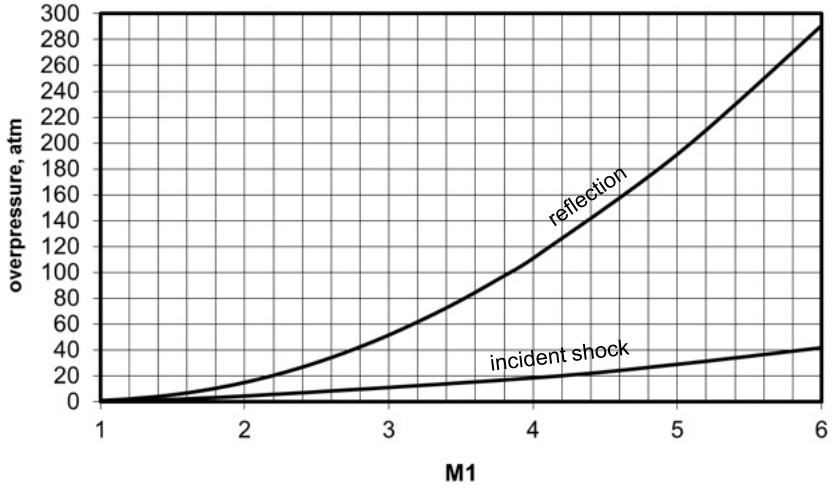

Figure 150: Normal-shock wave reflection over–pressure in air with $T_1 = 293$ K.

Summary – Reflected Shocks

Notes

- The reflected shock problem can easily be solved
  - Solve moving incident shock wave problem
  - Solver moving reflected shock wave problem, with $u_p = 0$.
- Boundary conditions of the reflected shock are driven by conservation of mass
- Properties continue to rise after each shock reflection
- It is not necessary to remember formulas for reflected shocks
  - Just use moving shock formulas

Thought experiment

- What happens if a shock wave keeps reflected within an enclosed pipe?
- What happens to shock waves that enter aircraft engine inlets?

Pitot-Static Probes in Supersonic Flow

- Previously developed theory for compressible flow and Pitot-static tubes
- Turn our attention to the theory and practice of Pitot-static tubes in supersonic flow.
- Previous equations do not apply because a normal shock wave will form if probe is placed in a flow with $M > 1$.
- Need to account for formation of shock and creation of entropy
- Classic marching problem

Henri Pitot

May 3, 1695 – December 27, 1771, French

- Hydraulic engineer and the inventor of the Pitot tube
- Assigned the task of measuring the flow in the river Seine
- Built Aqueduc de Saint-Clément near Montpellier and the extension of Pont du Gard in Nîmes
- Member of the French Academy of Sciences, and in 1740 a fellow of the Royal Society

S.A.E. Miller, Ph.D., saem@ufl.edu

Pitot Probes in Supersonic Flow

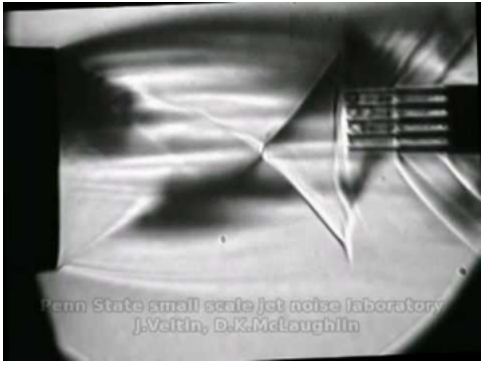

Figure 151: Four probe Pitot probe within supersonic jet flow. Note shocks in front of probe. Experiment conducted by McLaughlin and Veltin.

A short video is at https://www.youtube.com/watch?v=q6GoqZt-KBA

Rayleigh-Pitot Probe

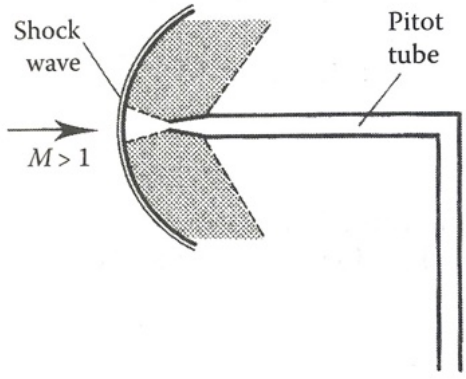

Figure 152: Diagram of a probe inserted into a supersonic flow.

Rayleigh-Pitot Probe

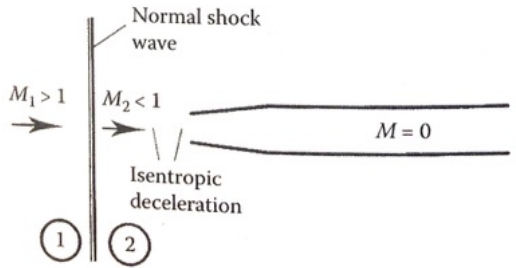

Figure 153: Diagram of a probe inserted into a supersonic flow.

Rayleigh-Pitot Probe

How would these probes be used within a wind tunnel?

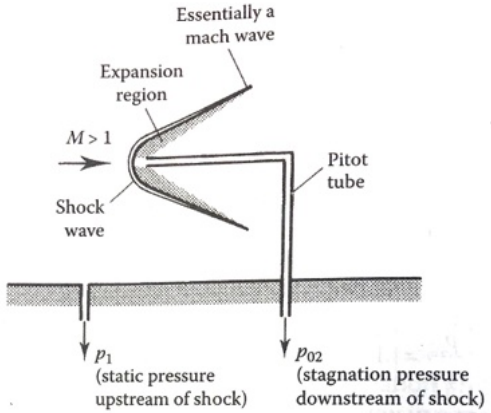

Figure 154: A wall mounted Rayleigh-Pitot probe.

Rayleigh-Pitot Probe

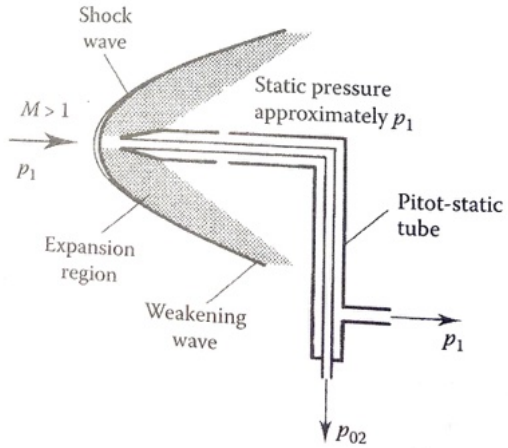

Figure 155: Diagram and notation of the Rayleigh-Pitot tube.

Rayleigh-Pitot Probe

- The introduction of the probe into the flow induces a shock wave
- If the probe was not present there is no shock wave
- The shock wave is standing
- Normally characterize the shock by M_1, but we wish to measure M_1. Problem is inverted.
- Seek a method to relate measurement with the probe to find M_1 and other properties

Recall the equation for stagnation pressure, static pressure, and Mach number

$$\frac{p_o}{p} = \left(1 + \frac{\gamma - 1}{2} M^2\right)^{\frac{\gamma}{\gamma - 1}} \tag{445}$$

Remember this is an equation for isentropic flow. We solve the equation for M^2

$$M^2 = \frac{2}{\gamma - 1}\left(\left(\frac{p_o}{p}\right)^{\frac{\gamma - 1}{\gamma}} - 1\right) \tag{446}$$

Rayleigh-Pitot Probe

Relate dynamic pressure to unknown quantities (we measure it)

$$\begin{aligned}\frac{1}{2}\rho u^2 &= \frac{\gamma}{2}\left(\frac{u^2}{\gamma p/\rho}\right)p = \frac{\gamma}{2}\left(\frac{u^2}{c^2}\right)p = \frac{\gamma}{2}M^2 p \\ &= \frac{\gamma}{\gamma-1}\left[\left(\frac{p_o}{p}\right)^{\frac{\gamma-1}{\gamma}} - 1\right]p\end{aligned} \tag{447}$$

We also note that

$$p_{\text{measured}} = p_{o2} = \frac{p_{o2}}{p_2}\left(\frac{p_2}{p_1}\right)p_1 \tag{448}$$

where $p_1 = p_\infty$ and $M_1 = M_\infty$

Rayleigh-Pitot Probe

We write the stagnation to static pressure ratio as (using normal shock relations)

$$\begin{aligned}\frac{p_{o2}}{p_2} &= \left(1+\frac{\gamma-1}{2}M_2^2\right)^{\frac{\gamma}{\gamma-1}} \\ &= \left[1+\left(\frac{\gamma-1}{2}\right)\left(\frac{M_1^2+\frac{2}{\gamma-1}}{\frac{2\gamma}{\gamma-1}M_1^2-1}\right)\right]^{\frac{\gamma}{\gamma-1}}\end{aligned} \tag{449}$$

Recall the corresponding static pressure ratio across a shock

$$\frac{p_2}{p_1} = \left(\frac{2\gamma}{\gamma+1}\right)M_1^2 - \frac{\gamma-1}{\gamma+1} \tag{450}$$

Rayleigh-Pitot Probe

We combine these two equations and simplify

$$\frac{p_{o2}}{p_1} = \left(\frac{\frac{\gamma+1}{2} M_1^2}{\frac{2\gamma}{\gamma+1} M_1^2 - \frac{\gamma-1}{\gamma+1}} \right)^{\frac{\gamma}{\gamma-1}} \left(\frac{2\gamma}{\gamma+1} M_1^2 - \frac{\gamma-1}{\gamma+1} \right) \tag{451}$$

And under further manipulation (simplification)

$$\boxed{\frac{p_{o2}}{p_1} = \frac{\gamma+1}{2} M_1^2 \left[\frac{(\gamma+1)^2 M_1^2}{4\gamma M_1^2 - 2(\gamma-1)} \right]^{\frac{1}{\gamma-1}}} \tag{452}$$

which is the Rayleigh-Pitot formula. Note that $p_1 = p_\infty, M_1 = M_\infty$, etc.

Example

Find the flow Mach number using a Pitot-static tube. We perform two measurements

- We measure static pressure as 20 kPa and total pressure as 32 kPa.
- A second measurement is performed and the static pressure is 20 kPa and the total pressure is 80 kPa.

Assume that $\gamma = 1.4$. Find the Mach number for both measurements.

Solution

- First ascertain if the flow Mach number is subsonic or supersonic.
- Examining the critical pressure ratio for $\gamma = 1.4$

$$\left(\frac{p_o}{p}\right)_{\text{critical}} = \left(\frac{\gamma+1}{2}\right)^{\frac{\gamma}{\gamma-1}} = 1.89293 \tag{453}$$

- For the first case $\frac{32\,\text{kPa}}{20\,\text{kPa}} = 1.60$, which is less than 1.89.
- This means the flow is subsonic. Why?
- For subsonic case, use the previously developed approach.
- Remember, do not use the incompressible Bernoulli equation.

Solution

- Check M for second measurement using the critical pressure ratio $\frac{80\text{ kPa}}{20\text{ kPa}} = 4$, therefore, the flow is supersonic. Why?
- Unfortunately, we require an iterative method (numerical) to find the solution. Appropriate technique was taught in numerical methods class.

Rewrite the Rayleigh-Pitot formula as

$$f(M) = AM^{2\gamma} - BM^2 + C = 0 \tag{454}$$

where

$$A = \frac{(\gamma+1)^{\gamma+1}}{2^{\gamma-1}}, B = 4\gamma\left(\frac{p_{o2}}{p_1}\right)^{\gamma-1}, \text{ and } C = 2(\gamma-1)\left(\frac{p_{o2}}{p_1}\right)^{\gamma-1} \tag{455}$$

Solution

The derivative of this function is

$$\frac{df}{dM}(M) = 2\gamma A M^{2\gamma-1} - 2BM \tag{456}$$

Use the Newton-Raphson algorithm to find a solution

$$M_{\text{new}} = M_{\text{old}} - \frac{f(M_{\text{old}})}{\frac{df}{dM}(M_{\text{old}})} = \frac{(2\gamma-1)AM_{\text{old}}^{2\gamma} - BM_{\text{old}}^2 - C}{2(\gamma A M_{\text{old}}^{2\gamma-1} - BM_{\text{old}})} \tag{457}$$

Using the given pressure ratio we find

$$A = 6.195766, B = 9.750166, \text{ and } C = 1.392881 \tag{458}$$

Iterate with a first guess, $M = 2$.

Solution

The result of the first five iterations of the Newton-Raphson algorithm are

n	M_{old}	$f(M)$	$\frac{df}{dM}$	M_{new}
1	2	5.54	21.4	1.74
2	1.74	1.104	13.11	1.65
3	1.65	0.10122	10.74129	1.64748
4	1.64748	0.00121	10.485	
5	1.64736	0	10.4822	—

- Tables of the Rayleigh-Pitot equation relating M and the pressure ratio.
- Therefore, use the tables or a numerical solver.
- These are provided to you by myself in the tables handout

An Online Calculator for Rayleigh-Pitot Probe

$$\frac{p_{o2}}{p_1} = \frac{\left(\frac{\gamma+1}{2}M_1^2\right)^{\frac{\gamma}{\gamma-1}}}{\left(\frac{2\gamma}{\gamma+1}M_1^2 - \frac{\gamma-1}{\gamma+1}\right)^{\frac{1}{\gamma-1}}}$$

Look at the online calculator https://saemiller.com/flow/SAEMiller_Comp_Calc.html

Figure 156: Example Rayleigh-Pitot calculation.

An Online Calculator for Rayleigh-Pitot Probe

Click calculate. The last line, p_{o2}/p_1 is the numerical solution.

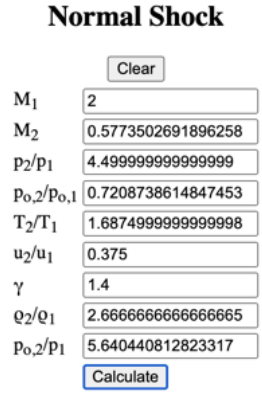

Figure 157: Example Rayleigh-Pitot calculation.

Are you able to write your own simple R-P calculator?

Class Summary

- Induced velocity behind shocks
- Reflected shock waves
- Rayleigh-Pitot equation

Next Time

- Air blast similarity theory
- Convergent-divergent nozzles and normal shock waves

Class Overview

- Air blast similarity theory
- Convergent-divergent nozzles and normal shock waves

“We knew the world would not be the same. A few people laughed, a few people cried, most people were silent. I remembered the line from the Hindu scripture, the Bhagavad-Gita: Vishnu is trying to persuade the Prince that he should do his duty and, to impress him, takes on his multi-armed form and says, Now I am become Death, the destroyer of worlds,”

Dr. J. Robert Oppenheimer

Blast Wave Theory

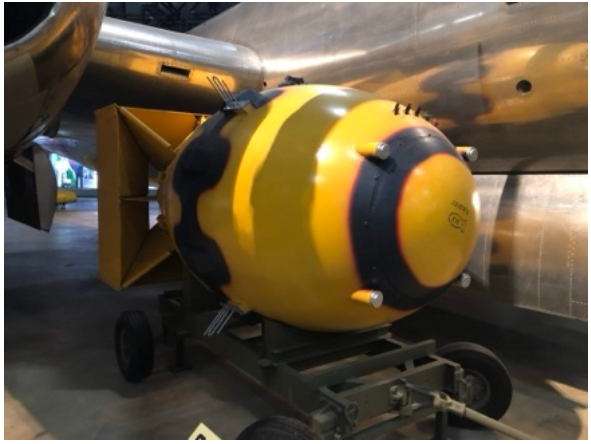

Figure 158: “Fat-Man,” Source: Miller.

Blast Wave Theory

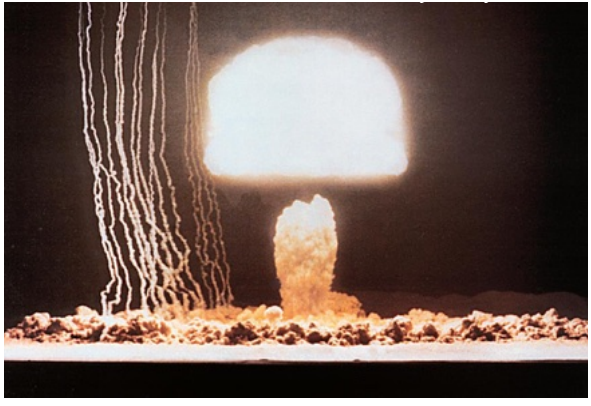

Figure 159: Bikini-Atoll blast.

Blast Wave Theory

The theory of the moving shock wave and flowfield produced by an intense spherical explosion in air – the airblast problem – was formulated by John von Neumann, Sir Geoffrey Taylor, and Leonid Sedov in the mid-20th century, and was driven by the development of the atomic bomb.

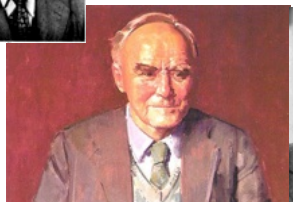

Figure 160: Various important figures at the time.

Blast Wave Theory

We seek to find a similarity theory for spherical shock waves created by points of energy

- Airblast problem examines the flow-field produced by an intense spherical explosion.
- See Thompson, Compressible Fluid Dynamics, Ch. 8.

To solve the problem, the following assumptions are made

- Perfect-gas atmosphere initially at rest
- Spherically-symmetric shock wave (isotropic)
- Strong shock wave, i.e. $p_2 >> p_1$ and $T_2 >> T_1$
- A large quantity of energy E is released at a point in space at $t = 0$

Blast Wave Theory

How do we provide such an energy release?

Consider the conventional explosives listed below:

- EGDN (ethylene glycol dinatrate) Nitrocellulose
- Nitroglycerin, PETN (Pentaerithrytol-tetranitrate)
- TNT (trinitrotoluene)
- RDX and C-4 (cyclo-trimethylene-trinitramine)
- ANFO (ammonium nitrate + fuel oil)

Some assumptions

- Assume that p_1 and T_1 of the undisturbed atmosphere compared with the much-larger p_2 and T_2
- Retain ρ_1, as ρ_2/ρ_1 approaches a value of six for infinite M_s as it goes to ∞

Blast Wave Theory

- Dimensional analysis
  - Method of repeating variables / Buckingham Π Theory
  - Independent variables are ρ_1 also called ρ_∞ , E, t, r is radius from blast center
  - Dependent variables are u, p, ρ, $T = p/\rho/R$.
  - The dimensions of the independent variables are: ρ_1, E, t, r
  - That is M/L3 ML2/T2 T L, respectively.
- Only one dimensionless combination of these variables

$$\eta = \frac{r}{\left(\frac{E}{\rho_\infty}\right)^{1/5} t^{2/5}} \tag{459}$$

Blast Wave Theory

- η is the similarity variable for the airblast problem
- A fusion detonation and a spec of dynamite produce similar flow-fields if they have the same value of η.
- Let $r = R$, the radius of the blast wave (moving normal shock wave)
- $\eta_{shock} = R/[(E/\rho_{atm})/t^{2/5}]$, describes the similarity solution for the blast wave itself. We can find
  - $Vs = dR/dt = (2/5)R/t$
  - The shock Mach number, $M_s = V_s/c_1$
- If the shock moves at constant speed, dR/dt is constant.
- As $dR/dt = 0.4R/t$, the shock wave slows down with increasing radius R, eventually decaying to an acoustic wave
  - Must be true, as it will require infinite energy E to drive a shock through the atmosphere at constant speed forever.

Blast Wave Theory

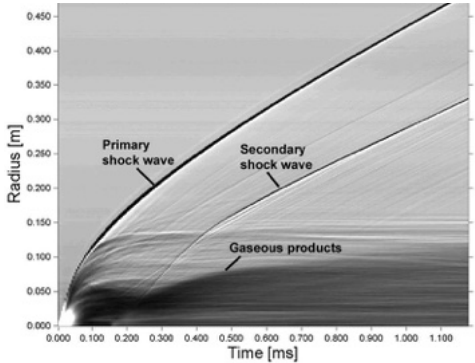

Figure 161: $x - t$ diagram of blast wave phenomenon. (image courtesy Penn State Gas Dynamics Lab)

Blast Wave Theory

- Previous figure shown was derived from a high-speed digital camera record of the explosion of 1 gram of PETN
- Incident shock wave follows η
- Shock wave slows down with increasing r
- Analysis is simpler than reality, but highly predictive
- Wave is weakened from by expansion that catch up to shock wave

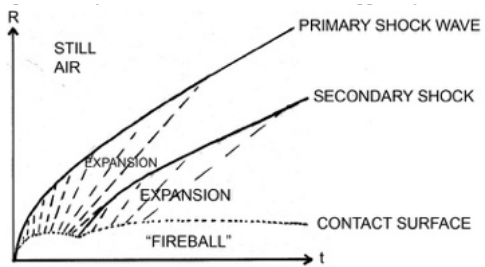

Figure 162: Schematic of spherical shock wave produced by point energy release.

Blast Wave Theory - Example

- Data on the shock-wave motion caused by the world's first atomic blast (Alamogordo NM, July 16, 1945).
- From the plot we see that at $t = 0.1$ sec the shock was at a radius $R = 210$ m from ground zero.
- We can use airblast similarity theory and the moving- shock calculation method described earlier to find the following:
- $V_s = 2/5(R/t) = 840$ m/s
- $M_s = 840/340 = 2.5$
- From the shock tables ($\gamma = 1.4$), $p_2/p_1 = 7.13$, $P_b > 7$ atm
- $T_2/T_1 = 2.14$, $T_b \approx 650$ K
- $\rho_2/\rho_1 = u_s/(u_s - u_g) = 3.33$
- $u_g = 588$ m/s
- $M_b = u_g/\sqrt{\gamma RT_b} = 1.15$
- M_b is the Mach number that would be seen by a fixed observer at $R = 210$ m, but no such observer would have survived the blast.

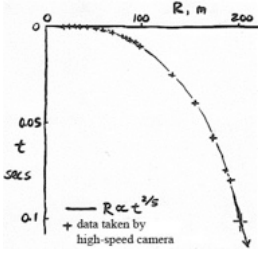

Figure 163: Blast wave position versus time.

Blast Wave Theory

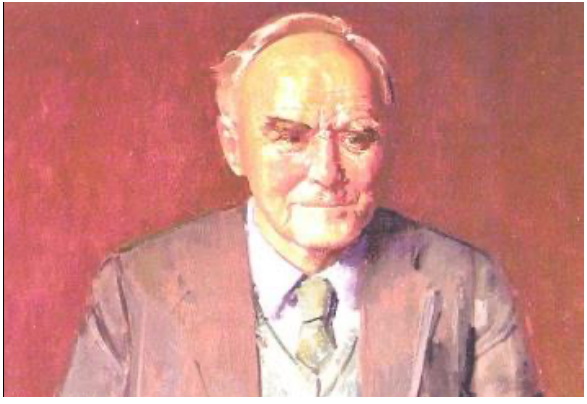

Figure 164: G. I. Taylor. Many discoveries in fluid dynamics, including one of three independent discoveries of spherical shock theory.

Blast Wave Theory

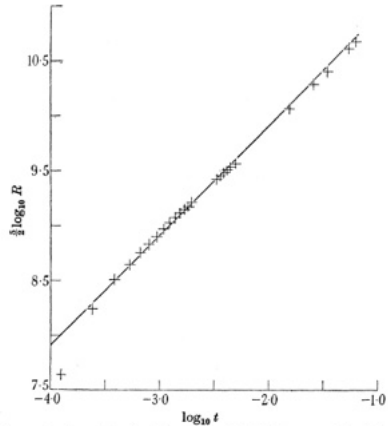

FIGURE 1. Logarithmic plot showing that $R^{\frac{5}{2}}$ is proportional to t.

Figure 165: History was made: Comparison of Alamogordo blast wave R versus t data with G. I. Taylor's similarity theory, derived more than 4 years before the blast occurred; a true prediction.

Blast Wave Theory

- Similarity theory further predicts that the density of the hot fireball of gas created by the explosion will be very small, almost zero.
- Thus the fireball is buoyant and rises in the colder surrounding atmosphere.
- The resulting circulation generates a rising toroidal vortex, the notorious mushroom cloud (not only for nuclear blasts, but also for any intense explosion).
- Circulation eventually causes u_g behind the shock to reverse, as seen by a fixed observer on the ground.

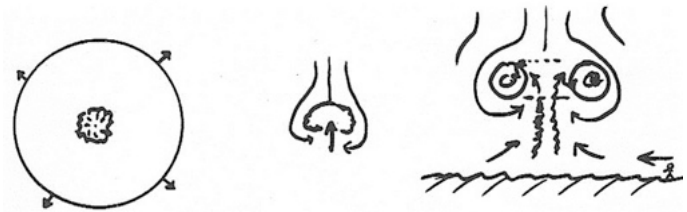

Figure 166: Sketches of the cloud.

Blast Wave Theory

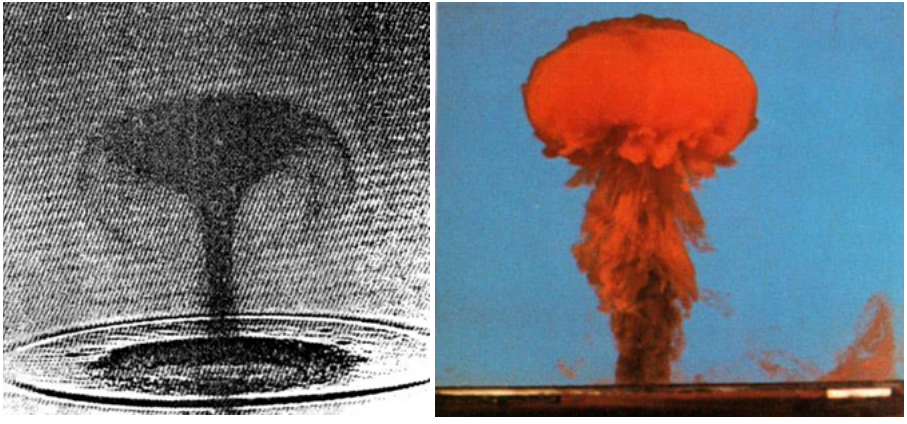

Figure 167: a) Llaser pulse deposits high energy density on the surface of water, creating a mushroom cloud on scale of $\approx$ 1 cm and b) Photo of the toroidal vortex generated in a water tank at CalTech for movie “The Day After”.

Blast Wave Theory

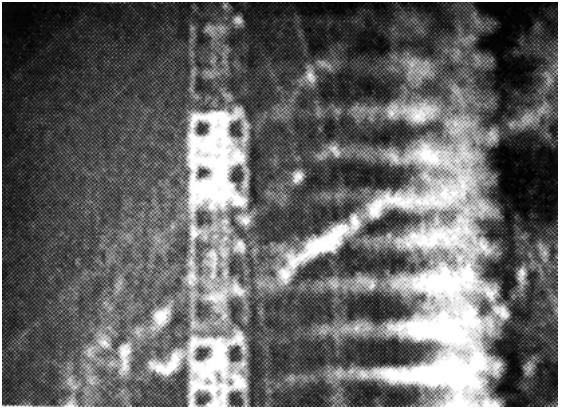

Figure 168: The shock wave from a nuclear blast, traveling left-to-right, passes a radio tower. Smoke trails form due to burning paint on the tower from the intense radiation. The smoke is then carried left-to-right by u_g after the shock. Slanted lines are burning, falling guy wires.

Blast Wave Theory

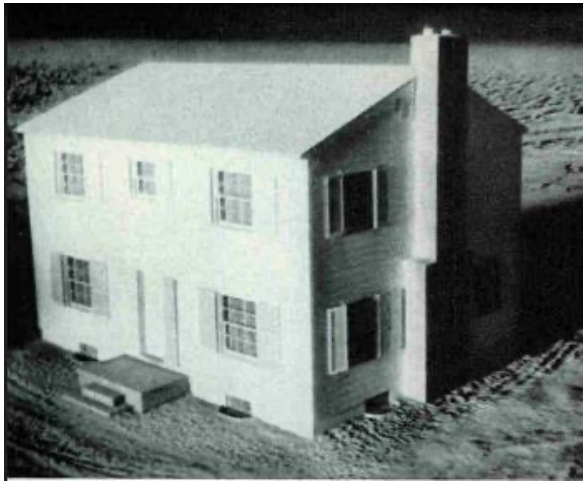

Figure 169: Before.

Blast Wave Theory

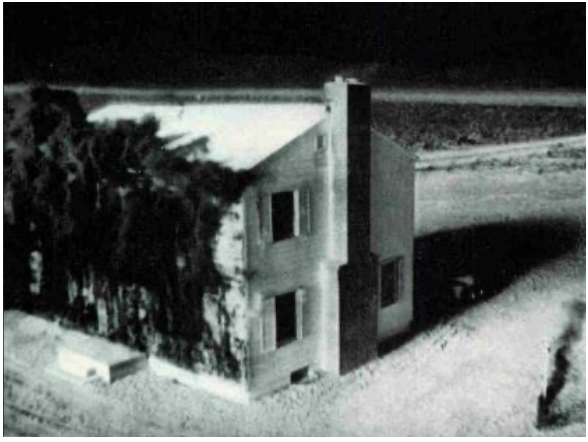

Figure 170: Immediately upon detonation, intense optical radiation burns the front of the house.

Blast Wave Theory

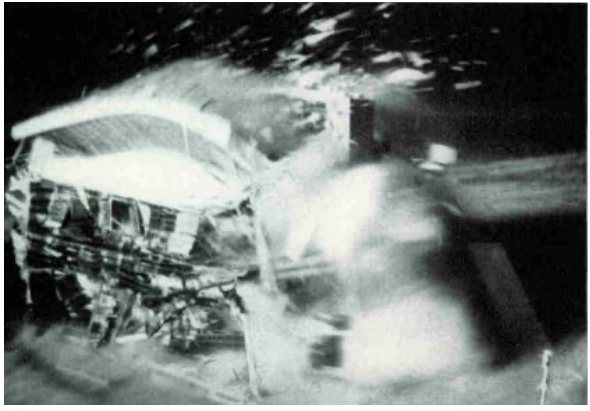

Figure 171: once the shock wave arrives, u_g behind the shock literally blows the house down. About a second later, the direction of u_g reverses and air rushes back toward ground zero.

Spherical Shock Theory - Considerations

- Solutions are self-similar
- Seek to match η between flow-fields
- Theory rests on instantaneous impulse of energy release
- What other aerospace flow-fields can be analyzed this way?
  - Hypersonic flow-fields can be considered by energy impulse methods
  - Shock tubes can be examined using impulse methods

Convergent-Divergent Nozzles and Shock Waves

- We previously examined isentropic flows through CD nozzles
- Examine non-isentropic flows with losses due to shock waves
- Shocks can stand or move through nozzles
  - What examples include moving shocks in nozzles?
  - When would we want a shock wave in a nozzle?

Convergent-Divergent Nozzles and Shock Waves

The schlieren shows shock waves and other phenomena within a nozzle. Let us identify them.

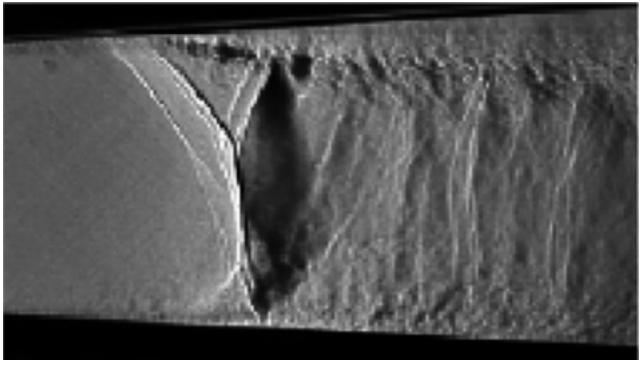

Figure 172: Schlieren image of a normal shock wave in a nozzle.

Video APS DFD Lele submission. In class we show a video produced by CFD of a time-dependent flow-field calculated with HPC.

Standing Shocks in Convergent-Divergent Nozzles

- How do we locate and analyze shock waves within nozzles?
- Consider the following flow and nozzle
  - A convergent-divergent nozzle has an exit area to throat area of $(A_e/A_t) = 3$
  - A normal shock stands at area location $A/A_t = 2$
- We seek to find the ratio of exit to reservoir pressure ratio
- Remember these notation

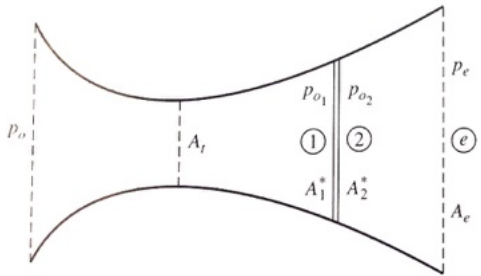

Figure 173: Diagram of standing normal shock within a nozzle.

Standing Shocks in Convergent-Divergent Nozzles

- Easiest to perform a numerical example
- Mach number at station one from tables is $\frac{A_1}{A_1^*} = 2 \rightarrow M_1 = 2.2$
- From normal shock table/equations for $M_1 = 2.2$, we find $\rightarrow M_2 = 0.547$ and $\frac{p_{o2}}{p_{o1}} = 0.628$
- Now at station $M_2 = 0.5471$ implies a new $A_2/A^* = 1.27$
- The value of A^* has changed across the shock wave!
- Why has A^* changed? Entropy increase across the shock wave

Standing Shocks in Convergent-Divergent Nozzles

Now

$$\frac{A_e}{A_2^*} = \frac{A_e}{A_2}\frac{A_2}{A_2^*} = \frac{A_e}{A_t}\frac{A_t}{A_2}\frac{A_2}{A_2^*} = 3\frac{1}{2}(1.27) = 1.905 \tag{460}$$

- Flow is subsonic behind standing shock wave
- Remaining portion of the nozzle is a divergent section
  - Therefore flow is subsonic in rest of section
- Subsonic isentropic flow tables shows

$$\frac{A_e}{A_2^*} = 1.905, M_e = 0.32, \text{ and } \frac{p_{oe}}{p_e} = 1.074 \tag{461}$$

Noting $p_o = p_{o1}$ and $p_{oe} = p_{o2}$,

$$\frac{p_e}{p_o} = \frac{p_e}{p_{oe}}\frac{p_{oe}}{p_{o2}}\frac{p_{o2}}{p_{o1}}\frac{p_{o1}}{p_0} = \left(\frac{1}{1.074}\right)(1)(0.6281)(1) = 0.585 \tag{462}$$

Standing Shocks in Convergent-Divergent Nozzles

Usually we know the pressure ratio of the nozzle and want to find shock wave location

Two approaches to analyze problem

- 1) Iterative approach
- 2) Direct approach

Iterative approach alters shock location until correct value of p_e/p_o is predicted (guess and check)

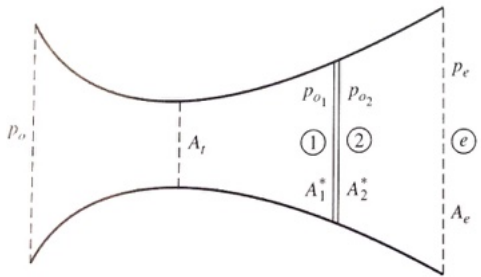

Figure 174: Shock wave location denoted in divergent section.

Standing Shocks in Convergent-Divergent Nozzles

The nozzle pressure ratio (NPR) is

$$NPR = \frac{p_o}{p_\infty} \approx \frac{p_o}{p_e} \tag{463}$$

We can conclude the following

$$p_{o1} = p_o \tag{464}$$

$$A_1^* = A_t \tag{465}$$

$$A_2^* = ? \tag{466}$$

We previously derived the mass flow rate for a choked nozzle

$$\dot{m} = \frac{p_o A^*}{T_o^{\frac{1}{2}}} \sqrt{\frac{\gamma}{R}\left(\frac{2}{\gamma+1}\right)^{\frac{\gamma+1}{\gamma-1}}} \tag{467}$$

Standing Shocks in Convergent-Divergent Nozzles

Recall how we found the equation for $\dot{m}$.

- $\dot{m} = \rho A u$ then substitute $A^* = A_t$
- p_o and T_o are total conditions

We find

$$\dot{m} \sim \frac{p_o A^*}{T_o^{\frac{1}{2}}} f(\gamma, R) \sim \frac{p_o A^*}{T_o^{\frac{1}{2}}} \tag{468}$$

Because T_o and $\dot{m}$ are constant across the shock we can say $p_o A^*$ is a constant based on our $\dot{m}$ equation

$$\boxed{p_{o1} A_1^* = p_{o2} A_2^*} \tag{469}$$

or

$$p_{o1} A_1^* = p_{oe} A_e^* \tag{470}$$

because of isentropic flow through nozzle (not across the shock).

Standing Shocks in Convergent-Divergent Nozzles

Rearranging

$$\frac{p_e A_e}{p_{oe} A_e^*} = \frac{p_e A_e}{p_{o1} A_1^*} = \underbrace{\frac{p_e}{p_{o1}} \frac{A_e}{A_1^*}}_{\text{known}} \tag{471}$$

Isentropic relation

$$\frac{p_e}{p_{oe}} = \left(1 + \frac{\gamma - 1}{2} M_e^2\right)^{\frac{-\gamma}{\gamma - 1}} \tag{472}$$

From the Area-Mach number relation

$$\frac{A_e}{A_e^*} = \frac{1}{M_e}\left[\left(\frac{2}{\gamma + 1}\right)\left(1 + \frac{\gamma - 1}{2} M_e^2\right)\right]^{\frac{\gamma + 1}{2(\gamma - 1)}} \tag{473}$$

Multiplying these two equations together yields

$$\frac{p_e}{p_{oe}} \frac{A_e}{A_e^*} = \frac{1}{M_e}\left(\frac{2}{\gamma + 1}\right)^{\frac{\gamma + 1}{2(\gamma - 1)}} \left(1 + \frac{\gamma - 1}{2} M_e^2\right)^{\frac{-1}{2}} \tag{474}$$

Standing Shocks in Convergent-Divergent Nozzles

Solve for M_e^2

$$M_e^2 = -\frac{1}{\gamma-1} + \left(\frac{1}{(\gamma-1)^2} + \left(\frac{2}{\gamma-1}\right)\left(\frac{2}{\gamma+1}\right)^{\frac{\gamma+1}{\gamma-1}} \times \left(\underbrace{\frac{p_{oe}A_e^*}{p_eA_e}}_{\text{known value} = \frac{p_e}{p_{o1}}\frac{A_e}{A_1^*}}\right)^2\right)^{\frac{1}{2}} \tag{475}$$

- Equation represents the exit Mach number for a standing shock wave within the divergent section.
- M_e must be subsonic, and we must enforce it (multi-value solution).
- Find M_e then p_{oe}/p_e from isentropic relation

Standing Shocks in Convergent-Divergent Nozzles

- Approache to find location of shock wave in CD nozzle
- One particular attack to solve the problem

First, find the total pressure ratio across the shock from

$$\frac{p_{o2}}{p_{o1}} = \frac{p_{oe}}{p_{o1}} = \frac{p_{oe}}{p_e} \underbrace{\frac{p_e}{p_{o1}}}_{\text{given!}} \tag{476}$$

From p_{o2}/p_{o1} find M_1 (shock table). Find A_1/A_1^* using M_1 (isentropic table). The location of the shock is a function of $A = A(x)$, which is defined by the nozzle contour.

Example

A convergent-divergent nozzle operates supersonically. A shock wave stands in the nozzle. Find the shock wave location. The area ratio of the nozzle is $A_e/A_t = 3$, total pressure in the nozzle plenum is $p_o = 1$ ATM, and the exit static pressure is $p_e = 0.5$ atm.

Solution

One strategy, seek M_e first

$$\frac{p_e}{p_{o1}}\frac{A_e}{A_1^*} = \left(\frac{0.5}{1.0}\right)(3) = 1.5 \tag{477}$$

and

$$\frac{p_e A_e}{p_{oe} A_e^*} = 1.5 \tag{478}$$

Find M_e^2

$$M_e^2 = -\frac{1}{\gamma - 1} + \left(\frac{1}{(\gamma-1)^2} + \left(\frac{2}{\gamma-1}\right)\left(\frac{2}{\gamma+1}\right)^{\frac{\gamma+1}{\gamma-1}}\left(\frac{p_{oe}A_e^*}{p_e A_e}\right)^2\right)^{\frac{1}{2}} \tag{479}$$

$$= -2.5 + \left[2.5^2 + 5(0.8333)^6\left(\frac{1}{1.5}\right)^2\right]^{\frac{1}{2}} \tag{480}$$

$$= 0.1447 \rightarrow M_e = 0.38 \tag{481}$$

Solution

Isentropic table for $M_e = 0.38 \rightarrow \frac{p_{oe}}{p_e} = 1.094$

$$\frac{p_{o2}}{p_{o1}} = \frac{p_{oe}}{p_e}\frac{p_e}{p_{o1}} = 1.094\left(\frac{0.5}{1}\right) = 0.547 \tag{482}$$

For normal shock relations we find

$$\frac{p_{o2}}{p_{o1}} \rightarrow M_1 = 2.38 \tag{483}$$

From isentropic relations

$$M_1 = 2.38 \rightarrow \frac{A}{A_1^*} = \boxed{\frac{A}{A_t} = 2.36} \tag{484}$$

Class Summary

- Air blast similarity theory
- Convergent divergent nozzles and normal shock waves

Next Time

- Off-design nozzles
- Shocks in nozzles and ducts
- Temperature-Entropy diagram
- Examples

Class Overview

- Off-design nozzles
- Shocks in nozzles and ducts
- Temperature-entropy diagram
- Examples

“The country (Germany) is like a man with a badly upset stomach who has not yet vomited enough.”

“The Kapp Putsch, also known as the Kapp-Luttwitz Putsch after its leaders Wolfgang Kapp and Walther von Luttwitz, was an attempted coup on 13 March 1920 which aimed to undo the German Revolution of 1918-1919, overthrow the Weimar Republic and establish a right-wing autocratic government in its place.”

Aurel Stodola in 1919 on right-wing putsch in Berlin two weeks earlier. CPAE Vol. 9 Dec. 16

Nozzle Pressure Ratio and Flow Inside Laval's Nozzle

- Examine how flow in convergent-divergent nozzle changes as we increase NPR from unity
- For fixed stagnation pressure, p_o, upstream of a Laval nozzle, we decrease back pressure p_b in order to establish supersonic flow
- NPR p_o/p_b determines the flow in the nozzle
  - What effect does T_o/T_∞ have?
- Can we graph p versus x?

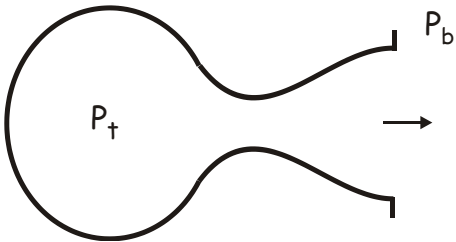

Figure 175: Simplified nozzle diagram.

Increasing NPR Pushes Shock Wave Downstream

- Increase NPR increases the mass flow, $\dot{m}$, through the nozzle until $M = 1$ at throat
- Higher NPR causes normal shock to form
- Normal shock then moves downstream until exits nozzle

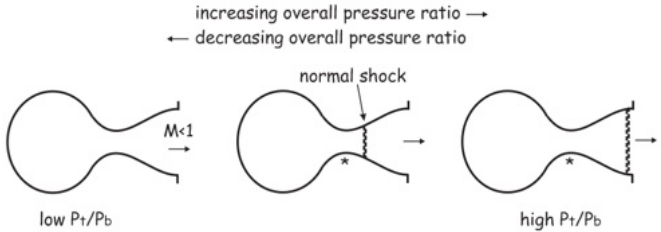

Figure 176: Variation of shock position with increasing NPR.

Lowering NPR from Supersonic Condition

- Decrease NPR and shock forms and moves towards throat
- Eventually shock wave hits throat and is gone
- Subsonic flow through nozzle obtained
- NPR reduces to unity and flow is stagnant

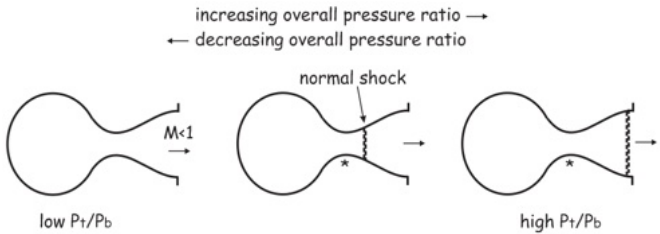

Figure 177: Variation of shock position with increasing NPR.

Full Range of Nozzle in terms of $p - x$

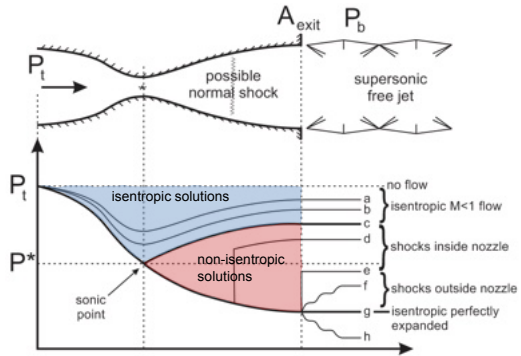

Figure 178: Various flows through a convergent-divergent nozzle.

Laval-Nozzle Isentropic Regions and Possible Normal Shocks

Drawn accurately for a nozzle with $M_e = 2.25$ by Prof. Luigi Crocco (1909-1986)

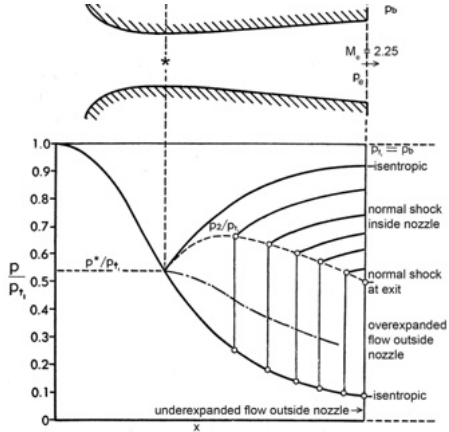

Figure 179: Pressure versus axial location, predictions of Prof. L. Crocco.

Stodola's Experiment

Stodola validated predictions experimentally of the CD nozzle, which eluded explanation of de Laval. Why is the pressure rise so gradual?

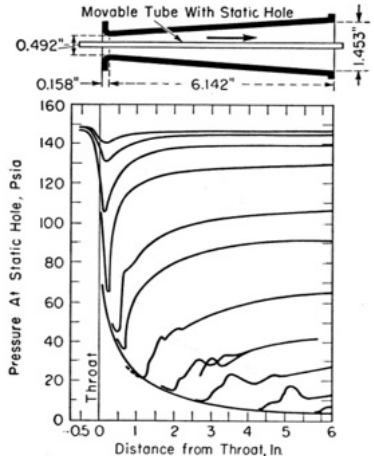

Figure 180: Diagram of the Stodola experiment. Notice the tube in the middle of the nozzle.

Aurel Boleslav Stodola

- Aurel Boleslav Stodola (10 May 1859 - 25 December 1942)
- Slovak engineer, physicist, and inventor.
- Pioneer in thermodynamics and its applications, and published his book Die Dampfturbine (the steam turbine) in 1903.
- Stodola was a professor of mechanical engineering at the Swiss Polytechnical Institute (now ETH) in Zurich.
- One of his students was Albert Einstein.
- In 1892, Stodola founded the Laboratory for Energy Conversion.

Prof. Aurel Stodola, 1859-1942, ETH Zurich

Figure 181

Multiple Throats or Local Minimum Areas

- Imagine we have a streamtube
- Multiple local minimums
- These might bet the same local minimum areas or they might differ
- What possible flow-fields do we have through this device?
- Where might we see these configurations in aerospace engineering?

Streamtubes with Multiple Throats

- Consider $A_1 = A_2$ as shown below, a normal shock cannot exist between throats 1 and 2 if flow is transonic between 1 and 2
- A normal shock must occur to initiate supersonic flow if the flow is initially at rest
- To achieve supersonic flow, we "open up" ... A_2 enough to "swallow" the shock wave, then close it back down to equal A_1
- Without such variable geometry, supersonic flow cannot occur between throats 1 and 2

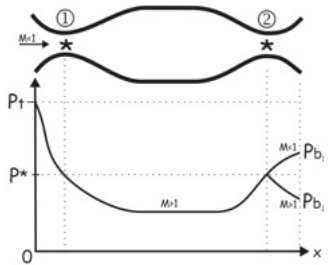

Figure 182: Supersonic isentropic flow through a nozzle.

Normal-Shock Stability in Converging and Diverging Ducts

- Supersonic flow enters a converging–diverging duct
- A normal shock stands at the local minimum area
- This is not a sonic throat, $M > 1$ ahead of the shock
- Flow expands and discharges to a variable back pressure p_b

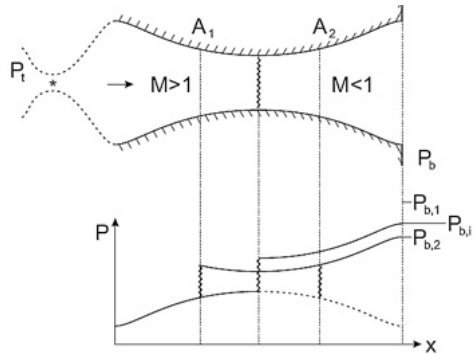

Figure 183: A supersonic diffuser.

Normal-Shock Stability in Converging and Diverging Ducts

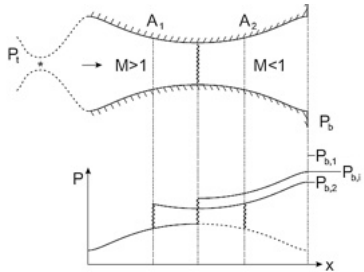

Figure 184: Potential shock positions.

- Initially, the normal shock is neutrally stable at the minimum area with the back pressure at $p_{b,i}$
- Now reduce back pressure to $p_{b,2}$, this increases the overall pressure ratio and moves the shock downstream to a new, stable position at A_2
- The shock loss is higher because M_1 in front of the shock is higher

Normal-Shock Stability in Converging and Diverging Ducts

- We start again with the normal shock neutrally stable at the minimum duct area with the back pressure at $p_{b,i}$
- Increase the back pressure to $p_{b,1}$
- This decreases the NPR and the shock moves upstream to a new position at A_1
  - The Mach number is higher
  - The loss across the shock is larger
  - Thus, p_b cannot be equal to $p_{b,1}$
- But instead returns to $p_{b,2}$.
- This cannot be a stable operating condition!

Normal-Shock Stability in Converging and Diverging Ducts

- This unstable position results in a pressure mismatch that drives the shock all the way back to the upstream nozzle
  - The new shock position resides at a location that is stable with p_b equal to $p_{b,1}$
- This process is called "disgorging the shock wave"
- This simple example shows why normal shocks do not stand in convergent ducts
- A rule – "normal shocks can only stand stably in a diverging duct and not in a converging duct"

Nomenclature and Notes

- A “blocked channel” is where two throats exist, a normal shock wave is trapped between them, and both throats are choked
  - The normal shock appears to tremble or jitter due to unstable downstream pressure conditions
- “Swallowing” the shock means providing a downstream restriction big enough to allow the shock to pass
  - Thus establishing supersonic flow in the entire passage
- The “terminal shock” wave is the normal shock or system of shock waves that terminates supersonic flow

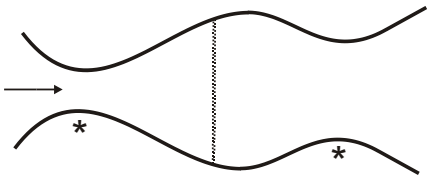

Figure 185: Standing shock in divergent-section.

Nomenclature and Notes

- "Unstart or disgorging" the shock wave is the reverse process of swallowing it
- A_1^*/A_2^* and the nozzle pressure ratio p_o/p_b (NPR) determine when shock swallowing and un-start occur
- Remember, shock wave cannot stand stably in a converging duct
  - Shock wave moves to a downstream diverging-duct location as the back pressure is lowered (shock swallowing)

$T - S$ Diagrams of Shocks

We now examine the variation of static temperature and entropy across shocks and their solutions.
Recall the equations of motion for a normal shock. Continuity

$$\rho_1 u_1 = \rho_2 u_2 \tag{485}$$

momentum

$$p_1 - p_2 = \rho_2 u_2^2 - \rho_1 u_1^2 \tag{486}$$

energy

$$h_1 + \frac{u_1^2}{2} = h_2 + \frac{u_2^2}{2} = h_o = c_p T_o \tag{487}$$

and state

$$p = \rho R T \tag{488}$$

$T - S$ Diagrams of Shocks

- Solution of three of the equations results in a locus of solutions in $T - s$ space
  - Combination of continuity, energy, and state equations produces a line on a $T - s$ diagram called a Fanno line, which momentum can be dissipated by friction
  - The continuity, momentum, and state equations produce a line called a Rayleigh line, which heat transfer occurs
- Normal shocks have both internal friction and heat transfer
- Their initial and final states in $T - s$ space are determined by the intersection of the Fanno and Rayleigh lines for a given mass flow rate.

$T - S$ Diagrams of Shocks

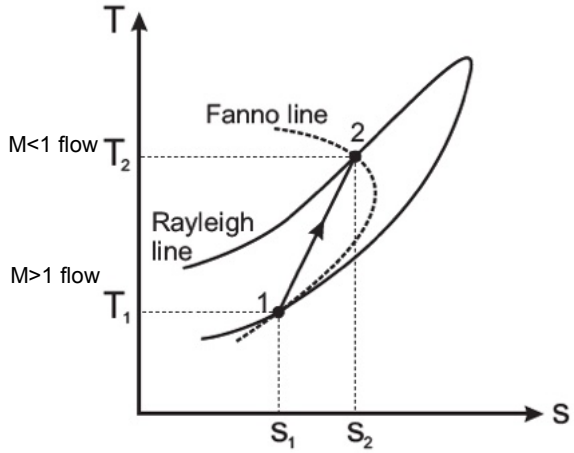

Figure 186: A $T - s$ diagram for a normal shock from state 1 to 2. The states 1 and 2 are defined by the intersection of the Fanno and Rayleigh lines for the same mass flow rate in $T - s$ space. The entropy level must always rise across a shock wave.

Properties Across A Shock

- Let us summarize the conditions across a shock
- Remember and understand these conditions across a normal shock

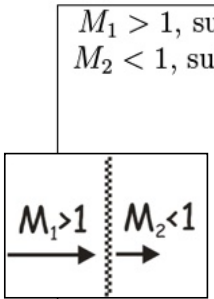

$M_1 > 1$, supersonic flow upstream at state 1

$M_2 < 1$, subsonic flow downstream at state 2

$$v_1 > v_2$$
$$\dot{m}_1 = \dot{m}_2$$
$$T_{t1} = T_{t2}$$
$$T_1 < T_2$$
$$P_{t1} > P_{t2}$$
$$P_1 < P_2$$
$$s_1 < s_2$$
$$\rho_1 < \rho_2$$
$$A_1^* < A_2^*$$

flow direction 1 = flow direction 2

Figure 187: Properties across a shock summarized.

Example

The Laval nozzle shown in the diagram has a throat-to-exit area ratio of 4.0. Under certain operating conditions the throat is choked and a normal shock wave stands at the location where the nozzle area is 3.0 times the throat area. Assuming isentropic airflow except across the shock, find the nozzle exit pressure and temperature, p_e and T_e, when the nozzle stagnation pressure and stagnation temperature are 2 MPa and 300K, respectively.

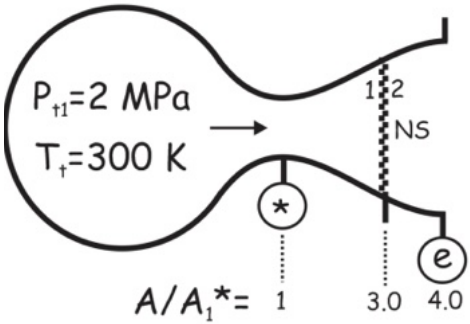

Figure 188: Example diagram for shock wave in CD nozzle.

Solution

- At the shock wave, $A_s/A_1^* = 3.0$. From the isentropic-flow tables this yields $M_1 = 2.64$.
- Find the conditions across the shock from the normal-shock tables at $M_1 = 2.64 \rightarrow M_2 = 0.5005$ and $p_{o2}/p_{o1} = 0.4452$, from which $p_{o2} = 0.445 \times 2$ MPA $= 0.8904$ MPa.
- Use isentropic table at $M_2 = 0.5005$, and find $A_s/A_2^* = 1.34$
  - Note that isentropic subsonic flow occurs from the shock wave to the nozzle exit due to the area change.

Solution Continued

- Find the change in area from shock to exit
  - $A_e/A_2^* = (A_e/A_s)(A_s/A_2^*) = (4/3)(1.34) = 1.79$
- Allowing us to find nozzle exit conditions from the isentropic theory
  - $M_e = 0.35$
  - $p_e/p_o = 0.9188$
  - $T_e/T_o = 0.9761$
- Finally, $p_e = 0.9188 \times p_{o2} = 0.818$ MPa, $T_e = 0.9671 \times T_o = 293$ K

Example – Channels with Two Throats

- A normal shock wave is blocked in a channel.
- Throats A_1^* and A_2^* are choked, but $A_1^* \neq A_2^*$ because a shock exists
- Let
  - $A_1 = 1$ m^2
  - $T_{o1} = 300$ K
  - $p_{o1} = 1010$ kPa
  - $\rho_{o2} = 3.71$ kg/m^3 (at second throat)
- Find
  - Area A_2^* of the second throat
  - Mach number M_x ahead of the shock

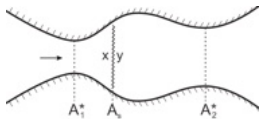

Figure 189: Shock trapped between two throats.

Solution

- We first seek, A_2^*, the area of the second throat
  - Find ρ_{o1}, which is the stagnation density at A_1^*
  - Recall that we have conservation of mass $\dot{m} = \rho_1 A_1 u_1 = \rho_2 A_2 u_2$
  - Based on Mach number definition, $u^* = \sqrt{(\gamma RT)}$ at $M = 1$
  - Also, $T_1 = T_2 = T^*$, because $T^*/T_o = f(\gamma, M = 1)$ is constant as T_o is conserved throughout the flow-field, so T^* must be constant at $M = 1$
  - Therefore, we eliminate u from mass conservation and solve for ρ_1^* in $A_2^*/A_1^* = \rho_1^*/\rho_2^*$

Solution cont.

- Stagnation gas law is conserved before shock,
  $\rho_o = p_o/R/T_o = (1010)/(287 \times 300) = 11.731$ kg/m^3, we find $\rho_o = 7.44$ kg/m^3.
  - Now $\rho_{o2}/\rho_{o1} = \rho_2^*/\rho_1^*$ because at both locations $M = 1$, therefore
    $\rho_{o1}/\rho_{o2} = 7.44/3.71 = A_2^*/A_1^* \approx 2$
  - We find $\boxed{A_2^* \approx 2}$ m^2
- We now look for M_x
  - From the tables or Calculator, we find $\boxed{M_x = 2.5}$ from $A_2^*/A_1^* = 2$

Video of Supersonic Flow in Wind Tunnel

Channel Flow of a Compressible Fluid https://www.youtube.com/watch?v=JhlEkEk7igs

Play from 22 minutes 10 seconds (plays about 10 min.).

Class Summary

- Off-design nozzles
- Shocks in nozzles and ducts
- Temperature-Entropy diagram
- Examples

Next Time

- Applications – Wind Tunnels

Class Overview

- Wind tunnel applications

Supersonic Wind Tunnels

- A supersonic wind tunnel is a facility for producing a controlled $M > 1$ air stream in the laboratory for testing and research.
- Depending on its size, a supersonic wind tunnel generally uses a lot of energy and is often a large, expensive facility.
- The largest supersonic wind tunnel in the world is located at the Arnold Engineering Development Center (AEDC), at Arnold Air Force Base, Tullahoma, Tennessee, has a 4.7 m square test section and is a closed circuit wind tunnel.
- This facility has some of the largest electric motors ever built and its own electric substation with enough power to light a small city.

Supersonic Wind Tunnels

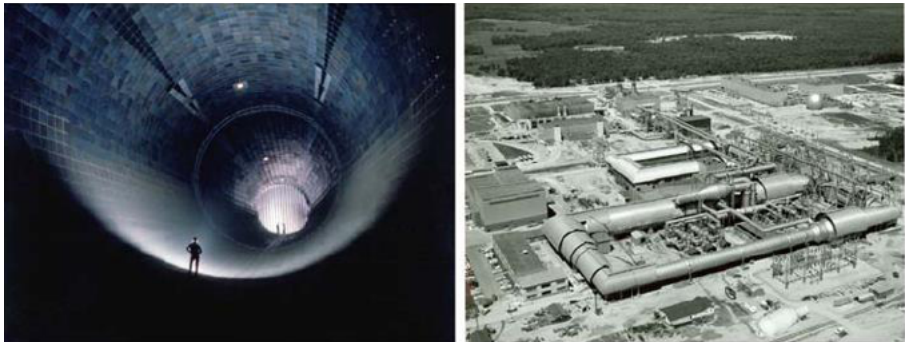

Figure 190: AEDC tunnels.

Supersonic Wind Tunnels

- Perhaps the smallest supersonic wind tunnel ever built was the high school science project of a student in Tennessee in 1966.
- His tunnel's test section was 0.5 x 1 inch in size and was powered with a 1/4 horsepower motor.
- It ran for a few seconds at a time and yielded schlieren images of the supersonic flow inside the nozzle. (Scientific American, October 1966, pages 120-125)

Supersonic Wind Tunnels

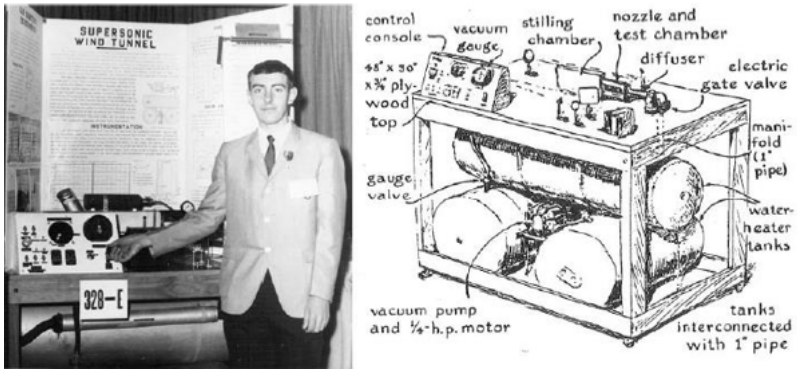

Figure 191: A science fair project which is superior to stupid volcanoes.

- For continuously-operating supersonic wind tunnels, the electrical power requirement goes up exponentially with the size of the test section.
- If you want a large test section, you'll need your own electric substation.
- Intermittent supersonic wind tunnels take a less-expensive route than this by storing energy over a comparatively long time and then discharging it intermittently for a brief test at supersonic speed.

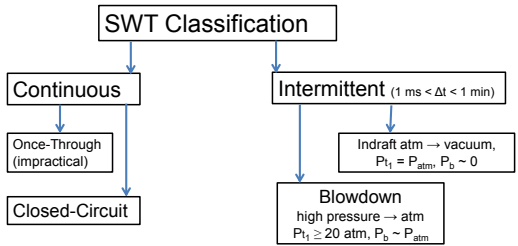

Figure 192: Simple flow-chart of wind-tunnel classification.

Intermittent Supersonic Wind Tunnels

- Blowdown type Pro's
  - High Reynolds number Small storage tank Easy to dry the air
- Blowdown type Con's
  - High-pressure hazard
  - Difficult to hold constant p_o Noisy
- Indraft type Pro's
  - No high-pressure hazard Constant p_o
  - Relatively quiet
- Indraft type Con's
  - Very limited Reynolds capability
  - Large vacuum tank required PSU SWT blowdown-type

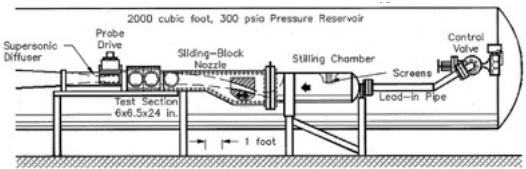

Figure 193: Blowdown wind tunnel.

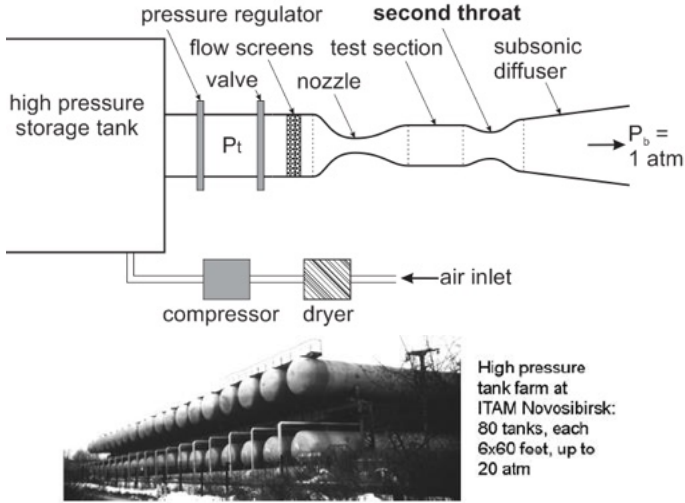

Figure 194: The bottle farm at Novosibirsk.

Novosibirsk

Novosibirsk is a city in Siberia, southern Russia, bisected by the Ob River. The Trans-Siberian Railway fueled much of the city's 19th-century growth, symbolized by the Novosibirsk Rail Bridge, which still stands today. In the city center is the 19th-century, Byzantine-style Alexander Nevsky Cathedral, with its golden domes. The expansive Novosibirsk Opera and Ballet Theatre borders Lenin Square.

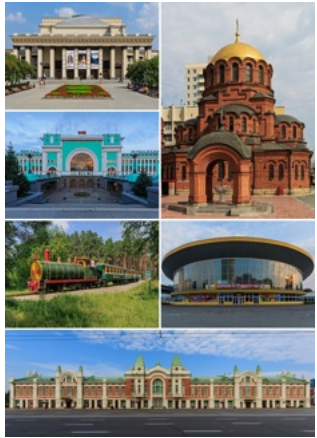

Figure 195: Novosibirsk

NASA Langley Tunnel

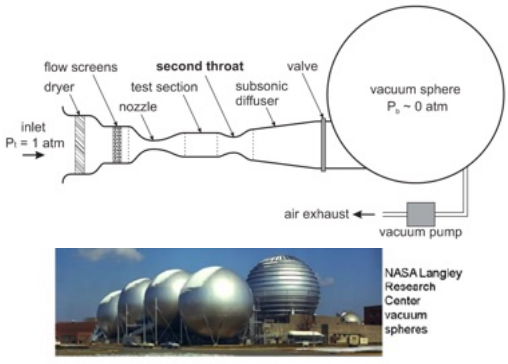

Figure 196: NASA Langley Vacuum Spheres

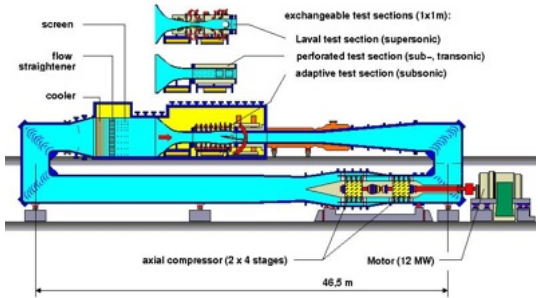

Figure 197: Transonic wind tunnel, DLR Gottingen, Germany. A closed circuit, variable density, continuous, subsonic, transonic and supersonic wind tunnel with three interchangeable test sections (courtesy DNW- German-Dutch-Wind Tunnels).

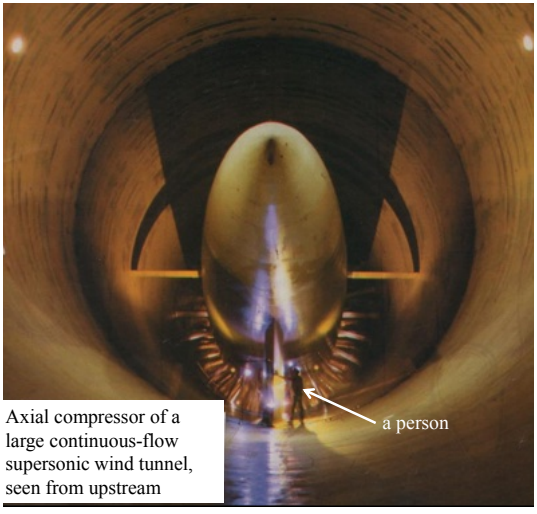

Figure 198: Axial compressor of a large continuous-flow supersonic wind tunnel, seen from upstream

Figure 199: F-111 model in the 16-foot (4.7m) transonic test section of the AEDC Propulsion Wind Tunnel. Note perforated walls.

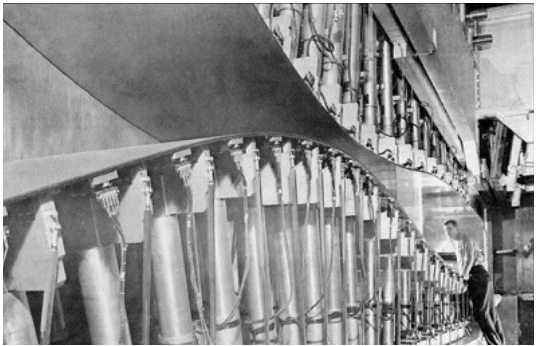

Figure 200: Variable-area nozzle using flexible hydraulic-actuated ceiling and floor plates (sidewall removed). USAF AEDC Tunnel A.

Supersonic Wind Tunnels with Second-Throat Diffusers

- Case 1: Fixed nozzle and second throat
- In order to establish supersonic flow in the test section, the second throat must be at least as large as A_2^* following a normal shock wave in the test section at station 1.
- The overall pressure ratio must be sufficient to support the shock wave in the test section.
- In this case the shock is 'swallowed' through the second throat to position 2, of the same area as position 1.
- Now the overall pressure ratio can be decreased to move the shock almost back to the second throat, position 3.
- This is the most efficient wind tunnel running condition for a fixed nozzle and second throat.
- The second-throat diffuser is needed because normal shocks above $M \approx 1.5$ are expensive in terms of wasted p_o.

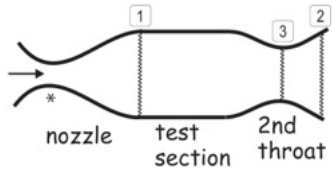

Figure 201

Adolf Busemann

- Adolf Busemann's supersonic wind tunnel from the early 1930's, the world's first practical supersonic wind tunnel, had an adjustable second throat for efficient operation.
- Busemann is best known for having invented the idea of sweeping back the wings of an airplane in order to make it perform better in the transonic flow regime.

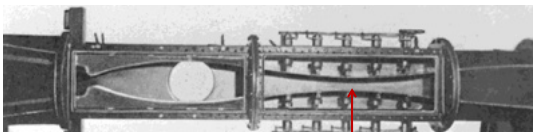

Figure 202: Adjustable second throat.

Figure 203: Adolf Busemann.

Supersonic Wind Tunnels with Second-Throat Diffusers

Case 2: Fixed nozzle, variable-area second throat

- Now, in order to establish supersonic flow, the second throat may be opened up to match the test section area.
- With sufficient overall pressure ratio, supersonic flow is established in the test section and a normal shock is 'swallowed' to a position downstream of the second throat.
- The adjustable second throat can now be closed almost to A_1^*, but not quite (due to friction losses in the boundary layers on the walls).
- The overall pressure ratio can be decreased to move the shock almost back to the second throat, where the Mach number ahead of the shock will be low and the loss small.
- This represents the most efficient wind tunnel running condition for a fixed nozzle and a variable second throat, which is more efficient than in Case 1.

Supersonic Wind Tunnels with Second-Throat Diffusers

Case 3: Variable nozzle, variable-area second throat

- Now the wind tunnel may be started and the normal shock swallowed at a low supersonic Mach number, say $M = 1.5$, with the second throat wide open.
- Both the adjustable nozzle throat and the adjustable second throat can be closed simultaneously in order to raise the test section Mach number while keeping the normal shock downstream of the second throat at an optimum location.
- Allows the highest test section Mach number for a given overall pressure ratio.
- Most complex and expensive of the three cases considered here.

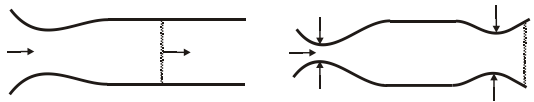

Figure 204

Figure 205: Vacuum chambers (spheres) of NASA Langley Research Center.

Figure 206: Test section.

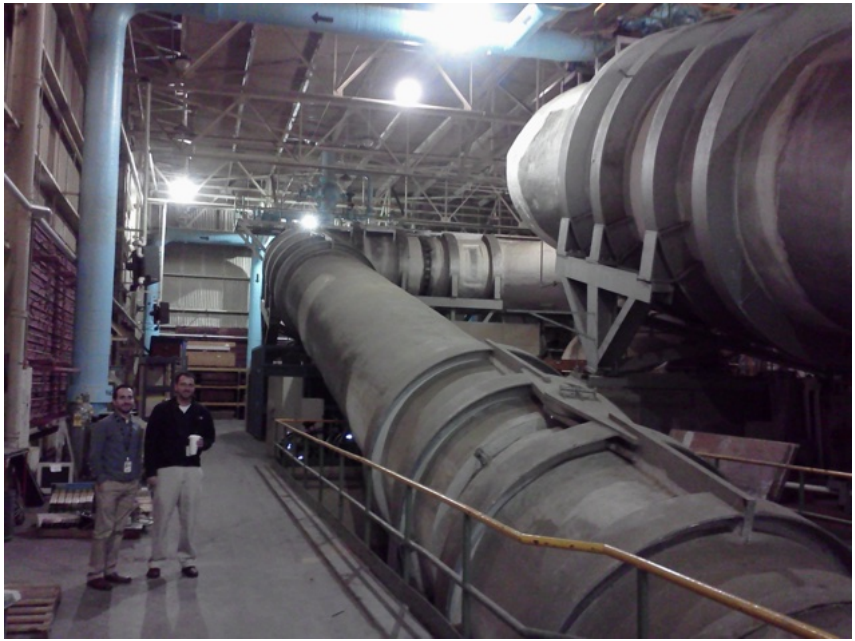

Figure 207: Prof. S. Miller at the NASA Langley Unitary Wind Tunnel

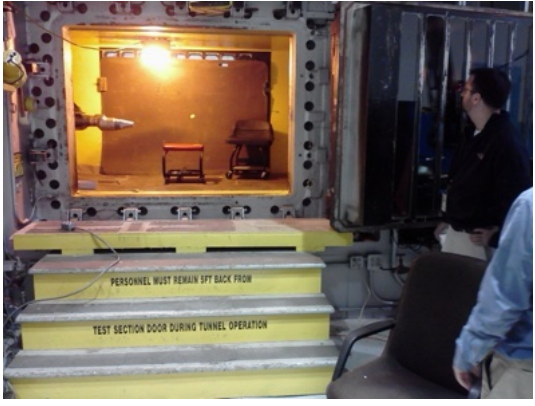

Figure 208: Prof. S. Miller at the NASA Langley Unitary Wind Tunnel.

Quick Thoughts

- Supersonic wind tunnels with large cross-sections require large amounts of power
- Diffusers are very important for reducing this power requirement
- Blow-down or intermittent tunnel reduces run-time

Blow-Down Tunnel

The atmosphere is pulled into a vacuum chamber. The vacuum chamber is often a large sphere.

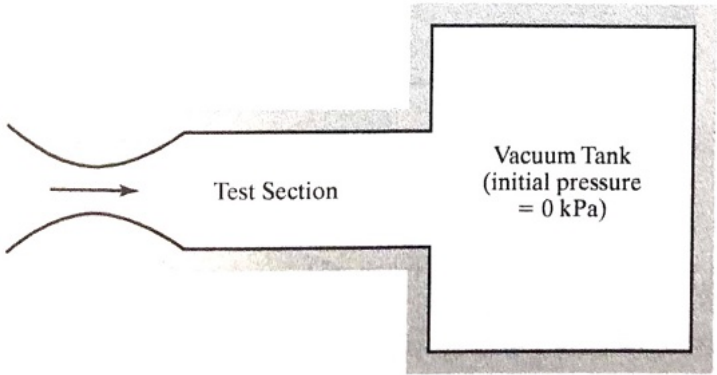

Figure 209

Blow-Down Tunnel

- Requires very large vacuum chamber
- Larger vacuum chambers lead to longer run-times
- Increase run-time of tunnel by adding a diffuser
- Diffuser also increases efficiency

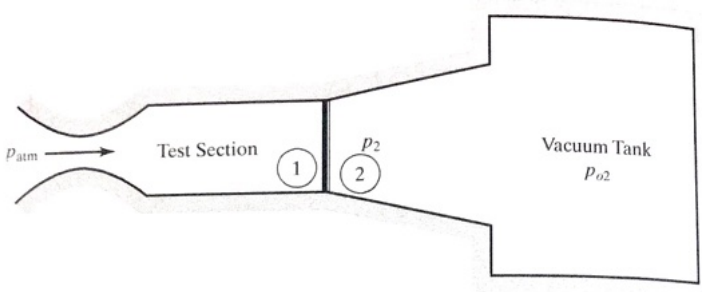

Figure 210

Wind Tunnels

- Isentropic flow through the diffuser provides some pressure recovery
- Typically blow-down supersonic tunnels provide relatively short test times
- Resolve short test times by making recirculating tunnel or continuous closed circuit tunnel
  - Obviously more expensive and complicated
  - Saves energy

Basic Recirculating Wind-Tunnel

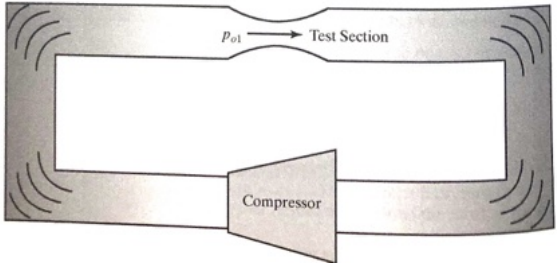

Figure 211

The addition of turning vanes greatly increases efficiency.

Wind-Tunnel Startup

- Recirculating test section is most ideal as diffuser helps with pressure recovery
- The startup of the tunnel is complicated
- At startup only a small pressure difference is maintained and then increased
- The increased pressure from the compressor forces a normal shock to form at the test section inlet

Wind-Tunnel Startup

A normal shock forms from the throat and is pushed down the tunnel

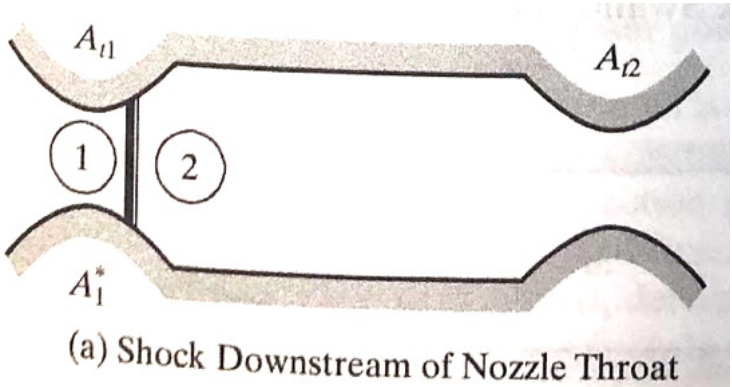

Figure 212

Wind-Tunnel Startup

- Still subsonic flow in test section
- No shocks present in test section
- Eventually shock moves downstream with increasing pressure ratio
- Want to remove shock from tunnel
- Second throat area must be at least A_2^* (while shock is propagating down test section.)
- As $\triangle p$ in tunnel is increased this shock moves to diffuser and is "swallowed"

Wind-Tunnel Startup

The shock moves into the test section.

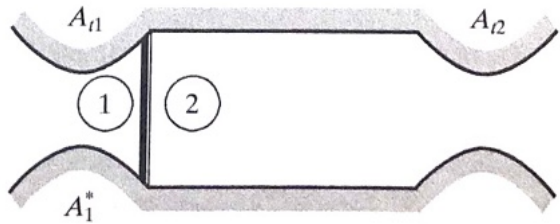

(b) Shock at Nozzle Exit

Figure 213

It eventually moves downstream through the diffuser and is swallowed.

Supersonic Wind Tunnel Operation

- Ideally want normal shock located at throat of the diffuser
- The shock strength will be at a minimum at this location
- As shock is swallowed, change diffuser area A_2^* to a smaller value and raise $\triangle p$ even more
  - Shock Mach number will approach unity

Final Phase of Supersonic Wind Tunnel Startup

Normal shock location is at the worst location.

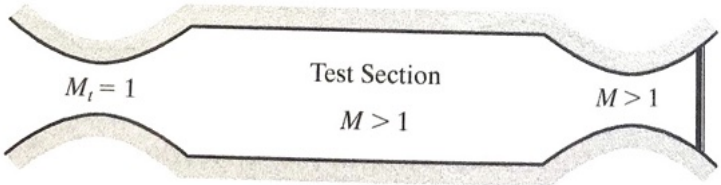

Figure 214

Ideal Supersonic Operation

Note location of normal shock, which is at an ideal location.

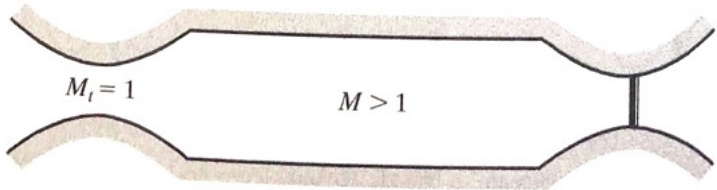

Figure 215

Example

A continuous supersonic wind tunnel designed with test section Mach number of 2, with γ= 1.4, and $c_p = 1.004$ kJ/kg K, is started and then run for tests. The test section $D = 0.25$ m. Find power requirements during startup and run.

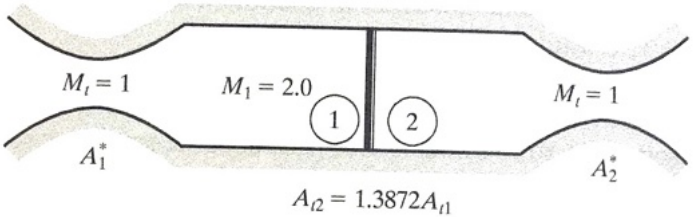

Figure 216

We define steady run as when shock stands in the diffuser throat. Worst case (startup) shock stands in the test section.

Solution

Startup is the worst case based on given M

$$\frac{p_{o2}}{p_{o1}} = 0.7209 = \frac{A_1^*}{A_2^*} = \frac{A_{t1}}{A_{t2}} \tag{489}$$

$$\therefore \frac{A}{A_{\text{test}}^*} = 1.6875 \tag{490}$$

We find the throat area of the diffuser

$$A_{t2} = \frac{A_{t2}}{A_{t1}} \frac{A_{t1}}{A_{\text{test}}^*} \frac{A_{\text{test}}^*}{A_{\text{test}}} A_{\text{test}} = \frac{1}{0.7209}(1)\frac{1}{1.6875} = 0.4035 \text{ m}^2 \tag{491}$$

During steady operations the mass flow through the test section is

$$\dot{m} = \rho A u = \frac{p}{RT} A M \sqrt{\gamma R T} \tag{492}$$

$\Longrightarrow$ $p = 5.5$ kPa and $T = 216.7$ K (Atmospheric tables)

Solution

We can find the mass flow rate

$$\dot{m} = \frac{5.5}{0.287(216.7)}\left(\frac{\pi}{4}0.25^2\right)2.0\sqrt{1.4(287)(216.7)} = 2.5619 \text{ kg/s} \tag{493}$$

- At $M = 2$, $T/T_o = 0.5556$ (isentropic) so test stagnation temperature is 390.0288 K
- Now at steady conditions $(\frac{A}{A^*})_{t2} = 1.3872$, we find $M_{2t} = 1.7506$ using Newton-Raphson method (shown previously)
- Across the shock we find $p_{o2}/p_{o1} = 0.8343$ (tables shock)
- The compressor must account for the loss in $\triangle p_o$

Solution

For the compressor

$$W = h_o - h_i = c_p(T_o - T_i) \tag{494}$$

If there are no losses

$$\frac{T_o}{T_i} = \left(\frac{p_o}{p_i}\right)^{\frac{\gamma-1}{\gamma}} \tag{495}$$

$$\therefore W = c_p(20.7197) = 20.8026 \text{ kJ/kg} \tag{496}$$

So power = $\dot{m}W = (2.5619)(20.8026) = 53.2941$ kW.
During startup recall $p_{o2}/p_{o1} = 0.7209$

$$W = c_p(T_o - T_i) = 1.004(38.2276) = 38.3805 \tag{497}$$

or

$$p = \dot{m}W = (2.5619)(38.3805) = 98.3269 \text{ kW} \tag{498}$$

(84.5% more power)

Wind Tunnel Videos

- NASA's Ames Research Center and NASA's Langley Research Center, in partnership with The Boeing Co., have completed wind tunnel testing of a full-scale Boeing 757 vertical tail model equipped with active flow control technology. https://www.youtube.com/watch?v=4PabZAx-4Yw
- NASA video showing October 2018 tests of Lockheed Martin's X-59A QueSST low-boom supersonic flight demonstrator in the 12ft low-speed tunnel at Langley Research Center https://www.youtube.com/watch?v=ZepnzFwXevg

Class Summary

- Wind tunnel applications

Next Time

- Applications - Isentropic flow and nozzles
- Applications - Supersonic inlets
- Applications - Ballistic range

Class Overview

- Applications - Isentropic flow and nozzles
- Applications - Supersonic inlets
- Applications - Ballistic range

Laval Nozzle Performance

- Let us reexamine the important static-pressure distributions along a Laval nozzle for fixed p_o and variable p_∞.
- Viscous effects have been neglected, but in a real nozzle the pressure rise at the wall due to a normal shock will not be discontinuous.
- A full understanding of the "over-expanded" flow outside the nozzle exit requires oblique-shock and Prandtl-Meyer theory (coming soon).
- 1D theory cannot give us the optimum shape of a Laval nozzle, which requires method of characteristics. $M = 2$ nozzle design below, from Harrop, 1953.

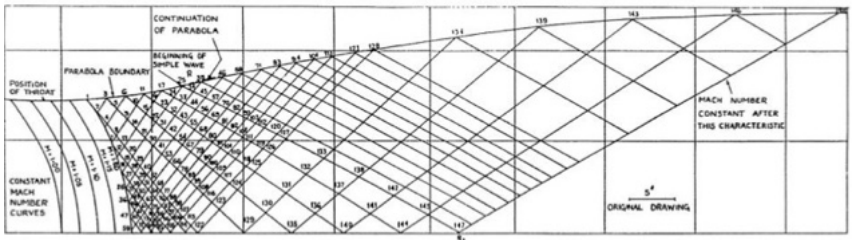

Figure 217: MOC design of nozzle.

Inlets

Figure 218: Two types of inlets.

Supersonic Inlets for air-breathing jet engines

- Supersonic airplanes with air-breathing jet engines, have specially-designed inlets for slowing the supersonic airstream to subsonic conditions.
- Most current turbojet engines require a subsonic inflow of air.
- For a plane traveling at supersonic speeds, this requires that the airstream be ingested and then slowed before it enters the jet engine.
- This air deceleration process is accomplished through a supersonic diffuser containing an isentropic compression and a normal shock wave.

Figure 219: Supersonic airplanes require specially-designed inlets to bring air into the jet engine, as shown here on the F-86 (left) and the F-15 (right).

MIG 17

Figure 220: Rossiyskaya samoletostroitel'naya korporatsiya 'MiG' – The prototype MiG-17 NATO code name Fres 20 first flew in January 1950 and was reported to have exceeded Mach 1 in level flight. Soviet production of the MiG-17 ended in 1958 with over 6,000 produced. It continued to be built under license: 1 → Poland as the Lim-5P and in China as the F-A The Mla-17 served with nearly 30 air forces worldwide, inciting the Soviet Union, Warsaw Pact countries, China Afghanistan, North Korea, Sri Lanka, Syria, Morocco, Cuba, Indonesia, and Cambodia. Though smaller than the USAF F-86 Sabre of Korean War fame its weight and performance favorably compared to that aircraft The MiG-1i was flown by most of the top North Vienamese pilots, including the leading ace. Colonel Tomb.

MIG 17

Figure 221: MiG 17 inlet.

MIG 21

Figure 222: MiG 21 inlet Source: Miller.

Inlets

- 1-D 'ideal case,' the inlet of an aircraft flying at supersonic design Mach number M_d ingests a stream-tube of air
  - Ideally isentropically back to Mach 1 through a throat of area A_D^*
  - Subsonic airflow into compressor
- Unfortunately this is unstable and impractical.
- If the aircraft slows down even a little, then A_D^* is no longer large enough to swallow the flow and suddenly a normal shock wave appears in front of inlet
- We say that the normal shock is "disgorged" from the inlet, and this unwanted process is known as inlet "unstart."

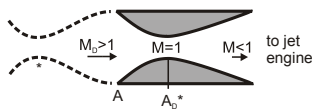

Figure 223: Situation 1

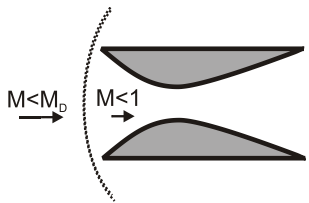

Figure 224: Situation 2

Inlets

- Inlet of an aircraft flying at supersonic M_d ingests the stream-tube of air
- Air moves through a normal shock wave to subsonic airflow that then proceeds to the jet engine.
- This case is stable, since the shock sits in a diverging channel and can adjust its strength to small variations in flight Mach number.
- The problem with this design lies in how to establish such a flow in the first place.

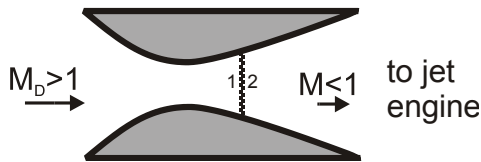

Figure 225: Normal shock in divergent section.

Inlets

- If one simply accelerates from rest up to M_d, a normal-shock forms ahead of the inlet and is not swallowed.
- The loss across the shock causes A_2^* after the shock to always be too large compared to the throat of the inlet.
- It would be necessary to overspeed to $M > M_d$ in order to swallow the shock, and this is completely impractical given the enormous drag of the normal shock in front of a stalled inlet.
- A practical solution is to use a variable-geometry inlet
  - Open throat at a low supersonic Mach number to swallow the shock
  - Gradually close the throat down as M increases in order to keep the shock swallowed

Inlets

- This process is what high-speed inlets accomplish
- Above about $M_d = 2$, every high-speed aircraft has a variable-geometry inlet.
- Supersonic aircraft inlets are not designed by the one-dimensional methods described above.
- They are designed with oblique shock waves, which can have small losses even at high supersonic Mach numbers.
- After we cover oblique shocks, we'll revisit this topic of supersonic inlet design.

Shock Tubes

- A shock tube is a device to produce high-pressure and high-temperature conditions using a shock wave traveling through a fixed pipe.
- Shock tubes are inherently moving-shock devices, and thus produce unsteady flow-fields.
- In its simplest form a shock tube has a high-pressure driver section which produces a shock wave and a driver section through which the shock propagates, and where the experiment is performed.
- The two sections are separated by a diaphragm that bursts at a given pressure, thus producing a shock wave.
- The properties of the driver and driven section gases (T, p, and another variable) determine the shock wave strength and all other test flow conditions.

Shock Tubes

- Schematic of a shock tube. When the diaphragm between the high- and low-pressure sides bursts, a shock will propagate down the tube from left to right.
- The shock will also reflect from the end wall, thus further increasing the temperature and pressure.
- Shock tubes are used to produce high shock Mach numbers (up to 15) and high temperature ratios ($T_2/T_1 = 40$) which are outside the range of conventional wind tunnels.

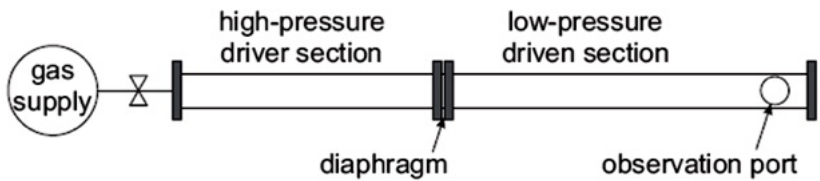

Figure 226: A shock tube schematic.

Shock Tubes

- A shock tube experiment typically lasts on the order of microseconds before shock reflections and the contact surface propagation cause non-uniform conditions to appear, requiring modern high- speed digital instrumentation.
- These facilities are useful for depositing a known amount of energy into a homogeneous test section and are used to study unsteady shock interactions (e.g. blast wave effects), aerothermodynamics (e.g. re-entry heating and ablation), chemical kinetics (e.g. ionization, dissociation, combustion), plasmas, and gas dynamic lasers.
- They are very useful one-dimensional compressible flow test facilities.

Shock Tubes

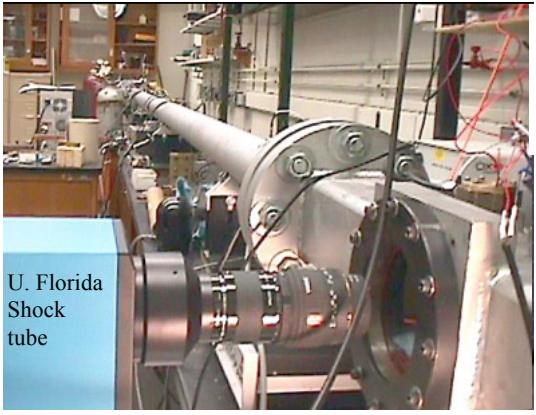

Figure 227: University of Florida Shock Tube.

Ballistic Range

- In a ballistic range (see diagram below), a gun fires a test model at high speed through a firing range containing still air.
- This is analogous to a wind tunnel where the model is held fixed while high-speed air flows over it.
- Often the model is contained in a plastic boot or sabot for firing down the gun barrel.
- The sabot splits after exiting the gun muzzle and only the model flies down the ballistic range.

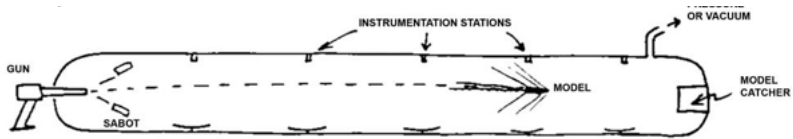

Figure 228: Schematic of a ballistics range.

Ballistic Range

- Fast instrumentation images the model's flight and collects other data before the model impacts the model-catcher and is destroyed.
- Some ballistic-range experiments study such high-speed impacts.
- It is possible to fire models down a ballistic range at hypersonic speeds, and even to obtain atmospheric re-entry conditions up to model speeds of around 10 km/sec.
- Since there is no model support mechanism, the wake of the flying model can be studied.

Ballistics

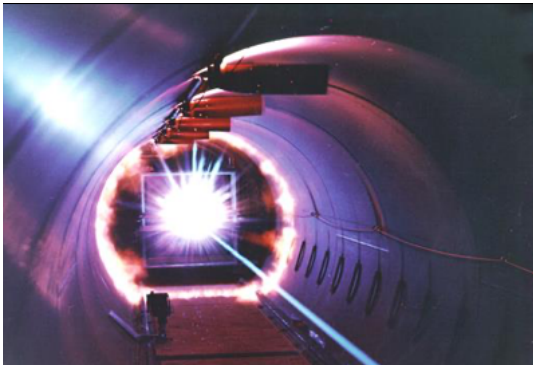

Figure 229: Energy flash when a projectile launched at speeds up to 17,000 miles an hour impacts a solid surface at the Hypervelocity Ballistic Range at NASA's Ames Research Center.

Ballistics

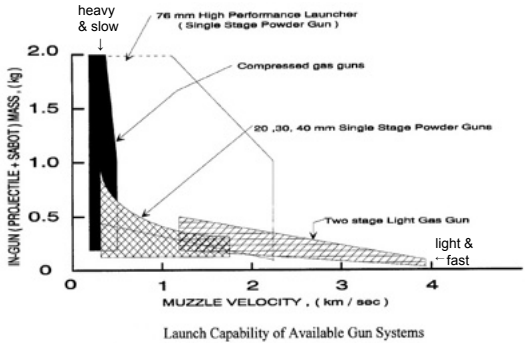

Figure 230: Mass of projectile and sabot with velocity.

Class Summary

- Applications - Isentropic flow and nozzles
- Applications - Supersonic inlets
- Applications - Ballistic range

Next Time

- Oblique Shock Waves

Class Overview

- Oblique shock wave examples
- Mach angle
- Oblique shock wave diagrams
- Oblique shock wave theory
- $\theta - \beta - M$ diagram

“If people do not believe that mathematics is simple, it is only because they do not realize how complicated life is.” John von Neumann

Oblique Shock Waves (OSW)

We study oblique shock waves as they are prevalent in external and internal aerodynamics

- A shock wave where the incoming flow angle is not normal relative to the wave front
- Normal shock waves are a special case of oblique shock waves
- Flow is turned “into itself”
- Contain many of the same properties as normal shock waves

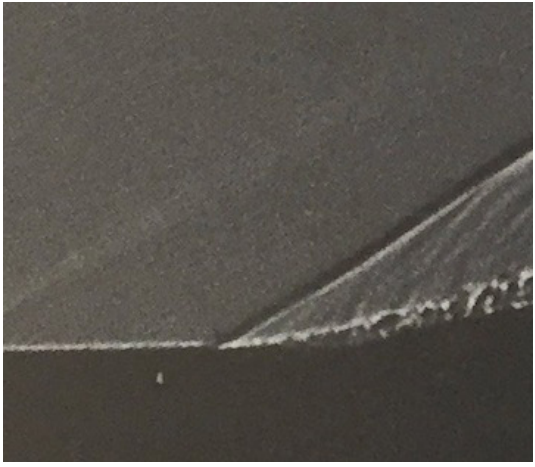

Figure 231: A schlieren of an oblique shock wave attached to a corner flow.

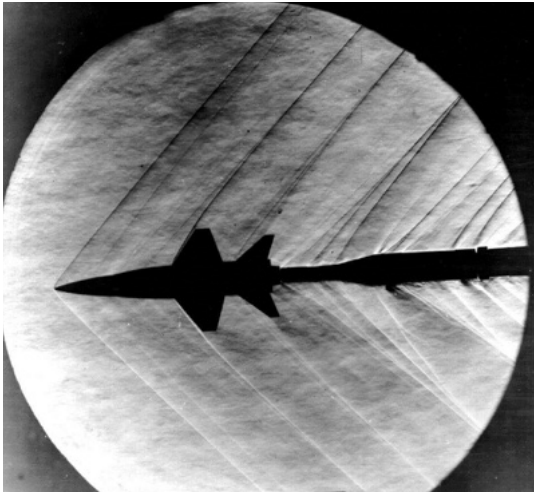

Figure 232: NASA X-15 wind tunnel test. As before, understand the phenomenon of these oblique-shock flows and the calculations will then be easy.

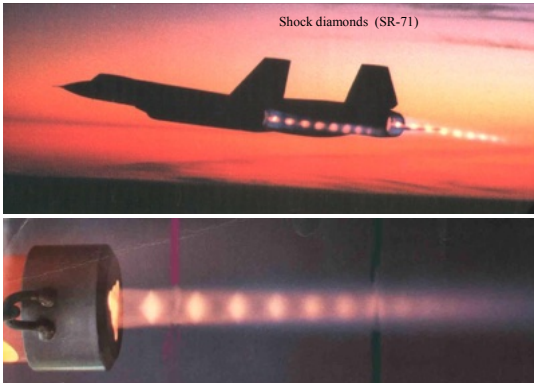

Figure 233: SR-71 in flight and model nozzle (bottom). Oblique shock waves are apparent in the jet (exhaust).

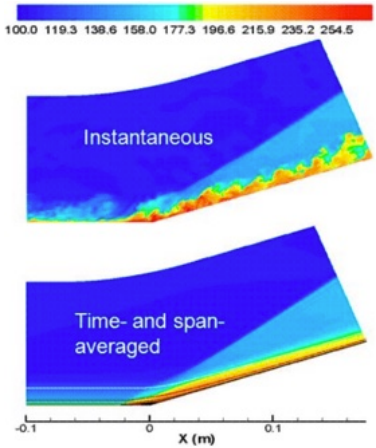

Figure 234: Instantaneous and time-averaged computational fluid dynamic solutions of oblique shock waves in a corner flow.

Oblique Shock Wave Diagram

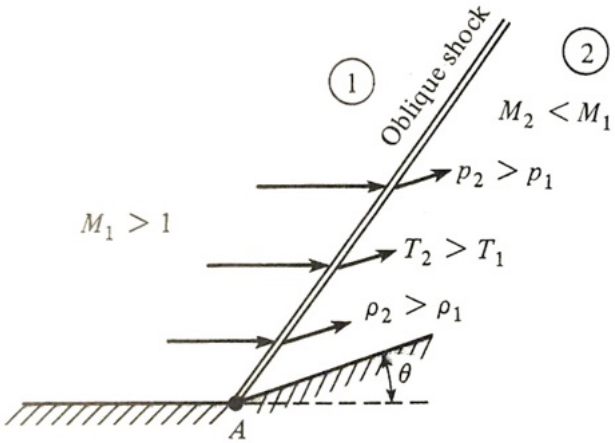

Figure 235: Diagram of an oblique shock wave in a corner flow.

Notes on the Oblique Shock Wave

- Oblique shock waves are prevalent in supersonic 3D flows
- Development of theory based on flow bounded by one side
- Flow is deflected by angle θ
- Stationary oblique shocks are functions of x and y
- Source is same as normal shock waves
  - Disturbances coalesce at speed of sound
  - Pressure mismatch within the domain
  - Please recall the moving point source example

A Disturbance in the Field

Moving point source and formation of Mach waves

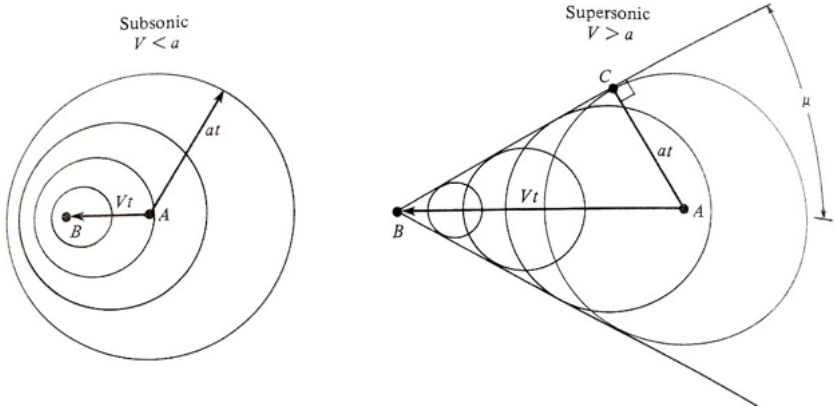

Figure 236: Diagram of waves coming from a moving disturbance.

Mach Wave

In the supersonic case a wave front is formed. Mach angle is

$$\sin \mu = \frac{ct}{ut} = \frac{c}{u} = \frac{1}{M} \tag{499}$$

$$\mu = \sin^{-1}\left(\frac{1}{M}\right) \tag{500}$$

- Coalescence of Mach waves (weak) disturbances into an oblique shock wave
- If disturbance is stronger, e.g. a wedge, then the wave is stronger than a Mach wave
- Coalescence occurs at an angel β to the free stream

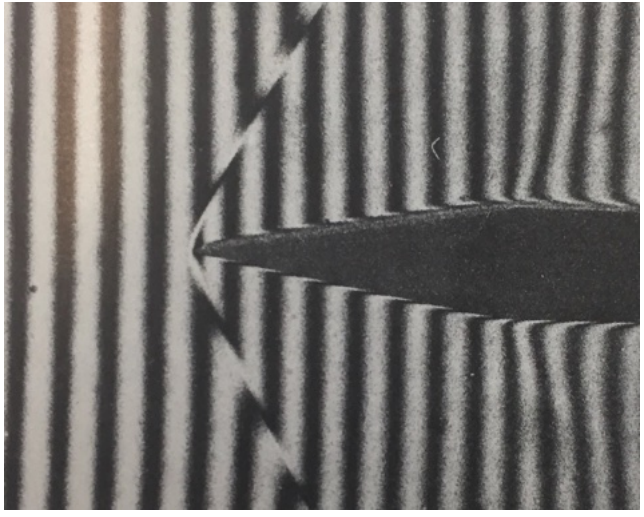

Figure 237: Shadowgraph.

Note that the Mach wave angle is smaller than the shock wave angle.

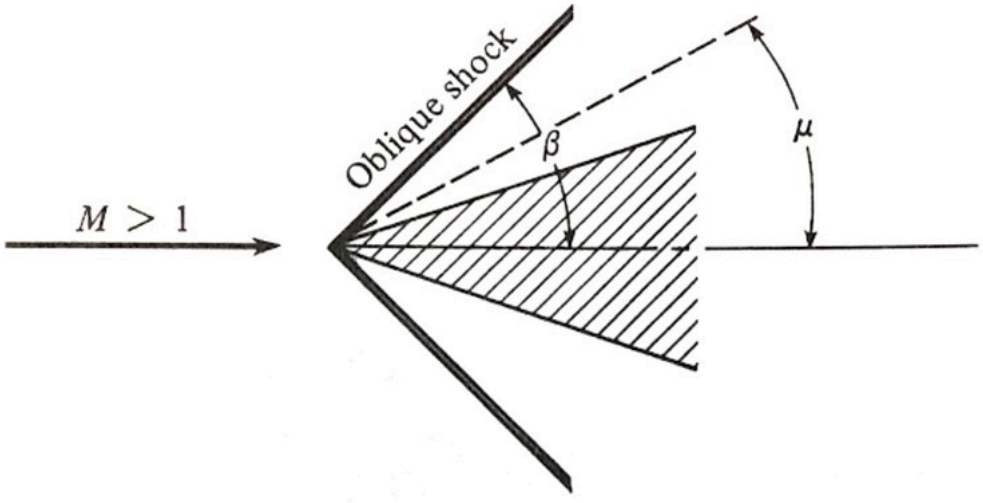

Figure 238: Diagram comparing the wave angle β and the Mach angle μ.

- Mach wave is a limiting weak shock case of the oblique shock wave
- Let us examine a diagram of the problem

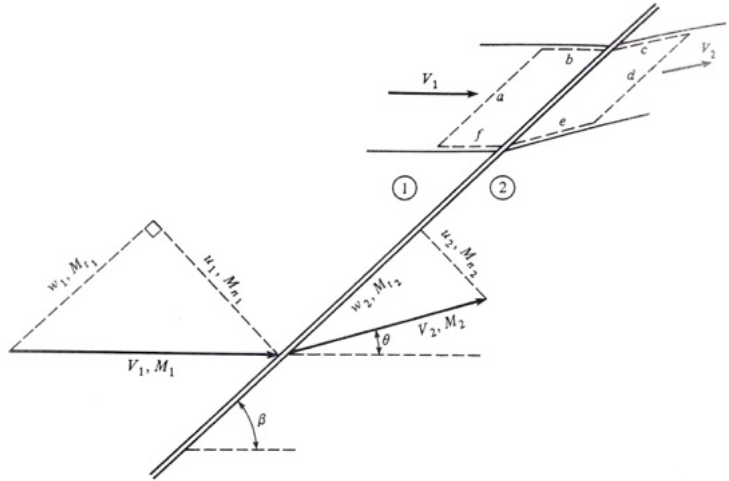

Figure 239: Oblique shock schematic.

Notation

- u_1, M_1 – velocity and Mach number upstream of the shock
- β – wave angle of oblique shock wave
- θ – flow is deflected by this angle (flow deflection angle)
- u_2, M_2 – velocity and Mach number behind the shock
- v_i, w_i – velocities normal and tangential to the shock front
- M_{ni}, M_{ti} – corresponding normal and tangential Mach numbers

Application of the Control Volume

Apply control volume theory to regions before and after the shock Find $\rho_1 v_1 = \rho_2 v_2$

$$\underline{u} \cdot d\underline{S} = 0 \tag{501}$$

Velocity does not cross dotted lines. Therefore

$$\rho_1 v_1 = \rho_2 v_2 \text{ (continuity)} \tag{502}$$

We assume there are no body forces.

Notation of underline denotes vector.

Application of the Control Volume

The tangential component of momentum in integral form

$$-(\rho_1 v_1)w_1 + (\rho_2 v_2)w_2 = 0 \tag{503}$$

Divide the equation by continuity

$$w_1 = w_2 \tag{504}$$

We now have the tangential component of velocity preserved across an oblique shock wave. Examine normal component of the differential equation

$$(-\rho_1 v_1)v_1 + (\rho_2 v_2)v_2 = -(-p_1 + p_2) \tag{505}$$

or

$$p_1 + \rho_1 v_1^2 = p_2 + \rho_2 v_2^2 \tag{506}$$

Application of the Control Volume

Let us examine the normal components. Integral form of the energy equation applied to control volume is

$$-(-p_1 v_1 + p_2 v_2) = -\rho_1 \left(e_1 + \frac{u_1^2}{2} \right) v_1 + \rho_2 \left(e_2 + \frac{u_2^2}{2} v_2 \right) v_2 \tag{507}$$

or

$$\left(h_1 + \frac{u_1^2}{2} \right) \rho_1 v_1 = \left(h_2 + \frac{u_2^2}{2} \right) \rho_2 v_2 \tag{508}$$

Application of the Control Volume

Dividing by the continuity equation yields

$$h_1 + \frac{u_1^2}{2} = h_2 + \frac{u_2^2}{2} \tag{509}$$

Recall that $u^2 = v^2 + w^2$ and $u_1^2 - u_2^2 = (v_1^2 + w_1^2) - (v_2^2 + w_2^2)$ and $w_1 = w_2$. We have

$$h_1 + \frac{v_1^2}{2} = h_2 + \frac{v_2^2}{2} \text{ (energy equation)} \tag{510}$$

Notes

- Our equations are almost identical to the standing normal shock relations.
- Particular velocity components are normal to the wave.
- Property changes across the wave are dependent on normal component of free-stream velocities
- Same mathematical procedure for a normal shock wave can be used to solve these equations.

Summary of our Relations for Oblique Shock Waves

We have

$$M_{n1} = M_1 \sin \beta \tag{511}$$

For calorically perfect gas we previously developed

$$\frac{\rho_2}{\rho_1} = \frac{(\gamma+1)M_{n1}^2}{(\gamma-1)M_{n1}^2+2} \tag{512}$$

$$\frac{p_2}{p_1} = 1 + \frac{2\gamma}{\gamma+1}\left(M_{n1}^2 - 1\right) \tag{513}$$

$$M_{n2}^2 = \frac{M_{n1}^2 + (2/(\gamma-1))}{(2\gamma/(\gamma-1))M_{n1}^2 - 1} \tag{514}$$

$$\frac{T_2}{T_1} = \frac{p_2}{p_1}\frac{\rho_1}{\rho_2} \tag{515}$$

Some Thoughts on Normal versus Oblique Waves

M_2 can be found through geometry and M_{n2} relation as

$$M_2 = \frac{M_{n2}}{\sin(\beta - \theta)} \tag{516}$$

Note the following

- Normal shock waves are only a function of one variable, M_1.
- Oblique shock waves are only a function of two variables, M_1 and β.
- Also, M_2 is dependent on θ (is this always the case?).
- We need to develop equations to find these relations.

Relation Between θ and β

From geometry

$$\tan\beta = v_1/\omega_1 \tag{517}$$

and

$$\tan(\beta-\theta) = \frac{v_2}{w_2} \tag{518}$$

Combining $w_1 = w_2$ these equations we find

$$\frac{\tan(\beta-\theta)}{\tan\beta} = \frac{v_2}{v_1} \tag{519}$$

Now combine with the integral relations for continuity, momentum, and energy

$$\frac{\tan(\beta-\theta)}{\tan\beta} = \frac{2+(\gamma-1)M_1^2\sin^2\beta}{(\gamma+1)M_1^2\sin^2\beta} \tag{520}$$

The $\theta - \beta - M$ Relation

Simplifying with trigonometric identities

$$\boxed{\tan\theta = 2\cot\beta\left[\frac{M_1^2\sin^2\beta - 1}{M_1^2(\gamma + \cos(2\beta)) + 2}\right]} \tag{521}$$

- We have found the $\theta - \beta - M$ relation, which gives θ as function of M_1 and β.
- But how does this function behave?

θ-β-M Diagram

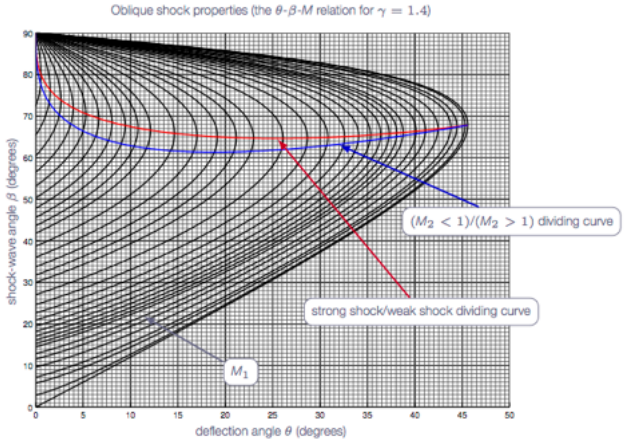

Figure 240: θ-β-M diagram.

θ-β-M Diagram

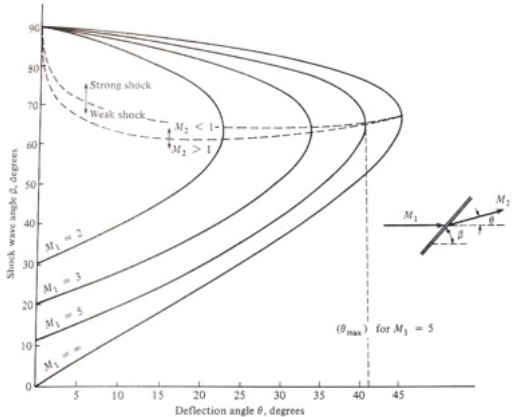

Figure 241: The θ-β-M diagram. Numerically generated from our derived θ-β-M equation.

Additional Notes for the θ-β-M Equation

- For any M_1 there is a max deflection angle $\theta_{\max}$.
- If geometry $\theta > \theta_{\max}$ then no solution exists for planar oblique shock wave
  - Instead shock wave will be strong and detached
- For $\theta < \theta_{\max}$ there are two valid values of β for each M_1.
  - Larger value of β implies the strong shock
  - Small value of β is weak shock solution
- Note – weak shock solution usually occurs (why?)
  - Determined by back pressure
- Strong shock implies $M_2 < 1$
- Weak shock implies $M_2 > 1$ (except near $\theta_{\max}$)

Class Summary

- Oblique shock wave examples
- Mach angle
- Oblique shock wave diagrams
- Oblique shock wave theory
- $\theta - \beta - M$ diagram

Next Time

- Attached versus bluff body shocks
- $\theta - \beta - M$ equation solutions
- Shock polar diagrams
- Hodographs
- Reflections

Class Overview

- Attached versus bluff body shocks
- $\theta - \beta - M$ equation solutions
- Shock polar diagrams
- Hodographs
- Reflections

“There’s no sense in being precise when you don’t even know what you’re talking about”
John von Neumann

Attached Versus Detached Shocks

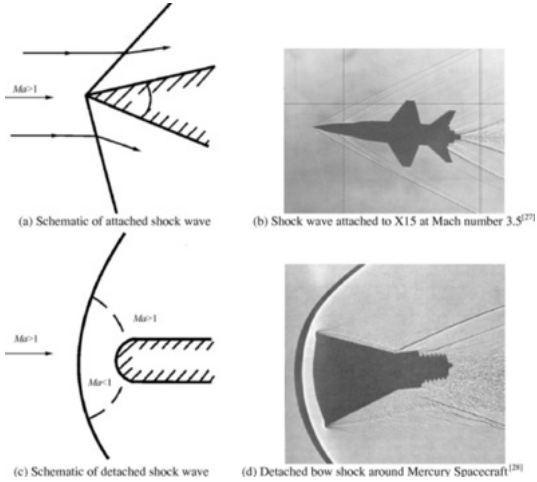

Figure 242: The attached and detached oblique shock waves.

Attached Versus Detached Shocks

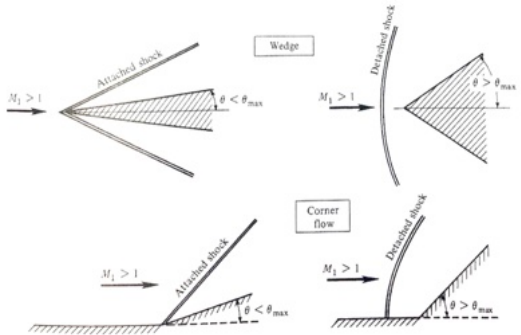

Figure 243: Oblique shock wave examples.

Detachment of Shocks and Other Notes

Physics to remember based on theory

- If $\theta = 0$ then $\beta = \frac{\pi}{2}$ implies a normal shock
- If $\beta = \mu$ then Mach wave
- If θ is constant while decreasing M_1 then wave angle β increases
- At very low Mach numbers the shock may detach
- No solution for $\theta - \beta - M$ equation for

$$\theta > \theta_{\max} \tag{522}$$

How can you find $\theta_{\max}$?

Analysis of $\theta - \beta - M$ Relation

- Results from oblique shock wave calculations reflect the nonlinear behavior of the equations e.g. often have M^2 terms
- Especially true of $\theta - \beta - M$ relation

Recalling $\theta - \beta - M$ equation

$$\tan\theta = 2\cot\beta\left[\frac{M_1^2\sin^2\beta - 1}{M_1^2(\gamma + \cos(2\beta)) + 2}\right] \tag{523}$$

- θ is easy to find, but usually know θ and seek β and M
- Usually can observe or measure these
- Predicting β involves numerics or advanced analytical solution

Sixth Order $\theta - \beta - M$ Equation

There is one analytical method to find β. Write $\theta - \beta - M$ as cubic equation then find roots

$$\sin^6\beta - \left(\frac{M^2+2}{M^2} + \gamma\sin^2\theta\right)\sin^4\beta + \left\{\frac{2M^2+1}{M^4} + \left[\left(\frac{\gamma+1}{2}\right)^2 + \frac{\gamma-1}{M^2}\right]\sin^2\beta\right\}\sin^2\beta - \frac{\cos^2\theta}{M^4} = 0 \tag{524}$$

In another form

$$\left(1 + \frac{\gamma-1}{2}M^2\right)\tan\theta\tan^3\beta - (M^2-1)\tan^2\beta + \left(1 + \frac{\gamma+1}{2}M^2\right)\tan\theta\tan\beta + 1 = 0 \tag{525}$$

Sixth Order $\theta - \beta - M$ Equation

Notes about this form of the equation

- 3 real unequal roots for attached shock wave for θ and M
- One root is negative, not useful
- Two positive roots correspond to weak and strong shocks

The Roots

We find

$$\tan\beta = \frac{M^2 - 1 + 2\lambda\cos[(4\pi\delta + \cos^{-1}\chi)/3]}{3\left(1 + \frac{\gamma-1}{2}M^2\right)\tan\theta} \tag{526}$$

$\delta = 0 \rightarrow$ Strong shock solution, and $\delta = 1 \rightarrow$ weak shock solution. Here

$$\lambda = \left[(M^2-1)^2 - 3\left(1 + \frac{\gamma-1}{2}M^2\right)\left(1 + \frac{\gamma+1}{2}M^2\right)\tan^2\theta\right]^{\frac{1}{2}} \tag{527}$$

and

$$\chi = \frac{(M^2-1)^3 - 9\left(1 + \frac{\gamma-1}{2}M^2\right)\left(1 + \frac{\gamma-1}{2}M^2 + \frac{\gamma+1}{4}M^4\right)\tan^2\theta}{\lambda^3} \tag{528}$$

Represents the "Alternative" form of the $\theta - \beta - M$ relation.
Allows explicit calculation for β given θ and M.

Shock Polar Diagrams

- Traditional approach in the field
- Excellent physical view-point of the oblique shock wave family
- Shock polar is a graphical representation of the solutions
- Graphically visualize mathematical solutions of the equations of motion for shock waves

Physical Plane

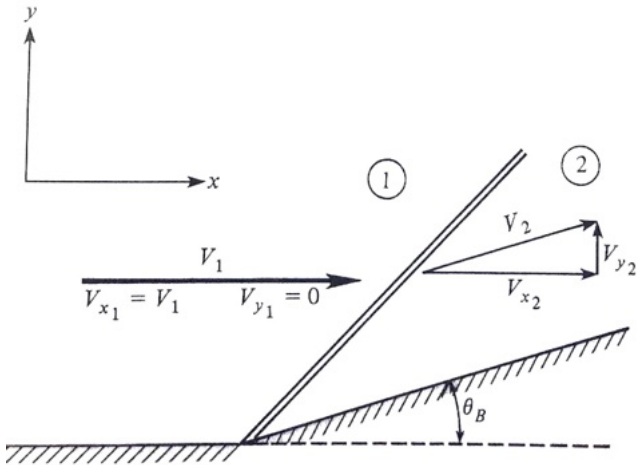

Figure 244: Physical plane coordinates and notation for the oblique shock.

Shock Polar Diagrams

Use u_x and u_y as axes, where u_x and u_y are velocity components. Plot the "hodograph" plane (graph of velocity components)

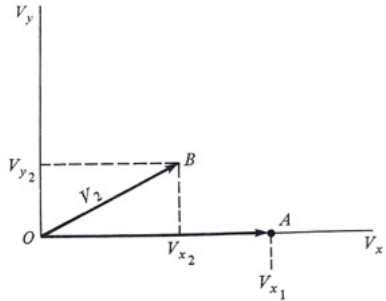

Figure 245: Hodograph of the oblique shock wave.

Tidbit: Hodographs are one of the only mathematical methods to construct nonlinear three-dimensional flow-field solutions!

Notation

Notes and notation for Fig. 245.

- Line OA is velocity ahead of shock
- Line OB is velocity behind shock
- Point A is state representation of flow-field ahead of the shock
- Point B is state representation of flow-field behind the shock
- Next consider new hodograph, where "θ_c" is increased to a higher value and u_2 is decreased because shock is stronger

Tracing the Shock Polar

Varying θ for all $\theta < \theta_{\max}$ we trace a line, which is the shock polar.

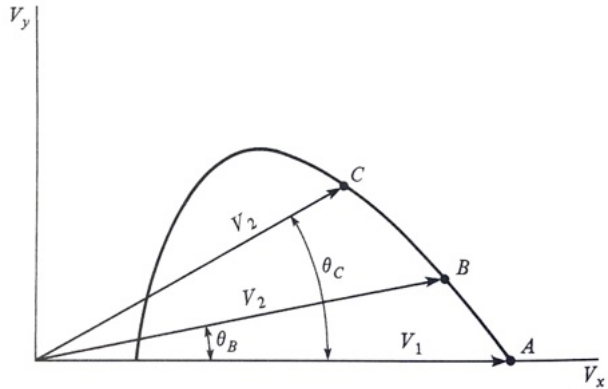

Figure 246: Create traces for a shock-polar diagram.

Shock Polar Diagram

Now, trace many lines for various solutions.

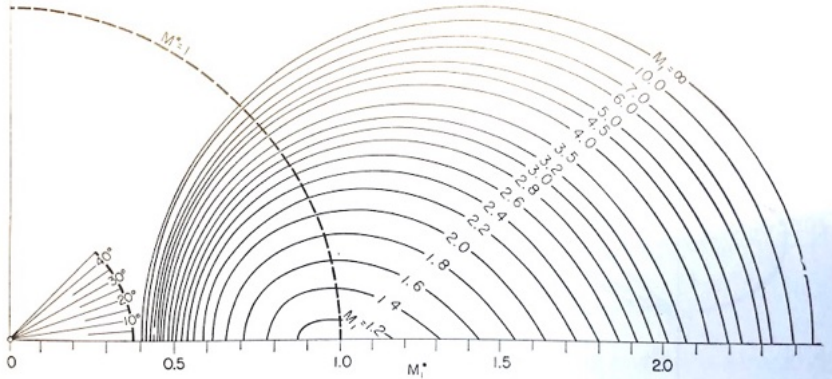

Figure 247: Family of hodograph shock polars from Shapiro.

Shock Polar Diagram

- Shock polar diagram that shows locus of all possible M_2^* for given values of M_1^*
- Now limit of $M \to \infty, M^* \to 2.45 (\gamma = 1.4$, air)
- Wide range of Mach numbers fit in a single diagram
- Circle of $M^* = 1$ encompasses all subsonic values

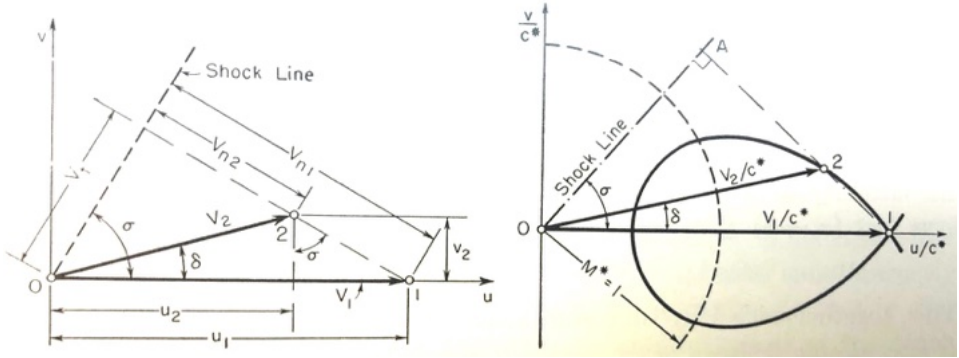

Figure 248: Shapiro's diagrams of shock polars.

Construction of the Shock Polar from Geometry

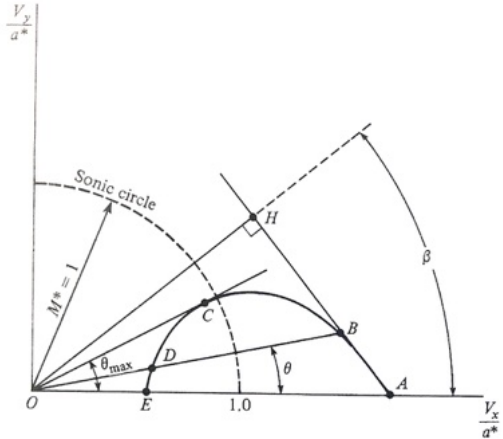

Figure 249: Geometric construction using the shock polar.

Shock Polar in Non-Dimensional Format

Seek a non-dimensional hodograph with a^* being hypothetical speed of sound at $M = 1$

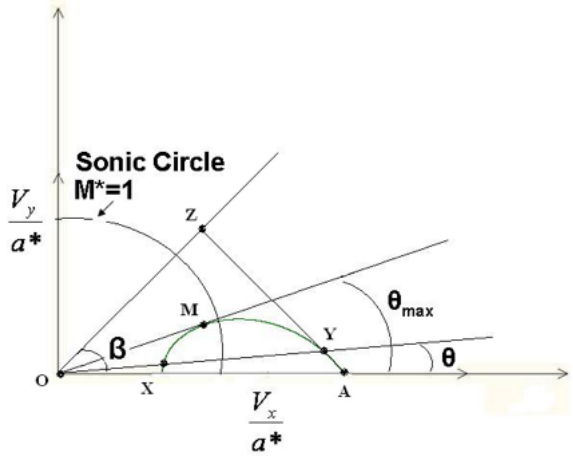

Figure 250

Important Points

1. For given θ, points y and x represent weak and strong shock solutions. Note D is inside sonic circle
2. Line $O7$ represents $\theta_{\max}$, for given M_1^*. No oblique shock for $\theta > \theta_{\max}$
3. Points x and A represent flow with no deflection $x \rightarrow$ normal shock, $A \rightarrow$ Mach wave
4. Line from A to y can be used to find angle β e.g. β is angle of HOA triangle
5. Shock polars for different Mach numbers form a family of curves. $M_1^* = 2.45$ is the circle

A Family of Shocks in the Polar Diagram

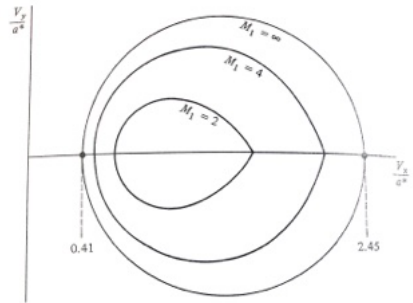

Figure 251: Shock polars for different Mach numbers.

An analytic expression for the shock polar is

$$\left(\frac{u_y}{c^*}\right)^2 = \frac{(M_1^* - u_x/c^*)^2[(u_x/c^*)M_1^* - 1]}{\frac{2}{\gamma+1}M_1^{*2} - (\frac{u_x}{c^*})M_1^* + 1} \tag{529}$$

Oblique Shock Wave Reflection on Solid Walls

Earlier in the class we considered reflections of normal shock waves. We now examine reflections of oblique shock waves.

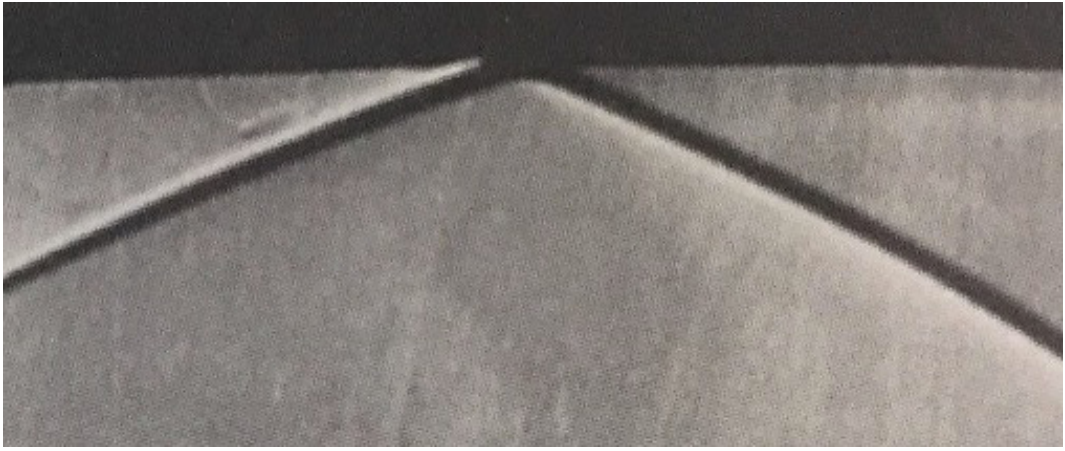

Figure 252: Schlieren image of a shockwave reflecting from a wall. Flow is obviously from left to right. Why?

Oblique Shock Wave Reflection on Solid Walls

- Recall our discussions of normal shock reflections
- Boundary condition (inviscid) Flow must be parallel to the wall.
- Analogy to a shock wave reflection of the previous moving shock problems

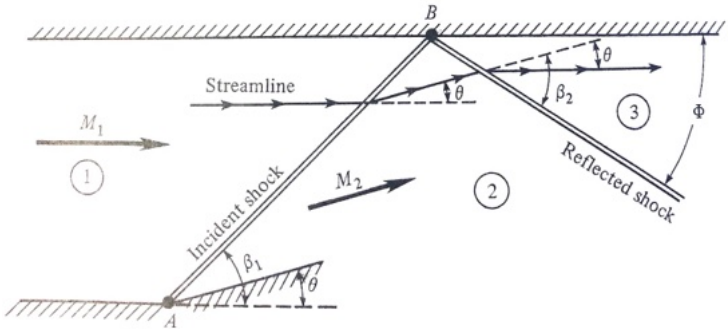

Figure 253: Reflected oblique shock wave.

Oblique Shock Wave Reflection on Solid Walls

- Reflected shock wave must turn flow again by angle θ after first shock wave
- All flow conditions are a function of θ and M_1
- At point B, the flow must be deflected by θ again (to keep flow parallel to wall).
- What happens if shock impinges on a corner?
- Second shock is defined by θ and M_2.
- M_2 must be less than M_1.
- $\beta_2 \neq \beta_1$ (unless unique wall angle)
- ϕ is angle reflected shock makes with the upper wall

How can we use our developed theory to solve these problems?

Example

Consider an oblique shock wave generated by a compression corner with a 10 deg. deflection angle. The Mach number of the flow ahead of the corner is 3.6; the flow pressure and temperature are standard sea level conditions. The oblique shock wave subsequently impinges on a straight wall opposite the compression corner. The geometry for this flow is given in Fig. 253. Calculate the angle of the reflected shock wave Φ relative to the straight wall. Also, obtain the pressure, temperature, and Mach number behind the reflected wave. (Example from Anderson)

Solution I

From the $\theta - \beta$ - M diagram, for $M_1 = 3.6$ and $\theta = 10°$, $\beta_1 = 24°$. Hence,

$$M_{n,1} = M_1 \sin\beta_1 = 3.6 \sin 24° = 1.464$$

$$M_{n,2} = 0.7157 \quad \frac{p_2}{p_1} = 2.32 \quad \frac{T_2}{T_1} = 1.294$$

Also,

$$M_2 = \frac{M_{n,2}}{\sin(\beta - \theta)} = \frac{0.7157}{\sin(24 - 10)} = 2.96$$

These are the conditions behind the incident shock wave. They constitute the upstream flow properties for the reflected shock wave. We know that the flow must be deflected again by $\theta = 10°$ in passing through the reflected shock. The $\theta - \beta - M$ diagram, for $M_2 = 2.96$ and $\theta = 10°$, we have the wave angle for the reflected shock, $\beta_2 = 27.3°$. Note

Solution II

that β_2 is not the angle the reflected shock makes with respect to the upper wall; rather, by definition of the wave angle, β_2 is the angle between the reflected shock and the direction of the flow in region 2 . The shock angle relative to the wall is, from the geometry

$$\Phi = \beta_2 - \theta = 27.3 - 10 = 17.3^\circ$$

Also, the normal component of the upstream Mach number relative to the reflected shock is $M_2 \sin \beta_2 = (2.96) \sin 27.3^\circ = 1.358$.

$$\frac{p_3}{p_2} = 1.991 \quad \frac{T_3}{T_2} = 1.229 \quad M_{n,3} = 0.7572$$

Hence,

$$M_3 = \frac{M_{n,3}}{\sin(\beta_2 - \theta)} = \frac{0.7572}{\sin(27.3 - 10)} = 2.55$$

Solution III

For standard sea level conditions, $p_1 = 2116\text{lb/ft}^3$ and $T_1 = 519°\text{R}$. Thus,

$$p_3 = \frac{p_3}{p_2}\frac{p_2}{p_1}p_1 = (1.991)(2.32)(2116) = 9774\text{lb/ft}^3$$
$$T_3 = \frac{T_3}{T_2}\frac{T_2}{T_1}T_1 = (1.229)(1.294)(519) = 825°\text{R}$$

Note that the reflected shock is weaker than the incident shock, as indicated by the smaller pressure ratio for the reflected shock, $p_3/p_2 = 1.991$ as compared to $p_2/p_1 = 2.32$ for the incident shock.

Class Summary

- Attached versus bluff body shocks
- $\theta - \beta - M$ equation solutions
- Shock polar diagrams
- Hodographs
- Reflections

Next Time

- Multiple shock systems
- Slip lines
- λ-shocks
- Mach intersections

Class Overview

- Multiple shock systems
- Slip lines
- λ-shocks
- Mach intersections

“The information needed by design engineers of either aircraft or flow machinery is the pressure, the shearing stress, the temperature, and the heat flux vector imposed by the moving fluid over the surface of a specified solid body or bodies in a fluid stream of specified conditions. To supply this information is the main purpose of the discipline of gasdynamics.” H. S. Tsien, 1953

Multiple Shock Systems - Inlet

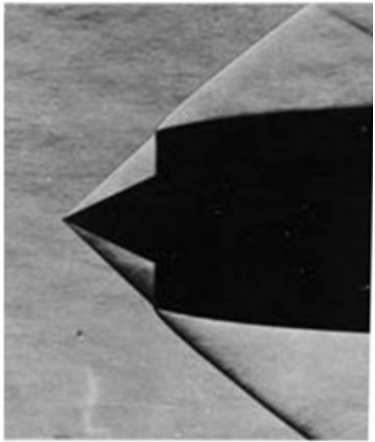

Figure 254: Schlieren image of an early fighter aircraft inlet.

Schematic of an Inlet

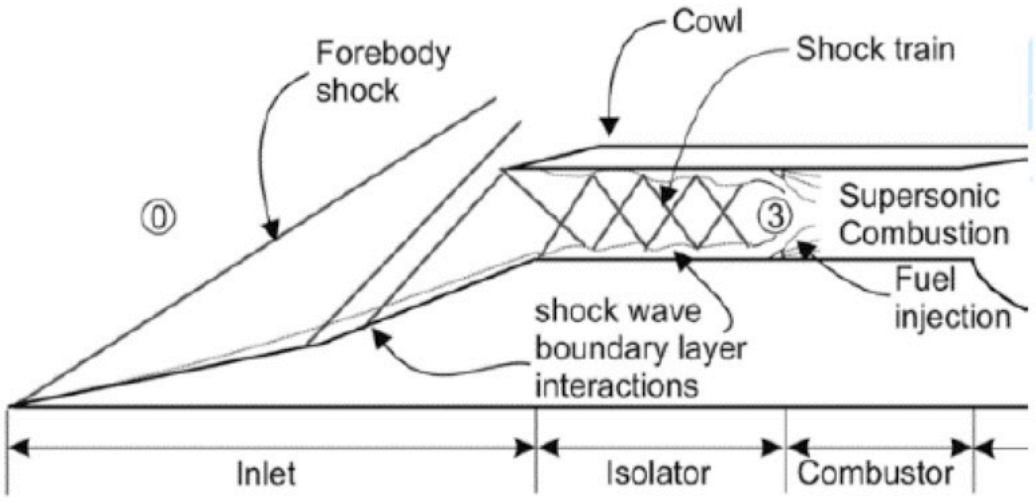

Figure 255: Basic drawing of concepts for the supersonic inlet.

Figure 256: SR 71

Figure 257: F22

Notes on Inlets

- Desire to increase pressure flow before compressor
  - Most efficient to move through system of oblique shocks
  - Single normal shock is highly inefficient
- Implications for supersonic wind tunnels within the diffuser
- Higher p_o recovery results in more efficient engines
- Smaller Δs across many weaker oblique shocks than single strong shock

Intersection of Shocks of Multiple Families

A “Left” and “Right” running shock intersect.

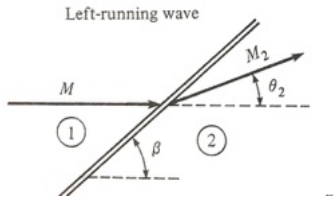

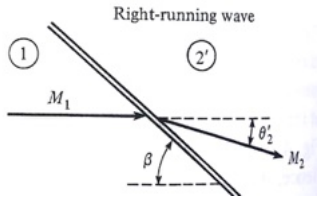

What happens?

CFD Example

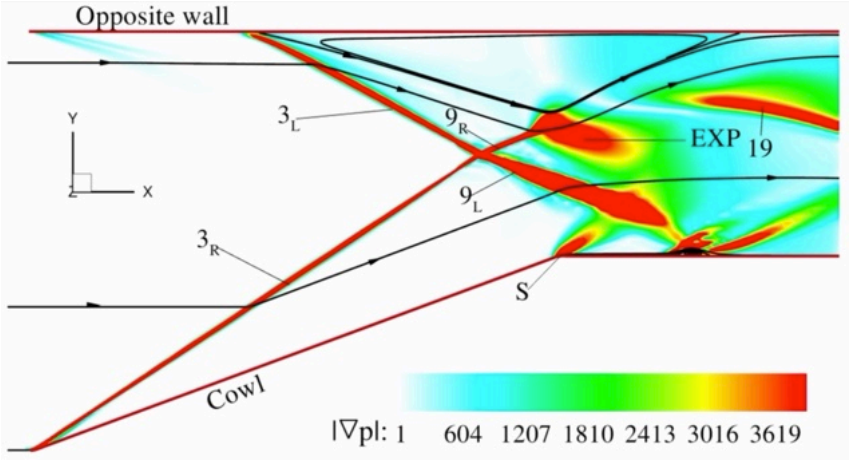

Figure 258: Contours of the magnitude of ∇p.

A Schematic of Shock Intersection

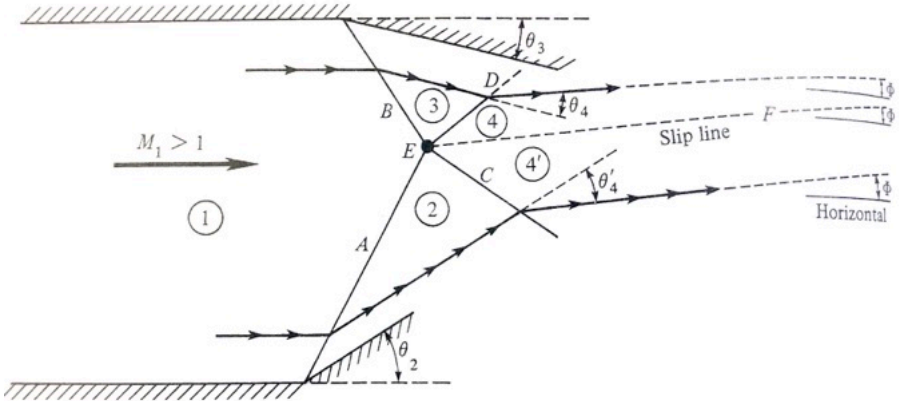

Figure 259: Schematic of intersecting shocks.

Notes on the Shock Intersection

- If $\theta_2 > \theta_3$ then shock A is stronger than B
- Streamlines undergo different entropy generation – Entropy in 4 and $4'$ differ
- "slip line" has a discontinuity in entropy
- Pressure across slip line must be constant, otherwise has curvature
  - We sometimes see slip lines that are curved
- Velocities in 4 and $4'$ are in same direction but have different magnitudes
- $\therefore$ Properties with known θ_2, θ_3, completely determine flow-field
- Thermodynamic values in 4 and $4'$ are different
- Solving these problems is easy, they are marching problems

Intersection of Shocks of the Same Family

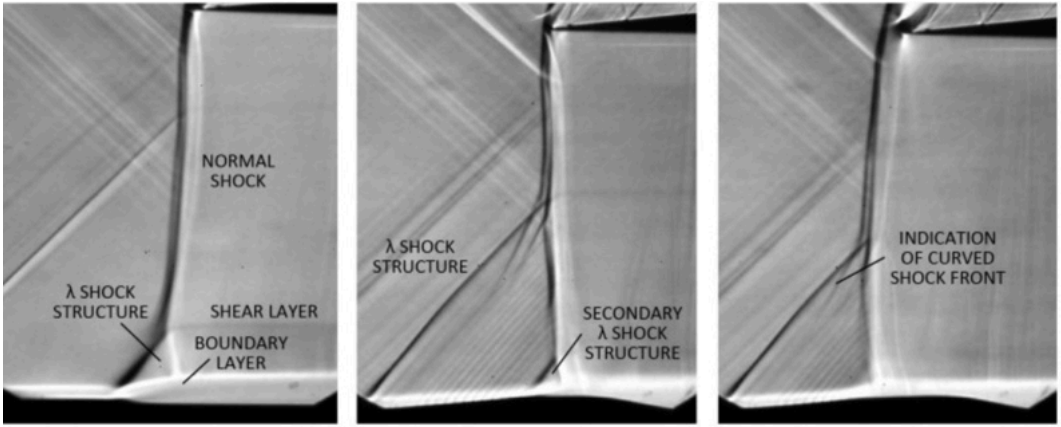

Figure 260: λ shockwaves.

A Corner Oblique Shock

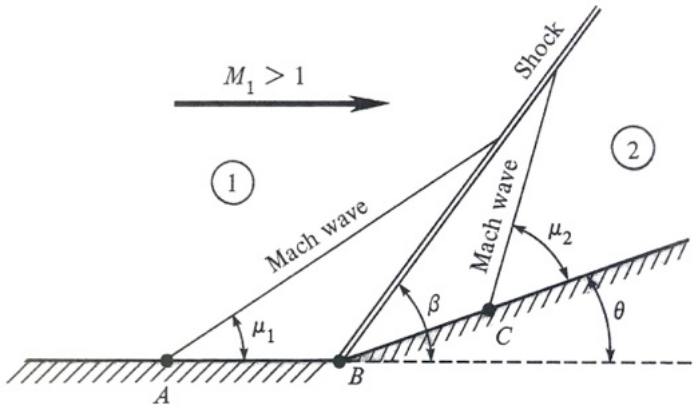

Figure 261: Corner oblique shock.

Intersection of Mach Waves

- Consider case where two Mach waves are generated
- Mach wave must intersect the shock because

$$v_1 = w_1 \sin\beta \rightarrow \sin\beta = \frac{v_1}{w_1} \;\&\; \sin\mu_1 = \frac{c_1}{w_1} \tag{530}$$

- We know $v_1 > c_1$ because shock normal component must be supersonic.
- Implies that $\underline{\beta > \mu_1}$
- Mach wave must intersect shock wave

Intersection of Mach Waves

What about the Mach wave behind the shock? We know

$$v_2 = w_2 \sin(\beta - \theta) \tag{531}$$

$$\& \ \sin(\beta - \theta) = \frac{v_2}{w_2} \ \& \ \sin \mu_2 = \frac{c_2}{u_2} \tag{532}$$

- Normal component is subsonic, $v_2 < c_2$
- Implies $\beta - \theta < \mu_2$
- Mach wave after the shock also intersects
- We can now extend this analysis to a more specific case....

Intersection of a Shock Family

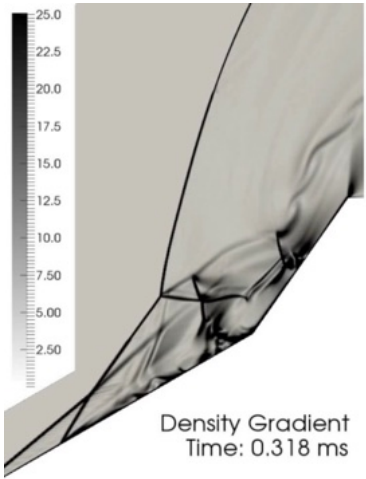

Figure 262: Schlieren of a shock family.

Extension of the Mach Intersection

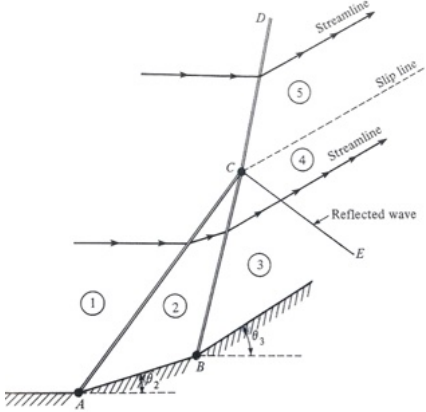

Figure 263: Schematic of the intersection.

Mach Intersection and λ Shock

- We observe a "λ" shock (lambda)
- Two left running oblique shock waves
- Region 5 properties are governed by a single oblique shock
- Region 4 governed by two oblique shocks
- Slip line shown develops between 4 and 5
- Entropy difference across the slip stream

Mach Intersection and λ Shock

- Different thermodynamic properties
- Velocity vector is in the same direction
- Originates at point C
- It is not possible for $p_4 = p_5$, but need this requirement, so a weak shock propagates in the "right" direction. (or expansion wave)
- Enforces $p_4 = p_5$ and $\theta_4 = \theta_5$
- Note system must be solved numerically by iterating waves CD and CE

Note on Mach Reflections

Consider again the reflection of an oblique shock near a wall.

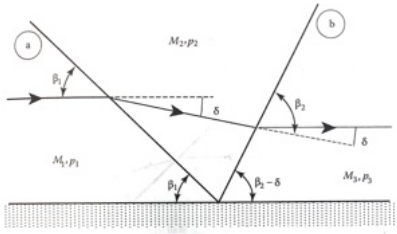

Figure 264: Diagram of a right running shock wave within corner.

- Streamlines are parallel to the wall pre- and post-reflection
- $\theta < \theta_{\max}$ for $M_2 \rightarrow$ solution of $\theta - \beta - M$ curve is valid
- Consider $\theta_{\max}$ for $M_2 < \theta < \theta_{\max}$ for M_1

Note on Attachment of Shock in Corner

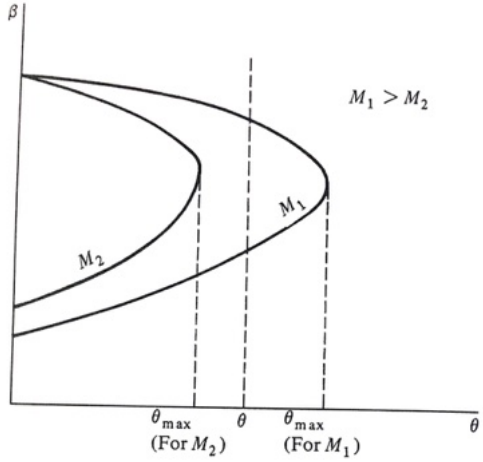

Figure 265: θ-β-M chart for reflection.

Incident shock is oblique, $\theta < \theta_{max}$

Shock Wave Wall Reflection

If flow is turned again by the wall after the shock, what happens when $\theta > \theta_{\max}$?

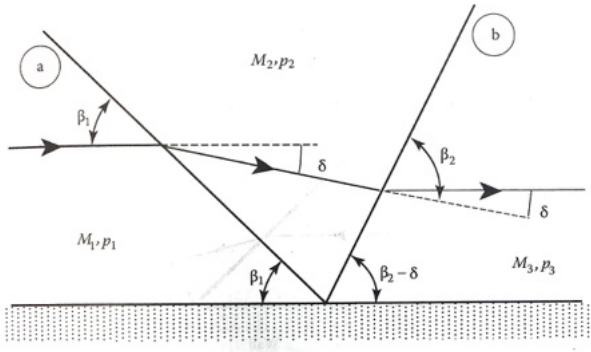

Figure 266

A normal shock is formed at the wall.

Notes

- Mach number always decreases across a shock wave
- Multiple shocks of the same family in the same flow must become progressively less swept back
- Shocks must eventually coalesce
- This happens for two reasons
  - 1) shock angles tend to be progressively less swept back
  - 2) each new wave angle is measured from the changed flow direction after the shock wave ahead of it

Example

$M_1 = 3.0$ and $\gamma = 1.4$ flow over a double-wedge compression corner with $\theta_1 = \theta_2 = 10$ deg. and $L = 5$ cm, determine:

- The height h of the oblique-shock coalescence point
- The Mach number in region 3, near the wall
- The Mach number in region 4, after shock coalescence

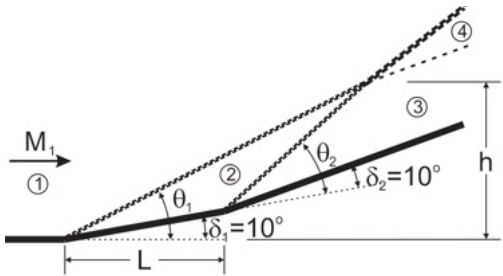

Figure 267: Shock waves of the same family (here left-running) will coalesce to form a single oblique shock.

Solution

- Begin by identifying the shock angles β_1 and β_2.
- Find β_1 from the oblique-shock charts or Calculator at $M_1 = 3.0$ and $\theta_1 = 10$ deg.
  - We find $\beta_1 = 27.4$ deg. and $M_2 = 2.51$
- Next find β_2 at $M_2 = 2.51$ and $\theta_2 = 10$ deg.
  - $\beta_2 = 31.9$ and $M_3 = 2.09$
- Remember that the angle β_2 is measured from the flow direction of M_2.
- Solve for h using trigonometry or graphically, obtaining $\boxed{h = 4.87}$ cm.

Solution

- The Mach number in region 3 has already been found, $\boxed{M_3 = 2.09}$, and was obtained by stepping through the two initial oblique shock waves.
- The Mach number in region 4 is different from M_3
  - The flow in region 4 has passed through only one shock wave
  - Whereas the flow in region 3 has passed through two shocks
- The coalesced shock wave has $M_1 = 3.0$ and a total turning angle $\theta = 20$ deg. in order to satisfy continuity.
- Looking up this oblique shock wave, $\boxed{M_4 = 1.99}$ and β coalesced shock = 37.8 deg.

Notes on Example

- Shows an important concept about coalescing shock waves
  - Flow discontinuities occur when parts of the flow pass through different combinations of shock waves.
  - The flow in region 3 is not the same as in region 4
- The flow is in the same direction in both regions 3 and 4, as it has been turned through a total of 20 deg.
- The flow is at a higher Mach number in region 3, $M_3 > M_4$
  - Shock strength increases with increasing incoming Mach number and increasing wave angle.
  - By turning the flow through two increments, there is less loss than turning the flow through the entire 20 deg. in one jump.

Notes on Example

- We can also calculate the change in p_o between region 1 and regions 3 and 4.
- $p_{o3}/p_{o1} = p_{o3}/p_{o2}(p_{o2}/p_{o1}) = (0.976)(0.963) = 0.940$ (Calculator)
- $p_{o4}/p_{o1} = 0.796/0.940 - 0.796 = 0.144$
- Thus there is 14.4% less p_o loss through 2 weak shocks then through a single (stronger) shock in this particular example

In general, to minimize the loss through oblique shocks, always turn through multiple small angles, not just one big turn.

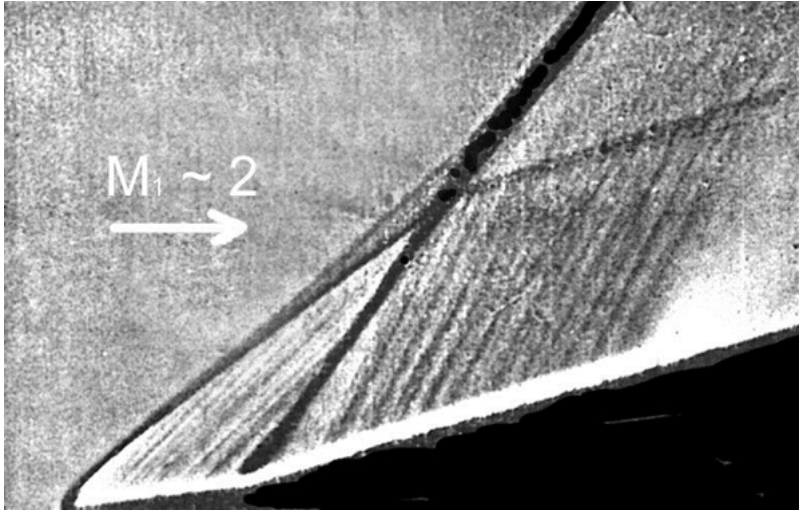

Figure 268: Compression corner involving multiple oblique and merged shocks. Notice the slip line.

The Slip Line

- Above and below the slip line the after-shock conditions are different, including the velocity.
- Flow direction and static pressure must be the same across the slip line, since the slip line is a streamline
- Velocity ‘slip’ causes a local normal velocity gradient, allowing viscosity to take over.
- Once the Reynolds number is high enough, the laminar slip line undergoes transition to turbulence. This can be seen in the regular Kelvin-Helmholtz vortices that form in the example above.

Figure 269: Slip line behind a λ shock.

Families of Oblique Shock Wave Reflections

Three types of oblique shock wave reflections are important to understand in basic gas dynamics:

- Reflection from a solid boundary or wall
- Reflection from a free boundary such as a jet boundary or shear layer
- Irregular or Mach reflection

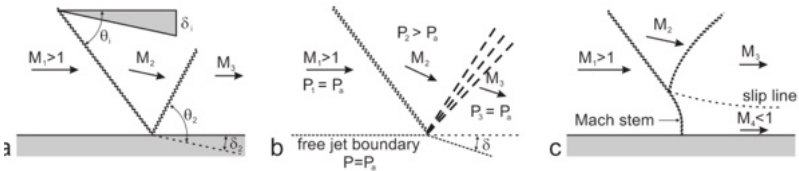

Figure 270: The three types of shock reflection are (a) a regular reflection from a solid boundary, (b) a regular reflection from a free boundary, and (c) an irregular or Mach reflection.

Oblique Shocks Changing Families

An oblique shock reflects from a solid boundary as an oblique shock of the opposite family, but it reflects from a free boundary as it is opposite: a Prandtl-Meyer expansion wave

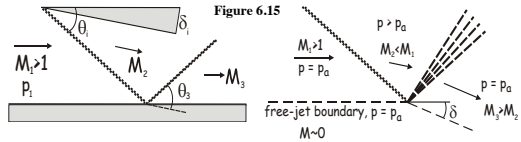

Figure 271

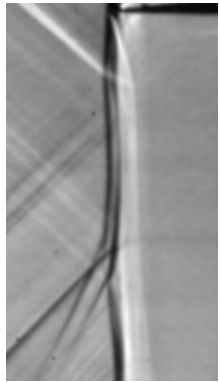

Figure 272: Oblique shock wave interacts with the upper wall, but a strong shock is formed instead of an oblique reflection.

Enforces streamlines to be parallel to the wall. This is a “Mach” reflection. Large subsonic flow values after this shock.

Class Summary

- Multiple shock systems
- Slip lines
- λ-shocks
- Mach intersections

Next Time

- Shock detachment
- Three-dimensional shocks
- Discussion of charts and figures

Class Overview

- Shock detachment
- Three-dimensional shocks
- Discussion of charts and figures

Detachment of Shock Waves in Front of Blunt Bodies

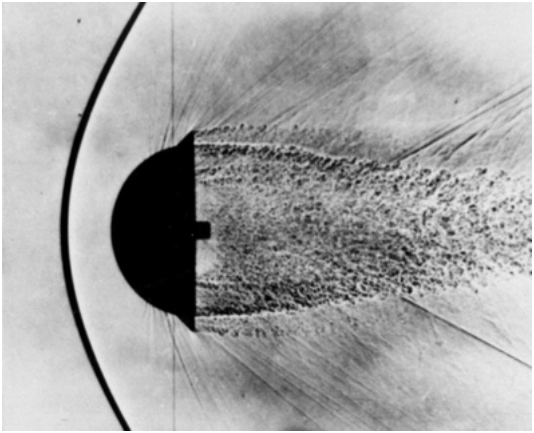

Figure 273: Bow shock with wake visualization through schlieren image.

Detached Shock Waves

Simple solutions of the oblique shock equations, as found in the charts and tables, are for straight shock waves attached to bodies with sharp leading-edges. If either

- a) the body is blunt, or
- b) the deflection angle θ is greater than θ_{max}, the maximum value permitted by the oblique shock equations

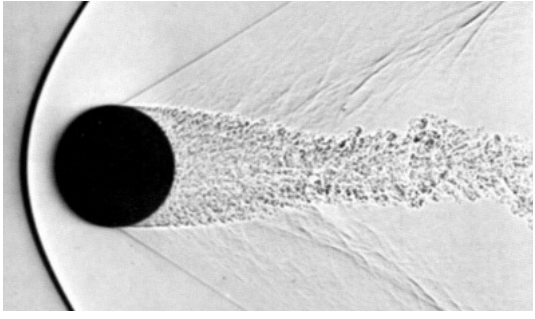

Figure 274: Supersonic cross-flow over a cylinder.

Detached Shock Waves

A curved detached shock wave stands ahead of the body

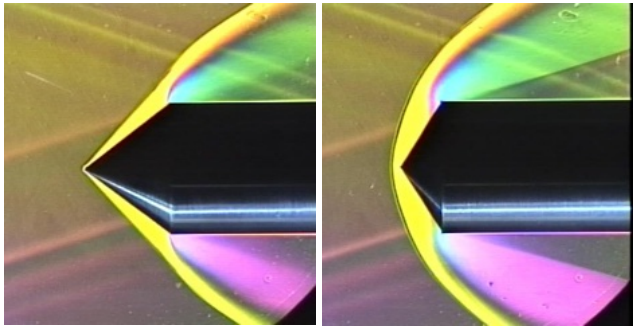

Figure 275: Note the detachment with larger deflection angle θ. Also, note the expansion in the left image that alters the oblique shock.

θ_{max} for a cone at Mach 3 in air is about 50 deg.

Detached Shock Waves

- The detached shock case is vastly more complicated than the attached-shock case.
- The governing equations for the supersonic and subsonic regions of this flow are different in nature with varying boundary conditions, There are no charted or tabulated solutions here.
- Computational fluid dynamics is required.

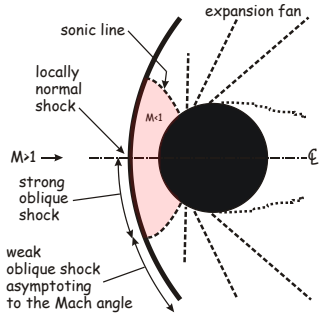

Figure 276

Detached Shock Waves

- As shown, the flow-field contains transonic, supersonic, and subsonic regions.
- δ - Detachment distance of the shock.
- These locations depend only on M_1 and shape of the body.

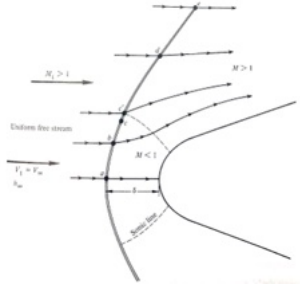

Figure 277

Between points “a through e”, the shock goes through all possible conditions for oblique shock waves.

$\theta - \beta - M_1$ Curve of Detached Shock

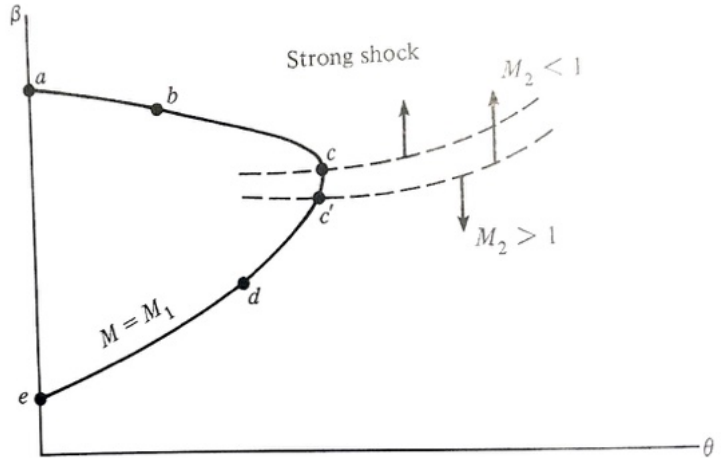

Figure 278: $\theta - \beta - M$ diagram illustrating the detached shock case. Remember the curve only represents the solution of the attached shock case.

Notation for the Previous Figure

- a – Normal shock
- b – Oblique shock but is strong shock solution
- c – Point dividing strong from weak shocks
- c – Point contains maximum deflection, θ_{max}
- c’ – Flow is sonic behind point
- a-c’ – Flow is subsonic
- c’ – Just above flow is supersonic

Three-Dimensional Shock Waves

- We have thus far only considered flow of 2D oblique shock waves
- For 3D flows, shock properties immediately after the shock can still be obtained with our approach
  - Realize that it is an additional approximation

The Three-Dimensional Oblique Shock

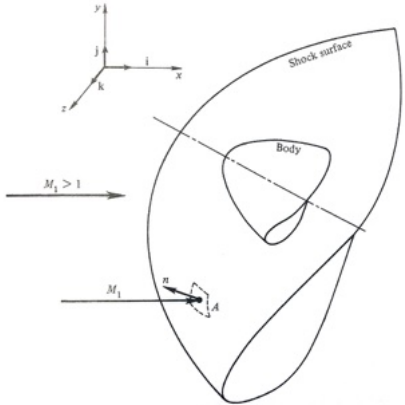

Figure 279: Schematic of a detached shock in front of a body.

Normal Components for 3D Shocks

The normal component of the Mach number is

$$M_{n1} = (M_1 \boldsymbol{i}) \cdot \boldsymbol{n} \tag{533}$$

- Now values of p_2, ρ_2, T_2, h_2 and M_{n2} can easily be found.
- Note that for 3D oblique shocks attached to cones, the Ames tables show solutions.

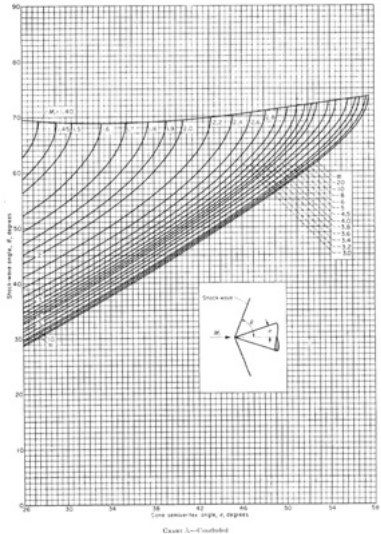

Figure 280: The Ames table for the cone.

Cones

- Once a cone is placed at an angle of attack to the freestream, the flow-field is no longer axisymmetric but rather fully three-dimensional.
- Full-scale computational solutions are now required.
- For large-enough angles of attack the flow becomes even more complicated by boundary layer separation on the leeward side of the cone due to strong crossflow, at which point CFD must be used.

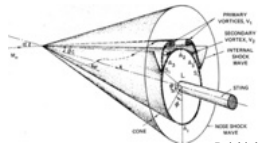

Rainbird, 1968

Interferogram of a cone in free flight at Mach 2 and an angle-of-attack of 37°. Kovalev & Mende, St. Peters-burg, Russia

Figure 281: Interferogram of a cone in free flight at Mach 2 and an angle-of-attack of 37 deg. Kovalev & Mende, St. Petersburg, Russia.

Examples of Cones

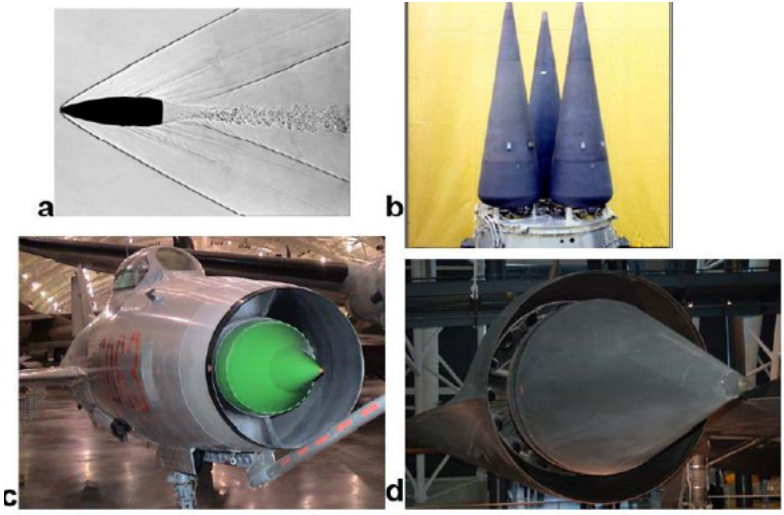

Figure 282: (a) bullets, (b) ballistic missiles and multiple independent re-entry vehicles (MIRVs), (c) the inlet of a MIG-21 and (d) the inlet of the SR-71.

Figure 283: LGM–118A Peacekeeper MIRV – source – Prof. Miller.

- Using the charts for planar oblique shocks (the pre-computer, 20th-century way)
- Example 1: Given $M_1 = 3.0$ and $\theta = 20$ in a $\gamma = 1.4$ flow, find the corresponding shock angle β.
- Solution: Enter the chart on $\theta = 20$ and follow the line upward until it crosses the line for $M_1 = 3.0$, then read across to find β.
- There are 2 solutions:$\beta = 37.8$ deg. (weak oblique shock) and $\beta = 82.2$ deg. (strong oblique shock)

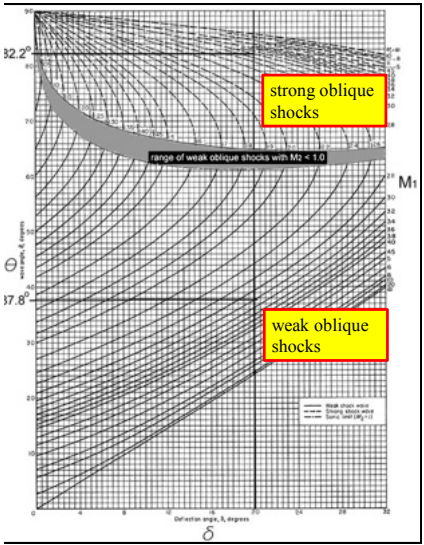

Figure 284

- Example 2: Given $M_1 = 3.0$ and $\beta = 38$ in a $\gamma = 1.4$ flow, find the corresponding wedge angle β
- Solution: Enter the chart at $\theta = 38$ deg. and follow the line upward until it crosses the line for $M_1 = 3.0$.
- Oops! It doesn't cross the line for $M_1 = 3.0$ because 38 deg. $> \theta_{max}$ at Mach 3. Thus there are NO attached oblique-shock solutions in this case.
- Use 2 clear straight-edges to stay on the lines!

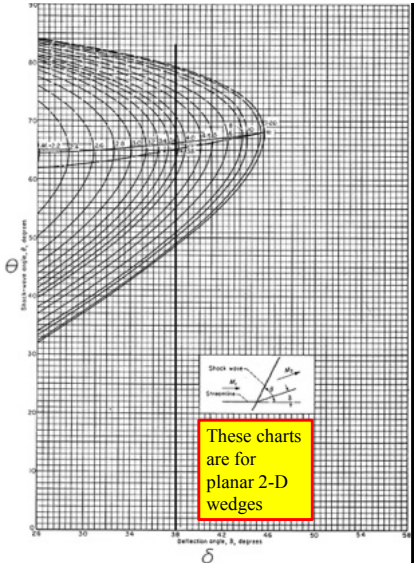

Figure 285

- Example 3: Given $M_1 = 2.8$ and $M_2 = 2.2$ in a $\gamma = 1.4$ flow, find the corresponding wedge angle θ
- Solution: Enter the chart at $M_2 = 2.2$, read across to the intersection with the line for $M_1 = 2.8$, then read down to find $\theta = 13$
- Since the given conditions uniquely define a weak-oblique-shock solution, there is no strong solution in this example

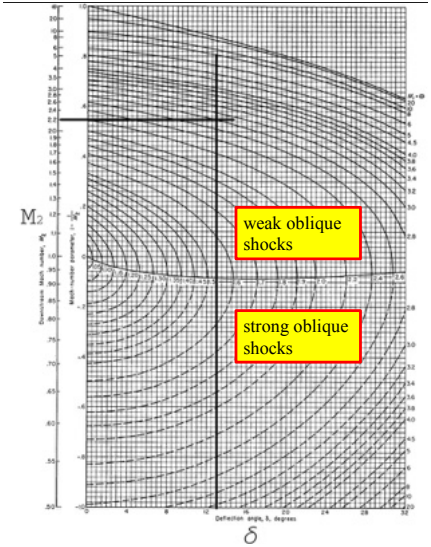

Figure 286

Strong solution → 82.2°

Q: How do I know whether to use the solid or the dashed lines on the oblique shock charts?

Weak solution → 37.8°

A: The solid lines are for the weak oblique shock solution. The dashed lines are dashed to warn you that you are looking up a strong oblique shock solution.

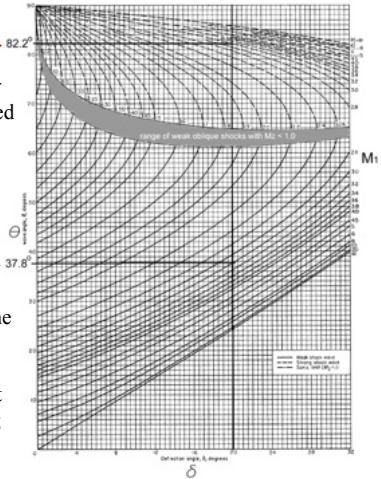

Figure 287

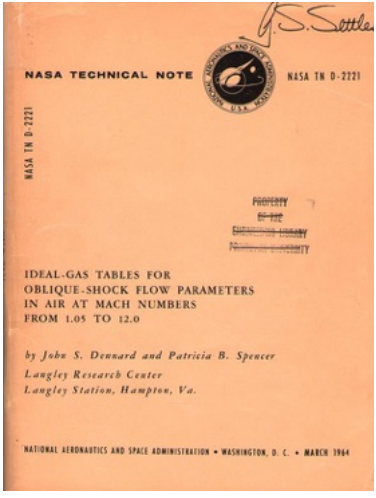

Figure 288: With the computing capacity we all now have available, it's a simple matter to program the oblique shock equations and let the machine do the work. At the dawn of the computer age in 1964 it was done for $\gamma = 1.4$ by Dennard and Spencer NASA TND-2221. Each of approximately 160 pages contains an oblique-shock table for a given M_1.

($\gamma = 1.4$, weak oblique shocks only)

note range of values

δ deg	θ deg	M_2	(ignore)	$\frac{p_2}{p_1}$	$\frac{\rho_2}{\rho_1}$	$\frac{T_2}{T_1}$	$\frac{p_{t2}}{p_{t1}}$	$\frac{\Delta s}{R}$
.0000E-99	1.9815E-01	2.9500E+00	7.0693E-01	1.0000E+00	1.0000E+00	1.0000E+00	1.0000E+00	.0000E-99
1.0000E-00	2.3520E+01	2.9007E+00	7.9199E-01	1.0789F-01	1.0554E+00	1.0218E+00	9.9999E-01	7.5233E-04
2.0000E-00	2.6220E+01	2.8488E+00	7.8863E-01	1.1634E+00	1.1140E+00	1.0443E+00	9.9984E-01	8.0684E-04
3.0000E-00	2.8950E+01	2.8012E+00	7.8175E-01	1.2519E+00	1.1737E+00	1.0666E+00	9.9988E-01	1.9832E-00
4.0000E-00	3.1671E+01	2.7521E+00	7.7611E-01	1.3446E+00	1.2358E+00	1.0895E+00	9.9732E-01	4.6345E-00
5.0000E-00	3.4490E+01	2.7041E+00	7.7065E-01	1.4413E+00	1.2997E+00	1.1128E+00	9.9490E-01	8.7722E-00
6.0000E-00	3.7290E+01	2.6572E+00	7.6512E-01	1.5513E+00	1.3658E+00	1.1364E+00	9.9143E-01	1.4238E+01
7.0000E-00	4.0122E+01	2.6087E+00	7.5927E-01	1.6630E+00	1.4326E+00	1.1608E+00	9.8675E-01	2.2899E+01
8.0000E-00	4.2972E+01	2.5613E+00	7.5328E-01	1.7802E+00	1.5014E+00	1.1856E+00	9.8075E-01	3.3324E+01
9.0000E-00	4.5884E+01	2.5120E+00	7.4694E-01	1.9032E+00	1.5721E+00	1.2113E+00	9.7335E-01	4.6934E+01
1.0000E+01	4.8775E+01	2.4637E+00	7.4049E-01	2.0344E+00	1.6437E+00	1.2376E+00	9.6453E-01	6.1975E+01
1.1000E+01	5.1698E+01	2.4160E+00	7.3390E-01	2.1720E+00	1.7161E+00	1.2645E+00	9.5429E-01	7.8628E+01
1.2000E+01	5.4620E+01	2.3689E+00	7.2691E-01	2.3134E+00	1.7899E-00	1.2922E+00	9.4253E-01	1.0156E+02
1.3000E+01	5.7600E+01	2.3186E+00	7.1951E-01	2.4684E+00	1.8649E+00	1.3213E+00	9.2925E-01	1.2597E+02
1.4000E+01	6.0590E+01	2.2687E+00	7.1221E-01	2.6193E+00	1.9393E+00	1.3508E+00	9.1480E-01	1.5282E+02
1.5000E+01	6.3622E+01	2.2179E+00	7.0422E-01	2.7836E+00	2.0153E+00	1.3813E+00	8.9881E-01	1.8306E+02
1.6000E+01	6.6708E+01	2.1678E+00	6.9607E-01	2.9546E+00	2.0911E+00	1.4126E+00	8.8167E-01	2.1615E+02
1.7000E+01	6.9850E+01	2.1169E+00	6.8749E-01	3.1319E+00	2.1673E+00	1.4450E+00	8.6333E-01	2.5216E+02
1.8000E+01	7.3060E+01	2.0653E+00	6.7870E-01	3.3175E+00	2.2436E+00	1.4786E+00	8.4391E-01	2.9120E+02
1.9000E+01	7.6350E+01	2.0145E+00	6.6934E-01	3.5088E+00	2.3192E+00	1.5129E+00	8.2373E-01	3.3275E+02
2.0000E+01	7.9730E+01	1.9619E+00	6.5953E-01	3.7092E+00	2.3951E+00	1.5488E+00	8.0259E-01	3.7743E+02
2.1000E+01	8.3270E+01	1.9080E+00	6.4918E-01	3.9185E+00	2.4712E+00	1.5856E+00	7.8054E-01	4.2515E+02
2.2000E+01	8.6810E+01	1.8542E+00	6.3837E-01	4.1383E+00	2.5468E+00	1.6237E+00	7.5803E-01	4.7536E+02
2.3000E+01	9.0410E+01	1.7995E+00	6.2697E-01	4.3727E+00	2.6215E+00	1.6633K+00	7.3500E-01	5.2831E+02
2.4000E+01	9.4210E+01	1.7444E+00	6.1511E+00	4.6208E+00	2.6958E+00	1.7036E+00	7.1168E+01	5.8378E+02
2.5000E+01	9.8090E+01	1.6872E+00	6.0233E+01	4.8371E+00	2.7703E+00	1.7460E+00	6.8771E+01	6.4243E+02
2.6000E+01	1.0220E+02	1.6295E+00	5.8895E+01	5.0905E+00	2.8441E+00	1.7896E+00	6.6363E+01	7.0379E+02
2.7000E+01	1.0650E+02	1.5700E+00	5.7463E+01	5.3557E+00	2.9178E+00	1.8355E+00	6.3925E+01	7.6785E+02
2.8000E+01	1.1100E+02	1.5084E+00	5.5932E+01	5.6338E+00	2.9915E+00	1.8832E+00	6.1463E+01	8.3522E+02
2.9000E+01	1.1590E+02	1.4442E+00	5.4255E+01	5.9283E+00	3.0699E+00	1.9337E+00	5.8988E+01	9.0662E+02
3.0000E+01	1.2120E+02	1.3760E+00	5.2410E+01	6.2442E+00	3.1415E+00	1.9876E+00	5.6482E+01	9.8271E+02
3.1000E+01	1.2660E+02	1.3023E+00	5.0330E+01	6.5878E+00	3.2194E+00	2.0461E+00	5.3758E+01	1.0651E+03
3.2000E+01	1.3200E+02	1.2197E+00	4.7888E+01	6.9745E+00	3.3024E+00	2.1117E+00	5.0948E+01	1.1572E+03
3.3000E+01	1.3700E+02	1.1183E+00	4.4872E+01	7.4455E+00	3.3988E+00	2.1935E+00	4.7690E+01	1.2570E+03
3.3725E+01	1.4193E+01	9.5281E+01	3.9200E+01	8.1990E+00	3.5350E+00	2.3101E+00	4.3149E+01	1.4422E+03
detached shocks		M2↓		$\frac{p_2}{p_1}$↑	$\frac{\rho_2}{\rho_1}$↑	$\frac{T_2}{T_1}$↑	$\frac{p_{t2}}{p_{t1}}$↓	∞↑

Figure 289

Example

As shown in the sketch, an oblique shock wave has an angle $\beta = 36.9$ with respect to an oncoming airflow at Mach 2.6. M_1, β, and γ define the jump conditions.

- a) Find the 2D planar wedge angle θ that would cause such a shock wave
- b) Find the circular-cone angle θ (also called σ for cones) that would cause such a shock wave

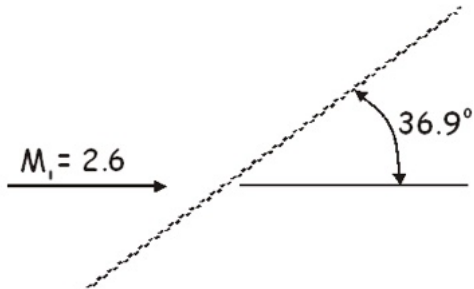

Figure 290

Solution

- Solve for p_2/p_1 across the shock using normal components and the normal shock tables,
  - Compare the result with that obtained from the p_2/p_1 chart, and with that obtained from the calculator
- Given $T_1 = 286$ K at M_1, find T_2 after the shock wave
- From the planar oblique-shock or Calculator, $\theta = 16.0$
- From the conical shock chart, $\sigma = 25.2$ deg.
  - Always takes a bigger cone than wedge angle to generate a shock of a given angle)

Class Summary

- Shock detachment
- Three-dimensional shocks
- Discussion of charts and figures

Next Time

- Prandtl-Meyer Expansion Fans

Class Overview

- Analysis of flows over cones

Taylor-Maccoll: Analysis of Flow-Fields Over Cones I

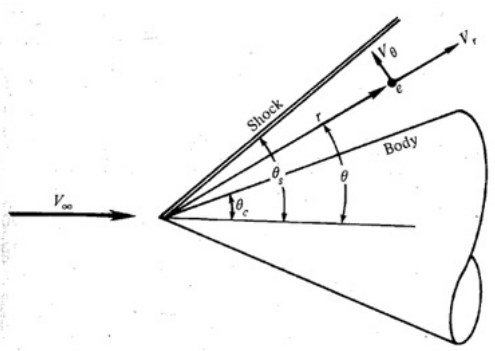

Figure 291: Coordinate system of flow-field over cone.

Taylor-Maccoll: Analysis of Flow-Fields Over Cones II

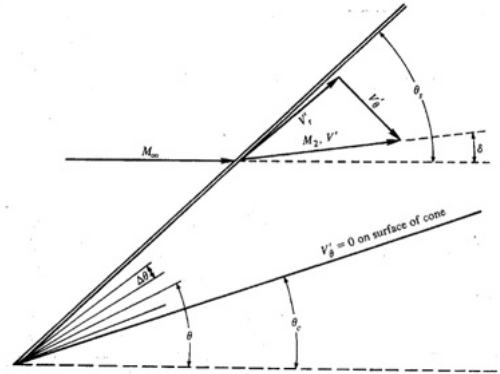

Figure 292: Shock wave centered velocity decomposition.

- Body of revolution, cylindrical co-ordinate system $(\mathrm{r}, \phi, \mathrm{z})$

Taylor-Maccoll: Analysis of Flow-Fields Over Cones III

- Axisymmetric $\frac{\partial}{\partial \phi} = 0$
- $\frac{\partial}{\partial \mathrm{r}} = 0$ (properties constant along rays)
- Background
  - Graphical solution: Buseman, 1929
  - Numerical solution: Taylor-Maccoll, 1933
- Consider a sharp cone at half angle θ_{c}.
- Streamlines are curved behind the shock
- Pressure is constant along the surface of the cone $\rightarrow$ length scale not important in this problem
- Flow properties constant along rays from a given vertex

Taylor-Maccoll: Analysis of Flow-Fields Over Cones IV

- Spherical co-ordinate system

$$r, \phi, \theta$$

Continuity equation

$$\nabla \cdot (\rho \mathbf{V}) = 0$$

$$\nabla \cdot \rho(\mathbf{V}) = \frac{1}{\mathrm{r}^2} \frac{\partial}{\partial \mathrm{r}} \left(\mathrm{r}^2 \rho \mathrm{V}_\mathrm{r} \right) + \frac{1}{\mathrm{r} \sin\theta} \frac{\partial}{\partial \theta} \left(\rho \mathrm{V}_\theta \sin\theta \right) + \frac{1}{\mathrm{r} \sin\theta} \frac{\partial \left(\rho \mathrm{V}_\phi \right)}{\partial \phi} = 0 \tag{534}$$

Taylor-Maccoll: Analysis of Flow-Fields Over Cones V

for axisymmetric conical flow

$$\frac{1}{r^2}\left[r^2\frac{\partial\left[\rho V_r\right]}{\partial r}+\rho V_r(2r)\right]+\frac{1}{r\sin\theta}\left[\rho V_\theta\cos\theta+\sin\theta\frac{\partial\left(\rho V_\theta\right)}{\partial\theta}\right]+\frac{1}{r\sin\theta}\frac{\partial\left(\rho V_\theta\right)}{\partial\phi}=0$$

$$\frac{2\rho V_r}{r}+\frac{\rho V_\theta}{r}\cot\theta+\frac{1}{r}\left(\rho\frac{\partial V_\theta}{\partial\theta}+V_\theta\frac{\partial\rho}{\partial\theta}\right)=0$$

$$2\rho V_r+\rho V_\theta\cot\theta+\rho\frac{\partial V_\theta}{\partial\theta}+V_\theta\frac{\partial\rho}{\partial\theta}=0 \tag{535}$$

Shock wave is straight - entropy increase same for all streamlines

$$\Rightarrow \nabla_s = 0$$

Taylor-Maccoll: Analysis of Flow-Fields Over Cones VI

adiabatic steady flow $\Rightarrow \nabla h_o = 0$

Crocco's Theorem: $T\nabla S = \nabla h_o - \mathbf{V} \times (\nabla \times \mathbf{V})$

$\Rightarrow \nabla \times \mathbf{V} = 0$ (Irrotational flow)

Crocco's theorem is a combination of continuity and momentum equation, $\Rightarrow \nabla \times \mathbf{V} = 0$ can be used in place for either one

$$\nabla \times \mathbf{V} = \frac{1}{r^2 \sin\theta} \begin{vmatrix} \mathbf{e_r} & re_\theta & (r\sin\theta)\mathbf{e}_\phi \\ \frac{\partial}{\partial r} & \frac{\partial}{\partial \theta} & \frac{\partial}{\partial \phi} \\ V_r & rV_\theta & (r\sin\theta)V_\phi \end{vmatrix} = 0$$

($\mathbf{e}_r, \mathbf{e}_\theta, \mathbf{e}_\phi$ are unit vectors in r, θ, ϕ directions)

$$\Rightarrow \nabla \times \mathbf{V} = \frac{1}{r^2 \sin\theta} \left\{ e_r \left[\frac{\partial}{\partial \theta}(rV_\phi \sin\theta) - \frac{\partial}{\partial \phi}(rV_\theta) \right] \right.$$

Taylor-Maccoll: Analysis of Flow-Fields Over Cones VII

$$-\mathrm{re}_\theta\left[\frac{\partial}{\partial \mathrm{r}}\left(\mathrm{rV}_\phi \sin\theta\right)-\frac{\partial}{\partial\phi}\left(\mathrm{V_r}\right)\right]+\left(\mathrm{r}\sin\theta\right)\mathrm{e}_\phi\left[\frac{\partial}{\partial \mathrm{r}}\left(\mathrm{rV}V_\theta\right)-\frac{\partial \mathrm{Vr}}{\partial\theta}\right]\Bigg\}=0 \quad (536)$$

for axisymmetric conical flow $\quad (V_\phi = 0)$

$$\frac{\partial}{\partial r}\left(rV_\theta\right)=\frac{\partial V_r}{\partial\theta} \Rightarrow \quad \mathrm{V}_\theta=\frac{\partial \mathrm{V_r}}{\partial\theta}$$

Euler's equation can be applied in any direction

$$\begin{aligned} dp &= -\rho V dV \\ V^2 &= V_r^2 + V_\theta^2 \end{aligned} \quad \Rightarrow dp = -\rho\left(V_r dV_r + V_\theta dV_\theta\right)$$

Taylor-Maccoll: Analysis of Flow-Fields Over Cones VIII

for isentropic flow $\left(\frac{dp}{d\rho}\right) = a^2$

$$\Rightarrow \frac{d\rho}{\rho} = -\frac{1}{a^2}\left(V_r dV_r + V_\theta dV_\theta\right)$$

define reference velocity $V_{\max}$: ($\mathrm{V} = \mathrm{V}_{\max}$ when $\mathrm{T} = 0$ and $\mathrm{h} = 0$)

$$\mathrm{h_O} = \text{constan}\, t = \mathrm{h} + \frac{\mathrm{V}^2}{2} = \frac{\mathrm{V}_{\max}^2}{2}$$

Here, $V_{\max} = \sqrt{2h_0}$, For a calorically perfect gas

$$\frac{a^2}{\gamma - 1} + \frac{V^2}{2} = \frac{V_{\max}^2}{2}$$

$$\Rightarrow a^2 = \frac{\gamma - 1}{2}\left(V_{\max}^2 - V^2\right) = \frac{\gamma - 1}{2}\left(V_{\max}^2 - V_r^2 - V_\theta^2\right)$$

Taylor-Maccoll: Analysis of Flow-Fields Over Cones IX

Substitution

$$\frac{d\rho}{\rho} = -\frac{2}{\gamma - 1}\left(\frac{V_r dV_r + V_\theta dV_\theta}{V_{\max}^2 - V_r^2 - V_\theta^2}\right)$$

- Euler's equation in a form useful for conical flow
- We now have three equations and three unknowns of ρ, V_r, V_θ
- One dependent variable, θ $\quad \Rightarrow$ with no partial derivatives

$$2V_r + V_\theta \cot\theta + \frac{dV_\theta}{d\theta} + \frac{V_\theta}{\rho}\frac{d\rho}{d\theta} = 0$$

and

$$\frac{d\rho}{d\theta} = -\frac{2\rho}{\gamma - 1}\left(\frac{V_r \frac{dV_r}{d\theta} + V_\theta \frac{dV_\theta}{d\theta}}{V_{\max}^2 - V_r^2 - V_\theta^2}\right)$$

Taylor-Maccoll: Analysis of Flow-Fields Over Cones X

$$\Rightarrow \frac{\gamma-1}{2}\left(\mathrm{V}_{\max}^2-\mathrm{V}_{\mathrm{r}}^2-\mathrm{V}_\theta^2\right)\left(2\,\mathrm{V}_{\mathrm{r}}+\mathrm{V}_\theta\cot\theta+\frac{\mathrm{dV}}{\mathrm{d}\theta}\right)- V_\theta\left(V_r\frac{dV_r}{d\theta}+V_\theta\frac{dV_\theta}{d\theta}\right)=0 \tag{537}$$

$$\mathrm{V}_\theta=\frac{d\,\mathrm{V}_{\mathrm{r}}}{\mathrm{d}\theta}\Rightarrow\frac{d\,\mathrm{V}_\theta}{\mathrm{d}\theta}=\frac{\mathrm{d}^2\,\mathrm{V}_{\mathrm{r}}}{\mathrm{d}\theta^2}$$

$$\frac{\gamma-1}{2}\left[\mathrm{V}_{\max}^2-\mathrm{V}_{\mathrm{r}}^2\left(\frac{\mathrm{dV_r}}{\mathrm{d}\theta}\right)^2\right]\left[2\,\mathrm{V}_{\mathrm{r}}+\frac{\mathrm{dV_r}}{\mathrm{d}\theta}\cot\theta+\frac{\mathrm{d}^2\,\mathrm{V}_{\mathrm{r}}}{\mathrm{d}\theta^2}\right] -\frac{\mathrm{dV_r}}{\mathrm{d}\theta}\left[\mathrm{V}_{\mathrm{r}}\frac{\mathrm{dV_r}}{\mathrm{d}\theta}+\frac{\mathrm{dV_r}}{\mathrm{d}\theta}\left(\frac{\mathrm{d}^2\,\mathrm{V}_{\mathrm{r}}}{\mathrm{d}\theta^2}\right)\right]=0 \tag{538}$$

which is the Taylor-Maccoll ODE.

Taylor-Maccoll: Analysis of Flow-Fields Over Cones XI

- This equation is solved numerically for the flow-field.

Class Summary

- Analysis of flows over cones

Next Time

- Prandtl-Meyer Flow-fields

Class Overview

- Prandtl-Meyer Expansion Fans - Introduction
- Theory
- Meyer function, ν (not viscosity)
- Solution approach

“It would be difficult to create the right mood under the present circumstances, but perhaps by accident another beautiful differential equation will come along again, as it once did when I worked with you.”

Letter from Meyer to Prandtl, May 5, 1918. Ref. no. GOAR:2647, DLR-Gottingen Archives

Prandtl-Meyer Expansion Waves

- Previously examined compression waves in the form of shock waves
- Turn our attention to Prandtl-Meyer expansion waves
- They form when supersonic flow is “turned out of itself”
- Opposite of shock wave

Prandtl-Meyer Expansion Wave Properties

- $M_2 > M_1$, expansions increase flow Mach number
- $p_2/p_1 < 1, \rho_2/\rho_1 < 1, T_2/T_1 < 1 \rightarrow$ pressure, density, and temperature decrease through the expansion wave
- Expansion is a continuous region of the flow
- Consists of an infinite number of Mach waves
- Streamlines are curved and smooth
- Expansions are isentropic because flow moves through Mach waves
  - $\triangle S = 0$ or $dS = 0$
- Theory developed by Prandtl's student Meyer in 1908 PhD dissertation – 46 pages (with a few figures)

Ludwig Prandtl

4 February 1875 – 15 August 1953, German

- Aerodynamics, transonics, boundary layers, thin-airfoils, lifting-line theories, Prandtl-Glauert correction, and more!
- Technische Hochschule Munich, earned Ph.D.
- Paper, "Fluid Flow in Very Little Friction," in which he described the boundary layer
- Student, Theodor Meyer developed the first theories of supersonic shock waves
- Director of the Kaiser Wilhelm Society
- Doctoral students Ackeret, Blasius, Busemann, Munk, Nikuradse, Pohlhausen, Schlichting, Tietjens, Tollmien, von Kármán, Vishnu Madav Ghatage, and many others (85 in total).
- At Göttingen until he died on 15 August 1953

Ludwig Prandtl 1904 with his fluid test channel

S.A.E. Miller, Ph.D., saem@ufl.edu

Theodor Meyer
July 1, 1882 – 1972, German

- Born, Lutheran family in Bevensen
- Wrote Ph.D. at 26, 46 pages long (PM-Expansion waves, Shock Waves, etc.), doctoral dissertation was the cornerstone of a modern scientific discipline
- Likely first MOC development for wind tunnel creation at end of WW1
- Called to military duty and served from the beginning of WWI as a captain in the German infantry (later chemical)
- Theodor Meyer married Frieda Buscher ¨Koopmann, did not participate in WW2, children
- After wars, mainly a school teacher, which he hated

Photograph of Theodor Meyer at the Munsterlager troop encampment in Germany during World War I, courtesy Christoph Meyer

S.A.E. Miller, Ph.D., saem@ufl.edu

Prandtl-Meyer Expansion Wave

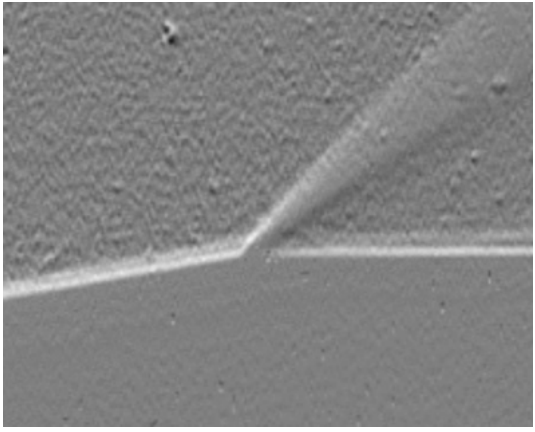

Figure 293: Schlieren of a Prandtl-Meyer expansion wave.

Prandtl-Meyer Expansion Wave

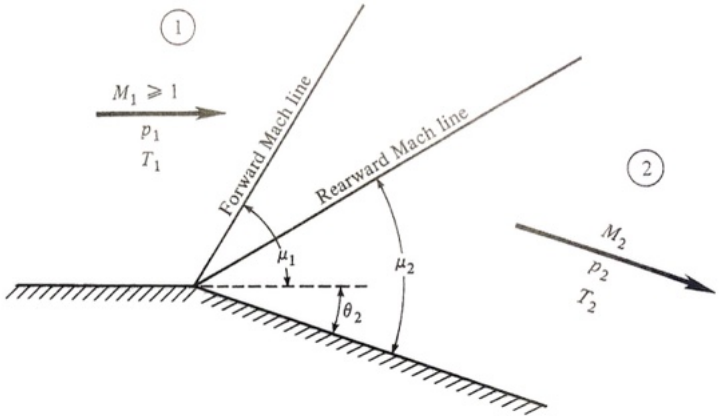

Figure 294: Expansion wave schematic.

Analysis

- Expansions occur in many different flows and situations
- Examples - Jet flows, supersonic external aerodynamics, internal aerodynamics, or corner flows
  - Can you think of more?
- Analyze this problem
  - For given flow properties M_1, p_1, T_1, and θ_2, find changes through the flow-field
  - Consider a small change of properties across a very weak wave
  - Wave deflection angle of $d\theta$

Notation for Prandtl-Meyer Expansion Wave

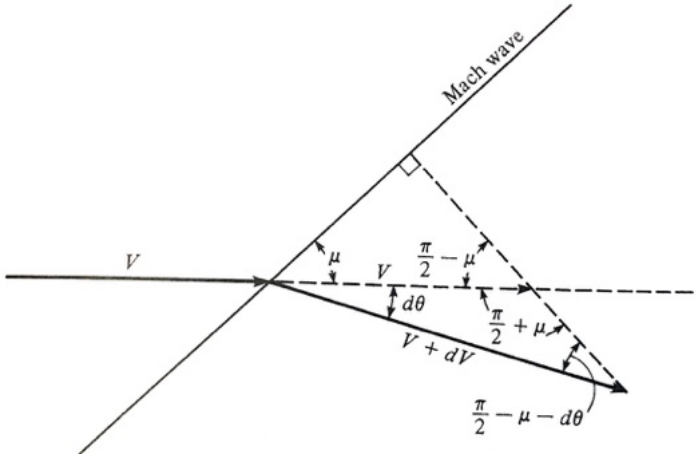

Figure 295: Differential changes within an expansion wave.

The law of sines states

$$\frac{u + du}{u} = \frac{\sin(\pi/2 + \mu)}{\sin(\pi/2 - \mu - d\theta)} \tag{539}$$

Using trigonometric identities

$$\sin\left(\frac{\pi}{2} + \mu\right) = \sin\left(\frac{\pi}{2} - \mu\right) = \cos\mu \tag{540}$$

and

$$\sin\left(\frac{\pi}{2} - \mu - d\theta\right) = \cos(\mu + d\theta) = \cos\mu\cos d\theta - \sin\mu\sin d\theta \tag{541}$$

Analysis

Substituting Eqns. 540 and 541 into Eqn. 539 yields

$$1 + \frac{du}{u} = \frac{\cos\mu}{\cos\mu\cos d\theta - \sin\mu\sin d\theta} \tag{542}$$

Note $d\theta$ is small, we can make use of the small angle assumption

$$\sin d\theta \approx d\theta \text{ and } \cos d\theta \approx 1 \tag{543}$$

Then we have

$$1 + \frac{du}{u} = \frac{\cos\mu}{\cos\mu - d\theta\sin\mu} = \frac{1}{1 - d\theta\tan\mu} \tag{544}$$

Analysis

Recall the series expansion

$$\frac{1}{1-x} = 1 + x + x^2 + x^3 ... \tag{545}$$

Likewise we expand our equation

$$1 + \frac{du}{u} = 1 + d\theta \tan\mu + ... \tag{546}$$

We now note $d\theta = \frac{du/u}{\tan\mu}$ and $\mu = \sin^{-1}(1/M)$ which we write as $\tan\mu = \frac{1}{\sqrt{M^2-1}}$. Now substitute this $\tan\mu$ relation into the $d\theta$ relation. We find

$$\boxed{d\theta = \left(M^2 - 1\right)^{1/2} \frac{du}{u}} \tag{547}$$

This is the governing differential equation for Prandtl-Meyer flow.

Analysis

Observations of Prandtl-Meyer equation

- An approximate equation for $d\theta$ (finite) and is exact as $d\theta \to 0$
- Derived based on geometry alone
- No gas assumptions
  - Valid for perfect, real, and chemically reacting gases
- Only valid for one small angle $d\theta$

Analysis

We must integrate to account for the entire turning angle. Integrating our function yields

$$\boxed{\int_{\theta_1}^{\theta_2} d\theta = \int_{M_1}^{M_2} \sqrt{M^2-1}\frac{du}{u}} \tag{548}$$

We can integrate this if we know du/u in terms of M. We choose to perform the natural log operation

$$\ln u = \ln M + \ln c \tag{549}$$

Now differentiate

$$\frac{du}{u} = \frac{dM}{M} + \frac{dc}{c} \tag{550}$$

Write the adiabatic energy equation as function of stagnation c and static c

$$\left(\frac{c_o}{c}\right)^2 = \frac{T_o}{T} = 1 + \frac{\gamma-1}{2}M^2 \tag{551}$$

Analysis

Solving for c

$$c = c_o \left(1 + \frac{\gamma - 1}{2} M^2\right)^{\frac{-1}{2}} \tag{552}$$

Differentiate c yields

$$\frac{dc}{c} = -\left(\frac{\gamma - 1}{2}\right) M \left(1 + \frac{\gamma - 1}{2} M^2\right)^{-1} dM \tag{553}$$

Substitute this relation into $\frac{du}{u} = \frac{dM}{M} + \frac{dc}{c}$ gives

$$\frac{du}{u} = \frac{1}{1 + \frac{\gamma - 1}{2} M^2} \frac{dM}{M} \tag{554}$$

We now know du/u as a function of M. So, substituting

$$\int_{\theta_1}^{\theta_2} d\theta = \theta_2 - 0 = \int_{M_1}^{M_2} \frac{\sqrt{M^2-1}}{1+\frac{\gamma-1}{2}M^2}\frac{dM}{M} \tag{555}$$

Let

$$\nu(M) = \int \frac{\sqrt{M^2-1}}{1+\frac{\gamma-1}{2}M^2}\frac{dM}{M} \tag{556}$$

be the Prandtl-Meyer Function, $\nu(M)$. The integration yields

$$\boxed{\nu(M) = \sqrt{\frac{\gamma+1}{\gamma-1}}\tan^{-1}\sqrt{\frac{\gamma-1}{\gamma+1}(M^2-1)} - \tan^{-1}\left(\sqrt{M^2-1}\right)} \tag{557}$$

Let the integration constant be zero. Now $\nu(M)$ for $M = 1$ and $\theta_2 = \nu(M_2) - \nu(M_1)$. The Prandlt-Meyer function is tabulated in tables for $\gamma = 1.4$, with μ.

Prandtl-Meyer Solution Approach

Step 1 Obtain $\nu(M_1)$ from table or use PM function for given M_1

Step 2 Calculate $\nu(M_2)$ from $\boxed{\theta_2 = \nu(M_2) - \nu(M_1)}$ from θ_2 and $\nu(M_1)$.

Step 3 Find M_2 from PM function or table using value of $\nu(M_2)$.

Step 4 Use isentropic relations as p_o and T_o are constant through the Prandtl-Meyer expansion to recover other variables.

TABLE II.—SUPERSONIC FLOW—Concluded

$\gamma = 1.4$

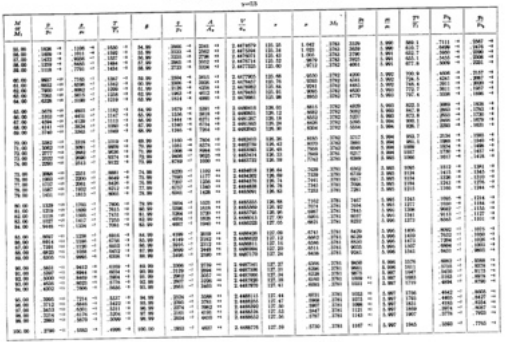

NOTATIONS FOR TABLES I AND II

M or M_1 local Mach number or Mach number upstream of a normal shock wave

$\frac{p}{p_0}$ ratio of static pressure to total pressure

$\frac{\rho}{\rho_0}$ ratio of static density to total density

$\frac{T}{T_0}$ ratio of static temperature to total temperature

β $\sqrt{M^2-1}$

$\frac{q}{p}$ ratio of dynamic pressure, $\frac{1}{2}\rho V^2$, to total pressure

$\frac{A}{A_*}$ ratio of local cross-sectional area of an isentropic stream tube to cross-sectional area at the point where $M=1$

$\frac{V}{a_*}$ ratio of local speed to speed of sound at the point where $M=1$

ν Prandtl-Meyer angle (angle through which a supersonic stream is turned to expand from $M=1$ to $M>1$), deg

μ Mach angle, $\sin^{-1}\frac{1}{M}$, deg

M_2 Mach number downstream of a normal shock wave

$\frac{p_2}{p_1}$ static pressure ratio across a normal shock wave

$\frac{\rho_2}{\rho_1}$ static density ratio across a normal shock wave

$\frac{T_2}{T_1}$ static temperature ratio across a normal shock wave

$\frac{p_{02}}{p_{01}}$ total pressure ratio across a normal shock wave

$\frac{p_2}{p_{01}}$ ratio of static pressure upstream of a normal shock wave to total pressure downstream

Figure 296: NASA Ames Tables

Theodore Meyer Original Dissertation

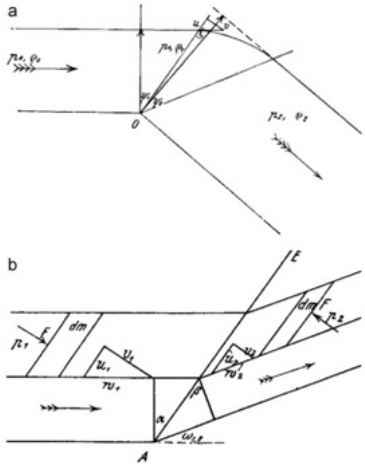

Figure 297: Meyer's dissertation – (a) the supersonic expansion and (b) the oblique shock wave.

Theodore Meyer Original Dissertation

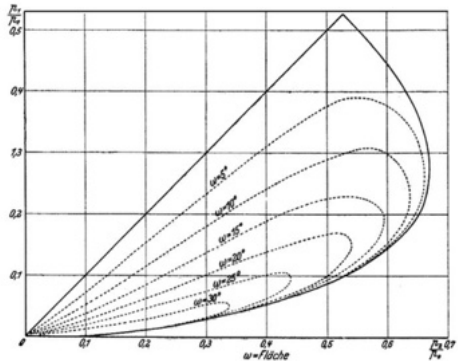

Figure 298: Meyer's dissertation – original oblique-shock polar diagram, in which the pressure ratio p_1/p_o before the shock wave is plotted versus p_2/p_o after the shock, with the flow-turning angle as a parameter, here solved for $\gamma = 1.4$.

Theodore Meyer Original Dissertation

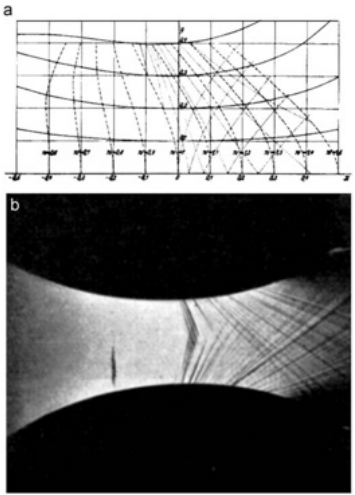

Figure 299: Meyer's dissertation – (a) solution for streamlines and constant-velocity lines in transonic flow at a Laval-nozzle throat and (b) schlieren image of Mach lines in the corresponding experiment.

Class Summary

- Prandtl-Meyer Expansion Fans - Introduction
- Theory
- Meyer function (ν)
- Solution approach

Next Time

- Shock expansion theory
- Diamond airfoils
- Wave drag
- Maximum expansion

Class Overview

- Shock expansion theory
- Diamond airfoils
- Note on downwash
- Wave drag
- Maximum expansion wave angle

“Mythologists and experimental theologians are needed for the development of a new method of attack”

Telegram to Meyer while in trenches after recovery which was mistranslated from “Meteorologists and experimental physicists,” where Meyer then traveled and met Fritz Haber (german Gas warfar pioneer)

Shock Expansion Theory

We will now combine our analysis of shock waves and expansions into a unified flow-prediction theory.

- Combination of oblique and expansion waves for calculation of aerodynamic forces.
- Analysis typically involves two-dimensional sections such as airfoils.
- More complicated analysis will involve three-dimensional calculations, often performed with computers.

Diamond Airfoil

One example is the diamond shaped airfoil, which is very illustrative and historic for this topic.

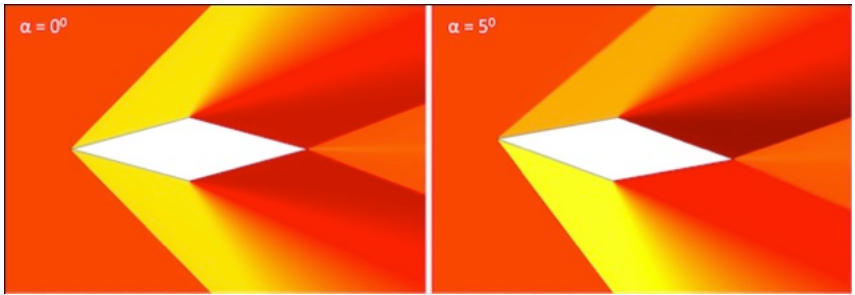

Figure 300: CFD solutions for diamond shape airfoil at two α at constant $M_\infty > 0$.

What flow-field features do we observer?

Diamond Airfoil

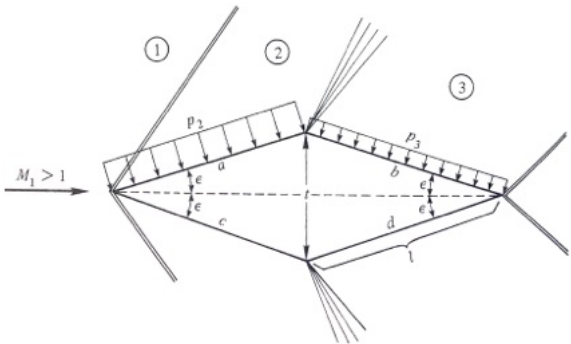

Figure 301: Forces on a diamond airfoil.

Notes on the Diamond Airfoil

- Illustration is symmetric in geometry, but only in specific cases
- The flow is also symmetric, but if $\alpha \neq 0$ then flow is not symmetric about x
- Flow is initially deflected by angle ϵ and compressed
- Flow is then expanded at mid-chord by angle 2ϵ
- At trailing edge the flow is deflected and compressed by angle ϵ
- Last deflection required for flow to be parallel, to the free-stream direction. e.g. – symmetry, but not the case for $\alpha \neq 0$
- Only force is drag because symmetry – lift is created for non-symmetric flow
- Combine our theories to solve these problems

The Pressure Drag

- We can concisely write the drag, due to the pressures induced by the shocks and expansions
- This is the wave drag of the vehicle
- The drag will be the x-component of the force
- Integrate the pressure on the vehicle

$$D_{wave} = -\oint p d\underline{S} \tag{558}$$

And for the symmetric diamond airfoil shown previously we find

$$\begin{aligned} D_{wave} &= (p_2 l \sin\epsilon - p_3 l \sin\epsilon) = 2(p_2 - p_3)t/2 \\ &= (p_2 - p_3)t \end{aligned} \tag{559}$$

This is more complicated for $\alpha \neq 0$

Jean-Baptiste le Rond d'Alembert's Paradox

- Supersonic flow with the existence of wave drag alters the most traditional theories of aerodynamics
- For example, d'Alembert's Paradox states that,

  "drag is zero for inviscid flow over an airfoil of finite span at subsonic speed."

- This theory used the assumption of incompressible flow

... which leads to my very favorite person in mathematics and science!

Jean-Baptiste le Rond d'Alembert

16 November 1717 – 29 October 1783, French

"time destroyed all models which the ancients may have left us in this genre"

- Mathematician, physicist, philosopher, and music theorist
- d'Alembert solution to wave equation
- Mother left him on the steps of the Saint-Jean-le-Rond de Paris church. Named after the patron saint of the church. Education secretly paid for by his father of royalty.
- 1740 Mémoire sur la réfraction des corps solides, theoretically explained refraction
- 1752, wrote D'Alembert's paradox: that the drag on a body immersed in an inviscid, incompressible fluid is zero.
- Participant in several Parisian salons
- A known 'unbeliever,' was buried in a common unmarked grave.

S.A.E. Miller, Ph.D., saem@ufl.edu

Wave Drag

- For supersonic flow, drag is finite in the context of traditional theory
- This new source of drag is called “wave drag”
- Dependent on loss of total pressure and increase of entropy across the oblique shock waves

XKCD - Lift

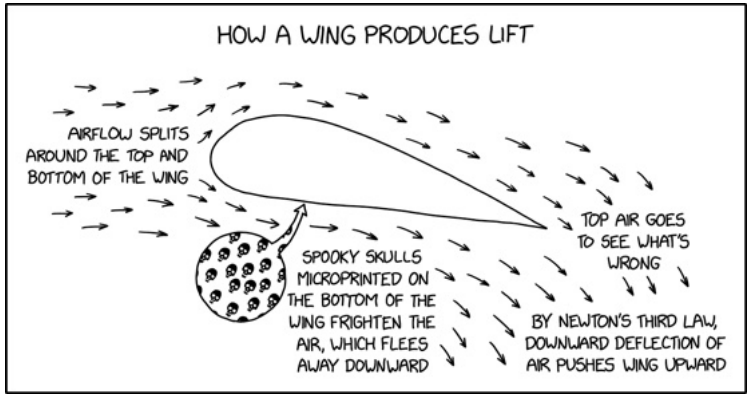

Figure 302: Source: https://xkcd.com/2678.

Example

Consider a thin plate at $\alpha = 5$ deg. in a $M_\infty = 2.6$ flow. Find c_l and c_d

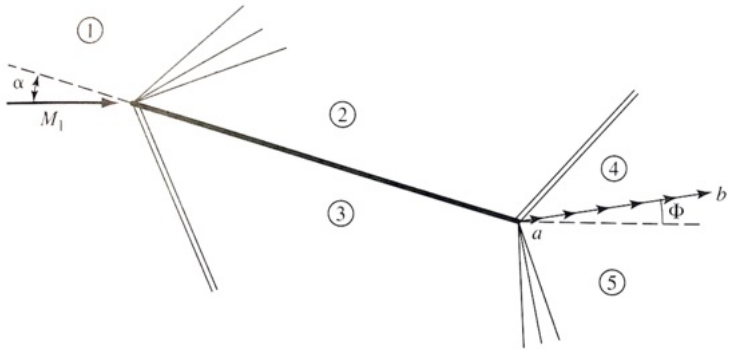

Figure 303: Simplified flow over a flat plate.

Solution

- Seek solution in region 2
  - Using Prandtl-Meyer table look at $M_1 = 2.6$
  - We find the PM function at 1, and find that $\nu = 41.41^\circ$
  - We need to march downstream. Using $\theta_2 = \nu(M_2) - \nu(M_1)$, we find

$$\nu_2 = \nu_1 + \alpha = 41.41 + 5 = 46.41^\circ \tag{560}$$

  - From Prandtl-Meyer table for $\nu_2 = 46.41^\circ$, we find $M_2 = 2.85$
  - Now from isentropic table for $M_1 = 2.6, p_{o1}/p_1 = 19.95$
  - For $M_2 = 2.85$, $\frac{p_{o2}}{p_2} = 29.29$

$$\therefore \frac{p_2}{p_1} = \frac{p_2}{p_{o2}} \frac{p_{o2}}{p_{o1}} \frac{p_{o1}}{p_1} = \frac{1}{29.29}(1)(19.95) = 0.681 \tag{561}$$

Solution

- Seek solution in region 3
  - Now using $\theta - \beta - M$ diagram for $M_1 = 2.6$, and $\theta = \alpha = 5^\circ$
  - $\rightarrow \beta = 26.5^\circ$

$$\therefore M_{n1} = M_1 \sin\beta = 2.6 \sin 26.5^\circ = 1.16 \tag{562}$$

  - From normal shock table for $M_{1n} = 1.16$

$$\therefore \frac{p_3}{p_1} = 1.403 \tag{563}$$

Solution

Now seek coefficients

- Lift $L' = (p_3 - p_2)c\cos\alpha$ per unit span
- Drag $D' = (p_3 - p_2)c\sin\alpha$ per unit span
- Let $q_1 = \frac{\gamma}{2}p_1 M_1^2$

$$c_l = \frac{L'}{q'c} = \frac{2}{\gamma M_1^2}\left(\frac{p_3}{p_1} - \frac{p_2}{p_1}\right)\cos\alpha \tag{564}$$

$$= \frac{2}{1.4(2.6)^2}(1.403 - 0.681)\cos 5^\circ = 0.152 \tag{565}$$

$$c_d = \frac{D'}{q_1 c} = \frac{2}{\gamma M_1^2}\left(\frac{p_3}{p_1} - \frac{p_2}{p_1}\right)\sin\alpha \tag{566}$$

$$= \frac{2}{(1.4)(2.6)^2}(1.403 - 0.681)\sin 5^\circ = 0.0133 \tag{567}$$

Notes on Flat Plate Wake in Supersonic Flow

- Entropy in region 4 is different than in region 5
- Flow is again turned at the trailing edge of the airfoil
  - Why? Due to difference of pressure
- Recall that pressure is the same in region 4 and 5
- Velocities have different magnitudes but same direction in wake
- ϕ is generally small and is a function of α and M_1
- Flow is turned 'up' 10 deg.
- Does this generate lift?

Generalization of Diamond Airfoil Flow to Practice

Let us construct a new type of flight-vehicle. We split the traditional diamond airfoil

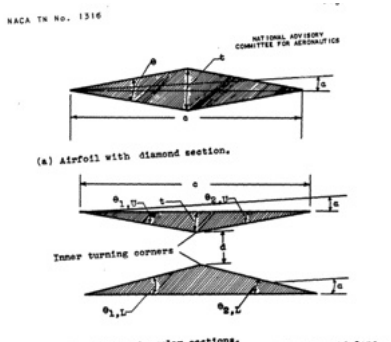

Figure 304: Moeckel, W. E., "Theoretical Aerodynamic Coefficients of Two-Dimensional Supersonic Bi-Planes," NACA Technical Note 1316, 1947.

Generalization of Diamond Airfoil Flow to Practice

We find a supersonic biplane.

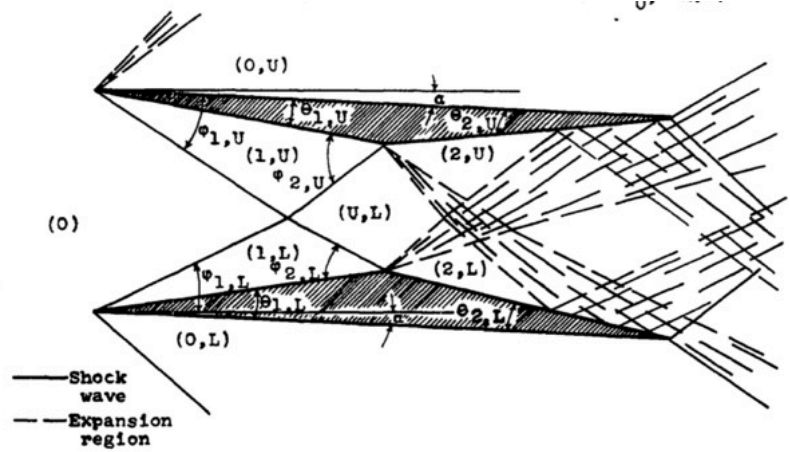

Figure 305: Moeckel, W. E., "Theoretical Aerodynamic Coefficients of Two-Dimensional Supersonic Bi-Planes," NACA Technical Note 1316, 1947.

Generalization of Diamond Airfoil Flow to Practice

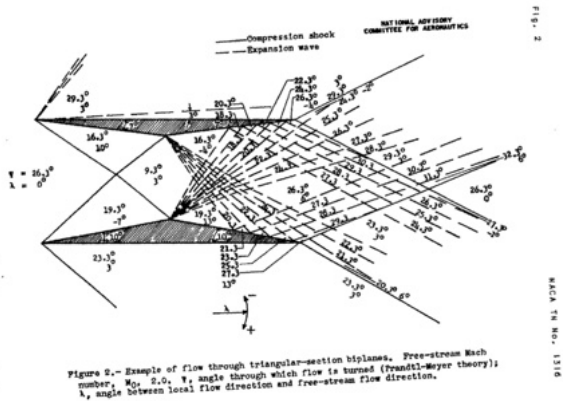

Figure 2.- Example of flow through triangular-section biplanes. Free-stream Mach number, M_0, 2.0. ν, angle through which flow is turned (Prandtl-Meyer theory); λ, angle between local flow direction and free-stream flow direction.

Figure 306: Moeckel, W. E., "Theoretical Aerodynamic Coefficients of Two-Dimensional Supersonic Bi-Planes," NACA Technical Note 1316, 1947.

Generalization of Diamond Airfoil Flow to Practice

Examine L/D versus α theoretical predictions. What do we find?

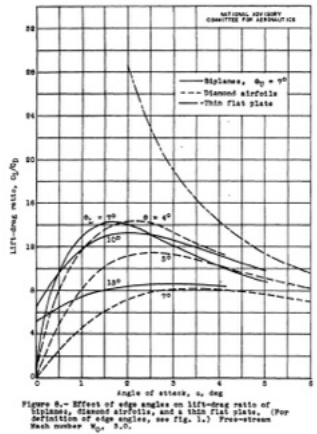

Figure 8.- Effect of edge angles on lift-drag ratio of biplanes, diamond airfoils, and a thin flat plate. (For definition of edge angles, see fig. 1.) Free-stream Mach number M_0, 3.0.

Figure 307: Moeckel, W. E., "Theoretical Aerodynamic Coefficients of Two-Dimensional Supersonic Bi-Planes," NACA Technical Note 1316, 1947.

Generalization of Diamond Airfoil Flow to Practice

Let us modify the supersonic bi-plane concept. What does this profile look like and what does it inspire?

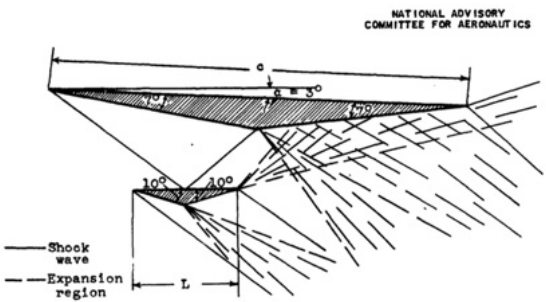

Figure 12.- Sketch of single triangular airfoil with shock-reflection surface. Free-stream Mach number M_0, 2.0.

Figure 308: Moeckel, W. E., "Theoretical Aerodynamic Coefficients of Two-Dimensional Supersonic Bi-Planes," NACA Technical Note 1316, 1947.

Advanced Application

Wind tunnel tests were a necessary step before the first flight attempt, as in this Mach 7 test of a full-scale model with spare flight engine in Langley's 8-Foot High Temperature Tunnel.

Figure 309: https://www.nasa.gov/centers/langley/pdf/142891main_X43A_2006.pdf

Advanced Application

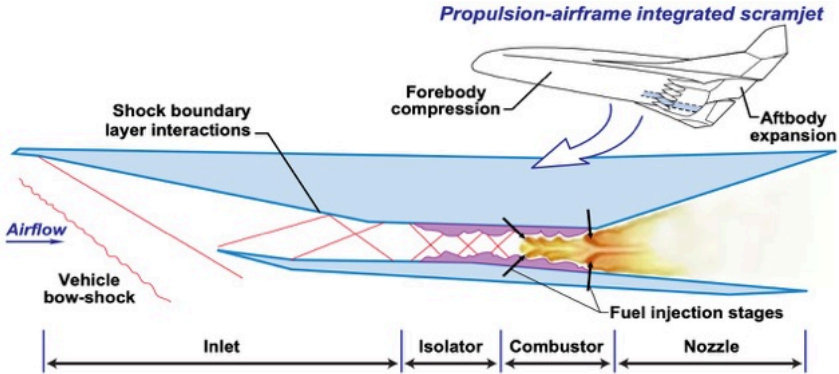

Figure 310: https://www.nasa.gov/centers/langley/pdf/142891main_X43A_2006.pdf

Downwash

Examine a new kind of physics, “downwash.” Induced by high-speeds and large-angles of attack.

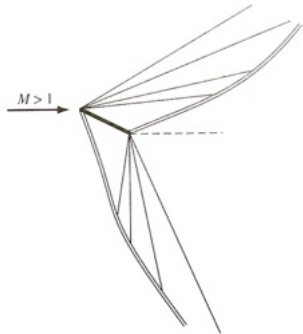

Figure 311: This view is called the overall “downwash.”

Expansions Over Very Large Angles

Extreme turns of flow-fields alter aerodynamics in unexpected ways. For example, expansion waves can turn strongly supersonic flows over large angles.

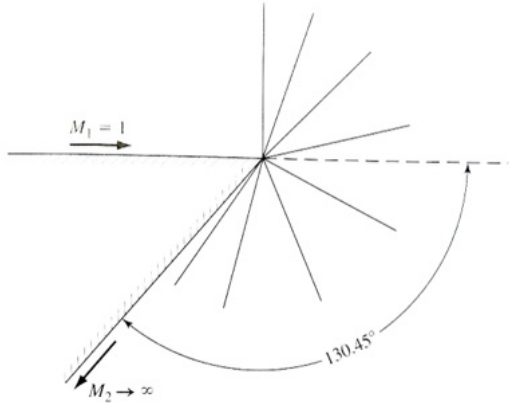

Figure 312: Prandtl-Meyer expansion over a large angle.

Expansions Over Very Large Angles

Recall the Prandtl-Meyer function is given by

$$\nu(M) = \sqrt{\frac{\gamma+1}{\gamma-1}}\tan^{-1}\sqrt{\frac{\gamma-1}{\gamma+1}(M^2-1)} - \tan^{-1}\sqrt{M^2-1} \tag{568}$$

In the limit of $M \to \infty$ we find

$$\lim_{M\to\infty}\nu = \left(\left(\frac{\gamma+1}{\gamma-1}\right)^{1/2}\frac{\pi}{2} - \frac{\pi}{2}\right) = 130.45^\circ \tag{569}$$

- An initially sonic flow might be expanded by 130.454 deg. for $\gamma = 1.4$
- But p and T downstream are zero, which is unlikely in practice.

Class Summary

- Shock expansion theory
- Diamond airfoils
- Note on downwash
- Wave drag
- Maximum expansion wave angle

Next Time

- Prandtl-Meyer Wave Expansions in Nozzles
- Prandtl-Meyer Waves and Maximum Turning Angles
- Application of shock-expansion systems for Inlets (revisited)

Class Overview

- Prandtl-Meyer Wave Expansions in Nozzles
- Prandtl-Meyer Waves and Maximum Turning Angles
- Application of shock–expansion systems for Inlets (revisited)

“A wave of sudden rarefaction, though mathematically possible, is an unstable condition of motion; any deviation from absolute suddenness tending to make the disturbance become more and more gradual. Hence the only wave of sudden disturbance whose permanency of type is physically possible, is one of sudden compression.” W. J. M. Rankine, 1870, attributed by him to a comment from Sir William Thomson

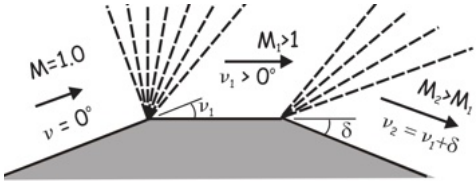

Figure 313: A double turning angle flow consisting of P-M waves.

- Illustration of the definition of the Prandtl-Meyer turning angle ν
- Flow turns Mach 1.0, where $\nu = 0$ deg.
- After expanding around a first corner, M is now supersonic
- Imagine that the corner(s) be replaced by the expansion section of a Laval nozzle
- Supersonic flow at M_1 expands through a second corner to $M_2 > M_1$
- P-M angle ν_1 is increased by the angle of the second turn, δ, so that now $\nu_2 > \nu_1$.

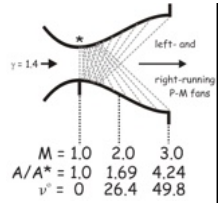

Figure 314: Two-dimensional flow through a nozzle.

- Angle ν is a cumulative angle, starting at $M = 1$, through which a flow must turn in order to expand to a particular M
- In a nozzle, how does the flow turn through such an angle and still remain parallel to the wall?
  - Conflicts with one-dimensional theory
  - Learned in one-dimensional flow, where we went from $M = 1$ to $M > 1$ in a nozzle without turning.
  - One-dimensional analysis neglects the turning that actually occurs in a Laval nozzle.
  - Examine a two-dimensional view to understand physics

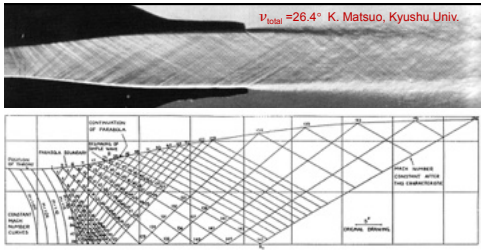

Figure 315: Schlieren image and expansion waves within the nozzle.

- Two-dimensional de Laval nozzles, flow expands in diverging nozzle section through both left- and right-running Prandtl-Meyer expansion waves
- Fans contribute to total turning angle required to reach the desired M_j
- Top image is a schlieren photo of a $M = 2$ nozzle flow, and bottom image is de Laval nozzle designed by the "method of characteristics" (Harrop, 1953).

Solving Prandtl-Meyer Flows

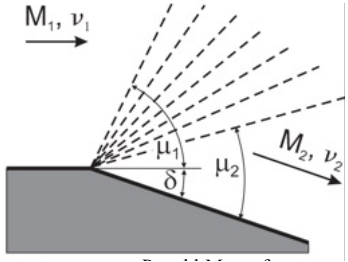

Figure 316: Schematic of flow parameters across a Prandtl-Meyer fan.

- Relatively simple since the entire fan is isentropic
- For a flow as sketched with an initial Mach number M_1, one can use the isentropic flow tables, equations, or use numerical method to find corresponding values of ν_1 and μ_1.

If flow is turned through an expansion angle θ, the total turning angle of the flow after the Prandtl-Meyer expansion fan is

$$\nu_2 = \nu_1 + \theta \tag{570}$$

Solving Prandtl-Meyer Flows

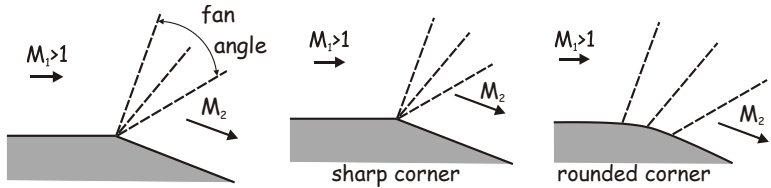

Figure 317: Types of P-M fans with the same outcome.

- Value ν_2 can be found in the isentropic tables, equations, or calculator to determine the Mach number M_2 after the expansion fan
- Property changes across the fan can then be determined by multiplying property ratios together as needed
- Note that stagnation pressure and temperature are both constant across an isentropic expansion fan

Solving Prandtl-Meyer Flows

- The fan angle can be determined as the difference between the Mach angles μ on either side of the fan
- A correction for the change in flow direction

$$\text{fan angle} = \mu_1 - \mu_2 + \theta = \nu_2 - \nu_1 + \mu_1 - \mu_2 \tag{571}$$

Because $\theta = \nu_2 - \nu_1$.

- The solution is independent of geometry (in general) e.g.
  - A sharp corner
  - A rounded corner
- Only beginning and end states matter

Example and Solution

- Example
  - A $M_1 = 2.0$ flow with $p_1 = 3$ atm and $T_1 = 300$ K is expanded through a $\theta = 30$ deg. corner.
  - Determine the downstream conditions: M_2, p_2, T_2, $p_{o,2}$, and $T_{o,2}$
- Solution
  - Entering the isentropic equations at $M_1 = 2.0$ and obtain $\nu_1 = 26.38$ deg., $p/p_{o,1} = 0.1278$, and $T/T_{o,1} = 0.5556$.
  - Find $p_{o,1} = p_1/0.1278 = 23.5$ atm and $T_{o,1} = T_1/0.5556 = 540$ K
  - Determine the value of ν_2 using $\theta = \nu_2 - \nu_1 \rightarrow 2 = 26.38$ deg. $+ 30$ deg. $= 56.38$ deg.
  - Using the Eqn. or tables at $\nu_2 = 56.38$ deg., find the value $M_2 = 3.37$, $p_2/p_{o,2} = 0.0158$, and $T_2/T_{o,2} = 0.3059$.

Solution Cont.

Finally, remembering that both stagnation pressure and temperature are constant in an isentropic Prandtl-Meyer flow, we can apply the chain rule to find the remaining flow properties p_2 and T_2

$$p_2 = p_1 \frac{p_{o1}}{p_1} \frac{p_{o2}}{p_{o1}} \frac{p_2}{p_{o2}} = p_{o2} \frac{p_2}{p_{o2}} = 0.3713 \text{ atm} \tag{572}$$

$$T_2 = T_1 \frac{T_{o1}}{T_1} \frac{T_{o2}}{T_{o1}} \frac{T_2}{T_{o2}} = T_{o2} \frac{T_2}{T_{o2}} = 165 \text{ K} \tag{573}$$

Example

- A weak oblique shock with $\theta = 44$ deg. in a horizontal planar supersonic jet at $M_1 = 2.0$ strikes the free-jet boundary as shown.
- After the reflection of this wave (as an expansion fan), find the flow direction with respect to the horizontal and the Mach number M_3.

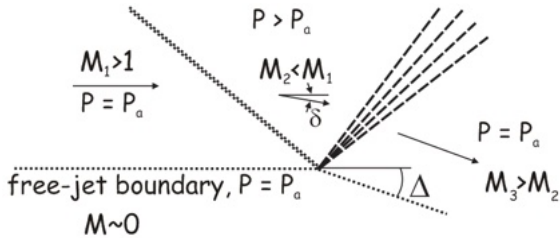

Figure 318: An oblique shock reflects from a free boundary as an expansion fan. The reflection causes the free boundary to be deflected though an angle Δ.

Solution I

- Begin by using the oblique shock charts to move from region 1 to region 2.
- Enter shock angle $\theta = 44$ deg. and $M_1 = 2.0$ to obtain $\delta = 14$ deg., $M_2 = 1.49$, and $p_2/p_1 = 2.1$, which is needed to analyze the free boundary.
- Expansion fan results in the pressure $p_3 = p_1$ to satisfy the free-jet boundary condition, no pressure change across the free boundary.
- We find that $p_3/p_2 = p_1/p_2 = 0.48$.
- Enter the isentropic tables at $M_2 = 1.49$ and obtain $p_2/p_{o2} = 0.276$ and $\nu_2 = 11.61$ deg.

Across an expansion fan p_o is a constant, so we write a chain

$$\frac{p_3}{p_{o3}} = \frac{p_2}{p_{o2}}\frac{p_{o2}}{p_{o3}}\frac{p_3}{p_2} = (0.276)(1)(0.48) = 0.132$$

- Enter the isentropic tables at $p_3/p_{o3} = 0.132$ to obtain $M_3 = 1.98$ and $\nu_3 = 25.83$ deg.

Solution II

- Use the Prandtl-Meyer equation to determine the deflection of the free boundary, measured clockwise from the horizontal

$$\Delta = \delta + (\nu_3 - \nu_2) = 14 \text{ deg. } + (25.83 \text{ deg. } - 11.61 \text{ deg. }) = 28.2 \text{ deg.}$$

Prandtl-Meyer Turning Angle as M

Graph the variation of angle ν for increasing M

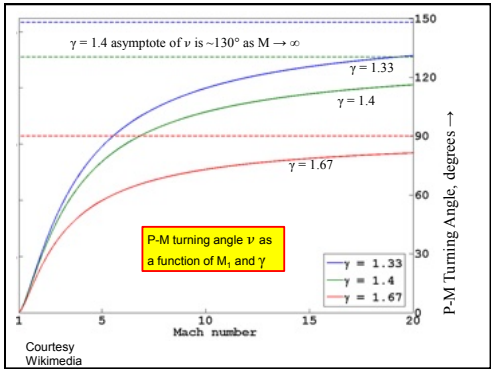

Figure 319: Asymptotic of P-M angle.

Maximum Turning Angle

- Previously showed limit of ν by examining the limit of ν as $M = \infty$.
  - Limit for $\gamma = 1.4$ and find a maximum $\nu_{max} = 130.4$ deg.
  - Angle through which a flow would have to be turned to produce an infinite Mach number
- This has a practical application if we consider a nozzle ejecting into space, where $p_\infty = 0$ and $M = \infty$.
- In space, as a gas is ejected supersonically from a nozzle (assuming it does not liquefy and violate ideal gas behavior), it will be turned back toward the direction from which it came!

Maximum Turning Angle

- Hollywood rarely gets the physics of this correct, however this can be seen in the moon-landing footage during liftoff of the crew capsule from the moon's surface.
- This also can be a problem for attempting to dock a spacecraft at a space station, where the exhaust from maneuvering rockets will tend to be vectored toward the station.

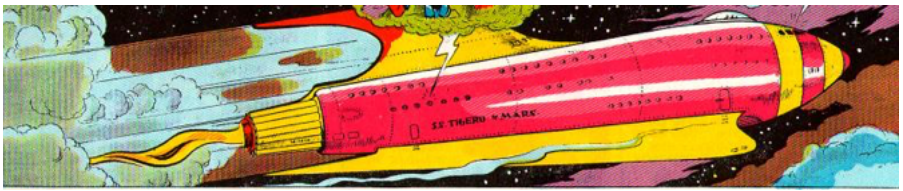

Figure 320: Buck Rogers in the 25th century.

Source: Prof. Settles

Turning Angle in Low Density Environments

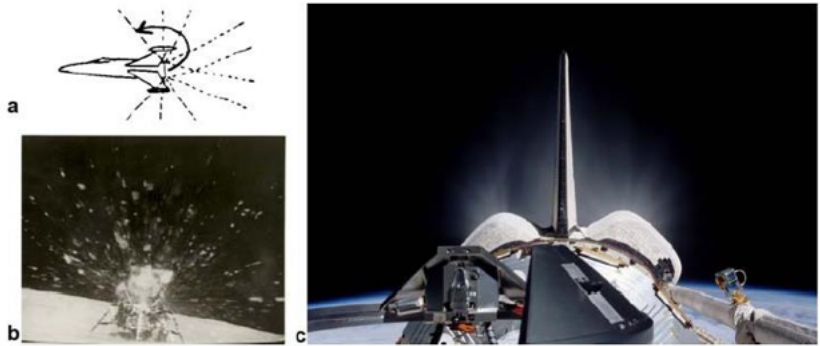

Figure 321: (a) A schematic showing the maximum turning angle vectoring a rocket nozzle exhaust forward. (b) An image from takeoff from the moon of the Apollo 16 Orion capsule. (c) An image of the space shuttle in orbit showing the exhaust from the maneuvering rockets expanding through a large angle.

Oblique-Shock Inlets for High-Speed Aircraft

- Simple normal-shock inlets (diffusers) are not an adequate solution to problem of jet propulsion.
- Losses are too large for Mach numbers M_1 significantly above 1 (≈ 1.4 and higher)
- Purpose of an aircraft inlet, or supersonic diffuser, is to slow the flow to subsonic speed with minimum loss, in order to promote efficiency and raise pressure isentropically, before it enters a turbojet engine.
- Small losses arise from oblique shock waves of small turning angle θ, even when M_1 is large.

Oblique-Shock Inlets for High-Speed Aircraft

- Combination of these ideas shows ideas for supersonic inlets
  - A series of relatively-weak oblique shocks, reduce the incoming flow Mach number from M_1 to a value less than ≈ 1.40
  - Proceed to subsonic flow through a relatively-weak normal shock wave that is stabilized in a diverging duct
- Works in practice and is used in high-speed aircraft
- Examine interesting examples, including both inlets with rectangular cross-sections and round (axisymmetric) inlets

Oblique-Shock Inlets for High-Speed Aircraft

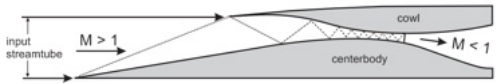

Figure 322

- Variable geometry is a challenge in design
  - No supersonic aircraft has luxury of efficient performance at only one value of M_∞
  - Inlet design is a problem for engineers, where the oblique-shock angles change with M_∞
- Below $M_\infty \approx 1.4$, it is possible to obtain good efficiency with a fixed-geometry inlet
  - Designs work well for military jet fighters that maneuver at transonic speeds and cruise up to about Mach 1.70

Oblique-Shock Inlets for High-Speed Aircraft

- At higher Mach numbers, a variable-geometry inlet is usually required.
- The shape of the inlet is hydraulically varied in flight in order to optimize its performance as the flight Mach number varies
- Earlier we saw simple 1-D normal-shock inlets, but now let us examine some vintage aircraft with more sophisticated inlets
- Inlets are often derived directly from the simple 2-D wedge and cone flows that you have learned

F-104 Starfighter 1/2-cone inlet

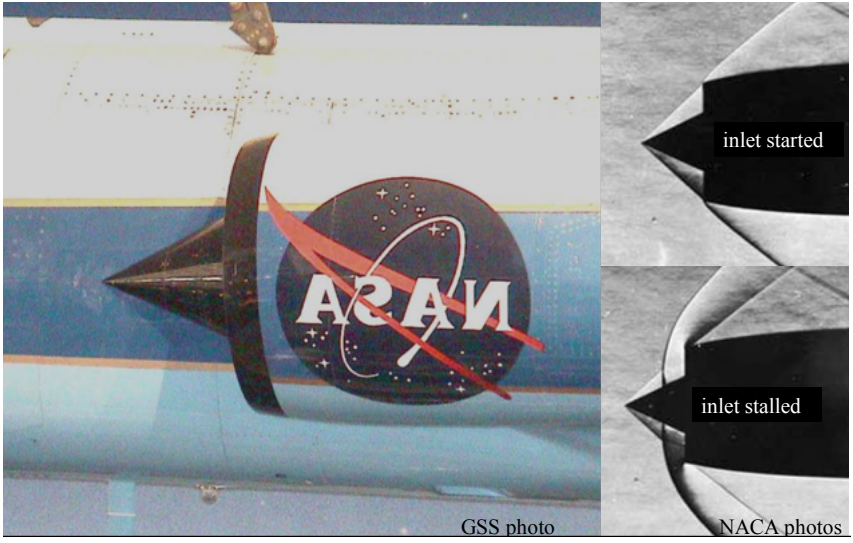

Figure 323: F-104 Starfighter inlet and associated schlieren images.

F-111 1/4-Cone Inlet

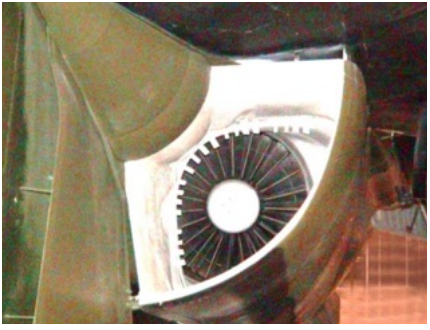

Figure 324

- Vortex generators inside inlet attempt to control boundary-layer separation
- Generators and suction through holes in the inlet walls (boundary-layer 'bleed') are often used, but boundary-layer control is a complex topic that is not well understood
- Inlet is far from from the aircraft fuselage in order to avoid ingesting the boundary-layer

Figure 325: F-15

- F-15 rectangular or wedge-type inlet
- Inlet features variable geometry depending upon flight Mach number
- Left inlet shown here is configured for subsonic flight, limiting the mass flow into the engine
- Right inlet is set up as a multiple-oblique-shock inlet for supersonic flight

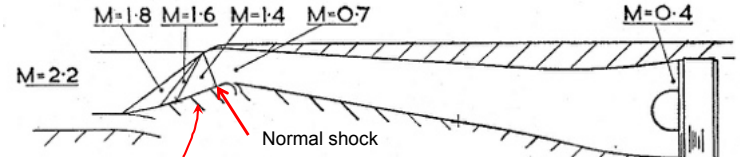

The *Concorde*'s engine inlet, shown above, was designed to compress the flow through several oblique shocks and a normal shock *before* the flow actually enters the duct leading to the engine: an *external-compression inlet* with a variable geometry ramp. The inlet shown below is a *mixed-compression* type, wherein supersonic flow is admitted inside the inlet and further compressed, terminating in an internal normal shock wave. Mixed-compression inlets require *starting* the supersonic flow in the duct, and they can *unstart* if viscous effects lead to *disgorging* the normal shock (e.g. 2 mins. into SR-71.avi –shown already).

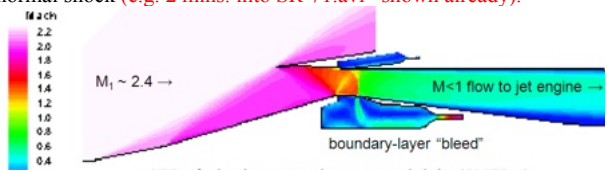

Figure 326

Figure 327: Inlet of the Concorde.

Figure 328: Potential design from Boeing for future supersonic transport aircraft.

- Concorde was the world's first commercial supersonic transport.
- Second was created in the USSR – TU-144.
- Economic competitiveness and fuel efficiency are almost as serious as the sonic boom problem.
- US law currently prohibits supersonic flight over land.

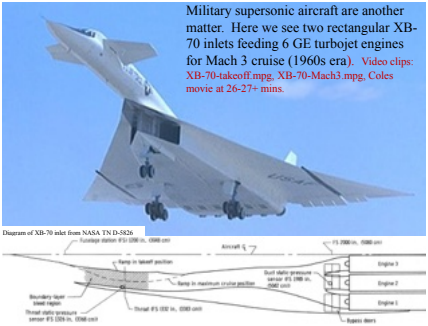

Figure 329

- Military supersonic aircraft are another matter
- Observer two rectangular XB-70 inlets feeding 6 GE turbojet engines for Mach 3 cruise (1960s era)

SR-71 Aerospikes

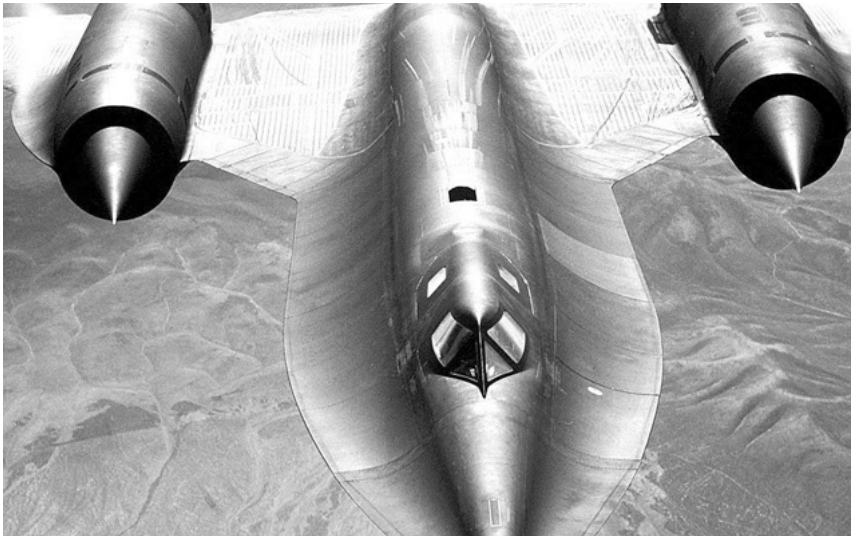

Figure 330: SR-61 in flight.

SR-71

Figure 331: SR-71 in museum.

Kelly Johnson

Kelly Johnson
(P-38, P-80, F-104, U-2, SR-71)

Figure 332: An incredible and influential engineer.

Inlet

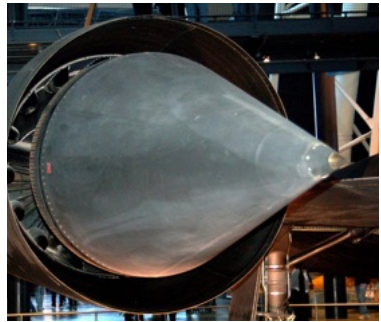

Figure 333: SR-7 inlet.

- An ingeniously-simple approach to variable geometry for Mach numbers well into the supersonic range
- Less complicated than the X-B70 inlet.
- Counter-intuitively, the cone is at full extension during takeoff and moves back inside the cowl as M_∞ increases.

SR-71 Inlet Diagram

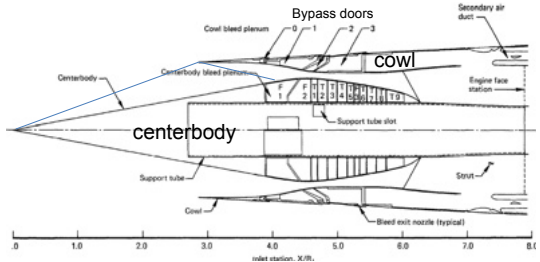

Figure 334: SR-71 engine inlet cross-section.

- SR-71 inlet diagram, with centerbody in rear position for efficient $M = 3.2$ cruise
- Centerbody is set so that the oblique shock exactly intersects the cowl lip at the optimum inlet adjustment for flight at a given $M > 1$
- Centerbody moves full forward at takeoff to allow maximum subsonic air inflow into the engine

SR-71 Inlet

- At Mach 1.6 the inlet should self-start (swallow the supersonic flow) with the centerbody fully forward
- Around 30,000 feet altitude the centerbody begins its motion aft
- At cruise Mach number, the inlet is positioned as shown in the previous diagram.
- The boundary layers are bled off both centerbody and cowl to prevent shock-induced flow separation.
- Compared to takeoff, in this position the throat area is reduced by 54% and the captured streamtube area is increased by 112%.
- Aerodynamic forces on the centerbody spike can be as much as 12 tons.
- Boundary-layer bleed, or suction of the bottom of the boundary layer through slots in the centerbody and cowl surfaces, is an attempt to prevent boundary-layer separation due to the pressure rise caused by impinging shock waves.

Inlet Design using Method of Characteristics

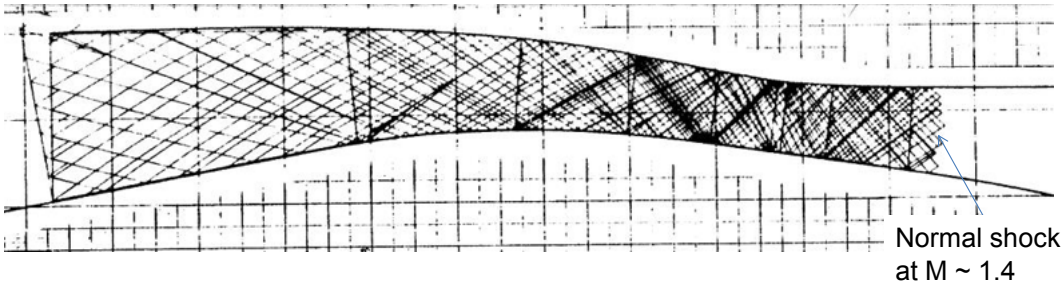

Figure 335: Method of characteristics flow-field inside an engine inlet.

- Flow separation inside the inlet can result in the normal shock wave being expelled out the front of the inlet–a phenomenon known as an ‘inlet unstart’
- This causes an instantaneous loss of engine thrust, explosive banging noises, and violent yawing of the aircraft

SR-71 J-58 Engine

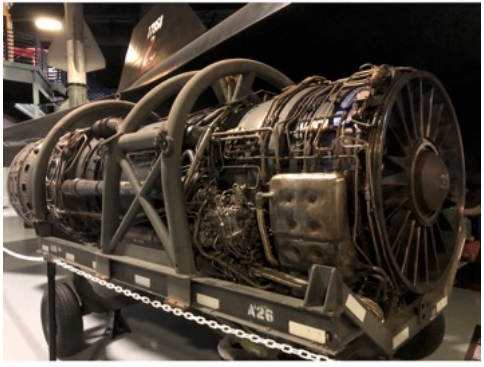

Figure 336: SR-71 J-58 engine.

SR-71

Figure 337: Prof. Miller and the SR-71 J-58 engine.

SR-71 Nozzle

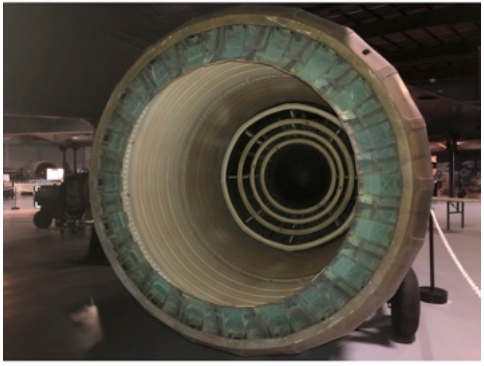

Figure 338: J-58 engine exit.

SR-71 Modes of Operation

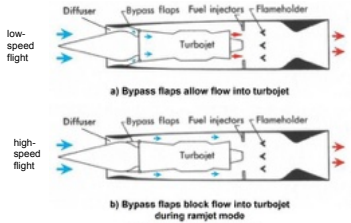

Figure 339: Operations of the SR-71 J-58 engine.

- In the Mach 3 to 4 range and above, the compressor and turbine of a turbojet engine are superfluous
- Inlet provides ram compressed air directly to the SR- 71's combustion chamber by way of bypass flaps
- The turbojet is carried along for the purpose of takeoff and landing only

Example

- Rectangular cross-section inlet shown above in side view functions similarly to the SR-71 inlet just described
- Planar two-dimensional wedge flow occurs instead of the conical flow around the SR-71's spike inlet
- Given the inlet geometry shown here, find the flight Mach number that yields peak inlet efficiency

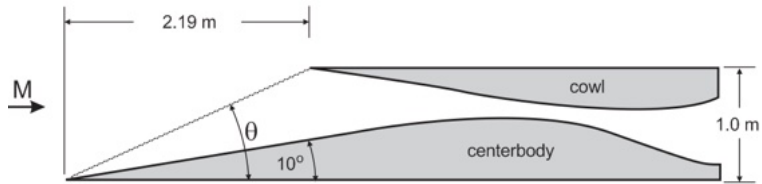

Figure 340: Supersonic engine inlet with rectangular cross-section.

Solution

- For peak efficiency the oblique shock wave from the center-body must exactly meet the cowl lip
- This line is shown in the diagram
- The solution is found via trigonometry
  - $\tan \beta = 1.0$ m / 2.19 m = 0.457
  - Therefore the shock angle β must be 24.54 deg
- Either the charts, equations, or numerically and find the Mach number at which a 10 deg. wedge produces a weak oblique shock at this angle, $M = 3.5$

Class Summary

- Prandtl-Meyer Wave Expansions in Nozzles
- Prandtl-Meyer Waves and Maximum Turning Angles
- Application of shock-expansion systems for Inlets (revisited)

Next Time

- Off-design shock-expansions from nozzles
- Shock impingement on aerodynamic bodies

Class Overview

- Off-design shock-expansions from nozzles
- Shock impingement on aerodynamic bodies

Figure 341: Images of all Saturn V Launches.

"There is just one thing I can promise you about the outer space program: Your tax dollar will go farther.," Dr. Wernher von Braun.

Off-Design Exit Flow from Laval Nozzles

- Recall the variation of static pressure along a Laval nozzle with fixed p_o and variable p_b
- We observed cases where the exit pressure is not equal to atmospheric pressure
  - Over-expanded flow occurs where the exit pressure is lower than atmospheric
  - Under-expanded flow occurs where the exit pressure is higher than atmospheric
- We will examine both of these important cases

Off-Design Exit Flow from Laval Nozzles

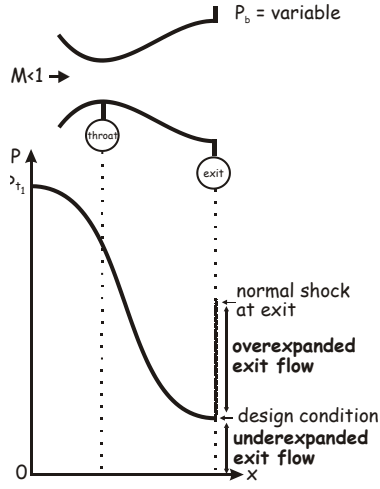

Figure 342: Ranges of flow-fields for supersonic nozzle flow.

Convergent-Divergent Nozzle and Shock Polar Diagram

- Over-expanded flow means that the nozzle expanded the flow too far to match ambient pressure
  - Exit pressure is lower than the back pressure, so a shock wave raises the pressure of the exiting jet until it matches the back pressure
  - A shock appears outside the nozzle
  - Shock polar diagram shows all possible shock waves at the exit Mach number
  - From a normal shock at ‘A’ through strong oblique shocks
  - To the discriminator between weak and strong shocks at ‘B’
  - Through weak oblique shocks eventually to the design condition ‘C,’ where no shock is needed so only a Mach wave appears

Convergent-Divergent Nozzle and Shock Polar Diagram

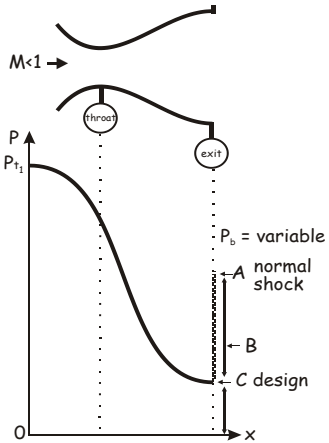

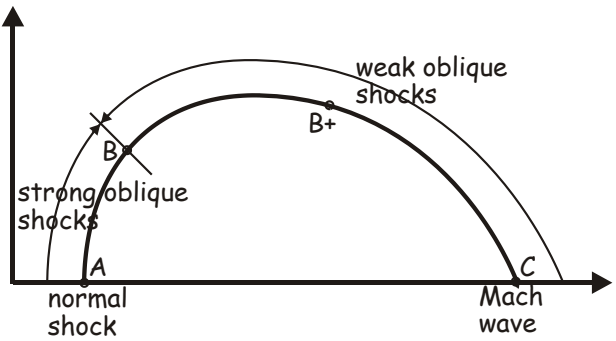

Figure 343: Shock polar diagram for shocked nozzle.

Jet Plume with Increasing Nozzle Pressure Ratio

- 5 nozzle exit flows shown above on the shock polar for over-expanded exit flow.
- A: normal shock, A-B: strong oblique shocks with irregular crossing, B-B+: weak oblique shocks with irregular crossing, B+-C: weak oblique shocks that cross regularly, and C: Mach waves only.

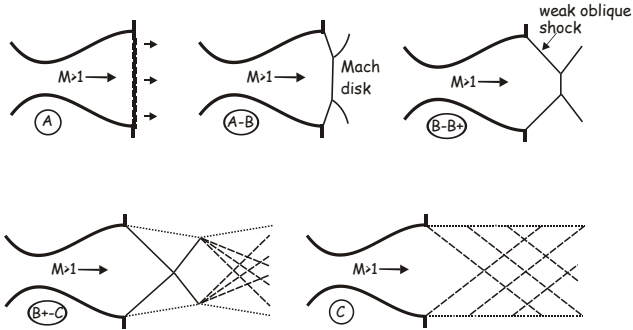

Figure 344: Flow-fields in the jet plume.

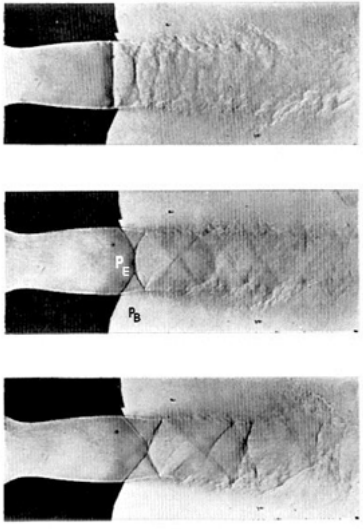

Figure 345: Schlieren of off-design jets.

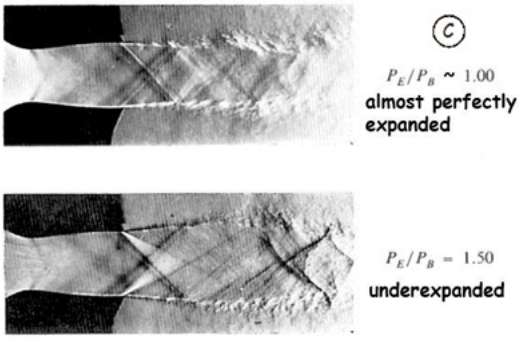

Figure 346: Schlieren of off-design jets.

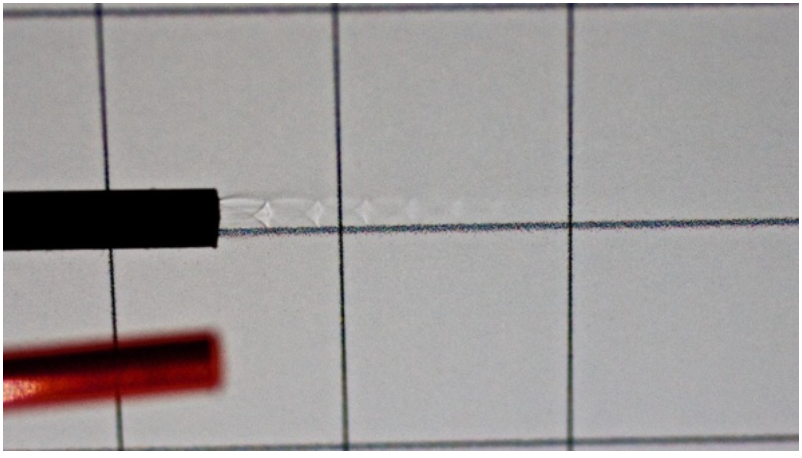

Figure 347: Picture of a shadowgraph of an off-design supersonic jet from a compressed air can. Experiment by Prof. Miller. Photography Jacob Klos, NASA Langley Research Center.

Important Points

- Compressions reflect from a free-jet boundary as expansions, and vice versa
- If $\theta > \theta_{max}$ for a given M_1, then an irregular oblique shock crossing occurs.
  - This corresponds to the Mach disk phenomenon shown in cases $A - B$ and $B - B+$
- All along the free-jet boundary beyond the nozzle exit, $p = p_\infty$, and thus the waves must adjust to satisfy this boundary condition
- A series of repeated compression and expansions, known as shock-cells or "shock-diamonds" due to their shape
- Shock-expansion appearance is shown below for a few cycles of over-expanded flow, where $p_e < p_\infty$

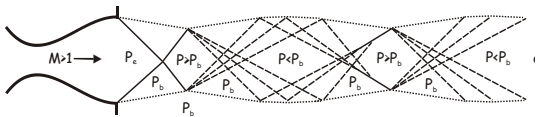

Figure 348: Static pressures within the shock-cell structure.

Under-Expanded Jet Flow

- A similar phenomenon occurs when $p_e > p_\infty$
- Nozzle has not expanded the flow enough to drop p_e to the outside pressure level p_∞
- An additional expansion is required at the nozzle exit in order to match the pressure
- Except for this different initial condition, the repeated compression and expansion cells (shock cells) look the same in this under-expanded flow

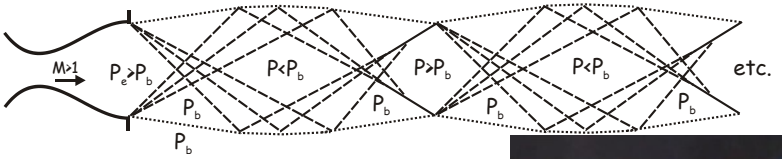

In the outer atmosphere P_b approaches zero and the overall pressure ratio driving a rocket nozzle outflow becomes very large, causing a spectacular jet expansion outside the nozzle: ***highly-underexpanded flow***:
(Saturn 5 rocket, Apollo 11 headed for orbit)

Figure 349: In the outer atmosphere p_b approaches zero and the overall pressure ratio driving a rocket nozzle outflow becomes very large, causing a spectacular jet expansion outside the nozzle: highly-under-expanded flow: (Saturn 5 rocket, Apollo 11 headed for orbit)

Figure 350: Schlieren and photograph of off-design jets.

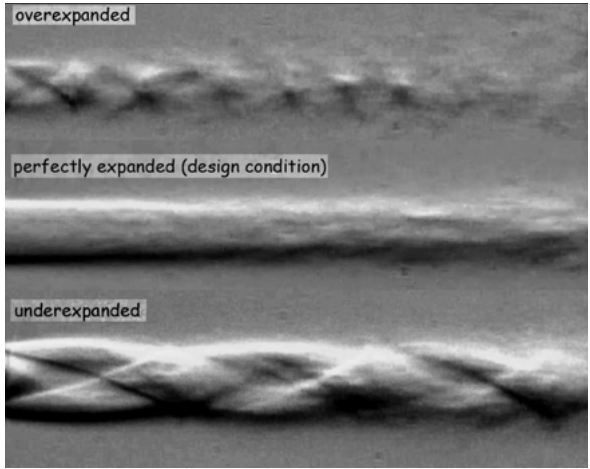

Figure 351: Over-expanded, under-expanded, and on-design jet flows.

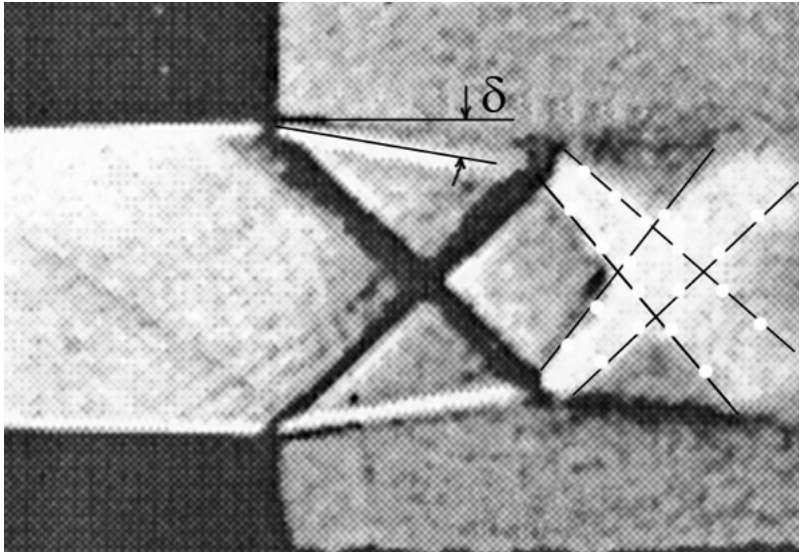

Figure 352: Schlieren image of an over-expanded 2*D* planar free jet, showing oblique-shock reflection as a Prandtl-Meyer fan from a free boundary. From Prandtl's lab, conducted during Wright Brothers' first flights.

Worked Example: Over-Expanded nozzle exit flow

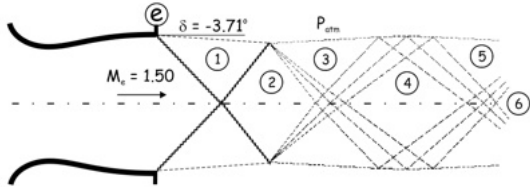

Figure 353: Example problem - shock cell structure of off-design jet.

- The sketch, drawn to scale, shows a planar 2D nozzle discharging a jet of helium to the atmosphere at $M_e = 1.50$.
- $p_{atm} > p_e$ so the jet is over-expanded, and must match the back pressure through an oblique shock that turns the flow inward through an angle $\theta = -3.71$ deg.
- Find the Mach numbers of regions 1-6 shown in the sketch.

Solution: Over-Expanded Nozzle Exit Flow

- The flow is symmetric about the centerline shown
- $M_e = 1.50$ and $\theta = 3.71$ deg., we find $M_1 = 1.346$
- The left-running oblique shock from 1-2 is found by requiring the flow to turn back to horizontal, just as in the oblique-shock reflection from a solid wall (centerline symmetry).
- $M_1 = 1.346$ and $\theta = 3.71$ deg. yield $M_2 = 1.182$ and $p_2/p_1 = 1.252$.
- Now note that $p_1 = p_{atm} = p_3 = p_5$ because the free shear layer above regions 1, 3, and 5 cannot support a pressure difference.
- An expansion fan is needed to make region 3 equal to atmospheric pressure
- Find M_3 using a static-pressure chain after looking up $p_2/p_o = 0.384$ at M_2 in the isentropic section of table

Solution: Over-Expanded Nozzle Exit Flow

$$\frac{p_3}{p_o} = \frac{p_3}{p_2}\frac{p_2}{p_o} = \frac{0.384}{1.252} = 0.307 \tag{574}$$

- $p_3/p_o = 0.307$ yields $M_3 = 1.35$ from the isentropic table, which gives the P-M turning angles $\nu_3 = 6.477$ deg. and $\nu_2 = 2.760$ deg.
- Now, $\Delta\nu$ from regions 2-3 is 6.477-2.760 = 3.717 deg.
- The turning angle across a P-M fan is not changed by the crossing of another fan
- $\nu_4 - \nu_3 = \Delta\nu = 3.717$ deg., so $\nu_4 = 10.194$ deg., from which isentropic flow gives $M_4 = 1.50$
- The loss across both oblique shocks is $\approx 0.2\%$, at such low Mach numbers and small ν, the flow essentially returns in region 4 to the nozzle exit conditions
- The reflected P-M compression from 4-5 subtracts $\Delta\nu$ and returns M_5 to the same value as M_3, which is 1.35. Similarly $M_6 = M_2 = 1.182$.

Effect of Shock Impingement on Heat Transfer Around Bodies

- Shock impingement on a blunt body in hypersonic flow is observed to greatly increase heat transfer
- A hemispherical model is used with platinum thin-film thermometer is placed into a hypersonic tunnel
- An impingement shock is imposed on the model and measurements of heat transfer are conducted
- Where might we see this phenomenon in practice?

Adapted from Edney, B. E., "Effects of Shock Impingement on the Heat Transfer around Blunt Bodies," AIAA Journal, Vol. 6, No. 1, 1968, pp. 15-21.

Effect of Shock Impingement on Heat Transfer around Bodies

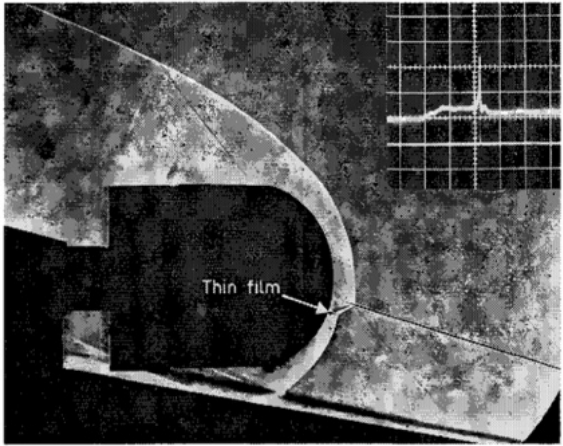

Figure 354: Schlieren of a shock-shock impingement experiment. Edney AIAAJ 1968.

Effect of Shock Impingement on Heat Transfer around Bodies

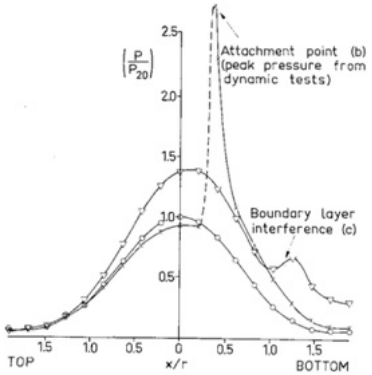

8 Measured pressure distributions. Hemisphere fixed relative to shock; $M = 4.6$, $\alpha = 5°$.

Figure 355: Edney AIAAJ 1968.

Effect of Shock Impingement on Heat Transfer around Bodies

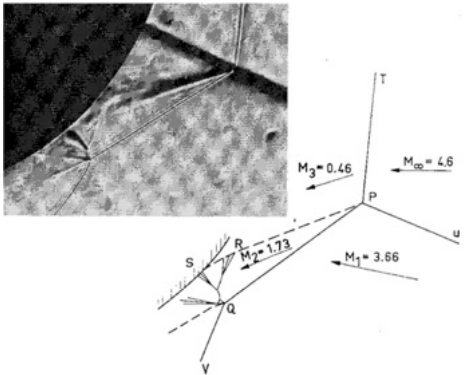

ig. 12. Attaching shear layer. Comparison with theoretical pattern. $M = 4.6$, $\alpha = 10°$.

Figure 356: Edney AIAAJ 1968.

Effect of Shock Impingement on Heat Transfer around Bodies

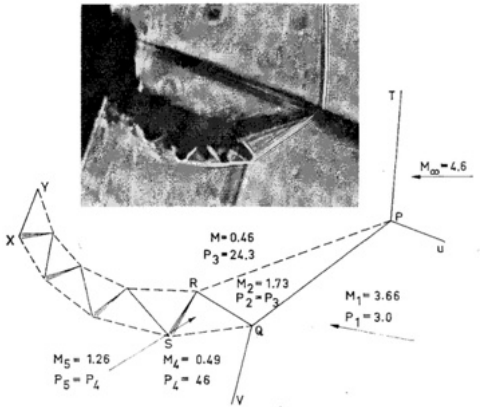

Fig. 13. Supersonic; embedded jet. Comparison with theoretical pattern. $M = 4.6, \alpha = 10°$

Figure 357: Edney AIAAJ 1968.

Class Summary

- Off-design shock-expansions from nozzles
- Shock impingement on aerodynamic bodies

Next Time

- Method of characteristics (MOC)

Class Overview

- Method of characteristics (MOC)
- Short example problem for nozzles

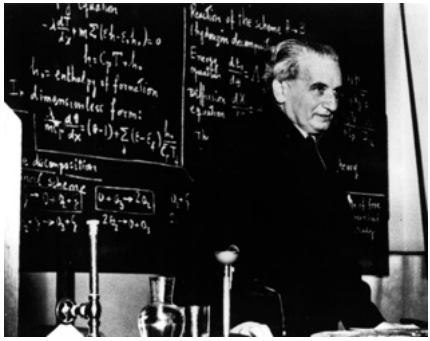

Figure 358: Theodore von Karman.

“Everyone knows it takes a woman nine months to have a baby. But you Americans think if you get nine women pregnant, you can have a baby in a month.,”

November 1957 - Told to Joseph G. Martin, then Aide-de-Camp to Maj. Gen. Daniel E. Hooks, as Lt. Martin escorted Dr. von Karman from New York City to lead a secret symposium on space flight in Cloudcroft, NM. Sputnik had been launched a month before and every branch of the US military had a separate space program and were desperately trying to get off a successful launch.

Sputnik

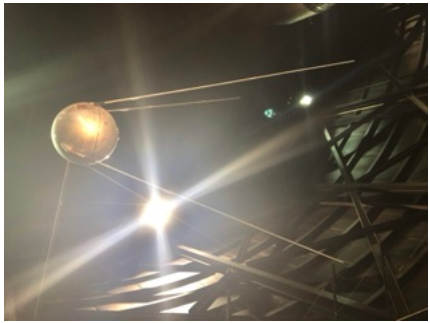

Figure 359: Sputnik Source: Miller.

The space age began on October 4, 1957, when the Soviet Union launched Sputnik 1, the first artificial Earth satellite. The event was a milestone in space exploration and a defining moment of the Cold War. It caused great anxiety in the United States because the public equated space achievements with military and technological power. To many, Sputnik represented the threat of superior Soviet space and missile technology. Sputnik, which means "satellite" in Russian, was the Soviet entry in a scientific race to launch the first satellite. In 1954, the International Council of Scientific Unions urged governments to design, build, and launch Earth-mapping satellites during the "International Geophysical Year" (IGY), planned for 1957-58. Both the United States and the USSR announced they would orbit satellites. The IGY was an opportunity for both the USSR and the US to demonstrate world leadership in space and rocket technology-and though the IGY focused on international cooperation and the peaceful use of space, satellites and rockets had obvious military implications.

MOC Philosophy

We will illustrate the method before developing a more rigorous approach. Consider the Taylor series expansion of u

$$u_{i+1,j} = u_{i,j} + \left(\frac{\partial u}{\partial x}\right)_{i,j} \Delta x + ... \tag{575}$$

We can find the value of the derivative from the conservation equation. For example consider a 2D irrotational flow

$$\left(1 - \frac{u^2}{c^2}\right)\frac{\partial u}{\partial x} + \left(1 - \frac{v^2}{c^2}\right)\frac{\partial v}{\partial y} - \frac{2uv}{c^2}\frac{\partial u}{\partial y} = 0 \tag{576}$$

and solving the equation for $\partial u/\partial x$ results in

$$\frac{\partial u}{\partial x} = \left(\frac{2uv}{c^2}\frac{\partial u}{\partial y} - \left(1 - \frac{v^2}{c^2}\right)\frac{\partial v}{\partial y}\right) / \left(1 - \frac{u^2}{c^2}\right) \tag{577}$$

MOC Philosophy

- Assume know velocity at a point i and j on a vertical line and all other adjoining points along the line.
- Can calculate $\partial u/\partial y$, and can calculate the RHS of our developed equation and find $\partial u/\partial x$.
- If the denominator is zero, then we have the sonic condition of $u = c$.
- Also define the angle μ by $\sin\mu = u/U = c/U = 1/M$, where μ is the Mach angle

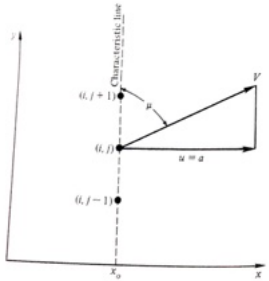

Figure 360

MOC Philosophy

- Derivatives of other flow variables are indeterminate along these lines
  - Lines are called characteristic lines.
- Outline the general process of MOC.
  - Consider a region of supersonic flow in $x - y$ space
  - Flow-field is solved in three major steps

MOC Philosophy

- 1) Find lines in space where flow variables are continuous and where derivatives are indeterminate
  - These are the characteristic lines
- 2) Combine the partial differential conservation equations where ordinary differential equations are obtained that hold along the characteristic lines.
  - These ODEs are called compatibility equations
- 3) Solve the compatibility equations step by step along the characteristic lines starting from an initial condition.
  - The entire flow-field can be mapped with this method.
  - The lines, make a net that are called the characteristic net and depend on the geometric locations.
  - Usually this is done numerically but results in explicit algebraic equations for irrotational 2D flow

Characteristic Lines in Two-Dimensional Irrotational Flow

Consider the steady, adiabatic, two-dimensional, irrotational supersonic flow. The governing compressible full potential velocity is

$$\left(1-\frac{\Phi_x^2}{c^2}\right)\Phi_{xx}+\left(1-\frac{\Phi_y^2}{c^2}\right)\Phi_{yy}-\frac{2\Phi_x\Phi_y}{c^2}\Phi_{xy}=0 \tag{578}$$

Here, $\Phi_x = u$, $\Phi_y = v$, and $\boldsymbol{U} = u\hat{i} + v\hat{j}$. The derivative of Φ is the x direction is a function of x and y, therefore

$$d\Phi_x = \frac{\partial \Phi_x}{\partial x}dx + \frac{\partial \Phi_x}{\partial y} = \Phi_{xx}dx + \Phi_{xy}dy \tag{579}$$

$$d\Phi_y = \frac{\partial \Phi_y}{\partial x}dx + \frac{\partial \Phi_y}{\partial y} = \Phi_{xy}dx + \Phi_{yy}dy \tag{580}$$

Characteristic Lines in Two-Dimensional Irrotational Flow

We have the system of simultaneous linear algebraic equations in Φ_{xx}, Φ_{yy}, and Φ_{xy}

$$\left(1 - \frac{u^2}{c^2}\right)\Phi_{xx} - \frac{2uv}{c^2}\Phi_{xy} + \left(1 - \frac{v^2}{c^2}\right)\Phi_{yy} = 0 \tag{581}$$

$$\Phi_{xx}dx + \Phi_{xy}dy = du \tag{582}$$

and

$$\Phi_{xy}dx + \Phi_{yy}dy = dv \tag{583}$$

Characteristic Lines in Two-Dimensional Irrotational Flow

There are many approaches to solving these equations and we adopt the method of Cramer's rule and find

$$\Phi_{xy} = \frac{det\begin{bmatrix} 1-u^2/c^2 & 0 & 1-v^2/c^2 \\ dx & du & 0 \\ 0 & dv & dy \end{bmatrix}}{det\begin{bmatrix} 1-u^2/c^2 & -2uv/c^2 & 1-v^2/c^2 \\ dx & dy & 0 \\ 0 & dx & dy \end{bmatrix}} = N/D \tag{584}$$

- Now consider the following, where the derivative of Φ_{xy} has a specific value at A.
- Solution gives Φ_{xy} at point A for arbitrary dx and dy in an arbitrary direction from A defined by dx and dy.

Characteristic Lines in Two-Dimensional Irrotational Flow

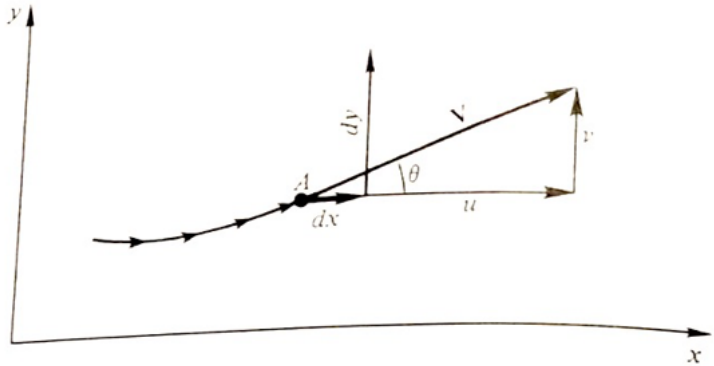

Figure 361: MOC on a Line.

Characteristic Lines in Two-Dimensional Irrotational Flow

- The direction from A given dx and dy is chosen so that $D = 0$ then $N = 0$ to keep Φ_{xy} finite, eg Φ_{xy}.
  - That is $\Phi_{xy} = \partial u/\partial y = \partial v/\partial x$ is the indeterminate.
- The lines in the $x - y$ space for which $D = 0$ are characteristic lines.
- We set $D = 0$ and find the following equations

$$\left(1 - \frac{u^2}{c^2}\right) dy^2 + \frac{2uv}{c^2} dxdy + \left(1 - \frac{v^2}{c^2}\right) dx^2 = 0 \tag{585}$$

or written as

$$\left(1 - \frac{u^2}{c^2}\right) \left(\frac{dy}{dx}\right)^2 + \frac{2uv}{c^2} + \left(1 - \frac{v^2}{c^2}\right) = 0 \tag{586}$$

Characteristic Lines in Two-Dimensional Irrotational Flow

The term dy/dx is the slope of the characteristic line, and we solve for dy/dx using the quadratic formula and find after simplification

$$\left(\frac{dy}{dx}\right)_{characteristic} = \frac{-uv/c^2 \pm \sqrt{\left[\left(u^2+v^2\right)/c^2\right]-1}}{1-u^2/c^2} \tag{587}$$

This equation represents the characteristic curves in physical space.

Characteristic Lines in Two-Dimensional Irrotational Flow

Note the terms inside the square root

$$\frac{u^2+v^2}{c^2}-1=\frac{U^2}{c^2}-1=M^2-1 \tag{588}$$

We can state

- If $M>1$ there are two real characteristics through each point of the flow-field. The equation is hyperbolic PDE.
- If $M=1$ there are one real characteristic through each point in the flow and the PDE is parabolic
- If $M<1$ the characteristics are imaginary, and the PDE is elliptic.

We therefore seek steady inviscid supersonic flow that is hyperbolic in nature. The method can not be used for subsonic flows

Characteristic Lines in Two-Dimensional Irrotational Flow

Let us examine the characteristic lines

$$\frac{dy}{dx}_{characteristic} = \frac{\frac{-U^2 \cos\theta \sin\theta}{c^2} \pm \sqrt{\frac{U^2}{c^2}(\cos^2\theta + \sin^2\theta)} - 1}{1 - \frac{U^2}{c^2}\cos^2\theta} \tag{589}$$

where μ is the Mach angle and we can simplify to

$$\frac{dy}{dx}_{characteristic} = \frac{\frac{-\cos\theta \sin\theta}{\sin^2\mu} \pm \sqrt{\frac{\cos^2\theta \sin^2\theta}{\sin^2\mu} - 1}}{1 - \frac{\cos^2\theta}{\sin^2\mu}} \tag{590}$$

Characteristic Lines in Two-Dimensional Irrotational Flow

Based on trigonometry

$$\sqrt{\frac{\cos^2\theta + \sin^2\theta}{\sin^2\mu} - 1} = \frac{1}{\tan\mu} \tag{591}$$

We can now simplify our equation as

$$\frac{dy}{dx}_{characteristic} = \frac{-\cos\theta\sin\theta/\sin^2\mu \pm 1/\tan\mu}{1 - \cos^2\theta/\sin^2\mu} \tag{592}$$

Which after additional simplification is

$$\frac{dy}{dx}_{characteristic} = \tan(\theta \mp \mu) \tag{593}$$

Characteristic Lines in Two-Dimensional Irrotational Flow

Let us interpret this result graphically

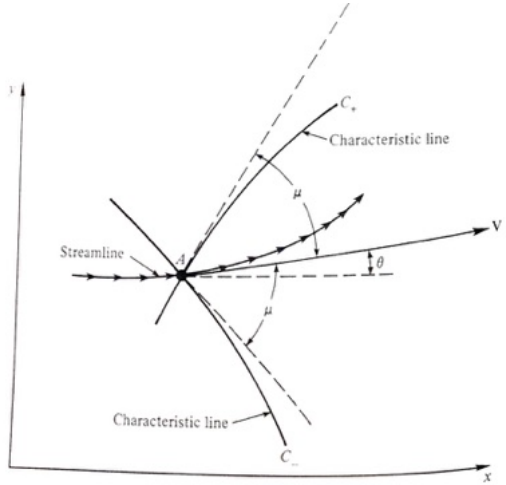

Figure 362

Characteristic Lines in Two-Dimensional Irrotational Flow

- At A, the streamlines make an angle θ with the x axis
- There are two characteristics passing through A at angle μ above the streamline and at angle μ below the streamline
- The characteristic lines are Mach lines.
- We define characteristic of angle $\theta + \mu$ as C_+, which is left running
- $\theta - \mu$ is called C_-, which is called right running.
- These form curves as the flow evolves.

Determination of the Compatibility Equation

We find the compatibility equations by setting $N = 0$. For $N = 0$, we find the determinant of the numerator as (after rearranging)

$$\frac{dv}{du} = \frac{-1 + u^2/c^2}{1 - v^2/c^2}\frac{dy}{dx} \tag{594}$$

Remember this equation holds only on the characteristic lines. Combining this equation the previously developed equation

$$\frac{dv}{du} = -\frac{1 - u^2/c^2}{1 - v^2/c^2}\left[\frac{-uv/c^2 \pm \sqrt{(u^2 + v^2)/c^2 - 1}}{1 - u^2/c^2}\right] \tag{595}$$

We can simplify the equation to

$$\frac{dv}{du} = \frac{uv/c^2 \mp \sqrt{(u^2 + v^2)/c^2 - 1}}{1 - v^2/c^2} \tag{596}$$

Determination of the Compatibility Equation

Recall that $u = U\cos\theta$ and $v = U\sin\theta$ then we can write the previous equation as

$$\frac{d(U\sin\theta)}{d(U\cos\theta)} = \frac{M^2\cos\theta\sin\theta \mp \sqrt{M^2-1}}{1 - M^2\sin^2\theta} \tag{597}$$

after some manipulation and simplification we find

$$d\theta = \mp\sqrt{(M^2-1)}\frac{dU}{U} \tag{598}$$

which is called the compatibility equation.

- This equation describes the variation of the flow along characteristic lines.
- Note that this is also the equation that appears in Prandtl-Meyer flow!

Determination of the Compatibility Equation

We integrate the equation to find the algebraic compatibility equations

$$\theta + \nu(M) = K_{-}(constant) \tag{599}$$

$$\theta - \nu(M) = K_{+}(constant) \tag{600}$$

where $K_{\mp}$ are constants along their characteristics and are analogous to Riemann invariants for unsteady flow.

Unit Processes

- The solution of the MOC is typically called the 'unit process,' which is an antiquated name.
- If we know the flow-field conditions at two-points in the flow then we can find the conditions at a third point.
- Values of ν_1 and θ_1 at point 1, ν_2 and θ_2 are known at point 2, and point 3 is located at an intersection C_- through 1 and C_+ through 2.

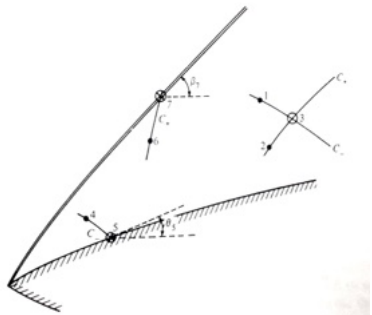

Figure 363

Unit Processes

Remember we know the equations hold

$$\theta_1 + \nu_1 = K_- \tag{601}$$

and

$$\theta_2 - \nu_2 = K_+ \tag{602}$$

We also know that at point 3

$$\theta_3 + \nu_3 = K_{-,3} = K_{-,1} \tag{603}$$

and

$$\theta_3 - \nu_3 = K_{+,3} = K_{+,2} \tag{604}$$

Unit Processes

Solving the equations for subscripts 3 in terms of $K_{\mp}$ yields

$$\theta_3 = \frac{1}{2}\left[K_-|_1 + K_+|_2\right] \tag{605}$$

and

$$\nu_3 = \frac{1}{2}\left[K_-|_1 - K_+|_2\right] \tag{606}$$

- The conditions at point 3 are now known from values 1 and 2
- We can recover M_3 from ν_3 (P-M relation)
- M_3 determines p, T, and ρ through isentropic relations

Unit Processes

Our method uses linear lines between points, so we must choose sufficiently small *dx* and *dy* to form curves and hope our method converges. In practice, we take averages to find new points through an average slope like

$$\frac{1}{2}(\theta_1 + \theta_3) - \frac{1}{2}(\mu_1 + \mu_3) \tag{607}$$

and for C_+

$$\frac{1}{2}(\theta_2 + \theta_3) - \frac{1}{2}(\mu_2 + \mu_3) \tag{608}$$

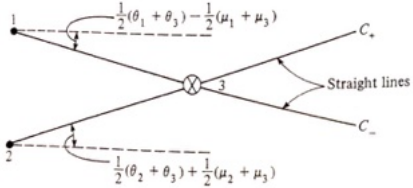

Figure 364

At the Wall

- We can find conditions at the wall if we know the flow conditions within the flow-field.
- Consider a point 4 off the wall with a characteristic connecting it to point 5 at the wall
- The characteristic is $K_{-,4} = \theta_4 + \nu_4$
- Then at point 5 we have $K_{,4-} = K_{,5} = \theta_5 + \nu_5$
- Because the flow at the wall must be tangent (velocity vector) then ν_5 is the only unknown and can be written $\nu_5 = \nu_4 + \theta_4 - \theta_5$

Regions of Influence and Domains of Dependence

- Our analysis shows that disturbances are restricted to certain regions
- We define the domain of dependence and the region of influence
- Remember, in steady flow disturbances in supersonic flow do not propagate upstream

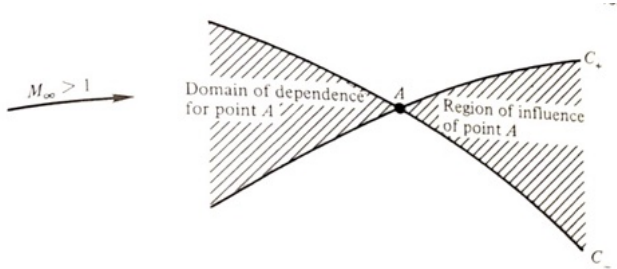

Figure 365: Domain of dependence and region of influence.

Nozzle Design

- Require knowledge of the nozzle contour beyond the typical area ratio found from one-dimensional theory
- Use the method of characteristics to design the divergent section of the nozzle from throat to exit
- Need to know exit conditions (when to stop marching in space) and throat conditions
- We assume that the sonic line is straight but in reality it follows Meyer's finding that it is quadratic
- Let θ_w be the angle of the wall with respect to x
- for θ_w increasing the nozzle is in the expansion region and otherwise is in the straightening section

Nozzle Design

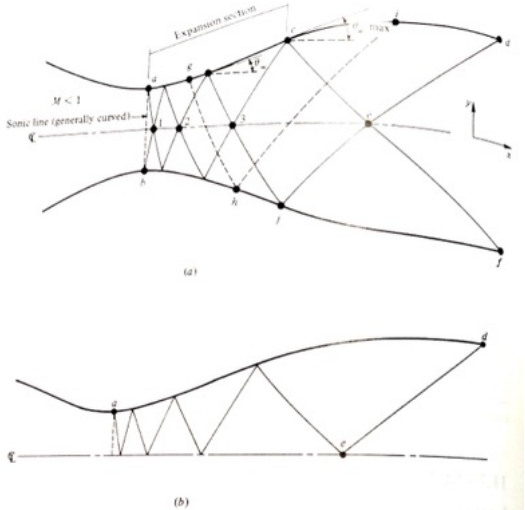

Figure 366: Illustration of the nozzle design process using method of characteristics.

Nozzle Design Sample Solution Process

- We seek to compute and graph the contour of a 2D nozzle for design Mach number 2.4
- We assume that there is a linear sonic line at the throat
- We find a resultant area ratio of 2.33 which is within 3% of the one-dimensional theory
- More accurate solutions will result within smaller increments in the network

Nozzle Design

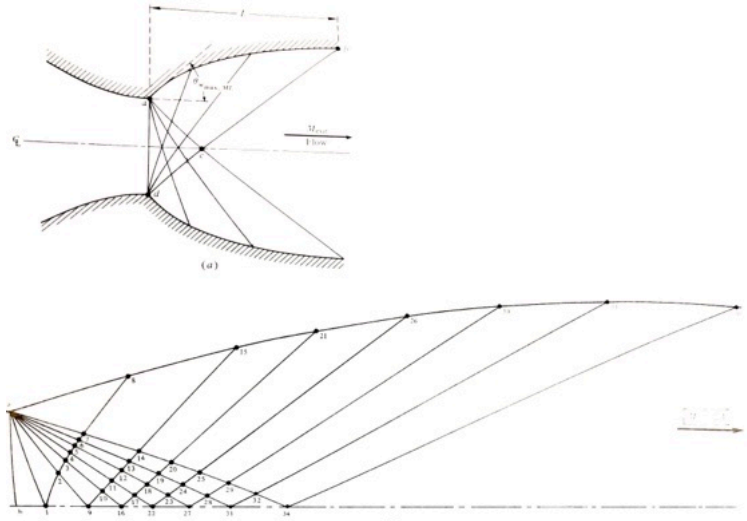

Figure 367: Example result from MOC design of a convergent-divergent nozzle.

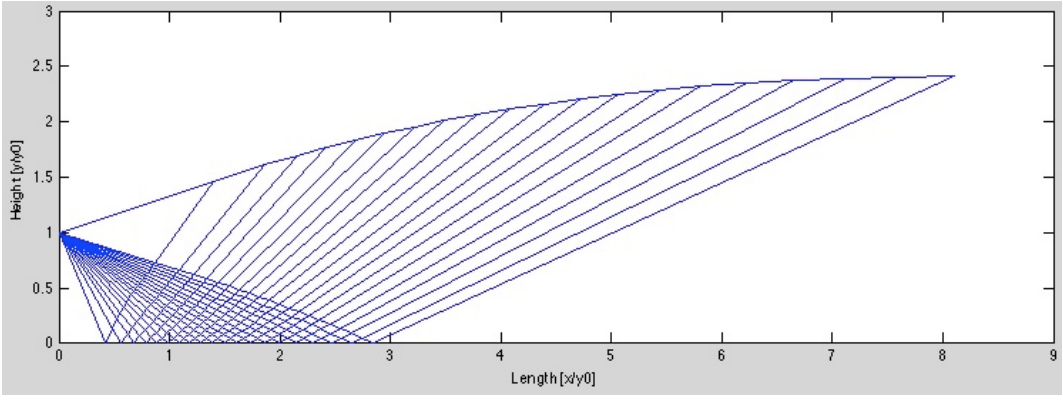

Figure 368: Example nozzle design program using MOC.

Class Summary

- Method of characteristics (MOC)
- Short example problem for nozzles

Next Time

- Compressible Stream Tubes and Pipe Flow

Class Overview

Purpose of the class is to introduce flow with heat addition. We cover.

- Rayleigh flow
- Examples
- Theory

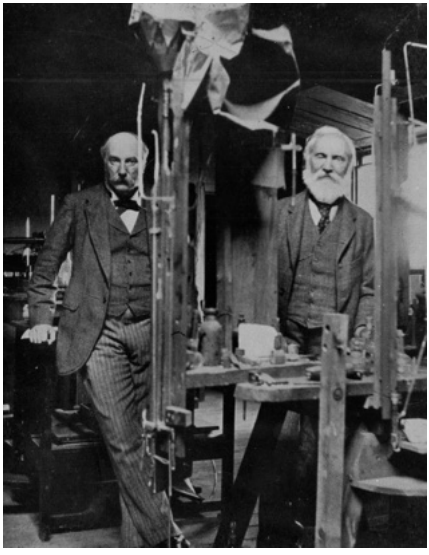

Figure 369: Lord Kelvin (right) and Lord Rayleigh (left) in the laboratory at Terling. Photograph by A.G. Webster, From: Rayleigh, Robert John Strutt, Baron. John William Strutt Third Baron Rayleigh, New York: Longmans, Green & Co., 1924; Air Force Cambridge Research Laboratory Tech Photo Branch, courtesy AIP Emilio Segre Visual Archives

“Examples ... show how difficult it often is for an experimenter to interpret his results without the aid of mathematics.”

Sir John William Strutt, Lord Rayleigh, Quoted in E. T. Bell, Men of Mathematics, xvi.

Examples

Figure 370: Alaska pipeline

Examples

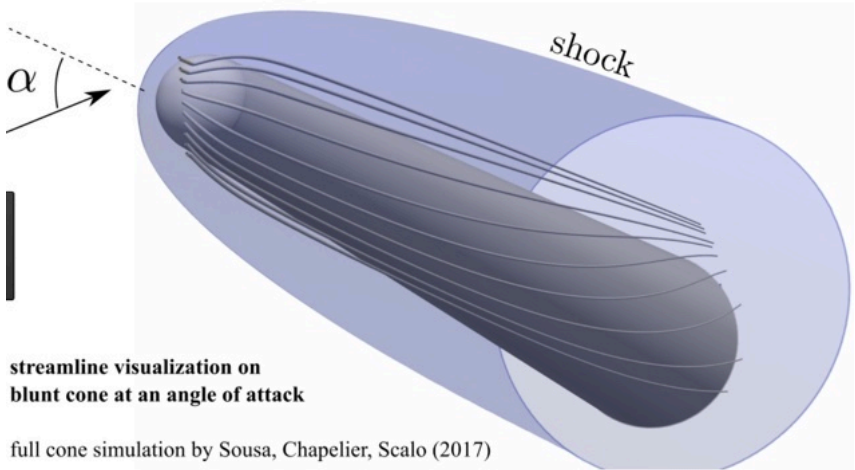

Figure 371: A bow shock with streamlines at an angle of attack.

Control Volume for One-Dimensional Flow

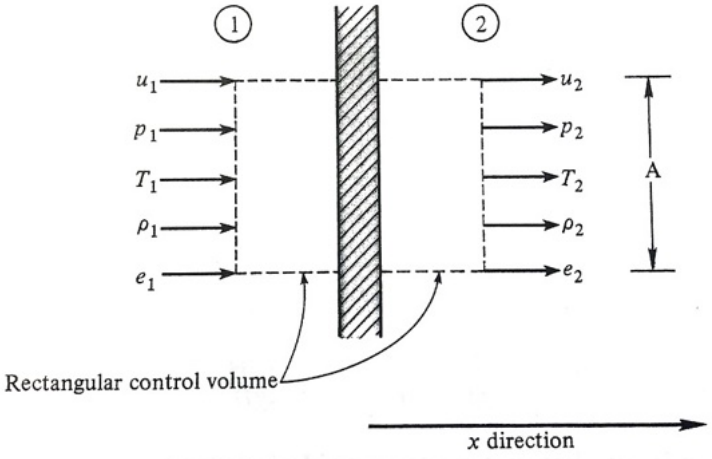

Figure 372: Differential control volume of one-dimensional Rayleigh flow.

Notes on the Control Volume

- Within control volume some change must occur to change properties
- Before the shock caused increase in entropy (disorder)
- Though no terms directly account for viscous (friction) or heating effects (conduction)
- Viscous effects such as friction might cause changes between regions 1 and 2
- Heat addition can also cause changes
- These can occur without presence of a shock
- Examples
  - Very long pipes transporting gases
  - Lasers heating portions of fluids (heating of small compressible wind tunnels)
  - Certain kinds of chemical reactions

3rd Baron Rayleigh,, John William Strutt,
12 November 1842 – 30 June 1919, English

- Physicist
- Argon, Rayleigh waves, Rayleigh scattering, Rayleigh criterion ,Rayleigh–Ritz method, Duplex theory, Sound theory, Rayleigh flow, Rayleigh problem, Rayleigh-Plesset equation, Rayleigh–Schrödinger perturbation theory, Rayleigh–Taylor instability, Rayleigh–Jeans law, Rayleigh's equation
- Cavendish Professor of Physics at the University of Cambridge
- 1904 Nobel Prize
- Deeply religious person that influenced his work
- Interestingly, also president of Society for Psychical Research

S.A.E. Miller, Ph.D., saem@ufl.edu

Rayleigh Analysis

We want to find properties at states one and two. Consider a flow with heat addition or extraction. The governing equations are

$$\rho_1 u_1 = \rho_2 u_2 \tag{609}$$

$$p_1 + \rho_1 u_1^2 = p_2 + \rho_2 u_2^2 \tag{610}$$

$$h_1 + \frac{u_1^2}{2} + q = h_2 + \frac{u_2^2}{2} \tag{611}$$

where h is enthalpy and q is heat added per unit mass. We also require an equation of state to solve for region 2. Generally a numerical approach is required.

Rayleigh Analysis

For calorically perfect gases we do not require a numerical approach. For $h = c_p T$ we can solve

$$q = \left(c_p T_2 + \frac{u_2^2}{2} \right) - \left(c_p T_1 + \frac{u_1^2}{2} \right) \tag{612}$$

The terms on the right hand side will simplify to

$$q = c_p T_{o2} - c_p T_{o1} = c_p (T_{o2} - T_{o1}) \tag{613}$$

We find that the effect of heat addition is to directly change the total temperature of the flow. e.g. $q \rightarrow$ increase of T_o.

Rayleigh Analysis

Examine properties of the flow between regions 1 and 2 in terms of M_1 and M_2. Note

$$\rho u^2 = \rho c^2 M^2 = \rho \frac{\gamma p}{\rho} M^2 = \gamma p M^2 \tag{614}$$

and based upon the momentum equation

$$p_2 - p_1 = \rho_1 u_1^2 - \rho_2 u_2^2 = \gamma p_1 M_1^2 - \gamma p_2 M_2^2 \tag{615}$$

Rayleigh Analysis

We now find the ratio of static thermodynamic pressures

$$\frac{p_2}{p_1} = \frac{1 + \gamma M_1^2}{1 + \gamma M_2^2} \tag{616}$$

Using the perfect gas law and continuity equation

$$\frac{T_2}{T_1} = \frac{p_2}{p_1}\frac{\rho_1}{\rho_2} = \frac{p_2}{p_1}\frac{u_2}{u_1} \tag{617}$$

Recall the speed of sound

$$c = \sqrt{\gamma R T} \tag{618}$$

Rayleigh Analysis

We are able to find the ratio of velocities

$$\frac{u_2}{u_1} = \frac{M_2}{M_1}\frac{c_2}{c_1} = \frac{M_2}{M_1}\left(\frac{T_2}{T_1}\right)^{\frac{1}{2}} \tag{619}$$

using this ratio and the ratio for pressures we find the ratio of temperatures

$$\frac{T_2}{T_1} = \left(\frac{1+\gamma M_1^2}{1+\gamma M_2^2}\right)\left(\frac{M_2}{M_1}\right)^2 \tag{620}$$

Using relation for $\rho_2/\rho_1 = f(p, T)$ yields

$$\frac{\rho_2}{\rho_1} = \left(\frac{1+\gamma M_2^2}{1+\gamma M_1^2}\right)\left(\frac{M_1}{M_2}\right)^2 \tag{621}$$

Rayleigh Analysis

Recall our equation relating total pressure with Mach number, which we substitute into the relation for the ratio of static pressures

$$\frac{p_o}{p} = \left(1 + \frac{\gamma - 1}{2} M^2\right)^{\frac{\gamma}{\gamma - 1}} \text{ and sub. into } \frac{p_2}{p_1} = \frac{1 + \gamma M_1^2}{1 + \gamma M_2^2} \tag{622}$$

yields

$$\frac{p_{o2}}{p_{o1}} = \frac{1 + \gamma M_1^2}{1 + \gamma M_2^2} \left(\frac{1 + \frac{\gamma - 1}{2} M_2^2}{1 + \frac{\gamma - 1}{2} M_1^2}\right)^{\frac{\gamma}{\gamma - 1}} \tag{623}$$

and ratio of total temperatures can be found from

$$\frac{T_o}{T} = 1 + \frac{\gamma - 1}{2} M^2 \tag{624}$$

and T_2/T_1 as

$$\frac{T_{o2}}{T_{o1}} = \frac{1 + \gamma M_1^2}{1 + \gamma M_2^2} \left(\frac{M_2}{M_1}\right)^2 \left(\frac{1 + \frac{\gamma - 1}{2} M_2^2}{1 + \frac{\gamma - 1}{2} M_1^2}\right) \tag{625}$$

Rayleigh Analysis

Next we seek to find the change in entropy in the system. Recall the developed equation for entropy change (please recall the assumptions)

$$S_2 - S_1 = c_p \ln\left(\frac{T_2}{T_1}\right) - R \ln\left(\frac{p_2}{p_1}\right) \tag{626}$$

where we have previously found the ratios of T and p. Now that we have found these ratios we need a method to find the state in region 2. Let us assume that we are aware of the state in region 1.

Rayleigh Analysis

For a given q, we can find T_{o2} using

$$q = c_p(T_{o2} - T_{o1}) \tag{627}$$

Then M_2 can be found using the $\frac{T_{o2}}{T_{o1}}$ equation.

- Now remaining ratios can be found using these developed equations.
- Unfortunately, M_2 requires a numerical methodology (maybe).

A Direct Method

Is there a more direct method that does not require particular numerics?

- Let us use a reference value, which is similar to the critical conditions that we used previously
- Let $M_1 = 1, p_1 = p^*, T_1 = T^*, \rho_1 = \rho^*, p_{o1} = p_o^*$, and $T_{o1} = T_o^*$
- Flow properties at other values of M can be found by using $M_1 = 1$ and $M_2 = M$ with our developed equations

A Direct Method

We find

$$\frac{p}{p^*} = \frac{1+\gamma}{1+\gamma M^2} \tag{628}$$

$$\frac{T}{T^*} = M^2\left(\frac{1+\gamma}{1+\gamma M^2}\right)^2 \tag{629}$$

$$\frac{\rho}{\rho^*} = \frac{1}{M^2}\left(\frac{1+\gamma M^2}{1+\gamma}\right) \tag{630}$$

$$\frac{p_o}{p_o^*} = \frac{1+\gamma}{1+\gamma M^2}\left[\frac{2+(\gamma-1)M^2}{\gamma+1}\right]^{\frac{\gamma}{\gamma-1}} \tag{631}$$

and

$$\frac{T_o}{T_o^*} = \frac{(\gamma+1)M^2}{(1+\gamma M^2)^2}[2+(\gamma-1)M^2] \tag{632}$$

Evaluations of these equations are tabulated in the tables in the back of most compressible flow books and labeled “one-dimensional flow with heat addition” or “Rayleigh flow”’

Example Rayleigh Flow

γ =	1.4000			Rayleigh		
M	p/p^*	$p_0/p_0{}^*$	T/T^*	ρ/ρ^* μ^*/μ	$T_0/T_0{}^*$
0.000	2.400E+00	1.268E+00	0.000E+00	-	0.000E+00
0.025	2.398E+00	1.267E+00	3.594E-03	6.673E+02	2.995E-03
0.050	2.392E+00	1.266E+00	1.430E-02	1.673E+02	1.192E-02
0.075	2.381E+00	1.263E+00	3.190E-02	7.466E+01	2.661E-02
0.100	2.367E+00	1.259E+00	5.602E-02	4.225E+01	4.678E-02
0.125	2.349E+00	1.254E+00	8.619E-02	2.725E+01	7.205E-02
0.150	2.327E+00	1.249E+00	1.218E-01	1.910E+01	1.020E-01
0.175	2.301E+00	1.242E+00	1.622E-01	1.419E+01	1.360E-01
0.200	2.273E+00	1.235E+00	2.066E-01	1.100E+01	1.736E-01
0.225	2.241E+00	1.226E+00	2.543E-01	8.814E+00	2.140E-01
0.250	2.207E+00	1.218E+00	3.044E-01	7.250E+00	2.568E-01
0.275	2.170E+00	1.208E+00	3.562E-01	6.093E+00	3.013E-01
0.300	2.131E+00	1.199E+00	4.089E-01	5.213E+00	3.469E-01
0.325	2.091E+00	1.188E+00	4.617E-01	4.528E+00	3.929E-01
0.350	2.049E+00	1.178E+00	5.141E-01	3.985E+00	4.389E-01
0.375	2.005E+00	1.167E+00	5.654E-01	3.546E+00	4.845E-01
0.400	1.961E+00	1.157E+00	6.151E-01	3.188E+00	5.290E-01
0.425	1.916E+00	1.146E+00	6.628E-01	2.890E+00	5.723E-01
0.450	1.870E+00	1.135E+00	7.080E-01	2.641E+00	6.139E-01
0.475	1.824E+00	1.124E+00	7.506E-01	2.430E+00	6.537E-01
0.500	1.778E+00	1.114E+00	7.901E-01	2.250E+00	6.914E-01

Figure 373: A portion of the Rayleigh table.

Let us examine the table developed for this class. Note the validity of the table via γ.

Notes on Rayleigh Flow

We can use tables, equations, or numerics.

- Remember – the stared (*) quantities are the same no matter what the local flow properties are
- * quantities are not like those before as this is a non-adiabatic process
- * quantities correspond to achieving Mach one through heat addition

The Rayleigh Technique in Pictures

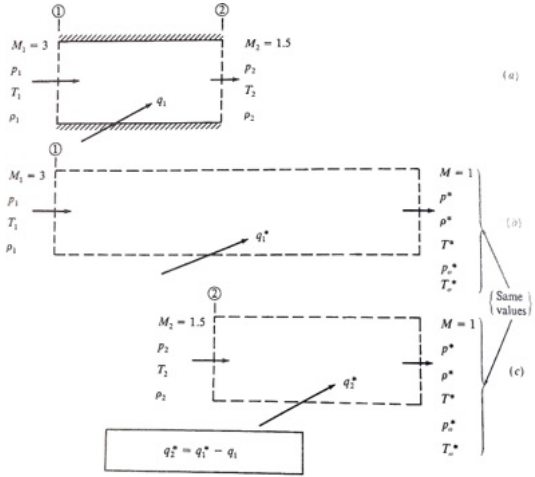

Figure 374: A diagram of the Rayleigh problem and solution approach.

Summary of Rayleigh Flow Trends in Subsonic Regime

- Mach number increases, $M_2 > M_1$
- Pressure decreases, $p_2 < p_1$
- Temperature increases for $M_1 < \gamma^{-1/2}$ and decreases for $M_1 > \gamma^{-1/2}$
- Total temperature increases, $T_{o2} > T_{o1}$
- Total pressure decreases, $p_{o2} < p_{o1}$
- Velocity increases, $u_2 > u_1$

Note, that if heat is extracted, then use inverse of all relations

Summary of Rayleigh Flow Trends in Supersonic Regime

- Mach number decreases, $M_2 < M_1$
- Pressure increases, $p_2 > p_1$
- Temperature increases, $T_2 > T_1$
- Total temperature increases, $T_{o2} > T_{o1}$
- Total pressure decreases, $p_{o2} < p_{o1}$
- Velocity decreases, $u_2 < u_1$

Mollier Diagram for Rayleigh Flow

A Mollier diagram is enthalpy versus entropy.

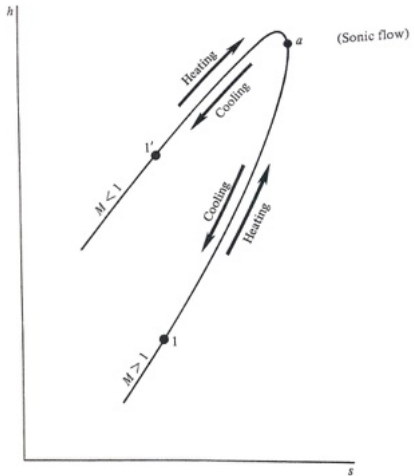

Figure 375: Mollier diagram for Rayleigh flow.

Notes on Rayleigh Flow Mollier Diagram

- At a the flow is choked.
- Additional q added to the flow will cause a normal shock to form
- If initially subsonic at 1, then choking flow, lowering q will lower conditions at 1 instead of a normal shock forming
- Possible to heat and cool a flow to make it supersonic from rest conditions
- At all speeds, adding q decreases p_o

Aerodynamic Calculator for Rayleigh Flow

Rayleigh Flow

Clear

M	2
p/p^*	0.36363636363636365
p_o/p_o^*	1.5030959785260414
T/T^*	0.5289256198347108
T_o/T_o^*	0.7933884297520661
u/u^*	1.4545454545454546
γ	1.4
ρ/ρ^*	0.6875

Supersonic | Calculate

Figure 376

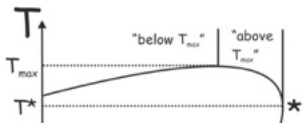

Figure 377

The Most Simple Rayleigh Flow Example

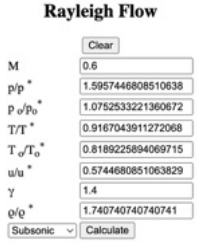

Figure 378

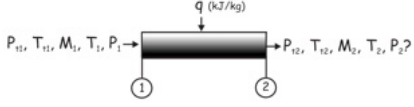

Figure 379

For a Rayleigh flow problem where flow conditions at the inlet to a duct are given and the heating rate q is known, the general solution approach is as follows...

The Most Simple Rayleigh Flow Example

- Using stagnation temperature at the entrance T_{o1}, find the stagnation temperature at the exit T_{o2} using the given heat transfer rate q.
- Enter the Rayleigh flow table or Calculator at M_1 to find T_{o1}/T_o^* at the pipe entrance.
- The quantity T_o^* is a reference condition for Rayleigh flow problems (whether or not the pipe is actually choked by heat transfer)

The Most Simple Rayleigh Flow Example

- Determine T_{o2}/T_o^*

$$\frac{T_{o2}}{T_o^*} = \frac{T_{o2}}{T_{o1}} \frac{T_{o1}}{T_o^*} \tag{633}$$

- Enter the Rayleigh flow table or calculator at T_{o2}/T_o^* to find M_2, T_2/T^*, and other property ratios
- Use chains to obtain the flow properties at the pipe exit, such as

$$T_2 = T_1 \frac{T^*}{T_1} \frac{T_2}{T^*} \tag{634}$$

Here we use $q = c_p \Delta T_o$.

Class Summary

- Rayleigh flow solutions
- Examples
- Trends

Next Time

- Fanno flow

Class Overview

- Boundary layers
- Fanno flow
- Theory
- Solution approach

One-Dimensional Flow with Friction (Fanno-Flow)

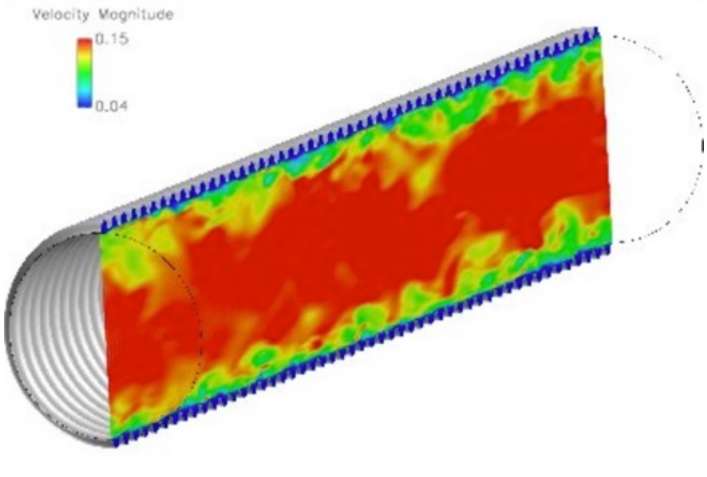

Figure 380: A computational fluid dynamics visualization of turbulent flow within a pipe.

“A very satisfactory explanation of the physical process in the boundary layer [Grenzschicht] between a fluid and a solid body could be obtained by the hypothesis of an adhesion of the fluid to the walls, that is, by the hypothesis of a zero relative velocity between fluid and wall. If the viscosity was very small and the fluid path along the wall not too long, the fluid velocity ought to resume its normal value at a very short distance from the wall. In the thin transition layer [Ubergangsschicht] however, the sharp changes of velocity, even with small coefficient of friction, produce marked results.”

L. Prandtl, in Verhandlungen des dritten internationalen Mathematiker-Kongresses in Heidelberg 1904, A. Krazer, ed., Teubner, Leipzig, Germany (1905), p. 484. English trans. in Early Developments of Modern Aerodynamics, J. A. K. Ackroyd, B. P. Axcell, A. I. Ruban, eds., Butterworth-Heinemann, Oxford, UK (2001), p. 77.

Boundary Layer – Law of the Wall

An empirical theory

Likely most famous similarity relationship within fluid dynamics and is applicable towards boundary layer turbulence

The streamwise velocity component near the wall varies logarithmically with the distance from the surface

The energy cascade of Kolmogorov also exists in BL flows (in fact all turbulent flows)

We derive a velocity scale of a turbulent boundary layer as the friction velocity

$$u_T \equiv \sqrt{\frac{\tau_w}{\rho}}$$

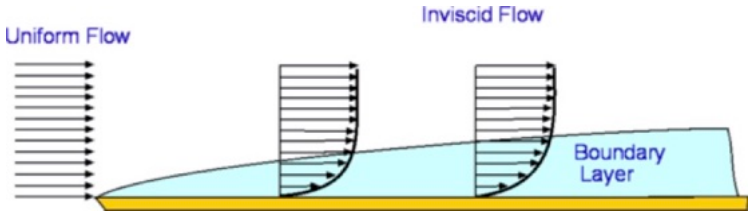

Boundary Layer – Law of the Wall

- Friction velocity is representative of the velocity scale close to a solid boundary
- We postulate that the mean velocity gradient, $\partial u/\partial y$, can be correlated as a function of u_τ , ν, and y as

$$\frac{\partial U}{\partial y} = \frac{u_\tau}{y} F(u_\tau y/\nu)$$

where F is some universal function. For F, experiments elude to a form like

$$F(u_\tau y/\nu) \to \frac{1}{\kappa} \quad \text{as} \quad u_\tau y/\nu \to \infty$$

Now if F varies with u_τ/y it would only depends on ν as viscous effects dissipate from from the surface, so we would find a relation such as

$$\frac{U}{u_\tau} = \frac{1}{\kappa} \ell n \frac{u_\tau y}{\nu} + C$$

where C is a dimensionless integration constant and experiments show that $C \sim 5$ and $\kappa \sim 0.41$ (which is the von Karman constant)

Boundary Layer – Law of the Wall

Typical profile of a TBL

$$u^+ \equiv \frac{U}{u_\tau} \quad \text{and} \quad y^+ \equiv \frac{u_\tau y}{\nu}$$

Velocity profile matches the law of the wall for values of y^+ in excess of 30.

Three main regions

- Viscous Sublayer
- Log Layer
- Defect Layer

Log layer separates inner and outer regions of the flow

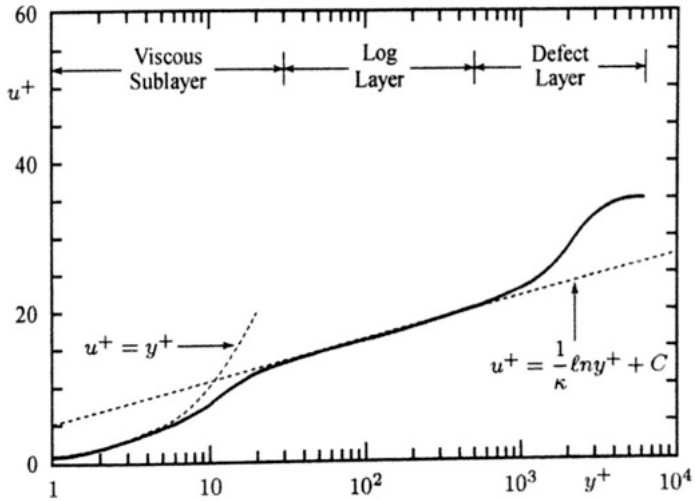

Boundary Layer – Law of the Wall

We assume that the velocity in the viscous sublayer depends on u_τ, ν, and y

$$U = u_\tau f(y^+)$$

where y^+ is a dimensionless function. This form is the law of the wall.
Experimentally, velocity data correlate very well with the so-called velocity-defect law or Clauser defect law

$$U = U_e - u_\tau g(\eta), \qquad \eta \equiv \frac{y}{\Delta}$$

where $g(\eta)$ is a dimensionless function. Δ is a thickness of the outer layer. We now have two length sales, the inner and outer

$$\nu/u_\tau \qquad \text{and} \qquad \Delta$$

There is a large disparity in the size of the scales $\frac{\nu}{u_\tau} \ll \Delta$

An overlap region must exist between them that obeys

$$u_\tau f(y^+) = U_e - u_\tau g(\eta) \quad \text{for} \quad y^+ \gg 1 \ \text{ and } \ \eta \ll 1$$

Boundary Layer – Law of the Wall

We can complete the matching by differentiating the previous equation w.r.t y

$$\frac{u_\tau^2}{\nu} f'(y^+) = -\frac{u_\tau}{\Delta} g'(\eta) \quad \text{for} \quad y^+ \gg 1 \ \text{ and } \ \eta \ll 1$$

Now multiply through by y/u_τ

$$y^+ f'(y^+) = -\eta g'(\eta) \quad \text{for} \quad y^+ \gg 1 \ \text{ and } \ \eta \ll 1$$

A wide separation of scales means we can regard y^+ and η as independent variables. Only way a function of y^+ can equal a function of η is for both to be equal to a constant

$$y^+ f'(y^+) = \text{ constant } = \frac{1}{\kappa} \implies f(y^+) = \frac{1}{\kappa} \ell n y^+ + c$$

Boundary Layer – Law of the Wall

For the velocity defect region we can formulate a departure from the logarithmic region a composite profile (profile for the entire BL) might be

$$U^+ = \frac{1}{\kappa}\ell n y^+ + C + \frac{2\Pi}{\kappa}\sin^2\left(\frac{\pi}{2}\frac{y}{\delta}\right)$$

where Π is Coles' wake-strength parameters and Δ is the BL thickness
Π varies with pressure gradient and for constant pressure is $\Pi \sim 0.60$
Let's examine a graph of Coles' wake strength parameter

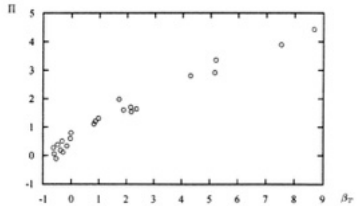

Figure 1.7: *Coles' wake-strength parameter, Π, as a function of pressure gradient; ∘ based on data tabulated by Coles and Hirst (1969).*

Gino Girolamo Fanno

18 November 1882 –23 March 1962, Italian

- Italian mechanical engineer who developed the Fanno flow model
- Pretended to be catholic to avoid concentration camp, in 1939 Fanno was denounced as a Jew and lost his Ph.D
- After WWII, Fanno was only able to work in agriculture and agricultural engineering
- Fanno died without recognition for his model

S.A.E. Miller, Ph.D., saem@ufl.edu

Fanno Flow

- One-dimensional flow of compressible fluid that is shockless, steady, and adiabatic.
- Consider viscous forces that create friction between the wall and fluid.
- Slight modification to our models allows us to account for this effect.

Fanno Flow Control Volume

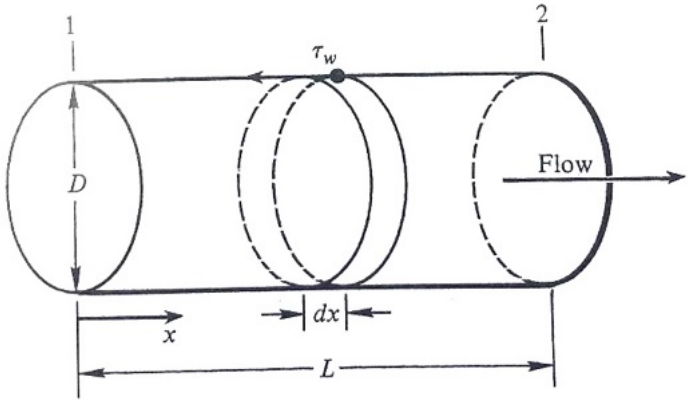

Figure 381: Diagram of Fanno flow.

Fanno Flow Analysis

We modify our momentum control volume approach to account for shear stress. Our conservation equation is

$$\oint_S (\rho \underline{u} \cdot d\underline{S}) u = -\oint_S (p dS)_x - \oint_S \tau_w dS \tag{635}$$

Applying this equation about the surface above yields

$$-\rho_1 u_1^2 A + \rho_2 u_2^2 A = p_1 A - p_2 A - \int_0^L \pi D \tau_w dx \tag{636}$$

Area is $A = \pi D^2/4$

$$(p_2 - p_1) + (\rho_2 u_2^2 - \rho_1 u_1^2) = -\frac{4}{D}\int_0^L \tau_w dx \tag{637}$$

Fanno Flow Analysis

τ_w is a function of x. Take limit of L as it approaches dx. We find

$$dp + d(\rho u^2) = -\frac{4}{D}\tau_w dx \tag{638}$$

Let us differential ρu

$$d(\rho u^2) = \rho u du + u d(\rho u) = \rho u du + u(0) = \rho u du \tag{639}$$

Fanno Flow Analysis

Using the relation $d(\rho u^2) = \rho u du$ we find

$$dp + \rho u du = -\frac{4}{D}\tau_w dx \tag{640}$$

Let the friction coefficient be $\tau_w = \frac{1}{2}\rho u^2 f$,

$$dp + \rho u du = -\frac{1}{2}\rho u^2 \frac{4 f dx}{D} \tag{641}$$

We now assume that we are working with a calorically perfect gas. We can then imply

$$c^2 = \frac{\gamma p}{\rho}, M^2 = u^2/c^2, p = \rho R T, \ \& \ \rho u = \text{ a constant} \tag{642}$$

$$c_p T + u^2/2 = \text{const.} \tag{643}$$

Fanno Flow Analysis

Using these relations we can simplify our equation as

$$\frac{4fdx}{D} = \frac{2}{\gamma M^2}(1-M^2)\left[1+\frac{1}{2}(\gamma-1)M^2\right]^{-1}\frac{dM}{M} \tag{644}$$

Now integrate this equation between $x = x_1$ and x_2 from $M = M_1$ to $M = M_2$

$$\int_{x_1}^{x_2}\frac{4fdx}{D} = \left[-\frac{1}{\gamma M^2} - \frac{\gamma+1}{2\gamma}\ln\left[\frac{M^2}{1+\frac{\gamma-1}{2}M^2}\right]\right]_{M_1}^{M_2} \tag{645}$$

This equation relates the Mach numbers at two locations to the integrated effect of friction. We can now easily find thermodynamic ratios (T_o= constant) adiabatic.

$$\frac{T_2}{T_1} = \frac{T_o/T_1}{T_o/T_2} = \frac{2+(\gamma-1)M_1^2}{2+(\gamma-1)M_2^2} \tag{646}$$

Fanno Flow Analysis

Also because $\rho_1 u_1 = \rho_2 u_2$ and $c^2 = \gamma p/\rho$

$$\frac{\gamma p_1 u_1}{c_1^2} = \frac{\gamma p_2 u_2}{c_2^2} \tag{647}$$

or

$$\frac{p_2}{p_1} = \frac{M_1}{M_2}\frac{c_2}{c_1} = \frac{M_1}{M_2}\sqrt{\frac{T_2}{T_1}} \tag{648}$$

Combining the relations for p_2/p_1 and T_2/T_1 yields

$$\frac{p_2}{p_1} = \left(\frac{M_1}{M_2}\right)\left[\frac{2+(\gamma-1)M_1^2}{2+(\gamma-1)M_2^2}\right]^{\frac{1}{2}} \tag{649}$$

Noting that $\rho_2/\rho_1 = (p_2/p_1)(T_1/T_2)$ we find that

$$\frac{\rho_2}{\rho_1} = \frac{M_1}{M_2}\left[\frac{2+(\gamma-1)M_1^2}{2+(\gamma-1)M_2^2}\right]^{\frac{1}{2}}\frac{2+(\gamma-1)M_2^2}{2+(\gamma-1)M_1^2} \tag{650}$$

Fanno Flow Analysis

We also find the ratios of total pressure to be

$$\frac{p_{o2}}{p_{o1}} = \frac{p_{o2}/p_2}{p_{o1}/p_1}\frac{p_1}{p_2} = \left[\frac{2+(\gamma-1)M_2^2}{2+(\gamma-1)M_1^2}\right]^{\frac{\gamma}{\gamma-1}}\frac{M_1}{M_2}\left[\frac{2+(\gamma-1)M_1^2}{2+(\gamma-1)M_2^2}\right]^{\frac{1}{2}} \tag{651}$$

and simplifying we find

$$\frac{p_{o2}}{p_{o1}} = \frac{M_1}{M_2}\left[\frac{2+(\gamma-1)M_2^2}{2+(\gamma-1)M_1^2}\right]^{\frac{\gamma+1}{2(\gamma-1)}} \tag{652}$$

- This is all very much like our results for Rayleigh flow
- Attempt approach with '*' reference theory $\rightarrow$ * quantities
- Sonic flow references of p^*, ρ^*, T^* and p_o^*.
- We find (as we did in Rayleigh flow) a set of equations

Fanno Flow Analysis

We find a set of equations relative to the reference value

$$\frac{T}{T^*} = \frac{\gamma + 1}{2 + (\gamma - 1)M^2} \tag{653}$$

$$\frac{p}{p^*} = \frac{1}{M}\left[\frac{\gamma + 1}{2 + (\gamma - 1)M^2}\right]^{\frac{1}{2}} \tag{654}$$

$$\frac{\rho}{\rho^*} = \frac{1}{M}\left[\frac{2 + (\gamma - 1)M^2}{\gamma + 1}\right]^{\frac{1}{2}} \tag{655}$$

$$\frac{p_o}{p_o^*} = \frac{1}{M}\left[\frac{2 + (\gamma - 1)M^2}{\gamma + 1}\right]^{\frac{\gamma+1}{2(\gamma-1)}} \tag{656}$$

Fanno Flow Analysis

If we define $x = L^*$ at point where $M^* = 1$ then

$$\int_0^{L^*} \frac{4f dx}{D} = \left[\frac{-1}{\gamma M^2} - \frac{\gamma+1}{2\gamma} \ln \left(\frac{M^2}{1 + \frac{\gamma-1}{2} M^2} \right) \right]_M^1 \tag{657}$$

or

$$\frac{4\bar{f}L^*}{D} = \frac{1 - M^2}{\gamma M^2} + \frac{\gamma+1}{2\gamma} \ln \left[\frac{(\gamma+1)M^2}{2 + (\gamma-1)M^2} \right] \tag{658}$$

where $\bar{f}$ is the average friction coefficient defined as

$$\bar{f} = \frac{1}{L^*} \int_0^{L^*} f dX. \tag{659}$$

Fanno Flow Table

The numerical results of these equations are tabulated in the back of almost all compressible flow books and provided in the equation sheet.

- Here local friction coefficient, f, depends on turbulent flow, R_e, surface roughness, etc.
- f is typically found empirically and is available in books
- Typically $f \cong 0.005$ for $R_e > 10^5$ and $\eta \approx 0.01D$, where η is the roughness

$\gamma =$	1.4000										
	Rayleigh					Fanno					
M	p/p^*	p_0/p_0^*	T/T^*	ρ/ρ^* u^*/u	T_0/T_0^*	p/p^*	p_0/p_0^*	T/T^*	ρ/ρ^*	$4fL^*/D$	
0.000	2.400E+00	1.268E+00	0.000E+00	-	0.000E+00	-	-	1.200E+00	-	-	
0.025	2.398E+00	1.267E+00	3.594E-03	6.673E+02	2.995E-03	4.382E+01	2.316E+01	1.200E+00	3.652E+01	1.136E+03	
0.050	2.392E+00	1.266E+00	1.430E-02	1.673E+02	1.192E-02	2.190E+01	1.159E+01	1.199E+00	1.826E+01	2.800E+02	
0.075	2.381E+00	1.263E+00	3.190E-02	7.466E+01	2.661E-02	1.460E+01	7.742E+00	1.199E+00	1.218E+01	1.220E+02	
0.100	2.367E+00	1.259E+00	5.602E-02	4.225E+01	4.678E-02	1.094E+01	5.822E+00	1.198E+00	9.138E+00	6.692E+01	
0.125	2.349E+00	1.254E+00	8.619E-02	2.725E+01	7.205E-02	8.750E+00	4.673E+00	1.196E+00	7.314E+00	4.159E+01	
0.150	2.327E+00	1.249E+00	1.218E-01	1.910E+01	1.020E-01	7.287E+00	3.910E+00	1.195E+00	6.099E+00	2.793E+01	
0.175	2.301E+00	1.242E+00	1.622E-01	1.419E+01	1.360E-01	6.241E+00	3.368E+00	1.193E+00	5.232E+00	1.977E+01	
0.200	2.273E+00	1.235E+00	2.066E-01	1.100E+01	1.736E-01	5.455E+00	2.964E+00	1.190E+00	4.583E+00	1.453E+01	
0.225	2.241E+00	1.226E+00	2.543E-01	8.814E+00	2.140E-01	4.844E+00	2.651E+00	1.188E+00	4.078E+00	1.090E+01	
0.250	2.207E+00	1.218E+00	3.044E-01	7.250E+00	2.568E-01	4.355E+00	2.403E+00	1.185E+00	3.674E+00	8.483E+00	
0.275	2.170E+00	1.208E+00	3.562E-01	6.093E+00	3.013E-01	3.954E+00	2.201E+00	1.182E+00	3.345E+00	6.661E+00	
0.300	2.131E+00	1.199E+00	4.089E-01	5.213E+00	3.469E-01	3.619E+00	2.035E+00	1.179E+00	3.070E+00	5.299E+00	
0.325	2.091E+00	1.188E+00	4.617E-01	4.528E+00	3.929E-01	3.336E+00	1.896E+00	1.175E+00	2.838E+00	4.260E+00	
0.350	2.049E+00	1.178E+00	5.141E-01	3.985E+00	4.389E-01	3.092E+00	1.778E+00	1.171E+00	2.640E+00	3.452E+00	
0.375	2.005E+00	1.167E+00	5.654E-01	3.546E+00	4.845E-01	2.881E+00	1.677E+00	1.167E+00	2.468E+00	2.816E+00	

Figure 382: Fanno flow table.

Fanno Flow in Subsonic Regime

- Mach number increases, $M_2 > M_1$
- Pressure decreases, $p_2 < p_1$
- Temperature decreases $T_2 < T_1$
- Total pressure decreases, $p_{o2} < p_{o1}$
- Velocity increases, $u_2 > u_1$
- We see that friction always drives M toward unity.

Fanno Flow in Supersonic Regime

- Mach number decreases, $M_2 < M_1$
- Pressure increases, $p_2 > p_1$
- Temperature increases, $T_2 > T_1$
- Total pressure decreases, $p_{o2} < p_{o1}$
- Velocity decreases, $u_2 < u_1$

Mollier Diagram for Fanno Flow

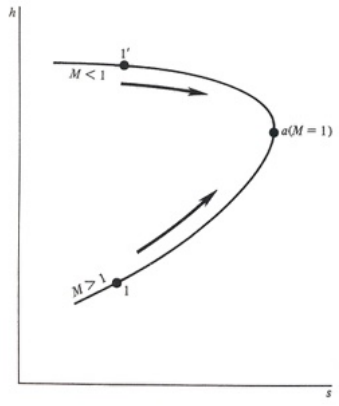

Figure 383: The Fanno curve.

Notes on Fanno Flow Curve

- Point *a* is maximum entropy
- Upper curve is subsonic and lower curve is supersonic
- Points on curve correspond to certain duct lengths, *L*
- For very large *L* the flow will eventually go through a normal shock
- Friction always causes the total pressure to decrease
- Not possible to decelerate flow from supersonic to subsonic or vice versa like in Rayleigh flow
  - Violates the second law of thermodynamics

All of the analysis up to this point assumes a constant value of friction coefficient f. An average friction coefficient is assumed over the length of a Fanno pipe:

$$\bar{f} = \frac{1}{L_{max}} \int_0^{L_{max}} f(x) dx \tag{660}$$

- The value of f can be found from the Moody chart, which is available on the Internet, in basic fluids texts
- It gives f as a function of Reynolds number and the relative roughness of the pipe wall.
- It assumes fully-developed flow, so in short pipes with $L < 10D$ the actual value of f will likely be higher than that found in the Moody chart.

Lewis Ferry Moody

5 January 1880 – 21 February 1953, American

- Lewis F. Moody as professor of fluid mechanics and machine design taught at Princeton University starting in 1930
- Best known for the Moody chart, a diagram capturing relationships between several variables used in calculating fluid flow through a pipe
- ASME created an Award to his honours: The Lewis F. Moody award

S.A.E. Miller, Ph.D., saem@ufl.edu

Class Summary

- Boundary layers
- Fanno flow
- Theory
- Solution approach

Next Time

- Fanno and Rayleigh flow additional examples with complexities

Class Overview

- Fanno and Rayleigh flow
- Additional examples with complexities

“Young man, in mathematics you don’t understand things. You just get used to them.”

Reply, according to Dr. Felix T. Smith of Stanford Research Institute, of von Neumann to a physicist friend who had said “I’m afraid I don’t understand the method of characteristics,” as quoted in The Dancing Wu Li Masters: An Overview of the New Physics (1979) by Gary Zukav, Bantam Books, p. 208, footnote.

Example

Air enters a constant area duct with $M_1 = 0.2$, $p_1 = 1$ atm, and $T_1 = 273$ K. Inside the duct $q = 1 \times 10^6$ J/kg.

Calculate at station 2, $M_2, p_2, T_2, \rho_2, T_{o,2}$ and $p_{o,2}$.

Solution

From the isentropic table we find conditions at state 1

- $M_1 = 0.2, T_{o1}/T_1 = 1.008, p_{o1}/p_1 = 1.028$
- Therefore, $T_{o1} = 1.008 T_1 = 1.008(273) = 275.2$ K
- $p_{o1} = 1.028 p_1 = 1.028$ ATM
- $c_p = \frac{\gamma R}{\gamma - 1} = \frac{1.4(287)}{0.4} = 1005$ J/kg K

Using the thermodynamic relation $q = c_p \Delta T_o$

$$T_{o2} = \frac{q}{c_p} + T_{o1} = \frac{1 \times 10^6}{1005} + 275.2 = 1270 \text{ K} \tag{661}$$

Solution

Using Rayleigh table at $M_1 = 0.2$

$$\rightarrow \frac{T_1}{T^*} = 0.2066, \frac{p_1}{p^*} = 2.273, \frac{p_{o1}}{p_o^*} = 1.235, \frac{T_{o1}}{T_o^*} = 0.1736 \tag{662}$$

$$\therefore \frac{T_{o2}}{T_o^*} = \frac{T_{o2}}{T_{o1}} \frac{T_{o1}}{T_o^*} = \frac{1270}{275.2}(0.1736) = 0.8013 \tag{663}$$

Rayleigh table for $\frac{T_{o2}}{T_o^*} \rightarrow M_2 = 0.58$

Solution

At $M_2 = 0.58$ we find from the Rayleigh table

$$\frac{T_2}{T^*} = 0.8955, \frac{\rho_2}{\rho^*} = 1.632, \frac{p_{o2}}{p_o^*} = 1.083 \tag{664}$$

$$\therefore T_2 = \frac{T_2}{T^*}\frac{T^*}{T_1}T_1 = 1183 \text{ K and } p_2 = \frac{p_2}{p^*}\frac{p^*}{p_1}p_1 = 0.718 \text{ atm} \tag{665}$$

$$p_{o2} = \frac{p_{o2}}{p_o^*}\frac{p_o^*}{p_{o1}}p_{o1} = 0.902 \text{ ATM} \tag{666}$$

Finally

$$\rho_2 = \frac{p_2}{RT_2} = 0.214 \text{ kg/m}^3 \tag{667}$$

Example

- Air enters a constant area duct at $M_1 = 0.50$, with a static temperature of $T_1 = 300$ K, and a static pressure $p_1 = 100$ kPa.
- The duct is 10 cm in diameter and 100 cm long
- If heat is added to the flow at a rate of $q = 90$ kJ/kg, determine the Mach number M_2, static pressure p_2, and static temperature T_2 at the duct exit.
- Assume frictionless flow and a constant specific heat of $c_p = 1004$ J/kg K

Solution

- Begin by determining the stagnation temperature at the duct entrance. Enter the subsonic isentropic flow tables at M_1 and obtain $T_1/T_{o1} = 0.9524$, from which $T_{o1} = 315$ K.
- Determine T_{o2}
- Enter the Rayleigh flow table or Calculator at $M_1 = 0.5$ and obtain the normalized property ratios $T_{o1}/T_{o^*} = 0.6914$, $T_1/T^* = 0.7901$, and $p_1/p^* = 1.778$.

Determine T_{o2}/T_o^* using a simple chain

$$\frac{T_{o2}}{T_o^*} = \frac{T_{o2}}{T_{o1}} \frac{T_{o1}}{T_o^*} = 0.889 \tag{668}$$

Example Continued

- Enter the Rayleigh flow tables or calculator at $T_{o2}/T_{o^*} = 0.889$ and obtain $M_2 = 0.67$, $T_2/T^* = 0.975$ and $p_2/p^* = 1.4738$.
- Seek the static temperature and pressure at the pipe exit

$$T_2 = \frac{T_2}{T^*}\frac{T^*}{T_1}T_1 = 370.2 \text{ K} \tag{669}$$

$$p_2 = \frac{p_2}{p^*}\frac{p^*}{p_1}p_1 = 82.9 \text{ kPa} \tag{670}$$

- The given pipe L and D are, of course, irrelevant
- Remember you can use isentropic flow at the entrance and exit of a Rayleigh duct, just not across the heat transfer region.

Example Continued

- Here is the $T - s$ diagram for the example problem just solved
- Understanding and being able to sketch Rayleigh lines in $T - s$ space is important

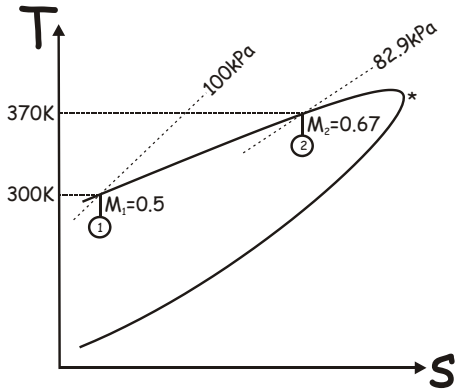

Figure 384: $T - s$ diagram.

Rayleigh-Fanno Flow Notes

- As in Fanno flow, we can make arguments that the effect of heat addition is similar to slowly convergent streamtubes
- This is also true in Rayleigh flow, where short streamtubes with heat addition cause expansion or displacement of the surface of a boundary layer.
- For supersonic flows, Rayleigh flows act as a diffuser that drives M towards unity
  - Here, T_o, T, and p increase and u decreases toward the duct exit

Rayleigh-Fanno Flow Notes

- For a subsonic inlet, the Rayleigh duct acts as a weakly-converging nozzle that accelerates the flow toward $M = 1$.
- Heat addition always causes T_o to increase, but p drops as the flow accelerates.

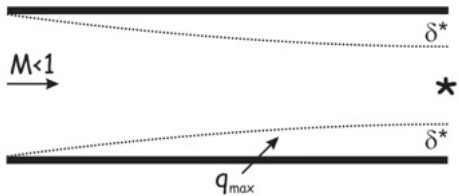

Figure 385: Heat addition with frictional effects.

Example

Consider the flow of air through a pipe of inside diameter of 0.15 m and length 30 m. At the inlet $M = 0.3$, p =1 atm, $T_1 = 273$ K. Assume that $\bar{f} = 0.005$. Calculate M_2, p_2, T_2, and p_{o2}.

Solution

Using an isentropic table $M_1 = 0.3 \rightarrow \frac{p_{o1}}{p_1} = 1.064$
So, $p_{o1} = 1.064(1 \text{ atm}) = 1.064 \text{ atm}$.

Using a Fanno table
$M_1 = 0.3 \rightarrow 4\bar{f}^*/D = 5.299, p_1/p^* = 3.619, T_1/T^* = 1.179,$
$p_{o1}/p^* = 2.035$

Now $L = 30 \text{ m} = L_1^* - L_2^*$, So $L_2^* = L_1^* - L$

Solution

Now seek the condition at state two via $\frac{4\bar{f}L_2^*}{D}$

$$\frac{4\bar{f}L_2^*}{D} = \frac{4\bar{f}L_1^*}{D} - \frac{4\bar{f}L}{D} = 5.2993 - \frac{4(0.005)(30)}{0.15} = 1.2993 \tag{671}$$

From Fanno table for $4\bar{f}L/D = 1.2993 \rightarrow M_2 = 0.475$

$$p_2 = \frac{p_2}{p^*}\frac{p^*}{p_1}p_1 = 2.258\frac{1}{3.169}(1 \text{ ATM}) = 0.713 \text{ ATM} \tag{672}$$

$$T_2 = \frac{T_2}{T_1^*}\frac{T^*}{T_1}T_1 = 1.148\frac{1}{1.179}273 = 265.8 \text{ K} \tag{673}$$

$$p_{o2} = \frac{p_{o2}}{p_o^*}\frac{p_o^*}{p_{o1}}p_{o1} = 1.392\frac{1}{1.035}1.064 = 0.728 \text{ ATM} \tag{674}$$

Example

Question: Airflow enters a constant area insulated duct at $M_1 = 0.60, p = 150$ kPa, and $T = 300$ K. The duct length is $L = 0.45$ m, with a diameter $D = 0.03$ m, and a friction coefficient $f = 0.02$. Find M, p, and T at the duct exit.

Solution I

- Solution: Begin by determining whether the outlet of the duct is choked or not. For the pipe entrance Mach number, enter the Fanno tables or Calculator and find $fL_{\max}/D = 0.4908$ at $M_1 = 0.60$.
- Note the different notation in the calculator for $fL_{\max}/D$.
- Now find the actual value of fL/D for the pipe you are attempting to analyze: $fL/D = (0.02)(0.45)/(0.03) = 0.3$
- Comparing the actual value to the choked-by-friction value, $0.3 < 0.4908$, which means that the duct is not choked: The combination of f, L, and D is less than $fL_{\max}/D$ for the inlet M of 0.6.

Solution II

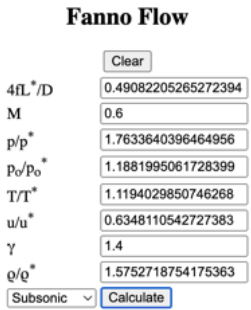

Figure 386: Example numerical prediction.

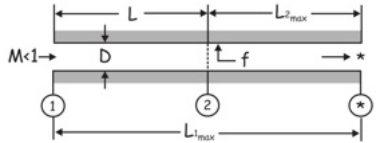

Since friction is evenly distributed along the length of the pipe, a simple geometric rule allows us to solve Fanno flows like this one. Here, L is too short to choke for a given mass flow rate, but we use as a reference the longer duct of length $L1_{max}$, which is choked by friction with the same inlet M, D, and f as the pipe of length L under consideration.

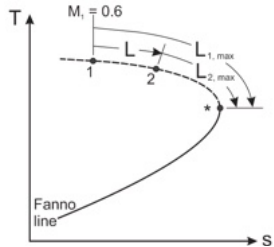

Figure 387

Now determine the fL_{max}/D at location 2 using:

$$\left(\frac{fL_{max}}{D}\right)_2 = \left(\frac{fL_{max}}{D}\right)_1 - \frac{fL}{D} \qquad (7.10)$$

$(fL_{max}/D)_2 = 0.4908 - 0.30 = 0.1908$. Now use this value to determine the flow properties at location 2 by looking it up in the tables or Calculator, and finding $M_2 = 0.709$.

Fanno Flow Perfect Gas, Gamma = 1.4

INPUT: 4fL*/D (sub) = 0.1908 Calculate

M=	0.70926946	T/T*=	1.09030185	P/P*=	1.47218407
P_o/P_o*=	1.08779856	U/U*=	0.74060158	4fL*/D=	0.19080000
(s*-s)/R=	0.08415598				

Notice that tabulated static pressures and temperatures are normalized by their values P* and T* at the exit of a duct choked by friction, whether or not that actually occurs in a given problem. We can use these tabulated property ratios at M_1 and M_2 to find P_2 and T_2 by way of simple chains:

$$P_2 = P_1 \frac{P^*}{P_1} \frac{P_2}{P^*} = 125\text{kPa} \qquad T_2 = T_1 \frac{T^*}{T_1} \frac{T_2}{T^*} = 292\text{K}$$

Figure 388

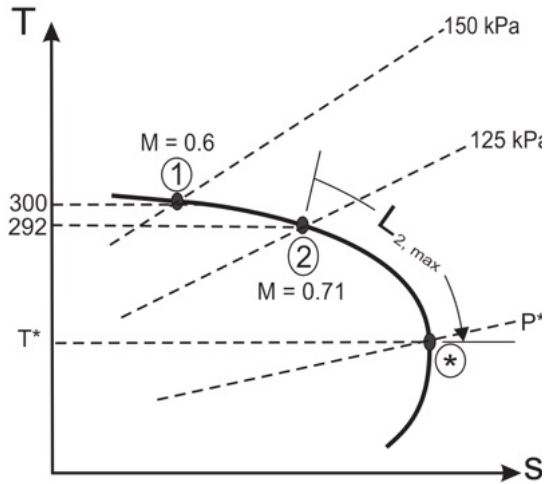

Figure 389: The $T - s$ diagram of the current problem.

Example continued

2) How to find the maximum mass flow rate through an existing subsonic Fanno pipe.

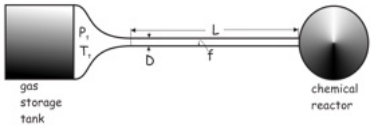

Figure 390

- Design: Imagine that you are a chemical-plant engineer
- There is an existing long frictional pipe between the high-pressure gas tank in the back lot and a chemical reactor that is hungry for more gas as a feedstock.
- What is the maximum mass flow rate through this existing pipe?
- For given storage tank p_o and T_o and a given pipe length L, diameter D and friction factor f, the maximum mass flow occurs when the exit of the pipe is choked by friction.

Why? Because if the flow is not choked, you can get more mass flow by dropping the back pressure (increasing the overall pressure ratio) until it does choke. Afterwards, mass flow is the same unless we raise p_o, lower T_o, or replace the pipe.

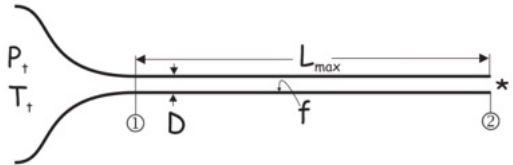

Figure 391

So, find fL/D of the pipe and look that up as fL_{max}/D, which gives you M_1. Now, for a short isentropic nozzle feeding the pipe, get p_1/p_o and T_1/T_o from the isentropic tables or Calculator at M_1. Finally, find the mass flow rate as station one

$$\dot{m}_{max} = \rho A V = \frac{p}{RT}_1 A_1 M_1 \sqrt{\gamma R T_1} \tag{675}$$

Example

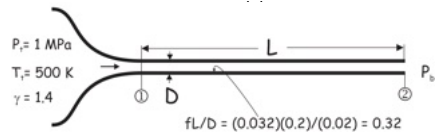

Figure 392

- A constant-area duct, 20 cm long by 2 cm in diameter, $f = 0.032$, is connected to a reservoir by a converging nozzle (see diagram).
- For the stagnation conditions shown, determine the maximum mass flow rate in kg/s of air through this duct, and the range of back pressures p_b over which this mass flow rate is realized.
- Repeat these calculations for the nozzle only, with no frictional duct.
- Solution: Maximum mass flow occurs when the nozzle exit is choked by friction.
- In this case fL/D of the pipe $= 0.32 = f_{Lmax}/D_1$

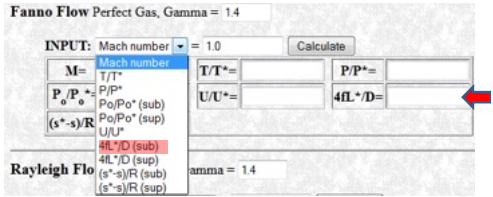

For the current problem input “4FL*/D (sub)”= 0.32 a

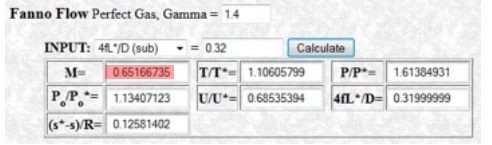

Figure 393: The pipe in this problem will be choked by friction when the inlet Mach number is 0.652. Thus the isentropic converging nozzle must supply $M_1 = 0.652$ to the pipe. Find Mach number in the isentropic section and find $p/p_o = 0.752$ and $T/T_o = 0.922$. Given $p_o = 1$ Mpa and $T_o = 500$ K, the nozzle will therefore deliver $p_1 = 752$ kPa and $T_1 = 461$ K to the pipe.

Now plug these numbers into the mass flow equation

$$\begin{aligned}\dot{m}_{\max} &= \left(\frac{p}{RT}\right)_1 A_1 M_1 \sqrt{\gamma R T_1} \\ &= \left[\frac{\left(751.5\text{kN/m}^2\right)}{(0.2870\text{kJ/kg}\cdot\text{K})(460.9\text{K})}\right]\left[\frac{\pi}{4}\left(4\times10^{-4}\right)\text{m}^2\right] \\ &\times\left[0.652\sqrt{1.4(287\text{J/kg}\cdot\text{K})460.9\text{K}}\right]\end{aligned} \tag{676}$$

$$= \left(5.681\text{kg/m}^3\right)\left(0.0003142\text{m}^2\right)\left(280.6\text{m/s}\right) = 0.5009\text{kg/s}$$

- Also $p_2/p_1 = p^*/p_1 = 1/1.6130$, or $p* = 465.9$ kPa, so the nozzle plus Fanno duct is choked over the range of back pressure from 0 to 465.9 kPa.
- Without the Fanno duct, the nozzle alone would choke with $M = 1$ at its exit.
- $p_1 = 0.5283(1000kPa) = 528.3$ kPa and $T_1 = 0.8333(500K) = 416.7$ K, so the maximum mass flow is 0.5679 kg/s.
- The nozzle alone is choked over the range of back pressure from 0 to 528.3 kPa.

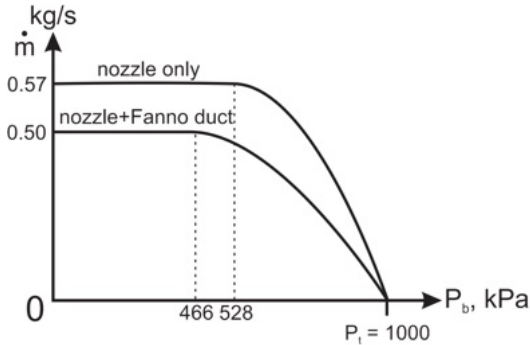

Figure 394: This plot of mass flow rate vs. pressure shows how the nozzle-only flow and the nozzle + Fanno duct flow are related. Both start with no flow at $p_b = p_o = 1000$ kPa, but the nozzle alone chokes at $p_b = 528$ kPa, and has the higher maximum mass flow rate, 0.57 kg/s. The nozzle plus Fanno duct requires a lower back pressure to choke, $p_o = 466$ kPa, due to the frictional loss in the pipe. In that case the maximum mass flow rate is also lower, only 0.50 kg/s.

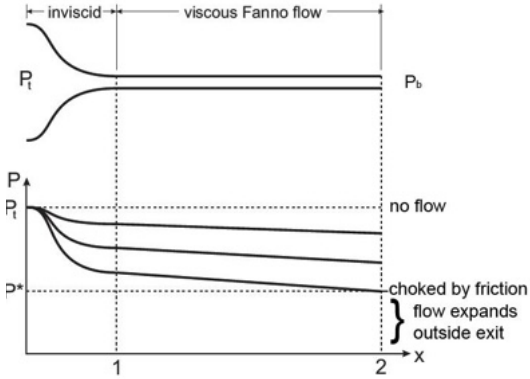

Figure 395: On occasion Fanno duct is fed by a nozzle, in which we neglect friction because it is short. Here are static pressure distributions through the combination for fixed p_o and variable p_b. Note that the pressure drop along the Fanno duct is linear. This illustrates how to draw static pressure distributions in Fanno ducts.

Class Summary

- Fanno and Rayleigh flow additional examples with complexities

Next Time

- Flows with heat addition and friction
- Prandtl number and Reynold's Analogy
- Isothermal Flow
- Some examples

Class Overview

- Flows with heat addition and friction
- Prandtl number and Reynold's Analogy
- Isothermal Flow
- Some examples

Derivation for Frictional Flow with Heat Addition I

- When heat is added to a gas flowing in a duct the effect of wall friction is present.
  - Example is heat exchanger, where designer must compromise the heat transfer design to minimize pressure drops due to friction and hence minimize pumping-power requirements.

Derivation for Frictional Flow with Heat Addition II

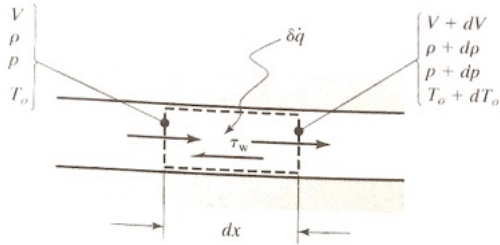

Figure 396: Differential Control Volume for Flow in a Constant-Area Duct with Friction and Heat Addition.

Derivation for Frictional Flow with Heat Addition III

For flow in a constant-area duct with heat transfer and friction for conservation of mass is

$$\frac{d\rho}{\rho} + \frac{du}{u} = 0 \tag{677}$$

and for momentum

$$dp + \frac{1}{2}\rho u^2 \frac{fdx}{D} + \rho u du = 0 \tag{678}$$

Here, $u = M\sqrt{\gamma RT}$, logarithmic differentiation is

$$\frac{du}{u} = \frac{dM}{M} + \frac{1}{2}\frac{dT}{T} \tag{679}$$

We can show

$$\frac{dp}{p} + \frac{1}{2}\gamma M^2 \frac{fdx}{D} + \gamma M^2 \frac{dM}{M} + \frac{1}{2}\gamma M^2 \frac{dT}{T} = 0 \tag{680}$$

Derivation for Frictional Flow with Heat Addition IV

Energy equation

$$\delta q = c_p dT_o \tag{681}$$

Recall from isentropics

$$T_o = T\left(1 + \frac{\gamma - 1}{2} M^2\right) \tag{682}$$

Combining we find

$$\frac{\delta q}{c_p T} = \left(1 + \frac{\gamma - 1}{2} M^2\right) \frac{dT}{T} + (\gamma - 1) M dM \tag{683}$$

We previously showed for perfect gases

$$\frac{dp}{p} = \frac{d\rho}{\rho} + \frac{dT}{T} \tag{684}$$

Derivation for Frictional Flow with Heat Addition V

Combining this expression with the differential version of the continuity equation, we obtain

$$\frac{dp}{p} = -\frac{du}{u} + \frac{dT}{T} \tag{685}$$

and combine it with the definition of Mach number, we obtain

$$\frac{dp}{p} = -\frac{dM}{M} + \frac{1}{2}\frac{dT}{T} \tag{686}$$

Now substitute this equation for dp/p and dT/T, we find

$$\frac{\delta q}{c_p T_o}\frac{1}{2}\left(1+\gamma M^2\right) + \frac{1}{2}\gamma M^2 \frac{fdx}{D} \tag{687}$$

$$= \left[\frac{1-\gamma M^2}{M} + \frac{\left(\gamma-1\right)\left(1+\gamma M^2\right)\frac{1}{2}M}{1+\frac{\gamma-1}{2}M^2}\right] dM \tag{688}$$

Derivation for Frictional Flow with Heat Addition VI

and can be rewritten simply as

$$\frac{1}{2}\left(1+\gamma M^2\right)\frac{\delta q}{c_p T_o}+\frac{1}{2}\gamma M^2\frac{f dx}{D}=\left[\frac{2\left(1-M^2\right)}{2+(\gamma-1)M^2}\right]\frac{dM}{M} \tag{689}$$

Notes on Recovery Factor I

- This equation shows effects of heat addition and friction
- We express δq in terms of mean convection heat transfer, $\overline{h}$
- For compressible flows, heat transfer between a differential wall area $dA_p = \pi D dx$ for circular streamtubes and gas can be given by

$$\delta \dot{q} = \bar{h} \left(T_w - T_{aw} \right) dA_p \tag{690}$$

  where T_w is the duct wall temperature and T_{aw} the adiabatic wall temperature.
- Viscous effects make recovery of temperature impossible, and we can now define the recovery factor

$$r = \frac{T_{aw} - T}{T_o - T} \tag{691}$$

Since $T_o/T = 1 + (\gamma - 1)M^2/2$, it is easy to show that

$$T_{aw} = \left[\frac{2 + r(\gamma - 1)M^2}{2 + (\gamma - 1)M^2} \right] T_o \tag{692}$$

Notes on Recovery Factor II

- Recovery factor shows
  - Laminar flow: $r = \text{Pr}^{1/2}$
  - Turbulent flow: $r = \text{Pr}^{1/3}$
- Here, Pr is the Prandtl number, a non-dimensional parameter that is the product of the specific heat at constant pressure, c_p, and the dynamic viscosity of the gas, μ, divided by the thermal conductivity k (i.e., $\text{Pr} \equiv c_p \mu / k$).

Prandtl Number and Reynold's Analogy I

- Prandtl number can be written as the ratio of kinematic viscosity $\nu = \mu/\rho$ to the thermal diffusivity $\alpha = k/\rho c_p$ (i.e., $\mathrm{Pr} = \nu/\alpha$)
- Prandtl number of gases is close to unity
- Hence, $r = 1$, and therefore $T_{aw} = T_o$ For gase

$$\begin{aligned} \delta\dot{q} &= \bar{h}\,(T_w - T_o)\,\pi D dx \\ \delta q &= \frac{\delta\dot{q}}{\dot{m}} = \frac{\delta\dot{q}}{\rho A u} \end{aligned} \tag{693}$$

- A relation between the mean convective heat transfer coefficient $\bar{h}$ and the friction factor f is given by Reynolds's analogy
- For Prandtl numbers close to unity

$$\bar{h} = \frac{\rho u c_p f}{8} \tag{694}$$

Constant Area Ducts I

- Note that for flow in a constant-area duct, ρu is a constant
- Variable-area ducts, ρu defined at a given location.
- Making this assumption we find

$$\frac{dM}{dx} = \left[\frac{2+(\gamma-1)M^2}{2\left(1-M^2\right)}\right] M \left[\left(\frac{1+\gamma M^2}{2}\right)\frac{1}{T_o}\frac{dT_o}{dx} + \left(\frac{1}{2}\gamma M^2\right)\frac{f}{D}\right] \tag{695}$$

- Numerical solutions must be used to solve this equation with knowledge of variation of T_o with x
- Fall into two categories
  - Constant-wall-temperature problems (i.e., $T_w =$ constant - these situations occur in heat exchangers where the heat transfer coefficient on the external surface is very large, a condition that can arise because of condensation or evaporation);
  - Constant-heat-rate problems (i.e., $q =$ constant - these situations occur when the duct wall is heated using electric resistance heating or radiant heating).

Constant Wall Temperature Problems I

We consider each of these cases to determine $T_n(x)$ for the flow in a circular duct of diameter D.

$$\delta\dot{q} = \dot{m}c_p dT_o = \bar{h}\left(T_w - T_o\right)\pi D dx$$
$$\frac{dT_o}{T_w - T_o} = \frac{\bar{h}\pi D dx}{\dot{m}c_p} \tag{696}$$

$$\bar{h} = \frac{\rho u c_p f}{8} = \frac{\rho A u c_p f}{8A} = \frac{\dot{m}c_p f}{8A}$$
$$\frac{\bar{h}\pi D}{\dot{m}c_p} = \frac{\pi D f}{8\frac{\pi D^2}{4}} = \frac{f}{2D} \tag{697}$$

$$\frac{dT_o}{T_w - T_o} = \frac{f}{2D}dx \tag{698}$$

Integration and simplification with a exponential distribution of stagnation temperature yields

$$\frac{1}{T_o}\frac{dT_o}{dx} = \frac{\left(T_w - T_{o1}\right)}{T_w e^{(f/2D)x} - \left(T_w - T_{o1}\right)}\frac{f}{2D} \tag{699}$$

Constant-Heat-Rate Problems I

We have

$$\frac{1}{c_p}\frac{\delta q}{dx} = \frac{dT_o}{dx} = \beta \tag{700}$$

via integration

$$T_o = T_{o1} + \beta x \tag{701}$$

We find

$$\frac{1}{T_o}\frac{dT_o}{dx} = \frac{\beta}{T_{o1} + \beta x} \tag{702}$$

where $\beta = \left(T_{o2} - T_{o1}\right)/L = q/\left(c_p L\right)$.

Variations of other Properties I

Determine variations in pressure and other flow properties, we modify theory for Rayleigh and Fanno flow to account for the fact that the stagnation temperature is not constant and that the area varies in the flow direction. The derivation follows the previous one and we summarize fundings here ...

$$\frac{T_k}{T_j} = \left(\frac{T_{ok}}{T_{oj}}\right) \frac{2 + (\gamma - 1)M_j^2}{2 + (\gamma - 1)M_k^2} \tag{703}$$

$$\frac{p_k}{p_j} = \frac{A_j M_j}{A_k M_k}\sqrt{\frac{T_k}{T_j}} = \left(\frac{A_j}{A_k}\right) \frac{M_j}{M_k} \left[\frac{2 + (\gamma - 1)M_j^2}{2 + (\gamma - 1)M_k^2}\right]^{1/2} \tag{704}$$

$$\frac{p_{ok}}{p_{oj}} = \frac{p_{ok}}{p_k}\frac{p_k}{p_j}\frac{p_j}{p_{oj}} = \left(\frac{A_j}{A_k}\right) \frac{M_j}{M_k} \left[\frac{2 + (\gamma - 1)M_k^2}{2 + (\gamma - 1)M_j^2}\right]^{\frac{\gamma+1}{2(\gamma-1)}} \tag{705}$$

Variations of other Properties II

$$\frac{\rho_k}{\rho_j} = \frac{p_k}{p_j}\frac{T_j}{T_k} = \left(\frac{A_j}{A_k}\right)\frac{M_j}{M_k}\left[\frac{2+(\gamma-1)M_k^2}{2+(\gamma-1)M_j^2}\right]^{1/2} = \left(\frac{A_j}{A_k}\right)\frac{u_j}{u_k} \tag{706}$$

$$\frac{s_k - s_j}{R} = -\ln\left(\frac{p_{ok}}{p_{oj}}\right) = \frac{\gamma}{\gamma-1}\ln\left(\frac{T_k}{T_j}\right) - \ln\left(\frac{p_k}{p_j}\right) \tag{707}$$

Isothermal Flow I

- Gas flow in long, non-insulated ducts and pipes, the gas is able to achieve temperature equilibrium with the surroundings.
- Temperature of the flow reaches a constant value and is therefore isothermal.
- Flow possesses characteristics that are different from either Fanno or Rayleigh flow because it involves both heat transfer and friction.
- A common misconception is to regard isothermal flow as flow that does not require any heat exchange.
- Exchange of heat that allows the temperature to remain constant.

Differential control volume of isothermal flow in a constant-area duct. The continuity, momentum, and energy equations are

$$\frac{d\rho}{\rho} + \frac{du}{u} = 0 \tag{708}$$

Isothermal Flow II

$$dp + \rho u du + \frac{f dx}{2D_h} \rho u^2 = 0 \tag{709}$$

and

$$\delta \dot{q} = \dot{m} \left(dh_o \right) = \dot{m} \left(c_p dT_o \right) = \dot{m} \left[c_p dT + d \left(\frac{u^2}{2} \right) \right] = \dot{m} d \left(\frac{u^2}{2} \right) \tag{710}$$

Isothermal Flow III

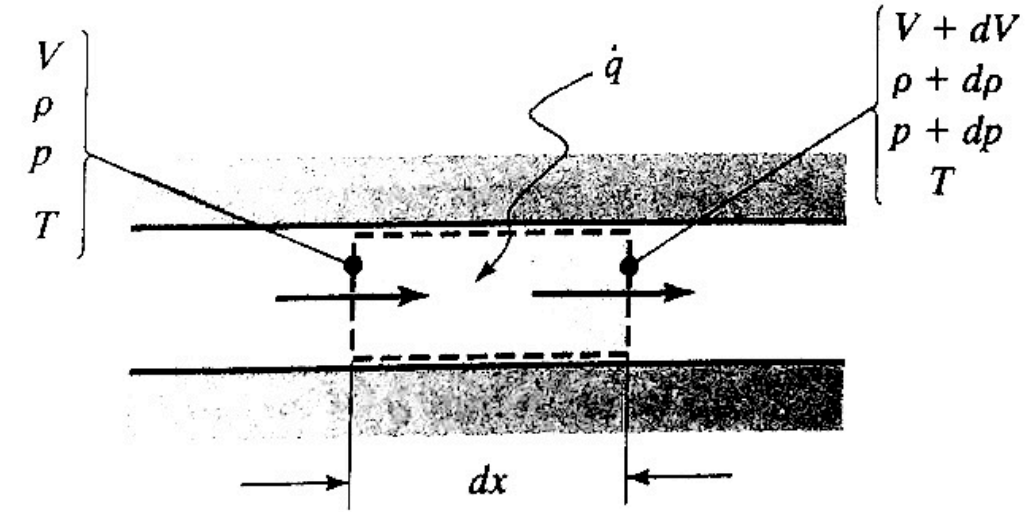

Figure 397: Differential Control Volume Used for Isothermal Flow Analysis.

Isothermal Flow IV

Isothermal Flow V

The differential momentum equation

$$\frac{dp}{p} + \frac{\gamma M^2}{2}\frac{f dx}{D_h} + \gamma M^2 \frac{du}{u} = 0 \tag{711}$$

Dividing by the mass-flow rate, which is constant, we find that the energy equation becomes

$$\frac{\delta \dot{q}}{\dot{m}} = \delta q = dh_o = c_p dT_o \tag{712}$$

The perfect-gas law expressed in differential form is

$$\frac{dp}{p} = \frac{d\rho}{\rho} + \frac{dT}{T} \tag{713}$$

Isothermal Flow VI

Since the temperature is constant, $dT/T = 0$, and therefore

$$\frac{dp}{p} = \frac{d\rho}{\rho} \tag{714}$$

From the definition of the Mach number, $M = u/c$. Since the temperature is constant, the speed of sound is also constant. Therefore, logarithmic differentiation yields

$$\frac{dM}{M} = \frac{du}{u} \tag{715}$$

Combining equations yields

$$\frac{dp}{p} = -\frac{dM}{M} \tag{716}$$

Isothermal Flow VII

then

$$\frac{dM}{M} = \frac{\left(\gamma M^2/2\right) \frac{fdx}{D}}{1 - \gamma M^2} \tag{717}$$

- This equation shows that the critical Mach number for isothermal flow is not Mach 1
  - $M = 1/\sqrt{\gamma} (= 0.8452 \text{ for } \gamma = 1.4)$
  - If $M < (1/\sqrt{\gamma})$, this flow is termed subcritical flow, indicates that M increases with x
  - If $M > (1/\sqrt{\gamma})$, we have supercritical flow, and M decreases with x

To determine the heat transfer necessary to maintain isothermal flow we must examine equation

$$\delta q = c_p dT_o = \frac{c_p T_o (\gamma - 1) M^4 \frac{\gamma}{2}}{\left(1 + \frac{\gamma - 1}{2} M^2\right)(1 - \gamma M^2)} \left(\frac{fdx}{D}\right) \tag{718}$$

Isothermal Flow VIII

- $M \to 1/\sqrt{\gamma}$, it can be seen that $q \to \infty$, indicating that an infinite rate of heat transfer is necessary to maintain the isothermal flow at the critical Mach number.
- It is impossible to isothermally accelerate flow in a constant-area duct from a low Mach number up to $M = 1/\sqrt{\gamma}$.
- The assumption of isothermal flow is valid, however, and can be realized physically for small-velocity, low-Mach-number flows.

For such flows, it is desirable to obtain an expression for pressure drop and Mach-number variation as a function of x. We can integrate our previous equation

$$\frac{fL}{D} = \int_{M_1}^{M_2} \frac{1-\gamma M^2}{(\gamma M^2/2)} \left(\frac{dM}{M}\right) \tag{719}$$

$$= 2\int_{M_1}^{M_2} \left(\frac{1}{\gamma M^3} - \frac{1}{M}\right) dM = -\left[\frac{1}{\gamma M^2} + 2\ln(M)\right]\Bigg|_{M_1}^{M_2} \tag{720}$$

Isothermal Flow IX

Which can be written

$$\frac{fL}{D} = \frac{1-\gamma M_1^2}{\gamma M_1^2} - \frac{1-\gamma M_2^2}{\gamma M_2^2} + \ln\frac{M_1^2}{M_2^2} = \frac{M_2^2 - M_1^2}{\gamma M_1^2 M_2^2} + \ln\frac{M_1^2}{M_2^2} \tag{721}$$

and shown that

$$\frac{T_{o1}}{T_{o2}} = \left(\frac{T_{o1}}{T_1}\right)\left(\frac{T_2}{T_{o2}}\right) = \frac{1+\frac{\gamma-1}{2}M_1^2}{1+\frac{\gamma-1}{2}M_2^2} = \frac{2+(\gamma-1)M_1^2}{2+(\gamma-1)M_2^2} \tag{722}$$

Integrating with cont. equation we find

$$\frac{p_1}{p_2} = \frac{M_2}{M_1} = \frac{\rho_1}{\rho_2} = \frac{u_2}{u_1} \tag{723}$$

Isothermal Flow X

This equation with the stagnation-to-static-pressure ratio expression, yields

$$\frac{p_{o1}}{p_{o2}} = \frac{p_{o1}}{p_1}\frac{p_1}{p_2}\frac{p_2}{p_{o2}} \tag{724}$$

$$= \left(1+\frac{\gamma-1}{2}M_1^2\right)^{\gamma/(\gamma-1)} \frac{M_2}{M_1} \left(1+\frac{\gamma-1}{2}M_2^2\right)^{-[\gamma/(\gamma-1)]} \tag{725}$$

Simplifies to

$$\frac{p_{o1}}{p_{o2}} = \frac{M_2}{M_1}\left[\frac{2+(\gamma-1)M_1^2}{2+(\gamma-1)M_2^2}\right]^{\gamma/(\gamma-1)} \tag{726}$$

The reference state can be chosen as $1/\sqrt{\gamma}$, which is noted as $*$. Using the usual solution approach with a reference state as shown in previous sections, we can write

$$\frac{T_{o1}}{T_{o2}} = \frac{T_o}{T_o^*} = \frac{2+(\gamma-1)M^2}{2+(\gamma-1)\left(\frac{1}{\sqrt{\gamma}}\right)^2} = \left(\frac{\gamma}{3\gamma-1}\right)\left[2+(\gamma-1)M^2\right] \tag{727}$$

Isothermal Flow XI

$$\frac{p}{p^*} = \frac{\rho}{\rho^*} = \frac{u^*}{u} = \frac{1}{\sqrt{\gamma}M} \tag{728}$$

$$\frac{fL_{\max}}{D} = \frac{1-\gamma M^2}{\gamma M^2} + \ln\left(\gamma M^2\right) \tag{729}$$

and

$$\frac{p_o}{p_o^*} = \frac{1}{\sqrt{\gamma}M}\left\{\frac{\gamma}{(3\gamma-1)}\left[2+(\gamma-1)M^2\right]\right\}^{\gamma/(\gamma-1)} \tag{730}$$

Example I

Methane enters a gas pipeline with a velocity of 15 m / s and static pressure of 500 kPa. The pipeline is 200 m long and 8 cm in diameter, with the gas temperature essentially constant at 288 K over the pipe length. Determine the pressure drop. For methane, $\gamma = 1.32$, and the molecular mass is 16. Assume that $f = 0.025$.

Solution

The inlet Mach number is

$$M_1 = \frac{u_1}{\sqrt{\gamma RT}} = \frac{15}{\sqrt{1.32\left(\frac{8{,}314}{16}\right)288}} = 0.033749 \tag{731}$$

and

$$\frac{fL}{D} = (0.025)\frac{(200)}{(0.08)} = 62.5 \tag{732}$$

Example II

Now as with Fanno flow

$$\left(\frac{fL_{\max}}{D}\right)_2 = \left(\frac{fL_{\max}}{D}\right)_1 - \frac{fL}{D} \tag{733}$$

or

$$\left(\frac{fL_{\max}}{D}\right)_2 = 657.6265 - 62.5 = 595.1265 \tag{734}$$

Thus, $M_2 = 0.035459$

$$\frac{p_2}{p_1} = \frac{M_1}{M_2} = \frac{0.033749}{0.035459} = 0.9518 \tag{735}$$

We find

$$p_1 - p_2 = p_1\left(1 - \frac{p_2}{p_1}\right) = 500(1 - 0.9518) = 24.1124kPa \tag{736}$$

Example III

$$\frac{fL}{D} = \frac{2}{\gamma M_1^2}\left(\frac{p_1 - p_2}{p_1}\right)\left[\left(1 - \gamma M_1^2\right) - \frac{\left(1 + \gamma M_1^2\right)}{2}\left(\frac{p_1 - p_2}{p_1}\right)\right] \tag{737}$$

Inserting values produces an fL/D of 62.4742, which is only 0.041 percent below the correct value of 62.5.

Class Summary

- Flows with heat addition and friction
- Prandtl number and Reynold's Analogy
- Isothermal Flow
- Some examples

Next Time

- Transonics

Class Overview

- Transonic flow definitions
- Theory in three main developments
- Historical context

Notes on Transonics

"We call the speed range just below and just above the sonic speed - Mach number nearly equal to one - the transonic range. Hugh Dryden and I invented the word transonic. We had found that a word was needed to denote the critical speed range of which we were talking. We could not agree whether it should be written with one s or two. Dryden was logical and wanted two s's. I thought it wasn't necessary and always to be logical in aeronautics, so I wrote it with one s. I introduced the term in this form in a report to the Air Force. I am not sure whether the general who read it knew what it meant, but his answer contained the word, so it seemed to be officially accepted. I well remember this period (1941) when designers were rather frantic because of the unexpected difficulties of transonic flight. They thought the troubles indicated a failure in aerodynamic theory."

Theodore von Karman at Cornell in lecture, 1953.

Notes on Transonics

- Characterized by drag divergence phenomena - rapid shift of center of pressure and unsteady and somewhat unpredictable effect of shock waves on control surfaces
- Most commercial airlines fly in the range of Mach 0.75 to 0.88
- Wish to push Mach numbers closer to unity but require greater understanding of transonic drag
- One conceptual transonic aircraft is ...

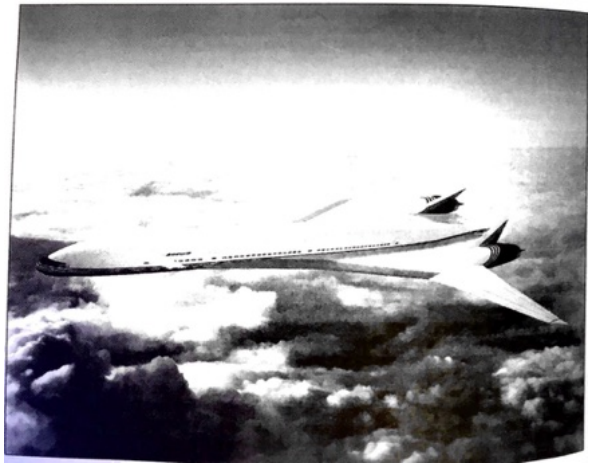

Figure 398: Conceptual artwork of a Boeing transonic aircraft.

Notes on Transonics

- Is a sonic cruiser that departs from classical configurations
- Departure from classic tube-and wing configurations
- Notice engine placement, wing placement, etc.
- Integrated engines in wing

Notes on Transonics

- In the 1940's there was a serious lack of aerodynamic data in the range of the transonic condition
- Very rapid changes in Mach number near sonic conditions caused extreme difficulty in measurement

According to subsonic and supersonic linearized theory the pressure coefficient correction for slender bodies is

$$c_p = \frac{c_{p,o}}{\sqrt{1 - M_\infty^2}} \tag{738}$$

and

$$c_p = \frac{c_{p,o}}{\sqrt{M_\infty^2 - 1}} \tag{739}$$

Note that denominators approach zero as Mach approaches unity that yield extremely large impossible pressure coefficients.

Transonic Notes

- Thus the transonic regime is very sensitive to the Mach number
- Now the use of slotted throat wind tunnels, that is test sections with holes, is prevalent in modern transonic tunnels - why is this?
- CFD has also helped find transonic results
- Transonic flow is still a challenge to modern engineers - examine commercial airliners and most contemporary fighter aircraft that operate at low supersonic speeds - why is this?
- Transonic flow is also important for space applications - Ascent and descent occur during flight to space!

Observations

Let us make some physical observations of transonic flow

- Definition - Critical Mach number M_{cr} is the free-stream Mach number at which sonic flow is first obtained on a body - thus the transonic regime could be viewed as beginning when critical Mach number is reached
- Transonic flow is mixed regions of locally subsonic and supersonic flow that occur in space and time
- We will examine transonic flow in an example of flow over an airfoil of NACA 64A006 which is 6 percent thick
- Note the various shock wave patterns as well as regions of flow separation

Observations

- Superimposed are the pressure coefficient distributions over the top of each surface
- Examine the ‘supersonic pocket’ of flow that is the nearly white regions in the flow, which has weak expansion waves terminating at the sonic line
- Note the separation of the boundary layer

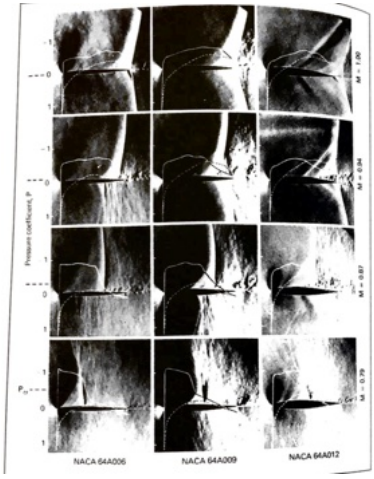

Figure 399: Schlieren photographs of increasing free-stream Mach number for transonic flow over an airfoil.

Observations

- The separation of flow is caused by the shock wave boundary layer interaction
- The pressure increased across the shock wave and represents a strongly adverse pressure gradient
- We know that regular boundary layers separate when the surface has an adverse pressure gradient
- When the shock wave is near the surface the boundary layer encounters an adverse pressure gradient and it will almost always separate
- Shock boundary layers cause a very large rise in drag which is called the drag-divergence phenomenon and is always associated with transonic flow
- Let us examine a figure of the drag divergence phenomenon where the curves correspond to different angles of attach

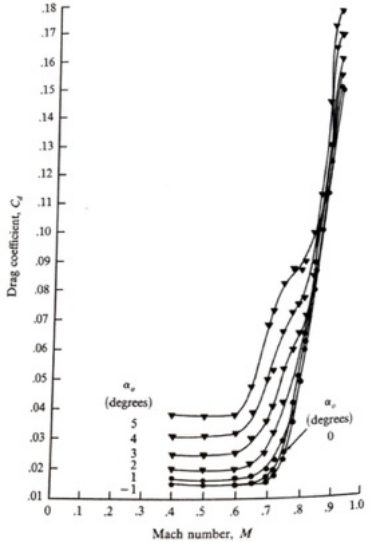

Figure 400: Variation of the drag coefficient with Mach number for an NACA 2315 airfoil. The drag diverges as Mach one is approached. Experimental ranges from -1 to 5 deg. α.

Analysis

We will perform our basic analysis using inviscid theory. We examine the Euler equations

$$\frac{\partial \rho}{\partial t} + \nabla \cdot (\rho u) = 0 \tag{740}$$

$$\rho \frac{Du}{Dt} = -\nabla p \tag{741}$$

$$\rho \frac{Dh_o}{Dt} = \frac{\partial p}{\partial t} \tag{742}$$

- We assumed that the flow is inviscid, adiabatic, and there are no body forces
- Also assumed that the flow has large entropy losses and that the flow is rotational according to Crocco's theorem

Analysis

We also must account for entropy changes across shocks. We recall that $c_p = \gamma R/(\gamma - 1)$. Then the entropy across a normal shock becomes

$$\frac{\Delta S}{R} = \frac{1}{\gamma - 1} \log \left[1 + \frac{2\gamma}{\gamma + 1}(M_1^2 - 1) \right] + \frac{\gamma}{\gamma - 1} \log \left[\frac{2 + (\gamma - 1)M_1^2}{(\gamma + 1)M_1^2} \right] \tag{743}$$

- We now let $m = M_1^2 - 1$ and the term in the second brackets to be equal to $\frac{1}{m+1}\left[\frac{\gamma-1}{\gamma+1}m + 1\right]$
- For transonic flows we know that $M_1 \approx 1$ and therefore $m << 1$. Each log term is of the form $1 + \epsilon$, where $\epsilon << 1$.
- The series expansion is known for $\log(1 + \epsilon) = \epsilon - \epsilon^2/2 + \epsilon^3/3 + ...$

Analysis

Using these definitions and simplifications we find

$$\frac{s_2 - s_1}{R} \approx \frac{2\gamma}{3(\gamma+1)^2}(M_1^2 - 1)^3 \tag{744}$$

- This shows that the entropy increases across a weak shock is of third order in terms of $M_1^2 - 1$
- Note that $M_1^2 - 1 << 1$ for transonic flows then the entropy increase across a shock is very small
- The strength of the shock is given by $\Delta p/p_1$ and is proportional to $M_1^2 - 1$, therefore entropy rise is approximately third order in shock strength
- We assume that the flow is nearly isentropic (essentially) and in turn assume that the flow is essentially irrotational

Analysis

We can then write a velocity potential Φ such that $\boldsymbol{u} = \nabla\Phi$ and the Euler equations can be written as

$$\left(1 - \frac{\Phi_x^2}{c^2}\right)\Phi_{xx} + \left(1 - \frac{\Phi_y^2}{c^2}\right)\Phi_{yy} + \left(1 - \frac{\Phi_z^2}{c^2}\right)\Phi_{zz} - \frac{2\Phi_x\Phi_y}{c^2}\Phi_{xx} - \frac{2\Phi_x\Phi_z}{c^2}\Phi_{xz} - \frac{2\Phi_y\Phi_z}{c^2}\Phi_{yz} = 0 \tag{745}$$

This equation (given its assumptions) holds for any body shape, thick or thin, at any angle of attack.

Analysis

If we assume that the perturbations of velocity potential are small then we can find a perturbation velocity potential equation. Performing a small perturbation analysis yields the equation

$$(1 - M_\infty^2)\phi_{xx} + \phi_{yy} + \phi_{zz} = M_\infty^2 \left[(\gamma + 1) \frac{\phi_x}{u_\infty} \right] \phi_{xx} \tag{746}$$

which is the transonic small perturbation equation.

Analysis

- Let us non-dimensionalize this equation using $\tau = b/c$, where b and c are the maximum thickness and length scales of the body.
- τ is small.
- We transform our coordinates as $\bar{x} = x/c$, $\bar{y} = y\tau^{1/3}/c$, and $\bar{z} = z\tau^{1/3}/c$ (they are on the order of c).

We then define the non-dimensional perturbation velocity potential as

$$\overline{\phi} = \frac{\phi}{cu_\infty \tau^{2/3}} \tag{747}$$

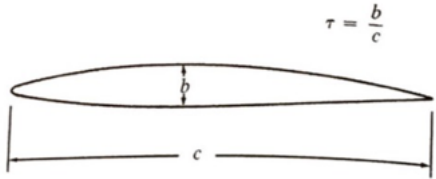

Figure 401: Slenderness ratio definition, τ.

Analysis

We substitute our dimensional forms of the variables in the equation for perturbation velocity potential and find after combining terms

$$\left[\frac{1-M_\infty^2}{\tau^{2/3}} - M_\infty^2(\gamma+1)\overline{\phi}_{\overline{x}}\right]\overline{\phi}_{\overline{xx}} + \overline{\phi}_{\overline{yy}} + \overline{\phi}_{\overline{zz}} = 0 \tag{748}$$

We define the transonic similarity parameter K as

$$K = \frac{1-M_\infty^2}{\tau^{2/3}} \tag{749}$$

By assuming that Mach numbers are near unity

$$\left[K-(\gamma+1)\right]\overline{\phi}_{\overline{xx}} + \overline{\phi}_{\overline{yy}} + \overline{\phi}_{\overline{zz}} = 0 \tag{750}$$

which is the transonic similarity equation. This equation shows that for two-different flows with the same K but with different values of τ then the solution fo both flows in terms of $\overline{\phi}$ will be the same.

Analysis

The pressure coefficients are then related between the two flows as

$$c_p/\tau^{2/3} = -2\overline{\phi}_{\overline{x}} = f(K, \overline{x}, \overline{y}, \overline{z}) \tag{751}$$

There are three major ways of examining transonic inviscid flow theory

- Solutions of the Euler equations
- Solutions of the potential equation, which gives approximate solutions with a weak normal shock
- Solutions of the small perturbation potential equation, which give further approximations for thin bodes at small angle of attack. Here, the transonic similarity principle holds.

Note that all three equations are nonlinear. This nonlinear nature of the equations is what leads to traditional linearized aerodynamic theory to fail. We must solve these equations with numerical methods.

Historical Viewpoints of Transonic Flow

- Chuck Yeager was the pilot of the XS-1 which obtained a Mach number of 1.06 and was the first manned aircraft to fly faster than c_∞ at sea level
- Success of XS-1 was followed by 30 years of research in aerodynamics of transonic flight
- Leonardo da Vinci and Galileo postulated that the drag of vehicles goes as the first power of velocity (which is wrong)

Figure 402: Chuck Yeager in the cockpit of the Bell XS-1.

Historical Viewpoints of Transonic Flow

- Edme Mariotte and Christiaan Huygens (both French academy of sciences) found the velocity squared law, which works well for low subsonic speeds
- Benjamin Robins was a mathematician and ballistician who examined the first transonic aerodynamic effects and wrote that “the velocity at which the moving body shifts resistance is nearly the same with which sound is propagated through the air.”
- In Germany in the journal Artillerische Monatshefte, Bensberg and Cranz showed the graph of c_d versus u in the range between 300 and 400 m/s.
  - This viewpoint helps explain why the fuselage of the Bell XS-1 is the shape of a 50-caliber machine gun bullet.
  - This was the first curve of transonic drag rise. They showed that the drag actually decreases after Mach one!

Historical Viewpoints of Transonic Flow

- Caldwell and Fales at the US Army Engineering Division at McCook Field near Dayton, Ohio (now Air Force Research and Development facilities at Wright-Patterson Air Force Base) conducted a series of experiments on airfoils for the purpose of studying propellor blades that were residing in the transonic regime.
  - Conducted the first wind-tunnel test involving the high-speed flow over a stationary airfoil that showed large decreases in lift and major increases in c_D.
  - Measured the compressibility effects on an airfoil, which they called the “critical speed.”

Historical Viewpoints of Transonic Flow

Not soon after H. Dryden and collaborators performed experiments published in NACA report no 207 “We may suppose that the speed of sound represents an upper limit beyond which an additional loss of energy take space. If at any point along the wing the velocity of sound is reached the drag will increase. From our knowledge of the flow around airfoils at ordinary speeds we know that the velocity near the surface is much higher than the general stream velocity .. the increase being greater for larger angles and thicker sections. This corresponds very well with the earlier flow breakdowns for the thicker wings and all of the wings at high angles of attack.”

Historical Viewpoints of Transonic Flow

- 1920s the NACA started a major research program into transonic flows.
- Briggs and Dryden built new smaller high-speed wind tunnel with a 2 in diameter jet.
- Mach number of the jet was 1.08.
- Using the same airfoils as their earlier work they executed the first supersonic experiments in the united states. They showed that:
  - Flow separated from the upper surface but did not know that it was due to the shock wave boundary layer interactions.
  - Drag coefficient for the airfoil followed the same type of drag divergence encountered by projectiles between $M = 0.95$ and $M = 1.08$
  - Observed for the first time ever the bow shock standing in front of the leading edge!

Their work lead to researchers such as Eastman Jacobs, John Stack, and most importantly the theoretician Theodore Theodorsen to produce major breakthroughs and the first widely viewed transonic schlieren image.

Theodore Theodorsen

1897 – 1 November 1978, Norwegian (American Immigrant)

- Born Sandefjord, Norway
- Doctorate at Johns Hopkins University
- Dr. Joseph Ames, President of Johns Hopkins University recommend he go to NACA/Langley
- Theoretician
- First noise research at NACA/NASA
- Bomb detection, wind-tunnel development, aeroelasticity, turbulence, Chief Scientist for the U.S. Air Force from 1950 to 1954, relativity development
- Theodorsen married Johanne Magdelene Hoem, in Trondheim, Norway, in 1922, before coming to the United States. Their daughter, Muriel Gerd-Preutz, and sons, Theodore Elliott and John Willman, were all born in the United States.

S.A.E. Miller, Ph.D., saem@ufl.edu

Historical Viewpoints of Transonic Flow

Early models inserted into transonic tunnels choked the tunnels and research was unable to be conducted. The model wingspan was 1 ft and the tunnel span was 8 ft. This was enough for the data to be practically useless due to transonic choking effects!

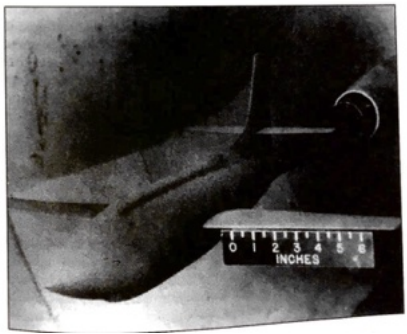

Figure 403: Wind tunnel model of the Bell XS-1 at NASA Langley - 1947

Historical Viewpoints of Transonic Flow

Figure 404: The world's first transonic tunnel located at NASA Langley (now preserved) – photo by Miller.

Historical Viewpoints of Transonic Flow

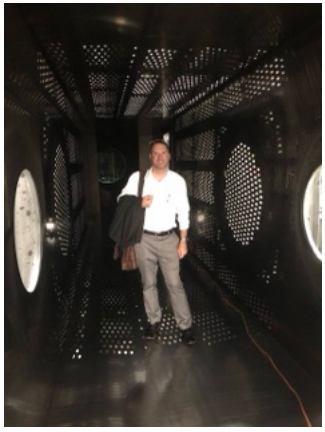

Figure 405: Miller in NASA Glenn Research Center Supersonic Wind Tunnel 2019.

Historical Viewpoints of Transonic Flow

A slotted wind-tunnel test section.

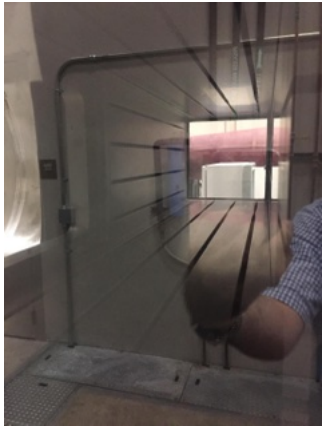

Figure 406: The slotted test section of the FSU Polysonic wind tunnel take by Prof. Miller, 2018.

Historical Viewpoints of Transonic Flow

- In 1946 Ray Wright, a theoretician at NACA Langley argued that a test section with long thin rectangular slots parallel to the flow with about 12 percent open area, then the blockage problem would be alleviated.
- John Stack, administrator at Langley, approved slotting of the 16 ft high speed tunnel of Langley. The slotted throat concept allowed for the smooth transition of the tunnel through Mach one and removed the problem of blockage
- This resulted in the first functional transonic tunnels - the slotting of the tunnels remained a state secret for decades!
- There was no theoretical, analytical, or numerical method useful for transonic calculations until the 1980s when CFD methods such as those of Murman and Cole came to use!

Class Summary

- Transonic flow definitions
- Theory in three main developments
- Historical context

Next Time

- The area rule and the supercritical airfoil
- Numerical solutions and examples

Class Overview

- The area rule
- Supercritical airfoil
- Numerical solutions and examples

“We built airplane models with Coke bottle-shaped fuselages and lo and behold the drag of the wing just disappeared. The wind tunnel showed it worked perfectly.”

Richard T. Whitcomb

https://youtu.be/oht43lM97jk

Also see https://www.nasa.gov/topics/people/features/richard_whitcomb.html

The Area Rule and the Supercritical Airfoil

- Discovered experimentally by Richard Whitcomb at NASA Langley Research Center
- Area rule found mathematically in USSR beforehand by Dr. Maslennikova.
- Both have objective of reducing drag
- Area rule (1950s) states that cross-sectional area of the body should have a smooth variation with longitudinal distance along the body
  - There should be no rapid or discontinuous changes in the cross sectional area distribution.

Richard T. Whitcomb

1921 - 2009, American

- NACA/NASA Langley
- Discovered area rule experimentally
- Invented super-critical airfoils
- Winglets
- Insane work ethic
- Made a branch head so that 'he could do whatever he wanted'
- Countless awards
- Excellent video interviews online – worth a watch to learn about NASA culture
- Never married… ashes spread over Chesapeake bay
- I had many personal indirect interactions!

S.A.E. Miller, Ph.D., saem@ufl.edu

Vera Nikolaevna Maslennikova
(Вера Николаевна Масленникова)
29 April 1926 – 14 August 2000, Soviet

- Mathematician
- Parents died at 11
- Served in the Great Patriotic War, defended Moscow, Artillery later
- Faculty of Mechanics and Mathematics at the University of Moscow, she graduated with distinction in 1951
- graduate student at the Steklov Institute of Mathematics, advised by Sergei Sobolev
- Doctorate in 1954 on the topic of "fundamental solutions of initial boundary-value problems for systems of hydrodynamics of rotating fluids with regard to compressibility."
- PDE expert
- Steklov Institute, working there for twenty two years
- Discovered via theory area rule well before known in the west
- State Prize of the USSR, Order of the Patriotic War

S.A.E. Miller, Ph.D., saem@ufl.edu

Supercritical Airfoil

- The supercritical airfoil (1960s) is shaped somewhat flat on the top surface in order to reduce the local Mach number, inside the supersonic region below what it would be for a conventional airfoil under the same flight conditions.
  - Shock wave strength is lower, the boundary layer separation is less severe, and free-stream Mach number is higher before the drag divergence phenomena occurs
- Supercritical airfoil tolerates larger increase in the free-stream Mach number above the critical value before drag divergence occurs
  - Supercritical airfoils are airfoils that operate far above the traditional critical Mach number.

Let's look at some examples of the area rule and supercritical airfoil.

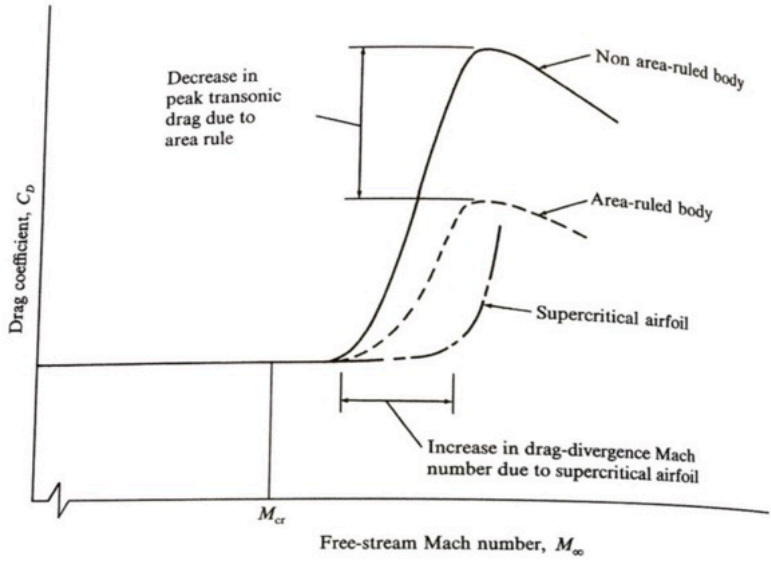

Figure 407: Illustration of separate effects of the area rule and the supercritical airfoil.

Note that before this production aircraft was ‘area-ruled’ at NASA Langley by Whitcomb, it could not fly supersonically!

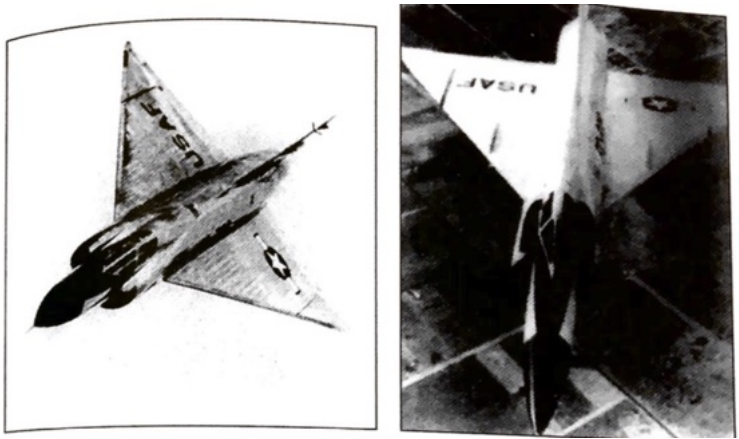

Figure 408: The Covair YF-12 with no area ruling and the Covair YF-102A with area ruling. Note the wasp or coke bottle like shape of the fuselage in comparison with the original.

The result of changes of the YF-102 by Whitcomb at NASA Langley. Resulted in 25% speed increase to supersonic regimes and 870 aircraft built.

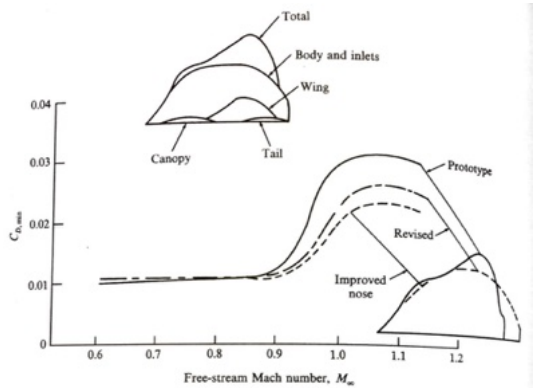

Figure 409: The effect of the area rule modifications made on the original non-area-ruled Convair YF-102 and the resulting area ruled YF-102A.

Almost all commercial aircraft and some military airplanes use supercritical airfoil. Usually results in 10% drag reduction at cruise Mach number.

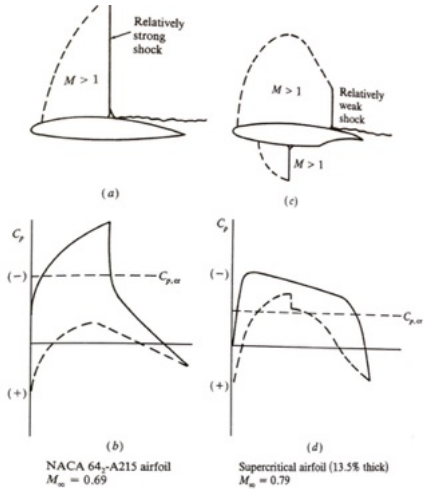

Figure 410: Standard NACA 64 series airfoil compared with supercritical airfoil at cruise lift conditions - R. T. Whitcomb.

The on-set of drag divergence is readily apparent between a traditional airfoil and a supercritical airfoil.

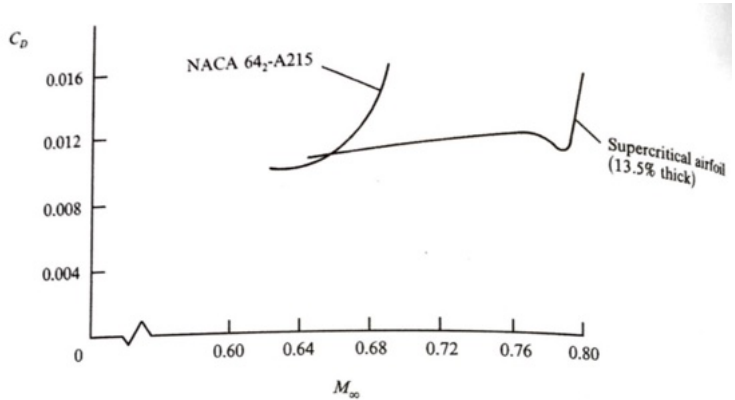

Figure 411: The drag divergence properties of a NACA 64 series airfoil and a supercritical airfoil

Small-Perturbation Velocity Potential Equation
Murman and Cole Method

- The method of Murman and Cole to solve the Small-Perturbation Velocity Potential Equation
- Consider an airfoil in physical space with zero angle of attack and symmetry
- Find the 2D inviscid transonic flow-field over this airfoil

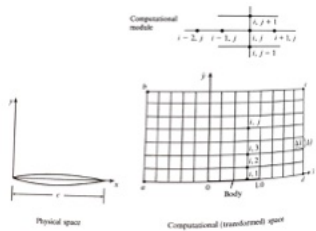

Figure 412: The physical and computational planes.

Small-Perturbation Velocity Potential Equation
Murman and Cole Method

We represent the shape of the body as a function f as

$$\frac{df}{dx} = \frac{v'}{u_\infty} \tag{752}$$

and with the transonic transformation previously defined we find

$$v' = \frac{\partial \phi}{\partial y} = \tau u_\infty \frac{\partial \overline{\phi}}{\partial \overline{y}} \tag{753}$$

Combining these two equations we find an equation for the boundary condition

$$\overline{\phi}_{\overline{y}}(\overline{x}, 0) = \frac{1}{\tau}\frac{df}{dx} \tag{754}$$

where df/dx is a known function of x and therefore $\overline{x}$. We also enforce flow-symmetry. We must find the solution with the method of finite-differences (an early form of CFD)!

Small-Perturbation Velocity Potential Equation
Murman and Cole Method

A second-order one-sided difference for $\overline{\phi}_{\overline{y}}$ at the surface is

$$\overline{\phi}_{\overline{y}} = \frac{\partial \overline{\phi}}{\partial y} = \frac{1}{2\Delta y}\left(-3\overline{\phi}_{i,1} + 4\overline{\phi}_{i,2} - \overline{\phi}_{i,3}\right) \tag{755}$$

where i is the grid point index. The corresponding discrete boundary condition is

$$\frac{1}{\tau}\frac{df}{dx}_i = \frac{1}{2\Delta y}\left(-3\overline{\phi}_{i,1} + 4\overline{\phi}_{i,2} - \overline{\phi}_{i,3}\right) \tag{756}$$

The other boundaries must account for the flow disturbances and takes into account the 'doublet singularity'

$$\overline{\phi}(\overline{x}, \overline{y}) = \frac{1}{2\pi K^{1/2}} \frac{\mathcal{D}\overline{x}}{\overline{x}^2 + K\overline{y}^2} \tag{757}$$

where $\mathcal{D}$ is the effective doublet strength obtained as part of the solution.

Small-Perturbation Velocity Potential Equation
Murman and Cole Method

The type of finite difference within the flow-field depends on the flow being supersonic or subsonic. This represents the advent of upwind differencing. For example for subsonic finite difference

$$\frac{\partial \overline{\phi}}{\partial \overline{x}}_{i,j} = \frac{\overline{\phi}_{i+1,j} - \overline{\phi}_{i-1,j}}{2\Delta x} \tag{758}$$

and for the supersonic flow

$$\frac{\partial \overline{\phi}}{\partial \overline{x}}_{i,j} = \frac{\overline{\phi}_{i,j} - \overline{\phi}_{i-2,j}}{2\Delta x} \tag{759}$$

Difference equations are found for locally subsonic and locally supersonic flow, respectively, at each grid point by substituting these (and similar) finite difference approximations into the governing equation.

Small-Perturbation Velocity Potential Equation
Murman and Cole Method

A system of equations is then formed and can be written compactly as

$$A\overline{\phi}_{i,j} = B \tag{760}$$

Solutions of this equation can be found using many numerical techniques of numerical linear algebra.

The original approached used the successive line relation technique.

Let us examine the result

Small-Perturbation Velocity Potential Equation
Murman and Cole Method

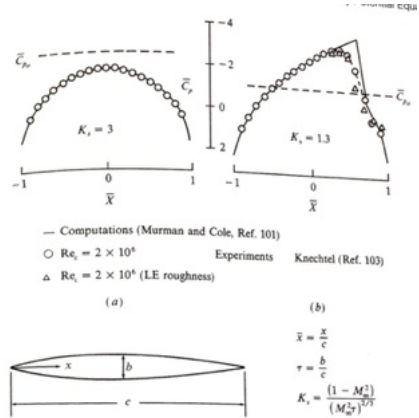

Figure 413: The pressure coefficient distribution for a circular arc airfoil. Comparisons between experiment and measurement. Free-stream Mach numbers correspond to subcritical and supercritical cases.

Solution of the Full Velocity Potential Equation

- Recall this approach assumes that the body is thin and resides at small α.
- We find 'good' results in both leading and trailing edge regions where there are large changes in the flow.
- There is some error near shocks
- We use the same numerical technique as previously described
- To save computational expense, a very unique computational grid is adopted

Let us examine some results

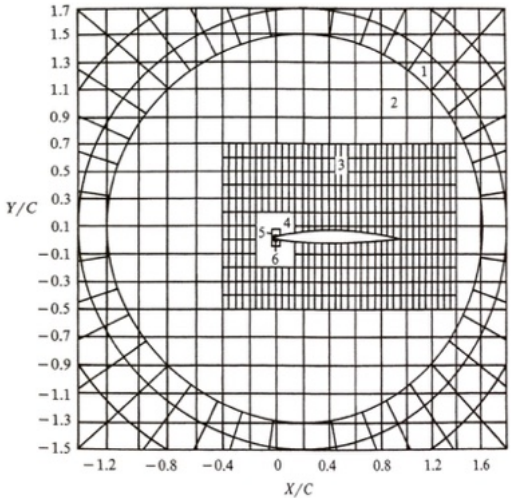

Figure 414: The patching of six different grids for the numerical calculation of transonic flow over an airfoil.

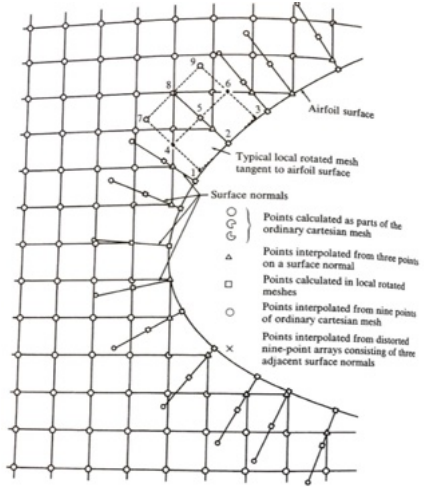

Figure 415: Detail of the grid shown of the previous figure in the vicinity of the leading edge.

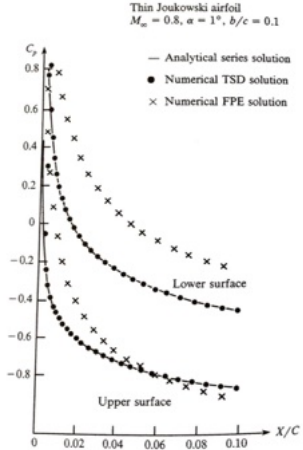

Figure 416: Analytical and numerical solutions for the pressure coefficient distributions near the leading edge of a thin Joukowski airfoil.

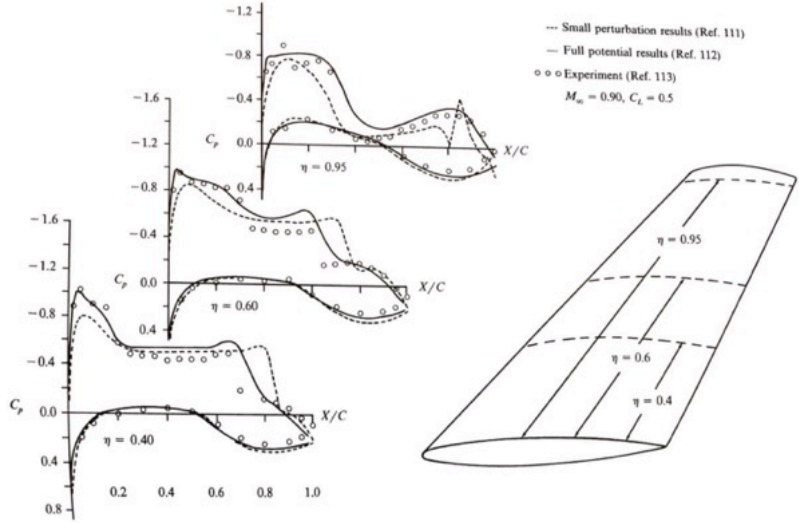

Figure 417: Transonic flow over a finite wing. Chordwise pressure coefficient distributions at three different spanwise locations. Comparison between small-perturbation and full potential results with experiment.

Numerical Solutions of the Euler Equations

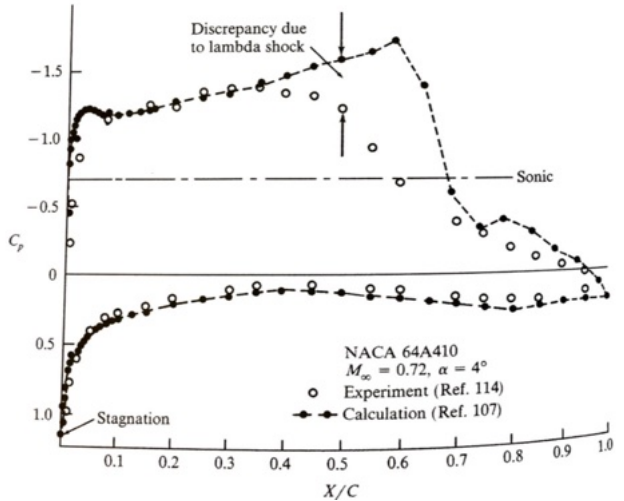

Figure 418: Finite difference solution of the complete Euler equations for transonic flow.

Numerical Solutions of the Euler Equations

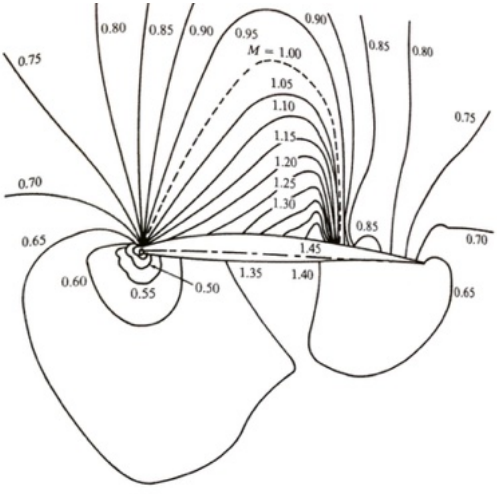

Figure 419: Contours of Mach number for an NACA 64A410 airfoil at $M_\infty = 0.72$ and $\alpha = 4$ deg.

Numerical Solutions of the Euler Equations

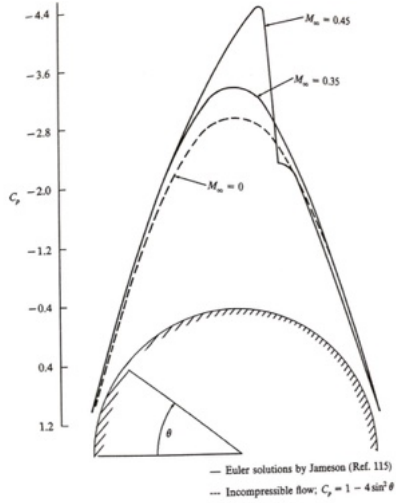

Figure 420: Transonic flow over a circular cylinder finite volume soutions of the Euler equations of Jameson where $M_\infty = 0.35$ and $M_\infty = 0.45$ is a supercritical case. The dashed line is the classical incompressible theory.

Numerical Solutions of the Euler Equations

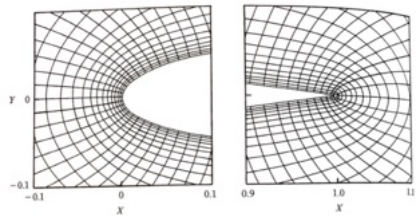

Figure 421: Boundary fitted curvilinear grid for the Euler solutions of Reddy and Jacobs.

Numerical Solutions of the Euler Equations

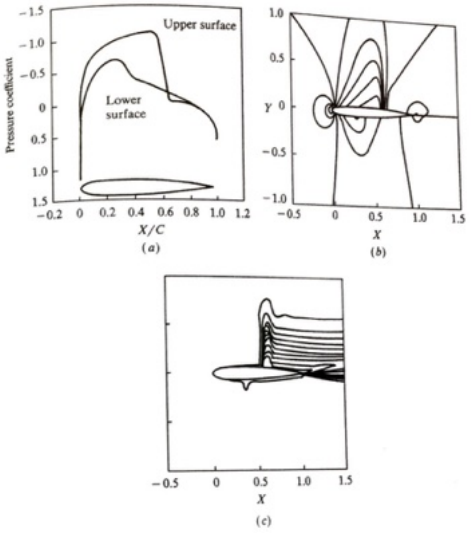

Figure 422: Transonic flow over an NACA 0012 airfoil with a $M_\infty = 0.80$ and $\alpha = 1.25$ deg of Reddy and Jacobs.

Numerical Solutions of the Euler Equations

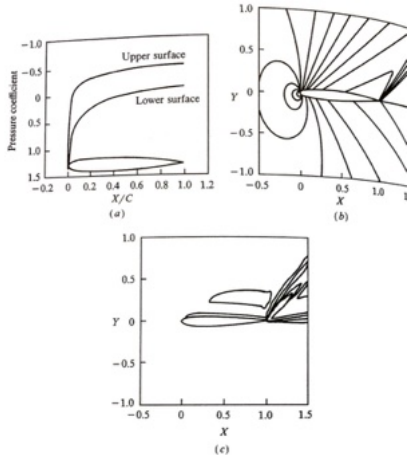

Figure 423: Transonic flow over an NACA 0012 airfoil with a supercritical free-stream $M = 1.2$ and $\alpha = 7$ deg. Contours are stagnation pressure.

Class Summary

- The area rule
- Supercritical airfoil
- Numerical solutions and examples

Next Time

- Hypersonics

Class Overview

- Introduction
- Examples
- Mach number independence
- Observations

“If you say why not bomb them tomorrow, I say why not today? If you say today at five o’ clock, I say why not one o’ clock?”

John von Neumann

As quoted in “The Passing of a Great Mind” by Clay Blair, Jr., in LIFE Magazine (25 February 1957), p. 96

Typical Hypersonics Nomenclature

NOMENCLATURE

a	angle of attack
c	speed of sound
C_p	pressure coefficient
C_{p_s}	pressure coefficient of shock
C_L	lift coefficient
C_D	drag coefficient
$\mathfrak{D}$	similarity function for C_D
f	function of ξ and η (Eq. 19.6)
h	dimensionless thickness distribution
k	ratio of specific heats
K	hypersonic similarity parameter, $\mathsf{M}_\infty\delta$
K_s	similarity parameter for shock, $\mathsf{M}_\infty\theta_s$
K_e	similarity parameter for simple-wave expansion, $\mathsf{M}_\infty\theta_e$
l	chord
$\mathfrak{L}$	similarity function for C_L
M	Mach Number
$\mathfrak{M}$	similarity function for C_{p_s}
p	pressure
$\mathcal{P}$	similarity function for C_p
$\mathcal{P}_s$	see Eq. 19.24
t	maximum thickness
u, v	Cartesian velocity components
U_∞	free-stream velocity
x, y	Cartesian coordinates
δ	thickness ratio
η	y/t
θ_s	deflection angle across shock
θ_e	deflection angle of simple-wave expansion
ξ	x/t
σ	shock angle
φ	perturbation velocity potential
ω	angle of turn through a wave; positive for compressions, negative for expansions
$(\ )_\infty$	signifies free-stream conditions
$(\ )_0$	signifies stagnation state
$(\ )_1$	signifies condition before shock
$(\ )_2$	signifies condition after shock
$(\ )_i$	signifies conditions at beginning of simple-wave expansion

Figure 424: N. Armstrong by North American X-15

Figure 425: NASA Hyper-X Program X-43. A winged booster rocket with the X-43 placed on top, called a ”stack”, was drop launched from a Boeing B-52 Stratofortress. After the booster rocket (a modified first stage of the Pegasus rocket) brought the stack to the target speed and altitude, it was discarded, and the X-43 flew free using its own engine, a scramjet. The first plane in the series, the X-43A, was a single-use vehicle. Three of them were built. The first was destroyed after malfunctioning in flight; the other two flew successfully, with the scramjet operating for approximately 10 seconds, followed by a 10-minute glide and intentional crash into the ocean.

Waveriders

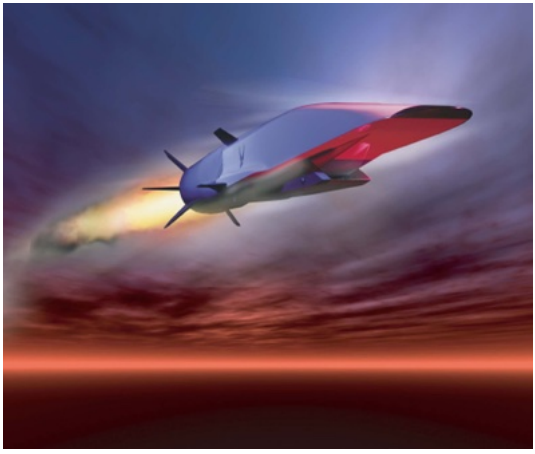

Figure 426: X-51A Waverider, U.S. Air Force graphic

Waveriders

Figure 427: X-51A Waverider on B-52 2009

Waveriders

Figure 428: NASA Langley - The SJX61-2 engine successfully completes ground tests simulating Mach 5 flight conditions.

Waveriders

Figure 429: The Chinese Project 0901 Flying Vehicle of CASIC shows another configuration of waverider.

Hypersonics Test Facility

Figure 430: NASA Langley Research Center – the bottle-field. Photography by Prof. Miller.

Hypersonics Test Facility

Figure 431: NASA Langley Research Center – the vacuum sphere. Photography by Prof. Miller.

Hypersonics Test Facility

Figure 432: NASA Langley Research Center – the hypersonic engine test cells – number one and two. Photography by Prof. Miller.

Natural Astrophysical Object Reentry

Figure 433: Meteor reentry in Russia. Fireball from a meteor that exploded over Chelyabinsk, Russia, on Feb. 15, 2013, creating a shockwave that shattered windows and injured more than 1,000 people

Figure 434: Hypersonic projectile.

Figure 435: Shadowgraph of flow past 60 deg. cone at Mach 6.7.

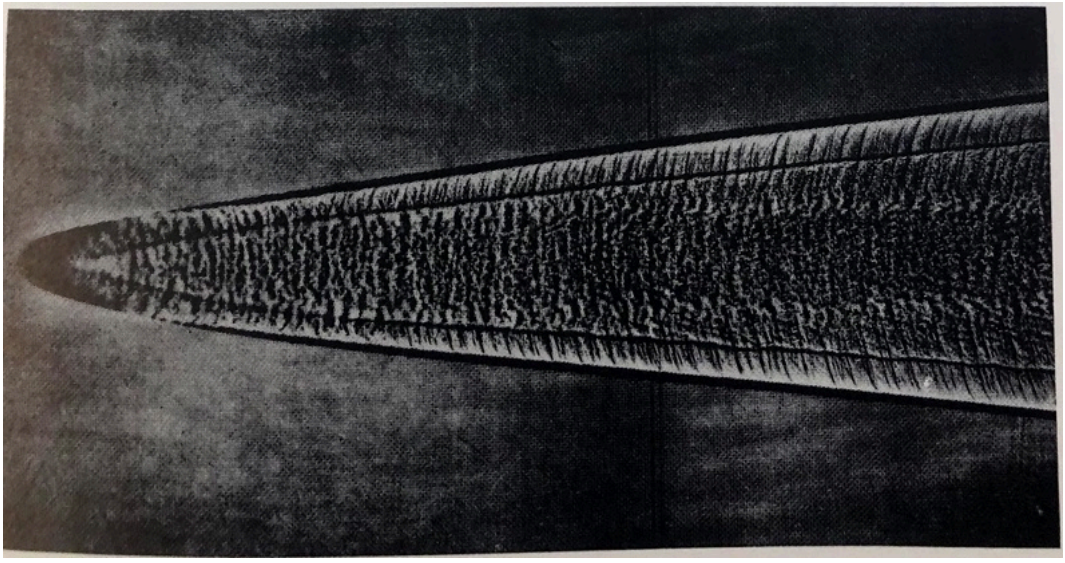

Figure 436: Schlieren photograph of flow pst a sphere at Mach 12.1

Melting of Models by Aerodynamic Heating

NASA Langley CRGIS Published on Jul 9, 2009
Test conducted in the 1950s at NASA Langley Research Center's 11 inch Hypersonic Tunnel. The models start to disintegrate as the air flow becomes heated.
https://www.youtube.com/watch?v=RChlt5wdqBs

The 8-Foot High-Temperature Tunnel (HTT) is the nation's largest hypersonic blow down test facility. The facility supports large-scale thermal protection system testing, flight qualification testing, and hypersonic engine testing. The HTT duplicates as near as possible, the flight conditions that would be encountered by hypersonic vehicles in the atmosphere. The facility test stream is produced by burning methane, air, and liquid oxygen and expanding the combustion products through any one of several nozzles into the test section. The facility currently provides testing capability at Mach 3, 4, 5, and 6.5.

The test section accommodates very large (5 by 9 ft) thermal protection system models. The facility has been heavily utilized for hypersonic engine testing and has tested the National Aerospace Plane Concept Demonstration Engine, the X43 Hyper-X engine, the Office of Naval Research HyFly Dual Combustor Ramjet Engine, the X43C program's Ground Demonstrator Engine No. 2, and the Air Force Research Laboratory SJX61–1 and SJX61–2 engines. The facility has an array of test support systems that include hydrogen system, silane system, JP–7 and JP–10 systems, ethylene system, model hydraulic system, water cooling systems, and nitrogen purge systems.

www.nasa.gov

Facility Benefits

- Proven experienced hypersonic test team
- Close working relationship with NASA Langley's Hypersonic Air-Breathing Propulsion Branch
- Nozzle calibration data available at all test Mach numbers
- Numerous test support systems available to meet varied test requirements
- All test data supplied to customers on a CD or DVD in customer selectable format
- Unlimited optical access for photography and video systems

Facility Applications

- National Aerospace Plane Concept Demonstration Engine test
- Office of Naval Research HyFly Dual Combustor Ramjet Engine test
- X43C program's Ground Demonstrator Engine No. 2 test and X43 Hyper-X engine test
- Air Force Research Laboratory SJX61–1 and SJX61–2 engines test
- U.S. Missile Defense Agency/Japanese Defense Agency missile nosecone flight qualification test
- NASA Next Generation Launch Transportation (NGLT) program metallic thermal protection system test
- NASA program for the Advancement of Inflatable Decelerators for Atmospheric Entry thermal protection system test
- Large Scramjet Engine Test Technology (LSETT)

Characteristics

Nozzle exit dimension	96 in. (2.4 m)
Speed	Mach 3, 4, 5, or 6.5
Reynolds number	0.44 to 5.09×10⁶ per ft (Mach dependent)
Plenum stagnation temperature	900 to 3500 °F (480 to 1950 °C) (Mach dependent)
Plenum stagnation pressure	50 to 2000 psia (340 kPa to 13.8 MPa) with oxygen enrichment (Mach dependent)
Plenum stagnation pressure	50 to 4000 psia (340 kPa to 27.5 MPa) with no oxygen (for thermal protection system testing) (Mach dependent)

Data Acquisition and Processing

Low frequency system	512 channels at 50 samples per second
High frequency system	96 channels at up to 200 K samples per second
Classified capability	Yes

Instrumentation

Strain gauge balances	Six-component force and moment measurement system
Available corrections	Interactions, temperature effects, attitude tares, axes orientation, pressure tares, momentum (flow) tares
Thermocouples	288 available channels at 50 samples per second
Strain-gauge-based devices	144 available channels at 50 samples per second
Electronically scanned pressure (ESP) system	1000 available channels at 10 samples per second

Contact Information

www.aerospace.nasa.gov/atp
Stephen Harvin
NASA Langley Research Center
Phone: 757–864–3237
E-mail: who+the_fifth@larc.nasa.gov

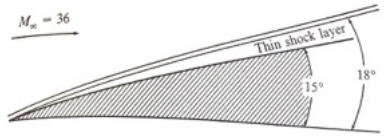

Figure 15.3 | Illustration of a thin shock layer at hypersonic Mach numbers.

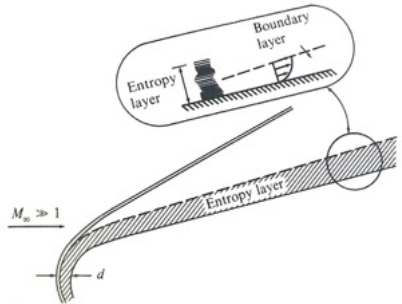

Figure 437: Illustration of the entropy layer of a blunt-nosed slender body at hypersonic speeds.

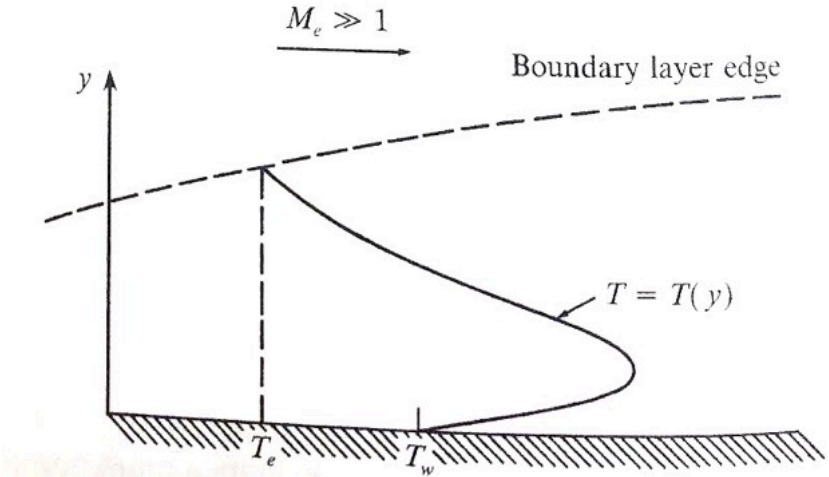

Figure 438: Schematic of a temperature profile in a hypersonic boundary layer.

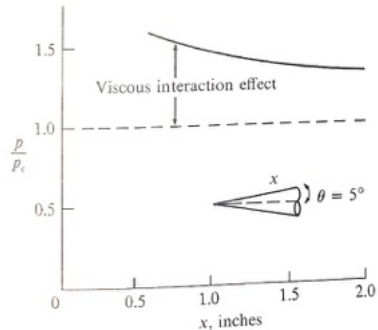

Figure 439: Viscous interaction effect. Induced pressure on a sharp cone at Mach 11 and Re 188000.

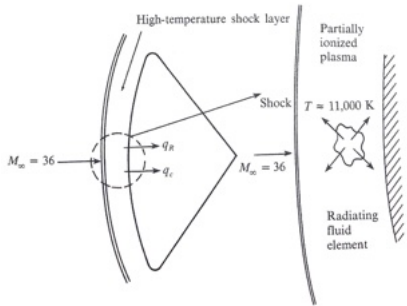

Figure 440: Illustration of a high temperature shock layer on a blunt body moving at hypersonic speeds.

Mach Number Independence

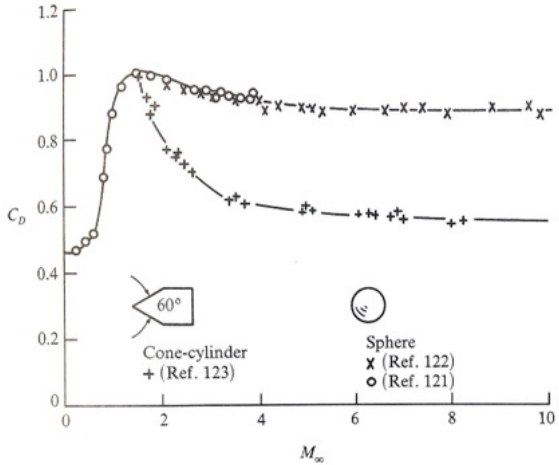

Figure 441: Drag coefficient for a sphere and a cone-cylinder from ballistic range measurements; an illustration of Mach number independence.

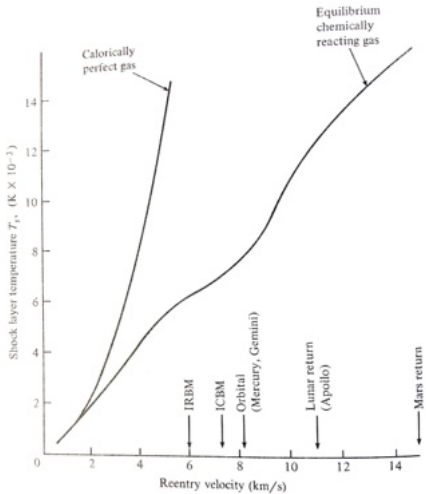

Figure 442: T behind a normal shock versus velocity for air at a standard altitude of 52 km. Comparison between calorically perfect and equilibrium gas results.

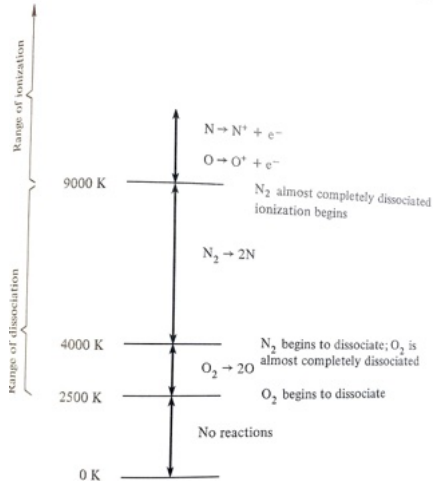

Figure 443: Ranges of dissociation and ionization for air at approximately 1 atm pressure.

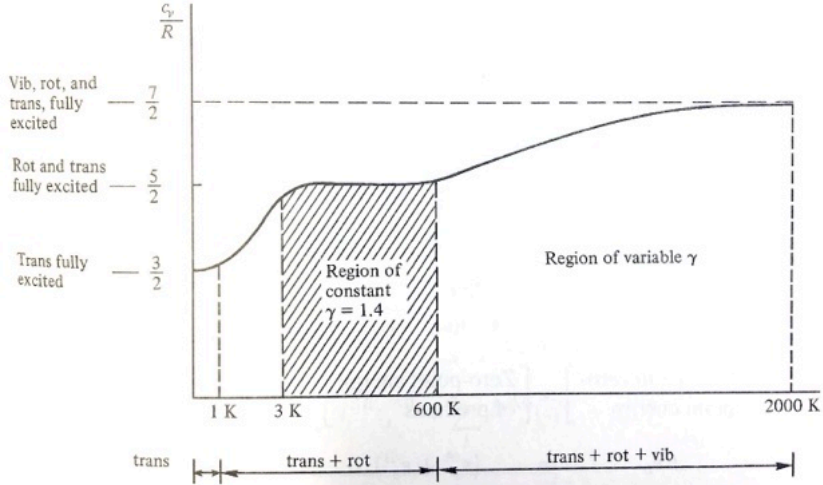

Figure 444: Schematic of the temperature variation of the specific heat for a diatomic gas.

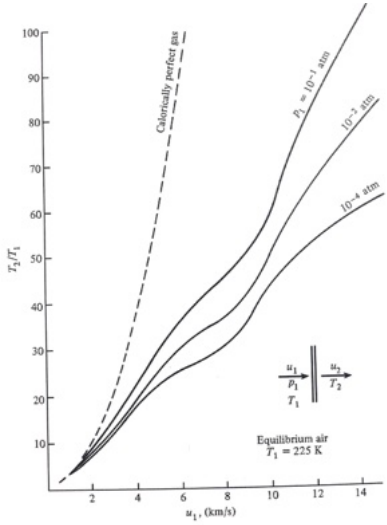

Figure 445: Influence of pressure on the normal shock temperature in equilibrium air.

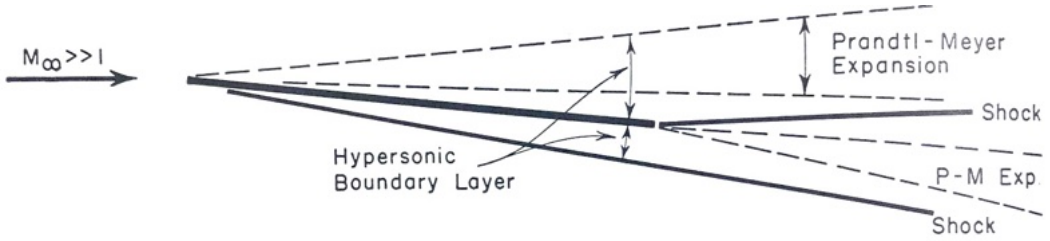

Figure 446: Hypersonic flow over an ideal slender body

Hypersonic Notes

- Linearized velocity potential theory is not applicable
- Pressure coefficient varies non-linearly with thickness ratio and angle of incidence
- Sometimes continuum assumption is invalid
- Mach angle is very small and waves often follow surface of the body
- Flow gives rise to a hypersonic boundary layer

Hypersonic Notes

- Pressure rise across shocks is very large
- Shock pressure is much larger than that across expansions
- Sometimes the volume behind the expansion is nearly or a vacuum
- We will see that these flows can sometimes be approximated using Isaac Newton's "corpuscular theory"

Class Summary

- Introduction
- Examples
- Mach number independence
- Observations

Next Time

- Newton
- K and similarity law
- Isentropic relations
- Oblique shocks
- Expansions

Class Overview

Hypersonics

- Newton
- *K* and similarity law
- Isentropic relations
- Oblique shocks
- Expansions

“I do not plan to come back. I have no reason to come back. I plan to do my best to help the Chinese people build up the nation to where they can live with dignity and happiness.”

Qian (1955) to reporters after returning to China. Cited in: “Qian Xuesen dies at 98; rocket scientist helped establish Jet Propulsion Laboratory” Obituary Nov 1, 2009

“It was the stupidest thing this country ever did. He was no more a Communist than I was, and we forced him to go.”

Dan A. Kimball in 1950s as cited in: Iris Chang (2008) Thread Of The Silkworm. p. 200

“That the government permitted this genius, this scientific genius, to be sent to Communist China to pick his brains is one of the tragedies of this century.”

Grant Cooper, CALTECH appointed attorney in 1950s

Corpuscular Flow

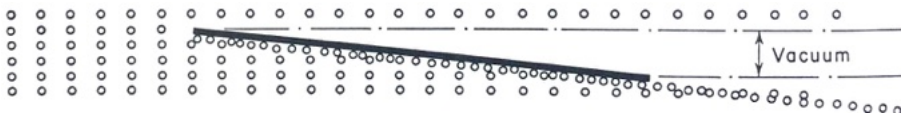

Figure 447: Corpuscular flow over a flat plate.

Isaac Newton

25 December 1642 – 20 March 1726, English

- Mathematician, astronomer, theologian, physicist
- 1687 - Mathematical Principles of Natural Philosophy
- Theoretical calculation of the speed of sound, and introduced the notion of a Newtonian fluid
- *Corpuscular theory of fluid*
- Countless accomplishments

"Was never sensible to any passion, was not subject to the common frailties of mankind, nor had any commerce with women—a circumstance which was assured me by the physician and surgeon who attended him in his last moments" ~Voltaire

S.A.E. Miller, Ph.D., saem@ufl.edu

Implications of Newton's Theory

Newton's theory leads to

$$c_l \cong 2\sin^2\alpha \text{ and } c_d \cong 2\sin^3\alpha \tag{761}$$

There is approximately no change in velocity of particles

- Method of characteristics does work sometimes for solving hypersonic problems
- We assume that hypersonic flow consists of small perturbations of the flow relative to a parallel uniform flow
- Seek similarity laws for 2D and axisymmetric flow
- Consider two-dimensional, irrotational motion past a thin profile
- Stream is initially uniform and parallel

Implications of Newton's Theory - Error in Theory for Large Disturbances

- Error is observed to go as τ^2, $\tau =$ thickness ratio
- For supersonic, τ
- For transonic $\tau^{2/3}$
- Newton's theory suggests that particles striking surface lose their cross-stream momentum.

Major Forces on a Plate

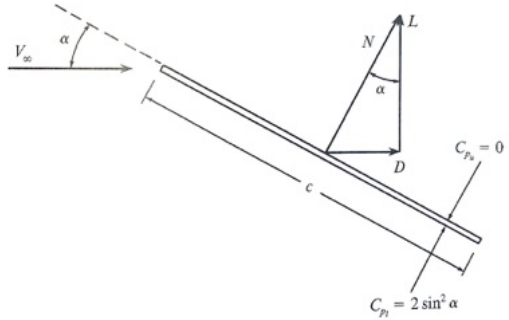

Figure 448: Flat plate at angle of attack illustrating the major aerodynamic forces.

Newtonian Results on the Flat Plate

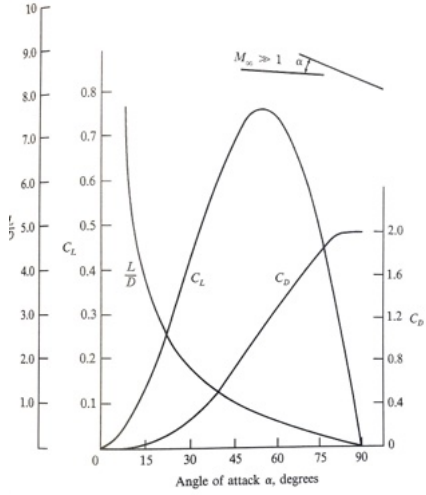

Figure 449: Newtonian results for a flat plate.

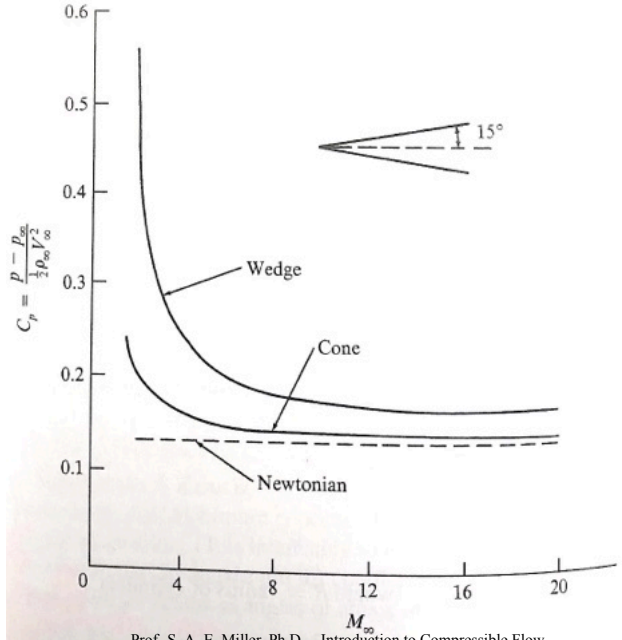
0.6
0.5
0.4
0.3
0.2
0.1
0
4
8
12
16
20
M_∞
$C_p = \frac{p - p_\infty}{\frac{1}{2}\rho_\infty V_\infty^2}$
15°
Wedge
Cone
Newtonian

Qian Xuesen or Hsue-Shen Tsien

December 1911 – 31 October 2009, Chinese

- Genius in aerodynamics / hypersonics and many other subjects
- MIT Ph.D., joined Theodore von Karman's group at Caltech, including the founding of the Jet Propulsion Laboratory
- 1950s, the United States government accused Tsien of communist sympathies. In 1950, despite protests by his colleagues, he was stripped of his security clearance. Tsien decided to return to China, but was detained at Terminal Island near Los Angeles.
- Five year house arrest, Tsien was released in exchange for the repatriation of American pilots
- Return, Tsien helped lead the Chinese nuclear weapons program. This effort ultimately led to China's first successful atomic bomb test and hydrogen bomb test, making China the fifth nuclear weapons state, and achieving the fastest fission-to-fusion development in history
- Tsien married Jiang Ying a famed opera singer

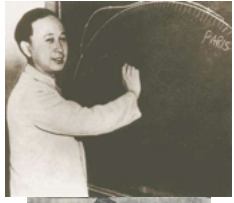

Ludwig Prandtl (German scientist), Hsue-Shen Tsien, Theodore von Kármán.

S.A.E. Miller, Ph.D., saem@ufl.edu

Compressible Perturbation of Velocity Potential

Analyze hypersonics with the velocity potential approach. For compressible perturbation of velocity potential ϕ_s

$$\left(1-\frac{u^2}{c^2}\right)\frac{d^2\phi}{dx^2}-2\frac{uv}{c^2}\frac{d^2\phi}{dxdy}+\left(1-\frac{v^2}{c^2}\right)\frac{d^2\phi}{dy^2}=0 \tag{762}$$

where

$$u=u_\infty+\frac{d\phi}{dx} \tag{763}$$

and

$$r=\frac{d\phi}{dy} \tag{764}$$

Compressible Perturbation of Velocity Potential

Local speed of sound is related to ambient speed of sound

$$\begin{aligned} c^2 &= c_\infty^2 - \frac{\gamma-1}{2}\left[\left(u^2-v^2\right)-u_\infty^2\right] \\ &= c_\infty^2 - \frac{\gamma-1}{2}\left[2u_\infty\frac{d\phi}{dx}+\left(\frac{d\phi}{dx}\right)^2+\left(\frac{d\phi}{dy}\right)^2\right] \end{aligned} \tag{765}$$

Remember $u_\infty >> c_\infty, u_\infty >> \frac{d\phi}{dx}$, and $u_\infty >> \frac{d\phi}{dy}$. Now substitute these relations into perturbation of velocity potential equation

$$\begin{aligned} &\left[1-(\gamma+1)\frac{M_\infty}{c_\infty}\frac{d\phi}{dx}-\frac{\gamma-1}{2}\frac{1}{c_\infty^2}\left(\frac{d\phi}{dy}\right)^2-M_\infty^2\right]\frac{d^2\phi}{dx^2} \\ &-2\frac{M_\infty}{c_\infty}\frac{d\phi}{dy}\frac{d^2\phi}{dxdy}+\left[1+(\gamma-1)\frac{M_\infty}{c_\infty}\frac{d\phi}{dx}-\frac{\gamma+1}{2}\frac{1}{c_\infty^2}\left(\frac{d\phi}{dy}\right)^2\right]\frac{d^2\phi}{dy^2}=0 \end{aligned} \tag{766}$$

Compressible Perturbation of Velocity Potential

Let our non-dimensional variables be

$$\xi = \frac{x}{l} \text{ and } \eta = \frac{y/l}{\delta} = y/t \text{ (substitutions)} \tag{767}$$

where l is chord, δ is thickness ratio, and η is normal to the body. Now ϕ can be non-dimensionalized as

$$\phi = \frac{c_\infty l}{M_\infty} f(\xi, \eta) \tag{768}$$

Using these definitions we find

$$\left[1 - (\gamma - 1)\frac{df}{d\xi} - \frac{\gamma + 1}{2(M_\infty \delta)^2}\left(\frac{df}{d\eta}\right)^2\right]\frac{d^2 f}{d\eta^2} = (M_\infty \delta)^2 \frac{d^2 f}{d\xi^2} + 2\frac{df}{d\eta}\frac{d^2 f}{d\xi dy} \tag{769}$$

Similarity Rule

If a series of profiles having the same thickness distribution but different thickness ratios are placed in flows of different Mach numbers such that M_∞ is held constant, then flow patterns are similar in the sense that they are governed by the function $f(\xi, y)$

Hypersonic Sensitivity Parameter

We define $M_\infty \delta$ as the hypersonic sensitivity parameter. Let

$$K = M_\infty \delta \tag{770}$$

where δ thickness ratio and about unity for most flows.

- We can define hypersonic flow as "a supersonic flow with small perturbations for which $M_\infty \delta$ is unity or greater."
- This equation can be related to affinely connected profiles as shown by Tsien.
- Affinely - Allowing for or preserving parallel relationships.

Hypersonic Sensitivity Parameter

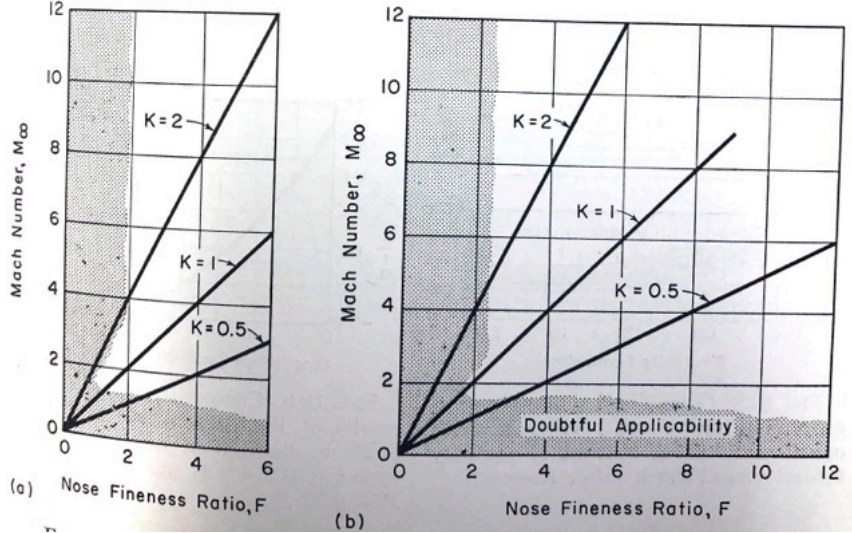

Figure 451: Range of applicability of similarity law for cone-cylinders and give-cylinders.

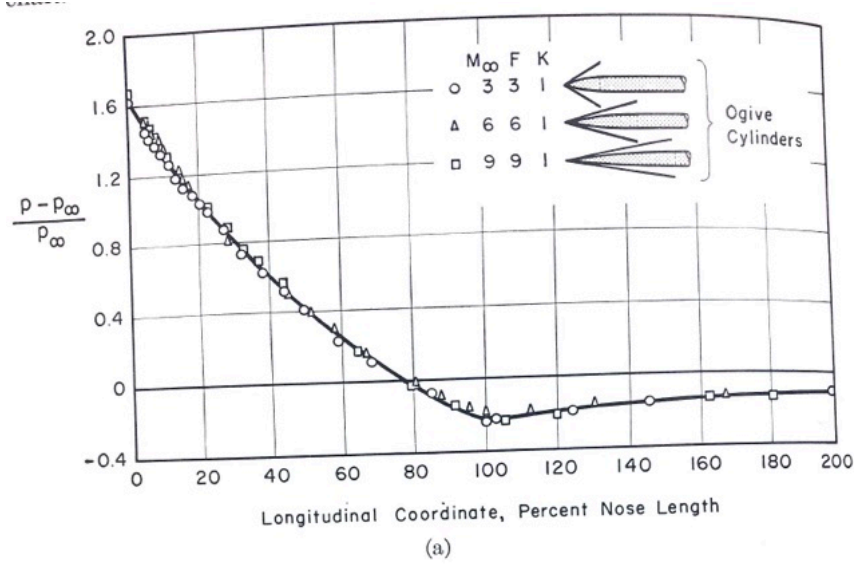

Figure 452: Pressure distributions plotted against hypersonic similarity law - ogive-cylinders.

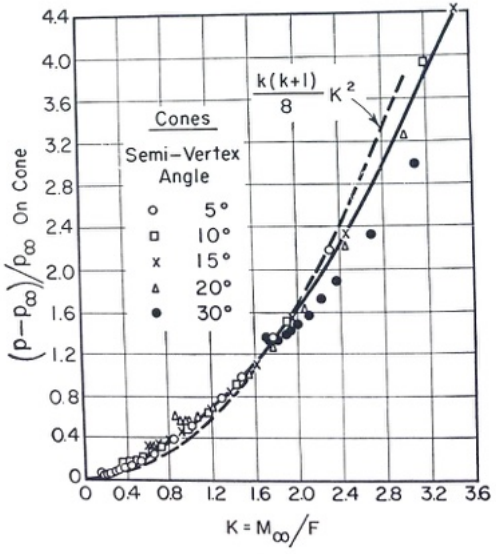

Figure 453: Pressure Distributions plotted against hypersonic similarity law - five cones with different vertex angles.

Isentropic Relations for Hypersonic Flow

$$\frac{p}{p_\infty} = \frac{p/p_o}{p_\infty/p_o} = \frac{(1 + \frac{\gamma-1}{2}\frac{u^2+v^2}{c^2})^{\frac{-\gamma}{(\gamma-1)}}}{(1 + \frac{\gamma-1}{2}M_\infty^2)^{\frac{-\gamma}{(\gamma-1)}}} \tag{771}$$

and for c_p using $u = u_\infty \frac{\partial \phi}{\partial x}$ and $v = \partial\phi/\partial y$, c^2 with ξ, η, $\phi = c_\infty lf/M_\infty$.

$$c_p = \frac{p - p_\infty}{\frac{1}{2}\rho_\infty u_\infty^2} = \frac{2}{\gamma M^2}\left(\frac{p}{p_\infty} - 1\right) \tag{772}$$

Expand expression for c_p in power series and disregard higher-order terms, which can be related to the thickness distribution.

$$\begin{aligned} c_p &= \frac{2}{\gamma K^2}\frac{K^2}{M_\infty^2} \\ &\times \left[\left\{1 - (\gamma-1)\frac{df}{d\xi} - \frac{\gamma-1}{2K^2}\left(\frac{df}{d\eta}\right)^2\right\}^{\frac{\gamma}{\gamma-1}} - 1\right] \end{aligned} \tag{773}$$

Isentropic Relations for Hypersonic Flow

- $f(\xi, \eta)$ only depends on ξ, η, and c_p/δ^2 and $c_p M_\infty^2$ are only dependent on K for profiles with same thickness distribution.
- Camber and angle of attack proportional to δ

If we approximate the bodies as very thin then we have two affinely related profiles

$$c_l = \frac{1}{M_\infty^2} K^2 \mathcal{L}(K_s, \gamma) \tag{774}$$

$$c_d = \frac{1}{M_\infty^3} K^2 D(K_s, \gamma)) \tag{775}$$

and

$$c_m = \frac{1}{M_\infty^2} K^2 \mathfrak{M}(K_s, \gamma) \tag{776}$$

Example

Let a symmetric profile with thickness ratio $\delta = 0.10$ be tested at $M_\infty = 5$ and $\alpha = 5^\circ$, measurements yield corresponding values of c_{L1} and c_{D1}. What can we say about same profile with $\delta = 0.05$?

Solution

We set $M_{\infty 1}\delta_1 = M_{\infty 2}\delta_2$. $\therefore$ Data of second profile depends on at least @ $M_{\infty 2} = 10$. Also,

$$\frac{\alpha_2}{\alpha_1} = \frac{\delta_2}{\delta_1} \tag{777}$$

So

$$\alpha_2 = 2.5^\circ. \tag{778}$$

$\therefore$ Lift and drag coefficients corresponding to $\delta_2 = 0.05, M_{\infty,2} = 10$, and $\alpha_2 = 2.5^\circ$ are related to the first condition, by the ratios

$$\frac{c_{L2}}{c_{L1}} = \left(\frac{\delta_2}{\delta_1}\right)^2 = \frac{1}{4} \text{ and } \frac{c_{D2}}{c_{D1}} = \left(\frac{\delta_2}{\delta_1}\right)^3 = \frac{1}{8}. \tag{779}$$

Obliques Shock Relations for Hypersonic Flow

Exact shock relations for hypersonics.

$$\frac{p_2}{p_1} = \frac{2\alpha}{\alpha+1} M_1^2 \sin^2\beta - \frac{\alpha-1}{\alpha+1}, \tag{780}$$

when β is shock angle and θ_s is turning angle. A pressure coefficient can be derived

$$c_{ps} = \frac{4}{\alpha+1}(\sin^2\beta - 1/M_1^2) \tag{781}$$

We can find $M_1^* = M_1(\beta, \alpha, \theta_s)$ as

$$\frac{1}{M_1^2} = \sin^2\beta - \frac{\alpha+1}{2}\frac{\sin\beta\sin\theta_s}{\cos(\beta-\theta_s)} \tag{782}$$

We can now observe another form for c_p

$$\frac{1}{4}c_{ps}^2\cos^2\beta = \left[1 - \frac{c_{ps}}{2}\right]^2 \sin^2\beta\tan^2\theta_s \tag{783}$$

Obliques Shock Relations for Hypersonic Flow

Now introduce assumption that M_1 is large and θ_s is small.
Implies

- c_p is small relative to unity
- β is small $\implies \cos\sigma \cong 1$
- $\tan\theta_s \cong \theta_s$

These approximations imply

$$\frac{1}{4}c_p = \theta_s^2 \sin^2\beta = \theta_s^2\left(\frac{\alpha+1}{4}c_p + \frac{1}{M_1^2}\right) \tag{784}$$

Place in form suggested by Hypersonic similarity relations.
Note that c_d is approximate θ_s and $K_s = M_1\theta_s$.

$$c_p = \theta_s^2 P(K,\alpha) \tag{785}$$

where $K = M_1\theta_s$

Obliques Shock Relations for Hypersonic Flow

Now substitute Eqn. (785) into (784). We find

$$p_s^2 - (\gamma + 1)p_s - \frac{4}{K_s^2} = 0. \tag{786}$$

This equation has a quadratic solution

$$p_s = \frac{\gamma + 1}{2} + \sqrt{\left(\frac{\gamma + 1}{2}\right)^2 + \left(\frac{2}{K}\right)^2} \tag{787}$$

Only the positive solution is useful. With the same approximations we find

$$\frac{M_2}{M_1} \cong \frac{1}{\sqrt{1 + \frac{\gamma}{2}K^2 P}} \tag{788}$$

which is the the form form of the function for special geometry of an oblique shock.

Obliques Shock Relations for Hypersonic Flow

Let us examine the limiting case. For large Mach number

- $M_1 \implies \infty, K_s \to \infty$
- $c_p \to (\gamma + 1)\theta_s^2$
- $c_l = (\gamma + 1)\theta_s^2$
- $c_d \cong c_l$
- $\theta_s \cong (\gamma + 1)\theta_s^3$
- For $\gamma = 1$ we recover Newton's corpuscular theory exactly

Obliques Shock Relations for Hypersonic Flow

As $M_\infty \to \infty$, c_d goes to a limiting finite value

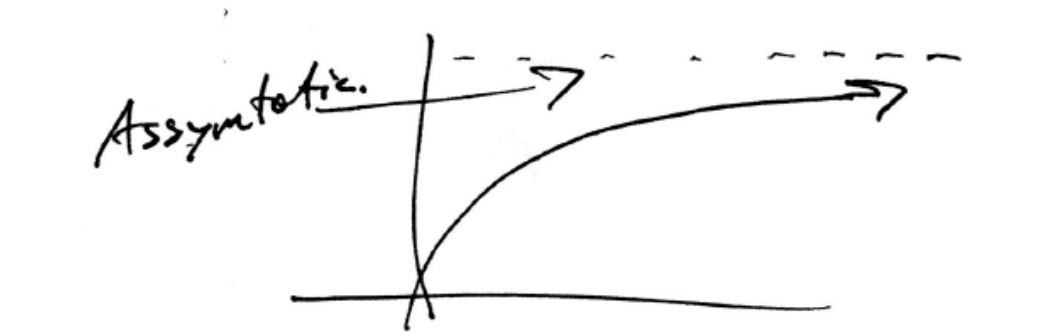

And M_2 goes as a limiting value also as $M_\infty \to \infty$

$$M_2 \to \frac{1}{\theta_s} \frac{2}{\sqrt{\gamma(\gamma+1)}} \tag{789}$$

Oblique Shock Wave Geometry and Ratios

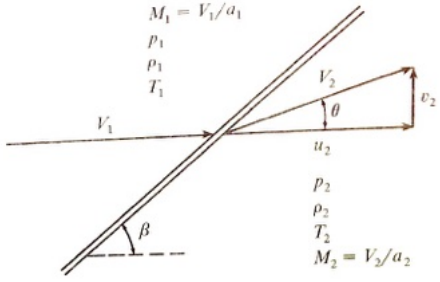

$$\frac{p_2}{p_1} \to \frac{2\gamma}{\gamma+1} M_1^2 \sin^2\beta$$

$$\frac{\rho_2}{\rho_1} \to \frac{\gamma+1}{\gamma-1}$$

$$\frac{T_2}{T_1} \to \frac{2\gamma(\gamma-1)}{(\gamma+1)^2} M_1^2 \sin^2\beta$$

$$\frac{u_2}{V_1} \to 1 - \frac{2\sin^2\beta}{\gamma+1}$$

$$\frac{v_2}{V_1} \to \frac{\sin(2\beta)}{\gamma+1}$$

$$C_p \to \left(\frac{4}{\gamma+1}\right)\sin^2\beta$$

In the hypersonic limit and for small θ:

$$\beta \to \frac{\gamma+1}{2}\theta$$

Figure 454: Oblique shock wave geometry and hypersonic ratios.

Expansion Waves in Hypersonic Flow

We note

- Incoming Mach number is very large and becomes even larger
- Recall the exact theory

$$\theta = \sqrt{\frac{\gamma+1}{\gamma-1}}\left(\tan^{-1}\sqrt{\frac{\gamma-1}{\gamma+1}}\sqrt{M^2-1}\right.$$
$$\left.-\tan^{-1}\sqrt{\frac{\gamma-1}{\gamma+1}}\sqrt{M_i^2-1}\right)-(\tan^{-1}\sqrt{M^2-1}-\tan^{-1}\sqrt{M_i^2-1}) \tag{790}$$

where M is local Mach number and M_i is at beginning of the expansion. Employ the approximations

$$\sqrt{M^2-1}\cong M \;\&\; \sqrt{M_i^2-1}\cong M_1 \tag{791}$$

Expansion Waves in Hypersonic Flow

Make this substitution and expand in an infinite series

$$\theta_e = \frac{2}{\gamma-1}\left(\frac{1}{M_i}-\frac{1}{M}\right) - \frac{1}{3}\left(\left(\frac{\gamma+1}{\gamma-1}\right)^2 - 1\right)\left(\frac{1}{M_i^3}-\frac{1}{M_3}\right) + \ldots \tag{792}$$

We can do the same for the pressure ratio

$$\frac{p}{p_i} = \frac{p/p_o}{p_i/p_o} = \left(\frac{1+\frac{\gamma-1}{2}M_i^2}{1+\frac{\gamma-1}{2}M^2}\right)^{\frac{\gamma}{\gamma-1}} \cong \left(\frac{M_i}{M}\right)^{\frac{2\gamma}{\gamma-1}} \tag{793}$$

Solving for M and placing in Eqn. θ_e yields

$$\begin{aligned} M_i\theta_i = {} & \frac{2}{\gamma-1}\left[1-\left(\frac{p}{p_i}\right)^{\frac{\gamma-1}{2\gamma}}\right] \\ & -\frac{1}{3M_i^2}\left[\left(\frac{\gamma+1}{\gamma-1}\right)^2 - 1\right]\left[1-\left(\frac{p}{p_i}\right)^{\frac{3(\gamma-1)}{2\gamma}}\right] + \ldots \end{aligned} \tag{794}$$

Expansion Waves in Hypersonic Flow

Recall M_i is large so first term is dominant and $K_e = M_i\theta_e$. We find

$$\frac{p}{p_i} = \left(1 - \frac{\gamma-1}{2}K_e\right)^{\frac{2\gamma}{\gamma-1}} \tag{795}$$

and

$$c_p = \frac{2}{\gamma M_i^2}\left(\frac{p}{p_i} - 1\right) = \frac{2}{\gamma M_i^2}\left[\left(1 - \frac{\gamma-1}{2}K\right)^{\frac{2\gamma}{\gamma-1}} - 1\right] \tag{796}$$

$$= \frac{2}{\gamma K^2}\left[\left(1 - \frac{\gamma-1}{2}K\right)^{\frac{2\gamma}{\gamma-1}} - 1\right]\theta_e^2. \tag{797}$$

- This equation holds for $K_e \leq \frac{2}{\gamma-1}$.
- We note that if $K = \frac{2}{\gamma-1}$, then the local pressure goes to zero, and local M is ∞.
- That is, physically a cavity (vacuum) exists within the flow.

Example Prediction of Oblique and Expansion Theory

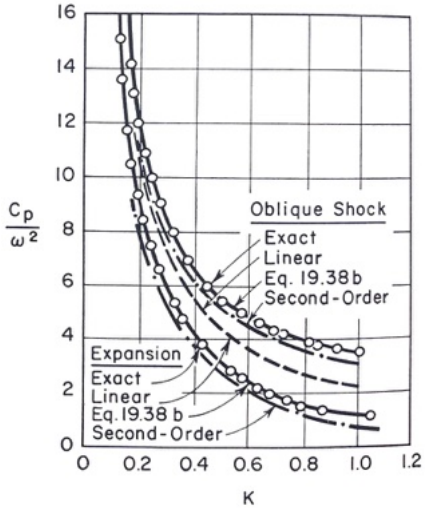

Figure 455: Pressure coefficient for oblique shocks and for Prandtl-Meyer waves.

Hypersonic Performance of 2D Profiles

Force and moment coefficients for a thin profile are found by first determining the c_p at each point on the surface. Integrate the profile and we can find the relations

$$c_l = \frac{1}{l} \oint c_p dx \tag{798}$$

$$c_d = \frac{1}{l} \oint c_p \frac{dy}{dx} dx \tag{799}$$

and

$$c_{\mathfrak{M}} = \frac{1}{l^2} \oint c_p x dx \tag{800}$$

Hypersonic Performance of 2D Profiles

For a plate with upper edge and no shock. Let $M_i = M_\infty, p_i = p_\infty$, and θ_e is ample of flow to the surface. From c_{pe} equation we find

$$c_p = \frac{2}{\gamma M_\infty^2}\left(\frac{p}{p_\infty} - 1\right) = \frac{2}{\gamma M_\infty^2}\left[\left(1 - \frac{\gamma - 1}{2}K\right)^{\frac{2\gamma}{\gamma-1}} - 1\right] \tag{801}$$

Recall $K = \delta M_\infty$. $\delta =$ thickness ratio. $\delta \propto$ angle of attack. We can then find

$$\frac{c_p}{\delta^2} = \frac{2}{\gamma K^2}\left[\left(1 - \frac{\gamma - 1}{2}K_e\right)^{\frac{2\gamma}{\gamma-1}} - 1\right] \tag{802}$$

Hypersonic Performance of 2D Profiles

- For a plate with lower edge with attached shock.
- Need to know conditions just behind the shock.
- Using the developed hypersonic relations we find the local pressure coefficient

$$c_p = \frac{2}{\gamma M_\infty^2}\left(\frac{p}{p_\infty} - 1\right) = \frac{2}{\gamma M_\infty^2}\left(\frac{p}{p_i}\frac{p_2}{p_1} - 1\right) \tag{803}$$

Substituting the relation for the ratio of pressures, $\frac{p}{p_i} = \left(1 - \frac{\gamma-1}{2}K\right)^{\frac{2\gamma}{\gamma-1}}$, $\frac{p_2}{p_1}$ with $c_{ps} = \frac{4}{\gamma+1}(\sin^2\sigma - 1/M_1^2)$ and use $K = M_\infty\delta$

Hypersonic Performance of 2D Profiles

We obtain

$$\frac{c_p}{\delta^2} = \left(\frac{K_s^2}{K^2}p_s + \frac{2}{\gamma K^2}\right)\left(1 - \frac{\gamma - 1}{2}K_e\right)^{\frac{2\gamma}{\gamma-1}} - \frac{2}{\gamma K^2} \tag{804}$$

where K_s and K_e are related to K, $K_e = M_i\theta_e$.

Similarity of simple wave expansion, K_s is the similarity for shock M_1, θ_s.

Let us Examine Some Results of our Theories

- Let $\alpha =$ angle of attack, then $K = M_\infty \alpha$
- For upper surface, $\delta = \alpha$ and $K_e = K$
- For lower surface, $\delta = \alpha$ and $K_s = K$

Making these substitutions we obtain

$$\frac{c_l}{\alpha^2} = \frac{c_d}{\alpha^3} = \frac{\gamma+1}{2} + \left(\left(\frac{\gamma+1}{2}\right)^2 + \frac{4}{K^2}\right)^{\frac{1}{2}} + \frac{2}{\gamma K^2}\left[1 - \left(1 - \frac{\gamma-1}{2}K\right)^{\frac{2\gamma}{\gamma-1}}\right] \tag{805}$$

The Flat Plate

- Lift curve is very linear for low M_∞
- Rapidly becomes parabolic
- As $M_\infty \to \infty$ then $c_l \to (\gamma + 1)\alpha^2$
- Recall incompressible case shows $c_l = 2\pi\alpha$

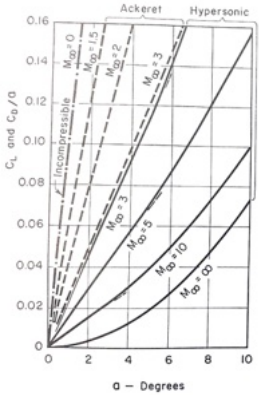

Figure 456

Profiles with Thickness

No easy way to find these analytically but measurements show the following. For a value of δ, maybe regarded as plots of c_l versus α for constant M_∞.

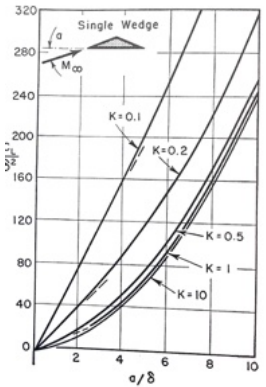

Figure 457: Variation of c_l with angle of attack (here denoted as a).

Important Aspects of Hypersonic Flows

- Single wedge is best performance
- Double wedge is the worst performance
- Pressure rise across shock is much greater than recovery through an expansion! (of equal turning angle)
- Aerodynamic forces most influenced by pressure via shocks
- Do not want shocks that radiate from upper surfaces of vehicle
- Best profiles have flat lower surfaces

Select Results

Experimental lift and drag of wings with double-wedge profiles and with delta and square planforms at $M_\infty = 6.9$.

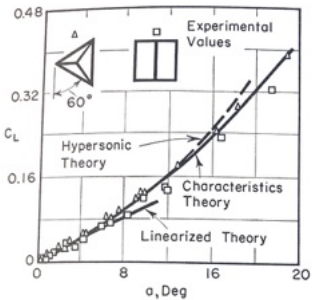

Figure 458

Select Results

Experimental lift and drag of wings with double-wedge profiles and with delta and square planforms at $M_\infty = 6.9$.

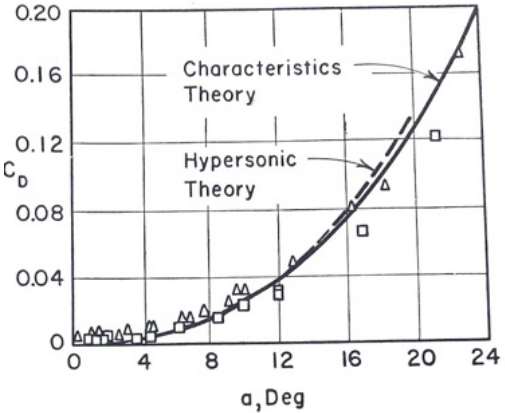

Figure 459

Select Results

Experimental lift and drag of wings with double-wedge profiles and with delta and square planforms at $M_\infty = 6.9$.

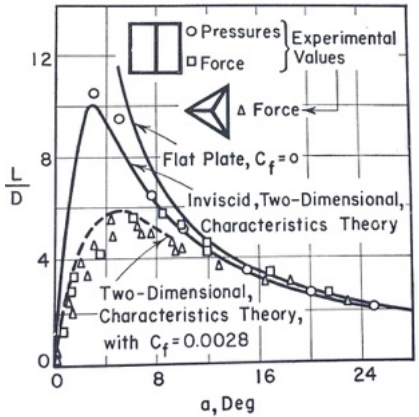

Figure 460

Select Results

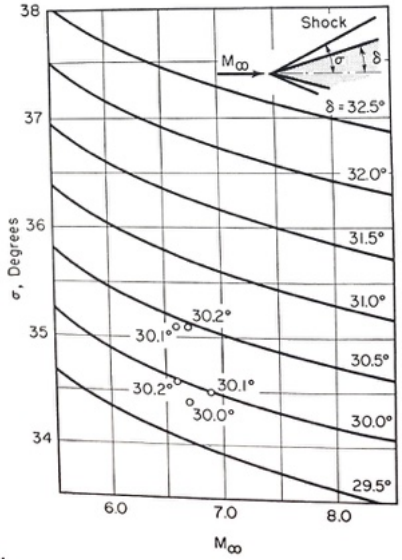

Figure 461: Experimental and theoretical shock wave angles for cones. Curves indicate theoretical results. Points indicate

Select Results

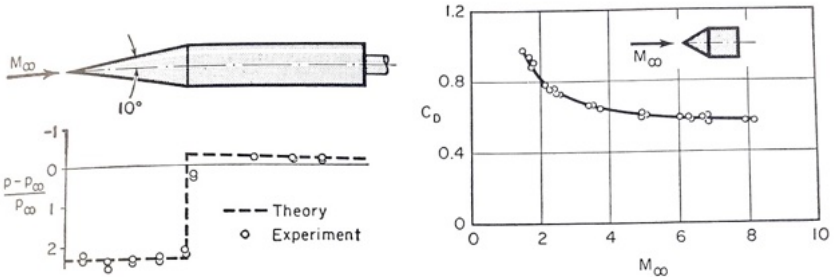

Figure 462: Experimental and theoretical pressure distributions on cone-cylinder at Mach 6.9. And drag coefficient of cone-cylinder versus Mach number.

Class Summary

- Newton
- *K* and similarity law
- Isentropic relations
- Oblique shocks
- Expansions

Next Time

- Leading edge bluntness
- Shock wave interaction
- Vorticity effects

Class Overview

Hypersonics

- Hypersonic heat-transfer
- Leading edge bluntness
- Shock wave interaction

“An engineering science aims to organize the design principles used in engineering practice into a discipline and thus to exhibit the similarities between different areas of engineering practice and to emphasize the power of fundamental concepts. In short, an engineering science is predominated by theoretical analysis and very often uses the tool of advanced mathematics.”

Qian Xuesen (in English Hsue-Shen Tsien or H.S. Tsien)

Heating Flight-Vehicles

Figure 463: Untested and tested Minuteman 1A reentry vehicle Source: Miller.

Hypersonic Heat Transfer

A few important points regarding work and heat transfer

- The drag work ultimately shows up as heat
- Work can be done over short or long periods of time
- Let us calculate the viscous heating for the boundary layer

Recall Newton's first law applied to an object decelerating in an atmosphere at hypersonic speed

$$\frac{W}{g}\frac{dV}{dt} = -D \tag{806}$$

where W is weight of the object, V is the flight velocity, g is the gravitational constant, and D is the total drag.

Hypersonic Heat Transfer

We define a heat transfer coefficient $\overline{C}_H$ through

$$\frac{dQ}{dt} = \overline{C}_H \rho V S \Delta h_o \tag{807}$$

where Q is the heat transferred to the object, ρ is the atmospheric density, S is the area the object is exposed to high-temperature gas, and ΔI is the enthalpy potential representing temperature difference which results in heat transfer from hot gas to cooler body.

We define $\Delta I = I_\infty - I_w$, where I_∞ is the stagnation enthalpy and I_w is the enthalpy of the air mixture at the object's surface temperature.

Hypersonic Heat Transfer

We define I_w is the enthalpy of the air mixture at the object's surface T

$$I_w = \int_0^{T_\infty} c_p dT \tag{808}$$

where c_p is the specific heat at constant pressure of the mixture and T_∞ is the ambient gas T.

The heat transfer rate is dependent on the body geometry, density or flight altitude, and flight velocity.

Hypersonic Heat Transfer

We are concerned with hypersonic speeds so our Mach numbers are large and we can approximate

$$\frac{u^2}{2c_pT_\infty} = \frac{\gamma - 1}{2}M^2 \geq 7.2 \text{ for } \gamma = 1.4 \tag{809}$$

where M is the Mach number as

$$M^2 = \frac{u^2}{\gamma RT_\infty} \tag{810}$$

We also note that T_w is on the same order of magnitude of T_∞, therefore

$$\delta I \approx u^2/2 \tag{811}$$

and $\overline{C}_H$ is proportional to the skin friction coefficient C_{DF}, we can write $C_H \approx C_{Df}$.

Hypersonic Heat Transfer

Combining equations we find a new law

$$dQ = -\frac{1}{2}\frac{C_{Df}}{C_D} D \left(\frac{W}{2g} u^2 \right) \tag{812}$$

where D is the drag given as

$$D = D_p + D_f = C_D \rho u^2 S/2 \tag{813}$$

and D_p is the drag due to stresses.

Hypersonic Heat Transfer

Integrating Eqn. 812 and finding Q_f

$$Q_f = \frac{1}{2}\frac{C_{Df}}{C_D}\frac{1}{2}\frac{W}{g}u_i^2 \tag{814}$$

where the subscript f denotes the final value of the heat transferred to the body after it has spent its kinetic energy and i denotes the initial value.

- As a first approximation, we assume that $u_f = 0$ and $q_i = 0$.
- The heat transferred to an object decelerating at hypersonic speeds within an atmosphere is proportional to the product of its initial kinetic energy and the ratio of the friction drag coefficient to the total drag coefficient.
- Try to minimize c_{Df}/c_D to lower heating.

Let us examine the implication of this equation.

Hypersonic Heat Transfer

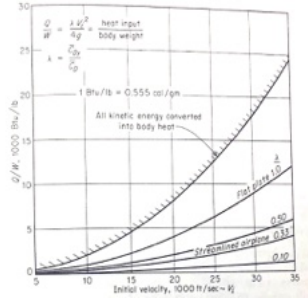

Figure 464: Heat transferred to a decelerating body at hypersonic speeds.

- Typical values of c_{Df}/c_D are 0.01 for a sphere, 0.33 for a streamlined airplane, and 1.0 for a flat plate.
- Total heat transferred can exceed the heat capacity of most known refractory materials,
- Examine typical values of heat capacity of aerospace materials.

Hypersonic Heat Transfer

Material	Total heat capacity from 312°K through vaporization, in cal/g	Total heat capacity† from 560°R through vaporization, in Btu/lb
Graphite	15,950 (up to 3980°K)	28,700 (up to 7160°R)
Beryllium oxide	7,450	13,400
Magnesium oxide	5,600	10,090
Silicon carbide	3,920	7,050
Titanium	2,145	3,865
Molybdenum	1,990	3,580
Zirconium	1,522	2,740
Tantalum	1,232	2,220
Tungsten	1,040	1,870

† Heat capacities except for that of graphite provided by AVCO Research and Development Division, Wilmington, Mass.

Figure 465: Heat capacities of some refractory materials.

Hypersonic Heat Transfer

- Theoretical maximum heat capacity of any material is never realized in applications of the type being discussed due to the non-uniform heat distribution
- Our analysis shows that blunt and non-streamlined objects are to be used if high amounts of heating are to be avoided
- A sphere might serve the shape of such object
- Communication with such objects are difficult due to ionization of the gas and luminosity of the gas in the wake of the object!
- Streamlining the object may result in excessive high heat transfer rates and a compromise must be made between the heat protection system and the shape of the object

Hypersonic Heat Transfer

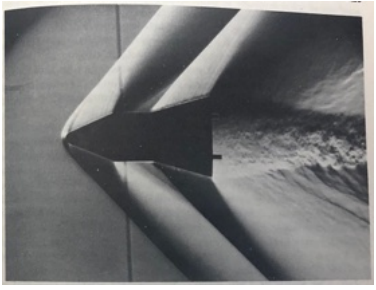

Figure 466: Model reentry shape in ballistic range. Shadowgraph of AVCO Corp.

Hypersonic Heat Transfer

- The nose is blunted in order to reduce heat transfer rates in that region
- The aft cone frustum (the portion of a cone or pyramid that remains after its upper part has been cut off by a plane parallel to its base, or that is intercepted between two such planes) provides aerodynamic stability
- Majority of heating occurs in the thin viscous boundary layer next to the body
- We care about the amount of heat and heat transfer rate to the body

Bluntness and Shockwave Interaction

- We shall now concern ourselves with problems associated with heating of the leading edge
- We will derive equations for the effect of the interaction of the leading edge shock and the boundary layer upon the skin friction and heat transfer
- The boundary layer has a displacement effect in the sense that the shape of the body is altered or enlarged because of the reduced mass flux in the BL
- This displacement is the thickness δ^*

Bluntness and Shockwave Interaction

We define the following

$$\rho_e u_e(\delta - \delta^*) = \int_0^\delta \rho u dy \text{ with } \delta \to \infty \tag{815}$$

and solving for δ^*

$$\delta^* = \int_0^\infty \left(1 - \frac{\rho u}{\rho_e u_e}\right) dy \tag{816}$$

Note that in a hypersonic turbulent boundary layer $T_W >> T_\infty$ and the displacement thickness approaches the δ

Bluntness and Shockwave Interaction

- p and M at the edge will vary with s as they would if replaced by a shape defined by the boundary layer edge.
- Let us determine the p at the edge of the boundary layer

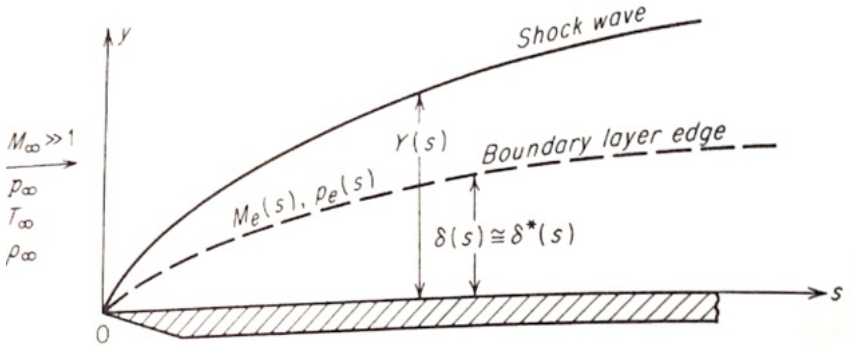

Figure 467: Interaction between the leading-edge shockwave and the boundary layer flow over a flat plate.

Bluntness and Shockwave Interaction

For 2D objects (similarly for 3D) if $M_\infty >> 1$ and $M_\infty d\delta^*/ds << 1$ then

$$\frac{p_e}{p_\infty} = 1 + \gamma M_\infty \frac{d\delta^*}{ds} + \frac{\gamma(\gamma+1)}{4}\left(M_\infty \frac{d\delta^*}{ds}\right)^2 + ... \tag{817}$$

and for $M_\infty >> 1$ and $M_\infty d\delta^*/ds >> 1$ using oblique shock relations

$$\frac{p_e}{p_\infty} \approx \frac{\gamma+1}{2}\gamma\left(M_\infty \frac{d\delta^*}{ds}\right)^2 \tag{818}$$

Unfortunately, p_e/p_∞ is also dependent by δ^*, which is the problem!

Bluntness and Shockwave Interaction

For laminar boundary layers that are compressible in the absence of leading edge shock interaction we can write

$$\delta^{*2} \approx \frac{\overline{\mu} s}{\overline{\rho} u_e} \tag{819}$$

where $\overline{u}$ and $\overline{\rho}$ are averages. Given some approximation that $u_e \approx u_\infty$ and $\overline{p} \approx p_e$ we can write the equation as

$$\delta^{*2} \approx C M_\infty^4 \frac{p_\infty}{p_e} \frac{s^2}{R_\infty} \tag{820}$$

where R is the Reynolds number. We can write

$$\frac{d\delta^*}{ds} \approx \frac{\delta^*}{s} \tag{821}$$

Bluntness and Shockwave Interaction

- From this analysis there are two extremes: The weak interaction case and the strong interaction case for $M_\infty d\delta^*/ds << 1$ and $M_\infty d\delta^*/ds >> 1$, respectively.
- There are now two major results for both these cases

For weak interactions

$$\frac{p_e}{p_\infty} - 1 \approx \overline{\Xi} \tag{822}$$

and for strong interactions

$$\frac{p_e}{p_\infty} \approx \overline{\Xi} \tag{823}$$

where $\overline{\Xi} = C^{1/2} M_\infty^3 Re_\infty^{-1/2}$

Bluntness and Shockwave Interaction

We have three major conclusions from this analysis

- $\overline{\Xi} = C^{1/2} M_\infty^3 Re_\infty^{-1/2}$ is the similarity parameter for the theory of hypersonic leading edge shock waves
- For strong interactions $\delta^* \propto s^{3/4}$
- Distance from leading edge is s
- For strong interactions $p_e/p_\infty \propto s^{-1/2}$

This relation holds for similarity solutions beyond the boundary layer and is valid between the boundary layer and shock front

Bluntness and Shockwave Interaction

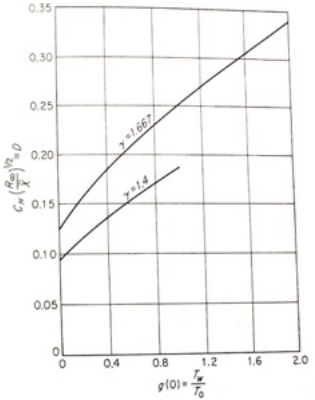

Figure 468: Variation of heat transfer coefficient with surface temperature in the strong-interaction region.

Bluntness and Shockwave Interaction

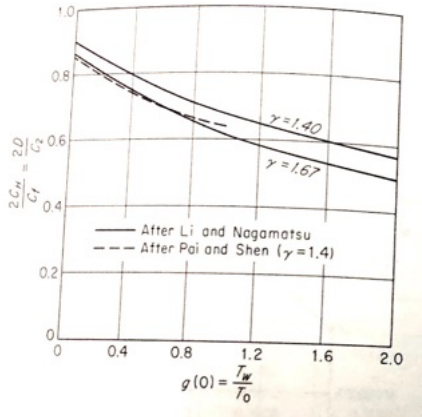

Figure 469: Effect of surface temperature on the ratio $2c_H/c_f$ in the strong interaction region.

Bluntness and Shockwave Interaction

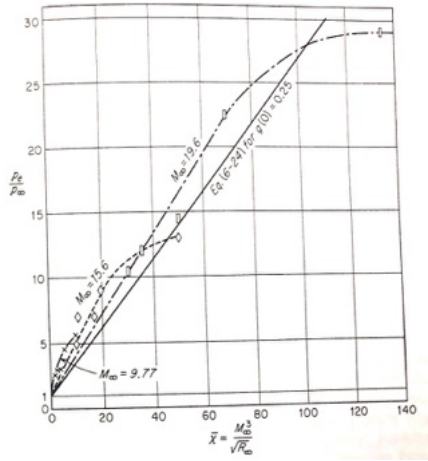

Figure 470: Comparison between theory and measurements of flat-plate surface pressure.

Bluntness and Shockwave Interaction

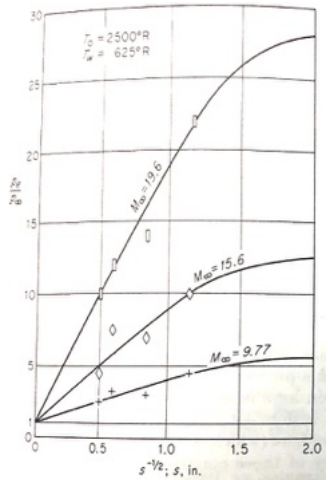

Figure 471: Measured variations of flat surface pressure with distance from the leading edge.

Bluntness and Shockwave Interaction

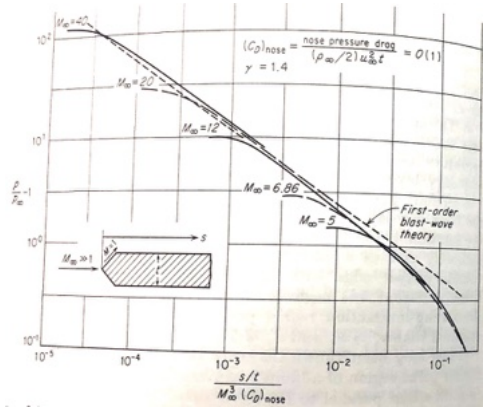

Figure 472: Effect of leading edge bluntness upon pressure distribution of inviscid flow over a flat plate.

Class Summary

- Hypersonic heat-transfer
- Leading edge bluntness
- Shock wave interaction

Next Time

- Special topics

Class Overview

Supersonic Flow Past Wings of Finite Span

- Regions of Two-Dimensional Flow on Supersonic Wings
- Supersonic and Subsonic Leading and Trailing Edges
- Sweep
- Similarity Theory for Supersonic Wings

“It makes me happy to remember that long ago, at the beginning of aviation, Heaven granted me the opportunity to make significant contributions to aerodynamics.” Max Munk, NACA (NASA Langley)

Basic History

- Wing sweep at high speeds was first investigated in Germany as early as 1935
- Swept wings became common on advanced first-generation jet fighters like the MiG-15 and F-86 Sabre
- Delta wing also incorporates the same advantages
- The idea of using swept wings to reduce high-speed drag was developed in Germany in the 1930s. At a Volta Conference meeting in 1935 in Italy, Dr. Adolf Busemann
- Albert Betz immediately suggested the same effect would be equally useful in the transonic regime
  - The host of the meeting, Arturo Crocco, jokingly sketched“Busemann’s airplane of the future” on the back of a menu

Adolf Busemann

20 April 1901 – 3 November 1986, German (American Immigrant)

- Joined the team led by Ludwig Prandtl, including Theodore von Kármán, Max Munk and Jakob Ackeret
- Discovered benefits of swept wings
- Operation paperclip
- Busemann started studies of airflow around delta wings
- Moved to the United States in 1947 and started work at NACA Langley Research Center
- Busemann - later a professorship at the University of Colorado and suggested the use of ceramic tiles on the space shuttle

S.A.E. Miller, Ph.D., saem@ufl.edu

Examples of Swept Wings

Figure 4.75: A-B-47 (public domain photo).

Examples of Swept Wings

Figure 474: A Grumman X-29. The aerodynamic instability of the X-29's airframe required the use of computerized fly-by-wire control (Source NASA).

Supersonic Flow Past Wings of Finite Span

- With MOC, we can find the supersonic flow past two-dimensional infinite span airfoils
- Will survey methodologies to find supersonic flow past wings of finite span
- Only analytical method is the method of small perturbations
  - Assume - Only first order effects in fluids are important and that the airfoil is very thin
  - Assume - Viscous effects are not important
  - Assume - The flow is irrotational and isentropic
- We will find good approximations to actual aerodynamic forces
  - Unless the BL separates or exhibits rapid growth
- Recall the region of influence, that disturbances in supersonic flow only occur within the Mach cone

Regions of Two-Dimensional Flow on Supersonic Wings

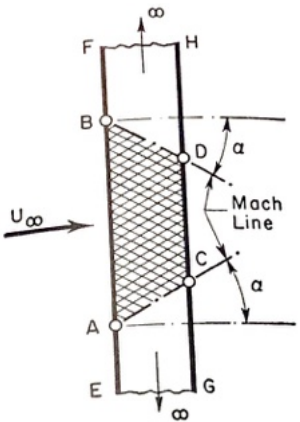

Figure 475: Wing of finite span which is thin. Note that wake is three-dimensional. Note region of influence of wing which is two-dimensional. Shaded regions represent two-dimensional flow.

Regions of Two-Dimensional Flow on Supersonic Wings

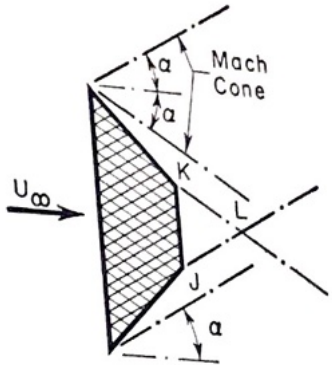

Figure 476: An unswept wing with ends that are un-raked, the flow over the entire plane-form is entirely in two-dimensions.

Regions of Two-Dimensional Flow on Supersonic Wings

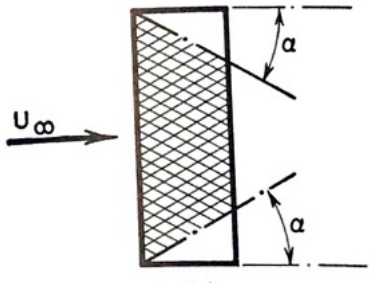

Figure 477: An unswept wing with ends within the tip Mach cone, the flow is two-dimensional except within the tip Mach cones.

Regions of Two-Dimensional Flow on Supersonic Wings

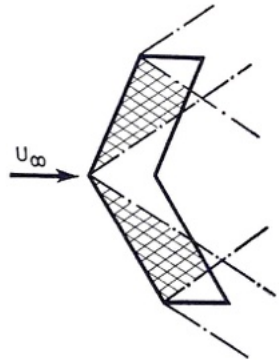

Figure 478: An infinite span wing that is swept back then the flow will appear two-dimensional to an observer moving along the span at such a speed that in the observer's coordinate system the oncoming flow was normal to the spanwise direction.

Regions of Two-Dimensional Flow on Supersonic Wings

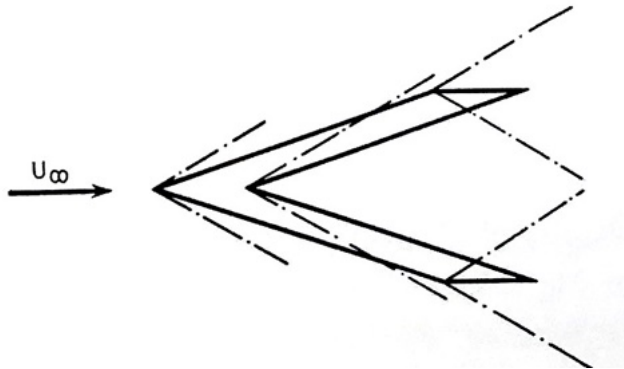

Figure 479: If the leading edges of a swept wing were swept behind the Mach line from the forward point then no part of the flow would be two-dimensional.

Regions of Two-Dimensional Flow on Supersonic Wings

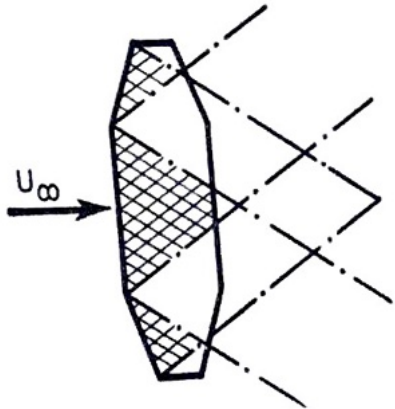

Figure 480: Remember the disturbances originate and propagate in the region of influence of the Mach cones.

Supersonic and Subsonic Leading and Trailing Edges

- Consider a swept wing of infinite span
- We resolve the free-stream velocity into components of u_∞
- A fluid parcel moving along the span with uniform speed $u_{\infty,n}$ observes a two-dimensional flow with free-stream velocity $u_{\infty,n}$ past an unswept wing

Recall that $c_\infty = u_\infty \sin \alpha_\infty$ (α is free-stream Mach angle, μ is sweep angle) and $u_{\infty,n} = u_\infty \sin \mu$, we find the following

$$M_{\infty,n} = \frac{u_{\infty,n}}{c_\infty} = \frac{\sin \mu}{\sin c_\infty} \tag{824}$$

- The equivalent two-dimensional flow is supersonic if μ exceeds the Mach angle
  - It is subsonic if $\mu < \infty$
- For example, we state that the leading edge is supersonic while the other is subsonic (though it is supersonic flow!)

Supersonic and Subsonic Leading and Trailing Edges

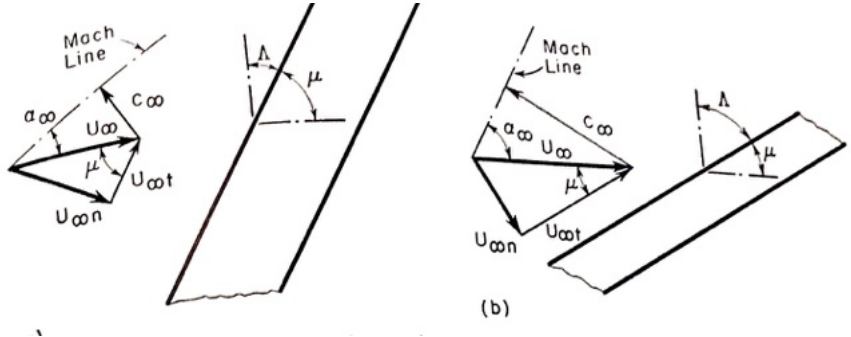

Figure 481: In (a) we observer the so-called supersonic leading edge and in (b) we observe the so-called subsonic leading edge.

Supersonic and Subsonic Leading and Trailing Edges

This notation is significant due to how lift is generated.
Let us illustrate on the flat plate case

- The pressure at the trailing edge of the airfoil is equal
- The circulation is determined by the Kutta-Joukowski condition
- In supersonic flow, the lift distribution is constant over the chord (in the context of this simplified theory)
- This leads to the following
  - Supersonic leading and trailing edges have finite lift loading
  - A subsonic leading edge tends to have a very high lift loading and a negative drag force
  - A sharp subsonic trailing edge has zero lift loading

Supersonic and Subsonic Leading and Trailing Edges

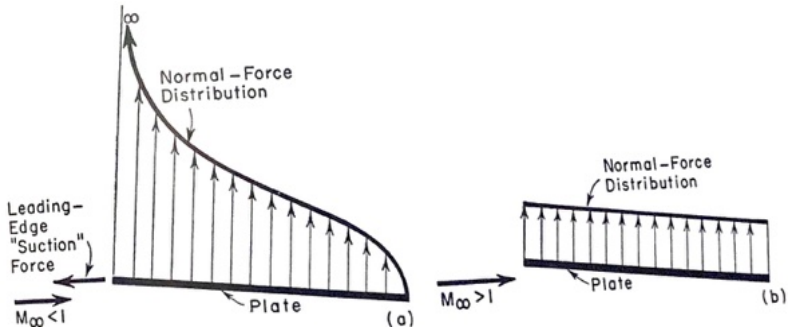

Figure 482: The chordwise distribution of p on a flat plate at non-zero α. (a) subsonic and (b) supersonic.

Superposition Effects

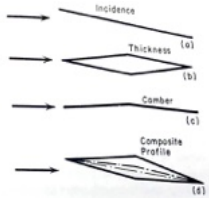

Figure 483: Summation of effects using a linearized decomposition.

- If we use a perturbation theory of aerodynamics we can superimpose solutions
- We can add effects due to incidence, thickness, camber, and find the perturbed pressure distribution of the composite profile
- Portion of the boundary which has a subsonic leading edge should have a rounded nose to avoid a large drag
- Supersonic leading edges should have a sharp shape to avoid the large pressure drags due to detached shocks

Supersonic and Subsonic Leading and Trailing Edges

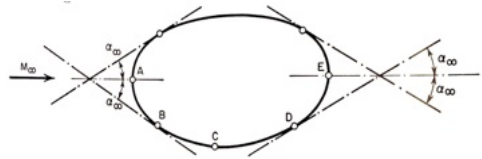

Figure 484

- Curve $A - B$ is the supersonic leading edge as flow is like that near the leading edge of a supersonic normal wing of infinite span
- Line $D - E$ is the supersonic trailing edge for the same reasons
- Boundary $B - C$ is a subsonic leading edge as the velocity component normal to the edge is less than c
- Between C and D the boundary is a subsonic trailing edge
- Disturbances propagate from points along $C - D$, cover part of the planform, and the flow can adjust as to satisfy the Kutta-Joukowski condition

Sweptback Wings

Swept wing at angle A and angle of attack α, where we resolve M_∞ into three components:

- On the plane of the wing and normal to the edge
- Normal to the plane of the wing
- In the plane of the wing and tangential to the leading edge

Sweptback Wings

An observer moving in the span direction the flow appears two-dimensional and may be treated (except the BL).

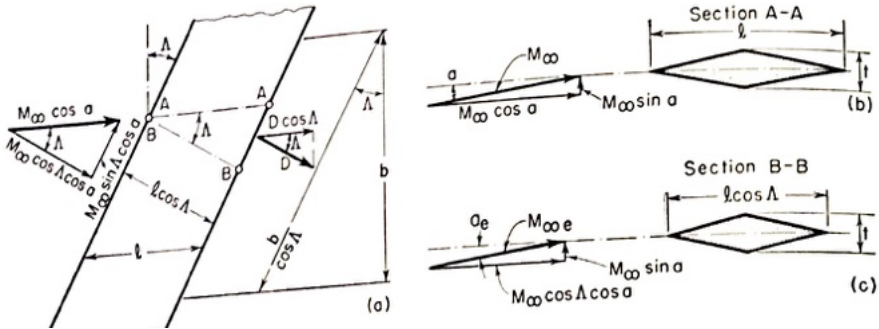

Figure 485

Sweptback Wings

Let subscript e denote flow quantities observed by the moving observer. Using the previous figure we can write

$$\begin{aligned} M_{\infty,e} &= \sqrt{(M_\infty \sin a)^2 + (M_\infty \cos a \cos A)^2} \\ &= M_\infty \sqrt{1 - \sin^2 A \cos^2 a} \end{aligned} \tag{825}$$

Solving for a_e the angle of attack observed by the observer yields

$$a_e = \tan^{-1} \frac{\tan a}{\cos A} \tag{826}$$

and

$$\delta_e = \frac{t}{l \cos A} = \frac{\delta}{\cos A} \tag{827}$$

where δ is the thickness ratio in the plane parallel to u_∞.

Sweptback Wings

The lift is not changed by a observer's motion we can write lift as

$$c_l = \frac{L}{\gamma p_\infty M_\infty^2 lb/2} \tag{828}$$

and

$$c_{le} = \frac{L}{kp_\infty M_{\infty e}^2 l \cos Ab/\cos A/2} \tag{829}$$

which can be simplified to

$$c_l = c_{le} = (M_{\infty,e}/M_\infty^2 = c_{l,e}(1 - \sin^2 A \cos^2 a) \tag{830}$$

Sweptback Wings

If we neglect the tangential velocity influence on drag then we can write the drag coefficients as

$$c_D = \frac{D \cos A}{\gamma p_\infty M_\infty^2 lb/2} \tag{831}$$

or

$$c_{D,e} = \frac{D}{\gamma p_\infty M_\infty^2 l \cos A b/\cos A/2} \tag{832}$$

and written concisely as

$$c_D = c_{D,e} \cos A \frac{M_{\infty,e}}{M_\infty}^2 = c_{D,e} \cos A (1 - \sin^2 A \cos^2 a) \tag{833}$$

We have found equations that take the geometrical relationships and are correct for large angles of attack. We can find values of M_e, a_a, and δ_e from the properties of the incoming flow and wing angle.

Sweptback Wings - Small Angle of Attack

- The total drag coefficient is found from adding the skin friction coefficient c_f, eg $c_{D,total} = c_D + c_f$.
- When the angle of attack is small ($a \approx \epsilon$) then we can write the small angle approximations.
- $\cos a \approx 1$, $\tan a \approx a$, and $\arctan a_e \approx a_e$
- We can then write
  - $M_{\infty,e} \approx M_\infty \cos A$ and $a_e \approx a / \cos A$.

Then our lift and drag formulas become

$$c_l = c_{l,e} \cos^2 A \tag{834}$$

$$c_{D,total} = c_{D,e} \cos^2 A + c_f \tag{835}$$

Thin Airfoil at Small Angle of Attack

If the thickness is small and the angle of attack is small then linear theory yields

$$c_L = \frac{4\cos A}{\sqrt{M_\infty^2 \cos^2 A - 1}} a \tag{836}$$

and

$$C_{D,total} = \frac{4\cos A}{\sqrt{M_\infty^2 \cos^2 A - 1}} a^2 + \frac{4\cos^3 A}{\sqrt{M_\infty^2 \cos^2 A - 1}} K\delta_e^2 + c_f \tag{837}$$

The first term here represents induced drag due to lift. The second term is the wave drag due to thickness.

Thin Airfoil at Small Angle of Attack

Let us example the derivative dc_l/da (change of lift with angle of attack).

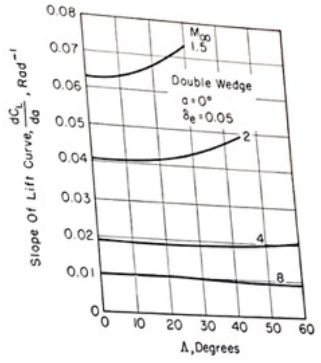

Figure 486: Ivey and Bowen of NACA.

Clearly there is a gain in lift due to increasing sweep at low supersonic Mach numbers! Sweepback is seen to yield substantial improvements in performance.

Similarity Theory for Supersonic Wings

- We will derive a rule by which the flow pattern around any thin wing at small incidence in a supersonic flow is related to the flow past an affinely related wing at $M_\infty = 2^{1/2}$.
- For supersonic flow with only small perturbations from the uniform flow in the x direction, the velocity potential perturbation equation is

$$-\beta^2 \frac{\partial^2 \phi}{\partial x^2} + \frac{\partial^2 \phi}{\partial y^2} + \frac{\partial^2 \phi}{\partial z^2} = 0 \tag{838}$$

where $\beta = \sqrt{M_\infty^2 - 1}$, which is often called the 'off-design parameter.' We now introduce transforms

$$x' = x;\ y' = \beta y;\ z' = \beta z;\ \phi'(x', y', z') = \beta^2 \phi(x, y, z) \tag{839}$$

Similarity Theory for Supersonic Wings

The transformed equation is now

$$-\frac{\partial^2 \phi'}{\partial x'^2} + \frac{\partial^2 \phi'}{\partial y'^2} + \frac{\partial^2 \phi'}{\partial z'^2} = 0 \tag{840}$$

- It is clear that the original equation and the transformed equation are the same when $M_\infty = \sqrt{2}$.
- It is inferred then that the factor β corresponds to dimensions of the lateral dimensions of the body that are larger than the original body.

Similarity Theory for Supersonic Wings

The linearized pressure coefficients at corresponding points in the two flows are affinely related as

$$c_p' = -\frac{2}{u_\infty}\frac{\partial \phi'}{\partial x'} = -\frac{2}{u_\infty}\beta^2\frac{\partial \phi}{\partial x} = \beta^2 c_p \tag{841}$$

where c_p' is the pressure coefficient at $M_\infty = 2^{1/2}$ for a body whose lateral dimensions are β times larger than the corresponding lateral dimensions of the body whose corresponding c_p at $M = 2^{1/2}$.

Similarity Theory for Supersonic Wings

The similarity rule summarized

$$c_p = \frac{1}{\beta} c_p \text{ at } M = \sqrt{2}; \text{ with } \beta AR \tag{842}$$

"The pressure coefficient at any given point for a flow at M past a given wing is greater by a factor of β^{-1} than the pressure coefficient at a corresponding point for a flow at Mach $\sqrt{2}$ past a wing which is alike in all respects expect that its aspect ratio is greater by a factor β than the original wing."
Note identical rules hold for c_m and c_d. All variables will form in a combination of $\beta \times AR$.

Similarity Theory for Supersonic Wings

Let us consider a geometric interpretation. For example, refer to the rectangular planform the fraction of the span at the trailing edge for which two-dimensional flow exists is given by

$$\frac{b_1}{b} = \frac{b - 2l/\sqrt{M_\infty^2 - 1}}{b} = 1 - \frac{2l}{b\sqrt{M_\infty^2 - 1}} = 1 - \frac{2}{AR\beta} \tag{843}$$

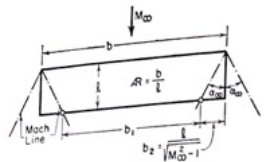

Figure 487: Proportion of two-dimensional flow depends on $AR\beta$.

For supersonics, solve for the supersonic flow past thin wings for the case of $M_\infty = 2^{1/2}$ then the general result is found by replacing the term AR by the term $AR\beta$.

Example Calculations Notation

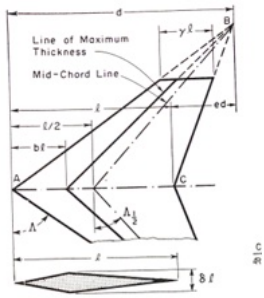

Figure 488

Example Calculations

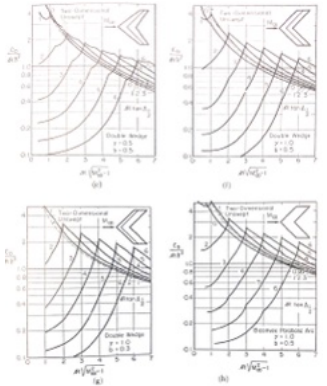

Figure 489: Wave drag of thin non-lifting wings having straight leading and trailing edges and the same dimensionless profile in all chordwise planes from Lawrence.

Class Summary

- Regions of Two-Dimensional Flow on Supersonic Wings
- Supersonic and Subsonic Leading and Trailing Edges
- Sweep
- Similarity Theory for Supersonic Wings

Next Time

- Schlieren concepts
- Types of schlieren
- Sensitivity

Class Outline

- Schlieren concepts
- Types of schlieren
- Sensitivity

This class is based on the book of Prof. G. S. Settles, “Schlieren and Shadowgraph Techniques,” Springer, 2001.

Introduction

- Our eyes do not perceive phase difference
- Light propagates uniformly through homogeneous media
- Inhomogeneity in atmosphere causes light to refract
- Light speed slows with interaction with matter
- $n = c_o/c$ is the refractive index where c is the speed of light in the medium and c_o is the speed of light in a vacuum
- There is a linear relationship between n and density of the gas ρ, $n - 1 = k\rho$, where k is the Gladstone-Dale coefficient which is 0.23 cm^3/g for air at standard conditions

Introduction

- In gasses k varies from 0.1 to 1.5
- Refractivity of a gas is defined as $n - 1$

Optical inhomogeneities refract or bend light in proportion to the gradients of refractive index in the $x - y$ plane and are governed by

$$\frac{\partial^2 x}{\partial z^2} = \frac{1}{n}\frac{\partial n}{\partial x} \tag{844}$$

and

$$\frac{\partial^2 y}{\partial z^2} = \frac{1}{n}\frac{\partial n}{\partial y} \tag{845}$$

Introduction

Upon integration we find components of the angular ray deflection in the x and y directions For two-dimensional schlieren of extend L along the optical axis we find

$$\epsilon_x = \frac{L}{n_o}\frac{\partial n}{\partial x} \tag{846}$$

and

$$\epsilon_y = \frac{L}{n_o}\frac{\partial n}{\partial y} \tag{847}$$

where n_o is the refractive index of the ambient gas.

- Note that knowledge of the inhomogeneous region does not rely on the knowledge of ray deflection
- This is the mathematical foundation of schlieren and shadowgraphy

Schlieren

- Schlieren are the name for the gradient disturbances of the inhomogeneous transparent media
- Schlieren occur in solids liquids and gases
- Shadowgraphs or shadowgrams are images of shadows
- Schlieren are responsive to the first partial derivative of the refractive index ($\partial n/\partial x$)
- Shadowgraphs are responsive to the second partial refractive index ($\partial^2 n/\partial x^2$)

Direct Shadowgraphy

Only a light source and point schlieren object projected onto a screen

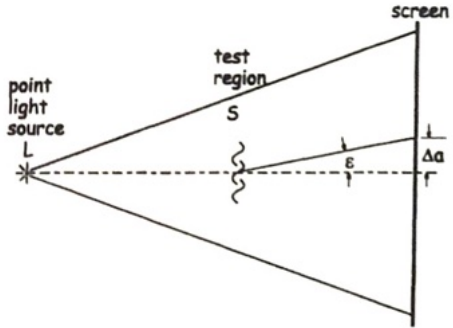

Figure 490: Direct shadowgraph method.

Some rays are bent by refraction angle ϵ which displaces it on the screen by Δa.

Direct Shadowgraphy

Adding a lens collimates the light from a point source into a series of parallel rays in the z direction over S

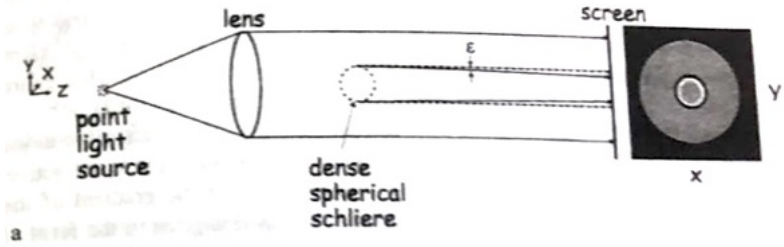

Figure 491: Parallel light shadowgraph of a dense transparent sphere.

This approach is called the ‘direct shadowgraphy’

Extended Light Source

A second lens focuses the beam to an image of a point source A knife edge is added to the focus of the second lens, which is often a razor blade.

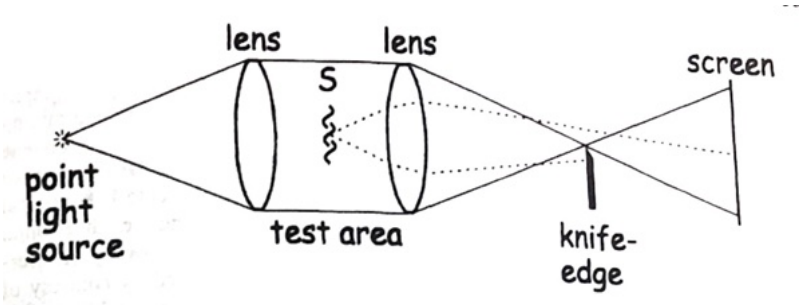

Figure 492: Simple schlieren with a point light source.

The knife edge blocks the entire image if *S* is not present. Adding *S* bends the light around the knife edge

Effect of Knife Edge Orientation

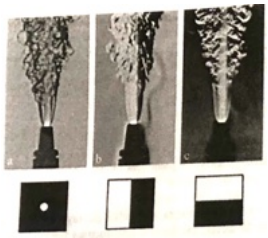

Figure 493: Schlieren showing a circular cut-off, vertical knife edge, and horizontal knife edge.

Extended Light Sources

- Now, an additional lens is added to the system.
- Incoherent beam of white light originates from the source in the form of a rectangular slit in the $x - y$ plane.

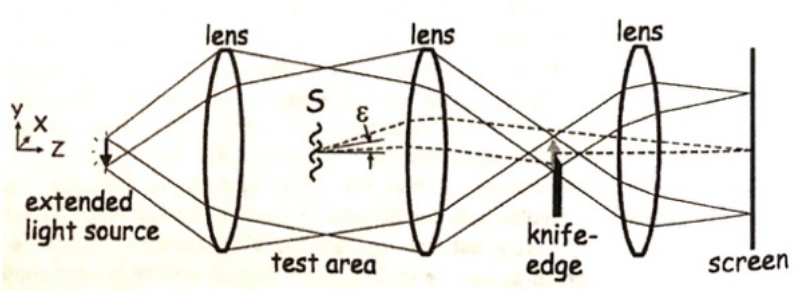

Figure 494: Diagram of a simple schlieren system with an extended light source.

Displaced Images

The amount of the knife-edge cut-off of the undisturbed source image sets the background level of the illuminance on the screen

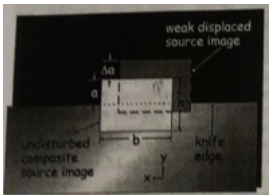

Figure 495: Knife-edge plane. Rectangular image is shown half cut-off with height a remaining obscured by a knife edge. Due to refraction a weak elemental source image is shifted to the upper right and is unobscured by height $a + \Delta a$.

The illuminance E is linearly proportional to the amount of the knife-edge cut-off, $\Delta a = f_2 \epsilon_y$, where f_2 is the focal length of the second lens.

Toepler's Schlieren Technique

- Toepler's technique denotes systems that have advanced from the time of simple lens and mirror systems
- Lays his system in three sections: illuminator, schlieren head, and analyzer
- Variety of modern techniques are possible with this approach in different configurations
- We seek to understand the basic steps of this process

Lens and Mirror Type Systems

- Modern multi-element lenses require high internal quality and surfaces to near-perfection
- Mirrors only need to be polished and need minor internal quality
- Mirrors are favored for los cost and when field-of-view are considered
- Largest lens type systems are typically in the range of 20 cm in diameter
- Larger systems are almost always mirror based

Mirror and Lens Cost

Exponential rise in cost with diameter

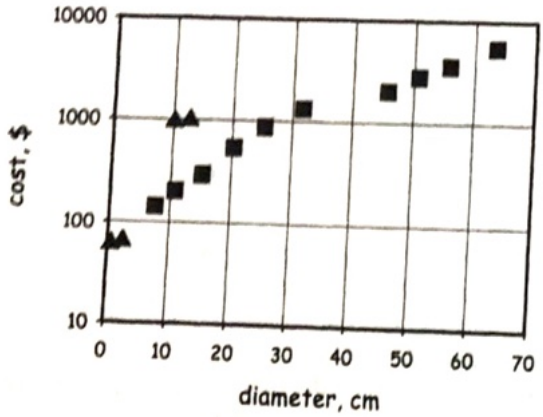

Figure 496: Cost in USD vs diameter for lenses (triangles) and parabolic mirrors (squares) from the year 2000. Need to adjust for today's figures!

Lens Systems

- Lens systems are prefered but unfortunately imperfections can mask sensitive density changes
- Because of the cost of lenses sometimes a single lens system is useful
- Unfortunately then only non-parallel light is used over the object *S*

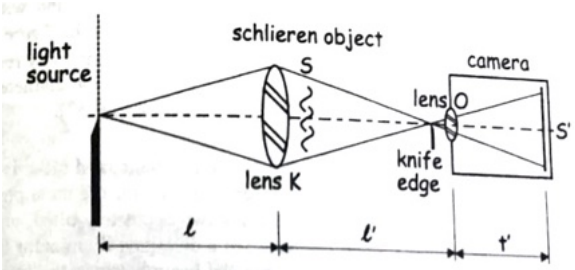

Figure 497: Toepler's single field lens schlieren arrangement.

Dual Lens

- A more improved setup uses dual field lens
- Parallel light in the test area is a major improvement
- Provides the least ambiguous interpretation of $\Delta a = f_2 \epsilon$
- Note also the use of a lamp with a condenser lens and slit to produce a well defined effective light source

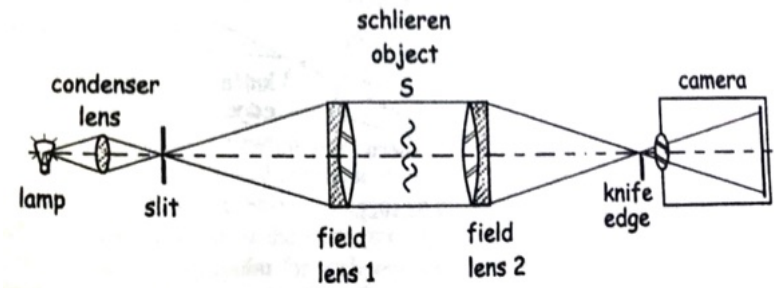

Figure 498: Dual field lens schlieren arrangement.

Mirror Systems

- Parabolic mirrors for telescopes also make wonderful schlieren mirrors
- The Z-Type 2 mirror schlieren system is one of the most popular types
- Parabolic off-axis concave mirrors are often used
- Consists of two oppositely titled on-axis telescopic parabolas
- The name ‘Z’ is derived from the shape of the system...

A Mirror

Figure 499: Professor Miller's Ph.D. student Mr. Alex Carr standing by a schlieren mirror at the FSU Polysonic Wind Tunnel in 2018.

Z-Type Schlieren Arrangement

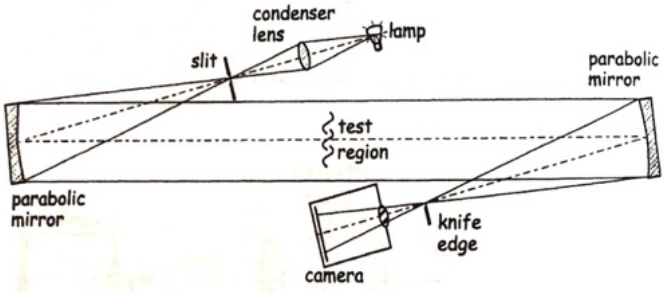

Figure 500: Z-Type Schlieren Arrangement

Aberrations

- The off-axis parabola mirrors are more expensive and are typically not used
- A minimum distance between mirrors is required at about $2f$, where f is the mirror focal length
- Use of on-axis parabola mirrors results in aberration errors that grow as a function of angle θ and the inverse square of the mirror f/n_o for given θ

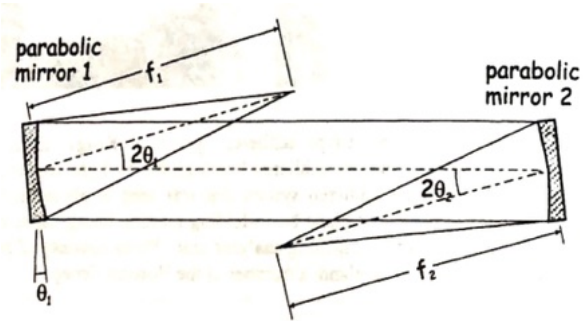

Figure 501: Z-type schlieren optics to illustrate aberrations.

Single Mirror Coincident System

- Other popular systems use mirrors but without the benefit of parallel light
- The most popular is the single mirror coincident system of Taylor and Waldram
- This is sometimes called the autocollimating system
- It uses a single spherical field mirror with light source at $R = 2f$
- A reflecting knife edge or beamsplitter is used to deflect the returning rays
- Ideally the test plane is transversed twice by the same ray
- Lack of parallel light in the test area is a disadvantage that hurts applications and accuracy
- Major advantage is use of only one mirror

Single Mirror Coincident System

Only one mirror but non-parallel light beams

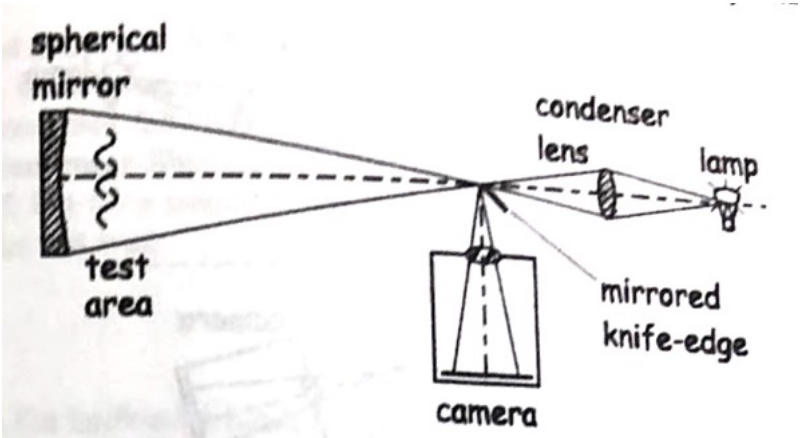

Figure 502: The single mirror coincident schlieren system

The Off-Axis Single Mirror System

- A single mirror can be used well-off axis
- The test area is positioned in the illuminator or analyzer beam
- Few have used it and it is rare
- The off-axis aberrations are worse than other systems
- Typically needs mirrors twice as large as normally required but can be used when other approaches are difficult

The Off-Axis Single Mirror System

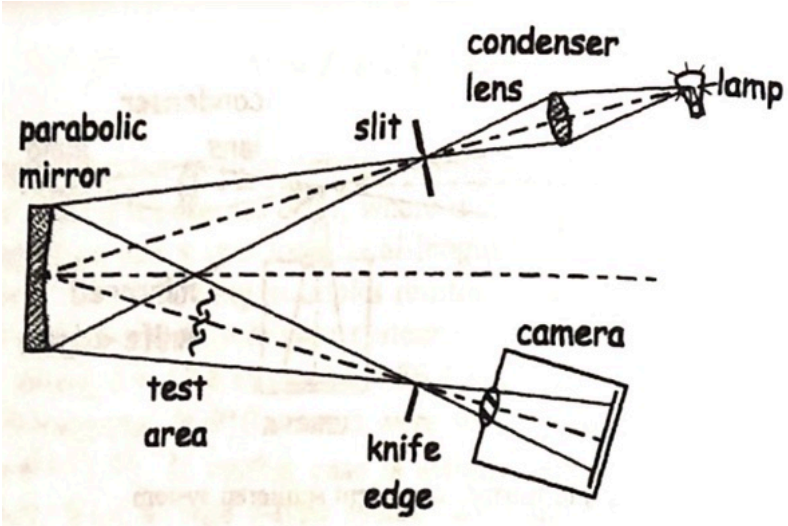

Figure 503: Single mirror off-axis schlieren system.

Sensitivity

- Let us examine the Z-type schlieren system
- We use a horizontal source slit and horizontal knife edge

The luminance B from the light source can be used to find the illuminance E_o upon the first mirror through the inverse square law

$$E_o = \frac{Bbh}{f_1^2} \tag{848}$$

where b and h are the breadth and height of the source slit and f_1 is the focal length of the first mirror If we include the magnification factor m that accounts for the size of the image relative to the test area then

$$E_o = \frac{Bbh}{m^2 f_1^2} \tag{849}$$

Sensitivity

If the knife edge blocks all but the part of the light at the second mirror focus which has part a then we replace h with $f_1/f_2 a$ to describe the unobstructed height of the light source

$$E = \frac{Bba}{m^2 f_1 f_2} \tag{850}$$

All schlieren images have a background illuminance or amplitude level E in the middle of the gray scale range.
If a object is placed at S then the image should shift by $\Delta a = \epsilon_y f_2$ then the change in illuminance from the ray is

$$\Delta E = \frac{f_2 \epsilon_y}{a} = \frac{\Delta E}{E} \tag{851}$$

We define the contrast sensitivity as the rate at which the change of image contrast with respect to refraction angle is

$$S = \frac{dC}{d\epsilon} = \frac{f_2}{a} \tag{852}$$

Sensitivity

$$S = \frac{dC}{d\epsilon} = \frac{f_2}{a} \tag{853}$$

- This equation represents a simple optical result that is sufficient for most systems
- It is a measure of schlieren sensitivity independent of any observing or recording means
- It shows that the sensitivity is proportional to the focal length of the second parabolic mirror in the z-type system
- Longer focal lengths are superior!

Sensitivity

The image contrast responds linearly to refraction angle ϵ and the background illumination level is linear with respect to the degree of the knife-edge cutoff.

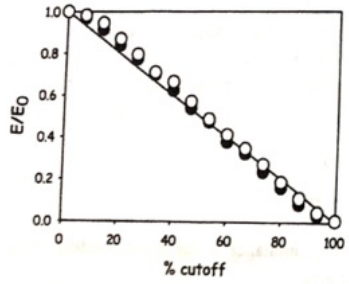

Figure 504: Plot of schlieren image illuminance ratio versus the percentage of knife-edge cut-off. Symbols are experimental data and the slid line is the prediction equation.

Departures from the linear theory we developed occur near 0 and 100 percent.

Sensitivity

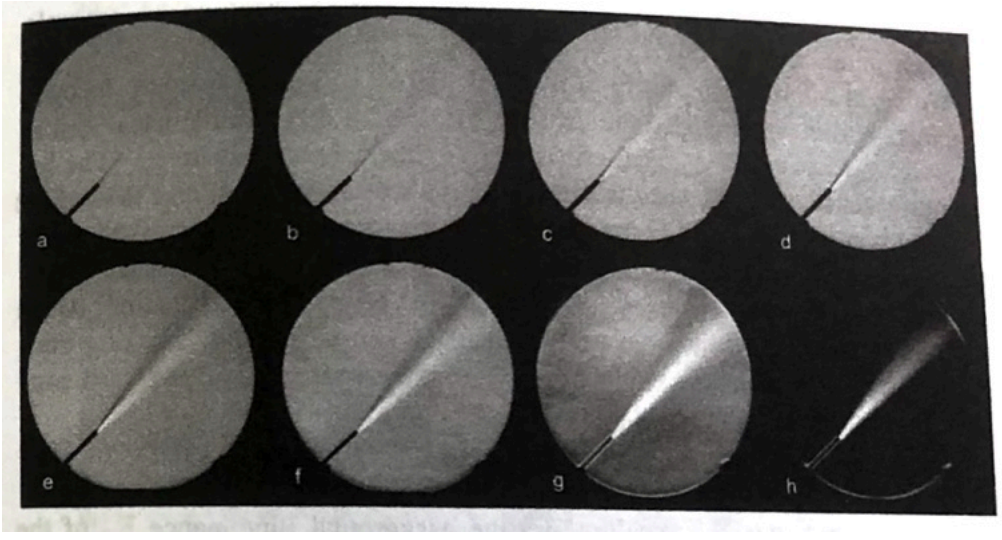

Figure 505: Long exposure schlieren of a jet. The degree of knife-edge cut-off of the sources images are a through h at 0, 20, 40, 60, 80, 90, 95 and 100%.

Sensitivity

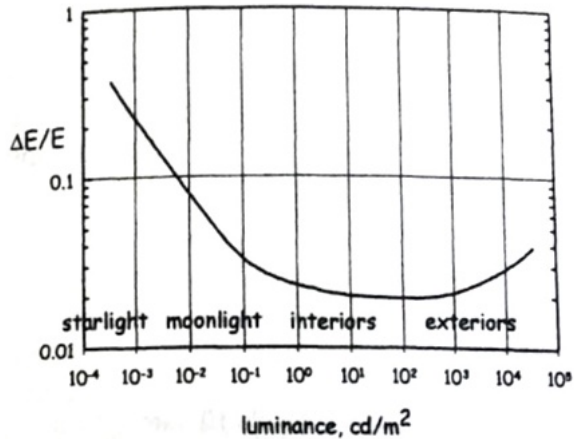

Figure 506: Contrast sensitivity of the human eye as a function of field luminance.

Class Summary

- Schlieren concepts
- Types of schlieren
- Sensitivity

Next Time

- Special Topics

Thank You

Class Outline

- Crash course in CFD
- Equations of motion and discretization
- Pre-processing
  - Geometry
  - Computational grid generation
- Solver
  - Solution of the discretized equations
  - Convergence and stability
- Post-processing
  - Inspection of solution
  - Graphing results

Crash Course in CFD

- *CFD is numerically solving an equation or set of equations that govern fluid motion*
  Throughout this class remember the following
  - CFD is a three step program
    - Pre-process - Setting up the problem
    - Solver - Solving the equations
    - Post-process - Analysis of the result
  - Skepticism - Is this result correct?

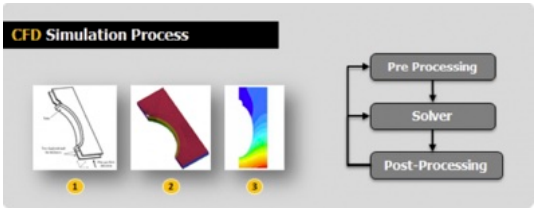

Equations of Motion and Discretization

- System of partial differential equations govern fluid dynamics
- For given boundary condition and domain the system of PDE do not have analytical solutions
- We should solve them numerically with digital computers
  - This is obviously easier stated than performed

$$\frac{\partial \rho}{\partial t} + \frac{\partial \rho u_j}{\partial x_j} = 0,$$

$$\frac{\partial \rho u_i}{\partial t} + \frac{\partial \rho u_i u_j}{\partial x_j} = -\frac{\partial p}{\partial x_j}\delta_{ij} + \frac{\partial \tau_{ij}}{\partial x_j},$$

$$\frac{\partial \rho e_o}{\partial t} + \frac{\partial \rho u_j e_o}{\partial x_j} = -\frac{\partial u_j p}{\partial x_j} - \frac{\partial q_j}{\partial x_j} + \frac{\partial u_j \tau_{ij}}{\partial x_j}$$

Subject to appropriate boundary conditions (BC)

Equations of Motion and Discretization

- Systems of PDE must be discretized for a discrete computer to solve them
- One example of discretization might involve replacing partial derivatives with their differenced form

$$\frac{\partial u(x)}{\partial x} = \lim_{\Delta x \to 0} \frac{u(x + \Delta x) - u(x)}{\Delta x} \qquad \left(\frac{\partial u}{\partial x}\right)_i = \frac{u_{i+1} - u_i}{\Delta x} + \mathcal{O}(\Delta x)$$

- We should also discretize time or just ignore it all together
- Our system of discretized PDE can now be solved with linear algebra or advanced nonlinear solvers
  - This is what the core of CFD computer programs execute

CFD Codes

- CFD Code - A suite of computer programs that solve fluid dynamic problems or a portion of the problem
- Commercial CFD codes provide pre-processors, solvers, and post-processors that work seamlessly
- Often integrate into a large aerospace companies workflow or can easily be used by individuals (eg: small groups like our class)
- In this class we are exercising the CD-Adaptco Star-CCM+ CFD code
- There are numerous codes available for free online, from governments (restricted), internal to companies (eg Boeing etc.)

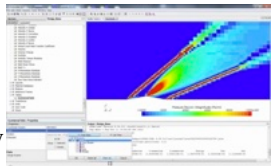

Defining the Problem

- Before trying out CFD, understand the underlying physics behind the problem.
- Check if CFD is feasible or not. Check if analytical solution is available or not.
- Get an idea on where grid refinement is needed, and where it is not needed.
- Classify the flow in various categories like laminar / turbulent, incompressible / compressible, etc based on non-dimensional numbers. Choose solvers accordingly.
- Verify and validate your results.

Pre-Processing - Geometry

- Discretized forms of the PDE must be solved at discrete points called grid points
- These grid points must conform (but not necessarily) to the domain and boundary conditions

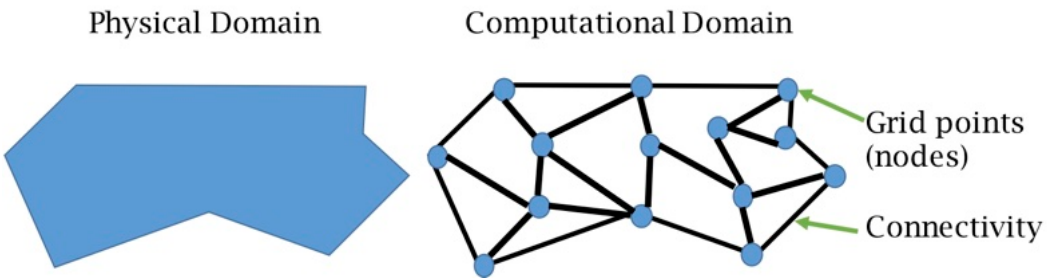

Pre-Processing - Computational Grid Generation

- Grid points and their connectivity can now easily number in the billions for large contemporary CFD simulations
- Large field of mathematics and engineering to create software or use software to make these grids - it is strangely fun
- As grid points are added to the solution should converge (hopefully)
- As grid points are added the computer power necessary to find a solution increases dramatically
- Expensive and specialized software has been created to create computational domains

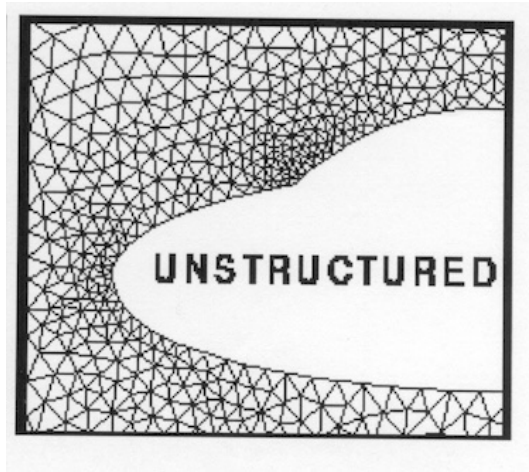

Solver - Solution of Discretized Equations

- Solvers responsible for finding solution of discretized form of equations
- Extremely complex and subject of much research over decades - even before the advent of digital computers
- Usually expressed as mathematical algorithms
- Implemented in high performance computing code such as C or Fortran along with MPI (parallel computing)

Solver - Solution of Discretized Equations

- In this class we will cover these are more!
  - Incompressible Flow Algorithms
    - ACM
    - SIMPLE
    - PISO
  - Compressible Flow Algorithms
    - PISO Compressible
    - Preconditioning
    - FDV
- It is easy to try various solver algorithms directly within our CFD code with a few clicks of the mouse
  - A poor choice of solver leads to no solution, the wrong solution, or a solution found very slowly
  - Remember, computational cost = money, keep costs down

Solver - Governing Equations

- Many choices of equations to solve
- Often a turbulence model is required for the problem of interest
- Often there are more unknowns then equations - as we need to find closure for these equations
  - This can constitute a turbulence model
- Many equations and models to choose
  - Know assumptions
  - Know when appropriate

Solver - Convergence and Stability

- Stability - The property of the solver where as it progresses towards finding the solution of the discretized equations the *error decays*
- Consistency - A finite difference representation of a PDE is consistent if the difference between the PDE and its discretized form representation vanishes as the mesh is refined
- Convergence - The discretized form of the equations of motions should approach that of the governing equations as the mesh is refined and the solver progresses

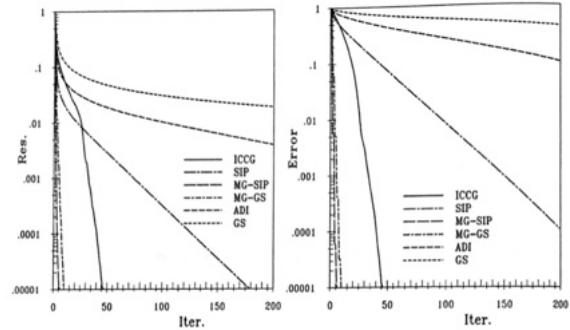

Fig. 5.5. Variation of the L_1 norm of residual (left) and iteration error (right) as a function of the number of performed iterations for various solvers and a 64×64 CV grid

$$Consistency + stability = convergence$$

Post-Processing - Inspection of Solution

- Post-Processing - Analysis, examination, plotting, visualization, and extraction of CFD solution
  - Solution is a numerical database containing the approximate solution of the discretized equations
- Visualization - Graphical or other representations of the solution for the understanding of physics and implication of the results
- Extraction - Process that derives quantitative or qualitative flow physics from CFD solutions
  - Typically this process is automated
- One typically examines the solution visually through various graphs
  - Experts, through experience, can observe when non-physical results are present

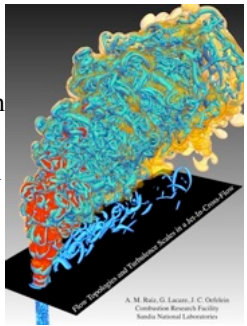

Post-Processing - Graphing Results

- There are many types of graphs
- Some are more helpful than others
- Qualitative vs Quantitative
- Graphs can be used to
  - Convey physical concepts
  - Compare predictions to experiments for quantitative validation

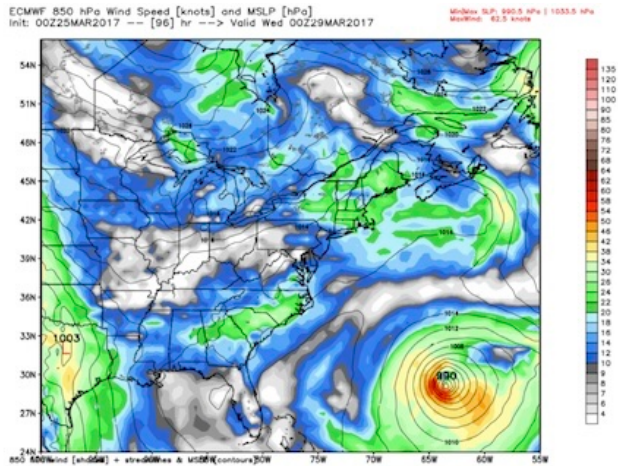

Post-Processing - Derived Quantities

- Remember that the solution only involves the field-variables
- Other quantities such as drag, lift, enstrophy, circulation, etc., must be derived from the field-variables

$$\Gamma = \int_{\partial S} \mathbf{V} \cdot dl = \int \int_{S} \omega \cdot d\mathbf{S}$$

Circulation

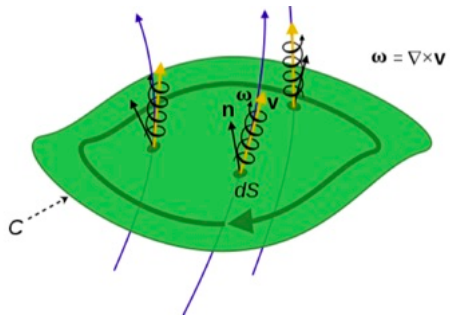

Class Summary and Conclusion

- Remember 3 Steps to CFD
  - Pre-process
  - Solver
  - Post-process
- Be skeptical
- Have fun exploring one contemporary CFD solver

Class Review

Class Review and Final Exam Information

Thank You